UNIVERSITEIT VAN PRETORIA
UNIVERSITY OF PRETORIA
YUNIBESITHI YA PRETORIA

CpMetal N-heterocyclic carbene complexes: Synthesis and applications

by

FREDERICK PIETER MALAN

Submitted in partial fulfilment of the requirements for the degree

PHILOSOPHIAE DOCTOR

in

CHEMISTRY

in the

FACULTY OF NATURAL AND AGRICULTURAL SCIENCES

of the

UNIVERSITY OF PRETORIA

Pretoria

October 2017

Table of Content

		Page
Declaration		VIII
Acknowledgements		IX
List of Abbreviations		X
List of Complexes		XII
Abstract		XVI
Preface		XVIII
Chapter 1		**1**
Half-sandwich transition metal complexes of normal and abnormal NHCs: Synergistic modulation of the steric and electronic metal environment		
1.	Introduction	1
2.	NHC as a class of ligands	3
3.	Nomenclature	5
4.	Chromium (Group 6 – Middle TM)	6
5.	Ruthenium (Group 8 – Late TM)	9
6.	Nickel (Group 10 – Late TM)	17
7.	Abnormal NHCs	23
8.	Catalytic applications	24
8.1	C-C and C-N bond formation	24
8.2	C-S bond formation	28
8.3	Oxidation/Reduction	28
8.4	Hydrosilylation	30
8.5	Miscellaneous	31

Chapter 2 33

Facile Suzuki-Miyaura coupling of activated aryl halides using new CpNiBr(NHC) complexes

Abstract 33

1. Introduction 34

2. Material and Methods 36

2.1 General 36

2.2 General synthesis of [CpNiBr(NHC)] complexes (**1**-**9**) 37

2.3 General procedure for the Suzuki-Miyaura coupling reactions 41

2.4 X-ray crystallography of compounds [H**L3**]Br, [H**L4**]Br, **1**, **2**, **3**, and **4** 41

3. Results and Discussion 41

3.1 Synthesis of cyclopentadienyl nickel(II) bromide NHC complexes 41

3.2 X-ray crystallographic studies 43

3.3 Suzuki-Miyaura coupling activity 46

4. Conclusion 50

Chapter 3 52

CpNiBr(NHC) complexes as pre-catalysts in the chemoselective anaerobic oxidation of secondary aryl alcohols: Experimental and DFT studies

Abstract 52

1. Introduction 53

2. Material and Methods 55

2.1 General 55

2.2 General synthesis of [CpNiBr(NHC)] complexes (**1**-**9**) 55

2.3 General procedure for the alcohol oxidation reactions 56

2.4 Computational methods 56

2.5 X-ray crystallography of **5**, **7**, and **8** 57

3. Results and Discussion 57

3.1 Synthesis of cyclopentadienyl nickel(II) bromide NHC complexes 57

3.2 X-ray crystallographic studies 58

3.3 Secondary alcohol oxidation activity 61

3.4 Mechanistic and computational considerations 67

4. Conclusion 73

Chapter 4 75

Synthesis, structure and DFT conformation analysis of CpNiX(NHC) and $NiX_2(NHC)_2$ (X = SPh or Br) complexes

Abstract 76

1. Introduction 76

2. Experimental 78

2.1 General 78

2.2 Synthesis 79

2.3 X-ray crystallography of **1**, **3**, **4** and **5** 81

2.4 Computational methods 81

3. Results and discussion 82

3.1 Synthesis of nickel(II) NHC complexes 82

3.2 X-ray crystallographic studies 85

3.3 DFT study 87

3.3.1 Conformational study 87

3.3.2 Electronic structure 91

3.3.3 Spectroscopy 93

4. Conclusion 93

Chapter 5 96

Electrochemistry of a series of symmetric and asymmetric CpNiBr(NHC) complexes: Probing the electrochemical environment due to push-pull effects

Abstract 97

1. Introduction 97

2. Experimental 99

2.1 General 99

2.2 Cyclic voltammetry 100

2.3 Computational methods 100

3. Results and Discussion 101

3.1 Synthesis of nickel(II) NHC complexes 101

3.2 Electrochemistry 103

3.2.1 Oxidation region 103

3.2.2 Reduction region 107

3.3 DFT studies 108

3.3.1 Non-NO_2-containing Ni(II)-NHCs 110

3.3.2 NO_2-containing Ni(II)-NHCs 111

3.3.3 Catalytic activities, redox potentials and DFT energies 114

4. Conclusion 116

Chapter 6 **119**

Base-free glucose dehydration catalysed by NHC-stabilised heterohalo cyclopentadienyl Cr(III) complexes

Abstract 119

1. Introduction 120

2. Results and Discussion 123

2.1 Synthesis of Cr(III)-NHC complexes 123

2.2 DFT studies 128

2.3 Electrochemistry 132

2.4 Glucose dehydration 135

3. Experimental 138

3.1 General considerations 138

3.2 General synthesis of [CpCrBrCl(NHC)] complexes 138

3.3 General (+)-D-glucose dehydration procedure 140

3.4 Cyclic voltammetry 141

3.5 Computational methods 141

3.6 X-ray crystallography of **1**-**7** 142

4. Conclusion 143

Chapter 7 **145**

Tandem transfer hydrogenation-epoxidation of ketone substrates catalysed by normal alkene-tethered Ru(II)-NHC complexes

Abstract 145

1. Introduction 146

2. Results and Discussion 148

2.1 Synthesis of the NHC ligands and metal precursors 148
2.2 Synthesis of the Ru(II)-NHC complexes 150
2.3 Catalytic studies 154
2.4 DFT studies 157
3. Experimental Section 158
3.1 General Procedures 158
3.2 General synthesis of half-sandwich Ru(II)-NHC complexes (**1**-**8**) 159
3.3 Transfer hydrogenation-epoxidation catalysis 162
3.4 X-ray crystallography of **L5**, **P2**, **P3**, **1**, **2**, **4**, **5**, **8**, and **1b** 163
4. Conclusion 163

Chapter 8 **166**

(De)hydrogenation catalysis by normal and abnormal alkene- and picolyl-tethered Ru(II)-NHC complexes

Abstract 166
1. Introduction 167
2. Results and Discussion 170
2.1 Synthesis of the NHC ligands 170
2.2 Synthesis of the normal and abnormal Ru(II) complexes 172
2.3 Acid stability studies 179
2.4 Transfer hydrogenation 181
2.5 Alcohol oxidation 184
3. Experimental Section 186
3.1 General Procedures 186
3.2 General synthesis of half-sandwich Ru(II) complexes (**1**-**10**) 186

3.3 Transfer hydrogenation catalysis 190

3.4 Secondary alcohol oxidation catalysis 191

3.5 X-ray crystallography of [H**L1**]Cl, [H**L4**]Cl, **1**, **3**, **4**, **5**, **6**, **7/8a**, **7/8b** and **10** 191

4. Conclusion 192

Chapter 9 **193**

Conclusion

Declaration

I, Frederick Pieter Malan hereby declare that the thesis titled "Cp-Metal *N*-heterocyclic carbene complexes: Synthesis and applications" which has been submitted to the University of Pretoria for the degree Philosophiae Doctor in Chemistry is my own work and has never been presented by me for the award of any degree or any examination at this or any other tertiary institution, and all sources of information contained herein have been accordingly acknowledged by means of complete references.

……..

Frederick Pieter Malan

October 2017

Acknowledgements

I would like to express my sincere gratitude to the following individuals:

The Lord Almighty for granting me the strength and perseverance to ensue this study. Without Him none of this would have been possible.

Prof Marilé Landman – Your continued guidance, advice and enthusiasm made all the work and effort that went into this work worthwhile. Thank you for giving me the opportunity to learn, for always making time available, and presenting me with many opportunities that would not have otherwise been possible.

Dr Eric Singleton – You remain one of the most influential people in my career. Thank you for always being willing to listen, advise, and share your invaluable knowledge. Prof Petrus van Rooyen – For always being willing to advise as our "wise and experienced" member of the group. Mr David Liles – For your willingness in helping me with problematic structures, and for teaching me the ways of X-ray diffractometry.

My parents Frederick and Magda Malan, my brother Francois Malan, and my extended family: Your love, patience, compassion and encouragement throughout my studies are greatly appreciated. Thank you for continually supporting and believing in me.

My friends (old and new) – Thank you for every contribution (major or minor) that helped me overcome the difficulties presented during this study. A special thanks to Nathan Antonels, Kariska Potgieter, Roan Fraser, Ozé Joubert, and Noël Joubert – all of your encouragement and special times together helped me see the positive side and reminded me to enjoy the ride.

Finally I am also grateful to the whole Chemistry Department of the University of Pretoria with special thanks to Prof PCB Forbes, Prof I Cukrowski, Dr Y Naudé, Dr M Selepe, Mrs R Swart, and Mrs N Steenkamp, for the contribution each of you have made during this study.

List of Abbreviations

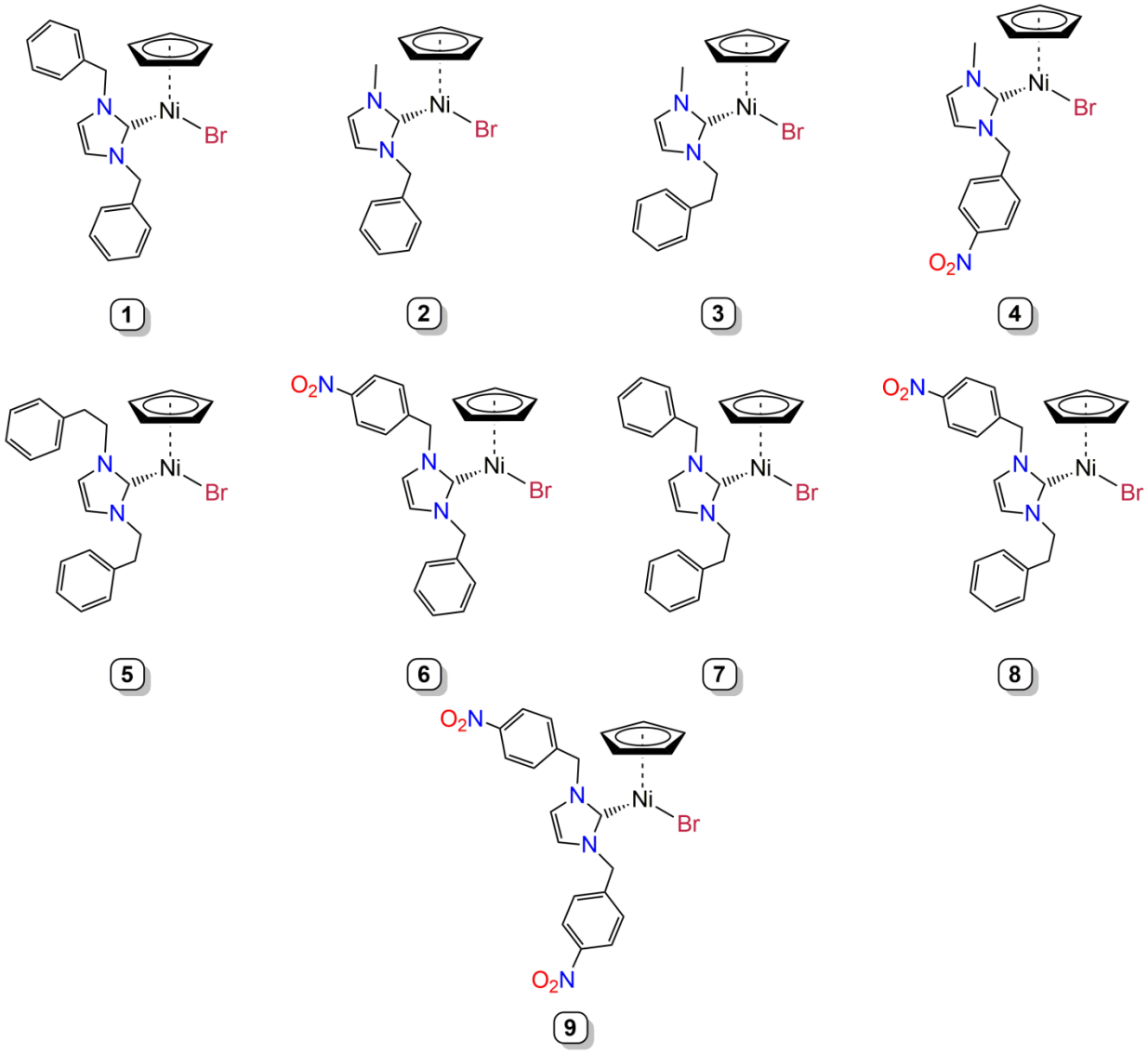
Å	Angström
acac	2,4-pentanedionato (acetylacetonate)
BAr_4^F	tetrakis[3,5-bis(trifluoromethyl)phenyl]borate
BIm	benzimidazole moiety
cod	1,5-cyclooctadiene
Cp	η^5-cyclopentadienyl
Cp*	η^5-pentamethylcyclopentadieniyl
CSD	The Cambridge Structural Database (May 2017 version)
dfppb	bis[di(2-fluorophenyl)phosphino]benzene
Fc	ferrocenyl
HOMO	Highest Occupied Molecular Orbital
HOTf	triflic acid
^{i}Pr	*iso*-propyl
IAd	*N*,*N'*-diadenyl imidazolylidene
I^{i}Pr	*N*,*N'*-diisopropyl imidazolylidene
I^{i}Pr^{Me2}	*N*,*N'*-diisopropyl-4,5-dimethyl imidazolylidene
ICy	*N*,*N'*-dicyclohexyl imidazolylidene
Idipp	*N*,*N'*-diisopropylphenyl imidazolylidene
Im	imidazole moiety
IMe	*N*,*N'*-dimethyl imidazolylidene
IMe^{Me2}	*N*,*N'*-dimethyl-4,5-dimethyl imidazolylidene

IMes	*N*,*N'*-dimesityl imidazolylidene
$IMes^{Cl2}$	*N*,*N'*-dimesityl-4,5-chloro imidazolylidene
IpClPh	*N*,*N'*-di-*para*-chlorophenyl imidazolylidene
IpTol	*N*,*N'*-di-*para*-tolyl imidazolylidene
IXy	*N*,*N'*-dixylyl imidazolylidene
LUMO	Lowest Unoccupied Molecular Orbital
^{n}Bu	*normal*-butyl
NHC	*N*-heterocyclic carbene
OTf	triflate (anion)
p-cym	*para*-cymene (1-methyl-4-(isopropyl) benzene)
ppm	parts per million
py	pyridine
SCXRD	Single Crystal X-Ray Diffractometry
SIdipp	*N*,*N'*-diisopropylphenyl imidazolinylidene
SIMe	*N*,*N'*-dimethyl imidazolinylidene
SIMes	*N*,*N'*-dimesityl imidazolinylidene
SImH	*N*,*N'*-dihydro imidazolinylidene
^{t}Bu	*tert*-butyl
THF	tetrahydrofuran
Tp	tris-pyrazolylborate, $[HB(pz)_3]^-$
Trip	tris-isopropylphenyl

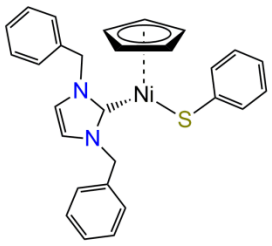
List of complexes

Only novel complexes are listed. Complex numbers are shown as they appear in each chapter. A total of 40 novel complexes have been synthesised.

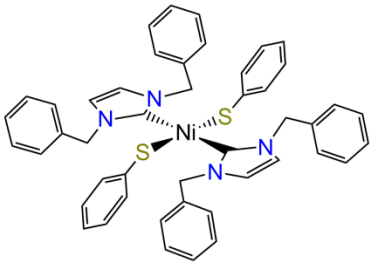
Chapter 2



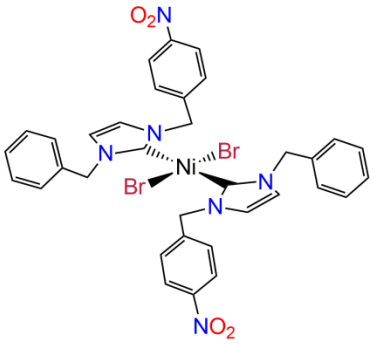
Chapter 4



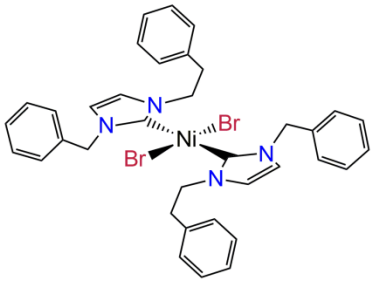
1



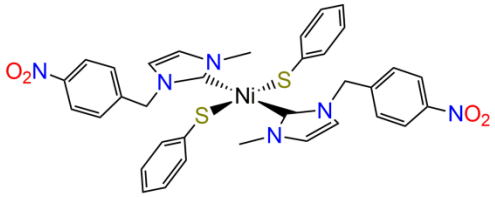
2



3

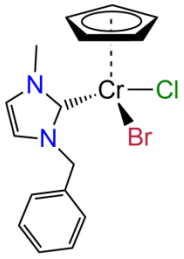


4

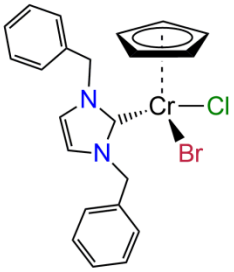


5

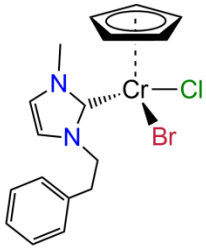
Chapter 6



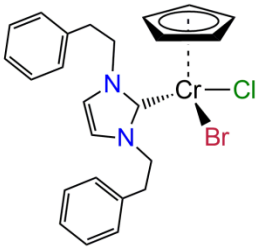
1



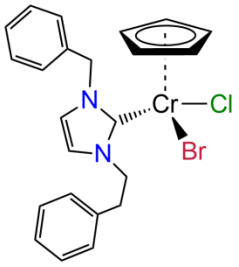
2



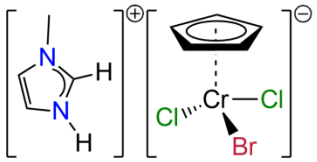
3



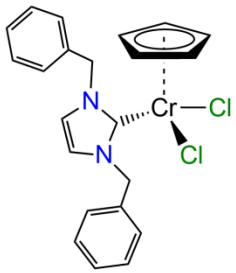
4



5

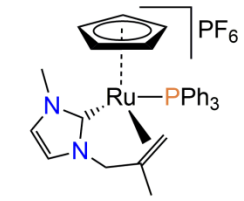


6

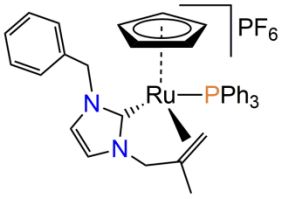


7

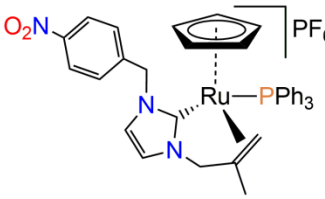
Chapter 7



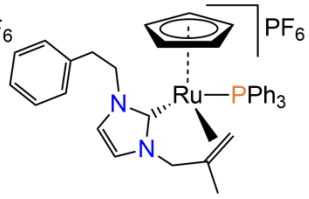
1



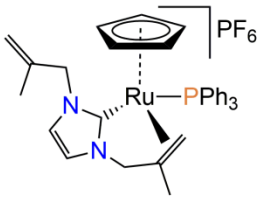
2



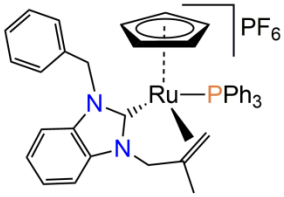
3



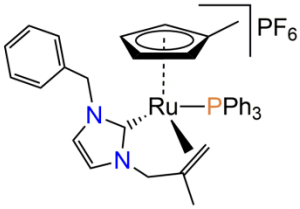
4



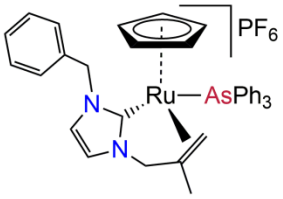
5



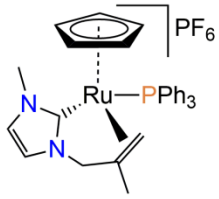
6



7

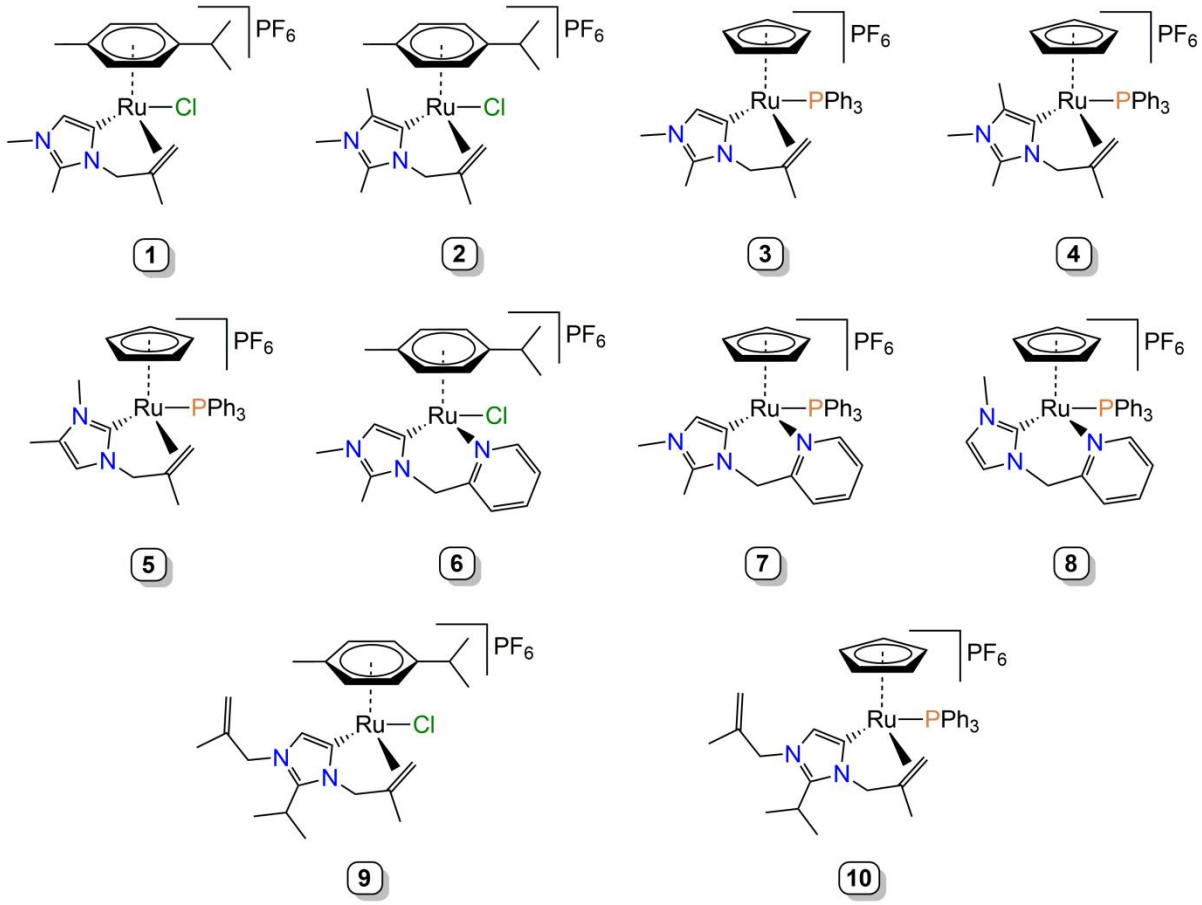


8



1b

Chapter 8



Abstract

The synthesis and catalytic application of new half-sandwich Ni(II), Cr(III), and Ru(II) complexes, all stabilised by either symmetric or asymmetric *N*-heterocyclic carbene (NHC) ligands, were investigated. The study entailed the synthesis of novel imidazolium halide salts as ligand precursors to the metal-NHC complexes. A range of nine (three symmetric, six asymmetric) imidazolium bromide salts were synthesised and characterized, with *N*-substituents including either electron-donating or electron-withdrawing groups. The ligands were reacted with nickelocene under inert conditions to form nine [CpNiBr(NHC)] complexes. These complexes were evaluated as catalysts in the Suzuki-Miyaura cross-coupling reaction for which moderate to good activity (53-79% conversion, maximum TOF = 320 h^{-1}) was observed. The catalytic activity of these complexes in the anaerobic oxidation of secondary alcohols was also assessed. Moderate activity (52-84% conversion, TOF = 14-86 h^{-1}) was observed using conventional heating, and excellent activity (90-98% conversion) using microwave heating. DFT studies provided insight into the better performance of the complexes featuring electron-donating NHCs as opposed to those with electron-withdrawing NHC ligands. In addition, DFT-supported energy profile studies explained the lack of formation of α-arylation byproducts, found for similar studies in the literature.

By-product formation of the type $[NiBr_2(NHC)_2]$ during synthesis of the above mentioned nickel NHC complexes led to the subsequent investigation of the reactivity and properties of the biscarbene complexes. Reaction of thiophenol with [CpNiBr(NHC)] or the biscarbene complexes, yielded complexes of the type [CpNi(SPh)(NHC)] and $[Ni(SPh)_2(NHC)_2]$. A detailed DFT study revealed structural preferences that were correlated with the experimentally observed structures. The electronic differences among the [CpNiBr(NHC)] complexes were further evaluated through a DFT-supported electrochemistry study, which showed some electrochemical variances due to the different *N*-alkyl substituents present in the nickel complexes.

Reaction of chromocene with the novel non-NO_2-containing imidazolium bromide salts, followed by chromium oxidation using CCl_4, allowed for the formation, purification and

characterisation of five [CpCrBrCl(NHC)] complexes. Exposure of these heterohalo complexes to excess $CHCl_3$ or CCl_4 leads to the formation of complexes [$CpCrCl_2$(NHC)]. Upon reaction of chromocene with the novel NO_2-containing imidazolium salts, a ligand decomposition reaction occurs. C-N bond cleavage and imidazole protonation result in the formation of [$C_4H_7N_2$][$CpCrBrCl_2$]. The catalytic activity of the six Cr(III)-NHC complexes was evaluated in the base-free glucose dehydration reaction for which moderate activity (52-81% conversion) was observed. Supplementary DFT studies added insight into the electrochemical properties of the Cr(III) complexes.

A range of six new bidentate (benz)imidazolium chloride salts (one symmetric, five asymmetric), each bearing an *N*-2-methylallyl substituent were synthesised and complexed to ruthenium(II) (three different Ru(II) precursors) *via* silver transmetallation. Eight new cationic complexes [(C_5H_4R)Ru(EPh_3)(NHC)]PF_6 (R = H, Me; E = P, As; NHC = Im(R')(2-methylallyl), BIm(Bn)(2-methylallyl); R' = alkyl) were isolated, purified and characterised. DFT studies illustrated the electronic properties of the complexes, while a catalytic study (tandem transfer hydrogenation-epoxidation of ketone substrates) showed moderate activity (39-62% conversion, TOF = 4-12 h^{-1}) for all of the complexes. Finally, a range of four new C(2)-protected bidentate imidazolium chloride salts (one symmetric, three asymmetric), each containing either an *N*-2-methylallyl or *N*-picolyl substituent, were synthesised and characterised. These ligands were found suitable as ligand precursors to abnormal NHCs, and hence were reacted with [(*p*-cym)$RuCl_2$]$_2$ or [$CpRuCl(PPh_3)_2$] to form ten new Ru(II)-NHC complexes (eight Ru-aNHC and two Ru-NHC complexes). The Ru-NHC complexes formed as by-products due to Ag-mediated C(2)-dealkylation in selected cases. The strength of the Ru-aNHC bond was probed in an ^{1}H-NMR titration study with DCl, which showed its superior bond strength when compared to analogous normally bound Ru-NHC complexes. The catalytic activity of the latter ten complexes was screened in both the transfer hydrogenation and alcohol oxidation reactions. The complexes are therefore more suitable as transfer hydrogenation catalysts (50-93% conversion, TOF = 22-60 h^{-1}) than for application in alcohol oxidation catalysis (56-77% conversion, TOF = 2-11 h^{-1}).

Preface

The aim of the research outlined in this thesis focuses on the development of robust, yet highly active catalysts for a variety of metal-specific catalytic transformations. The study evaluated the use of cyclopentadienyl and imidazolylidene (NHC) as ligands coordinating to nickel(II), chromium(III), and ruthenium(II) to stabilise the resultant complexes, as well as their corresponding sensitive catalytic intermediates. To this end, a number of objectives have been set out for this study in order to achieve this aim:

- The synthesis of new symmetric (R = R') and asymmetric (R ≠ R') imidazolium bromide salts, bearing different electron-donating and electron-withdrawing substituents as NHC ligand precursors for complexation.
- Subsequent synthesis and characterisation of [CpNiBr(NHC)] complexes.
- Evaluation of the catalytic activities of the Ni-NHC complexes in catalytic reactions associated with expensive PGM catalysts, i.e. Suzuki-Miyaura coupling reaction and the anaerobic secondary alcohol oxidation reaction, as a more economical option.
- Synthesis and characterisation of an analogous range of [CpCrBrCl(NHC)] complexes using the above mentioned new NHC ligands.
- Evaluation of the catalytic activity of the range of Cr-NHC complexes in a lesser-studied catalytic application, i.e. the dehydration of glucose to form 5-hydroxymethylfurfural.
- The synthesis of two novel ranges of alkene-tethered bidentate imidazolium chloride ligands: the one for use as normally bound NHC (nNHC) ligands and the other for employment as abnormally bound NHC (aNHC) ligands.
- Subsequent syntheses and characterisation of a range of Ru-nNHC and Ru-aNHC complexes.
- Assessment of the catalytic activities of the Ru-nNHC and Ru-aNHC in similar applications, to evaluate the effect of the mode (normal *versus* abnormal) of coordination of the NHC ligand.
- Identification of structure-activity relationships for each set of complexes and their metal-specific catalytic applications by means of DFT and electrochemical studies.

An extremely large body of work in the literature dealing with the use of NHCs features the standard, commercially available NHCs of IMes, IDipp, and I^{i}Pr in their investigations. Very few studies employ custom NHCs that vary both according to steric bulk en electronic properties. However, we were interested in synthesising a range of different NHCs that (i) is fluxional, (ii) bears different degrees of steric bulk, (iii) is electronically different in terms of their overall donor capacities, and (iv) exhibit potentially hemilabile *N*-moieties (Chapters 2, 7 and 8). In terms of Ni(II)-NHCs: Prior to our contributions (as presented in this thesis), relatively few CpNiBr(NHC) complexes were known as compared to analogous CpNiX(NHC) (X = Cl, I) complexes, with even less employed in catalytic processes. In Chapters 2 and 3 we addressed this by synthesizing a range of new CpNiBr(NHC) complexes for which we observed moderate to high catalytic activity. Furthermore, side-reactions observed that led to the isolation of interesting Ni(II) biscarbene species were also investigated and reported on (Chapter 4). Apart from one preliminary report on the electrochemistry of the CpNi(NHC) complexes, no detailed electrochemical study detailing the chemical nature of all oxidation and reduction processes observed exist. We address this research gap in Chapter 5 with a detailed, DFT-supported electrochemical study.

In terms of Cr(III)-NHC systems, only a select few $CpCrCl_2$(NHC) complexes exist, of which classic polymerization/oligomerisation catalysis is the only catalytic application these complexes were evaluated for. In Chapter 6 we investigated the synthesis of new heterohalo CrBrCl(NHC) complex systems, and employed it for the first time in the environmentally important reaction of glucose dehydration. In general, the activities of our Cr(III) complexes compared well to existing Cr(II) and Cr(III) halide salt systems employing ionic liquids. In Chapter 7 we address the lack of known [CpRuL(NHC)]X (L = pnictogen, X = anion) complexes and their catalytic application through the synthesis of 8 new complexes, which were all catalytically active in the tandem transfer hydrogenation/epoxidation of carbonyl substrates. With these complexes, we attempted to exploit the catalytic advantage of custom-designed potentially hemilabile NHC ligands through the employment of alkenyl-tether moieties. Chapter 8 deals with the serious lack of known abnormally bound Ru(II) complexes and their catalytic applications. The change in coordination mode of NHCs from normal (classic) to abnormally is well-known to have profound advantages in terms of catalyst stability, reactivity, and catalytic activity. We have

synthesized eight new abnormal Ru(II)-aNHC complexes, and evaluated their catalytic activity in the transfer hydrogenation of ketones, as well as the secondary alcohol oxidation reactions. Furthermore, we investigate the robustness of the Ru-aNHC bond by acid stability tests and successfully address the serious problem of normal *vs.* abnormal selectivity in Ag-NHC synthesis.

A major part of this thesis has, or is in the process of being published as separate publications. Each chapter starts with the relevant publication details. In addition, details pertaining to my personal contributions to the work contained within each chapter are included. Assigned complex numbers are unique for each chapter and do not follow from previous chapters.

1 Half-sandwich transition metal complexes of normal and abnormal NHCs: Synergistic modulation of the steric and electronic metal environment

Frederick P. Malan, Eric Singleton, Petrus H. van Rooyen, M. Landman*

Department of Chemistry, University of Pretoria, 02 Lynnwood Road, Hatfield, Pretoria, 0002, South Africa.

Abstract

As part of our continued interest in cyclopentadienyl complexes featuring highly stabilising *N*-heterocyclic carbene (NHC) ligands, we focus on the employment of earth-abundant and easily accessible middle to late transition metals. This aligns closely with global efforts to access, research, and further develop high-value chemicals synthesised using efficient, sophisticated, and economical catalysts. As part of our efforts, we have limited the focus on the use of the abundant chromium and nickel metals as alternatives to the more expensive literature examples (usually PGM metals), as well as the more expensive ruthenium metal, which serves as a convenient platform for the comparison of both normal and abnormally bound Ru-NHC complexes. To this end, an up-to-date review covering the organometallic chemistry of half-sandwich transition metal complexes bearing normal and abnormal *N*-heterocyclic carbenes of chromium, ruthenium, and nickel is presented. The work presented here is by no means exhaustive, but serves to report on the most notable reactions and isolated metal complex species published to date. In addition, the metal-specific syntheses and catalytic applications of these complexes are briefly discussed.

1. Introduction

Since the discovery of ferrocene more than six decades ago,[1] science, technology, and medicine in all their vastly different fields have seen tremendous advancement because of the breakthrough that organometallic chemistry has since provided.[2] Some of the major applications

[1] G. B. Kauffman, *J. Chem. Ed.*, 1983, **60**, 185-186.
[2] W. J. Evans, *Organometallics*, 2016, **35**, 3088-3100.

of *N*-heterocyclic carbene-containing organometallic complexes include luminescence,[3,4] electrophosphoresence,[5,6] inorganic synthesis,[7,8] organic synthesis *via* catalysis,[9,10] biocatalysis,[11,12] and bio-application as drugs.[13-15] Research on organometallic complexes and intermediates has also illustrated the important role that organo-ligands can play, which are often not simple spectator or "innocent" ligands.

The cyclopentadienyl ligand is one of the key ligands that allowed for the development and better understanding of the rich chemistry associated with the M-C bond. The importance stems from the early involvement of the Cp ligand in the synthesis of the first metallocene, ferrocene (Cp_2Fe), from which the field of metallocene chemistry has been developed further to include a multitude of functionalised cyclopentadienyl ligands that are tailored for refined and multi-functional catalysis.[16] Evans has aptly stated: "Although these advances should not be limited only to organometallic environments, it is the cyclopentadienyl ligand that made these discoveries possible for the first time. Bravo, Cp! It is a ligand that should not be overlooked just because it is very old." [16] Until about two decades ago, cyclopentadienyl and phosphine ligands were considered to be two main classes of ligands that were sterically and electronically tunable and found widespread use in organometallic catalysis.[17] The phosphine ligand series in particular is able to provide diverse steric modifications in a reliable and predictable fashion, mostly due to the pioneering work of Tolman and co-workers.[17] Since the discovery of the first isolated free

[3] L. Mercs, M. Albrecht, *Chem. Soc. Rev.*, 2010, **39**, 1903-1912.
[4] R. Visbal, M. C. Gimeno, *Chem. Soc. Rev.*, 2014, **43**, 3551-3574.
[5] V. A. Krylova, P. I. Djurovich, M. T. Whited, M. E. Thompson, *Chem. Commun.*, 2010, **46**, 6696-6698.
[6] V. J. Catalano, A. O. Etogo, *Inorg. Chem.*, 2007, **46**, 5608-5615.
[7] B. Royo, E. Peris, *Eur. J. Inorg. Chem.*, 2012, 1309-1318.
[8] C. M. Crudden, D. P. Allen, *Coord. Chem. Rev.*, 2004, **248**, 2247-2273.
[9] S. Díez-González, N. Marion, S. P. Nolan, *Chem. Rev.*, 2009, **109**, 3612-3676.
[10] E. Levin, E. Ivry, C. E. Diesendruck, N. G. Lemcoff, *Chem. Rev.*, 2015, **115**, 4607-4692.
[11] T. Liu, M. Y. Darensbourg, *J. Am. Chem. Soc.*, 2007, **129**, 7008-7009.
[12] G. A. N. Felton, C. A. Mebi, B. J. Petro, A. K. Vannucci, D. H. Evans, R. S. Glass, D. L. Lichtenberger, *J. Organomet. Chem.*, 2009, **694**, 2681-2699.
[13] P. V. Simpson, I. Casari, S. Paternoster, B. W. Skelton, *Chem. Eur. J.*, 2017, **23**, 6518-6521.
[14] M-L. Teyssot, A-S. Jarrousse, M. Manin, A. Chevry, S. Roche, F. Norre, C. Beaudoin, L. Morel, D. Boyer, R. Mahiou, A. Gautier, *Dalton Trans.*, 2009, 6894-6902.
[15] A. Gautier, F. Cisnetti, *Metallomics*, 2012, **4**, 23-32.
[16] W. J. Evans, *Organometallics*, 2016, **35**, 3088-3100.
[17] R. H. Crabtree, *J. Organomet. Chem.*, 2005, **690**, 5451-5457.

NHC in 1991 by Arduengo *et al.*,[18] a new class of highly stabilising ligands has made its debut in organometallic chemistry. Today NHCs is a widely electronically and sterically diverse, multi-functional, and multi-applicable ligand class that can no longer be considered merely as a phosphine analogue.[17,19,20] Many examples of organometallic complexes exploiting the advantages of both cyclopentadienyl and NHC ligand classes simultaneously have since emerged, with successful application in both organometallic[7] and bio-inorganic chemistry.[13-15]

In this literature review the syntheses and applications of numerous existing cyclopentadienyl transition metal complexes bearing imidazolylidene-based NHCs are described, including how the two ligand classes might function together to enhance complex stability, reactivity, and catalytic efficiency. The focus here revolves around chromium (group 6), ruthenium (group 8), and nickel (group 10) featuring both cyclopentadienyl (and their substituted analogues) and NHCs (imidazolylidenes), and their respective catalytic applications. Although numerous NHC-bearing half-sandwich complexes of the arene-type and/or tris-pyrazolyl borate (Tp) exist, it was decided to exclude these classes of half-sandwich complexes since they each constitute a wide range of unique $[(L_3)M(NHC)]^{n+}$ (L_3 = arene, Tp; n > 0) complexes with interesting applications that could form sizable contributions on their own.

2. NHC as a class of ligands

N-heterocyclic carbenes (NHCs) have developed over the last three decades into a class of one of the most catalytically useful ligands. Of these ligands, the five-membered imidazolylidenes remain by far the most popular and have been extensively derivatised to modulate steric, electronic, and other bi-functional requirements in transition metal catalysis. As seen in Chart 1, the number of papers published in a literature search using SciFinder[21] for the phrase '*N*-

[18] A. J. Arduengo, R. L. Harlow, M. Kline, *J. Am. Chem. Soc.*, 1991, **113**, 361-363.
[19] Z. Wang, L. Jiang, D. K. B. Mohamed, J. Zhao, T. S. Andy Hor, *Coord Chem. Rev.*, 2015, **293-294**, 292-326.
[20] R. H. Crabtree, *Coord. Chem. Rev.*, 2013, **257**, 755-766.
[21] SciFinder, version 2017; Chemical Abstracts Service: Columbus, OH, **2017**.

heterocyclic carbene' and 'NHC', along with the corresponding hits in the CSD database[22] is shown to have an exponential increase, especially over the last decade.

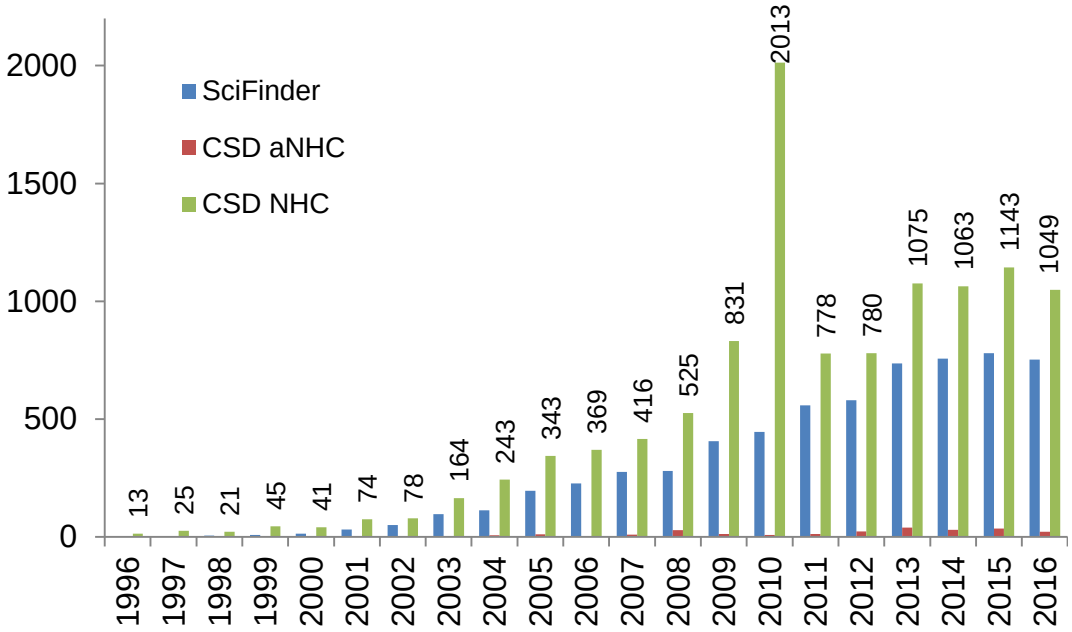


Chart 1: Plot of the number of publications found using '*N*-heterocyclic carbene' on SciFinder[21] (blue), and number of hits found of normally (green) and abnormally (red) bound transition metal NHC complexes on the CSD database,[22] between 1996-2016.

NHCs find widespread application mainly because of their strong σ-electron donating properties with little to no π-back donation of the NHC ligand, all of which helps form strong NHC-metal bonds and hence stabilise sensitive transition metal species.[4,19,20] A famous example of the successful utilisation of NHCs in catalysis is the Grubbs catalyst. The first generation Grubbs catalyst containing two phosphine ligands was found to be highly active in the metathesis of unsaturated hydrocarbons. The activity and stability of the catalyst was found to be greatly enhanced once one of the phosphine ligands were replaced by an NHC ligand.[23] Imidazolylidenes typically have nitrogen substituents that help donate π electrons to the carbene centre, and hence enhance its nucleophilicity and thermodynamic stability. The interaction of the *N*-substituent π electrons with the pπ-orbital of the carbene carbon atom leads to a four-electron-three-centre π system, generally with an associated multiple bond character for the carbene-

[22] The Cambridge Structural Database, C. R. Groom, I. J. Bruno, M. P. Lightfoot, S. C. Ward, *Acta Cryst.*, 2016, **B72**, 171-179.
[23] M. Scholl, S. Ding, C. W. Lee, R. H. Grubbs, *Org. Lett.*, 1999, **1**, 953-956.

substituent bond(s) (Figure 1).[24,25] In contrast, the metal-carbene bond found in Fischer carbenes is a donor-acceptor bond with σ-donation from the carbene carbon to the metal and π-back donation from the metal to the carbene moiety. Fischer carbenes are typically associated with low oxidation state metals with π-accepting ligands and π-donor substituents on the carbene ligand moiety.[26] However, Schrock carbene ligands are typically associated with high oxidation state metals with non-π-accepting ligands and without π-donor substituents on the carbene ligand moiety.[27] Fischer carbenes are encountered in the singlet spin state, whereas Schrock carbenes are usually in the triplet spin state.

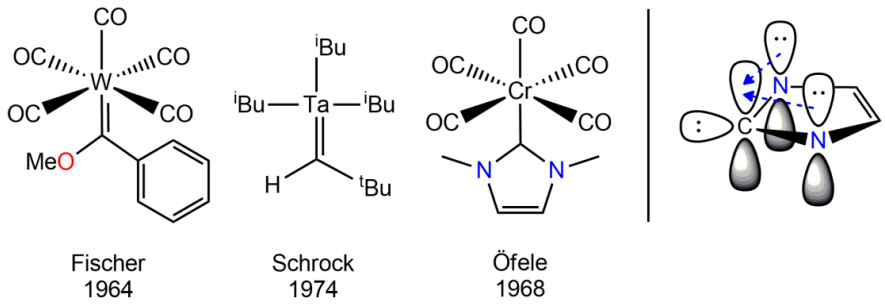


Figure 1: The first structurally characterised Fischer, Schrock, and NHC complexes. In NHC complexes, carbene stabilisation is supported through π-interactions.

3. Nomenclature

For clarity purposes, it is important that the nomenclature of imidazole derivatives and their carbene-adducts are reviewed. Due to several inconsistencies present in the literature, the nomenclature shown in Figure 2(a) will be followed throughout this thesis. In addition, selected examples of the most commonly employed NHC ligands are illustrated in Figure 2(b). The ligated normal NHC metal complexes have been depicted in various different ways in the literature (**I-IV** in Figure 2(c)), and therefore the indicated representation **I** will be followed throughout.

[24] F. E. Hahn, M. C. Jahnke, *Angew. Chem. Int. Ed.*, 2008, **47**, 3122-3172.
[25] D. Bourissou, O. Guerret, F. P. Gabbaï, G. Bertrand, *Chem. Rev.*, 2000, **100**, 39-91.
[26] R. Fraser, P. H. van Rooyen, M. Landman, *J. Coord. Chem.*, 2016, **69**, 2972-2987.
[27] S. Díez-González, S. P. Nolan, *Coord. Chem. Rev.*, 2007, **251**, 874-883.

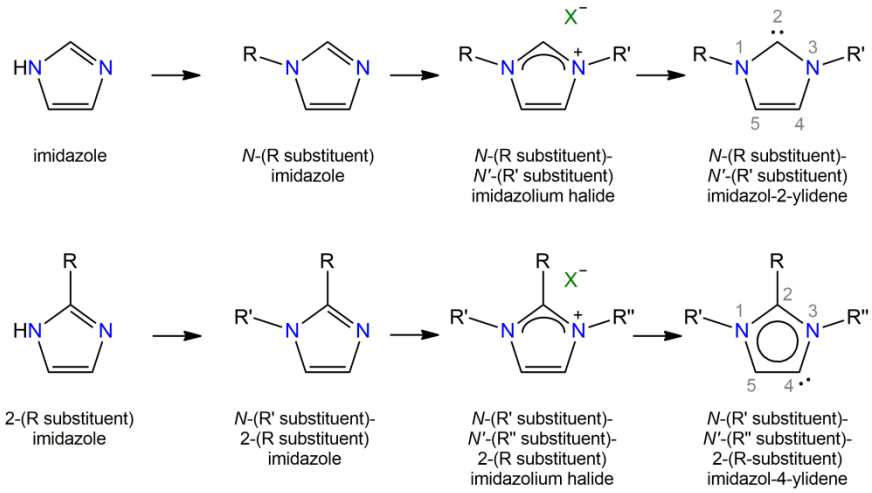


Figure 2(a): The different nomenclature of imidazole, imidazolium, and imidazolylidene derivatives.

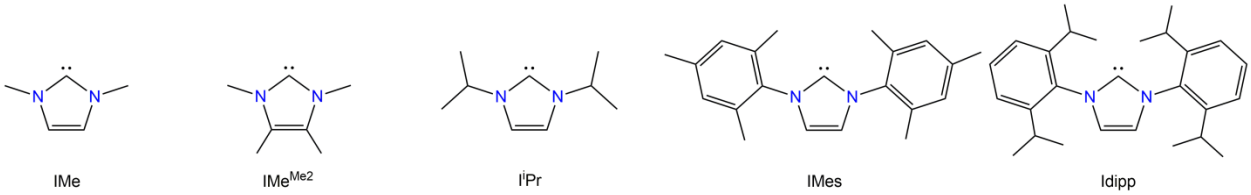


Figure 2(b): Selected examples of commonly employed NHC ligands in the literature.

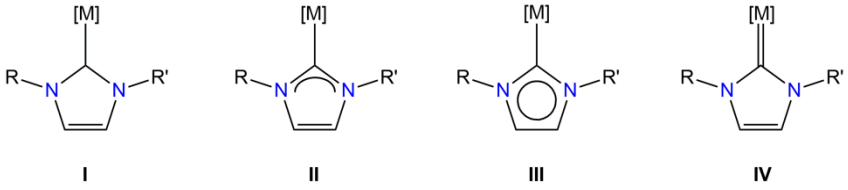


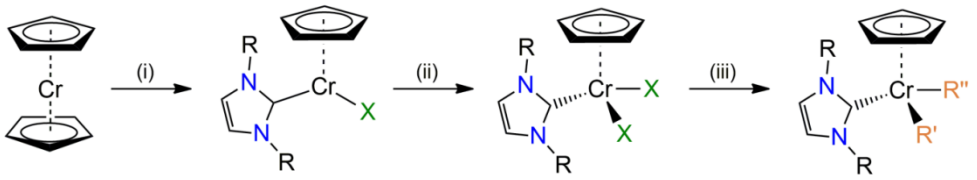
Figure 2(c): Different depictions (**I-IV**) of the metal-NHC moiety in the literature.

4. Chromium (Group 6 – Middle TM)

The first ever Cr-NHC complex synthesised, $[Cr(CO)_5(IMe)]$, was reported by Öfele[28] in 1968. Since then Cr-NHC chemistry has noticeably expanded such that complexes containing chromium in a variety of oxidation states (0),[19,28] (I),[19] (II),[29,30] (III),[29,32] (IV),[19] and (V),[19] are known to date (Figure 3). Despite this expansion, relatively few reports exist which specifically focus on half-sandwich complexes of Cr(II) and Cr(III) NHCs.[19] The first cyclopentadienyl Cr-

[28] K. Öfele, *J. Organomet. Chem.*, 1968, **12**, 42-44.

NHC complex was only reported in 1999, by the Tilset group.[29] They reported the protonolysis reaction of chromocene with the imidazolium salt [HIMes]Cl to yield the 14-electron Cr(II) complex [CpCrCl(IMes)] (**1**) (see Scheme 1 for general synthesis route). During this reaction a molecule of cyclopentadiene is eliminated, which could easily be removed through extraction with hexane. Complex **1** is highly air sensitive, although thermally stable, producing a melt without decomposition.[29] Chloride exchange of **1** with PhMgBr was also possible, and gave rise to [CpCr(Ph)(IMes)] (**2**). The Cr(II) centre could be oxidised to Cr(III) by addition of $CHCl_3$ to **1** to form [$CpCrCl_2$(IMes)] (**3**).[29] Also in 1999, Cowley and Jones' group[30] observed that the reaction of chromocene with the NHC (IMes or IMe^{Me2}), led to the formation of the highly air-sensitive 14-electron Cr(II) complexes [CpCr(η^1-C_5H_5)(IMes)] (**4**) and [CpCr(IMe^{Me2})$_2$]C_5H_5 (**5**).[30] Complex **4** served as the first example of a thermally stable [CpCr(η^1-C_5H_5)(NHC)] complex.



Scheme 1: General syntheses of CpCr(II)-NHC and CpCr(III)-NHC derivatives. (i) [HIm(R)$_2$]X, THF, reflux. (ii) $CHCl_3$/CCl_4/$PbCl_2$/I_2, stir. (iii) MeLi/PhMgBr/Bn_2Mg/Ph_2Mg, stir.

In 2011 Zhou *et al.*[31] reported the I^iPr derivative of **1**, [CpCrCl(I^iPr)] (**6**). The iodo derivative of IMe, [CpCrI(IMe)] (**7**), was obtained using chromocene and [HIMe]I. Further reaction of complex **6** with MesMgBr in Et_2O gave the complex [CpCr(Mes)(I^iPr)] (**8**).[31] In an attempt to further stabilise the sensitive Cr(II) species, oxidation of chromium(II) with $PbCl_2$ (for **6**) or I_2 (for **7**) produced the corresponding Cr(III)-NHC complexes [$CpCrCl_2$(I^iPr)] (**9**) and [CpCrI(Mes)(I^iPr)] (**10**), respectively. Other routes to Cr(III)-NHCs also exist, for example treatment of the Cr(III) complex [Cp_2Cr]I with [HIMe]I resulted in the formation of [$CpCrI_2$(IMe)] (**11**).[31] Similarly the complex [Cp'$CrCl_2$(THF)] (Cp' = Cp, Cp*) reacts with

[29] M. H. Voges, C. Rømming, M. Tilset, *Organometallics*, 1999, **18**, 529-533.
[30] C. D. Abernethy, J. A. C. Clyburne, A. H. Cowley, R. A. Jones, *J. Am. Chem. Soc.*, 1999, **121**, 2329-2330.
[31] W. Zhou, J. A. Therrien, D. L. K. Wence, E. N. Yallits, J. L. Conway, B. O. Patrick, K. M. Smith, *Dalton Trans.*, 2011, **40**, 337-339.

[HIMe^{Me2}]Cl to yield [Cp'CrCl$_2$(IMe^{Me2})] (Cp' = Cp (**12**), Cp* (**13**)).[32] Substitution reactions of **12** and **13** with the Grignard reagent MeMgCl or MeLi gave the corresponding alkylated complexes [Cp'Cr(Me)$_2$(IMe^{Me2})] (Cp' = Cp (**14**), Cp* (**15**)).

Several other cyclopentadienyl-derivative Cr-NHC complexes have since been reported, for example the indenyl-functionalised Cr(III)-NHC complexes, [(Indenyl-NHC)CrCl$_2$] (**16**, **17**) by Conde-Guadano *et al.*[33] in 2012. These complexes were prepared from CrCl$_3$(THF)$_3$ and the potassium salt of the indenyl-functionalised NHC ligands, which upon complexation form a distorted two-legged piano stool structure. A Cr(II) analogue of **16**, [(Indenyl-NHC)CrCl] (**18**), was prepared from CrCl$_2$ and the corresponding potassium salt of the indenyl NHC ligand. When CrCl$_2$(CH$_3$)(THF)$_3$ is used as Cr(III) source, mixed methyl chloride Cr(III)-NHC complexes of the type [(Indenyl-NHC)CrCl(Me)] (**19,20**) are isolated. Complex **16** could also be reacted with either Bn$_2$Mg or Ph$_2$Mg in a substitution reaction to form the isostructural Cr(III) complexes [(Indenyl-NHC)Cr(Bn)$_2$] (**21**) and [(Indenyl-NHC)CrCl(Ph)] (**22**), respectively.[33] THF solutions containing the neutral Cr-Me complexes **19** and **20**, and Cr-Bn complex **21**, were converted to the cationic complexes [(Indenyl-NHC)CrCl(THF)]B(C$_6$F$_5$)$_4$ (**22, 23**), and [(Indenyl-NHC)CrBn(THF)]B(C$_6$F$_5$)$_4$ (**24**), respectively. Interestingly, the methyl groups were exchanged and the chloride ligands left intact, contrary to the expected outcome of similar ligand exchange reactions. When subjected to a petroleum ether atmosphere, a concentrated THF solution of **18** dimerises to form the rare distorted tetrahedral complex [{(Indenyl-NHC)CrCl}$_2$(μ-O)] (**25**).

An interesting 17-electron chromium radical, [CpCr(CO)$_2$(IMe)]$^{\bullet}$ (**26**) formed in a comproportionation reaction of [CpCr(CO$_2$)]$_2$ with IMe, has been reported by Bullock and co-workers.[34] Complex **26** adopts a classical piano stool structure with three irregularly positioned legs whereby the C$_{CO}$-Cr-C$_{CO}$ bond angle is noticeably smaller than the C$_{NHC}$-Cr-C$_{CO}$ bond angles. Complex **26** was also found not to react with the radical scavenger 2,6-di-*tert*-butyl-1,4-dibenzoquinone (DBBQ) to form an adduct, as have been found with its tungsten analogue.[34]

[32] A. Döhring, J. Göhre, P. W. Jolly, B. Kryger, J. Rust, G. P. J. Verhovnik, *Organometallics*, 2000, **19**, 388-402.
[33] S. Conde-Guadano, A. A. Danopoulos, R. Pattacini, M. Hanton, R. P. Tooze, *Organometallics*, 2012, **31**, 1643-1652.
[34] E. F. van der Eide, M. L. Helm, E. D. Walter, R. M. Bullock, *Inorg. Chem.*, 2013, **52**, 1591-1603.

However, complex **26** can be reduced by KC_8 in THF to form the 18-electron Cr(II) complex K[CpCr(CO)$_2$(IMe)] (**27**). Addition of 18-crown-6 to **27** yields [K(18-crown-6)][CpCr(CO)$_2$(IMe)] (**28**) in which all of the six oxygen atoms bind to the potassium ion, while the potassium ion simultaneously interacts with the bound carbonyl and NHC moieties. Protonation of either **27** or **28** results in the formation of the corresponding hydride complex [CpCrH(CO)$_2$(IMe)] (**29**) which, however, has not been isolated to date.[34]

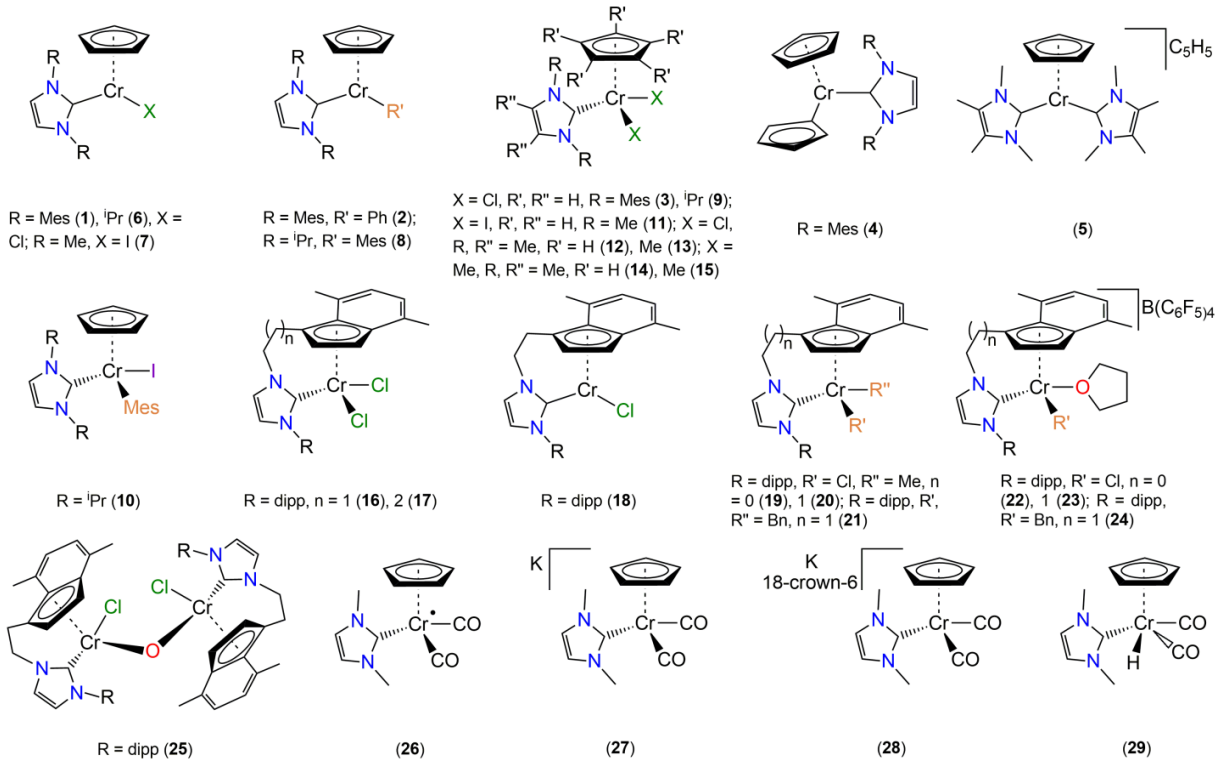


Figure 3: Cyclopentadienyl-based Cr-NHC complexes reported in literature.

5. Ruthenium (Group 8 – Late TM)

To date, ruthenium remains the most extensively studied of the half-sandwich NHC-bearing group 8 metals, with most of the complexes finding multi-functional use in organometallic chemistry, homogeneous catalysis, and as biologically active compounds.[35,36] This could be partly ascribed to the increasing number of routes to readily accessible ruthenium starting

[35] P. Kumar, R. K. Gupta, D. S. Pandey, *Chem. Soc. Rev.*, 2014, **43**, 707-733.
[36] V. Dragutan, I. Dragutan, L. Delaude, A. Demonceau, *Coord. Chem. Rev.*, 2007, **251**, 765-794.

materials, and the facile synthetic routes employed to produce catalytically active, stable, and chemoselective half-sandwich Ru-NHC complexes.[36] The first cyclopentadienyl Ru-NHC complexes were synthesised in 1999 by Nolan and co-workers[37,38] and were based on the reaction of the tetrameric $[Cp^*RuCl]_4$ with carbene ligands to afford coordinatively unsaturated complexes of the type [Cp*RuCl(NHC)] (NHC = IMes (**30**), ICy (**31**), IpTol (**32**), IpClPh (**33**), IAd (**34**), $IMes^{Cl2}$ (**35**), Idipp (**36**)) in high yields (> 80%).[37,38,39] Calorimetric studies on these complexes provided evidence for the strong binding nature of the NHCs as opposed to the related phosphines, e.g. a PCy_3 ligand in the complex $[Cp^*RuCl(PCy_3)]$ may be substituted for an ICy ligand to form **31** along with a loss of 10 kcal/mol.[38]

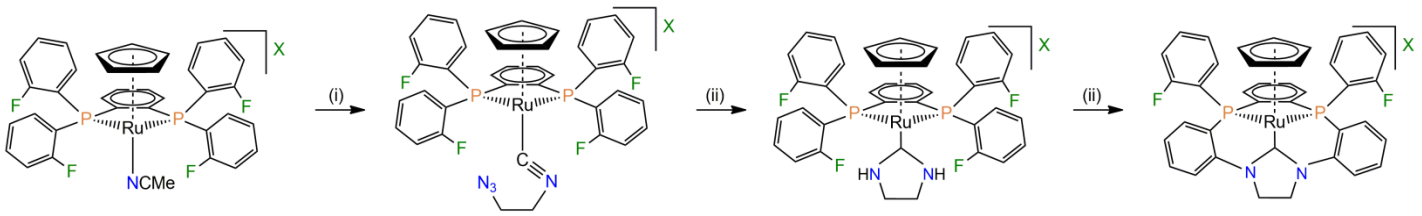
The series was later expanded by the same group to include chiral imidazolylidene ligands within the complexes [Cp*RuCl(NHC)] (NHC = ImR_2; R = *R*-1-1cyclohexylethyl (**37**), 1*S*,2*S*,3*S*,5*R*-isopinocamphenyl (**38**), *R*-α-methylbenzyl (**39**)).[40] Shortly after, Herrmann's group devised another route to complexes **30** (IMes) and **31** (ICy) in near quantitative yields.[41] In their route they made use of the versatile precursor $[Cp^*Ru(OMe)]_2$ which was reacted with the imidazolium chloride salt to give **30** and **31** respectively, along with concomitant MeOH elimination. Furthermore, they found complex **31** to be reactive to addition of CO, PPh_3, and pyridine in order to produce coordinatively saturated complexes of [Cp*RuCl(ICy)(L)] (L = CO (**40**), PPh_3 (**41**), py (**42**)). In 2002 the Herrmann group reported additional synthetic routes to CpRu-NHC complexes using the easily accessible ruthenium precursors $[Cp'RuCl(PR_3)_2]$ (Cp' = Cp, Cp*; R = Ph, 2-MeC_6H_4), $[CpRuCl(L)\{PPh_2(2\text{-}MeC_6H_4)\}]$ (L = CO, $=CPh_2$).[42] For example, treatment of either $[Cp'RuCl(PR_3)_2]$ or $[CpRuCl(L)\{PPh_2(2\text{-}MeC_6H_4)\}]$ (L = CO, $=CPh_2$) with NHC ligand (ICy), leads to the formation of $[CpRuCl(ICy)_2]$ (**43**), [Cp*RuCl(ICy)(L)] (L = CO (**40**), PPh_3 (**41**)), [CpRuCl(CO)(ICy)] (**44**), and $[CpRuCl(=CPh_2)(ICy)]$ (**45**), respectively. Interestingly, the second PPh_3 ligand is not substituted for a second NHC ligand during the formation of **41**, due to the steric demand presented by the Cp* ligand as opposed to the Cp

[37] J. Huang, E. D. Stevens, S. P. Nolan, J. L. Petersen, *J. Am. Chem. Soc.*, 1999, **121**, 2674-2678.
[38] J. Huang, H-J. Schanz, E. D. Stevens, S. P. Nolan, *Organometallics*, 1999, **18**, 2370-2375.
[39] L. Jafarpour, E. D. Stevens, S. P. Nolan, *J. Organomet. Chem.*, 2000, **606**, 49-54.
[40] J. Huang, L. Jafarpour, A. C. Hillier, E. D. Stevens, S. P. Nolan, *Organometallics*, 2001, **20**, 2878-2882.
[41] W. Baratta, W. A. Herrmann, P. Rigo, J. Schwarz, *J. Organomet. Chem.*, 2000, **593-594**, 489-493.
[42] W. Baratta, E. Herdtweck, W. A. Herrmann, P. Rigo, J. Schwarz, *Organometallics*, 2002, **21**, 2101-2106.

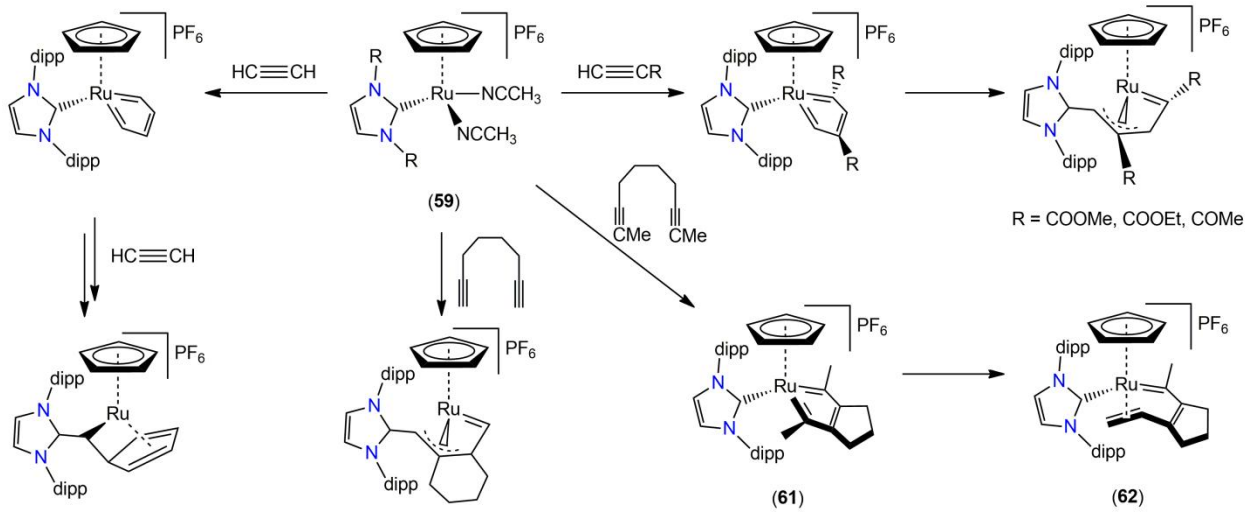
ligand. Complex **41** served as a suitable precursor for PPh_3 substitution reactions: Treatment of **41** with CO, pyridine, or ethyldiazoacetate all form the PPh_3-substituted complexes **40**, **42**, and [Cp*RuCl(=CHCO$_2$Et)(ICy)] (**46**), respectively. The first saturated NHC ligands on CpRu were reported by the group of Nolan,[43] in combination with calorimetric and quantum mechanics studies that revealed bond dissociation energies not much different from their unsaturated analogues. Following the route described above, $[Cp^*RuCl]_4$ reacts with NHC ligands (SIMes, SIdipp) to form the 16-electron complexes [Cp*RuCl(NHC)] (NHC = SIMes (**47**), SIdipp (**48**)).

In terms of chiral-at-metal complexes with built-in chiral NHC components, Ganter and co-workers[44] synthesised chiral phosphaferrocene NHCs and ligated them to ruthenium. Upon reaction of NHC ligands with $[Cp^*RuCl]_4$ in dry THF, complexes of type [Cp*RuCl(NHC)] (NHC = Im(Me)(CH$_2$FcP) (**49**), Im(CH$_2$FcP)$_2$ (**50**)) were synthesised. Interestingly, **50** could not be isolated due to the spontaneous further reaction (if heated, or in the presence of THF) of **50** to form **51**, [Cp*Ru(NHC)]Cl, bearing the bidentate phosphaferrocene NHC ligand.[44] Hahn and co-workers[45] reported the azide-containing isocyanide ring-closing reactions in CpRu systems (Scheme 2). In these reactions, the complexes $[CpRu(dfppb)(CNCH_2CH_2N_3)]^+$, containing bisphosphine and azido isocyanide ligands, react with Zn/NH_4Cl in a H_2O/MeOH mixture to reduce the azide to a primary amine moiety, followed by a ring-closing reaction to give the CpRu-NHC complexes [CpRu(dfppb)(SImH)]X (X= Cl (**52**), BF_4 (**53**), ½$ZnCl_4$ (**54**)). Subsequent reactions of **52**-**54** with KO^{t}Bu lead to intramolecular C-F activation and formation of a tridentate NHC ligand in the complexes [CpRu(dfppb-NHC)]X (X= Cl (**55**), BF_4 (**56**), ½$ZnCl_4$ (**57**)). Similar reactions by the same group using other mono- and bis-phosphine analogues were performed to give rise to imidazolinylidene and benzimidazolylidene-containing CpRu-NHC complexes.[46]

[43] A. C. Hillier, W. J. Sommer, B. S. Yong, J. L. Petersen, L. Cavallo, S. P. Nolan, *Organometallics*, 2003, **22**, 4322-4326.
[44] H. Willms, W. Frank, C. Ganter, *Chem. Eur. J.*, 2008, **14**, 2719-2729.
[45] A. Flores-Figueroa, O. Kaufhold, A. Hepp, R. Fröhlich, F. E. Hahn, *Organometallics*, 2009, **28**, 6362-6369.
[46] A. Flores-Figueroa, O. Kaufhold, K-O. Feldmann, F. E. Hahn, *Dalton Trans.*, 2009, 9334-9342.



Scheme 2: Ring-closing synthesis of complexes **52**-**57**. Reagents: (i) (2-azidoethyl)isonitrile (ii) Zn, NH_4Cl, H_2O (iii) KO^tBu.



Scheme 3: Reactions of **59** with various mono- and bis-acetylenes.

In 2006 Sun *et al.*[47] published a synthetic route in which a 1,5-cod ligand is displaced with an NHC in the complex containing a bidentate Cp-borane ($C_2B_{10}H_{10}$) ligand, to form the corresponding complex [(Cp-borane)Ru(IMe^{Me2})$_2$] (**58**) in moderate yield. In that same year, Kirchner and co-workers[48-50] published novel insertion reactions that coordinated NHC ligands undergo when CpRu-NHC species are reacted with acetylenes. When the complexes [CpRu(NHC)(CH_3CN)$_2$]PF_6 (NHC = Idipp (**59**); for SIdipp (**60**) analogue see Figure 5) are reacted with various mono- and bis-acetylenes, C-C coupling including NHC migration leads to the formation of the formal [2+2+1] cycloaddition products of the type [CpRu(η^4-C_5H_5-η^1-CH-Idipp)] (Scheme 3). The complexes **59** and **60** are synthesised from the corresponding NHC salts,

[47] Y. Sun, H-S. Chan, P. H. Dixneuf, Z. Xie, *J. Organomet. Chem.*, 2006, **691**, 3071-3082.
[48] E. Becker, V. Stingl, G. Dazinger, M. Puchberger, K. Mereiter, K. Kirchner, *J. Am. Chem. Soc.*, 2006, **128**, 6572-6573.
[49] E. Becker, V. Stingl, K. Mereiter, K. Kirchner, *Organometallics*, 2006, **25**, 4166-4169.
[50] E. Becker, V. Stingl, G. Dazinger, K. Mereiter, K. Kirchner, *Organometallics*, 2007, **26**, 1531-1535.

nBuLi as base, and $[CpRu(CH_3CN)_3]PF_6$ as ruthenium precursor. Following this methodology, the tris-carbene complex $[CpRu(Idipp)(=C_2(Me)_2C_2(CH_2)_3]PF_6$ (**61**), and its 1,2-H shift analogue **62** have been isolated and characterised.[49]

The first bidentate pyridyl-containing NHCs were reported by Araki *et al.*[51] Using similar routes as for **30**-**36** described above, $[Cp^*RuCl]_4$ reacts directly with *N*-pyridyl benzimidazole to form the complex [Cp*RuCl(BIm(H)(py))] (**63**) *via* a tautomerisation reaction of the imidazole in high yield. The bidentate NHC binding nature in **63** was confirmed with ^{1}H- and ^{13}C-NMR spectroscopy, as well as with X-ray structural analysis. Reaction of complex **63** with silver nitrite in CH_3CN affords the nitrosyl-imidazolyl complex *via* intramolecular proton migration, which after KOTf anion exchange, gave the complex [CpRu(NO)(BIm(py))]OTf (**64**). All characterisation data acquired for **64** point to the absence of carbene coordination. Only upon protonation of **64** with HOTf could the imidazolyl-functionality be transformed to a formal NHC ligand, shown in complex **65**. Kollipara[52] and Valerga[53] further expanded on the range of *N*-donor functionalised CpRu-NHCs through the syntheses of pyrimidyl- and picolyl-containing NHC complexes. The pyrimidyl complexes **66** and **67** by Kollipara were accessed through reaction of $[(X)RuCl(PPh_3)_2]$ (X = Cp, indenyl) with the carbene (*via* transmetallation from the silver-NHC complex).[52] The picolyl-substituted NHCs of Valerga and co-workers[53] were obtained by reaction of $[Cp^*Ru(CH_3CN)_3]PF_6$ with the deprotonated NHC ligands, to furnish complexes of the type $[Cp^*Ru(CH_3CN)(NHC)]PF_6$ (**68**-**73**). Anion exchange with $KBAr_4^F$ of **68** gave the BAr_4^F-analogue **74**, whereas the same reaction in air with **69** yielded the O_2-ligated complex $[Cp^*Ru(O_2)\{Im(^iPr)(picolyl)\}]BAr_4^F$ (**75**). The CH_3CN ligand of **68**-**73** proved labile enough to be substituted for the stronger binding CO ligand, from which complexes **76**-**81** were synthesised.[53]

Furthermore, various groups developed a variety of different N-, P-, C-, O-, and S-donor functionalised bidentate NHC ligands and coordinated them to the CpRu-fragment in various ways: Hahn[54] made use of the classical $[Cp^*RuCl]_4$ route to access P-donor functionalised

[51] K. Araki, S. Kuwata, T. Ikariya, *Organometallics*, 2008, **27**, 2176-2178.
[52] V. R. Anna, R. Pallepogu, Z-Y. Zhou, M. R. Kollipara, *Inorg. Chim. Acta*, 2012, **387**, 37-44.
[53] F. E. Fernández, M. C. Puerta, P. Valerga, *Organometallics*, 2011, **30**, 5793-5802.
[54] F. E. Hahn, A. R. Naziruddin, A. Hepp, T. Pape, *Organometallics*, 2010, **29**, 5283-5288.

CpRu-NHC complexes **82** and **83**, whereas Grotjahn[55] made use of the [CpRuCl(cod)] precursor to access related complexes **84-91**. Albrecht and co-workers[56] reacted [CpRuCl(PPh_3)$_2$] with olefin-, thioether-, and carboxylate-functionalised NHCs to form CpRu-NHC complexes **92-95** while Morris and co-workers[57,58] reported new complexes of the type [Cp*Ru{IMe($PhEtNH_2$)}(L)]PF_6 (L = py (**96**), CO (**97**)) functionalised with primary amine donor NHCs. Tilley and co-workers[59-62] reported a reactive group of silylene and stannylene-based CpRu-NHC complexes from the versatile complex [Cp*RuCl(IXy)] (**98**). Halide abstraction led to C-H activation of the NHC moiety to give complex [Cp*Ru(IXy-H)] (**99**), which binds N_2 stoichiometrically to form [Cp*Ru(N_2)(IXy-H)] (**100**).[59] Further reaction of **100** with substituted silanes $RSiH_3$ (R = H, Mes, Tol, Trip) or the stannyl compound $TripSnH_3$ gave rise to the thermally stable, colourless complexes [Cp*RuH(EH_2R)(IXy-H)] (E = Si, R = Mes (**101**), Tol (**102**), Trip (**103**); E = Sn, R = Trip (**104**)). Finally, subsequent reactions of complex **103** with ketones, secondary alcohols, or tosyl azides activate the silylene moiety for 1,2-hydrogen transfer to form the silylether-adduct complexes **105-116**.[59,60,61]

Nikonov and co-workers[63,64] reported the reactive complex, [CpRuCl(Idipp)] (**117b**), obtained from [CpRu(py)$_2$(Idipp)]PF_6 (**117a**) which is formed from [CpRu(py)$_3$]PF_6 and Idipp. Complex **117a** can be oxidised to the corresponding Ru(IV) complex with $LiAlH_4$, [CpRuH_3(Idipp)] (**118**), which is able to activate silanes to yield silyl dihydride complexes [CpRuH_2(Idipp)(SiR_3)] (R = Cl (**119**), Cl_2Me (**120**), $ClMe_2$ (**121**), H_2Ph (**122**), HMePh (**123**), Me_2Ph (**124**)).[63] Similarly, complex **117b** reacts with the same silanes to give the silyl derivative complexes of

[55] V. Miranda-Soto, D. B. Grotjahn, A. L. Cooksy, J. A. Golen, C. E. Moore, A. L. Rheingold, *Angew. Chem. Int. Ed.*, 2011, **50**, 631-635.
[56] C. Gandolfi, M. Heckenroth, A. Neels, G. Laurenczy, M. Albrecht, *Organometallics*, 2009, **28**, 5112-5121.
[57] W. W. N. O, A. J. Lough, R. H. Morris, *Organometallics*, 2012, **31**, 2137-2151.
[58] W. W. N. O, A. J. Lough, R. H. Morris, *Chem. Commun.*, 2010, **46**, 8240-8242.
[59] H-J. Liu, C. Raynaud, O. Eisenstein, T. D. Tilley, *J. Am. Chem. Soc.*, 2014, **136**, 11473-11482.
[60] H-J. Liu, C. Landis, C. Raynaud, O. Eisenstein, T. D. Tilley, *J. Am. Chem. Soc.*, 2015, **137**, 9186-9194.
[61] H-J. Liu, M. S. Ziegler, T. D. Tilley, *Angew. Chem. Int. Ed.*, 2015, **54**, 6622-6626.
[62] H-J. Liu, J. Guihaumé, T. Davin, C. Raynaud, O. Eisenstein, T. D. Tilley, *J. Am. Chem. Soc.*, 2014, **136**, 13991-13994.
[63] V. H. Mai, L. G. Kuzmina, A. V. Churakov, I. Korobkov, J. A. K. Howard, G. I. Nikonov, *Dalton Trans.*, 2016, **45**, 208-215.
[64] V. H. Mai, I. Korobkov, G. I. Nikonov, *Organometallics*, 2016, **35**, 936-942.

[CpRuClH(SiR_3)] (**125-129**).[64] Recently Nolan's group[65,66] expanded on the range of coordinatively unsaturated CpRu-NHC complexes by reporting the novel complexes [Cp*RuCl(Idipp*)] (**130**) and [Cp*Ru(OH)(NHC)] (NHC = Idipp (**131**), IMes (**132**)). Finally, Wang[67] and Peris' groups[68] independently synthesised indenyl- and cyclopentadienyl-functionalised Ru-NHC complexes directly from $Ru_3(CO)_{12}$ and the cyclopentadiene-containing NHC. The work of Wang focused on the use of indenyl-functionalised NHCs to oxidatively add onto Ru(0) to form the Ru(II) complexes of [(Indenyl-NHC)RuBr(CO)] (**133**, **134**) along with the loss of H_2(g).[67] Peris and co-workers[68] focused on the use of substituted cyclopentadienyl-functionalised NHCs to form the chiral complexes **135** and **136**. Upon employing a chiral amine as auxiliary ligand, the diastereomeric mixtures of complexes **135** and **136** could be separated using preparative thin-layer chromatography. The above synthetic protocol employed leads to a total of eight accessible routes to cyclopentadienyl-functionalised Ru-NHC complexes as reviewed in this chapter (Figure 4).

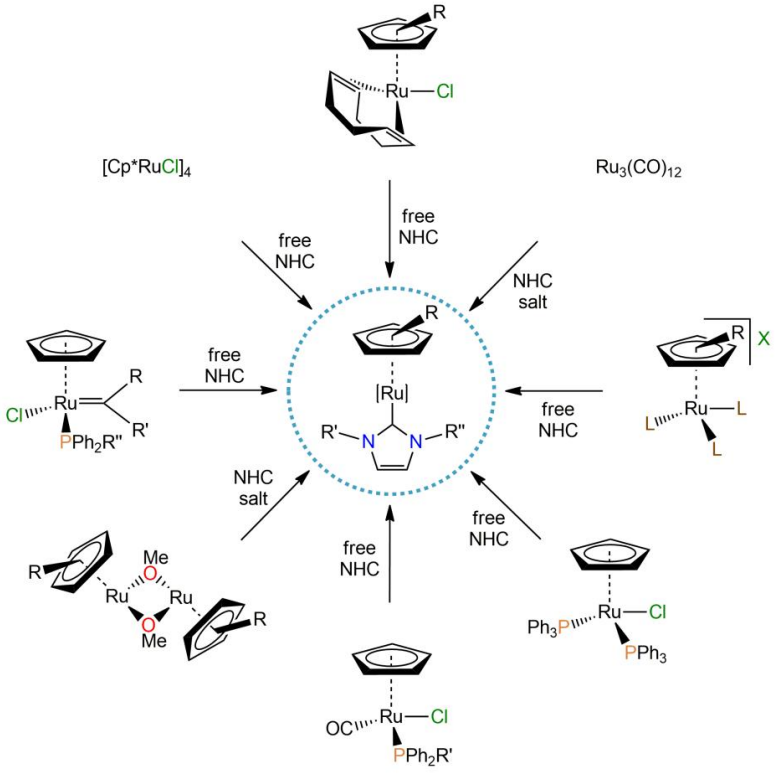


Figure 4: Synthetic routes employed to CpRu-NHC complexes.

[65] J. Balogh, A. M. Z. Slawin, S. P. Nolan, *Organometallics*, 2012, **31**, 3259-3263.
[66] P. Nun, G. C. Fortman, A. M. Z. Slawin, S. P. Nolan, *Organometallics*, 2011, **30**, 6347-6350.
[67] C. Zhang, F. Luo, B. Cheng, B. Li, H. Song, S. Xu, B. Wang, *Dalton Trans.*, 2009, 7230-7235.
[68] A. P. da Costa, J. A. Mata, B. Royo, E. Peris, *Organometallics*, 2010, **29**, 1832-1838.

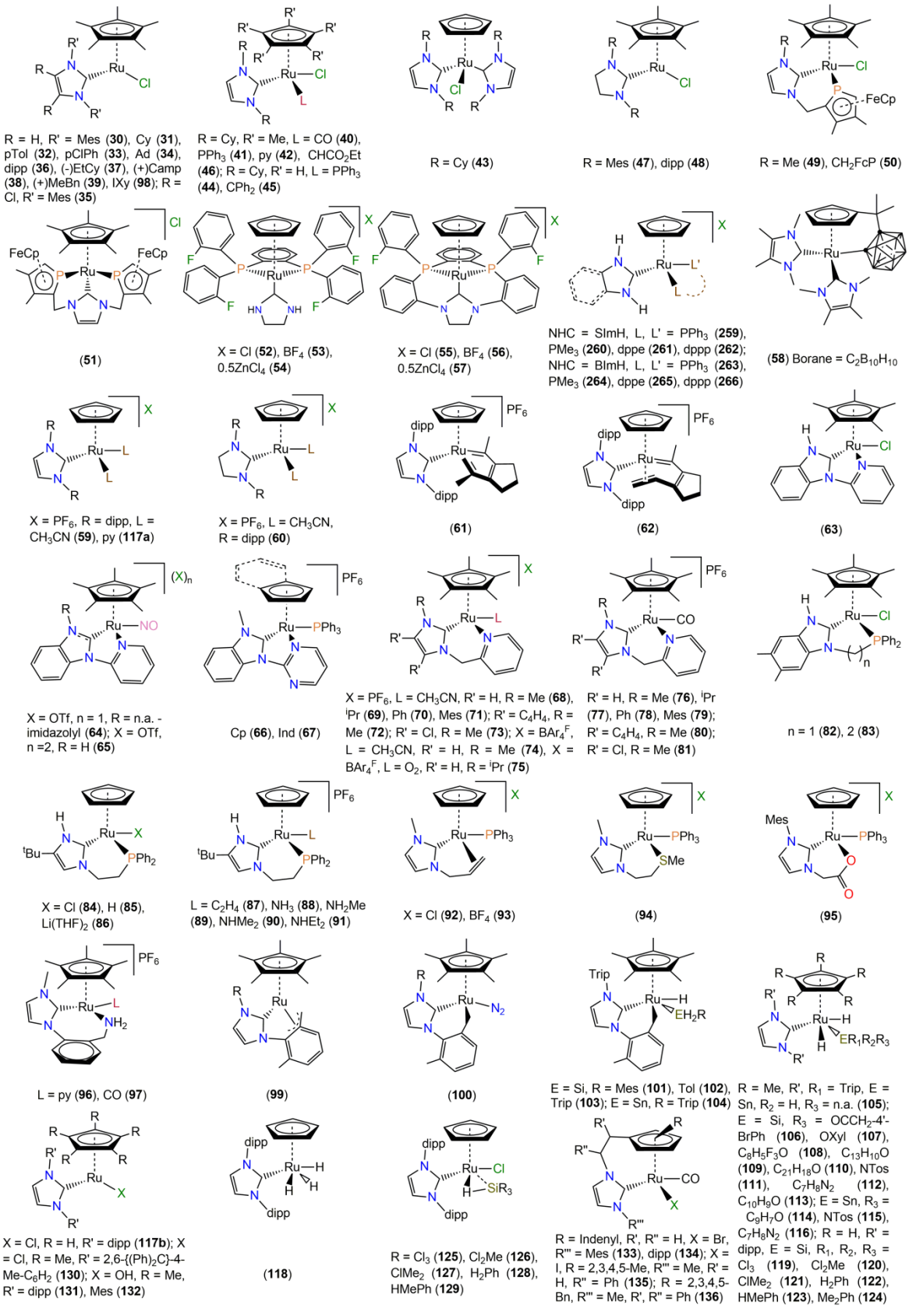
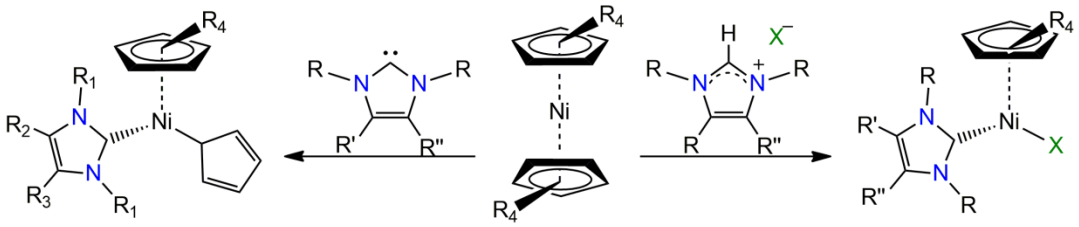


Figure 5: Cyclopentadienyl-based Ru-NHC complexes reported in the literature.

6. Nickel (Group 10 – Late TM)

Since the discovery of the facile synthesis for CpNi-NHC complexes in 1999 by Cowley and co-workers,[69] an extensive range of mono and multinuclear nickel NHC complexes have emerged in a period of 18 years.[70] Nickelocene (Cp_2Ni) reacts with a imidazolylidene (Scheme 4) to form the complex [CpNi(η^1-C_5H_5){Im($C_8H_8Br)_2$}] (**137**), which was proposed to correspond to an important intermediate for the reaction of nickelocene with phosphines.[69] Using the ligand IMe^{Me2} in the same reaction, the first cyclopentadienyl biscarbene nickel complex, [CpNi($IMe^{Me2})_2$] (**138**), was isolated. The same group later noted the spontaneous protonolysis reaction of nickelocene with imidazolium halide salts, a reaction from which the 18-electron complex [CpNiCl(IMes)] (**139**) was formed along with the loss of a cyclopentadiene molecule.[71] Treatment of **139** with MeLi yields the alkylated product, [CpNi(Me)(IMes)] (**140**).



Scheme 4: Synthetic routes of imidazolium salts and imidazolylidene compounds to form different CpNi-NHCs.

Studies by various groups followed: In 2003 Jones and co-workers[72] reported the first hydride complex [CpNiH(IMes)] (**141**), Sun *et al.*[73] reported on the first indenyl complexes [(Indenyl)NiX(I^iPr)] (X = Cl (**142**), Br (**143**)), Nolan and co-workers[74,75] prepared the complexes [CpNiCl(NHC)] (NHC = SIMes (**144**), Idipp (**145**), SIdipp (**146**)) as well as the thiophenolato

[69] C. D. Abernethy, J. A. C. Clyburne, A. H. Cowley, R. A. Jones, *J. Am. Chem. Soc.*, 1999, **121**, 2329-2330.
[70] A. P. Prakasham, P. Ghosh, *Inorg. Chim. Acta*, 2015, **431**, 61-100.
[71] C. D. Abernethy, A. H. Cowley, R. A. Jones, *J. Organomet. Chem.*, 2000, **596**, 3-5.
[72] C. D. Abernethy, R. J. Baker, M. L. Cole, A. J. Davies, C. Jones, *Trans. Met. Chem.*, 2003, **28**, 296-299.
[73] H. M. Sun, Q. Shao, D. M. Hu, W. F. Li, Q. Shen, Y. Zhang, *Organometallics*, 2005, **24**, 331-334.
[74] R. A. Kelly, N. M. Scott, S. Díez-González, E. D. Stevens, S. P. Nolan, *Organometallics*, 2005, **24**, 3442-3447.
[75] D. A. Malyshev, N. M. Scott, N. Marion, E. D. Stevens, V. P. Ananikov, I. P. Beletskaya, S. P. Nolan, *Organometallics*, 2006, **25**, 4462-4470.

complexes [CpNi(SR)(NHC)] (R = phenyl and similar, **147-152**), and Buchowicz *et al.*[76] published the substituted cyclopentadienyl halo and methyl complexes **153-155**.

In 2007 Shen and co-workers[77,78] reported the first *ansa*-derivative (indenyl)Ni-NHC complex **156**, as well as substituted indenyl Ni-NHC complexes **157** and **158**. During the same time, Hahn *et al.* reported the first bidentate NHC-containing nickel complex: The new allyl-functionalised NHC ligand was coordinated to nickel using nickelocene to form [CpNiBr{Im(allyl)(R)}] (R = Me (**159**), allyl (**160**)), which upon dehalogenation using $AgBF_4$ form the cationic complexes [CpNi{Im(allyl)(R)}]BF_4 (R = Me (**161**), allyl (**162**)), featuring bidentate NHC ligands.[79] The same group later embarked on the research of multinuclear CpNi-NHC complexes.[80,81] Dinuclear nickel(II) complex **163** was formed in the reaction of the bidentate NHC salt and nickelocene. Monodentate analogues **164** and **165**, with benzimidazolylidene ligands, were similarly synthesised. Further reaction of dinuclear **163** with 4,4'-bipyridine afforded the tetranuclear nickel(II) complex **166**, whereas reaction of the mononuclear **165** with 4,4'-bipyridine produced the dinuclear Ni(II) complex **167**.[80] Complexes **163**, **166** and **167** all represent the first examples of supramolecular CpNi-NHC complexes.

Chetcuti[82] and Radius[83] reported the first examples of Cp*Ni-NHC complexes **168-172**, making use of Cp*Ni(acac) and $NiBr_2(NHC)_2$ as precursors, respectively. Reactions using substituted cyclopentadienyl nickelocene are also possible. For example, Buchowicz *et al.*[84] made use of substituted nickelocene and asymmetric NHC salts to form the complexes [$(C_5H_4R)NiX(NHC)$] (R = alkyl, X = Cl, Br, **173-176**). Ritleng and Chetcuti provided more examples of substituted cyclopentadienyl Ni-NHC complexes (**177**, **178**), along with their cationic (C_5R_5)Ni-NHC analogues (R = H, Me; **179-181**), where a halide has been substituted for a molecule of

[76] W. Buchowicz, A. Kozioł, L. B. Jerzykiewicz, T. Lis, S. Pasynkiewicz, A. Pęcherzewska, A. Pietrzykowski, *J. Mol. Catal. A.*, 2006, **257**, 118-123.
[77] H-M. Sun, D-M. Hu, Y-S. Wang, Q. Shen, Y. Zhang, *J. Organomet. Chem.*, 2007, **692**, 903-907.
[78] L-Z. Xie, H-M. Sun, D-M. Hu, Z-H. Liu, Q. Shen, Y. Zhang, *Polyhedron*, 2009, **28**, 2585-2590.
[79] F. E. Hahn, B. Heidrich, A. Hepp, T. Pape, *J. Organomet. Chem.*, 2007, **692**, 4630-4638.
[80] F. E. Hahn, C. Radloff, T. Pape, A. Hepp, *Organometallics*, 2008, **27**, 6408-6410.
[81] C. Radloff, F. E. Hahn, T. Pape, R. Fröhlich, *Dalton Trans.*, 2009, 7215-7222.
[82] V. Ritleng, C. Barth, E. Brenner, S. Milosevic, M. J. Chetcuti, *Organometallics*, 2008, **27**, 4223-4228.
[83] P. Fischer, T. Linder, U. Radius, *Z. Anorg. Allg. Chem.*, 2012, **638**, 1491-1496.
[84] W. Buchowicz, W. Wojtczak, A. Pietrzykowski, A. Lupa, L. B. Jerzykiewicz, A. Makal, K. Woźniak, *Eur. J. Inorg. Chem.*, 2010, 648-656.

CH_3CN.[85] The same group observed the intramolecular C-H activation of CH_3CN when KO^{t}Bu is used as base (Scheme 5). In this reaction the neutral nitrile ligand from **179** and **181** is converted into an anionic cyanomethyl ligand to produce the neutral complexes [(C_5H_4R)Ni(IMes)(CH_2CN)] (R = Me (**182**), H (**183**)). In light of this, the nitrile moiety has been grafted onto the *N*-substituents of NHC ligands, which undergo the typical complexation route when reacted with nickelocene to produce complexes **184**-**187**.[86] Dehalogenation using KPF_6 or $AgBF_4$ leads to the formation of externally bound CH_3CN cationic complexes **188**-**190**, leaving the dangling *N*-nitrile substituents intact. Reaction of KO^{t}Bu with solutions containing **185**-**188**, leads to the formation of the novel C-H activated nickelacycles **191**-**194** in moderate yield.[86,87]

A similar C-H activation is observed when the neutral ligand acetone is used: Dehalogenation of **139** with $AgBF_4$ in the presence of acetone yields [CpNi(IMes)(C_3H_6O)]BF_4 (**195**). Complex **195** further reacts with KO^{t}Bu to undergo mono- and bis-alkylation of an acetone molecule form complexes **196** (mono-alkylated) and **197** (bis-alkylated).[88] The same group showed that the cationic complexes [CpNi(NHC)(CH_3CN)]X (NHC = IMes (**181**), X = PF_6; IMe (**198**), X = BF_4) may react with imidazolylidenes in THF to form the cationic biscarbene complexes (**199**-**201**).[89] However, upon reacting IMes with **198**, protonolysis occurs and yields the [HIMes]PF_6 along with the cyanomethyl-containing complex **183**. Ritleng and Chetcuti also reported a series of CpNi-NHC and Cp*Ni-NHC complexes featuring aliphatic nBu and trialkoxysilylpropyl *N*-substituents (**202**-**209**). The latter silyl-containing complex (**209**), as well as the resulting alumina-immobilised complex was synthesised, characterised, and comparatively employed in a catalytic study (*vide infra*).[90]

To date, several more examples of [CpNiX(NHC)] (X = halide) and [CpNi(L)(NHC)]X (L = neutral ligand, X = anion) complexes have been reported by various groups: Navarro and co-

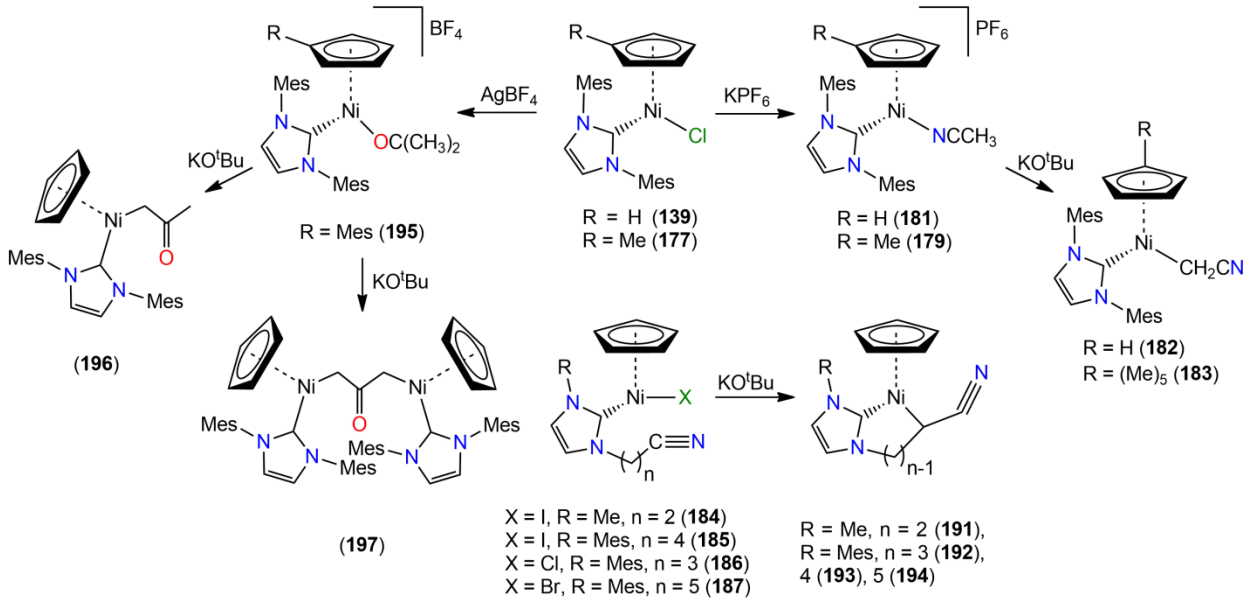
[85] V. Ritleng, A. M. Oertel, M. J. Chetcuti, *Dalton Trans.*, 2010, **39**, 8153-8160.
[86] A. M. Oertel, J. Freudenreich, J. Gein, V. Ritleng, L. F. Veiros, M. J. Chetcuti, *Organometallics*, 2011, **30**, 3400-3411.
[87] A. M. Oertel, V. Ritleng, M. J. Chetcuti, L. F. Veiros, *J. Am. Chem. Soc.*, 2010, **132**, 13588-13589.
[88] A. M. Oertel, V. Ritleng, A. Busiah, L. F. Veiros, M. J. Chetcuti, *Organometallics*, 2011, **30**, 6495-6498.
[89] A. M. Oertel, V. Ritleng, L. Burr, M. J. Chetcuti, *Organometallics*, 2011, **30**, 6685-6691.
[90] A. M. Oertel, V. Ritleng, M. J. Chetcuti, *Organometallics*, 2012, **31**, 2829-2840.

workers[91] reported increased yields for complexes **139** and **144**-**146** using microwave heating syntheses; Buchowicz *et al.*[92] reported additional examples of Im(R)(R') and SIm(R)(R') ligands on substituted cyclopentadienyl nickel complexes **210**-**213**; Crabtree and co-workers[93,94] reported CpNi complexes **214**-**216** with backbone-functionalised NHC ligands and performed electrochemical screening studies; Landman and co-workers[95] expanded on the CpNiBr(NHC) and CpNi(SPh)(NHC) complexes (**217**-**226**) in particular; Włodarska *et al.*[96] reported additional examples of neutral and cationic alkene-tethered CpNi-NHC complexes **227**-**229**; Chen *et al.*[97] reported the synthesis of the multinuclear biscarbene complexes **230**-**232**; Bielinski *et al.*[98] published new examples of mixed cyclopentadienyl, indenyl, and allyl-bearing Ni-NHC complexes **233**-**236**; Nolan and co-workers[99] reported the first examples of CpNiX(NHC) (X = halide) complexes **237**-**243** bearing exceptionally bulky NHC ligands; Ritleng and co-workers[100] reported examples of the first CpNiCl(NHC) complexes (**244**, **245**) featuring chiral substituents; and finally Manners and co-workers[101] produced an example of an *ansa*-type [Cp-C_3H_6-η^1-C_5H_3)Ni(IMes)] (**246**) complex.

The first series of cyclopentadienyl Ni(I)-NHC complexes were first reported by Hazari and co-workers[102]: starting from the dinuclear complex, [$Ni_2(NHC)_2(\mu\text{-}Cl)_2$], reaction of two equivalents of either NaCp or Li(Indenyl) produces the highly paramagnetic complexes [CpNi(NHC)] (**247**, **248**) or [(Indenyl)Ni(NHC)] (**249**, **250**), respectively. Wolf and co-workers[103,104] shortly

[91] B. Landers, O. Navarro, *Inorg. Chim. Acta*, 2012, **380**, 350-353.
[92] W. Buchowicz, J. Conder, D. Hryciuk, J. Zachara, *J. Mol. Catal. A.*, 2014, **381**, 16-20.
[93] O. R. Luca, B. A. Thompson, M. K. Takase, R. H. Crabtree, *J. Organomet. Chem.*, 2013, **730**, 79-83.
[94] O. R. Luca, D. L. Huang, M. K. Takase, R. H. Crabtree, *New J. Chem.*, 2013, **37**, 3402.
[95] F. P. Malan, E. Singleton, P. H. van Rooyen, M. Landman, *J. Organomet. Chem.*, 2016, **813**, 7-14.
[96] A. Włodarska, A. Kozioł, M. Dranka, A. Gryff-Keller, P. Szczeciński, J. Jurkowski, A. Pietrzykowski, *Organometallics*, 2015, **34**, 577-581.
[97] Y-H. Chen, K-E. Peng, G-H. Lee, S-M. Peng, C-W. Chiu, *RSC Adv.*, 2014, **4**, 62789-62792.
[98] E. A. Bielinski, W. Dai, L. M. Guard, N. Hazari, M. K. Takase, *Organometallics*, 2013, **32**, 4025-4037.
[99] A. R. Martin, Y. Makida, S. Meiries, A. M. Z. Slawin, S. P. Nolan, *Organometallics*, 2013, **32**, 6265-6270.
[100] M. Rocquin, V. Ritleng, S. Barroso, A. M. Martins, M. J. Chetcuti, *J. Organomet. Chem.*, 2016, **808**, 57-62.
[101] S. Baljak, A. D. Russel, S. C. Binding, M. F. Haddow, D. O'Hare, I. Manners, *J. Am. Chem. Soc.*, 2014, **136**, 5864-5867.
[102] J. Wu, A. Nova, D. Balcells, G. W. Brudvig, W. Dai, L. M. Guard, N. Hazari, P-H. Lin, R. Pokhrel, M. K. Takase, *Chem. Eur. J.*, 2014, **20**, 5327-5337.
[103] S. Pelties, D. Herrmann, B. de Bruin, D. Hartl, R. Wolf, *Chem. Commun.*, 2014, **50**, 7014-7016.

thereafter reported that the complexes [(C_5R_5)Ni(NHC)] (**251-254**) may be accessed *via* reduction of [(C_5R_5)NiCl(NHC)] with KC_8.



Scheme 5: Synthetic routes to C-H activated CpNi-NHC products.

In addition, a last few interesting examples of CpNi-NHC complexes have been reported: As part of their work on borane-functionalised cyclopentadienyl metal-NHC complexes, Liu *et al.*[105] investigated the nickel counterpart (**255**) of the ruthenium complex described above (**58**); Fischer and co-workers[106] reported the first examples of cyclopentadienyl nickel-NHC alkynyl (**256**) and allenylidene (**257**) complexes; and finally Varonka *et al.*[107] synthesised the first example of a Ni-NHC nitrosyl complex **258**.

[104] U. Chakraborty, F. Urban, B. Mühldorf, C. Rebreyend, B. de Bruin, N. van Velzen, S. Harder, R. Wolf, *Organometallics*, 2016, **35**, 1624-1631.
[105] D. Liu, Z. Qiu, H-S. Chan, Z. Xie, *Can. J. Chem.*, 2012, **90**, 108-117.
[106] T. Haas, K. Kaspar, K. Forner, M. Drexler, H. Fischer, *J. Organomet. Chem.*, 2011, **696**, 946-955.
[107] M. S. Varonka, T. H. Warren, *Organometallics*, 2010, **29**, 717-720.

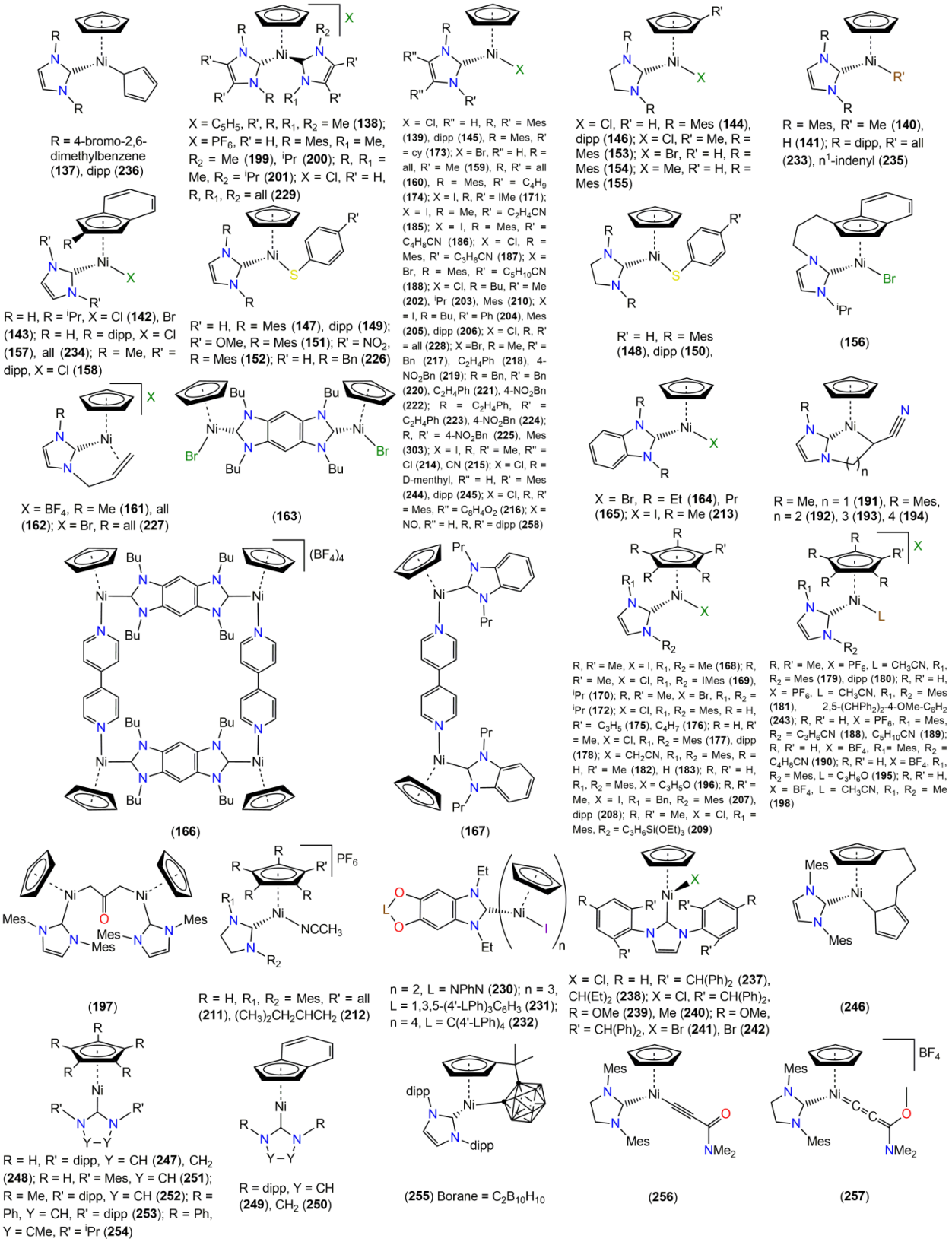


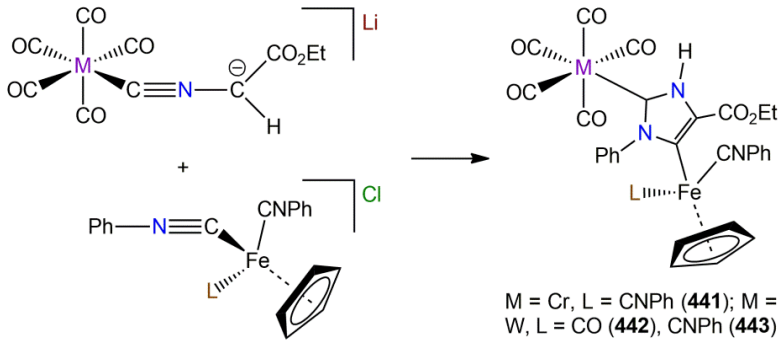
Figure 6: Cyclopentadienyl-based Ni-NHC complexes reported in the literature.

7. Abnormal NHCs

In contrast to the abundance of normally bound *N*-heterocyclic carbenes of the imidazolylidene type, corresponding abnormally bound NHCs (aNHC) are relatively scarce in literature.[108] This is despite the first report in 2001 by Crabtree and co-workers,[109] where C-H activation of the bidentate imidazolium salts [HIm(R)(picolyl)]BF_4 (R = ^{i}Pr, Bu) with [$IrH_5(PPh_3)_2$] was observed to form the cationic complex [$IrH_2(PPh_3)${Im(R)(picolyl)}]BF_4 along with concomitant loss of H_2(g). Some examples of CpM-aNHC complexes have since been reported, notably those of rhodium,[110,111] iridium,[112,113] and yttrium (1 example).[114] It is worth mentioning that abnormally bound NHCs of Ru(II) exist, although only complexes with a *para*-cymene co-ligand: Stephan and co-workers[115] synthesised the anionic abnormally-bound dimeric complex [(*p*-cym)RuCl{Im(BF_3)(dipp)$_2$}]$_2$. This complex then served as a reactive precursor for monomeric *para*-cymene complexes [(*p*-cym)RuCl{Im(BF_3)(dipp)$_2$}L] (L = PPh_3, CO) by reaction of various neutral donor ligands. Albrecht and co-workers[116] reported the complex [(*p*-cym)$RuCl_2$(aNHC)] (aNHC = *N*-methyl-[1,2-a]pyridinium-imidazolyl), whereas Peris and co-workers[117] described similar complexes [(*p*-cym)$RuCl_2$(aNHC)] (aNHC = 2-Me-IMe, 2-Ph-IMe). Among the group 6, 8, and 10 metal triads, only three examples of CpFe-NHC complexes reported by the same group could be found: Fehlhammer[118] reported the synthesis of abnormally bound Fe-NHC complexes [CpFe(CNPh)(L){$M(CO)_5$(NHC)}] (L = CNPh, CO; M = Cr, W; NHC = Im(H)(Ph)(CO_2Et); **441**-**443**) (Scheme 6). The imidazolylidenes were formed through the

[108] P. L. Arnold, S. Pearson, *Coord. Chem. Rev.*, **251**, 596-609.
[109] S. Gründemann, A. Kovacevic, M. Albrecht, J. W. Faller, R. H. Crabtree, *Chem. Commun.*, 2001, 2274-2275.
[110] D. Ghorai, J. Choudhury, *ACS Catal.*, 2015, **5**, 2692-2696.
[111] D. Ghorai, C. Dutta, J. Choudhury, *ACS Catal.*, 2016, **6**, 709-713.
[112] M. Viciano, M. Feliz, R. Corberán, J. A. Mata, E. Clot, E. Peris, *Organometallics*, 2007, **26**, 5304-5314.
[113] A. Petronilho, J. A. Woods, H. Mueller-Bunz, S. Bernhard, M. Albrecht, *Chem. Eur. J.*, 2014, **20**, 15775-15784.
[114] W. Yi, J. Zhang, S. Huang, L. Weng, X. Zhou, *Chem. Eur. J.*, 2014, **20**, 867-876.
[115] C. Pranckevicius, D. W. Stephan, *Chem. Eur. J.*, 2014, **20**, 6597-6602.
[116] A. Petronilho, H. Mueller-Bunz, M. Albrecht, *J. Organomet. Chem.*, 2015, **775**, 117-123.
[117] A. Prades, M. Viciano, M. Sanaú, E. Peris, *Organometallics*, 2008, **27**, 4254-4259.
[118] F. Schoder, U. Plaia, R. Metzner, W. Sperber, W. Beck, W. P. Fehlhammer, *Z. Anorg. Allg. Chem.*, 2010, **636**, 700-709.

[3+2] cycloaddition reactions of metallonitrile-ylides with cyclopentadiene iron carbonyl and isocyanide complexes.



Scheme 6: Synthesis of abnormally bound CpFe-NHC complexes.

8. Catalytic applications

Ancillary ligands have always played a fundamental role in catalysis by modulating the steric and electronic properties as well as the environment of the catalytically active metal centre in transition metal complexes. A large library of catalysis research exists in the literature that explicitly employs NHCs as ligands to almost every transition metal in the periodic table.[10] Below is a short review of cyclopentadienyl NHC complexes of chromium, ruthenium, and nickel that have been employed as catalysts in organic transformation reactions (Table 1).

8.1 C-C and C-N bond formation

Within the group 6 triad of metals, NHC complexes of mainly CpCr and CpMo were employed as polymerisation catalysts. All of the studied Cr-NHC complexes mentioned below were catalytically active in the polymerisation and oligomerisation reactions of unsaturated hydrocarbons, with the majority of studies employing ethylene gas as the monomeric unit. Depending on the oxidation state of chromium, the coordination environment, and the type of NHC ligand, a variety of activities ranging from low to excellent was reported.[32,33] The (C_5R_5)Cr-NHC (R = H, Me; **12-15**) complexes reported by Jolly[32] were employed as precursors for ethylene polymerisation using methylalumoxane (MAO) as co-catalyst (in a toluene/CH_2Cl_2 mixture with Cr:MAO (1:100)), which resulted in poor activity. A highly branched polymer that melts in two steps (89/120°C) was produced. The indenyl-functionalised Cr-NHC complexes

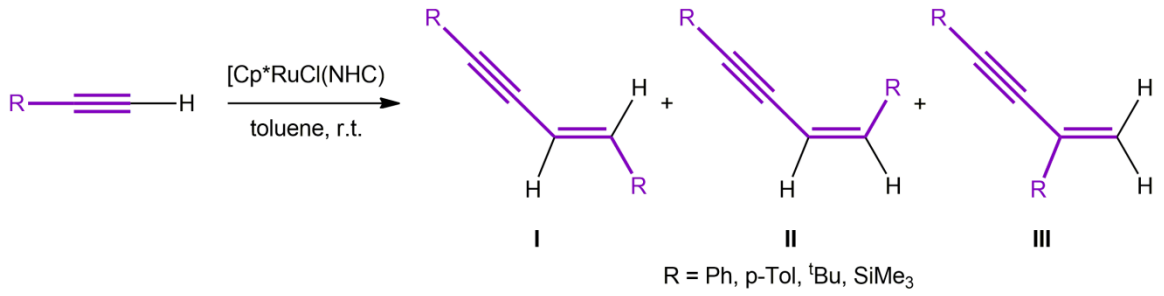
(**16**, **17**, **20**, and **21**) of Danopoulos[33] seemed more efficient in the ethylene oligomerisation/polymerisation using modified methylalumoxane (MMAO-3A) as co-catalyst in chlorobenzene.

Table 1: Catalytic applications of CpM-NHC complexes (M = Cr, Ru, Ni).

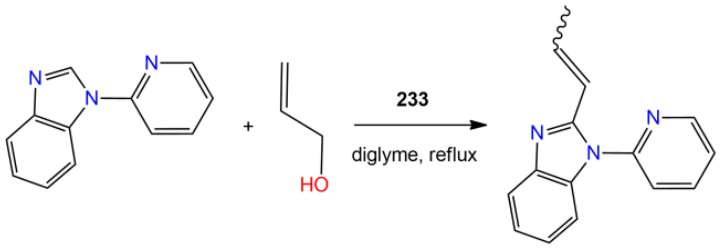
Element	Application	Activity	General conditions	Ref(s)
Cr	Ethylene polymerisation	Low-Med	Cr:MAO (1:100); Cr:MMAO (1:500); 2-8 bar C_2H_4	32,33
Ru	Transfer hydrogenation	High	0.1-1 mol% [Ru], KOH/KO^{t}Bu (0-10 mol%), ^{i}PrOH, 70-100°C	53,55,123,124
	Hydrogenation	Med-High	0.1-0.05 mol% [Ru], H_2 (8-60 bar), 25-80 °C	56,57,58
	Hydrosilylation	Med-Low	5 mol% [Ru], silane (1.4 eq), r.t	64
	Alkyne coupling	High	1 mol% [Ru], r.t.	41
	Dehydrogenative coupling	Med-High	2 mol% [Ru], 150°C	51
	Allylic alcohol isomerisation	High	0.2-1 mol% [Ru], 55-75°C	68
	Alcohol racemisation	Med-High	5 mol% [Ru], 50°C	66
Ni	Suzuki-Miyaura coupling	Med-High	1-3 mol% [Ni], 2-3 eq. KO^{t}Bu, 70-110°C	85,90,95, 102,119
	Kumada-Tamao-Corriu coupling	Med	1 mol% [Ni], r.t.	120
	Buchwald-Hartwig coupling	Low-High	5 mol% [Ni], KO^{t}Bu (2 eq), 110°C	74,99
	α-Arylation reactions	Med-High	1-5 mol% [Ni], 1.25 eq. KO^{t}Bu, 110°C	121
	Hydrosilylation reactions	Med-High	0.5-10 mol% [Ni], 0-10 mol% additive, silane (1-4 eq), 25-110°C	126,127, 128,129
	Polymerisation	Low-High	substrate:Ni:MAO (1000:1:100)-(15000:1:300); 50°C	76,78,84, 92,96 119
	Hydrothiolation of alkynes	Med-High	1.5-2.5 eq HSAr, 6 mol% NEt_3, 3 mol% [Ni], 60°C	75,97
	Anaerobic alcohol oxidation	Med-High	1-5 mol% [Ni], NaO^{t}Bu/KO^{t}Bu (1 eq), haloarene (excess), 25-110°C (conventional and microwave)	91,125

Using the latter complexes (**16**, **17**, **20**, and **21**)**,** ethylene was polymerised efficiently under high pressure and temperature (40 bar, 60°C). The best performing polymerisation catalyst, [{indenyl-C_3H_6-Im(dipp)}$CrCl_2$] (**17**), was reported to exhibit a TON of 271 100 mol.(molCr)$^{-1}$ and an activity of 1.179 × 10^6 mol.(molCr)$^{-1}$.h^{-1} under optimised conditions.

Over the last three decades numerous ruthenium-based organometallic complexes have found application as efficient catalysts, which are ascribed to ruthenium's propensity to easily change oxidation states and be compatible with a wide range of hard- and soft-donor ligands.[36] For instance, CpRu-NHC complexes (**30**, **31**) synthesised by Herrmann and co-workers[41] have been employed as catalysts in the coupling of terminal alkynes (Scheme 7). Phenyl acetylene could be dimerised quantitatively at room temperature within five minutes (TON = 860, maximum TOF = 10320 h^{-1}) to form the *E*-alkene isomer with moderately high selectivity (I(76%):II(16%):III(8%)). Araki *et al.*[51] found their complex, [CpRuCl(BIm(H)(py)] (**63**), catalytically active for the dehydrative condensation of *N*-(2-pyridyl)benzimidazole and allyl alcohol: a mixture of *E*- and *Z*-2-(1-propenyl)-*N*-(2-pyridyl)benzimidazole products (*E*(77%):*Z*(23%)) was obtained after 12 hours (Scheme 8).



Scheme 7: Ruthenium-catalysed coupling of terminal alkynes.

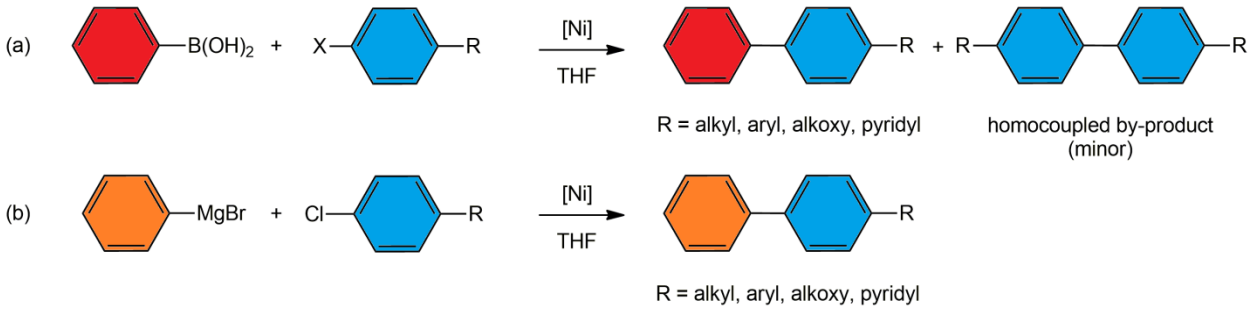


Scheme 8: Dehydrative condensation of *N*-(2-pyridyl)benzimidazole and allyl alcohol.

Complexes of CpNi-NHC have been extensively evaluated as catalysts or catalyst precursors in an impressive range of different organic transformations, with most proving to be successful.[70] For many of the CpNi-NHC complexes, the well-known Suzuki-Miyaura reaction has served as a suitable catalytic screening model to evaluate their activities (Scheme 9). Most notably, the best results reported matched some of the most developed analogous Pd catalysts. The groups that contributed to this field include: Hazari and co-workers[102] with their cyclopentadienyl and indenyl Ni(I) complexes **247**-**250** (maximum conversion = 71%, 3.5 hours, 10 mol% [Ni]); Chetcuti and co-workers[85,90] with a wide range of neutral and cationic CpNi(II)-NHC complexes **168**-**172**, **178**-**181**, and **281** (23-100% conversion (various examples of different catalysts and substrates), 15min-1hour, 1-3 mol% [Ni]); and Buchowicz *et al.*[119] with a wide range of neutral and cationic CpNi(II)-NHC complexes **153**-**155**, **175**-**177**, and **210**-**213** (38-88% conversion (different catalysts with 4'-bromoacetophenone), 1 hour, 3 mol% [Ni]).

Other interesting C-C coupling reactions for which medium to high catalytic activity have been observed include the Kumada-Tamao-Corriu coupling reaction (studied by Teo *et al.*[120]), α-arylation of ketones (studied by Ritleng and Chetcuti[121]), and ethylene dimerisation (studied by Sun *et al.*[73]). Alkene polymerisation (including ethylene, styrene, methyl methacrylate, ethyl diazoacetate) was also studied using a variety of different neutral and cationic CpNi-NHC complex systems by Buchowicz,[76,84,92,119] Pietrzykowski,[96] and Sun[78]: In general the neutral complexes bearing halide anions were (surprisingly) more active than the corresponding cationic complexes giving conversions of between 0-100% depending on the substrate:catalyst:aluminium activator ratio. In terms of C-N bond formation, Nolan and co-workers[74,99] was successful in employing [CpNiCl(NHC)] complexes as pre-catalysts (5 mol% [Ni]) in the arylamination reactions of various amines and arylchlorides (12 examples) to give low-high conversions (16-98%) in 3-10 hours.

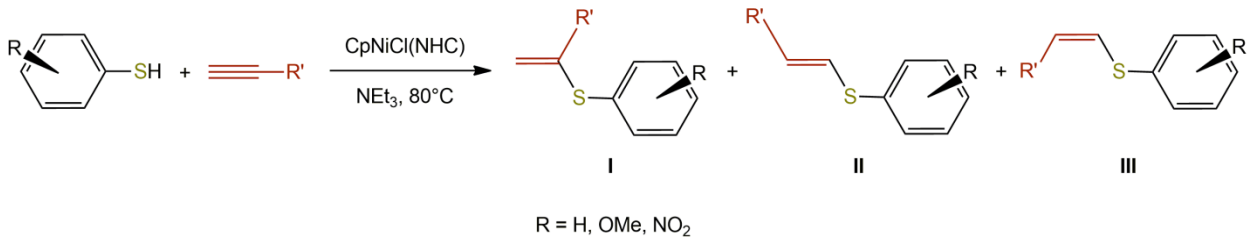
[119] W. Buchowicz, Ł. Banach, J. Conder, P. A. Guńka, D. Kubicki, P. Buchalski, *Dalton Trans.*, 2014, **43**, 5847-5857.
[120] W. J. Teo, Z. Wang, F. Xue, T. S. A. Hor, J. Zhao, *Dalton Trans.*, 2016, **45**, 7312-7319.
[121] M. Henrion, M. J. Chetcuti, V. Ritleng, *Chem. Commun.*, 2014, **50**, 4624-4627.



Scheme 9: The (a) Suzuki-Miyaura and (b) Kumada-Tamao-Corriu coupling reactions.

8.2 C-S bond formation

Catalytic hydrothiolation of alkynes is a catalytic reaction that is enjoying increasingly more attention: Nolan[75] and Chiu[97] investigated the use of [CpNiCl(NHC)] (NHC = IMes, SIMes, Idipp, SIdipp; **139**, **144-146** and **230-232**) in the hydrothiolation of various terminal alkynes (1-heptyne was employed as model substrate), whereas the complexes of Chiu (**230-232**) were less active (conversions < 72%, 36 hours, 3 mol% [Ni]) than those of Nolan (**139**, **144-146**; conversion = 20-87% (7 examples), 6 hours, 3 mol% [Ni]). Both groups found the use of the base NEt_3 crucial to inhibit byproduct (II and III) formation (Scheme 10).



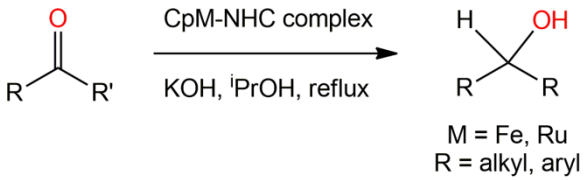
Scheme 10: Catalytic hydrothiolation of terminal alkynes.

8.3 Oxidation/Reduction

Transfer hydrogenation of different ketones and aldehydes using various CpFe-NHC and CpRu-NHC complexes have been reported to date (Scheme 11).[122] CpRu-NHC complexes have proven to be the more active series of complexes for the transfer hydrogenation of ketones, exhibiting activity at concentrations of 1-2 mol% at temperatures of 80-110°C, using base concentrations of

[122] K. Riener, S. Haslinger, A. Raba, M. P. Högerl, M. Cokoja, W. A. Herrmann, F. E. Kühn, *Chem. Rev.*, 2014, **114**, 5215-5272.

0-10 mol% (KOH/KO^{t}Bu). Many groups engaged in this field: Valerga and co-workers[53,123] (complexes **68-73**, conversion = 74-100% (12 examples), TON = 740-1000); Morris and co-workers[124] (complexes **96** and **97**, maximum conversion = 96%, maximum TOF = 880 h^{-1}); and Grotjahn and co-workers[55] (complexes **84-91**, conversion = 97% (3h), 100% (24h); TON = 97-2000). Peris and co-workers[68] found use for their *ansa*-type complexes **135** and **136** in the catalytic isomerisation of allylic alcohols. They found that allylic alcohol substrates are converted nearly quantitatively in a period of 1-4 hours (0.2 – 1 mol% [Ru]) in either THF (55°C) of water (75°C).



Scheme 11: Catalytic transfer hydrogenation of ketone substrates.

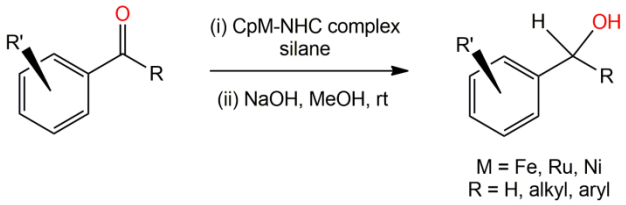
The hydrogenation of unsaturated hydrocarbon substrates using H_2(g) were evaluated by the following groups: Albrecht and co-workers[56] employed their bidentate-NHC Ru(II) complexes **92-95** (0.1 mol%) to hydrogenate styrene to ethylbenzene. Complexes **92-94** showed low to no activity (albeit higher activity for polystyrene formation under the hydrogenation conditions), except for the carboxylate-tethered complex **95**, which showed a conversion of 100% in 5 hours. The primary-amine tethered complexes of Morris and co-workers[57,58] (**96** and **97**) proved highly active (maximum TOF = 938 h^{-1}) for activated carbonyl substrates, with catalyst loadings of 0.1-0.05 mol% [Ru], under mild conditions (8 bar H_2, 25°C) in THF with KO^{t}Bu as base (8 eq).

Finally, the Navarro group[91,125] employed the series of [CpNiCl(NHC)] complexes as catalysts for the anaerobic oxidation of alcohols. In their catalytic study, they found that secondary alcohols are oxidised using 2,4-dichlorotoluene and NaO^{t}Bu/KO^{t}Bu with both conventional and microwave heating methods (conversion = 5-100% (various examples), 0.3-36 hours, 1-5 mol% [Ni]). Microwave heating was found to help yield higher conversions in shorter reaction times.[91]

[123] F. E. Fernández, M. C. Puerta, P. Valerga, *Organometallics*, 2012, **31**, 6368-6879.
[124] W. W. N. O., A. J. Lough, R. H. Morris, *Organometallics*, 2011, **30**, 1236-1252.
[125] C. Berini, D. F. Brayton, C. Mocka, O. Navarro, *Org. Lett.*, 2009, **11**, 4244-4247.

8.4 Hydrosilylation

Numerous CpM-NHC complexes have successfully been employed as catalysts for the hydrosilylation reactions of aldehydes, ketones, sulfoxides, and alcohols with different silanes, to furnish the corresponding alcohols, sulfides and silylethers after hydrolysis in moderate to high yields (Scheme 12). However, the study by Nikonov and co-workers,[64] employing the complex $[CpRu(Idipp)(CH_3CN)_2]B(C_6F_5)_4$ (NHC = Idipp, **59b**), was found to exhibit disappointingly low activity for a variety of substrates using different silanes (conversion = 11-47%, 5 mol% [Ru]). In contrast, CpNi-NHC complexes have found productive use in this class of catalytic reduction reactions, where Ritleng,[126,127] Royo,[128] and Watanabe[129] contributed to research in this field. Collectively, complexes belonging to the class of [CpNiX(NHC)] (X = halide, alkyl) and [(Cp-NHC)NiX] (X = halide) were found highly active in, amongst others, the hydrosilylation of aldehydes and ketones (conversion = 65-99% (17 examples), 1-24 hours, 0.5–5 mol% [Ni]), dehydrogenative silylation of alcohols (conversion = 3-99% (10 examples), 12 hours, 3–10 mol% [Ni]), hydrosilylation of imines (conversion = 40-99% (19 examples), 8-24 hours, 0.5–5 mol% [Ni]),[127] and the dehydrogenative hydrosilylation of thiols (conversion = 14-96% (9 examples), 18 hours, 1 mol% [Ni]).[128]



Scheme 12: Catalytic hydrosilylation of carbonyl substrates.

[126] L. P. Bheeter, M. Henrion, L. Brelot, C. Darcel, M. J. Chetcuti, J-B. Sortais, V. Ritleng, *Adv. Synth. Catal.*, 2012, **354**, 2619-2624.
[127] L. P. Bheeter, M. Henrion, M. J. Chetcuti, C. Darcel, V. Ritleng, J-B. Sortais, *Catal. Sci. Technol.*, 2013, **3**, 3111-3116.
[128] L. Postigo, B. Royo, *Dalton Trans.*, 2014, **43**, 853-858.
[129] H. Ohta, N. Miyoshi, Y. Sakata, Y. Okamoto, M. Hayashi, Y. Watanabe, *Tetrahedron Lett.*, 2015, **56**, 2910-2912.

8.5 Miscellaneous

Nolan and co-workers[66] employed their hydroxyl-functionalised complexes [Cp*Ru(OH)(NHC)] (NHC = Idipp (**131**), IMes (**132**)) as catalysts in the racemisation of enantiopure alcohols: A solution containing (*S*)-1-phenylethanol is racemised (0% *ee*) within 9 hours using either **131** or **132** (5 mol% [Ru]). A variety of other enantiopure alcohols have also been screened with similar results. Later other catalysts of [Cp*RuCl(NHC)] (**30**, **31**, **34**, **36**, **130**) were employed by the same group to find slightly enhanced activities: base (NaO^tBu, 5 mol%) was employed at a lower catalyst concentration (2 mol% [Ru]) to complete the reaction after 30 min, although complete racemisation could not be achieved (66-88% *ee*).

CHAPTER 2

Facile Suzuki-Miyaura coupling of activated aryl halides using new CpNiBr(NHC) complexes

Chapter 2 was adapted from an article published in the Journal of Organometallic Chemistry, with the following details:

Authors: Frederick P. Malan, Eric Singleton, Petrus H. van Rooyen, Marilé Landman

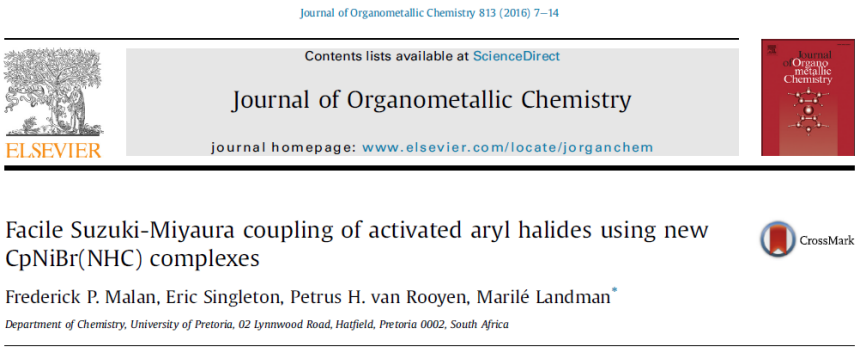
Year: 2016

Volume: 813

Pages: 7-14

Status: Published

Website: http://dx.doi.org/10.1016/j.jorganchem.2016.03.017



Journal of Organometallic Chemistry 813 (2016) 7–14

Contents lists available at ScienceDirect

Journal of Organometallic Chemistry

journal homepage: www.elsevier.com/locate/jorganchem

Facile Suzuki-Miyaura coupling of activated aryl halides using new CpNiBr(NHC) complexes

Frederick P. Malan, Eric Singleton, Petrus H. van Rooyen, Marilé Landman*

Department of Chemistry, University of Pretoria, 02 Lynnwood Road, Hatfield, Pretoria 0002, South Africa

Contributions:

Frederick P. Malan: Author, synthesis, characterisation, catalysis study

Eric Singleton: Co-author, co-supervisor

Petrus H. van Rooyen: Co-author, crystallography

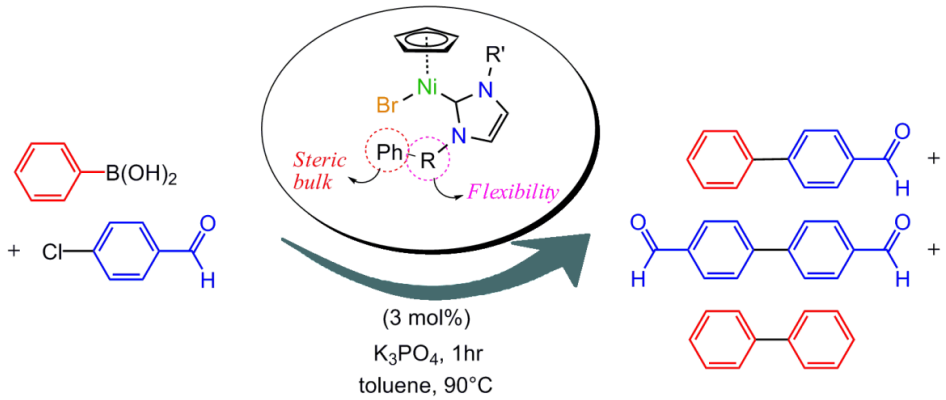
Marilé Landman: Corresponding author, supervisor

2

Facile Suzuki-Miyaura coupling of activated aryl halides using new CpNiBr(NHC) complexes

Frederick P. Malan, Eric Singleton, Petrus. H. van Rooyen and Marilé Landman*

Department of Chemistry, University of Pretoria, 02 Lynnwood Road, Hatfield, Pretoria, 0002, South Africa.



Abstract

Nine new Ni(II)-NHC complexes, [CpNiBr(NHC)], were synthesised from nickelocene and the corresponding symmetric or asymmetric alkyl/-benzyl/phenylethyl imidazolium bromide ligands in relatively high yield. Access to each of the synthesised symmetric or asymmetric alkyl/benzyl/phenylethyl imidazolium bromide salts was obtained through deprotonation of imidazole, followed by treatment with an alkyl or aryl halide, which is subsequently followed with reaction of a secondary alkyl-, benzyl-, or phenylethyl halide. The series of [CpNiBr(NHC)] exhibited catalytic activity in the Suzuki-Miyaura coupling of activated aryl halides with phenylboronic acid to give the respective biphenyl and biphenyl-containing products. In general, the more electron-donating NHC-bearing Ni complexes showed higher activity with aryl halides bearing electron-withdrawing functionalities including carboxaldehyde moieties. All complexes were characterised by ^{1}H- and ^{13}C-NMR spectroscopy, FT-IR spectroscopy, CHN and MS analyses, along with six selected single crystal X-ray structures that are reported here.

Keywords: Nickel; *N*-heterocyclic carbene; Suzuki-Miyaura coupling

1. Introduction

N-Heterocyclic carbenes (NHCs) as a class of metal-stabilising "wonder ligands" remain the ligands of choice in many organometallic complexes, with specific application in homogeneous catalysis, organocatalysis, and medicinal chemistry.[1-4] This is mainly due to the support that NHCs provide through the possibility of reliable, predictable, and extensive steric and electronic tuning[2,3(b),5-7] in the design of a model complex with the specific application in mind. With the ever-increasing number of transition metal-NHCs reported, NHC-complexes of Rh,[3(a),8] Ru,[9] Ni,[7-14] Pd,[4(a),6(b),15,16] Ag,[17] and Au[17,18] remain to be the most

[1] S. Gaillard, J-L. Renaud, *Dalton Trans.*, 2013, **42**, 7255-7270.
[2] O. Kühl, *Chem. Soc. Rev.*, 2007, **36**, 592-607.
[3] (a) B. K. Shaw, B. O. Patrick, M. D. Fryzuk, *Organometallics*, 2012, **31**, 783-786. (b) L. Mercs, G. Labat, A. Neels, A. Ehlers, M. Albrecht, *Organometallics*, 2006, **25**, 5648-5656.
[4] (a) T. Steinke, B. K. Shaw, H. Jong, B. O. Patrick, M. D. Fryzuk, *Organometallics*, 2009, **28**, 2830-2836. (b) W. A. Herrmann, *Angew. Chem. Int. Ed.*, 2002, **41**, 1290-1309. (c) K. M. Hindi, M. J. Panzner, C. A. Tessier, C. L. Cannon, W. J. Youngs, *Chem. Rev.*, 2009, **109**, 3859-3884. (d) A. Kumar, P. Ghosh, *Eur. J. Inorg. Chem.*, 2012, 3955-3969. (e) A. Gautier, F. Cisnetti, *Metallomics*, 2012, **4**, 23-32.
[5] (a) F. E. Hahn, M. C. Jahnke, *Angew. Chem. Int. Ed.*, 2008, **47**, 3122-3172. (b) O. Schuster, L. Yang, H. G. Raubenheimer, M. Albrecht, *Chem. Rev.*, 2009, **109**, 3445-3478.
[6] (a) R. H. Crabtree, *Coord. Chem. Rev.*, 2013, **257**, 755-766. (b) C-C. Ho, S. Chatterjee, T-L. Wu, K-T. Chan, Y-W. Chang, T-H. Hsiao, H. M. Lee, *Organometallics*, 2009, **28**, 2837-2847.
[7] O. R. Luca, B. A. Thompson, M. K. Takase, R. H. Crabtree, *J. Organomet. Chem.*, 2013, **730**, 79-83.
[8] (a) A. R. Naziruddin, A. Hepp, T. Pape, F. E. Hahn, *Organometallics*, 2011, **30**, 5859-5866. (b) J. Li, J. Peng, Y. Bai, G. Lai, X. Li, *J. Organomet. Chem.*, 2011, **696**, 2116-2121. (c) J. M. Praetorius, C. M. Crudden, *Dalton Trans.*, 2008, 4079-4094.
[9] (a) V. Miranda-Soto, D. B. Grotjahn, A. L. Cooksy, J. A. Golen, C. E. Moore, A. L. Rheingold, *Angew. Chem. Int. Ed.*, 2011, **50**, 631-635. (b) W. N. O. Wylie, A. J. Lough, R. H. Morris, *Chem. Comm.*, 2010, **46**, 8240-8242. (c) C. Pranckevicius, D. W. Stephan, *Chem. Eur. J.*, 2014, **20**, 6597-6602. (d) E. Becker, V. Stingl, G. Dazinger, M. Puchberger, K. Mereiter, K. Kirchner, *J. Am. Chem. Soc.*, 2006, **128**, 6572-6573. (e) D. Jantke, M. Cokoja, A. Pöthig, W. A. Herrmann, F. E. Kühn, *Organometallics*, 2013, **32**, 741-744. (f) J. Witt, A. Pöthig, F. E. Kühn, W. Baratta, *Organometallics*, 2013, 32, 4042-4045.
[10] A. P. Prakasham, P. Ghosh, *Inorg. Chim. Acta.*, 2015, **431**, 61-100.
[11] (a) W. Buchowicz, A. Kozioł, L. B. Jerzykiewicz, T. Lis, S. Pasynkiewicz, A. Pęcherzewska, A. Pietrzykowski, *J. Mol. Cat. A.*, 2006, **257**, 118-123. (b) V. Ritleng, C. Barth, E. Brenner, S. Milosevic, M. J. Chetcuti, *Organometallics*, 2008, **27,** 4223-4228. (c) R. A. Kelly III, N. M. Scott, S. Díez-González, E. D. Stevens, S. P. Nolan, *Organometallics*, 2005, **24**, 3442-3447. (d) M. Henrion, M. J. Chetcuti, V. Ritleng, *Chem. Commun.*, 2014, **50**, 4624-4627. (e) A. M. Oertel, V. Ritleng, A. Busiah, L. F. Veiros, M. J. Chetcuti, *Organometallics*, 2011, **30**, 6495-6498.
[12] A. R. Martin, Y. Makida, S. Meiries, A. M. Z. Slawin, S. P. Nolan, *Organometallics*, 2013, **32**, 6265-6270.
[13] A. Włodarska, A. Kozioł, M. Dranka, A. Gryff-Keller, P. Szczeciński, J. Jurkowski, A. Pietrzykowski, *Organometallics*, 2015, **34**, 577-581.
[14] W. Buchowicz, Ł. Banach, J. Conder, P. A. Guńka, D. Kubicki, P. Buchalski, *Dalton Trans.*, 2014, **43**, 5847-5857.

abundant in literature, noting that Ni-NHC complexes received considerable attention only during the last decade.[11,13,14] The reaction of nickelocene with bis(alkyl/aryl)imidazolium halides to yield the complexes [CpNiX(NHC)] (X = Cl, Br, I), represents one of the most frequently employed and facile routes to cyclopentadienyl nickel(II) NHC systems.[7,11-13,19-21] Since the discovery of this atom-economical reaction by Cowley and co-workers[22] in 2000, the series of substituted [(η^5-C_5R_5)NiX(NHC)] (R = H, Me; X = Cl, Br, I, SPh) complexes has expanded to constitute a relatively well studied class of Ni(II) NHC complexes, predominantly employed in synthetic and catalytic applications.[7,11-13,19-21]

In homogeneous catalysis, Ni-NHCs occupy an important position in carbon-carbon and carbon-heteroatom organic transformations offering access to an impressive array of valuable molecules which could previously be obtained only via expensive Ru and Pd catalysts.[10-12,15,19,23,24] In the plethora of C-C coupling reactions, the Suzuki-Miyaura reaction has become one of the most studied catalytic applications due to its tolerance of various functional groups and the low toxicity of its by-products.[4(d),15,19,24,25] Furthermore, [CpNiX(NHC)] (X = halide) and related systems have provided equal or improved catalytic activity in some C-C coupling

[15] M. Gholinejad, H. R. Shahsavari, M. Razeghi, M. Niazi, F. Hamed, *J. Organomet. Chem.*, 2015, **796**, 3-10.
[16] (a) S. Meiries, K. Speck, D. B. Cordes, A. M. Z. Slawin, S. P. Nolan, *Organometallics*, 2013, **32**, 330-339. (b) S. Budagumpi, R. A. Haque, A. W. Salman, *Coord. Chem. Rev.*, 2012, **256**, 1787-1830. (c) G. C. Fortman, S. P. Nolan, *Chem. Soc. Rev.*, 2011, **40**, 5151-5169.
[17] (a) R. Visbal, A. Laguna, M. C. Gimeno, *Chem. Commun.*, 2013, **49**, 5642-5644. (b) J. C. Y. Lin, R.T.W. Huang, C.S. Lee, A. Bhattacharyya, W.S. Hwang, I.J.B. Lin, *Chem. Rev.*, 2009, **109**, 3561-3598. (c) M. Pellei, V. Gandin, M. Marinelli, C. Marzano, M. Yousufuddin, H. V. R. Dias, C. Santini, *Inorg. Chem.*, 2012, **51**, 9873-9882.
[18] E. Schuh, C. Pflüger, A. Citta, A. Folda, M. P. Rigobello, A. Bindoli, A. Casini, F. Mohr, *J. Med. Chem.*, 2012, **55**, 5518-5528.
[19] (a) A. M. Oertel, V. Ritleng, M. J. Chetcuti, *Organometallics*, 2012, **31**, 2829-2840. (b) M. Henrion, V. Ritleng, M. J. Chetcuti, *ACS Catal.*, 2015, **5**, 1283-1302. (c) C-C. Lee, W-C. Ke, K-T. Chan, C-L. Lai, C-H. Hu, H. M. Lee, *Chem. Eur. J.*, 2007, **13**, 582-591. (d) J. Wu, A. Nova, D. Balcells, G. W. Brudvig, W. Dai, L. M. Guard, N. Hazari, P-H. Lin, R. Pokhrel, M. K. Takase, *Chem. Eur. J.*, 2014, **20**, 5327-5337.
[20] A. M. Oertel, J. Freudenreich, J. Gein, V. Ritleng, L. F. Veiros, M. J. Chetcuti, *Organometallics*, 2011, **30**, 3400-3411.
[21] (a) O. R. Luca, D. L. Huang, M. K. Takase, R. H. Crabtree, *New. J. Chem.*, 2013, **37**, 3402-3405. (b) W. Buchowicz, W. Wojtczak, A. Pietrzykowski, A. Lupa, L. B. Jerzykiewicz, A. Makal, K. Woźniak, *Eur. J. Inorg. Chem.*, 2010, 648-656.
[22] C. D. Abernethy, A. H. Cowley, R. A. Jones, *J. Organomet. Chem.*, 2000, **596**, 3-5.
[23] K. Matsubara, K. Ueno, Y. Shibata, *Organometallics*, 2006, **25**, 3422-3427.
[24] E. A. Standley, S. J. Smith, P. Müller, T. F. Jamison, *Organometallics*, 2014, **33**, 2012-2018.
[25] N. Debono, A. Labande, E. Manoury, J-C. Daran, R. Poli, *Organometallics*, 2010, **29**, 1879-1882.

reactions when compared to the traditional Pd catalysts.[10,12,19,24,26] In spite of this, bromo complexes in the series of [CpNiBr(NHC)] compounds reported are few when compared to their chloro- and iodo-analogues.[10,19(a)] The known [CpNiBr(NHC)] complexes (NHC = imidazolium backbone) reported to date are illustrated in Figure 1.

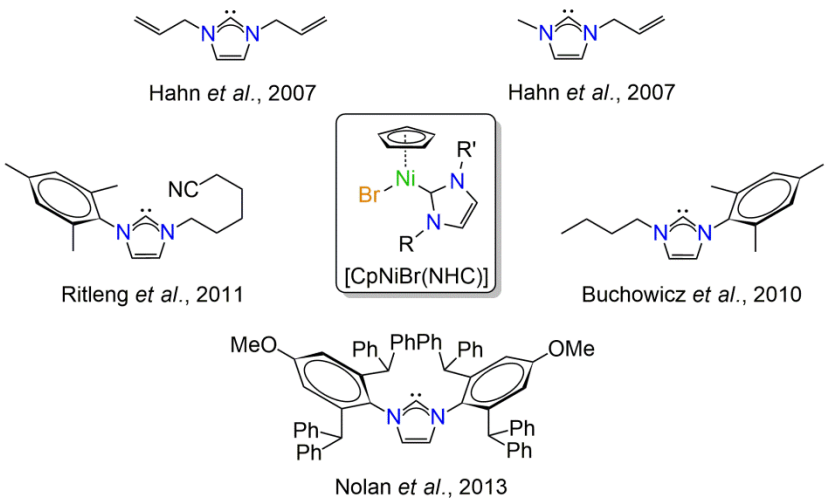


Figure 1: Known [CpNiBr(NHC)] complexes reported by various groups.[5(a),11(e),12,20,21(b)]

In this study, we expand the existing bromide series by reporting nine novel [CpNiBr(NHC)] complexes, where both symmetric and asymmetric NHC ligands are employed. All new complexes synthesised were characterised, and their catalytic activity evaluated in the Suzuki-Miyaura (SM) coupling reaction using activated aryl chlorides and bromides. One of these substrates, 4-chlorobenzaldehyde, bearing an electron-withdrawing functional group, has to date not been fully investigated previously as a substrate in [CpNiX(NHC)] (X = halide) catalysed SM reactions.

2. Material and Methods

2.1 General

All experiments were carried out under an argon atmosphere using standard Schlenk techniques. Solvents were dried prior to use using standard techniques.[27] Column

[26] D. A. Malyshev, N. M. Scott, N. Marion, E. D. Stevens, V. P. Ananikov, I. P. Beletskaya, S. P. Nolan, *Organometallics*, 2006, **25**, 4462-4470.
[27] (a) R. J. Errington, Advanced Practical Inorganic and Metalorganic Chemistry, Blackie Academic & Professional, London, 1997. (b) D. F. Shriver, M. A. Drezdzon, The Manipulation of Air-Sensitive Compounds, 2nd ed., Wiley, New York, 1986.

chromatography was carried out under inert argon atmospheres using silica gel (particle size 0.063-0.200 mm) as the stationary phase. The imidazolium bromide salts [H(**L1**-**L9**)]Br (Figure 2) with general formula [HImRR']Br with R, R' = Me, Bn, $(CH_2)_2Ph$, 4-NO_2Bn were synthesised and purified according to literature procedures.[2,13,14,19,20] NMR characterisation confirmed the molecular structures of the synthesised ligands (see Supplementary Information for data), which correlated with literature data. All other chemicals were purchased from Sigma-Aldrich and used without further purification. ^{1}H (300 MHz) and ^{13}C{H} (76 MHz) NMR spectra were recorded on a Bruker ARX-300 spectrometer using either $CDCl_3$, or $(CD_3)_2CO$ solutions. All measurements were performed at ambient temperature (~296 K), unless otherwise noted. Chemical shifts were referenced to the internal residual protio solvent impurity at δ_H 7.24 ($CDCl_3$) or 2.04 ($(CD_3)_2CO$); or carbon signals at δ_C 77.0 ($CDCl_3$), or 29.8 and 206.3 ppm ($(CD_3)_2CO$). Solid state FT-IR experiments were carried out on a Perkin Elmer Spectrum RXI FT-IR spectrometer as pressed KBr pellets in air. Microanalytical analyses (%CHNS) were obtained using a Thermo Scientific Flash 2000 elemental analyser fitted with a TCD detector. All GC/MS analyses were carried out on a Hewlett Packard (HP) GC 1530A coupled to an Agilent 5975C mass selective detector (MSD). MS (ESI) and MS/MS measurements were performed on a Waters SYNAPT G2 LC-MS spectrometer.

*2.2 General synthesis of [CpNiBr(NHC)] complexes (**1**-**9**)*

A suspension of the alkyl/benzyl/phenylethyl imidazolium bromide (3 mmol) in THF (10 mL) with $[Ni(C_5H_5)_2]$ (0.57 g, 3 mmol) was heated under reflux between 3-16 hours (depending on the NHC ligand). The reaction mixture was concentrated *in vacuo*, and purified by silica gel column chromatography, using gradient elution with hexane and dichloromethane. Red to red-brown powders were obtained in relatively high yields.

*[CpNiBr{Im(Bn)$_2$}] (**1**)*: Yield: 79%. IR (cm^{-1}): 3168 (ν(=CH), w), 3136 (ν(=CH), w), 3110 (ν(=CH), w), 3028 (ν(-CH), w), 2929 (ν(-CH), w), 1569 (ν(=CH), w), 1495 (δ(-CH), sym, m), 1453 (δ(-CH), sym, s), 1430 (δ(-CH), asym, m), 1404 (δ(-CH), asym, s), 1358 (δ(-CH), s), 1230 (ν(-CN), s), 1028 (ν(CN), w), 794 (δ(=CH), s), 755 (s), 725 (δ(-CH), s), 715 (s), 685 (s). ^{1}H-NMR ($CDCl_3$, δ_H) 5.12 (s, C_5H_5, 5H), 5.98 (d, $^2J_{HH}$ = 15 Hz, CH_2, 2H), 6.20 (d, $^2J_{HH}$ = 15 Hz, CH_2, 2H), 6.79 (s, NC*H*, 2H), 7.26-7.40 (m, C_6H_5, 10H). ^{13}C{^{1}H}-NMR ($CDCl_3$, δ_C) 55.6 (s, *C*H$_2$), 91.7 (s, *C*$_5$H$_5$), 122.8 (s, N*C*H), 127.3 (s, *C*$_6$H$_5$), 127.6 (s, *C*$_6$H$_5$), 128.0 (s, *C*$_6$H$_5$), 128.2 (s, *C*$_6$H$_5$), 128.8 (s, *C*$_6$H$_5$) 129.2 (s, *C*$_6$H$_5$), 136.3 (s, *ipso*-*C*$_6$H$_5$), 166.9 (s, N*C*N). CHN

(%): [$C_{22}H_{21}BrN_2Ni$]: C, 58.16 (58.46), H, 4.68 (4.68), N, 5.91 (6.20). MS (ESI): m/z 452.02 (M^+).

[CpNiBr{Im(Me)(Bn)}] ***(2)***: Yield: 77%. IR (cm^{-1}): 3168 (ν(=CH), w), 3132 (ν(=CH), w), 3104 (ν(=CH), w), 3053 (ν(-CH), w), 3029 (ν(-CH), w), 2924 (ν(-CH), w), 1564 (ν(=CH), w), 1518 (δ(-CH), sym, m), 1495 (δ(-CH), sym, m), 1454 (δ(-CH), sym, s), 1430 (δ(-CH), asym, m), 1404 (δ(-CH), asym, s), 1340 (δ(-CH), s), 1230 (ν(-CN), s), 1076 (ν(CN), w), 788 (δ(=CH), s), 725 (δ(-CH), s), 714 (s), 685 (s). ^{1}H-NMR ($CDCl_3$, δ_H) 4.25 (s, C*H*$_3$, 3H), 5.16 (s, C$_5$*H*$_5$, 5H), 5.91 (s, C*H*$_2$, 1H), 6.07 (s, C*H*$_2$, 1H), 6.75 (s, NC*H*, 1H), 6.91 (s, NC*H*, 1H), 7.20-7.31 (m, C$_6$*H*$_5$, 5H). ^{13}C{^{1}H}-NMR ($CDCl_3$, δ_C) 38.8 (s, *C*H$_3$), 55.1 (s, *C*H$_2$), 91.2 (s, *C*$_5$H$_5$), 121.9 (s, {Me}N*C*H), 123.6 (s, {Bn}N*C*H), 127.3 (s, *C*$_6$H$_5$), 127.6 (s, *C*$_6$H$_5$), 128.4 (s, *C*$_6$H$_5$), 136.0 (s, *ipso*-*C*$_6$H$_5$), 161.8 (s, N*C*N). CHN (%): [$C_{16}H_{17}BrN_2Ni$]: C, 50.96 (51.12), H, 4.31 (4.56), N, 7.75 (7.45). MS (ESI): m/z 375.99 (M^+).

[CpNiBr{Im(Me)((CH$_2$)$_2$Ph)}] ***(3)***: Yield: 74%. IR (cm^{-1}): 3156 (ν(=CH), w), 3124 (ν(=CH), w), 3100 (ν(=CH), w), 3054 (ν(-CH), w), 2922 (ν(-CH), w), 1604 (ν(=CH), s), 1519 (δ(-CH), sym, s), 1492 (δ(-CH), sym, m), 1460 (δ(-CH), sym, s), 1408 (δ(-CH), asym, s), 1339 (δ(-CH), s), 1233 (ν(-CN), s), 1081 (ν(CN), w), 786 (δ(=CH), s), 727 (δ(-CH), s), 714 (s), 697 (s). ^{1}H-NMR ({CD_3}$_2$CO, δ_H) 3.41 (br s, NC*H*$_2$, 2H), 4.28 (s, C*H*$_3$, 3H), 4.95 (d, $^3J_{HH}$ = 29 Hz, C*H*$_2$C$_6$H$_5$, 2H), 5.20 (s, C$_5$*H*$_5$, 5H), 7.13 (s, NC*H*, 1H), 7.20 (s, NC*H*, 1H), 7.23-7.38 (m, C$_6$*H*$_5$, 5H). ^{13}C{^{1}H}-NMR ({CD_3}$_2$CO, δ_C) 37.7 (s, *C*H$_3$), 39.1 (s, N*C*H$_2$), 53.9 (s, *C*H$_2$C$_6$H$_5$), 92.0 (s, *C*$_5$H$_5$), 123.4 (s, {Me}N*C*H), 124.5 (s, {PhEt}N*C*H), 127.3 (s, *C*$_6$H$_5$), 127.6 (s, *C*$_6$H$_5$), 129.3 (s, *C*$_6$H$_5$), 129.9 (s, *C*$_6$H$_5$), 139.7 (s, *ipso*-*C*$_6$H$_5$), 161.3 (s, N*C*N). CHN (%): [$C_{17}H_{19}BrN_2Ni$]: C, 52.49 (52.36), H, 4.58 (4.91), N, 6.90 (7.18). MS (ESI): m/z 388.19 (M^+).

[CpNiBr{Im(Me)(4-NO$_2$Bn)}] ***(4)***: Yield: 69%. IR (cm^{-1}): 3168 (ν(=CH), w), 3132 (ν(=CH), w), 3109 (ν(=CH), w), 3053 (ν(-CH), w), 2929 (ν(-CH), w), 1674 (ν(NO), asym, m), 1516 (δ(-CH), sym, s), 1454 (δ(-CH), sym, s), 1430 (δ(-CH), asym, m), 1404 (δ(-CH), asym, s), 1344 (δ(-CH), s), 1230 (ν(-CN), s), 1166 (ν(NO), sym, m), 1108 (m), 1013 (ν(CN), w), 858 (m), 795 (δ(=CH), s), 726 (δ(-CH), s), 715 (s), 685 (s). ^{1}H-NMR ($CDCl_3$, δ_H) 4.30 (s, C*H*$_3$, 3H), 5.19 (s, C$_5$*H*$_5$, 5H), 6.10 (s, C*H*$_2$, 1H), 6.23 (s, C*H*$_2$, 1H), 6.80 (s, NC*H*, 1H), 6.98 (s, NC*H*, 1H), 7.46 (s, C$_6$*H*$_4$, 2H), 8.22 (s, C$_6$*H*$_4$ adjacent to NO_2, 2H). ^{13}C{^{1}H}-NMR ($CDCl_3$, δ_C) 25.6 (s, *C*H$_3$), 39.3 (s, *C*H$_2$), 91.8 (s, *C*$_5$H$_5$), 122.2 (s, {Me}N*C*H), 124.2 (s, *C*$_6$H$_4$), 124.6

(s, {4-NO_2Bn}N*C*H), 128.6 (s, C_6H_4 adjacent to NO_2), 143.8 (s, *ipso*-C_6H_4), 147.8 (s, *ipso*-C_6H_4 containing NO_2), 164.8 (s, N*C*N). CHN (%): [$C_{16}H_{16}BrN_3NiO_2$]: C, 45.64 (45.66), H, 3.52 (3.83), N, 9.61 (9.98). MS (ESI): m/z 418.98 (M^+).

[CpNiBr{Im($(CH_2)_2$Ph)$_2$}] ***(5)***: Yield: 71%. IR (cm^{-1}): 3120 (ν(=CH), w), 3101 (ν(=CH), w), 3048 (ν(-CH), w), 2922 (ν(-CH), w), 2443 (w), 1675 (m), 1603 (ν(=CH), s), 1519 (δ(-CH), sym, s), 1459 (δ(-CH), sym, m), 1441 (δ(-CH), sym, s), 1408 (δ(-CH), asym, s), 1341 (δ(-CH), s), 1234 (ν(-CN), s), 1108 (ν(CN), m), 1013 (w), 859 (s), 786 (δ(=CH), s), 734 (δ(-CH), s), 679 (m). ^{1}H-NMR ($CDCl_3$, δ_H) 3.32 (m, NCH_2, 4H), 4.98 (m, C$H_2C_6H_5$, 2H), 5.17 (s, C_5H_5, 5H), 6.61 (s, NC*H*, 2H), 7.24-7.34 (m, C_6H_5, 10H). ^{13}C{^{1}H}-NMR ($CDCl_3$, δ_C) 37.2 (s, NCH_2), 53.5 (s, $CH_2C_6H_5$), 91.8 (s, C_5H_5), 122.2 (s, N*C*H), 126.8 (s, C_6H_5), 128.7 (s, C_6H_5), 129.0 (s, C_6H_5), 138.1 (s, *ipso*-C_6H_5), 161.3 (s, N*C*N). CHN (%): [$C_{24}H_{25}BrN_2Ni$]: C, 60.21 (60.05), H, 5.38 (5.25), N, 6.13 (5.84). MS (ESI): m/z 480.43 (M^+).

[CpNiBr{Im(Bn)(4-NO_2Bn)}] ***(6)***: Yield: 74%. IR (cm^{-1}): 3163 (ν(=CH), w), 3090 (ν(=CH), m), 3020 (ν(-CH), w), 2921 (ν(-CH), w), 2846 (w), 1674 (ν(NO), asym, m), 1597 (s), 1517 (δ(-CH), sym, s), 1496 (s), 1455 (δ(-CH), sym, s), 1435 (δ(-CH), asym, m), 1407 (δ(-CH), asym, s), 1343 (δ(-CH), s), 1230 (ν(-CN), s), 1208 (ν(NO), sym, m), 1108 (m), 1044 (ν(CN), w), 1011 (m), 859 (m), 838 (m), 788 (δ(=CH), s), 734 (δ(-CH), s), 714 (s), 684 (s). ^{1}H-NMR ($CDCl_3$, δ_H) 5.13 (s, C_5H_5, 5H), 6.08 (m, {Bn}CH_2, 2H), 6.23 (m, {4-NO_2Bn}CH_2, 2H), 6.82 (s, NC*H*, 1H), 6.85 (s, NC*H*, 1H), 7.28-7.50 (m, C_6H_4 and C_6H_5, 2H), 8.23 (s, C_6H_4 adjacent to NO_2, 2H). ^{13}C{^{1}H}-NMR ($CDCl_3$, δ_C) 55.1 (s, $CH_2C_6H_5$), 55.9 (s, $CH_2C_6H_4NO_2$), 91.9 (s, C_5H_5), 122.5 (s, {Bn}N*C*H), 123.4 (s, {4-NO_2Bn}N*C*H), 123.7 (s, C_6H_5), 124.2 (s, C_6H_5), 127.8 (s, C_6H_4), 128.4 (s, C_6H_5), 128.6 (s, C_6H_5), 129.1 (s, C_6H_4 adjacent to NO_2), 136.0 (s, *ipso*-C_6H_5), 143.7 (s, *ipso*-C_6H_4), 147.8 (s, *ipso*-C_6H_5 containing NO_2), 165.8 (s, N*C*N). CHN (%): [$C_{17}H_{15}BrN_3NiO_2$]: C, 53.41 (53.16), H, 4.19 (4.06), N, 8.10 (8.45). MS (ESI): m/z 465.08 (M^+).

[CpNiBr{Im(Bn)($(CH_2)_2$Ph)}] ***(7)***: Yield: 73%. IR (cm^{-1}): 3154 (ν(=CH), w), 3100 (ν(=CH), w), 3054 (ν(-CH), w), 2922 (ν(-CH), w), 2437 (w), 1674 (m), 1604 (ν(=CH), s), 1518 (δ(-CH), sym, s), 1459 (δ(-CH), sym, m), 1408 (δ(-CH), asym, s), 1340 (δ(-CH), s), 1233 (ν(-CN), s), 1108 (ν(CN), m), 1014 (w), 859 (m), 832 (m), 786 (δ(=CH), s), 734 (δ(-CH), s), 700 (m), 679 (m). ^{1}H-NMR ($CDCl_3$, δ_H) 3.36 (q, $^3J_{HH}$ = 9 Hz, NCH_2CH_2, 2H), 5.00 (t, $^3J_{HH}$ = 8 Hz, C$H_2C_6H_5$, 2H), 5.12 (s, C_5H_5, 5H), 5.90 (d, $^2J_{HH}$ = 15 Hz, NC$H_2C_6H_5$, 1H), 6.29 (d, $^2J_{HH}$

= 15 Hz, NC*H*$_2$C$_6$H$_5$, 1H), 6.74 (m, NC*H*, 2H), 7.18-7.39 (m, C$_6$*H*$_5$, 10H). ^{13}C{^{1}H}-NMR (CDCl$_3$, δ_C) 37.2 (s, *C*H$_2$CH$_2$C$_6$H$_5$), 53.5 (s, CH$_2$*C*H$_2$C$_6$H$_5$), 55.7 (s, *C*H$_2$C$_6$H$_5$), 91.8 (s, *C*$_5$H$_5$), 122.3 (s, {PhEt}N*C*H), 122.7 (s, {Bn}N*C*H), 126.9 (s, *C*$_6$H$_5$), 127.6 (s, *C*$_6$H$_5$), 128.1 (s, *C*$_6$H$_5$), 128.7 (s, *C*$_6$H$_5$), 128.9 (s, *C*$_6$H$_5$), 129.0 (s, *C*$_6$H$_5$), 136.6 (s, *ipso*-*C*$_6$H$_5$ of PhEt), 138.0 (s, *ipso*-*C*$_6$H$_5$ of Bn), 162.9 (s, N*C*N). CHN (%): [C$_{23}$H$_{23}$BrN$_2$Ni]: C, 59.01 (59.28), H, 4.86 (4.97), N, 6.29 (6.01). MS (ESI): m/z 495.45 (M$^+$).

[CpNiBr{Im((CH$_2$)$_2$Ph)(4-NO$_2$Bn)}] (***8***): Yield: 70%. IR (cm^{-1}): 3148 (ν(=CH), w), 3116 (ν(=CH), w), 3109 (ν(=CH), w), 2937 (ν(-CH), m), 2840 (ν(-CH), w), 1674 (ν(NO), asym, m), 1598 (s), 1516 (δ(-CH), sym, s), 1453 (δ(-CH), sym, s), 1412 (δ(-CH), asym, m), 1341 (δ(-CH), s), 1263 (m), 1233 (ν(-CN), s), 1183 (ν(NO), sym, m), 1108 (m), 1015 (ν(CN), w), 858 (m), 833 (m), 786 (δ(=CH), s), 739 (δ(-CH), s), 721 (s), 700 (s). ^{1}H-NMR (CDCl$_3$, δ_H) 3.40 (br s, NC*H*$_2$CH$_2$, 2H), 5.02 (br s, C*H*$_2$C$_6$H$_5$, 2H), 5.15 (s, C$_5$*H*$_5$, 5H), 6.24 (s, C*H*$_2$C$_6$H$_4$NO$_2$, 2H), 6.76 (d, $^3J_{HH}$ = 6 Hz, NC*H*, 2H), 7.24- 7.33 (m, C$_6$*H*$_5$, 5H), 7.43 (d, $^3J_{HH}$ = 7 Hz, C$_6$*H*$_4$, 2H), 8.25 (d, $^3J_{HH}$ = 8 Hz, C$_6$*H*$_4$ adjacent to NO$_2$, 2H). ^{13}C{^{1}H}-NMR (CDCl$_3$, δ_C) 37.2 (s, *C*H$_2$CH$_2$C$_6$H$_5$), 53.7 (s, CH$_2$*C*H$_2$C$_6$H$_5$), 55.3 (s, *C*H$_2$C$_6$H$_4$NO$_2$), 92.0 (s, *C*$_5$H$_5$), 123.7 (s, {PhEt}N*C*H), 124.3 (s, {4-NO$_2$Bn}N*C*H), 127.1 (s, *C*$_6$H$_5$), 128.5 (s, *C*$_6$H$_4$), 128.9 (s, *C*$_6$H$_5$), 129.1 (s, *C*$_6$H$_4$ adjacent to NO$_2$), 129.6 (s, *C*$_6$H$_5$), 132.3 (s, *C*$_6$H$_5$), 133.2 (s, *C*$_6$H$_5$), 137.8 (s, *ipso*-*C*$_6$H$_5$ of PhEt), 143.9 (s, *ipso*-*C*$_6$H$_4$ of 4-NO$_2$Bn), 147.9 (s, *ipso*-*C*$_6$H$_4$ containing NO$_2$), 164.8 (s, N*C*N). CHN (%): [C$_{18}$H$_{17}$BrN$_3$NiO$_2$]: C, 53.67 (54.06), H, 4.09(4.34), N, 8.39 (8.22). MS (ESI): m/z 509.26 (M$^+$).

[CpNiBr{Im(4-NO$_2$Bn)$_2$}] (***9***): Yield: 59%. IR (cm^{-1}): 3098 (ν(=CH), m), 3071 (ν(=CH), w), 2927 (ν(-CH), m), 2857 (ν(-CH), w), 1679 (ν(NO), asym, m), 1598 (s), 1515 (δ(-CH), sym, s), 1444 (δ(-CH), sym, s), 1409 (δ(-CH), asym, m), 1342 (δ(-CH), s), 1237 (ν(-CN), s), 1179 (ν(NO), sym, m), 1109 (m), 1014 (ν(CN), w), 858 (m), 798 (δ(=CH), s), 733 (δ(-CH), s). ^{1}H-NMR (CDCl$_3$, δ_H) 5.28 (s, C$_5$*H*$_5$, 5H), 6.09 (d, $^2J_{HH}$ = 15 Hz, C*H*$_2$C$_6$H$_4$NO$_2$, 2H), 6.32 (d, $^2J_{HH}$ = 15 Hz, C*H*$_2$C$_6$H$_4$NO$_2$, 2H), 6.42 (br s, NC*H*, 2H), 7.30- 7.53 (m, C$_6$*H*$_4$, 4H), 8.13 (d, $^3J_{HH}$ = 6 Hz, C$_6$*H*$_4$ adjacent to NO$_2$, 4H). ^{13}C{^{1}H}-NMR (CDCl$_3$, δ_C) 41.5 (s, *C*H$_2$), 43.1 (s, *C*H$_2$), 92.1 (s, *C*$_5$H$_5$), 123.6 (s, N*C*H), 123.7 (s, N*C*H), 128.6 (s, *C*$_6$H$_5$), 129.2 (s, *C*$_6$H$_5$), 144.0 (s, *ipso*-*C*$_6$H$_4$ of 4-NO$_2$Bn), 148.1 (s, *ipso*-*C*$_6$H$_4$ adjacent to NO$_2$), 164.8 (s, N*C*N). CHN (%): [C$_{17}$H$_{14}$BrN$_4$NiO$_4$]: C, 48.73 (48.75), H, 3.38 (3.53), N, 10.52 (10.34). MS (ESI): m/z 539.97 (M$^+$).

2.3 General procedure for the Suzuki-Miyaura coupling reactions

To a round-bottom flask containing the substrate (2.8×10^{-4} mol), K_3PO_4 (2.6 eq., 7.2×10^{-4} mol) and $PhB(OH)_2$ (1.3 eq, 3.6×10^{-4} mol), was added [CpNiBr(NHC)] (3 mol%, 8.3×10^{-6} mol) and toluene (4 mL) and the subsequent reaction mixture was stirred at 90°C for 60 minutes. The mixture was left to cool, and passed through a pad of silica. 1 mL of the resulting light yellow solution was then analysed directly by GC/MS using hexadecane as internal standard upon which the coupling yields were based. All yields are based on the average of three runs.

*2.4 X-ray crystallography of compounds [H**L3**]Br, [H**L4**]Br, **1**, **2**, **3**, and **4***

Single crystal diffraction studies of compounds [H**L3**]Br, [H**L4**]Br, **1**, **2**, **3**, and **4** were done using Quazar multi-layer optics monochromated Mo Kα radiation (k = 0.71069 Å) on a Bruker D8 Venture kappa geometry diffractometer with duo Iμs sources, a Photon 100 CMOS detector and APEX II control software.[28] All X-ray diffraction measurements were performed at 150(2) K. Data reduction was performed using SAINT+[28] and the intensities were corrected for absorption using SADABS.[29] All structures were solved by direct methods with SHELXS-97[30] using the OLEX2[31] interface. All H atoms were placed in geometrically idealised positions and constrained to ride on their parent atoms. For a table containing the data collection and refinement parameters, see Supplementary Information.

3. Results and Discussion

3.1 Synthesis of cyclopentadienyl nickel(II) bromide NHC complexes

Because of the continued interest in the synthesis and interesting application of the large range of [CpNiX(NHC)] (X = Cl, I) complexes, the inherent need to expand on the few existing bromo-analogues existed. In order to address this, we have synthesised a range of flexible symmetric and asymmetric NHC bromide ligands according to the reported methods[2,13,21] (see supplementary information), in high yields (> 85%). This synthetic route involves the initial *N*-functionalisation of imidazole with RBr (alkyl-, benzyl-, or phenylethyl

[28] APEX2 (including SAINT and SADABS), Bruker AXS Inc., Madison, WI, 2012.
[29] G. M. Sheldrick, SHELXL96, Program for the Refinement of Crystal Structures, University of Göttingen, Germany, 1996.
[30] G. M. Sheldrick, *Acta Cryst.*, 2008, **A64**, 112-122.
[31] O. V. Dolomanov, L. J. Bourhis, R. J. Gildea, J. A. K. Howard, H. Puschmann, *J. Appl. Cryst.*, 2009, **42**, 339-341.

halide) in the presence of KOH/K_2CO_3, which after purification is further reacted with R'Br to yield the respective *N*,*N'*-functionalised imidazolium bromide salts. Each of the resulting NHC ligands bears *N*-alkyl, *N*-benzyl or -*N*-phenethyl moieties that provide bulk through phenyl groups, as well as flexibility through sp^3 methylene carbon linkers (Figure 2).

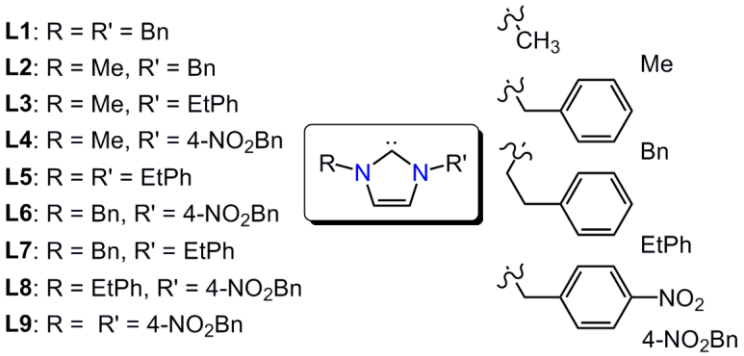


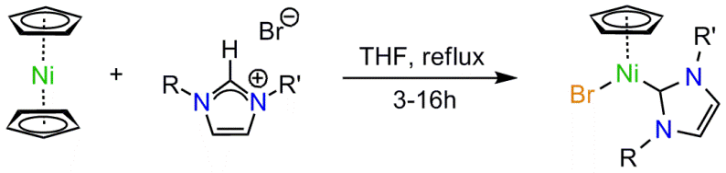
Figure 2: R and R' groups employed in ligand salts [H(**L1**-**L9**)]Br.

Each of these NHC ligands was reacted with $NiCp_2$[12,14,19] to form the complexes [CpNiBr(NHC)] (**1**-**9**) with the loss of a cyclopentadiene ligand (Table 1). During these complexation reactions, a typical colour change from emerald green to blood red/red-brown was observed, with reaction times that varied between 3 and 6 hours. The more electron withdrawing NHC ligands of **4**, **6**, **8**, and **9** proved to required longer reaction times, ranging from 6-18 hours to give the Ni(II) complexes in notably lower yields (59-74%). Nolan and co-workers[12] have previously pointed out that longer reaction times were required whenever bulkier, as opposed to electron-withdrawing, NHC ligands were employed. The [CpNiBr(NHC)] complexes synthesised showed sufficient stability in deoxygenated commercial grade solvents of acetone, chloroform, and DCM.

In general the ^{1}H-NMR spectra of complexes **1**-**9** correspond to those of similar complexes reported in literature.[11(b),13,14,19,32] The cyclopentadienyl protons were observed as singlets between 5.12 and 5.28 ppm, along with the NCH protons appearing either as one or a set of two singlets at 6.42-7.20 ppm, depending on the symmetrical nature of the NHC ligand employed. The ^{13}C-NMR spectra of **1**-**9** also conformed to those in the literature, with the carbene carbon signal resonating between 161.3 (electron-donating NHCs) and 166.9 (electron-withdrawing NHCs) ppm.

[32] V. Ritleng, A. M. Oertel, M. J. Chetcuti, *Dalton Trans.*, 2010, **39**, 8153-8160.

Table 1: Synthesis data of the [CpNiBr(NHC)] complexes (**1**-**9**)



Complex	[NHC]Br	Reaction time (h)	Yield (%)
1	[HIm(Bn)$_2$]Br	4	79
2	[HIm(Me)(Bn)]Br	3	77
3	[HIm(Me)((CH$_2$)$_2$Ph)]Br	4	74
4	[HIm(Me)(4-NO$_2$Bn)]Br	6	69
5	[HIm((CH$_2$)$_2$Ph)$_2$]Br	6	71
6	[HIm(Bn)(4-NO$_2$Bn)]Br	6	74
7	[HIm(Bn)((CH$_2$)$_2$Ph)]Br	6	73
8	[HIm((CH$_2$)$_2$Ph)(4-NO$_2$Bn)]Br	7	70
9	[HIm(4-NO$_2$Bn)$_2$]Br	16	59

3.2 X-ray crystallographic studies

The molecular structures of complexes [CpNiBr{Im(Bn)$_2$}] (**1**), [CpNiBr{Im(Me)(Bn)}] (**2**), [CpNiBr{Im(Me)((CH$_2$)$_2$Ph)}] (**3**), and [CpNiBr{Im(Me)(4-NO$_2$Bn)}] (**4**) were confirmed by single crystal X-ray diffraction, and are included in Figures 3 and 4 along with the structures of [H**L3**]Br and [H**L4**]Br. All crystallographic data and data collection parameters are included in the supplementary information. With the cyclopentadienyl ligand considered as a single ligand, complexes **1**-**4** may be considered to exhibit a distorted trigonal planar geometry around the central metal atom, with Cp$_{cent}$-Ni1-Br1 ≈ Cp$_{cent}$-Ni-C1 ≈ 133°. In addition, the angle between the mean imidazolyl (NHC) plane and Ni1-Br1 bond ranges between 92.865°-94.519° for **1**, **3** and **4**. This angle, however, increases to 96.687° for **2**, which contains the least bulky NHC ligand of the four complexes. This is the result of the Cp and Br ligands being more conveniently arranged around Ni1 with the smaller NHC ligand.

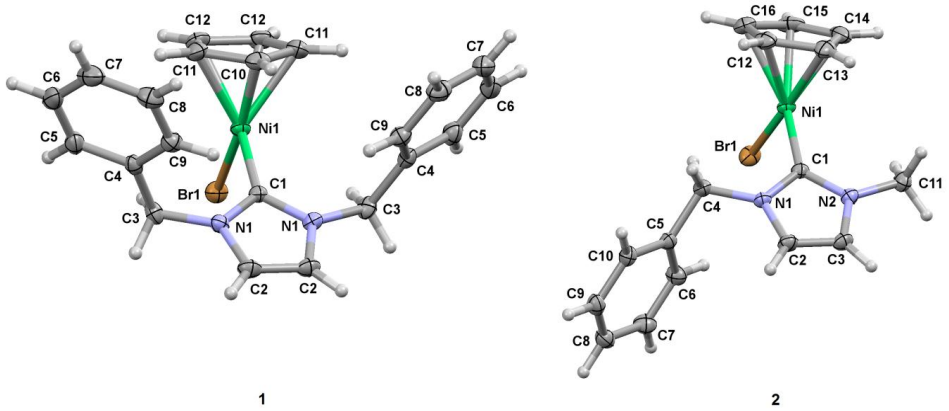


Figure 3: Perspective views of [CpNiBr{Im(Bn)$_2$}] (**1**) and [CpNiBr{Im(Me)(Bn)}] (**2**) with thermal ellipsoids drawn at 50% probability level.

The key descriptors of both structures compare well with similar [CpNiBr(NHC)] complexes[11(e),12,14,19,32], with Ni1-C1 (1.8688(1) Å (**1**); 1.8757(1) Å (**2**)), and Br1-Ni1-C1 (94.107(1)° (**1**); 96.201(3)° (**2**)) (Table 2). The molecular structures obtained for ligands [Im(Me)((CH$_2$)$_2$Ph)]Br ([H**L3**]Br) and [Im(Me)(4-NO$_2$Bn)]Br ([H**L4**]Br), and their corresponding Ni(II)-complexes (**3** and **4** respectively) are included in Figure 4. The Br1-Ni1-C1 angles of 93.965(3)° (**3**) and 94.227(6)° (avg.) (**4**) correspond well with those of **1** and **2**, and fall within the range 92.9(2)°-98.41(9)° reported for most of the [CpNiX(NHC)] (X = Cl, Br, I) analogues.[11(e),12,14,19,20,32] The flexibility in the range of NHC ligands employed, before and after coordination is structurally demonstrated through the N1-C1-X and N2-C1-X bond angles, as well as the C-N1-C1-X and C-N2-C1-X torsion angles, where X = H, Ni.

In sterically demanding environments the *N*-substituents tend to "fold-out", such that the bulky moieties are directed away from the metal centre, which is observed through the C-N-C and C-N-C-Ni angles. The N1-C1-X angles (123.969(1)° ([H**L3**]Br); 125.752(4)° ([H**L4**]Br)), as well as the N2-C1-X angles (127.823(2)° ([H**L3**]Br); 125.753(2)° ([H**L4**]Br)) in general increased after complexation to 127.623(4)° (**3**) and 127.469(9)° (avg.) (**4**), and 128.052(4)° (**3**) and 127.950(9)° (avg.) (**4**), respectively. This shows the compromise the benzyl (**1**, **2**), phenylethyl (**3**) and 4-NO$_2$-benzyl (**4**) groups make to fit around an already crowded nickel centre bearing cyclopentadienyl and bromide ligands. The C-N1-C1-X and C-N2-C1-X (X = H, Ni) torsion angles indicated planarity that can be associated with delocalisation of electron density from the ring system to the X atom (4.226(3)° and -

5.210(3)° ([H**L3**]Br); 2.132(7)° and -1.030(7)° ([H**L4**]Br); 1.020(9)° and 1.577(9)° (**3**); 2.313(2)° (avg.) and 1.961(2)° (avg.) (**4**)).

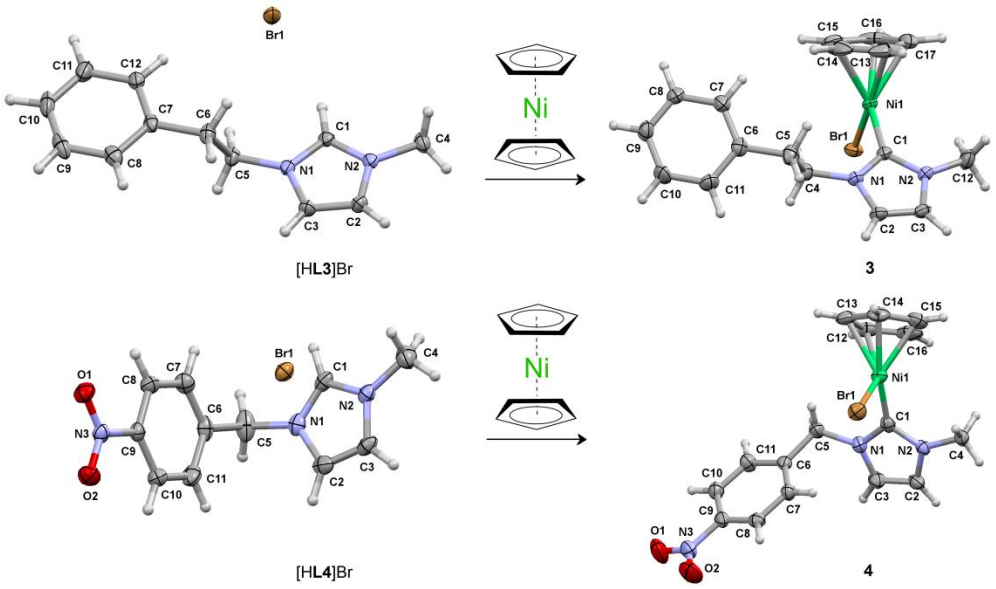


Figure 4: Perspective views of [HIm(Me)((CH$_2$)$_2$Ph)]Br ([H**L3**]Br), [HIm(Me)(4-NO$_2$Bn)]Br ([H**L4**]Br), along with their corresponding [CpNiBr(NHC)] complexes (**3**; **4**) with thermal ellipsoids drawn at 50% probability level. Half a molecule of C_6H_6 (solvent of crystallisation) in **3** has been omitted for clarity.

Table 2: Selected bond distances (Å) and angles (°) for compounds [H**L3**]Br, [H**L4**]Br, **1**, **2**, **3** and **4**.

Description	[H**L3**]Br	[H**L4**]Br	**1**	**2**	**3**[c]	**4**[d]
Ni-C1	--	--	1.8688(1)	1.8757(1)	1.8753(1)	1.8557(1), 1.8806(2)
Ni1-Br1	--	--	2.3427(1)	2.3253(1)	2.3272(1)	2.3166(2), 2.3154(2)
Br1-Ni1-C1	--	--	94.107(1)	96.201(3)	93.965(3)	94.528(6), 93.925(6)
N1-C1-X[a]	123.969(1)	125.752(4)	127.706(2)	127.189(4)	127.623(4)	127.279(8), 127.658(9)
N2-C1- X[a]	127.823(2)	125.753(2)	127.706(2)	128.375(4)	128.052(4)	129.040(9), 126.860(8)
C[b]**-N1-C1**	125.375(1)	125.600(3)	123.826(2)	124.104(3)	124.671(6)	123.199(9), 124.046(1)
C[b]**-N2-C1**	125.622(1)	125.994(2)	123.826(2)	124.661(3)	124.123(6)	122.975(1), 124.358(1)
C[b]**-N1-C1-X**[a]	4.226(3)	2.132(7)	6.267(3)	3.587(7)	1.020(9)	2.343(2), 2.282(2)
C[b]**-N2-C1-X**[a]	-5.210(3)	-1.030(7)	-6.267(3)	-4.400(7)	1.577(9)	0.053(2), -3.868(2)

[a] X = H, Ni. [b] Carbon atom of the substituent on the adjacent N-atom. [c] Contains half of a molecule of C_6H_6. [d] Two molecules per asymmetric unit.

No mentionable changes in the C-N1-C1 and C-N2-C1 bond angles were observed either before or after complexation, however. Collectively, the ability of the ligand salts ([H**L3**]Br,

[H**L4**]Br) to compensate for a decrease of spatial freedom when coordinated (**3**, **4**), is shown through the "folding-out" and flexibility of the *N*-substituted groups. This functionality of the ligands and corresponding complexes provide a unique way of introducing the required steric bulk and flexibility[12] in the ligand systems of Suzuki-Miyaura active catalyst complexes.

3.3 Suzuki-Miyaura coupling activity

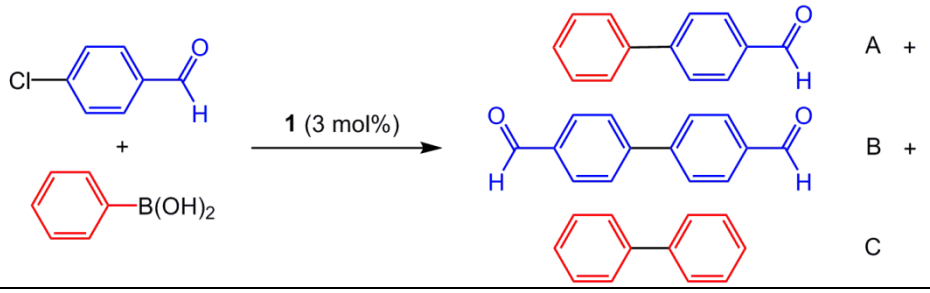
The Suzuki-Miyaura reaction is usually carried out with 4-halo acetophenone and phenylboronic acid as coupling partners to yield 4-acetylbiphenyl (major, 70-100% conversion) and very low yields of the homo-coupled by-product, 4,4'-diacetylbiphenyl (minor, 0-16%) in less than 60 minutes. Complexes **1**-**9** were employed as catalysts in the Suzuki-Miyaura (SM) coupling reaction of the aryl chloride, 4-chlorobenzaldehyde and $PhB(OH)_2$. This is the first instance where the more challenging[14,19(c),33] chloro-aryl carboxaldehydes are employed as substrates using CpNiBr(NHC) complexes, as opposed to the usual chloro and bromo aryl ketones with [CpNiX(NHC)] (X = Cl, I) complexes as catalysts.[14,19,32] All complexes **1**-**9** exhibited catalytic activity under optimised reaction conditions, i.e. stirred suspensions in toluene with 2.6 eq. K_3PO_4, 1.3 eq. $PhB(OH)_2$, and 3 mol% catalyst at 90°C, to give 4-carboxaldehydebiphenyl (CBP) (53-79% conversion) as the major product within one hour (Table 3). Surprisingly, formation of minute amounts of the homo-coupled product, 4,4'-dicarboxaldehydebiphenyl, and a significant amount of biphenyl as by-products (15-30%) were observed. This result was found to be directly related to the *N*-substituted groups of the different Ni(II)-NHC complexes involved in each isolated reaction, where the more electron-withdrawing benzyl groups tend to yield slightly higher yields of biphenyl, with consequential lower yields of CBP.

In the optimisation process of the SM reaction we found, as with other groups,[14,19,32] that K_3PO_4 as base is by far more effective compared to K_2HPO_4, K_2CO_3 or NEt_3 (entries 1-4). An increase in reaction time, or with increased temperature, led to increased yields (entries 5-6). We focused on a direct comparison of catalytic efficiencies with those reported and therefore employed similar reaction conditions (90°C, 60 min), for which we obtained moderate to high conversions. An immediate lowering in conversion was observed upon lowering of the reaction temperature (entries 7-8). A reaction time of 60 minutes is still

[33] H. M. Lee, P. L. Chiu, J. Y. Zeng, *Inorg. Chim. Acta.*, 2004, **357**, 4313-4321.

considered fast for Ni-catalysed SM reactions,[19] especially without added additives such as PPh_3,[19] whereas product formation occurred within the first 5 minutes.

Table 3: Suzuki-Miyaura reaction of 4-chlorobenzaldehyde with phenylboronic acid catalysed by [CpNiBr(NHC) complexes (**1**-**9**)



Entry	Cat. (mol%)	Solvent	Base	Time (min)	Temp (°C)	S:PBA:B[a]	Conv. (%)[b]	A:B:C [b]
1	**1** (3)	toluene	K_3PO_4	60	90	1:1.3:2.6	79	79:0:21
2	**1** (3)	toluene	K_2HPO_4	60	90	1:1.3:2.6	33	76:0:24
3	**1** (3)	toluene	K_2CO_3	60	90	1:1.3:2.6	62	75:0:25
4	**1** (3)	toluene	NEt_3	60	90	1:1.3:2.6	4	24:3:73
5	**1** (3)	toluene	K_3PO_4	30	90	1:1.3:2.6	43	73:0:27
6	**1** (3)	toluene	K_3PO_4	120	90	1:1.3:2.6	87	69:0:31
7	**1** (3)	toluene	K_3PO_4	60	60	1:1.3:2.6	46	65:0:35
8	**1** (3)	toluene	K_3PO_4	60	25	1:1.3:2.6	24	58:0:42
9	**1** (3)	DMP	K_3PO_4	60	90	1:1.3:2.6	42	65:0:35
10	**1** (3)	CH_3CN	K_3PO_4	60	90	1:1.3:2.6	23	43:0:57
11	**1** (0)	toluene	K_3PO_4	60	90	1:1.3:2.6	5	9:0:91
12	**1** (3)	toluene	K_3PO_4	60	90	1:1.1:2.2	59	81:0:19
13	**2** (3)	toluene	K_3PO_4	60	90	1:1.3:2.6	73	79:0:21
14	**3** (3)	toluene	K_3PO_4	60	90	1:1.3:2.6	69	70:0:30
15	**4** (3)	toluene	K_3PO_4	60	90	1:1.3:2.6	71	83:1:16
16	**5** (3)	toluene	K_3PO_4	60	90	1:1.3:2.6	76	78:0:22
17	**6** (3)	toluene	K_3PO_4	60	90	1:1.3:2.6	62	78:0:22
18	**7** (3)	toluene	K_3PO_4	60	90	1:1.3:2.6	73	78:0:22
19	**8** (3)	toluene	K_3PO_4	60	90	1:1.3:2.6	57	66:0:34
20	**9** (3)	toluene	K_3PO_4	60	90	1:1.3:2.6	53	77:0:23

General reaction conditions: 4-chlorobenzaldehyde (0.28 mmol), phenylboronic acid (0.36 mmol), base (0.72 mmol), catalyst (3 mol%), toluene (4 mL), 90°C, 60 min.[a] Molar ratio of substrate:phenylboronic acid:base. [b] Conversion based on internal standard, average value of three runs.

Polar aprotic CH_3CN and dimethoxypropane proved inefficient (entries 9-10), whereas toluene proved superior as the solvent of choice for aryl coupling reactions that can withstand the temperatures involved.Using toluene as solvent, a stabilisation effect might also be significant, especially if air and moisture sensitive Ni-NHC catalytic species are involved, through soft π-interactions of the *N*-phenyl-containing groups of the NHC ligands. This effect is further illustrated when lower catalyst concentrations are used providing lower CBP conversions (entry 11), and might indicate fast catalyst deactivation.[19] In an attempt to decrease the biphenyl product formation, separate decreases in K_3PO_4 (2.2 eq.) and $PhB(OH)_2$ amounts led to an immediate decrease of CBP yield, with no significant proportional decrease of biphenyl formation (entry 12).

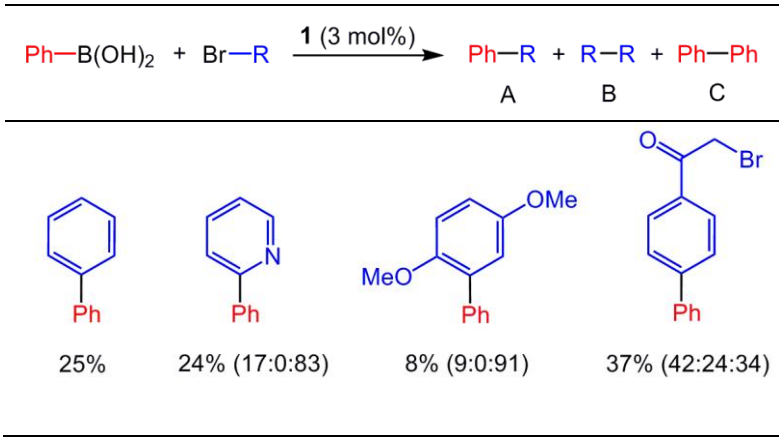
A significant variation of CBP yields was observed among each of the complexes **1**-**9**. Under the optimised conditions, [CpNiBr{Im(Bn)$_2$}] (**1**) performed best, with 79% conversion in 60 minutes. An initial turn-over frequency (TOF) of 320 h^{-1} was observed for **1**. This is much higher than the reported 190 h^{-1} ([Cp*Ni(NCMe){Im(iPr$_2$Ph)$_2$}]PF_6),[32] and comparable to 352 h^{-1} ([CpNiI{Im(Mes)(nBu)}]), observed to have the best TOF for a Ni(II)-catalysed SM coupling in the absence of reductant and/or co-catalysts.[19] Amongst complexes **1**-**9**, a general trend was observed where the more electron-withdrawing NHC-bearing complexes led to the lowest CBP yields, i.e. [CpNiBr{Im(4-NO_2Bn)$_2$}] (**9**) produced only 53% conversion (entry 20). This could be explained by the relative nickel complex stabilities once dehalogenation and reduction by K_3PO_4 and $PhB(OH)_2$ have taken place.[32] The more efficient electron-donating ancillary ligands stabilise the sensitive intermediates, and ultimately depress catalyst decomposition.[19(c)] This effect was also observed by Ritleng[19(a)] and Buchowicz,[14] where they found that electron-donating, bulky *N*-substituents lead to higher 4-acetylbiphenyl conversions, and the minimisation of the homocoupled product formation. Moreover, Nolan and co-workers[12] found that the use of bulky NHC ligands stabilises the intermediate nickel(0) species, while flexible NHC ligands proved even more useful to allow for unhindered substrate coordination.[34] The latter observation agrees with our findings, where accessibility to incoming substrates and the reductive elimination step in the catalytic cycle is better facilitated with bulky, flexible benzyl- and phenethyl-bearing NHCs. The sp^3-methylene carbon-linked NHCs allow for free rotation of the bulky phenyl groups, which could at any stage of the catalytic process find itself in close proximity to the metal centre

[34] (a) F-S. Han, *Chem. Soc. Rev.*, 2013, **42**, 5270-5298. (b) L. B. Junquera, F. E. Fernández, M. C. Puerta, P. Valerga, *Eur. J. Inorg. Chem.*, 2017, 2547-2556.

through ligand/substrate interactions. This creates intra-ligand strain, which could increase the rate of reductive elimination in order to relieve steric strain before the following substrate coordinates.

In addition, we also investigated the effect of employing the non-activated bromobenzene, as well as activated electron-donating substrates in these coupling reactions, and found that the results conform to those reported[6(b),19(a),33] in that all coupling yields decreased dramatically (Table 4). Little conversion was observed for bromobenzene, and only 24% conversion for 2-bromopyridine. The electron-withdrawing 4-bromophenacylbromide showed most promising with a conversion of 37% and little or no signs of side-reactions, even with an acetyl bromide functionality present.

Table 4: Suzuki-Miyaura reaction of other substrates with phenylboronic acid catalysed by complex **1**[a,b]



Reaction conditions: substrate (0.28 mmol), phenylboronic acid (0.36 mmol), base (0.72 mmol), **1** (3 mol%), toluene (4 mL), 90°C, 60 min. [a] GC yields based on internal standard, average value of three runs. [b] Molar ratio of products A:B:C, shown in parentheses.

According to the five important points required, as set out by Matsubara *et al.*[23] when designing a multi-functional nickel catalyst, the series [CpNiBr(NHC)] (**1**-**9**) conforms to the requirements. This is because complexes **1**-**9** (i) are prepared in a facile fashion, (ii) are thermally and relatively air and moisture stable, (iii) easily form a coordinatively unsaturated site with mild bases, (iv) possess electron-donating ligands to stabilise the unsaturated site which accelerates the oxidative addition process, and (v) exhibit a range of steric substituents on the NHC ligand to enhance the reductive elimination reaction.[12,24]

4. Conclusion

A new range of flexible, electron-withdrawing and -donating NHC ligands, as well as their relatively air and moisture stable [CpNiBr(NHC)] complexes were synthesised directly from nickelocene, and characterised. Molecular structures of two of these [NHC]Br ligand salts, and four of the corresponding [CpNiBr(NHC)] complexes were obtained and elucidated. This series of Ni(II)-NHC complexes serves as an interesting expansion on the current limited series of bromo-analogues when compared with the vast series of [CpNiX(NHC)] (X = Cl, I) complexes reported to date. The complexes **1**-**9** efficiently catalysed the SM reaction of, amongst others, 4-chlorobenzaldehyde, which under optimised conditions gave 4-carboxaldehydebiphenyl (major) and biphenyl (minor) in an average ratio of 80:20 respectively. The flexibility and bulkiness of the *N*-substituted groups on the NHC ligands provided accessibility to incoming substrates, while also facilitating the reductive elimination of the organic products. Among complexes **1**-**9**, the more electron-donating NHC-bearing complexes were more efficient at the coupling of activated aryl halides and phenylboronic acid in the SM reactions investigated, as opposed to the electron-withdrawing NHC-bearing complexes.

Acknowledgements

The National Research Foundation of South Africa (NRF) and the University of Pretoria (UP) are gratefully acknowledged for financial support (ML, FPM). Single crystal X-ray diffraction collections by Mr D. Liles are gratefully acknowledged as well as assistance with GC-MS studies by Dr Y. Naudé.

CHAPTER 3

CpNiBr(NHC) complexes as pre-catalysts in the chemoselective anaerobic oxidation of secondary aryl alcohols: Experimental and DFT studies

Chapter 3 was adapted from an article published in Molecular Catalysis, with the following details:

Authors: Frederick P. Malan, Eric Singleton, Bryan W. Bulling, Ignacy Cukrowski, Petrus H. van Rooyen, Marilé Landman

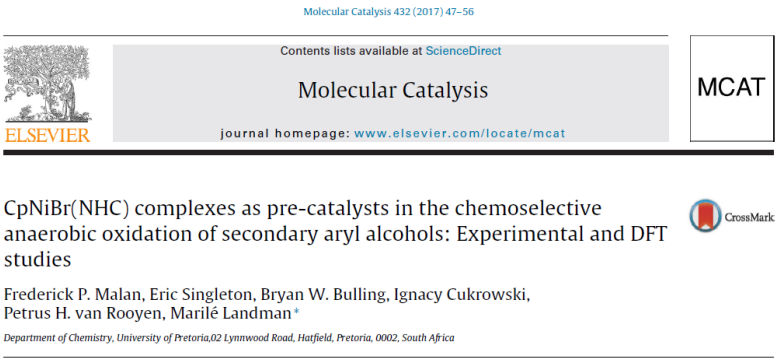
Year: 2017

Volume: 432

Pages: 47-56

Status: Published

Website: http://dx.doi.org/10.1016/j.mcat.2016.12.023



Molecular Catalysis 432 (2017) 47–56

Contents lists available at ScienceDirect

Molecular Catalysis

journal homepage: www.elsevier.com/locate/mcat

MCAT

CpNiBr(NHC) complexes as pre-catalysts in the chemoselective anaerobic oxidation of secondary aryl alcohols: Experimental and DFT studies

Frederick P. Malan, Eric Singleton, Bryan W. Bulling, Ignacy Cukrowski, Petrus H. van Rooyen, Marilé Landman*

Department of Chemistry, University of Pretoria,02 Lynnwood Road, Hatfield, Pretoria, 0002, South Africa

Contributions:

Frederick P. Malan: Author, synthesis, characterisation, catalysis study, DFT study (full optimisation, scanning for transition state species, full optimisation of transition state species, calculation of HOMOs/LUMOs, energy calculations)

Eric Singleton: Co-author, co-supervisor; Bryan W. Bulling and Ignacy Cukrowski: Co-authors, transition state calculation tutorials, provision of DFT facilities; Petrus H. van Rooyen: Co-author, crystallography;

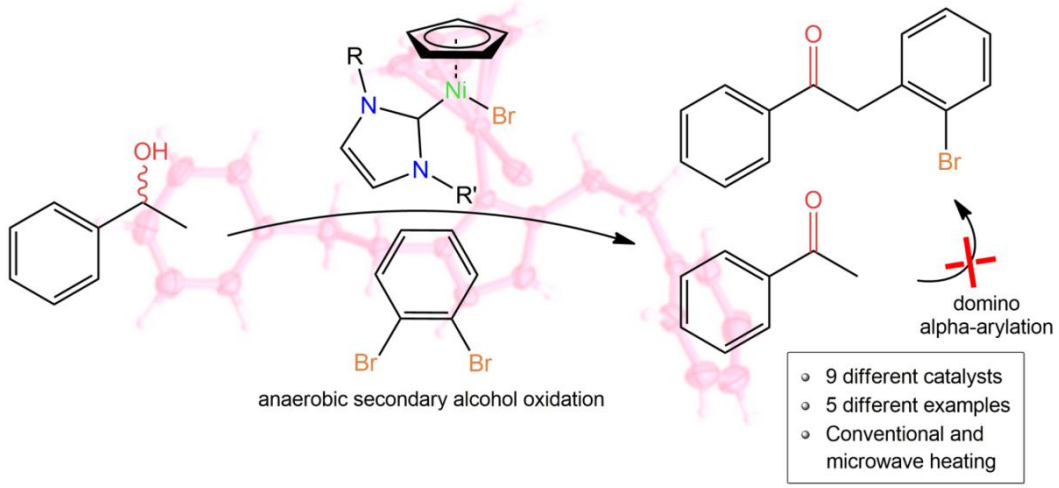
Marilé Landman: Corresponding author, supervisor

3

CpNiBr(NHC) complexes as pre-catalysts in the chemoselective anaerobic oxidation of secondary aryl alcohols: Experimental and DFT studies

Frederick P. Malan, Eric Singleton, Bryan W. Bulling, Ignacy Cukrowski, Petrus H. van Rooyen and Marilé Landman*

Department of Chemistry, University of Pretoria, 02 Lynnwood Road, Hatfield, Pretoria, 0002, South Africa.



Abstract

Nine Ni(II)-NHC complexes of the type [CpNiBr(NHC)], each containing either a symmetric or asymmetric alkyl/benzyl/phenylethyl imidazolium ligand, effectively catalysed the anaerobic oxidation of a series of secondary alcohols, including 1-phenylethanol to yield acetophenone. Catalytic reactions performed using KO^{t}Bu as a mild base and 1,2-dibromobenzene as both oxidant and solvent cleanly converted secondary alcohols to their corresponding ketones in high yield using conventional heating, and almost quantitatively using microwave heating. Catalytic activity of the nine [CpNiBr(NHC)] complexes were evaluated separately under optimised conditions, where the more electron-donating NHC-bearing Ni complexes (**1**, **2**, and **5**) proved to be more efficient than the electron-withdrawing NHC ligand analogues (**6**, **8**, and **9**). Substrate screening studies revealed that secondary alcohols bearing electron-withdrawing functional groups were less efficiently oxidised. Catalyst concentration optimisation studies were aimed at finding a catalyst concentration to limit the effects of catalyst deactivation, while also maintaining reasonable TONs. Additional

characterisation of selected Ni(II) complexes have been included, comprising three single crystal X-ray structure determinations, and a DFT study on the mechanistic reaction pathways of the alcohol oxidation reaction as well as α-ketone arylation, a potential secondary competitive catalytic reaction.

Keywords: nickel; *N*-heterocyclic carbene; alcohol oxidation; anaerobic

1. Introduction

The oxidation of secondary alcohols remains a topic of interest for both organic and inorganic chemists in the synthesis of sought after carbonyl-containing molecules.[1-4] While the majority of alcohol oxidation reactions are focused on employing molecular oxygen as oxidant (aerobic oxidation), where quantitative conversions may be achieved using low catalyst concentrations with fast reaction times, the potentially dangerous conditions under which these reactions occur remain to be a concern.[1,2,4,5] The anaerobic oxidation of primary and secondary alcohols only received considerable attention during the last decade, despite it being a much milder and safer route to yield functionalised ketones and aldehydes in high yields.[4,6] The elimination of the need to perform oxidations at high O_2 pressures and high temperatures, as well as the lack of formation of reactive species that give rise to side-reactions, allows for an attractive route for which large-scale application is possible.[1,6]

Many catalytically active zero-valent metal complexes require ligands to help stabilise these sensitive species and prevent catalyst decomposition.[2,3,7-9] *N*-heterocyclic carbenes (NHCs) remain to be a favourite class of ancillary ligands that provide additional steric and electronic

[1] C. Berini, O. H. Winkelmann, J. Otten, D. A. Vicic, O. Navarro, *Chem. Eur. J.*, 2010, **16**, 6857-6860.
[2] L. M. Dornan, G. M. A. Clendenning, M. B. Pitak, S. J. Coles, M. J. Muldoon, *Catal. Sci. Technol.*, 2014, **4**, 2526-2534.
[3] K. M. Gligorich, M. S. Sigman, *Angew. Chem. Int. Ed.*, 2006, **45**, 6612-6615.
[4] C. Berini, D. F. Brayton, C. Mocka, O. Navarro, *Org. Lett.*, 2009, **11**, 4244-4247.
[5] S. Manzini, C. A. Urbina-Blanco, S. P. Nolan, *Organometallics*, 2013, **32**, 660-664.
[6] M. N. Kopylovich, A. P. C., Ribeiro, E. C. B. A. Alegria, N. M. R. Martins, L. M. D. R. S. Martins, A. J. L. Pombeiro, *Advances in Organometallic Chemistry*, Elsevier Inc., 2015, 91-174.
[7] J. A. Mueller, C. P. Goller, M. S. Sigman, *J. Am. Chem. Soc.*, 2004, **126**, 9724-9734.
[8] R. H. Crabtree, *Chem. Rev.*, 2015, **115**, 127-150.
[9] L. P. Bheeter, M. Henrion, L. Brelot, C. Darcel, M. J. Chetcuti, J-B. Sortais, V. Ritleng, *Adv. Synth. Catal.*, 2012, **354**, 2619-2624.

ligand tuning options.[8-13] This is believed to be due to the stronger binding of NHCs to metal centres, which prevents rapid degradation under oxidising conditions, as is the case with most common ligands.[14,15] The oxidation of secondary alcohols has successfully been performed using mainly Pd[3,7,14-20] and Ru[5,21] NHC-bearing organometallic systems. The employment of the significantly cheaper analogue of Pd, *viz.* Ni, was only realised in 2009 for Ni(II)-NHC complexes,[1,4] and in 2013 using low-coordinated Ni(0) nanoparticles supported on alumina.[6] Furthermore, only one research group has actively investigated the anaerobic oxidation of alcohols using the catalytically versatile [CpNiX(NHC)] (X = halide) complexes.[1,11,12,15] During this process a secondary alcohol is dehydrogenated and used as hydrogen donor to an aryl halide to form the corresponding secondary ketone and unreactive dehalogenated arene as by-products.[15,20]

We have recently expanded the existing limited range[22-25] of [CpNiBr(NHC)] complexes to include bulky, flexible Ni(II)-NHC ligands that improve the efficiency of these complexes to

[10] (a) A. Collado, A. Gómez-Suárez, A. R. Martin, A. M. Z. Slawin, S. P. Nolan, Chem. Commun., 2013, **49**, 5541-5543. (b) R. H. Crabtree, *Coord. Chem. Rev.*, 2013, **257**, 755-766. (c) G. C. Fortman, S. P. Nolan, *Chem. Soc. Rev.*, 2011, **40**, 5151-5169. (d) O. Kühl, *Chem. Soc. Rev.*, 2007, **36**, 592-607.
[11] B. Landers, O. Navarro, *Inorg. Chim. Acta.*, 2012, **380**, 350-353.
[12] B. Landers, O. Navarro, *Eur. J. Inorg. Chem.*, 2012, 2980-2982.
[13] (a) S. R. Patrick, A. Collado, S. Meiries, A. M. Z. Slawin, S. P. Nolan, *J. Organomet. Chem.*, 2015, **775**, 152-154. (b) A. P. Prakasham, P. Ghosh, *Inorg. Chim. Acta.*, 2015, **431**, 61-100. (c) O. Santoro, A. Collado, A. M. Z. Slawin, S. P. Nolan, C. S. J. Cazin, *Chem. Commun.*, 2013, **49**, 10483-10485. (d) O. Schuster, L. Yang, H. G. Raubenheimer, M. Albrecht, Chem. Rev., 2009, **109**, 3445-3478. (e) R. Visbal, A. Laguna, M. C. Gimeno, *Chem. Commun.*, 2013, **49**, 5642-5644.
[14] L-Y. Wang, J. Li, Y. Lv, H-Y. Zhang, S. Gao, *J. Organomet. Chem.*, 2011, **696** 3257-3263.
[15] V. Ritleng, M. Henrion, M. J. Chetcuti, *ACS Catal.*, 2016, **6**, 890-906.
[16] M. Gholinejad, H. R. Shahsavari, M. Razeghi, M. Niazi, F. Hamed, J. Organomet. Chem., 2015, **796**, 3-10.
[17] S. Meiries, K. Speck, D. B. Cordes, A. M. Z. Slawin, S. P. Nolan, *Organometallics*, 2013, **32**, 330-339.
[18] Y. Li, Z. Lin, *Org. Chem. Front.*, 2014, **1**, 1188-1196.
[19] S. Dayan, N. O. Kalaycioglu, *Appl. Organometal. Chem.*, 2013, **27**, 52-58.
[20] B. Landers, C. Berini, C. Wang, O. Navarro, *J. Org. Chem.*, 2011, **76**, 1390-1397.
[21] (a) D. Jantke, M. Cokoja, A. Pöthig, W. A. Herrmann, F. E. Kühn, *Organometallics*, 2013, **32**, 741-744. (b) C. Pranckevicius, D. W. Stephan, *Chem. Eur. J.*, 2014, **20**, 6597-6602.
[22] (a) W. Buchowicz, W.Wojtczak, A. Pietrzykowski, A. Lupa, L. B. Jerzykiewicz, A. Makal, K. Woźniak, Eur. J. Inorg. Chem., 2010, 648-656. (b) F. E. Hahn, M. C. Jahnke, *Angew. Chem. Int. Ed.*, 2008, **47**, 3122-3172.
[23] A. R. Martin, Y. Makida, S. Meiries, A. M. Z. Slawin, S. P. Nolan, *Organometallics*, 2013, **32**, 6265-6270.
[24] A. M. Oertel, V. Ritleng, A. Busiah, L. F. Veiros, M. J. Chetcuti, *Organometallics*, 2011, **30**, 6495-6498.
[25] A. M. Oertel, J. Freudenreich, J. Gein, V. Ritleng, L. F. Veiros, M. J. Chetcuti, *Organometallics*, 2011, **30**, 3400-3411.

partake in catalytic addition and elimination processes.[26] Here we evaluate the catalytic activity of nine [CpNiBr(NHC)] complexes in the oxidation of a range of secondary alcohols using KO^{t}Bu as base and 1,2-dibromobenzene as oxidant. This serves as the first catalytic report on the use of [CpNiBr(NHC)] complexes in the oxidation of secondary alcohols to form their corresponding ketones. Furthermore, we evaluate the effect of catalyst concentration, and employ a DFT study to help elucidate the favoured secondary alcohol oxidation mechanism over the subsequent α-ketone arylation mechanism.

2. Material and Methods

2.1 General

All experiments were carried out under an argon atmosphere using standard Schlenk techniques. Solvents were dried prior to use using standard techniques.[27] Column chromatography was carried out under inert argon atmospheres using silica gel (particle size 0.063-0.200 mm) as the stationary phase. The synthesis, purification, and characterisation of complexes [CpNiBr(NHC)] **1**–**9** (Figure 1) were recently reported by our group.[26] All other chemicals were purchased from Sigma-Aldrich and used without further purification. GC analyses were carried out on a Shimadzu GC-2010 fitted with a flame ionisation detector (FID) using a TRB-780143 capillary column (30 m, 0.25 mm ID, thickness 0.25 µm) and an AOC-20i auto injector. Mass spectrometry measurements were performed using a Hewlett Packard (HP) GC 1530A coupled to an Agilent 5975C mass selective detector (MSD).

*2.2 General synthesis of [CpNiBr(NHC)] complexes (**1**-**9**)*

The syntheses of complexes **1**-**9** were accomplished as described in literature.[26] A suspension of the alkyl/aryl imidazolium bromide (3 mmol) in THF (10 mL) with [Ni(C_5H_5)$_2$] (0.57 g, 3 mmol) was heated under reflux between 3-16 hours (depending on the NHC ligand). The reaction mixture was concentrated *in vacuo*, and purified by silica gel column chromatography, using gradient elution with hexane and dichloromethane. The red bands were collected and concentrated *in vacuo* to give red to red-brown powders in relatively high yields.

[26] F. P. Malan, E. Singleton, P. H. van Rooyen, M. Landman, *J. Organomet. Chem.*, 2016, **81**, 7-14.
[27] (a) R. J. Errington, *Advanced Practical Inorganic and Metalorganic Chemistry*, Blackie Academic & Professional, London, 1997. (b) D.F. Shriver, M.A. Drezdzon, *The Manipulation of Air-Sensitive Compounds*, 2nd ed., Wiley, New York, 1986.

2.3 General procedure for the alcohol oxidation reactions

To a round-bottom flask containing the secondary alcohol substrate (0.3 mmol), KO^{t}Bu (2.6 eq., 0.7 mmol), 1,2-dibromobenzene (3 mL), was added [CpNiBr(NHC)] (3 mol%, 9 µmol) and the subsequent reaction mixture was purged with argon before being stirred at 110°C for 120 minutes before the mixture was left to cool. The resulting mixture was passed through a pad of silica, from which 2 mL of the resulting light yellow solutions were analysed by GC using heptane as internal standard. All products were confirmed by GC-MS, and by comparison of their GC retention times with those of the authentic samples. All conversions and concentrations were based on both consumption of starting material and the internal standard present, and are based on the average of three runs. The effluent was combusted using a H_2/air flame and detected using a FID. The following general GC conditions were employed: injection temperature, 250 °C; initial column temperature, 80 °C; initial hold time, 1 min; ion source temperature, 200 °C, interface temperature 250 °C. Retention times (min): acetophenone (5.560), ±1-phenylethanol (4.316), 4'-chloroacetophenone (6.179), 4'-chlorophenylethanol (5.565), benzophenone (16.287), benzhydrol (14.967), isonitrosoacetophenone (14.047), α-(hydroxyimino)acetophenone (10.869), 4'-bromophenacylbromide (7.792), 2-bromo-(4'-bromophenyl)ethanol (7.345).

2.4 Computational methods

All calculations were carried out using DFT with the B3LYP hybrid functional,[28,29] and were implemented in the gas phase using the Gaussian 09, Revision D01 program.[30] The triple-ζ basis set 6-311G* basis set was used for all atoms (C, H, N, Br, and O), whereas the Stuttgart/Dresden (SDD) pseudopotential was used to describe the nickel metal electronic core, while the metal valence electrons were described using the def2-TZVPP basis set.[31] The

[28] A. D. Becke, *J. Chem. Phys.*, 1993, **98**, 5648-5652.
[29] C. Lee, W. Yang, R. G. Parr, *Phys. Rev. B.*, 1988, **37**, 785-789.
[30] M. J. Frisch, G. W. Trucks, H. B. Schlegel, G. E. Scuseria, M. A. Robb, J. R. Cheeseman, G. Scalmani, V. Barone, B. Mennucci, G. A. Petersson, H. Nakatsuji, M. Caricato, X. Li, H. P. Hratchian, A. F. Izmaylov, J. Bloino, G. Zheng, J. L. Sonnenberg, M. Hada, M. Ehara, K. Toyota, R. Fukuda, J. Hasegawa, M. Ishida, T. Nakajima, Y. Honda, O. Kitao, H. Nakai, T. Vreven, J. A. Montgomery (Jr), J. E. Peralta, F. Ogliaro, M. Bearpark, J. J. Heyd, E. Brothers, K. N. Kudin, V. N. Staroverov, T. Keith, R. Kobayashi, J. Normand, K. Raghavachari, A. Rendell, J. C. Burant, S. S. Iyengar, J. Tomasi, M. Cossi, N. Rega, J. M. Millam, M. Klene, J. E. Knox, J. B. Cross, V. Bakken, C. Adamo, J. Jaramillo, R. Gomperts, R.E. Stratmann, O. Yazyev, A. J. Austin, R. Cammi, C. Pomelli, J. W. Ochterski, R. L. Martin, K. Morokuma, V. G. Zakrzewski, G. A. Voth, P. Salvador, J. J. Dannenberg, S. Dapprich, A. D. Daniels, O. Farkas, J. B. Foresman, J. V. Ortiz, J. Cioslowski, D. J. Fox, Gaussian 09, Revision D.01, Gaussian Inc., Wallingford CT, 2010.
[31] F. Weigend, R. Ahlrichs, Phys. *Chem. Chem. Phys.*, 2005, **7**, 3297-3305.

gas phase geometries of all intermediates and transition states were fully optimised at this level of theory without any symmetry restrictions, ensuring that the local minima had zero imaginary vibrational frequencies[32] and the transition state had exactly one and to provide the thermal correction to free energies at 298.15 K and 1 atm. Solvent effects have also been included for the theoretical TOF calculations where all intermediates and transition state have been reoptimised at the same level of theory and calculated using defined properties (dielectric constant, molar volume, solvent radius, and density) for 1,2-dibromobenzene as the solvent. The HOMOs and LUMOs of all reaction intermediates, as well as the energy gaps were calculated from the same DFT method and level of theory.

*2.5 X-ray crystallography of **5**, **7**, and **8***

Single crystal diffraction of compounds **5**, **7**, and **8** were done using Quazar multi-layer optics monochromated Mo Kα radiation (k = 0.71069 Å) on a Bruker D8 Venture kappa geometry diffractometer with duo Iμs sources, a Photon 100 CMOS detector and APEX II control software.[33] All x-ray diffraction measurements were performed at 150(2) K. Data reduction was performed using SAINT+[33] and the intensities were corrected for absorption using SADABS.[34] All structures were solved by direct methods with SHELXS-97[35] using the OLEX2[36] interface. All H atoms were placed in geometrically idealised positions and constrained to ride on their parent atoms. For tables containing the data collection and refinement parameters, see Supplementary Information.

3. Results and Discussion

3.1 Synthesis of cyclopentadienyl nickel(II) bromide NHC complexes

In our previous report[26] we described the synthesis and full characterisation of a range of [CpNiBr(NHC)] complexes bearing flexible symmetric and asymmetric NHC ligands. Each of these NHC ligands bears *N*-alkyl, -benzyl, and/or -phenylethyl moieties that exhibit steric bulk through phenyl groups, as well as flexibility through sp^3 methylene carbon linkers

[32] J. W. McIver, A. K. Komornicki, *J. Am. Chem. Soc.*, 1972, **94**, 2625-2633.
[33] APEX2 (including SAINT and SADABS), Bruker AXS Inc., Madison, WI, 2012.
[34] G. M. Sheldrick, SHELXL96, Program for the Refinement of Crystal Structures, University of Göttingen, Germany, 1996.
[35] G. M. Sheldrick, *Acta Cryst.*, 2008, **A64**, 112-122.
[36] O. V. Dolomanov, L. J. Bourhis, R. J. Gildea, J. A. K. Howard, H. Puschmann, *J. Appl. Cryst.*, 2009, **42**, 339-341.

(Figure 1). Briefly, to a slurry containing the imidazolium bromide ligand in dry THF, one equivalent of nickelocene was added, and the resulting mixture was heated under reflux for 3-16 hours (depending on the NHC salt).[26] After the loss of a cyclopentadiene ligand, both the neutral carbene ligand and bromide ligand coordinate to the nickel centre. All ^{1}H-NMR spectra of complexes **1-9** exhibited the disappearance of the acidic imidazolium (NC*H*N) proton (9.3-10.5 ppm) as well as the appearance of a significantly downfield shifted carbenic carbon on complexation (161.3-166.9 ppm from the ^{13}C-NMR spectra).

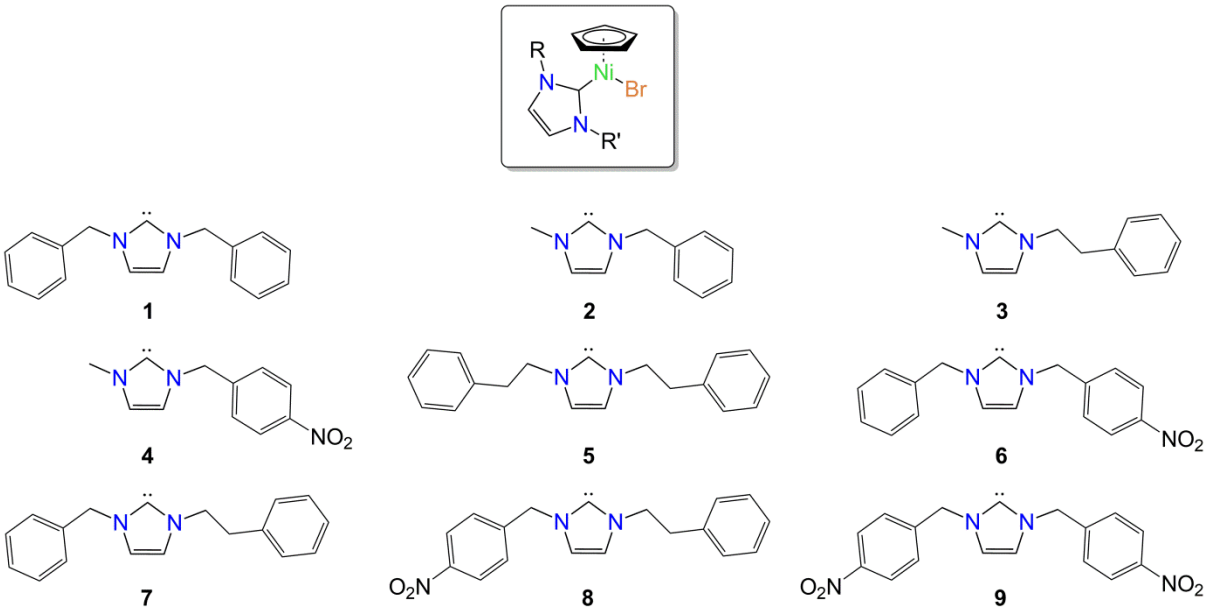


Figure 1: The range of synthesised [CpNiBr(NHC)] complexes **1-9**

3.2 X-ray crystallographic studies

The molecular structures of complexes [CpNiBr{Im(EtPh)$_2$}] (**5**, Figure 2), [CpNiBr{Im(Bn)(4-NO$_2$Bn)}] (**6**, Figure 3), and [CpNiBr{Im((CH$_2$)$_2$Ph)(4-NO$_2$Bn)}] (**8**, Figure 4) all serve as representative examples of the solid-state molecular geometry of the cyclopentadienyl, NHC, and bromo-ligands around the nickel centre, and how flexibility of the N-substituents influence the catalytic efficiency of the Ni(II) complexes. All crystallographic data and data collection parameters are included in the supplementary information. Complexes **5**, **6**, and **8** may each be considered to exhibit a distorted trigonal planar geometry around the central metal atom, with Cp$_{cent}$-Ni1-Br1 ≈ Cp$_{cent}$-Ni-C6 ≈ 133°.

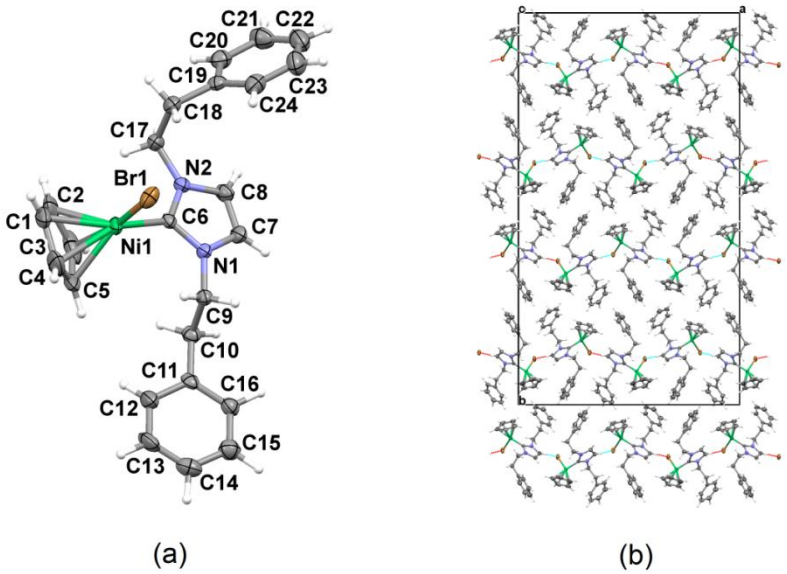


Figure 2: (a) Perspective view of [CpNiBr{Im(EtPh)$_2$}] (**5**) with thermal ellipsoids drawn at 50% probability level. (b) Packing diagram of **5** as viewed along the c axis. Hydrogen-bromide interactions are indicated with red and teal lines.

Typical bond lengths include Ni1-C6 (1.881(3)-2.15(2) Å), Ni1-Br1 (2.334(2)-2.355(5) Å), and Ni1-Cpcent (1.759(2)-1.768(2) Å), and compare well with similar [CpNiBr(NHC)] complexes.[23-26, 37 - 39] Other comparable descriptors include the bond angles Br1-Ni1-C6 (94.46(8)-161.0(5)°), N1-C6-Ni1 (127.2(3)-129.6(2)°), N2-C6-Ni1 (127.8(3)-127.9(7)°). The flexibility in the range of NHC ligands employed is clearly demonstrated through the methylene- and ethylene-phenyl containing *N*-substituents of **5**, **6**, and **8**, through the C_β-C_α-N1 (112.4(7)-113.8(2)°) and C_β-C_α-N2 (110.3(7)-112.8(3)°) (C_α and C_β are the primary and secondary methylene linker carbon atoms) bond angles, as well as the C_β-C_α-N1-C6 (from -103.6(3) up to 95.9(5)°), C_β-C_α-N2-C6 (from -140.3(8) up to 98.8(3)°), C_α-N1-C6-Ni1 (from -13(1) up to 0.7(6)°), C_α-N2-C6-Ni1 (from 1.2(4) up to 10(1)°) torsion angles.

[37] W. Buchowicz, Ł. Banach, J. Conder, P. A. Guńka, D. Kubicki, P. Buchalski, *Dalton Trans.*, 2014, **43**, 5847-5857.
[38] A. M. Oertel, V. Ritleng, M. J. Chetcuti, *Organometallics*, 2012, **31**, 2829-2840.
[39] V. Ritleng, A. M. Oertel, M. J. Chetcuti, *Dalton Trans.*, 2010, **39**, 8153-8160.

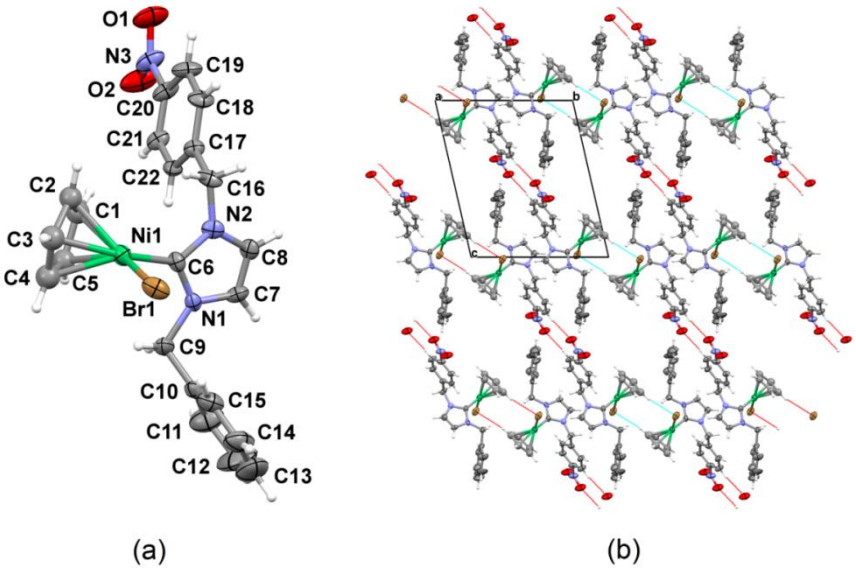


Figure 3: (a) Perspective view of [CpNiBr{Im(Bn)(4-NO_2Bn)}] (**6**) with thermal ellipsoids drawn at 50% probability level. (b) Packing diagram of **6** as viewed along the a axis. Hydrogen-bromide and hydrogen-oxo interactions are indicated with red and teal lines.

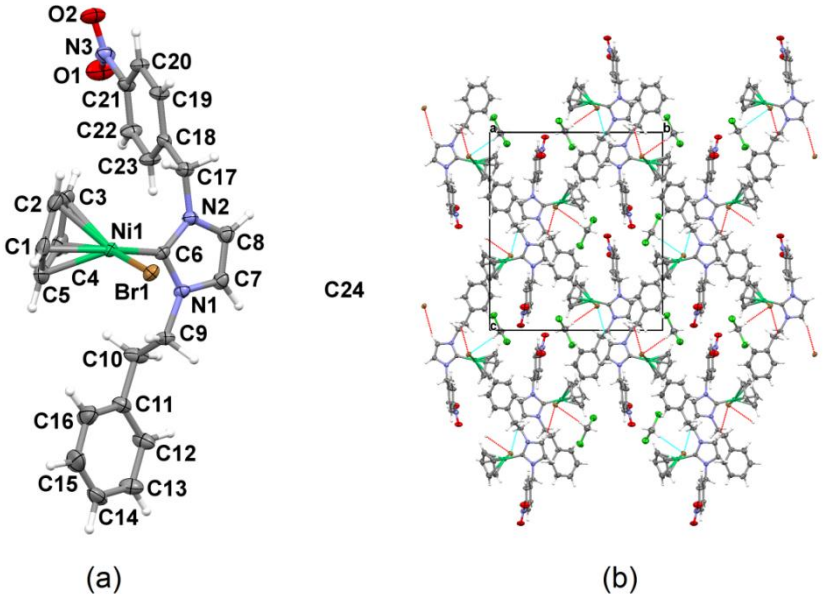


Figure 4 (a) Perspective view of [CpNiBr{Im($(CH_2)_2$Ph)(4-NO_2Bn)}] (**8**) with thermal ellipsoids drawn at 50% probability level. One molecule of CH_2Cl_2 has been omitted for clarity. (b) Packing diagram of **8** as viewed along the a axis. Hydrogen-bromide interactions are indicated with red and teal lines.

In sterically demanding environments the N-alkyl/-aryl groups tend to "fold-out", such that the bulky moieties are directed away from the metal centre. Interestingly, in **5** it is seen that

the N2-phenethyl chain is directed towards the nickel centre, whereas the N1-phenethyl chain is directed away through radically different C_γ-C_β-C_α-N2 (-74.1(5)°) and C_γ-C_β-C_α-N1 (-178.3(3)°) torsion angles (C_γ refers to the *ipso* carbon of the phenyl group adjacent to the ethylene linker). A similar structural effect is also observed in **6** and **8**, where the 4-NO_2-benzyl fragment is directed towards the nickel centre, whereas the remaining benzyl and phenylethyl fragments are directed away from the metal centre. In Figures 2-4, short contact interactions are observed between the bromide ligand, and the hydrogen atoms of the imidazolyl backbone as well as the methylene/ethylene linkers. This stabilisation effect is certainly only observed in the solid state. This is due to solvation effects, followed by dehalogenation as one of the first catalytic steps towards the formation of the catalytically active species.

3.3 Secondary alcohol oxidation activity

The anaerobic oxidation of secondary alcohols has been studied for several years now, with various synthetic and catalytic routes that exist in efficiently producing key ketones.[1,3,4] Nickel-NHC complexes, despite exhibiting competitive catalytic activities as pre-catalysts, have received little attention compared to the well-studied platinum group metals. We employed our recently reported series of [CpNiBr(NHC)] complexes as pre-catalysts in the oxidation of secondary alcohols using 1,2-dibromobenzene as oxidant. This is the first account of [CpNiBr(NHC)] complexes employed in the anaerobic alcohol oxidation reactions, whereas only four [CpNiCl(NHC)] complexes of the [CpNiX(NHC)] (X = halide) series have ever been employed.[11] Complexes **1-9** catalysed the oxidation of racemic 1-phenylethanol efficiently, and gave high yields of the corresponding acetophenone.

Complex **1**, [CpNiBr{Im(Bn)$_2$}], was employed as the catalyst for the optimisation of the anaerobic oxidation of ±1-phenylethanol (Table 1). We initially employed similar reaction conditions to Navarro and co-workers,[11] that is, stirred suspensions of the secondary alcohol in 1,2-dichlorobenzene (3 mL) with 2.6 eq. KO^{t}Bu, and 3 mol% catalyst at 110°C for 120 minutes. The use of 1,2-dibromobenzene as solvent and oxidant instead of 2,4-dichlorotoluene, which was used in the reported method,[11] allowed for easier oxidative addition to the Ni(0) centre. These changes were employed without sacrificing catalytic efficiency and substrate conversion, despite conventional heating methods that were employed (entry 5). Lower conversions were obtained compared to those reported by Navarro[11] for the given optimised temperature (110 ºC) and reaction time (120 min). They

employed microwave heating at the same temperatures in 30 min to give almost quantitative conversions. However, the same Ni-NHC systems of Navarro and co-workers[11] were able to effect secondary alcohol transformations with conversions of up to only 5% when conventional heating was applied. The effect of catalyst concentrations lower than 3 mol% was observed in dramatic lower alcohol conversions (entries 1 and 2). The mild base KO^{t}Bu was more effective in this study than K_3PO_4 (entry 4, which was found to be superior in similar arylhalide functionalisation and C-C coupling reactions.[26,37-39] Separate decreases in temperature (entries 6 and 7) and reaction time (entry 8) lead to the expected decrease in alcohol conversion, whereas slightly lower equivalents of KO^{t}Bu present in the reaction mixture did not notably affect alcohol oxidation product formation, or lead to any side-product formation (entry 9).

Table 1: Optimisation of reaction conditions in the oxidation of ±1-phenylethanol.

Entry	Cat. (mol%)	Solvent/ Oxidant[a]	Base	Time (hrs)	Temp (°C)	Base (equiv)	Conv. (%)[b]
1	**1** (0.5)	1,2-DBB	KO^{t}Bu	2	110	2.6	9
2	**1** (1)	1,2-DBB	KO^{t}Bu	2	110	2.6	56
3	**1** (3)	1,2-DBB	KO^{t}Bu	2	110	2.6	84
4	**1** (3)	1,2-DBB	K_3PO_4	2	110	2.6	49
5	**1** (3)	1,2-DCB	KO^{t}Bu	2	110	2.6	65
6	**1** (3)	1,2-DBB	KO^{t}Bu	2	80	2.6	58
7	**1** (3)	1,2-DBB	KO^{t}Bu	2	25	2.6	30
8	**1** (3)	1,2-DBB	KO^{t}Bu	1	110	2.6	76
9	**1** (3)	1,2-DBB	KO^{t}Bu	2	110	2.0	82

General reaction conditions: ±1-phenylethanol (0.3 mmol), KO^{t}Bu (0.78 mmol), catalyst (**1**, 3 mol%), 1,2-dibromobenzene (3 mL). [a] 1,2-DBB = 1,2-dibromobenzene. 1,2-DCB = 1,2-dichlorobenzene. [b] GC yields based on internal standard, average value of three runs.

Complexes **1-9** were all catalytically active in the anaerobic oxidation of racemic 1-phenylethanol. Screening of each separate complex in the catalytic reactions under optimised conditions showed that electronic and steric differences present in the *N*-substituents of the coordinated NHC ligands affect the performance and more notably the efficiency of the catalysts (Figure 5). Complexes **1**, **2**, and **5** were the most active in the oxidation of ±1-phenylethanol to give high conversions (> 80%) within 2 hours.

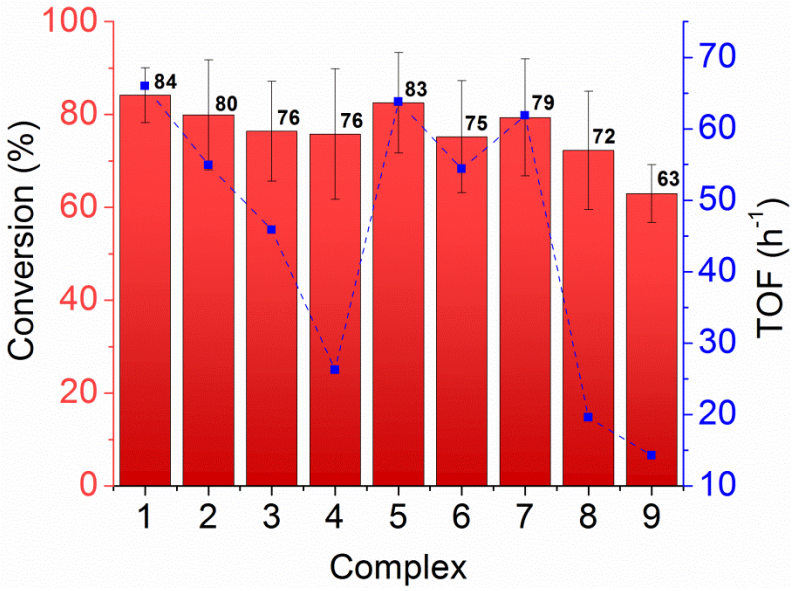


Figure 5: Anaerobic alcohol oxidation using complexes **1-9**. Reaction conditions: ±1-phenylethanol (0.3 mmol), KO^{t}Bu (0.78 mmol), catalyst (3 mol%), 1,2-dibromobenzene (3 mL), 110°C, 120 min. TOF (h^{-1}) indicated in the graph is the initial TOF (h^{-1}) calculated based on the amount of substrate converted within the first 5 minutes of the reaction. All GC yields are based on internal standard, average value of three runs.

A gradual decrease in oxidation activity is observed as the electron-donating character of the coordinating NHC ligand changes. The complexes bearing NHCs with electron-withdrawing 4-NO_2-benzyl moieties showed the poorest activity, with complex **9**, [CpNiBr{Im(4-NO_2Bn)$_2$}], only converting 63% of the secondary alcohol. This result was found to be directly related to the *N*-alkyl/benzyl/phenylethyl groups of the different Ni(II)-NHC complexes involved in each separate reaction, where the more electron-withdrawing aryl groups tend to destabilise the electron-donating character of the NHC ligand. This leads to a metal complex with less electron density to help stabilise air and moisture sensitive catalytically active Ni(0) species, and invariably hinders the oxidative addition of the substrate. This effect was also observed by Ritleng[38] and Buchowicz,[37] where they found that electron-donating, bulky *N*-substituents lead to more stable and catalytically active nickel species. Furthermore, the sp^3-carbon linkers on the *N*-substituents help provide flexibility to the relatively bulky phenyl-containing substituents to allow for unhindered substrate coordination and enhanced reductive elimination steps in the catalytic cycle.[23] The presence of aryl halides in the reaction mixtures may also provide additional stabilisation through soft π-interactions of the *N*-benzyl and phenylethyl groups, as well as close-contact hydrogen-

halide interactions. A similar trend is also observed in the initial TOFs of complexes **1-9**, where complexes **1-3**, **5**, **6**, and **7** were all very efficient during the first five minutes of the reaction. Complexes **4**, **8**, and **9** were all much less effective, resulting in lower atom efficiency of the catalyst and lower substrate conversion. It is interesting to note that although the latter complexes exhibited low TOFs, the eventual substrate conversions were not severely influenced and might indicate slow(er) catalyst decomposition.

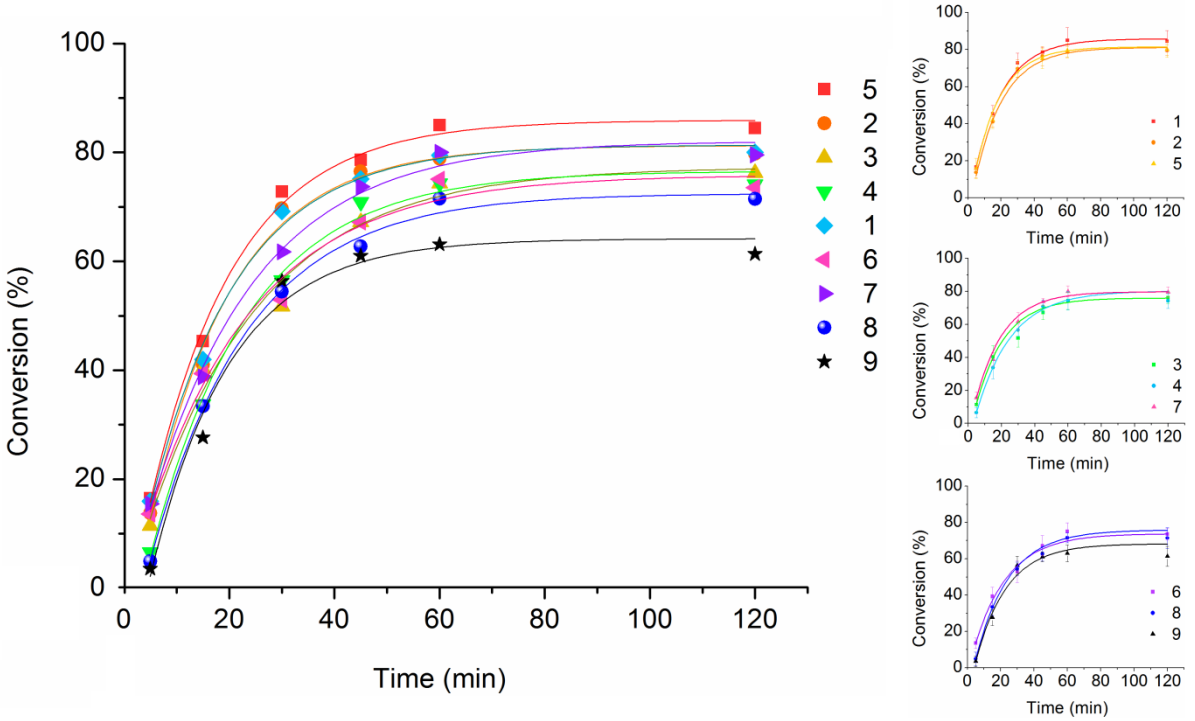
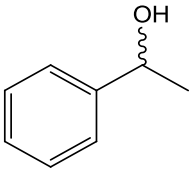
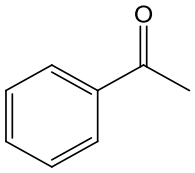
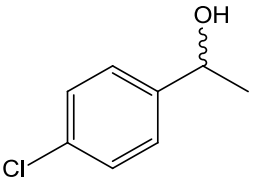
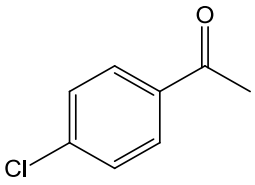
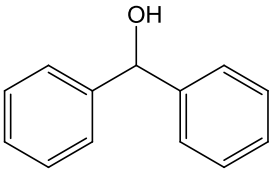
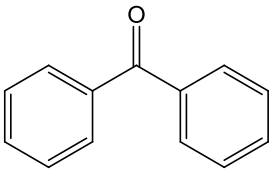
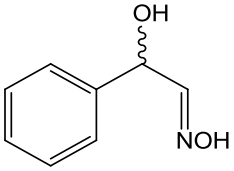
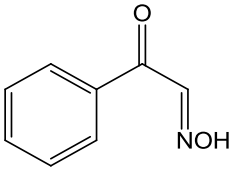
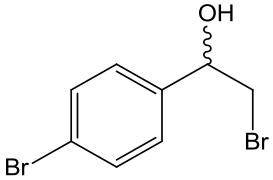
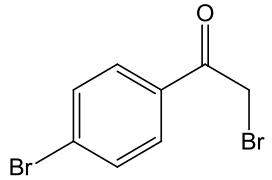


Figure 6: Time resolved plots of acetophenone conversion (%) using complexes **1-9**. Reaction conditions: ±1-phenylethanol (0.3 mmol), KO^{t}Bu (0.78 mmol), catalyst (3 mol%), 1,2-dibromobenzene (3 mL), 110°C, 120 min.

From the time resolved plots of ±1-phenylethanol conversion, more insight is obtained into catalyst decomposition and catalyst performance limitations (Figure 6). An initial fast conversion of alcohol is observed for all reactions (first 15 minutes), after which a gradual relaxation in the slopes are observed to reach an apparent reaction time of about 60 minutes. Thereafter the effects of catalyst decomposition become noticeable, inhibiting further conversion activity. Complexes **1-9** have been divided based on activity as insets in Figure 6 for clarity. From these it can be seen that complexes **1**, **2**, and **5** were the most active, followed by **3**, **4**, and **7**, and finally **6**, **8**, and **9**. These observations strongly correlate to the overall conversions and TOFs attained using each of these catalysts. A reaction time of 60

minutes could be considered fast for conventionally heated Ni-catalysed alcohol oxidation reactions,[1] especially without added additives such as PPh_3.[15,38]

Table 2: Conventional and microwave-heated oxidation of secondary alcohols

Entry	Cat. (mol%)	Solvent/ Oxidant[a]	Substrate	Product	Time (hrs)	Temp (°C)	Conv. (%)[b]
1	**1** (3)	1,2-DBB			2	110	84 (98)
2	**1**(3)	1,2-DBB			2	110	79 (97)
3	**1** (3)	1,2-DBB			2	110	71 (96)
4	**1** (3)	1,2-DBB			2	110	52 (90)
5	**1** (3)	1,2-DBB			2	110	60 (94)

General reaction conditions: alcohol (0.3 mmol), KO^{t}Bu (0.78 mmol), catalyst (**1**, 3 mol%), 1,2-dibromobenzene (3 mL), 110°C, 120 min. [a] 1,2-DBB = 1,2-dibromobenzene. [b] GC yields based on internal standard, average value of three runs. Values in parentheses are conversions when microwave heating (500W) was used for two hours.

Using **1**, several other secondary alcohol substrates were also evaluated for oxidation under optimised conditions (Table 2). The similar substrate ±1-(4'-Cl)-phenylethanol was oxidised to 4'-chloroacetophenone in slightly lower yields as compared to ±1-phenylethanol (entry 2), with even less of the more bulky benzhydrol converted to benzophenone (entry 3). This is surprising since a lower conversion has been associated with substrates bearing electron-donating *para*-substituents.[40] This is indicative of the important influence the electronic nature of the aromatic ring has in oxidation reactions. Interestingly, the presence of an aryl halide in the alcohol substrates (entries 2, 5) did not lead to any side product formation under optimised conditions, despite the possibility of the aryl halide-bearing alcohol or their oxidised species undergoing oxidative addition onto Ni(0) species present in the reaction mixture.[10(b),38,41]

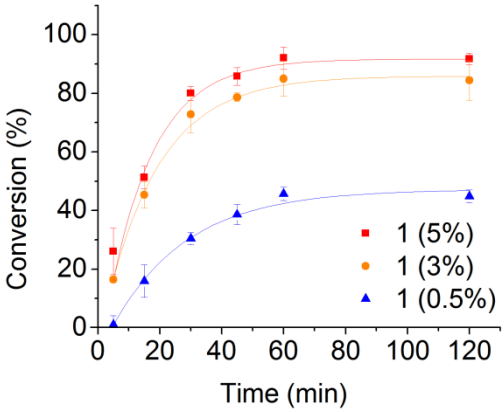


Figure 7: Effect of catalyst concentration on conversion of ±1-phenylethanol. General reaction conditions: ±1-phenylethanol (0.3 mmol), KO^{t}Bu (0.78 mmol), catalyst (**1**), 1,2-dibromobenzene (3 mL), 110°C, 120 min.

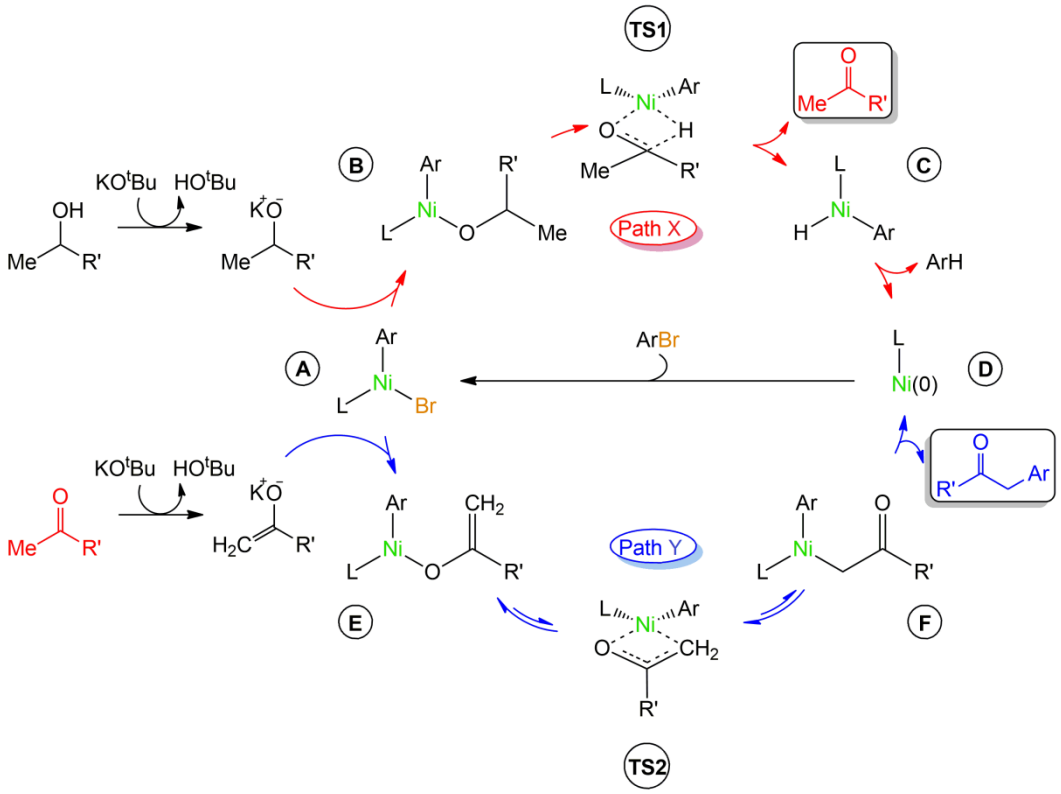
The relationship between secondary alcohol conversion over reaction time at various catalyst concentrations is illustrated in Figure 7. The notable effect of catalyst concentration on the conversion of the alcohol substrate is indicative of a relatively fast catalyst deactivation process.[38] At concentrations lower than 3 mol%, a significant decrease in alcohol conversion is seen, whereas a saturation point in activity and atom efficiency is quickly reached at catalyst concentrations higher than 5 mol%. At these high catalyst concentrations the turnover number (TON) (see Supplementary Information) and turnover frequency (TOF) of

[40] C-C. Lee, W-C. Ke, K-T. Chan, C-L. Lai, C-H. Hu, H. M. Lee, *Chem. Eur. J.*, 2007, **13**, 582-591.
[41] S. Thangavel, S. Boopathi, N. Mahadevaiah, P. Kolandaivel, P. B. Pansuriya, H. B. Friedrich, *J. Mol. Catal. A.*, 2016, **423**, 160-171.

the reactions decreases dramatically, leading to an inefficient and expensive catalytic reaction.

3.4 Mechanistic and computational considerations

In the seminal article by Navarro and co-workers,[20] they found that when 2 or more equivalents of the aryl chloride (oxidant) is used, a subsequent domino α-ketone arylation takes place once the ketone has formed. These α-arylated products were obtained in high yields (> 76%) when 2 mol% of [PdCl(allyl)(iPr)] (iPr = 2,6-diisopropylimidazolidene) was used at 80°C with 2.2 eq of KO^{t}Bu. They did not, however, observe formation of these species when complexes [CpNiCl(NHC)] (NHC = IMes, SIMes, IPr, SIPr) were employed,[11] which is in full agreement with our results.



Scheme 1: Mechanistic pathways for the anaerobic alcohol oxidation (Path X), and domino α-ketone arylation (Path Y)

In the anaerobic alcohol oxidation mechanism (Path X, Scheme 1), the [CpNiBr(NHC)] complex is reduced and dehalogenated by the base present, after which the aryl halide present undergoes oxidative addition to the Ni(0) species (**D**) to form the Ni(II) species (**A**). The secondary alcohol is deprotonated by the excess of base present, which substitutes the bromide anion on the nickel(II) centre to form **B**, through which, after β-hydride elimination,

the ketone formed is expelled from the nickel centre, leaving the nickel(II)-hydride species **C**. Reductive elimination of the arene leads to the **D** species, which after oxidative addition of another aryl halide molecule regenerates **A**. It has been shown that the π complexation of haloarenes with Ni(0) is irreversible and could initiate at any C-C bond of the aromatic ring.[42] A series of ringhopping steps take place before the final addition process on the preferred aromatic C-X bond. Furthermore, species **A** may then also react with the ethenoxide (formed from the ketone, Path Y) to form species **E**, followed by a tautomeric shift to oxidise the ethenoxide to a σ-bonded 2-oxo-2-phenylethyl moiety (**F**), through which after reductive elimination yields **D** and 2-(2-bromophenyl)-1-phenylethanone as the organic product.

Gibbs free energy calculations on **1** and its catalytic intermediates were carried out to support the two proposed paths and provide insight into the high selectivity of Path X over Path Y. In Figures 8 (singlet states) and 9 (triplet states) the relative Gibbs free energy over the course of Paths X (red) and Y (blue) have been illustrated. Both spin multiplicities with respect to the nickel species involved in the mechanistic pathways X and Y (Scheme 1) were taken into consideration, since no unambiguous assignment could be made given the chemical and geometrical nature of the species. Furthermore, notable energy discrepancies between identical species calculated using different spin multiplicities required further investigation and revealed that the lowest energy species were calculated for 10 species using singlet multiplicities, and 7 species using triplet multiplicities. Recognising that Ni(II) (d^8) species usually exhibit the triplet state (tetrahedral arrangement) and the singlet state (square planar arrangement) as favourable multiplicity states, and that formally no triplet state is expected for Ni(0) (d^{10}) species, both spin multiplicities for Ni(II) and Ni(0) were considered for completeness. Indeed, in selected cases we found that the singlet/triplet multiplicity for Ni(II)/Ni(0) species resulted in lower Gibbs energies. The crossover to the unusual singlet state for Ni(II) species is likely mediated by the relatively large spin-orbit coupling of the Ni-centre,[3] and effectively decreases the activation barrier. Spin-crossing or two-state reactivity is a concept in organometallic chemistry proposed by Shaik *et al*.[43] and has been used widely to explain and predict the reactivity of several organometallic and bioinorganic systems,[43,44,45(a)] including a report on Ni(II)-porphyrin complexes.[45(b)]

[42] T. Sperger, I. A. Sanhueza, I. Kalvet, F. Schoenebeck, *Chem. Rev.*, 2015, **115**, 9532-9586.
[43] S. Shaik, H. Hirao, D. Kumar, *Acc. Chem. Res.*, 2007, **40**, 532-542.
[44] B. K. Mai, Y. Kim, *Angew. Chem. Int. Ed.*, 2015, **54**, 3946-3951.

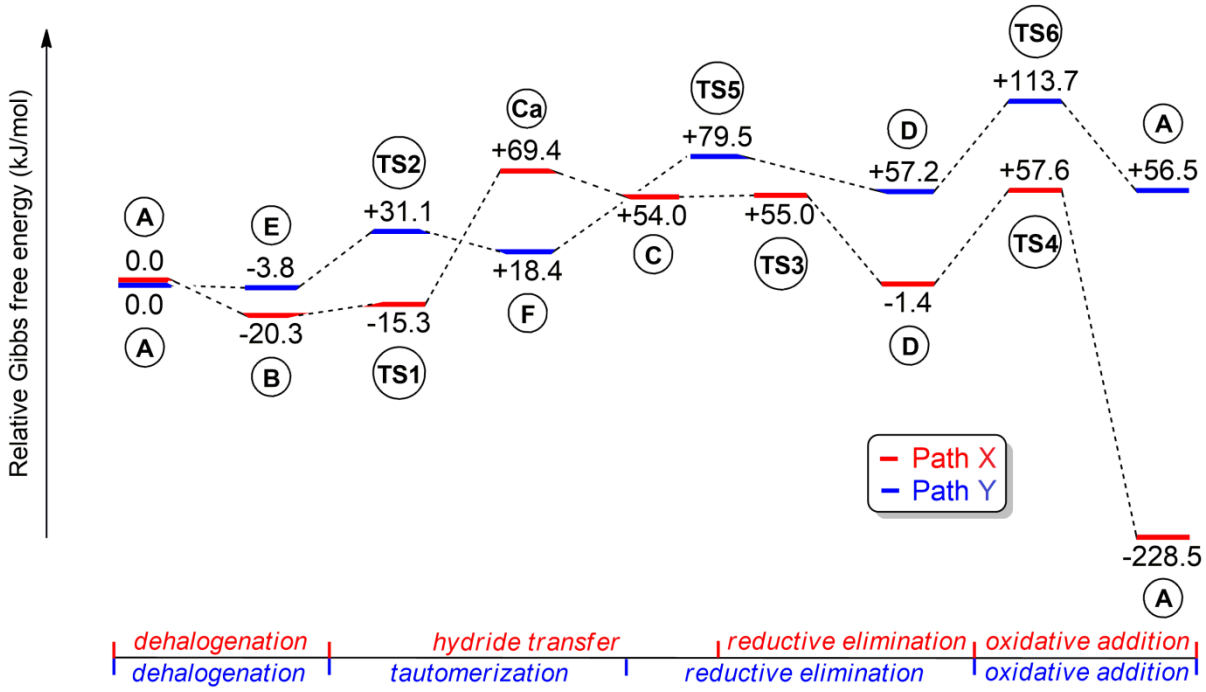


Figure 8: Relative Gibbs free energy profile for the Ni(II) singlet state of Paths X and Y

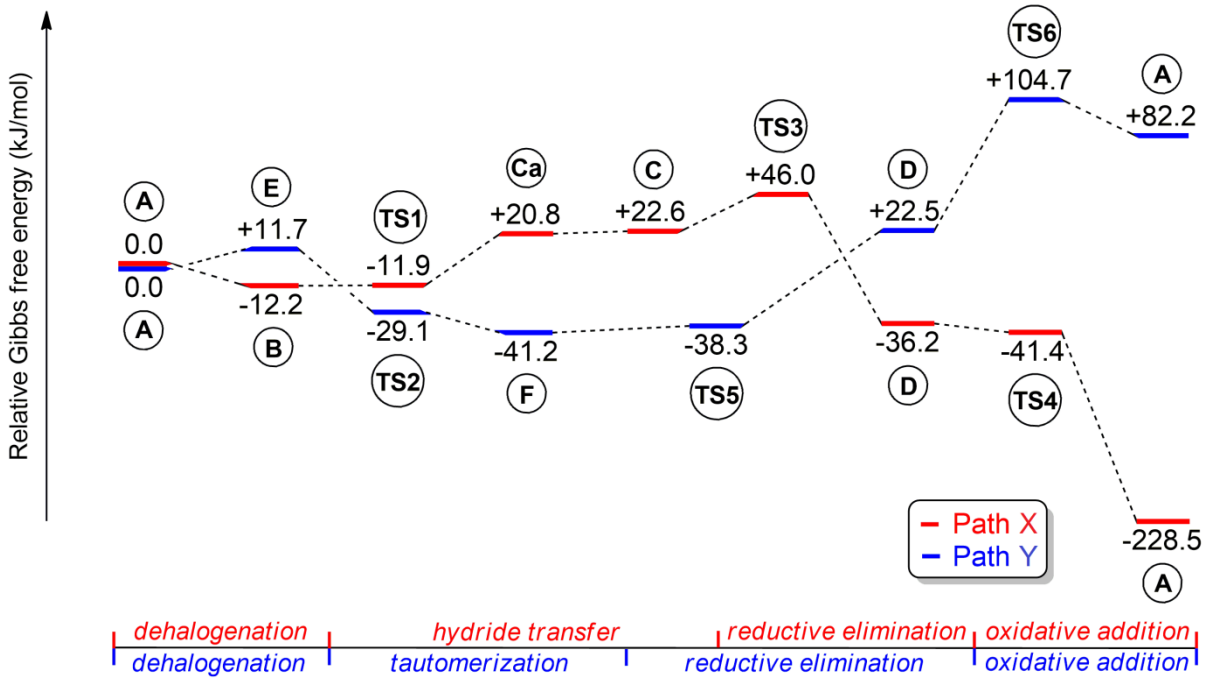


Figure 9: Relative Gibbs free energy profile for the Ni(II) triplet state of Paths X and Y

[45] (a) D. Schröder, S. Shaik, H. Schwarz, *Acc. Chem. Res.*, 2000, **33**, 139-145. (b) S. Thies, C. Bornholdt, F. Köhler, F. D. Sönnichsen, C. Näther, F. Tuczek, R. Herges, *Chem. Eur. J.*, 2010, **16**, 10074-10083.

With species **A** (Paths X and Y) taken as the reference, formation of **B** (Path X) is associated with a loss of 12.2 kJ/mol, whereas formation of **E** (Path Y) exhibits a barrier of +11.7 kJ/mol. This result, together with the energy costs involved in converting acetophenone into potassium 1-phenylethenolate (+24.6 kJ/mol) versus conversion of 1-phenylethanol into potassium 1-phenylethanolate (-98.7 kJ/mol) would inhibit formation of **E** from Path Y. Both intermediates **B** and **E** are characterised by shorter C-O bonds (1.851 Å (**B**), 1.817 Å (**E**)) in the singlet state, as compared to the (more stable) triplet states (1.876 Å (**B**), 1.872 Å (**E**)). Figures and additional bond lengths of the fully optimised intermediates and transition states are included in the Supplementary Information.

When only considering the singlet multiplicity case for Paths X and Y (Figure 8), Path X exhibits an activation barrier of +46.0 kJ/mol, associated with the rate-determining state of reductive elimination.[46] In contrast, Path Y exhibits an activation barrier of +228.1 kJ/mol, associated with the rate-determining state of oxidative addition. This leads to a favourable energetic span for Path X of δE = +58.2 kJ/mol, an exothermic pathway, as compared to the much higher δE = +269.3 kJ/mol for Path Y, an endothermic pathway. The oxidative addition step for Paths X and Y evaluated as either singlet or triplet multiplicities (-20.3 and +11.7 kJ/mol respectively) are all lower than similar oxidative addition steps of Pd-NHC species (> 60.5 kJ/mol)[18] and Ni-NHC species (> 23.8 kJ/mol),[47 (a)] and in the case of Path X (singlet/triplet) is indicative of a facile step.

Overall, Path X is highly exergonic with -228.5 kJ/mol, and Path Y endergonic with +82.2 kJ/mol, which leads to the conclusion that Path X is the preferred path. When considering triplet multiplicity for all the intermediates involved (Figure 9), the more stable **B** is formed (Path X) with a loss of 20.3 kJ/mol, whereas the more stable **E** (Path Y) is formed with a loss of 3.8 kJ/mol. For Path X, the rate-determining state shifts to the hydride transfer step with an activation barrier of +69.4 kJ/mol, and an associated δE of +89.7 kJ/mol. The latter is in clear contrast to Path Y, having the rate-determining state(s) remaining at the oxidative addition step, with an activation barrier of +174.0 kJ/mol and an associated δE of +177.9 kJ/mol. Similar to the singlet multiplicity, the triplet multiplicity shows Path X to be the preferred

[46] S. Kozuch, S. Shaik, *Acc. Chem. Res.*, 2011, **44**, 101-110.
[47] (a) T. Mesganaw, A. L. Silberstein, S. D. Ramgren, N. F. F. Nathel, X. Hong, P. Liu, N. K. Garg, *Chem. Sci.*, 2011, **2**, 1766-1771. (b) A. T. Normand, K. J. Hawkes, N. D. Clement, K. J. Cavell, B. F. Yates, *Organometallics*, 2007, **26**, 5352-5363.

path being highly exergonic at -228.5 kJ/mol, compared to Path Y being endergonic at +56.5 kJ/mol. Efficient catalysis relies on the minimisation of δE, as under steady-state conditions the rate of the reaction is strongly influenced by this parameter. Therefore, improvements in catalyst efficiency and atom economy would include stabilisation of the highest energy transition state, as well as destabilising the most abundant reaction intermediate.[47(b)] Hence, with all results considered, it is clear that Path X is preferred irrespective of the spin multiplicities of the intermediates involved, and agrees with our experimental findings that anaerobic alcohol oxidation is feasible under elevated temperatures.

Kozuch *et al.*[46] developed an elegant yet simplistic method of estimating the TOF of a given catalytic cycle. They showed that for exothermal reactions ($\Delta G < 0$) that the TOF could be defined as

$$\mathrm{TOF} = \frac{k_B T}{h} \mathrm{e}^{-\delta E/RT} \qquad (1)$$

where k_B is the Boltzmann constant, T is the temperature, h is Planck's constant, δE is the energetic span, and R is the universal gas constant. If we apply equation 1 to reoptimised reaction intermediates and transition states where solvent effects have been included, the TOF calculations are in agreement with the preferred Path X in both spin multiplicities, with TOF = 0.2 h^{-1} (X, singlet), 3.7 × 10^{-9} h^{-1} (Y, singlet), 0.1 h^{-1} (X, triplet), and 6.4 × 10^{-7} h^{-1} (Y, triplet). With the theoretical TOF of Path X (singlet) = 0.2 h^{-1}, resulting from a solvent-corrected δE = 94.5 kJ/mol (25°C), it is in fair agreement with our experimental TOF finding for **1** (84 h^{-1} at 110°C; 8 h^{-1} at 25°C) and furthermore shows the strong temperature dependence on the TOF of the reaction.

The molecular orbital diagrams of **A** and its dehalogenated products **B** and **E** (Figure 10) help to further illustrate the electronic differences of the intermediate products of Path X over Y. The HOMO of **A** is uniquely populated over the ArNiBr functionalities, and is the lowest in energy of all the species involved. Following Path X, the formation of alkoxy adduct **B** shifts the electron density in the HOMO away from the aryl towards the Ni(alkoxy)(NHC) functionalities, and in the case of **E** (Path Y), shifts toward the Ni(alkenoxy) functionalities (highest in energy). The LUMOs of **A** and its adducts **B** and **E** all have similar electronic character with Ni(NHC)(X) (X = Br, alkoxy, alkenoxy) involved. However, in **E** the LUMO is highly concentrated on the metal centre and ethenoxy moiety, bearing the highest LUMO energy (-4.78 eV) of the three intermediates. It is noteworthy that the largest HOMO/LUMO

energy difference (energy gap) is exhibited by the alkoxy adduct **B** (5.26 eV), while the smallest energy gap is exhibited by ethenoxide adduct **E** (2.82 eV), which further highlights the latter species' instability and higher reactivity.[40] In terms of the Principle of Maximum Hardness (PMH) related to the molecular orbital (MO) theory, the hardness of a molecule (η) is defined as half the energy gap between the HOMO and the LUMO.[48] Furthermore, a chemical system tends to arrange itself to maximise hardness of its respective molecules where a hard molecule tend to have a large energy gap,[48] Comparing intermediates **B** (η = 2.63 eV) and **E** (η = 1.41 eV), **E** is softer than **B**, and therefore is expected to be less stable and more reactive than intermediate **B**.[48]

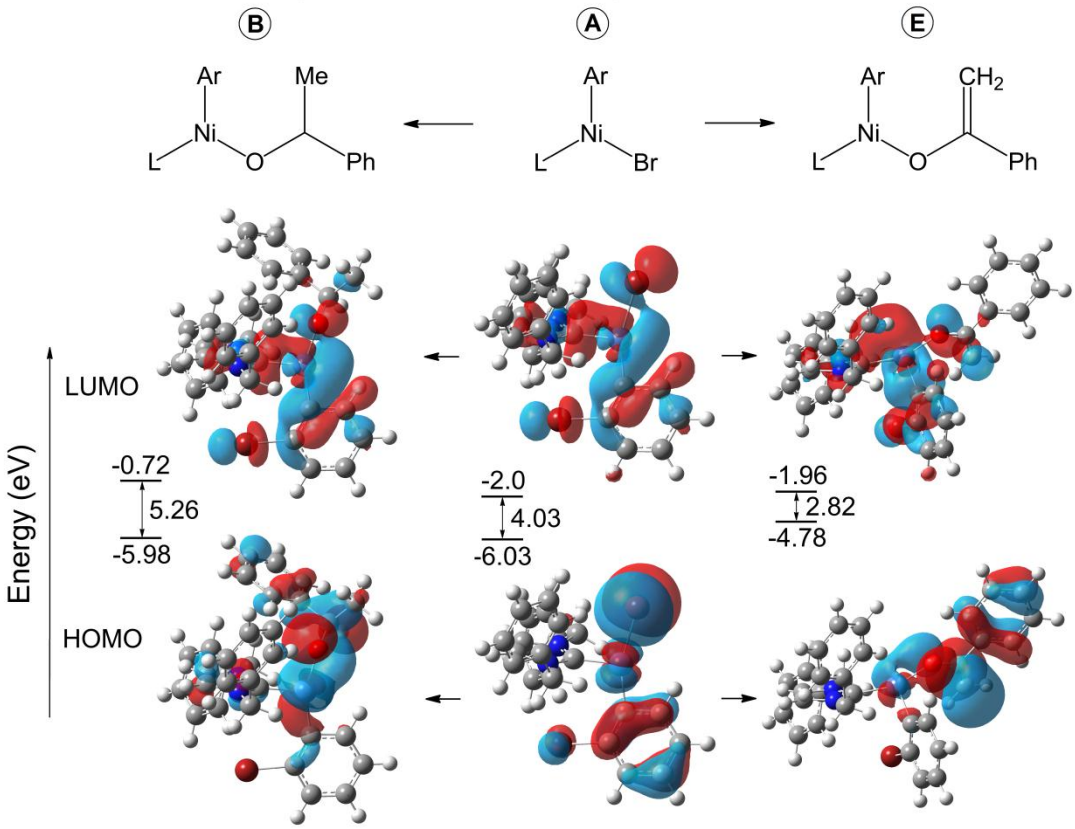


Figure 10: Molecular orbital diagrams of **A**, **B** (Path X) and **E** (Path Y) using singlet multiplicities

[48] R. G. Pearson, *Acc. Chem. Res.*, 1993, **26**, 250-255.

4. Conclusion

A range of nine [CpNiBr(NHC) complexes, each bearing flexible, electron withdrawing/donating NHCs were inexpensively synthesised. The molecular structures of three of these complexes were obtained and elucidated with X-ray crystallography. These Ni(II)-NHC were all catalytically active in the anaerobic alcohol oxidation reaction whereby a range of several secondary alcohols were oxidised to their corresponding ketones, along with concomitant dehalogenation of 1,2-dibromobenzene. Complexes **1**, **2**, and **5** were the most active, followed by **3**, **4**, and **7**, and finally **6**, **8**, and **9**. Among complexes **1-9**, the more electron-donating NHC-bearing complexes were more efficient, owing to their enhanced ability to better support sensitive Ni(0) species. The flexibility and bulkiness of the N-alkyl/aryl substituents on the NHC ligands provided accessibility to incoming substrates, while also aiding in the reductive elimination of the organic products. A strong catalyst concentration dependency was found, which is indicative of catalyst decomposition. Utilisation of microwave heating methods notably increased the alcohol conversions, by decreasing the reaction times to inhibit the effects of catalyst decomposition. Furthermore, DFT mechanistic studies gave more insight into the favoured ketone product formation, as opposed to their subsequent α-ketone arylated products.

Acknowledgements

The National Research Foundation of South Africa (NRF, grant number 93638) and the University of Pretoria (UP) are gratefully acknowledged for financial support (ML, FPM).

CHAPTER 4

Synthesis, structure and DFT conformation analysis of CpNiX(NHC) and $NiX_2(NHC)_2$ (X = SPh or Br) complexes

Chapter 4 was adapted from an article published in the journal of Molecular Structure:

Authors: Frederick P. Malan, Eric Singleton, Petrus H. van Rooyen, Jeanet Conradie, Marilé Landman

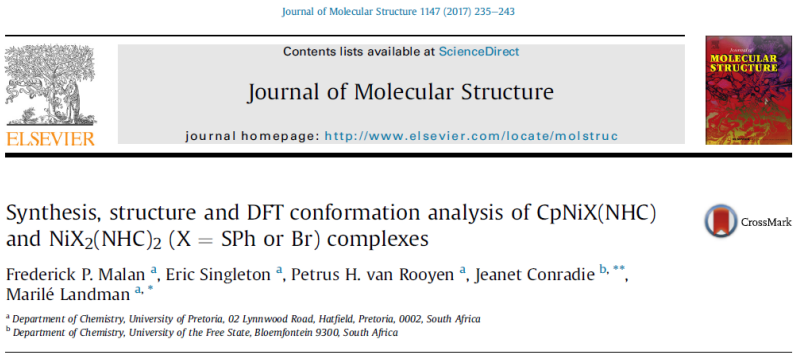
Year: 2017

Volume: 1147

Pages: 235-243

Status: Published

Website: http://dx.doi.org/10.1016/j.molstruc.2017.06.086



Journal of Molecular Structure 1147 (2017) 235–243

Contents lists available at ScienceDirect

Journal of Molecular Structure

journal homepage: http://www.elsevier.com/locate/molstruc

Synthesis, structure and DFT conformation analysis of CpNiX(NHC) and $NiX_2(NHC)_2$ (X = SPh or Br) complexes

Frederick P. Malan [a], Eric Singleton [a], Petrus H. van Rooyen [a], Jeanet Conradie [b, **], Marilé Landman [a, *]

[a] Department of Chemistry, University of Pretoria, 02 Lynnwood Road, Hatfield, Pretoria, 0002, South Africa
[b] Department of Chemistry, University of the Free State, Bloemfontein 9300, South Africa

Contributions:

Frederick P. Malan: Author, synthesis, characterisation, crystallography, DFT study (full optimisation, calculation of HOMOs/LUMOs, energy calculations)

Eric Singleton: Co-author, co-supervisor; Petrus H. van Rooyen: co-author; Jeanet Conradie: Corresponding author, DFT study (supervision of calculations, provision of DFT facilities and execution of input files created by FP Malan, electronic structure calculations)

Marilé Landman: Corresponding author, supervisor

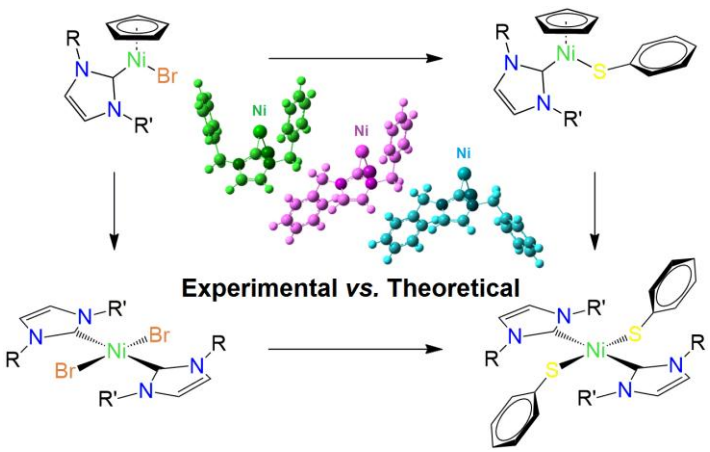
4 Synthesis, structure and DFT conformation analysis of CpNiX(NHC) and $NiX_2(NHC)_2$ (X = SPh or Br) complexes

Frederick P. Malan,[a] Eric Singleton,[a] Petrus H. van Rooyen,[a] Jeanet Conradie[b,*] and Marilé Landman[a,*]

[a] *Department of Chemistry, University of Pretoria, 02 Lynnwood Road, Hatfield, Pretoria, 0002, South Africa.*

[b] *Department of Chemistry, University of the Free State, Bloemfontein 9300, South Africa.*

Graphical abstract



Keywords

nickel; *N*-heterocyclic carbene; biscarbene; DFT; conformation

Highlights

- Five new Ni(II)-NHC complexes synthesised and characterised
- X-ray structures of four complexes reported
- DFT conformational analysis of all complexes
- DFT electronic structure comparison of mono- and bis-NHC complexes

Abstract

The synthesis, density functional theory (DFT) conformational study and structure analysis of novel two-legged piano stool Ni *N*-heterocyclic carbene complexes and square planar Ni bis-*N*-heterocyclic carbene complexes, all containing either bromido or thiophenolato ligands, are described. [CpNi(SPh)(NHC)] complexes were obtained from the neutral 18-electron [CpNiBr(NHC)] complexes by substitution of a bromido ligand with SPh, using NEt_3 as a base to abstract the proton of HSPh. The 16-electron biscarbene complexes $[Ni(SPh)_2\{NHC\}_2]$ were isolated when an excess of HSPh was added to the reaction mixture. Biscarbene complexes of the type $[NiBr_2(NHC)_2]$ were obtained in the reaction of $NiCp_2$ with a slight excess of the specific imidazolium bromide salt. The molecular and electronic structures of the mono- and bis-*N*-heterocyclic carbene complexes have been analysed using single crystal diffraction and density functional theory (DFT) calculations, to give insight into their structural properties.

1. Introduction

Nickel is continuously gaining interest in biological studies due to an increase in the number of its compounds that have found successful applications as metallodrugs, as well as its presence in nature where numerous nickel-containing enzymes have been identified to date.[1,2] Nickel(I)[1] and nickel(II)[3,4] complexes containing nitrogen- and sulfur-donor ligands have been used for the synthesis of active site models for oxidoreductases, including nitrogenases and CO dehydrogenases.[3,5,6] Equally important, nickel complexes with thiolato ligands continue to find application in catalysis due to their important roles in homogeneous C-S coupling reactions, hydrodesulfurisation methods, small molecule activation processes, and electron transfer reactions.[6-8]

[1] M. Ito, T. Matsumoto, K. Tatsumi, *Inorg. Chem.*, 2009, **48**, 2215-2223.
[2] M. T. H. Tarafder, N. Saravanan, K. A. Crouse, *Transition Metal Chemistry*, 2001, **26**, 613-618.
[3] S. Chattopadhyay, T. Deb, H. Ma, J. L. Petersen, V. G. Young, Jr., M. P. Jensen, *Inorg. Chem.*, 2008, **47**, 3384-3392.
[4] D. Sellmann, W. Prechtel, F. Knoch, M. Moll, *Organometallics*, 1992, **11**, 2346-2348.
[5] D. Sellmann, W. Prechtel, F. Knoch, M. Moll, *Inorg. Chem.*, 1993, **32**, 538-546.
[6] S. C. Holm, F. Rominger, B. F. Straub, *J. Organomet. Chem.*, 2012, **719**, 54-63.
[7] F. Olechnowicz, G. L. Hillhouse, R. F. Jordan, *Inorg. Chem.*, 2015, **54**, 2705-2712.
[8] T. Schaub, M. Backes, O. Plietzsch, U. Radius, *Dalton Trans.*, 2009, 7071-7079.

The soft and electron-rich thiolato ligands form some of the strongest metal-sulfur bonds, and help stabilise sensitive catalytically active metal species.[9,10] Our interest in employing these stabilising thiolato ligands in our Ni(II)-NHC systems forms part of an existing project on the use of Ni(II) NHC complexes in homogeneous catalysis and biological applications. Our group,[11,12] and others[13-15] have found excellent potential for cyclopentadienyl Ni(II)-NHC complexes as catalyst precursors. Numerous catalysed organic transformations are made more economical and versatile by using readily available and cheap Ni(II) precursors.[16] The choice of using NHCs as ancillary ligands in Ni(II) systems stems from their strongly donating properties, capable of forming strong M-C bonds and consequently stabilising Ni(II) complexes as well as *in situ* generated catalytically active nickel species.[16,17]

Following our recent report on the electrochemical properties of a series of [CpNiBr(NHC)] complexes containing different NHC ligands,[18] the reactivity and structural properties of the thiophenolato derivatives of these complexes were subsequently investigated. Interestingly, while a large number of [CpNiX(NHC)] (X = halogen) complexes have been structurally reported, only six crystal structures for the series of [CpNi(Y)(NHC)] (Y = thioarylate, disulfide, trisulfide) complexes could be found in the literature.[19] In this study, we report the use of [CpNiBr(NHC)] complexes[11] as precursors to synthesise complexes of the type [CpNi(SPh)(NHC)], [Ni(SPh)$_2${NHC}$_2$] and [NiBr$_2${NHC}$_2$]. The NHC ligands of this study are shown in Figure 1. Of particular interest is the reactivity patterns observed in the syntheses of 18-electron and 16-electron Ni(II)-thiophenolato complexes, along with the comparison between experimental molecular structures and DFT calculated conformational preferences as well as the calculated electronic configuration for each type of complex.

[9] D. Yuan, H. V. Huynh, *Inorg. Chem.*, 2013, **52**, 6627-6634.
[10] A. Bheemaraju, J. W. Beattie, E. G. Tabasan, P. D. Martin, R. L. Lord, S. Groysman, *Organometallics*, 2013, **32**, 2952-2962.
[11] F. P. Malan, E. Singleton, P. H. van Rooyen, M. Landman, *J. Organomet. Chem.*, 2016, **813**, 7-14.
[12] F. P. Malan, E. Singleton, B. Bulling, I. Cukrowski, P. H. van Rooyen, M. Landman, *Mol. Catal.*, 2017, **432C**, 56-67.
[13] D. A. Malyshev, N. M. Scott, N. Marion, E. D. Stevens, V. P. Ananikov, I. P. Beletskaya, S. P. Nolan, *Organometallics*, 2006, **25**, 4462-4470.
[14] A. R. Martin, Y. Makida, S. Meiries, A. M. Z. Slawin, S. P. Nolan, *Organometallics*, 2013, **32**, 6265-6270.
[15] M. Henrion, V. Ritleng, M. J. Chetcuti, *ACS Catal.*, 2015, **5**, 1283-1302.
[16] E. A. Standley, S. J. Smith, P. Müller, T. F. Jamison, *Organometallics*, 2014, **33**, 2012-2018.
[17] J. Li, J. Morris, W. W. Brennessel, W. D. Jones, *J. Chem. Crystallogr.*, 2014, **44**, 15-19.
[18] F. P. Malan, E. Singleton, M. Landman, J. Conradie, *Electrochim. Acta*, 2017, submitted.
[19] The Cambridge Structural Database, C. R. Groom, I. J. Bruno, M. P. Lightfoot, S. C. Ward, *Acta Cryst.*, 2016, **B72**, 171-179.

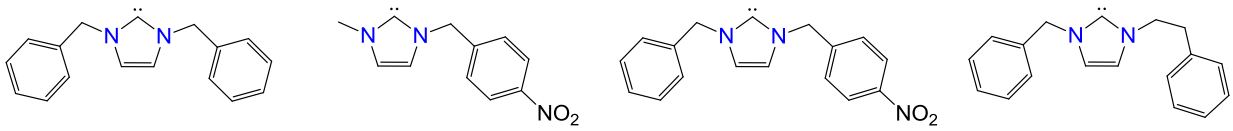


Figure 1. Structures of the imidazolylidene ligands used in this study. **NHC1** = {Im(Bn)$_2$}, **NHC2** = {Im(Me)(4-NO$_2$Bn)}, **NHC3** = {Im(Bn)(4-NO$_2$Bn)} and **NHC4** = {Im(Bn)(EtPh)}

2. Experimental

2.1 General

All experiments were carried out under an argon atmosphere using standard Schlenk techniques. Solvents were dried prior to use using standard techniques.[20] Column chromatography was carried out under inert argon atmospheres using silica gel (particle size 0.063-0.200 mm) as the stationary phase. Imidazolylidene ligands **NHC1**-**NHC4** (**NHC1** = {Im(Bn)$_2$}, **NHC2** = {Im(Me)(4-NO$_2$Bn)}, **NHC3** = {Im(Bn)(4-NO$_2$Bn)} and **NHC4** = {Im(Bn)(EtPh)}; see Figure 1), as well as their corresponding [CpNiBr(NHC)] (**A**-**D**) complexes were all synthesised and reported recently.[11,12] Figure 3 shows the complex numbering. Complexes **E**-**H** were prepared in this study but used *in situ* for the formation of the final [Ni(SPh)$_2$(NHC)$_2$] complexes (**2**, **5** and **I**). Complex **I** however, was isolated in too low yield to allow for full characterisation. All other chemicals were purchased from Sigma-Aldrich and used without further purification. ^{1}H and ^{13}C nuclear magnetic resonance (NMR) spectra were recorded on a Bruker ARX-300 spectrometer in CDCl$_3$, using the solvent residual peak as the internal reference, at 300.1 and 75.5 MHz, respectively. Infrared (IR) spectra were recorded on a Perkin Elmer Spectrum RXI FT-IR spectrophotometer as potassium bromide pellets, and only the vibration bands in the carbonyl-stretching region (1500 - 2200 cm^{-1}) are reported. Mass spectra were recorded on a SYNAPT G2 HDMS instrument, using electrospray ionisation as the ion source and a time-of-flight mass analyser. A sampling time of 3 minutes was used, with the direct infusion inlet method.

[20] R. J. Errington, *Advanced Practical Inorganic and Metalorganic Chemistry*, Blackie Academic & Professional, London, 1997.

2.2 Synthesis

*[CpNi(SPh){Im(Bn)$_2$}] (**1**):*

To a red solution of [CpNiBr{Im(Bn)$_2$}] (**A**) (0.26 g, 0.6 mmol) in toluene (10 mL) was slowly added a toluene solution (5 mL) of HSPh (64 µL, 0.7 mmol) and NEt_3 (90 µL, 0.7 mmol) in a drop-wise fashion over a period of one hour. The resulting mixture was stirred at room temperature for an additional 2 hours, after which the mixture was concentrated *in vacuo,* and washed with hexane. The residue was subjected to silica gel column chromatography (dichloromethane/acetone 4:1). The collected red-brown fraction was concentrated *in vacuo* to give a brown powder (0.25 g, 96 %). IR (cm^{-1}): 3094 (ν(=CH), w), 3058 (ν(-CH), w), 1941 (ν(-CH), w), 1866 (w), 1804 (w), 1572 (ν(=CH), w), 1495 (δ(-CH), sym, m), 1455 (δ(-CH), sym, m), 1407 (δ(-CH), asym, m), 1359 (δ(-CH), m), 1238 (ν(-CN), m), 1217 (m), 1165 (w), 1078 (w), 1021 (ν(CN), w), 783 (δ(=CH), s), 740 (s), 728 (δ(-CH), s), 693 (s), 685 (s). ^{1}H-NMR ($CDCl_3$, δ_H) 5.07 (s, C_5H_5, 5H), 5.47 (d, $^2J_{HH}$ = 15 Hz, CH_2, 2H), 6.28 (d, $^2J_{HH}$ = 15 Hz, CH_2, 2H), 6.65 (s, NC*H*, 2H), 6.90-6.92 (m, C_6H_5, 3H), 7.15 (s, SC_5H_5, 2H), 7.17 (m, SC_5H_5, 3H), 7.30-7.36 (m, C_6H_5, 6H), 7.42-7.46 (m, C_6H_5, 2H). ^{13}C{^{1}H}-NMR ($CDCl_3$, δ_C) 55.2 (s, CH_2), 91.6 (s, C_5H_5), 122.3 (s, NCH), 127.3 (s, C_6H_5), 127.6 (s, SC_6H_5), 128.0 (s, C_6H_5), 128.9 (s, C_6H_5), 134.8 (s, SC_6H_5), 136.6 (s, *ipso*-C_6H_5), 145.6 (s, *ipso*-SC_6H_5), 169.2 (s, NCN). MS (ESI): *m*/*z* 481.1213 (M^+).

*[Ni(SPh)$_2${Im(Bn)$_2$}$_2$] (**2**):*

To a red solution of [CpNiBr{Im(Bn)$_2$}] (**A**) (0.20 g, 0.4 mmol) in toluene (10 mL) was added a toluene solution (5 mL) of HSPh (100 µL, 1 mmol) and NEt_3 (140 µL, 1 mmol). The resulting mixture was stirred at room temperature overnight, after which the mixture was concentrated *in vacuo*, and washed with hexane. The residue was subjected to silica gel column chromatography (dichloromethane/acetone 4:1). The collected red-brown fraction was concentrated *in vacuo* to give a brown powder (0.25 g, 73 %). IR (cm^{-1}): 3097 (ν(=CH), w), 3059 (ν(=CH), w), 1605 (ν(=CH), w), 1572 (ν(-CH), w), 1519 (ν(=CH), w), 1455 (δ(-CH), sym, w), 1408 (δ(-CH), asym, m), 1342 (δ(-CH), m), 1233 (ν(-CN), m), 1165 (w), 1079 (w), 1021 (ν(CN), w), 784 (δ(=CH), m), 727 (δ(-CH), m), 693 (m), 685 (m). ^{1}H-NMR ($CDCl_3$, δ_H) 4.20 (s, CH_2, 4H), 4.37 (s, CH_2, 4H), 5.77 (s, NC*H*, 2H), 6.08 (s, NC*H*, 2H), 6.17 (m, SC_6H_5, 2H), 6.49 (d, $^3J_{HH}$ = 15 Hz, C_6H_5, 4H), 6.79 (m, C_6H_5, 6H), 7.00 (m, SC_6H_5, 6H), 7.56 (m, SC_6H_5, 2H), 7.72 (m, C_6H_5, 4H), 8.19 (m, C_6H_5, 6H). ^{13}C{^{1}H}-NMR ($CDCl_3$, δ_C) 37.9 (s, CH_2), 53.4 (s, CH_2), 120.0 (s, NCH), 122.9 (s, NCH), 123.8 (s, SC_6H_5), 127.2 (s,

C_6H_5), 129.4 (s, C_6H_5), 129.7 (s, SC_6H_5), 134.0 (s, SC_6H_5), 143.7 (s, C_6H_5), 145.1 (s, C_6H_5), 147.7 (s, *ipso* SC_6H_5), 147.8 (s, *ipso* C_6H_5), 179.5 (s, N*C*N). MS (ESI): *m*/*z* 772.2204 (M^+).

*[$NiBr_2${Im(Bn)(4-NO_2Bn)}$_2$] (**3**):*

To a green solution of [$Ni(Cp)_2$] (0.30 g, 1.6 mmol) in THF (10 mL) was added [H**NHC3**]Br (1.4 g, 2.4 mmol). The resulting mixture was heated under reflux overnight, after which the mixture was concentrated *in vacuo*, and washed with hexane. The residue was subjected to silica gel column chromatography (dichloromethane/acetone 2:1). The collected red fraction was concentrated *in vacuo* to give a red powder (0.46 g, 32 %). IR (cm^{-1}): 3098 (ν(=CH), w), 3058 (ν(-CH), w), 2353 (ν(-CH), w), 1673 (w), 1602 (ν(=CH), w), 1519 (δ(-CH), sym, m), 1449 (δ(-CH), asym, w), 1401 (δ(-CH), asym, w), 1339 (δ(-CH), s), 1233 (ν(-CN), w), 1164 (w), 1105 (w), 1009 (ν(CN), w), 786 (δ(=CH), w), 726 (δ(-CH), w). ^{1}H-NMR ($CDCl_3$, δ_H) 6.00 (d, $^2J_{HH}$ = 15 Hz, CH_2, 2H), 6.20 (s, CH_2, 4H), 6.44 (d, $^2J_{HH}$ = 15 Hz, CH_2, 2H), 6.88 (s, NC*H*, 2H), 6.95 (s, NC*H*, 2H), 7.39-7.43 (m, C_6H_5, 8H), 8.10-8.38 (m, C_5H_4 and C_5H_5, 10H). ^{13}C{^{1}H}-NMR ($CDCl_3$, δ_C) 46.8 (s, *C*H_2), 55.2 (s, *C*H_2), 123.7 (s, N*C*H), 124.1 (s, N*C*H), 127.0 (s, *C*$_6$H$_5$), 128.4 (s, *C*$_6$H$_5$), 128.7 (s, *C*$_6$H$_5$), 143.9 (s, *ipso*-*C*$_6$H$_5$), 148.2 (s, *ipso*-*C*$_6$H$_5$), 153.1 (s, N*C*N). MS (ESI): *m*/*z* 802.0049 (M^+).

*[$NiBr_2${Im(Bn)(EtPh)}$_2$] (**4**):*

Complex **4** was synthesised according to the method described for **3** above, using [H**NHC4**]Br and nickelocene as starting material (0.12 g, 64%). IR (cm^{-1}): 3104 (ν(=CH), w), 2930 (ν(=CH), w), 2863 (ν(-CH), w), 1681 (ν(=CH), w), 1601 (ν(=CH), w), 1519 (ν(-CH), s), 1410 (δ(-CH), m), 1346 (δ(-CH), s), 1259 (ν(-CN), m), 1183 (w), 1109 (w), 1015 (ν(CN), w), 857 (δ(=CH), w), 803 (δ(-CH), w). ^{1}H-NMR ($CDCl_3$, δ_H) 2.32 (m, CH_3, 3H), 2.93 (m, CH_3, 3H), 3.99 (d, $^2J_{HH}$ = 7 Hz, CH_2, 2H), 4.90 (d, $^2J_{HH}$ = 7 Hz, CH_2, 2H), 6.19 (s, NC*H*, 2H), 6.30 (s, NC*H*, 2H), 6.83 (m, SC_6H_5, 2H), 6.98 (t, $^3J_{HH}$ = 7 Hz, C_6H_4, 2H), 7.20 (m, C_6H_4, 3H), 7.42 (br s, SC_6H_5, 2H), 7.54 (m, SC_6H_5, 3H), 7.62 (m, SC_6H_5, 3H), 7.77 (m, C_6H_4, 2H), 8.12 (m, C_6H_4, 2H). ^{13}C{^{1}H}-NMR ($CDCl_3$, δ_C) 29.7 (s, *C*H_3), 30.4 (s, *C*H_3), 54.5 (s, *C*H_2), 54.8 (s, *C*H_2), 106.0 (s, N*C*H), 106.2 (s, N*C*H), 121.7 (s, SC_6H_5), 122.9 (s, SC_6H_5), 125.6 (s, *C*$_6$H$_4$), 134.8 (s, *C*$_6$H$_4$), 136.2 (s, SC_6H_5), 137.5 (s, *C*$_6$H$_4$), 141.7 (s, *ipso* SC_6H_5), 145.0 (s, *ipso* C_6H_5), 159.5 (s, N*C*N). MS (ESI): m/z 830.0256 (M^+).

*[Ni(SPh)$_2${Im(Me)(4-NO$_2$Bn)}$_2$] (**5**):*

Complex **5** was synthesised according to the method described for **3** above, using [CpNiBr{Im(Me)(4-NO$_2$Bn)}] (**B**) as starting complex. The yield of **5** was too little for NMR analysis. The structure of complex **5** has been confirmed by single crystal X-ray diffraction (see section 3.2 below). IR (cm^{-1}): 3149 (ν(=CH), w), 3087 (ν(=CH), w), 2958 (ν(=CH), w), 2925 (ν(-CH), w), 2857 (ν(-CH), w), 1664 (ν(=CH), w), 1603 (ν(=CH), w), 1572 (ν(-CH), w), 1455 (δ(-CH), s), 1409 (δ(-CH), w), 1261 (δ(-CH), m), 1165 (m), 1084 (w), 1027 (ν(CN), w), 806 (w), 749 (δ(=CH), m), 703 (δ(-CH), m). MS (ESI): m/z 710.1126 (M$^+$).

*2.3 X-ray crystallography of **1**, **3**, **4** and **5***

Single crystal diffraction of compounds **1**, **3**, **4** and **5** were performed using Quazar multi-layer optics monochromated Mo Kα radiation (k = 0.71069 Å) on a Bruker D8 Venture kappa geometry diffractometer with duo Iμs sources, a Photon 100 CMOS detector and APEX II control software.[21] All X-ray diffraction measurements were performed at 150(1) K. Data reduction was performed using SAINT+,[21] and the intensities were corrected for absorption using SADABS.[22] All structures were solved by direct methods with SHELXS-97[23] using the OLEX2[24] interface. All H atoms were placed in geometrically idealised positions and constrained to ride on their parent atoms. For data collection and refinement parameters, see Supplementary Information.

2.4 Computational methods

All calculations were carried out using DFT with the B3LYP hybrid functional[25,26] in the gas phase using the Gaussian 09 program.[27] The triple-ζ basis set 6-311G basis set was used for

[21] APEX2 (including SAINT and SADABS), Bruker AXS Inc., Madison, WI, 2012.
[22] G. M. Sheldrick, SHELXL96, *Program for the Refinement of Crystal Structures*, University of Göttingen, Germany, 1996.
[23] G. M. Sheldrick, *Acta Cryst.*, 2008, **A64**, 112-122.
[24] O. V. Dolomanov, L. J. Bourhis, R. J. Gildea, J. A. K. Howard, H. Puschmann, *J. Appl. Cryst.*, 2009, **42**, 339-341.
[25] A. D. Becke, *J. Chem. Phys.*, 1993, **98**, 5648-5652.
[26] C. Lee, W. Yang, R. G. Parr, *Phys. Rev. B.*, 1988, **37**, 785-789.

all atoms (C, H, N, Br, O), whereas the Stuttgart/Dresden (SDD) pseudopotential was used to describe the nickel metal electronic core, while the metal valence electrons were described using the def2-TZVPP basis set.[28] The gas phase geometries of all intermediates were fully optimised at the same level of theory without any symmetry restrictions, ensuring that the local minima had zero imaginary vibrational frequencies[29] and to provide the thermal correction to free energies at 298.15 K and 1 atm. The series of [CpNiBr(NHC)], [CpNi(SPh)(NHC)], [Ni(SPh)$_2$(NHC)$_2$], and [NiBr$_2$(NHC)$_2$] complexes were modelled as low spin diamagnetic (singlet multiplicity) d^8 complexes since the singlet calculations resulted in lower energies (0.001-0.782 eV) compared to triplet multiplicity calculations, for all complexes.

3. Results and discussion

3.1 Synthesis of nickel(II) NHC complexes

The synthesis and full characterisation of the [CpNiBr(NHC)] complexes (NHC = NHC1-NHC4, see Figure 1) needed to synthesise complexes **1**-**5** of this study, have previously been described.[11,12] An interesting addition to the series of [CpNiBr(NHC)] complexes, is complex **1**, [CpNi(SPh){Im(Bn)$_2$}], which was synthesised by reacting [CpNiBr{Im(Bn)$_2$}] (**A**) with HSPh and NEt$_3$ as per the published route (Figure 3).[13] The ^{1}H-NMR spectrum of **1** exhibits an upfield shift for the imidazolyl backbone protons (6.65 ppm) compared to [CpNiBr{Im(Bn)$_2$}] (**A**), (6.79 ppm), along with the cyclopentadienyl signal at 5.07 ppm (5.12 ppm for [CpNiBr{Im(Bn)$_2$}], **A**). Two sets of doublets are observed for the non-equivalent methylene protons at δ_H 5.98 and 6.20 ppm ($^2J_{HH}$ = 15 Hz each), separated by $\Delta\nu$

[27] M. J. Frisch, G. W. Trucks, H. B. Schlegel, G. E. Scuseria, M. A. Robb, J. R. Cheeseman, G. Scalmani, V. Barone, B. Mennucci, G. A. Petersson, H. Nakatsuji, M. Caricato, X. Li, H. P. Hratchian, A. F. Izmaylov, J. Bloino, G. Zheng, J. L. Sonnenberg, M. Hada, M. Ehara, K. Toyota, R. Fukuda, J. Hasegawa, M. Ishida, T. Nakajima, Y. Honda, O. Kitao, H. Nakai, T. Vreven, J. A. Montgomery (Jr), J. E. Peralta, F. Ogliaro, M. Bearpark, J. J. Heyd, E. Brothers, K. N. Kudin, V. N. Staroverov, T. Keith, R. Kobayashi, J. Normand, K. Raghavachari, A. Rendell, J. C. Burant, S. S. Iyengar, J. Tomasi, M. Cossi, N. Rega, J. M. Millam, M. Klene, J. E. Knox, J. B. Cross, V. Bakken, C. Adamo, J. Jaramillo, R. Gomperts, R. E. Stratmann, O. Yazyev, A. J. Austin, R. Cammi, C. Pomelli, J. W. Ochterski, R. L. Martin, K. Morokuma, V. G. Zakrzewski, G. A. Voth, P. Salvador, J. J. Dannenberg, S. Dapprich, A. D. Daniels, O. Farkas, J. B. Foresman, J. V. Ortiz, J. Cioslowski, D. J. Fox, Gaussian 09, Revision D.01, Gaussian Inc., Wallingford CT, 2010.
[28] F. Weigend, R. Ahlrichs, *Phys. Chem. Chem. Phys.*, 2005, **7**, 3297-3305.
[29] J. W. McIver, A. K. Komornicki, *J. Am. Chem. Soc.*, 1972, **94**, 2625-2633.

= 65 Hz for **A**. Interestingly, these doublets appeared more upfield at δ_H 5.47 and 6.28 ppm ($^2J_{HH}$ = 15 Hz each), separated by $\Delta\nu$ = 241 Hz for the strongly coupled, inequivalent methylene protons of the benzyl substituents of the NHC ligand (Figure 2) for **1**. The inequivalency of the H_a and H_b protons of the methylene moiety (of the *N*-benzyl substituents) is ascribed to the favoured conformation of the benzyl substituent such that H_a is situated in close proximity to both the metal bearing a higher electron density, as well as the electron-donating thiophenolato ligand. This leads to more shielding of this nucleus, and hence a more upfield ^{1}H-signal. It has been found that this conformation exists both in solid state and solution. H_b which is situated further away from the metal centre, experiences less shielding and hence its ^{1}H-NMR signal is shifted slightly downfield due to the lower electron density surrounding H_b. The presence of a significantly upfield shifted carbene carbon peak at 145.6 ppm (166.9 ppm for **A**) in the ^{13}C-NMR spectrum furthermore confirms the increased shielding of the methylene carbon nucleus, and overall increase in electron density on the metal centre upon coordination of the PhS^- ligand.

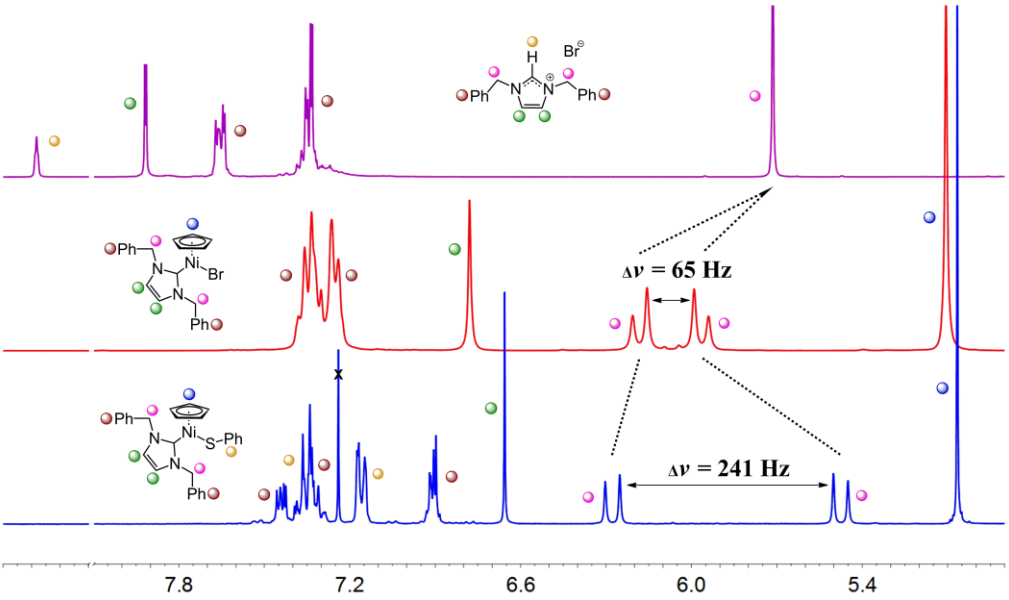


Figure 2. ^{1}H-NMR of (a) [H**NHC1**]Br, (b) [CpNiBr{Im(Bn)$_2$}] (**A**) and (c) [CpNi(SPh){Im(Bn)$_2$}] (**1**).

In the initial reactions of $NiCp_2$ with a slight excess of the particular imidazolium bromide ([HIm]Br) salt, a red biscarbene by-product was formed. It was concluded that $NiCp_2$ reacts with > 1.5 mol [HIm]Br to form complexes of the type $[NiBr_2(NHC)_2]$ in low yields (Figure 3). The formation of these biscarbene complexes follows from the spontaneous abstraction of the acidic protons of two [HIm]Br species by both cyclopentadienyl ligands to form the

neutral free carbene ligands, [Im], and two molecules of cyclopentadiene *in situ*. These free NHC ligands and bromide anions, from the respective [HIm]Br salts, subsequently coordinate to the Ni(II) centre in a *trans* fashion to form the neutral 16-electron [$NiBr_2(NHC)_2$] complexes. In this manner, the new complexes [$NiBr_2\{Im(Bn)(4\text{-}NO_2Bn)\}_2$] (**3**) and $NiBr_2\{Im(Bn)(EtPh)\}_2$] (**4**) were isolated. Further reaction of the bis-bromido complexes with excess HSPh and NEt_3 substitutes both bromido ligands to yield the relatively uncommon 16-electron bis-thiophenolato complexes of the type [$Ni(SPh)_2\{NHC\}_2$].[5,6,8,30] Analogues of the latter complexes, [$Ni(SPh)_2\{Im(Bn)_2\}_2$] (**2**) and [$Ni(SPh_2)\{Im(Me)(4\text{-}NO_2Bn)\}_2$] (**5**), were obtained from similar reactions using the complexes [$NiBr_2\{Im(Bn)_2\}_2$] (**E**) and [$NiBr_2\{Im(Me)(4\text{-}NO_2Bn)\}_2$] (**F**), respectively. Complexes **2** and **5** could also be synthesised in the reactions of the cyclopentadienyl complexes, [CpNi(SPh)(NHC)] (**1** and **G**), with excess HSPh and NEt_3, albeit in lower yields.

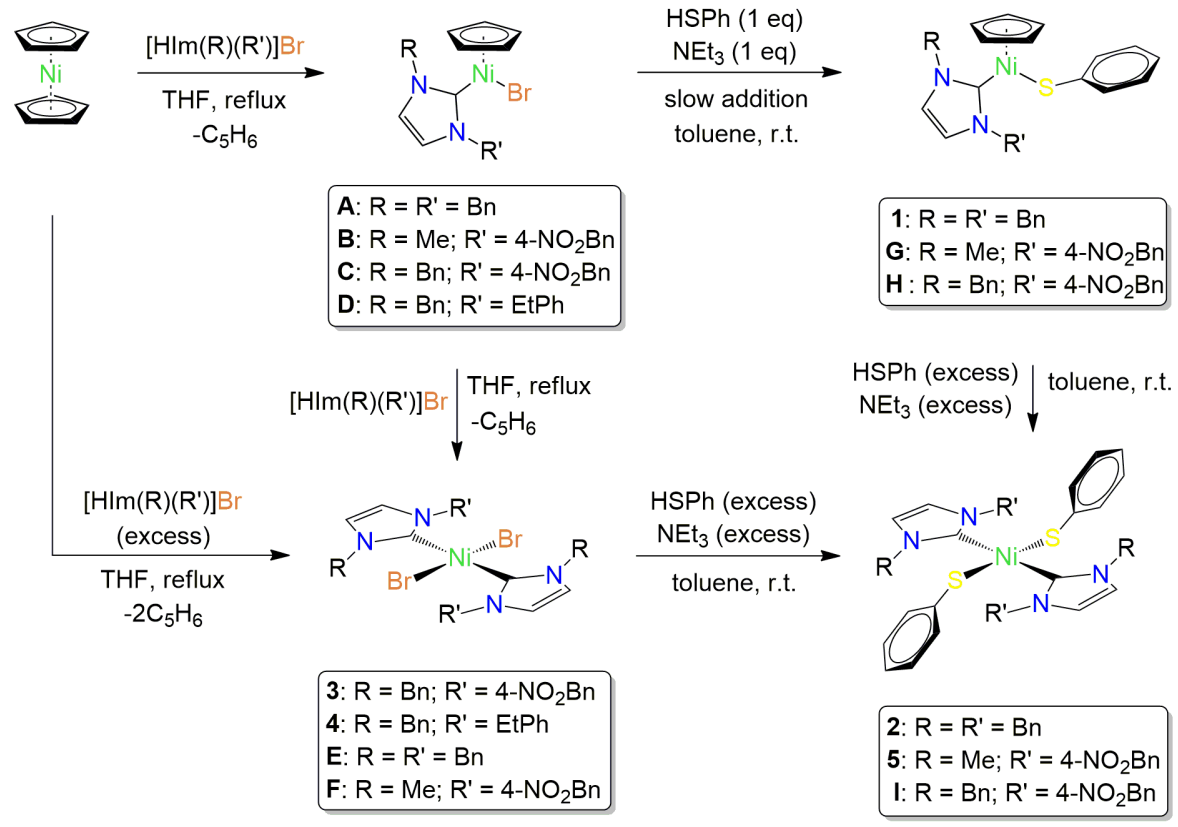


Figure 3. Synthetic routes to the 18-electron and 16-electron Ni(II) complexes of the type [CpNiBr(NHC)], [CpNi(SPh)(NHC)], [$Ni(SPh)_2\{NHC\}_2$] and [$Ni(Br)_2\{NHC\}_2$].

[30] D. Sellmann, C. Allmann, F. Heineman, F. Knoch, J. Sutter, *J. Organomet. Chem.*, 1997, **541**, 291-305.

The ^{1}H-NMR spectrum of **2**, containing the more electron-donating thiophenolato ligands, shows upfield-shifted imidazolyl backbone protons (5.77 and 6.08 ppm), and methylene protons (4.20 and 4.37 ppm), compared to the less electron-rich complex **3**, with signals resonating at 6.88 and 6.95 ppm (imidazolyl backbone protons), as well as a singlet at 6.20 ppm, and two doublets at δ_H 6.00 and 6.44 ppm ($^{3}J_{HH}$ = 15 Hz each) (methylene protons), respectively. The ^{13}C-NMR signal of the carbene carbon of the 16-electron complex **2** (179.5 ppm) is shifted downfield from the usual 161-167 ppm range of the 18-electron [CpNiBr(NHC)] complexes, although this same signal for **3** (153.1 ppm) is higher upfield from the usual range. This latter phenomenon is attributed to increased effective shielding of the carbene carbon of the NHC and the higher electron density from the bis-bromido ligands that are coordinated mutually *cis* to the carbene carbon atom.

3.2 X-ray crystallographic studies

The molecular structures of complexes [CpNi(SPh){Im(Bn)$_2$}] (**1**), [NiBr$_2$\{Im(Bn)(4-NO$_2$Bn)\}$_2$] (**3**), [NiBr$_2$\{Im(Bn)(EtPh)\}$_2$] (**4**), and [Ni(SPh)$_2$\{Im(Me)(4-NO$_2$Bn)\}$_2$] (**5**) are presented in Figure 4, together with other crystallographic data and data collection parameters in the supplementary information (Table S1). Complex **1** shows the typical pseudo-piano stool structure, whereas complexes **3**, **4**, and **5** display slightly distorted square planar conformations with the NHC ligands *trans* to one another. Complex **1** may be considered to exhibit a distorted trigonal planar geometry around the central metal atom, with Cp$_{cent}$-Ni1-S1 ≈ Cp$_{cent}$-Ni-C1 ≈ 133°. Notable bond lengths include Ni1-C1 (1.872(3) Å), Ni1-S1 (2.1934(7) Å), and Ni1-C$_{cent}$ (1.756(6) Å), which compare well with similar CpNi(II)-NHC complexes.[11,14]

During the formation of **3** and **4** from NiCp$_2$, as well as the formation of **2** (from [NiBr$_2$\{Im(Bn)$_2$\}$_2$] (**E**) or **1**) and **5** (from [NiBr$_2$\{Im(Me)(4-NO$_2$Bn)\}$_2$] (**F**)), the *trans*-NHC coordination is consistent. Complexes **3**, **4**, and **5** crystallised in such a manner that the nickel centre is located on a special position, and thus only half a molecule is present in the asymmetric unit. An apparent *trans*-effect could thus not be confirmed with the XRD results since the other half of each molecule is generated through symmetry, although a few structural features are notable: All three complexes (**3**, **4**, and **5**) crystallised in a slightly distorted square-planar geometry with 178.7(2)° ≤ C1-Ni1-C1' ≤ 180.00(1)°, 178.07(4)° ≤ Br1-Ni1-Br1' ≤ 180.0(0)°, and S1-Ni1-S1' = 180.00(2)° (**5**). The bond lengths of 1.872(3) Å ≤

Ni1-C1 ≤ 1.912(5) Å, 2.3160(9) Å ≤ Ni1-Br1 ≤ 2.3199(5) Å, and Ni1-S1 = 2.185(2) Å are all in excellent agreement with the respective bond lengths of similar complexes.[4,5,6,8,30,31]

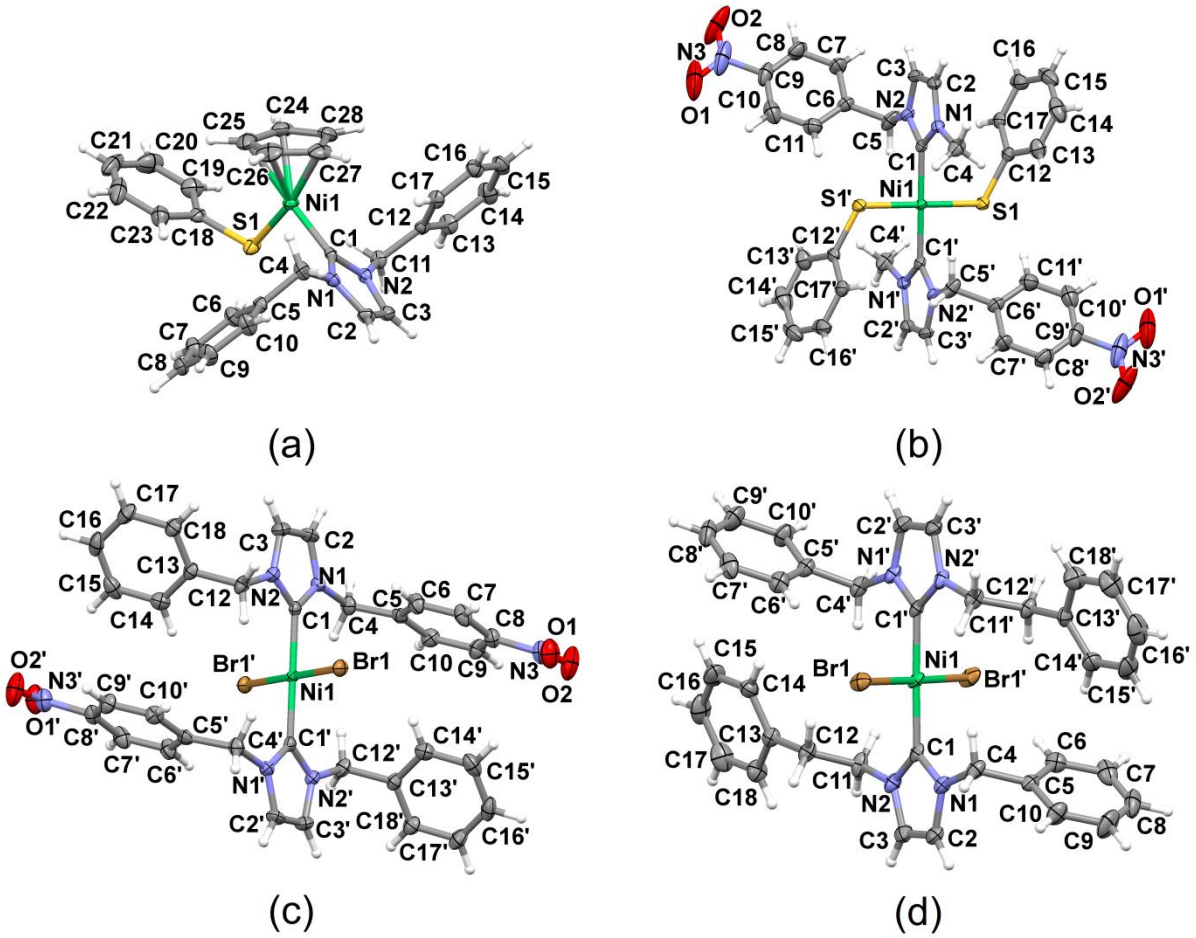


Figure 4. Perspective views of (a) [CpNi(SPh){Im(Bn)$_2$}] (**1**), (b) [Ni(SPh)$_2$}{Im(Me)(4-NO$_2$Bn)}$_2$] (**5**), (c) [NiBr$_2$}{Im(Bn)(4-NO$_2$Bn)}$_2$] (**3**), and (d) [NiBr$_2$}{Im(Bn)(EtPh)}$_2$] (**4**) – all with thermal ellipsoids drawn at 50% probability level.

An interesting "folding-out" effect of the phenyl substituents is observed in **1**, **3**, **4** and **5**. The benzyl/phenylethyl/4-NO$_2$benzyl substituents of each NHC are directed in opposite directions with respect to one another, and near perpendicular to the bonding direction of the thiophenolato ligands (where present). In sterically demanding environments the *N*-substituents tend to assume a conformation such that the bulky moieties are directed away from each other, and not necessarily away from the central metal atom. This is clearly demonstrated in **3** and **4**, with torsion angles C1-N1-C$_\alpha$-C$_\beta$ = 82.5(2) (**3**) and -113.8(5) (**4**); and C1-N2-C$_\alpha$-C$_\beta$ = 114.62(2) (**3**) and -79.1(7) (**4**), where C$_\alpha$ = the alpha carbon of the *N*-

[31] A. M. Oertel, V. Ritleng, M. J. Chetcuti, *Organometallics*, 2012, **31**, 2829-2840.

substituent adjacent to the nitrogen atom, and C_β = the beta carbon of the *N*-substituent adjacent to the C_α atom.

3.3 DFT study

3.3.1 Conformational study

In this study, two types of complexes are considered, namely two-legged piano stool *N*-heterocyclic carbene-Ni(II) complexes and square planar bis-*N*-heterocyclic carbene-Ni(II) complexes. These complexes, bearing NHC = Im(R)(R') (R, R' = methyl, benzyl, 4-NO_2benzyl, phenethyl) ligands, are symmetrically (R = R') or asymmetrically (R ≠ R') substituted. This fact, as well as the different mutual orientation(s) each of the *N*-substituents on the NHC-ligand can assume, leads to a number of possible conformations for each of the different complexes. For the *N*-substituents containing a benzyl, 4-NO_2Bn, or phenethyl substituent, the phenyl moiety of these substituents may be directed either above the imidazolylidene plane, or below. The in-plane conformation is energetically unfavourable, and is thus excluded from the possible conformations. This leads to a total of 3 conformations for symmetric NHCs (R = R'), whereas asymmetric NHCs (R ≠ R') have a total of 4 possible conformations (see Figure 5).

Table 1 contains the DFT calculated Gibbs free energies of each of the precursor complexes of the type [CpNiBr(NHC)], mono-thiophenolato complexes of the type [CpNi(SPh)(NHC)], bis-thiophenolato complexes of the type [$Ni(SPh)_2(NHC)_2$], and bis-bromido complexes of the type [$NiBr_2(NHC)_2$]. For each complex of the series [CpNiBr(NHC)], the lowest DFT calculated conformation was found to be conformation B, B, where both *N*-substituents were situated below the plane of the imidazolium ligand (*i.e.* further away from the cyclopentadienyl ring, isomers (c) and (g) in Figure 5). Conformation A,A consistently has the highest energy, only 0.05-0.1 eV higher than conformation B,B. The small energy differences generally obtained between the different conformations imply that most of the conformations are experimentally possible.

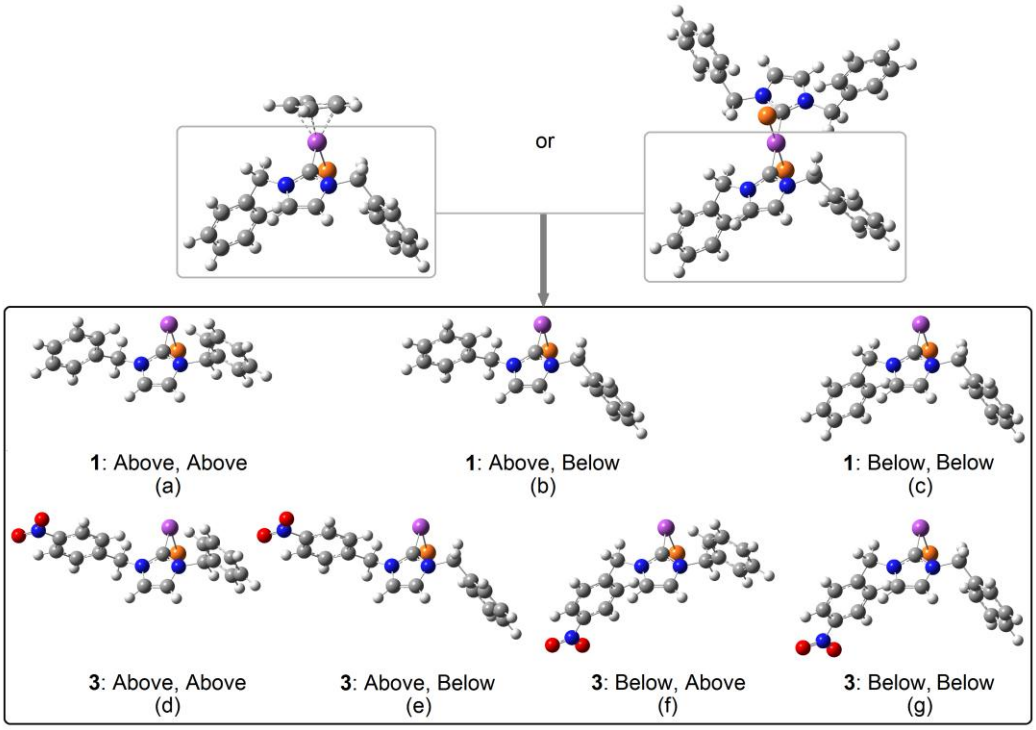


Figure 5. Various conformations that the *N*-substituents on the NHC-ligands can assume in complexes bearing symmetric NHCs (conformations for complex **1** shown in (a), (b) and (c)), and asymmetric NHCs (conformations for complex **3** shown in (d)-(g)). The terms 'above' and 'below' refer to the relative conformation of the relevant *N*-substituent with respect to the imidazolylidene ligand plane. Cp ring or second NHC-ligand bonded to Ni not shown for clarity in (a)-(g) Colour code used for atoms: Ni (violet), N (dark blue), O (red), Br/S (orange), C (grey) and H (white).

Interestingly, the lowest energy conformation was not obtained in the solid state x-ray structures of complexes [CpNiBr{Im(Bn)$_2$}] (**A**)[11] (conformation B,B; (c) in Figure 5) and [CpNiBr{Im(Bn)(4-NO$_2$Bn)}] (**C**)[12] (conformation B,B; (g) in Figure 5), as well as 16 of 20 x-ray structures of the other similar reported [CpNiX(NHC)] (X = halogen) complexes with aliphatic and benzyl-type *N*-substituents.[31-36] All of the 16 structures as well as [CpNiBr{Im(Bn)$_2$}] (**A**) and [CpNiBr{Im(Bn)(4-NO$_2$Bn)}] (**C**) adopted one of the

[32] M. Roquin, V. Ritleng, S. Barroso, A. M. Martins, M. J. Chetcuti, *J. Organomet. Chem.*, 2016, **808**, 57-62.
[33] F. E. Hahn, C. Radloff, T. Pape, A. Hepp, *Organometallics*, 2008, **27**, 6408-6410.
[34] A. M. Oertel, J. Freudenreich, J. Gein, V. Ritleng, L. F. Veiros, M. J. Chetcuti, *Organometallics*, 2011, **30**, 3400-3411.
[35] H. Valdes, M. Poyatos, G. Ujaque, E. Peris, *Chem. Eur. J.*, 2015, **21**, 1578-1588.
[36] Y.-H. Chen, K.-E. Peng, G.-H. Lee, S.-M. Peng, C.-W. Chiu, RSC Advances, 2014, 4, 62789-62792.

conformations A,A or A,B ((a), (b), (d), (e), and (f) in Figure 5). However, the solid state molecular structures of complexes [CpNiBr{Im(Me)(4-NO_2Bn)}] (**B**),[11] [CpNiBr{Im(Me)(Bn)}],[11] and the remaining 4 of 20 x-ray structures[31,37,38] all adopt conformations B or B,B which correlate the closest to the lowest energy conformation predicted in Table 1. A different result is observed with the substitution of the bromido ligand for the thiophenolato ligand in the series of [CpNi(SPh)(NHC)] complexes. Here, the lowest energy conformation is the asymmetric conformation of *N*-substituents (conformation A,B; (b), (e), and (f) in Figure 5, *i.e.* one *N*-substituent above and the other below the plane of the imidazolylidene ligand). This is postulated to result from a more favourable spatial arrangement of the *trans*-thiophenolato ligands with respect to the relatively bulky *trans*-NHC ligands, which is more prevalent than for the less bulky bromido ligands of the *trans*-$NiBr_2(NHC)_2$ species. The conformations of the *N*-substituents of **1** from its x-ray molecular structure corresponded well with the predicted lowest energy conformation A,B. Furthermore, the asymmetric conformation of *N*-substituents are also observed for the square planar *trans* bis-NHC Ni(II) complexes. For complex **3**, DFT studies predicted a conformation where only one of the four *N*-substituents are positioned above the plane of the two *trans* NHC ligands (A,B; A,A), whereas an inverted conformation of *N*-substituents (B,A; A,B) were predicted for complex **4**. The solid state conformations of complexes **3** and **4**, as well as 35 of 37 other similar reported [$NiX_2(NHC)_2$] (X = halogen) complexes[39-46] containing aliphatic and benzyl-type *N*-substituents, adopted the (B,A; A,B) conformation, which lead to the conclusion that the (B,A; A,B) conformation is indeed the preferred orientation of *N*-substituents.

[37] A. Włodarska, A. Kozioł, M. Dranka, A. Gryff-Keller, P. Szczeciński, J. Jurkowski, A. Pietrzykowski, *Organometallics*, 2015, **34**, 577-581.
[38] A. Włodarska, A. Kozioł, M. Dranka, J. Jurkowski, A. Pietrzykowski, *J. Mol. Catal. A*, 2014, **395**, 481-485.
[39] Y-P. Huang, C-C. Tsai, W-C. Shih, Y-C. Chang, S-T. Lin, G. P. A. Yap, I. Chao, T-G. Ong, *Organometallics*, 2009, **28**, 4316-4323.
[40] S. Hameury, P. de Fremont, P-A. R. Breuil, H. Olivier-Bourbigou, P. Braunstein, *Organometallics*, 2015, **34**, 2183-2201.
[41] S. Hameury, P. de Fremont, P-A. R. Breuil, H. Olivier-Bourbigou, P. Braunstein, *Dalton Trans.*, 2014, **43**, 4700-4710.
[42] H. V. Huynh, C. Holtgrewe, T. Pape, L. L. Koh, E. Hahn, *Organometallics*, 2006, **25**, 245-249.
[43] F. E. Hahn, B. Heidrich, A. Hepp, T. Pape, *J. Organomet. Chem.*, 2007, **692**, 4630-4638.
[44] A. V. Astakhov, O. V. Khazipov, E. S. Degtyareva, V. N. Khrustalev, V. M. Chernyshev, V. P. Ananikov, *Organometallics*, 2015, **34**, 5759-5766.
[45] A. C. Baclaj, G. G. Lavoie, *Organometallics*, 2012, **31**, 1103-1111.
[46] J. C. Bernhammer, H. V. Huynh, *Organometallics*, 2014, **33**, 5845-5851.

Table 1: (Relative) Gibbs free energies (eV) for the different conformations of Ni(II)-NHC complexes.

Complex	Rel. energy, G_{rel} (eV)	Conf.[a]	Conf. (secondary NHC)[a]	Ref[b]
[CpNiBr(NHC)]				
[CpNiBr{Im(Bn)$_2$}] **A**	0.075* 0.014 **0.000**	A,A* A,B B,B	- - -	11
[CpNiBr{Im(Me)(4-NO$_2$Bn)}] **B**	0.049 **0.000***	A B*	- -	11
[CpNiBr{Im(Bn)(4-NO$_2$Bn)}] **C**	0.058 0.041 0.020* **0.000**	A,A A,B B,A* B,B	- - - -	11,12
[CpNiBr{Im(Bn)(EtPh)}] **D**	0.096* 0.036 0.045 **0.000**	A,A* A,B B,A B,B	- - - -	11
[CpNi(SPh)(NHC)]				
[CpNi(SPh){Im(Bn)$_2$}] **1**	0.029 **0.000*** 0.004	A,A A,B* B,B	- - -	This work
[CpNi(SPh){Im(Bn)(4-NO$_2$Bn)}] **H**	0.014 0.001 **0.000** 0.007	A,A A,B B,A B,B	- - - -	This work
[Ni(SPh)$_2$(NHC)$_2$]				
[Ni(SPh)$_2${Im(Bn)$_2$}$_2$] **2**	0.161 0.204 **0.000**	A,B A,B B,B	A,A A,B A,A	This work
[Ni(SPh)$_2${Im(Bn)(4-NO$_2$Bn)}$_2$] **I**	0.087 **0.000** 0.105 0.187 **0.000**	A,B A,B B,A B,A B,B	A,A A,B A,A A,B A,A	This work
[Ni(SPh)$_2${Im(Me)(4-NO$_2$Bn)}$_2$] **5**	0.046 **0.000***	A B*	A A*	This work

$[NiBr_2(NHC)_2]$				
$[NiBr_2\{Im(Bn)_2\}_2]$ **E**	0.018 0.006 0.017 **0.000**	A,A A,B A,B B,B	A,A A,A A,B A,A	This work
$[NiBr_2\{Im(Bn)(4\text{-}NO_2Bn)\}_2]$ **3**	0.022 **0.000** 0.088 0.031 0.031* 0.014	A,A A,B A,B B,A B,A* B,B	A,A A,A A,B A,A A,B* A,A	This work
$[NiBr_2\{Im(Bn)(EtPh)\}_2]$ **4**	0.028 0.155 0.024 0.063 **0.000*** 0.064	A,A A,B A,B B,A B,A* B,B	A,A A,A A,B A,A A,B* A,A	This work

The conformation that agrees with the solid state crystal structure is indicated with an asterisk. [a] *N*-substituent conformation with respect to the imidazolium ligand plane: A = above, B = below. [b] Original report of synthesis and/or structural characterisation.

3.3.2 Electronic structure

In Figure 6 and Figure 7 the Kohn-Sham molecular orbital energy level diagrams of $[CpNiBr\{Im(Bn)_2\}]$ (**A**), $[CpNi(SPh)\{Im(Bn)_2\}]$ (**1**), $[Ni(Br)_2\{Im(Bn)_2\}_2]$ (**E**) and $[Ni(SPh)_2\{Im(Bn)_2\}_2]$ (**2**), are shown as representative complexes. All of these complexes have a d^8 Ni(II)-metal centre. Since the lowest energy state is a singlet state, all these complexes have four orbitals fully occupied, containing an α and a β electron each, and one unoccupied molecular orbital of mainly Ni-d character. However, the ordering of the orbitals of mainly Ni-d character differs slightly for the two types of complexes, the two-legged piano stool monocarbene complexes and the square planar biscarbene complexes:

d_{xy}, d_{π}, d_{z2}, d_{π} (HOMO), $d_{x2\text{-}y2}$ (LUMO) for [CpNiBr(NHC)] (**A**);

d_{xy}, d_{z2}, d_{π}, d_{π} (HOMO), $d_{x2\text{-}y2}$ (LUMO) for [CpNi(SPh)(NHC)] (**1**);

d_{xy}, d_{π}, d_{z2}, d_{π} (HOMO), $d_{x2\text{-}y2}$ (LUMO) for $[Ni(Br)_2\{NHC\}_2]$ (**E**) and $[Ni(SPh)_2\{NHC\}_2]$ (**2**).

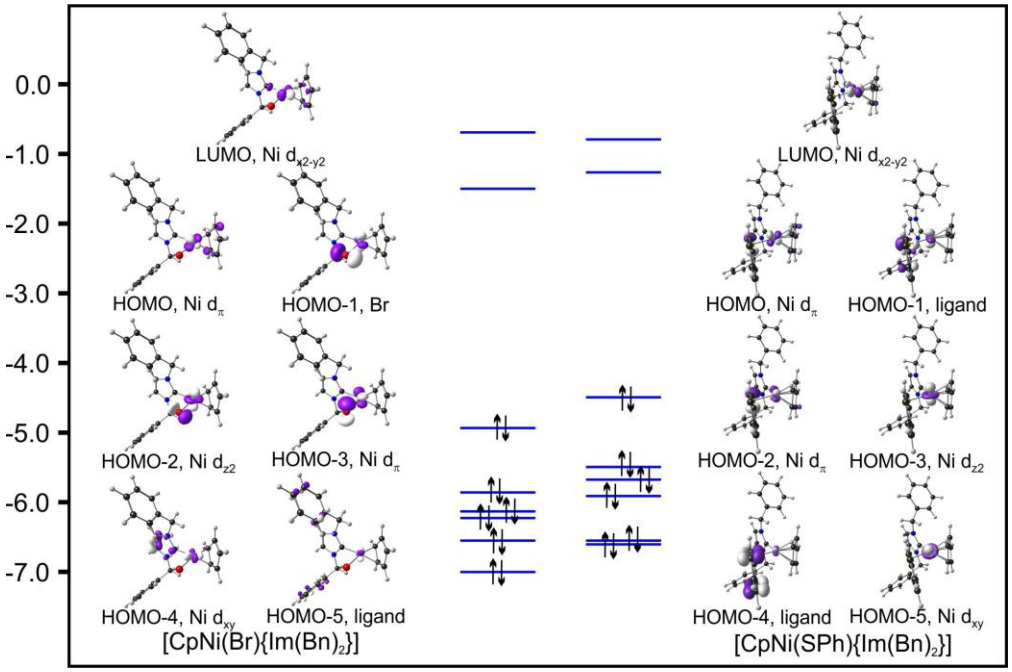


Figure 6. Kohn-Sham molecular orbital energy level diagram of [CpNiBr{Im(Bn)$_2$}] (**A**) and [CpNi(SPh){Im(Bn)$_2$}] (**1**).

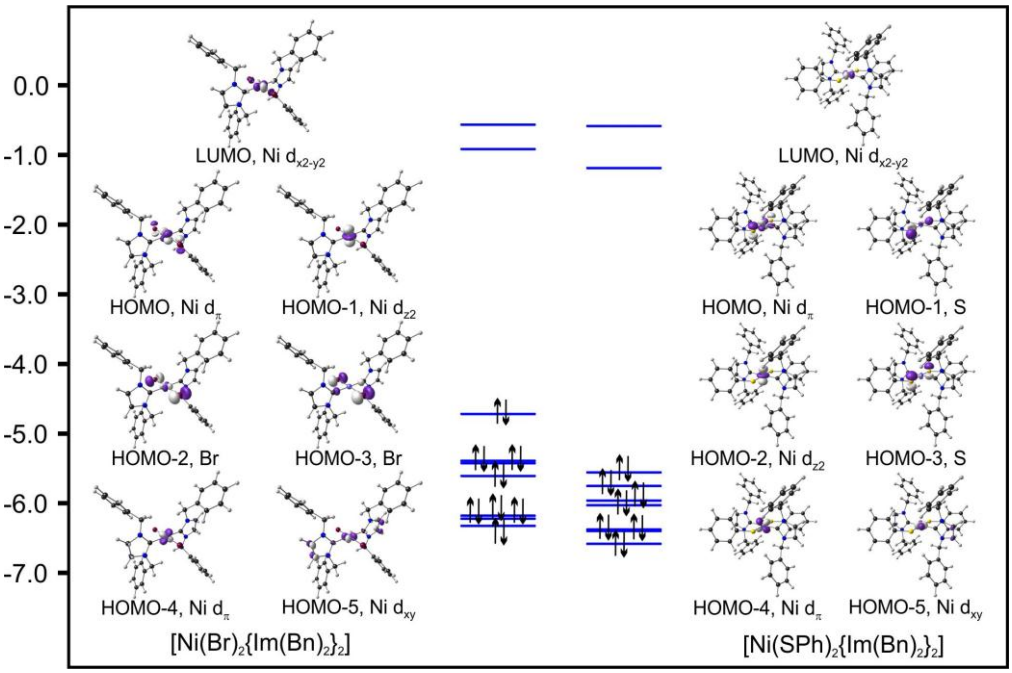


Figure 7. Kohn-Sham molecular orbital energy level diagram of [Ni(Br)$_2${Im(Bn)$_2$}$_2$] (**E**) and [Ni(SPh)$_2${Im(Bn)$_2$}$_2$] (**2**).

The x-y plane is chosen as the plane passing through Ni, the centre of Cp, C_{NHC} and Br for [CpNiBr(NHC)]; the plane through Ni, the centre of Cp, C_{NHC} and S for [CpNi(SPh){Im(Bn)$_2$}] (**1**); the plane through Ni, the two Br's and the two C_{NHC}'s for [Ni(Br)$_2${NHC}$_2$] and the plane through Ni, the two S's and the two C_{NHC}'s for

[Ni(SPh)$_2${NHC}$_2$]. The x and y directions are towards the S/Br and C_{NHC}. The Ni $d_{x^2-y^2}$-based LUMO thus has the highest energy, since the lobes of the $d_{x^2-y^2}$ orbital are directed towards the ligands for all four complexes (**A**), (**1**), (**E**) and (**2**). This leads to repulsion between the $d_{x^2-y^2}$ orbital and a p_x or p_y orbital on the ligands, thereby destabilising this Ni $d_{x^2-y^2}$-based LUMO. The Ni d_{xy}-based orbital with lobes positioned between the Ni-ligand bonds, is thus the most stable of the five Ni d-based orbitals. The Ni d_{z^2}-based orbital has its density directed mostly out of the x-y plane, but since there is a ring of electron density in the x-y plane, this orbital as well as the d_π orbitals (d_{xz} and d_{yz}), have energies lower than the Ni $d_{x^2-y^2}$-based LUMO, but higher than the Ni d_{xy}-based orbital. The d_π HOMO facing in the direction of the bromine or sulfur atoms, is destabilised relative to the other d_π orbital due to repulsion between the Ni-d_π orbital and the p_z orbital on Br/S.

3.3.3 Spectroscopy

In Table 2 the experimental infrared spectroscopy data for complexes **1**-**5** have been compared with the theoretically calculated data. In general, the data compare relatively well. The latter further corroborates the suitability of the chosen basis set and level of theory in the DFT studies conducted on these complexes. No scaling of the raw data was done.

4. Conclusion

Five new Ni(II)-NHC complexes of the type, [CpNi(SPh)(NHC)]; [Ni(SPh)$_2$(NHC)$_2$] and [NiBr$_2$(NHC)$_2$] have been synthesised and characterised. The conformational preferences of the *N*-substituents of the coordinated NHCs have been observed structurally by SXRD for four complexes. DFT conformational studies have shown for the majority of studied complexes that the predicted lowest energy conformers did correspond (or closely agreed) to the experimental solid state molecular structures. The solid state crystal data of the majority of complexes from the series of [CpNiBr(NHC)] complexes revealed the conformation of *N*-substituents of slightly higher energy was obtained, although the solid state crystal data of [CpNi(SPh)(NHC)] conformations agreed with the DFT calculated lowest energy conformations. The DFT calculated electronic structures of the mono- and bis-*N*-heterocyclic carbene complexes revealed that the Ni $d_{x^2-y^2}$-based orbital was the highest in energy

(LUMO), while the Ni d_{xy}-based orbital was the lowest in energy, and the Ni d_{π} was intermediate in energy.

Table 2: Experimental and Calculated IR data

Complex	Frequency (cm^{-1})[a]								
	ν(=CH), w	ν(-CH), w	δ(-CH), m	δ(-CH), w	δ(-CH), w	δ(-CH), m	ν(-CN), m	δ(=CH), m	δ(-CH), m
1	3094 (3171)	3058 (3047)	1495 (1500)	1455 (1451)	1407 (1390)	1359 (1374)	1238 (1242)	783 (765)	728 (726)
2	3097 (3154)	3059 (3048)	1519 (1531)	1455 (1430)	1408 (1391)	1342 (-)	1233 (1246)	784 (745)	727 (710)
3	3098 (3171)	3058 (3063)	1519 (1530)	1449 (1433)	1401 (-)	1339 (1378)	1233 (1253)	786 (818)	726 (727)
4	3104 (3179)	2930 (3063)	1519 (1529)	- (1437)	1410 (1387)	1346 (1376)	1259 (1236)	803 (750)	- (704)
5	3087 (3150)	2925 (3052)	1572 (1579)	1455 (1439)	1409 (-)	- (1379)	1261 (1252)	806 (820)	749 (701)

[a] Experimental frequencies, values in parentheses indicate calculated frequencies.

Acknowledgements

This work has received support from the Norwegian Supercomputing Program (NOTUR) through a grant of computer time (Grant nr. NN4654K) (JC), the South African National Research Foundation (JC Grant nr. 96111, ML Grant nr. 93638, FPM Grant nr. 88594) and the Central Research Fund of the University of the Free State, Bloemfontein (JC) and the University of Pretoria (ML). The High Performance Computing facility of the UFS is acknowledged for computer time.

CHAPTER 5

Electrochemistry of a series of symmetric and asymmetric CpNiBr(NHC) complexes: Probing the electrochemical environment due to push-pull effects

Chapter 5 contains work that has been prepared for publication in J. Electroanal. Chem.:

Authors: Frederick P. Malan, Eric Singleton, Jeanet Conradie, Marilé Landman

Status: To be submitted

Contributions:

Frederick P. Malan: Author, synthesis, characterisation, electrochemistry (experiment and analysis), DFT study (full optimisation, calculation of HOMOs/LUMOs, energy calculations)

Eric Singleton: Co-author, co-supervisor

Jeanet Conradie: Corresponding author, electrochemistry (supervision of results), DFT study (supervision of calculations, provision of DFT facilities and execution of input files created by FP Malan)

Marilé Landman: Corresponding author, supervisor

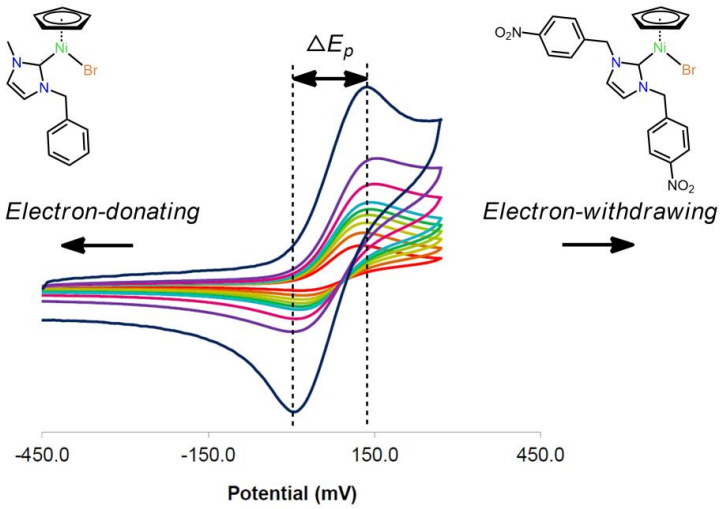
5 Electrochemistry of a series of symmetric and asymmetric CpNiBr(NHC) complexes: Probing the electrochemical environment due to push-pull effects

Frederick P. Malan,[a] Eric Singleton,[a] Jeanet Conradie[b,*] and Marilé Landman[a,*]

[a] *Department of Chemistry, University of Pretoria, 02 Lynnwood Road, Hatfield, Pretoria, 0002, South Africa.*

[b] *Department of Chemistry, University of the Free State, Bloemfontein 9300, South Africa.*

Graphical abstract



Highlights

- Cyclic voltammograms of nine [CpNiBr(NHC)] complexes show metal and ligand-based redox processes
- Three oxidation states of Ni (I, II, III) observed
- NO_2-containing NHC complexes exhibited cathodic shifts of 0.01-0.03 V relative to non-NO_2-containing NHC complexes
- DFT calculations confirm the redox centres associated with each of the redox processes

Abstract

The electrochemistry of nine Ni(II) *N*-heterocyclic carbene (NHC) complexes of general formula [CpNiBr(NHC)], bearing either a symmetric or asymmetric *N*-substituted alkyl/benzyl/phenethyl NHC ligand with Cp = cyclopentadienyl is described. Both metal and ligand-centred redox processes were observed and systematically evaluated. The quasi-reversible Ni(II)/Ni(III) couple (0.068 V $\leq$ $E^{\circ\prime}$ $\leq$ 0.120 V) is followed by the electrochemically and chemically irreversible ligand based oxidation peaks (E_{pa} ~ 0.35 V and ~0.405 V). The Ni(II)/Ni(I) and NHC ligand reduction processes are observed below -1.3 V. A comparison between the nine different Ni(II)-NHC complexes revealed that the electron-withdrawing NO_2-containing NHC ligands exhibit the most positive metal-oxidation redox processes. A DFT study complements the experimental findings by establishing where the oxidation and reduction centres are based.

Keywords:

nickel; cyclopentadienyl; *N*-heterocyclic carbene; electrochemistry; DFT

1. Introduction

Many of the catalytically active zero valent metal complexes employed in the literature require ligands to assist in stabilising these sensitive species and preventing catalyst decomposition.[1-5] *N*-heterocyclic carbenes (NHCs) remain a favourite class of ancillary ligands that provides additional steric and electronic ligand tuning options.[3,5-12] The stronger binding of NHCs to metal centres helps to avoid rapid degradation under oxidising

[1] L. M. Dornan, G. M. A. Clendenning, M. B. Pitak, S. J. Coles, M. J. Muldoon, *Catal. Sci. Technol.*, 2014, **4**, 2526-2534.
[2] J. A. Mueller, C. P. Goller, M. S. Sigman, *J. Am. Chem. Soc.*, 2004, **126**, 9724-9734.
[3] R. H. Crabtree, *Chem. Rev.*, 2015, **115**, 127-150.
[4] K. M. Gligorich, M. S. Sigman, *Angew. Chem. Int. Ed.*, 2006, **45**, 6612-6615.
[5] L. P. Bheeter, M. Henrion, L. Brelot, C. Darcel, M. J. Chetcuti, J-B. Sortais, V. Ritleng, *Adv. Synth. Catal.*, 2012, **354**, 2619-2624.
[6] R. H. Crabtree, *Coord. Chem. Rev.*, 2013, **257**, 755-766.
[7] O. Kühl, *Chem. Soc. Rev.*, 2007, **36**, 592-607.
[8] A. P. Prakasham, P. Ghosh, *Inorg. Chim. Acta.*, 2015, **431**, 61-100.
[9] R. Visbal, A. Laguna, M. C. Gimeno, *Chem. Comm.*, 2013, **49**, 5642-5644.
[10] O. Schuster, L. Yang, H. G. Raubenheimer, M. Albrecht, *Chem. Rev.*, 2009, **109**, 3445-3478.
[11] B. Landers, O. Navarro, *Inorg. Chim. Acta.*, 2012, **380**, 350-353.
[12] B. Landers, O. Navarro, *Eur. J. Inorg. Chem.*, 2012, 2980-2982.

conditions, as is the case with most common ligands.[13,14] Cyclopentadienyl nickel(II) halo complexes containing NHC ligands, [CpNiX(NHC)] (X = Cl, Br, I), have been actively studied by various research groups over the last two decades. Since their first reported synthesis by Cowley and co-workers[15] in 2000, this versatile class of complexes has expanded and been employed in numerous useful catalytic applications including Suzuki-Miyaura coupling reactions,[16 - 18] Kumada-Tamao-Corriu coupling reactions,[19] the hydrothiolation of alkynes,[20] hydrosilylation of aldehydes and ketones,[5] styrene[16] and phenylacetylene polymerisation reactions,[21] Buchwald amination,[22] secondary alcohol oxidation,[11] α-arylation of ketones,[23] dehalogenation reactions,[24] as well as energy storage applications.[25,26]

We have recently extended the existing limited range[21,27-29] of [CpNiBr(NHC)] complexes to include bulky, flexible symmetric and asymmetric NHC ligands, which were found to be catalytically active for Suzuki-Miyaura coupling[30] and anaerobic secondary alcohol oxidation reactions.[31] Despite their versatile application possibilities, electrochemical studies on the redox properties of this class of [CpNiX(NHC)] (X = Cl, Br, I) complexes, remain under-

[13] L-Y. Wang, J. Li, Y. Lv, H-Y. Zhang, S. Gao, *J. Organomet. Chem.*, 2011, **696**, 3257-3263.
[14] V. Ritleng, M. Henrion, M. J. Chetcuti, *ACS Catal.*, 2016, **6**, 890-906.
[15] C. D. Abernethy, A. H. Cowley, R. A. Jones, *J. Organomet. Chem.*, 2000, **596**, 3-5.
[16] W. Buchowicz, Ł. Banach, J. Conder, P. A. Guńka, D. Kubicki, P. Buchalski, *Dalton Trans.*, 2014, **43**, 5847-5857.
[17] A. M. Oertel, V. Ritleng, M. J. Chetcuti, *Organometallics*, 2012, **31**, 2829-2840.
[18] V. Ritleng, A. M. Oertel, M. J. Chetcuti, *Dalton Trans.*, 2010, **39**, 8153-8160.
[19] T. K. Macklin, V. Sniekus, *Org. Lett.*, 2005, **7**, 2519-2522.
[20] D. A. Malyshev, N. M. Scott, N. Marion, E. D. Stevens, V. P. Ananikov, I. P. Beletskaya, S. P. Nolan, *Organometallics*, 2006, **25**, 4462-4470.
[21] W. Buchowicz, W. Wojtczak, A. Pietrzykowski, A. Lupa, L. B. Jerzykiewicz, A. Makal, K. Woźniak, *Eur. J. Inorg. Chem.*, 2010, 648-656.
[22] A. R. Martin, Y. Makida, S. Meiries, A. M. Z. Slawin, S. P. Nolan, *Organometallics*, 2013, **32**, 6265-6270.
[23] M. Henrion, M. J. Chetcuti, V. Ritleng, *Chem. Commun.*, 2014, **50**, 4624-4627.
[24] R. A. Kelly III, N. M. Scott, S. Díez-González, E. D. Stevens, S. P. Nolan, *Organometallics*, 2005, **24**, 3442-3447.
[25] O. R. Luca, B. A. Thompson, M. K. Takase, R. H. Crabtree, *J. Organomet. Chem.*, 2013, **730**, 79-83.
[26] O. R. Luca, D. L. Huang, M. K. Takase, R. H. Crabtree, *New. J. Chem.*, 2013, **37**, 3402-3405.
[27] F. E. Hahn, M. C. Jahnke, *Angew. Chem. Int. Ed.*, 2008, **47**, 3122-3172.
[28] A. M. Oertel, V. Ritleng, A. Busiah, L. F. Veiros, M. J. Chetcuti, *Organometallics*, 2011, **30**, 6495-6498.
[29] A. M. Oertel, J. Freudenreich, J. Gein, V. Ritleng, L. F. Veiros, M. J. Chetcuti, *Organometallics*, 2011, **30**, 3400-3411.
[30] F. P. Malan, E. Singleton, P. H. van Rooyen, M. Landman, *J. Organomet. Chem.*, 2016, **813**, 7-14.
[31] F. P. Malan, E. Singleton, B. Bulling, I. Cukrowski, P. H. van Rooyen, M. Landman, *Mol. Catal.*, 2017, **432C**, 47-56.

explored. Only one report by Crabtree and co-workers[25] evaluates the preliminary electrochemical data on a series of six [CpNiX(NHC)] (X = Cl, I) complexes. The NHCs of their series contained a number of different substituents on the imidazolylidene backbone, including electron-withdrawing chloro and cyano moieties, and a conjugated benzimidazole or a triazolidene ligand system. All complexes showed two or more, generally electrochemically irreversible oxidation features (large peak separations at a scan rate of 0.1 V s^{-1}), the first assigned to Ni(II)/Ni(III) oxidation. Only [CpNiCl(IMes)] showed a electrochemically reversible Ni(II)/Ni(III) oxidation. A quasi-reversible reduction was also observed for the latter complex at -1.510 V *vs* FcH/FcH^{+}.

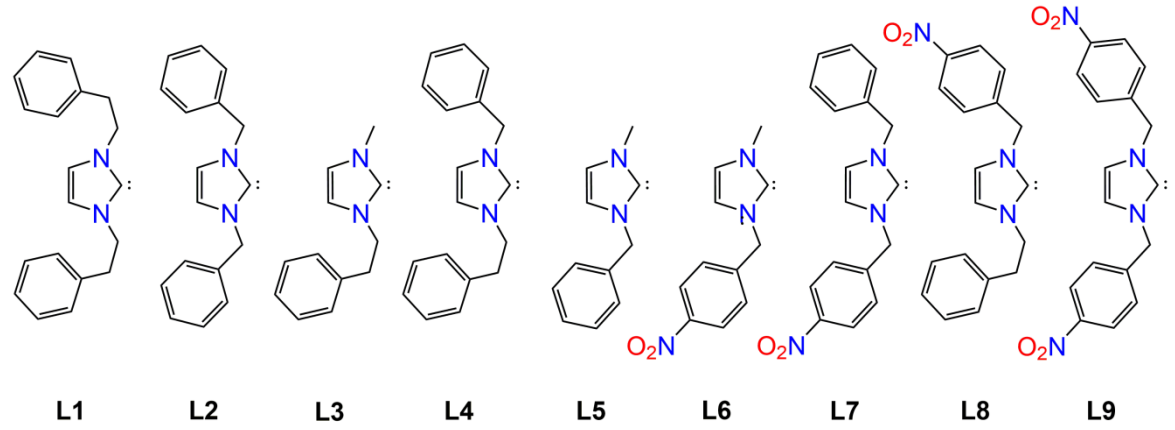


Figure 1: The ligands employed in the synthesis of the complexes [CpNiBr(NHC)] (**1**–**9**).

The main focus of this study is to investigate the effect of a series of unique NHC ligands featuring different *N*-substituents (see Figure 1) on the Ni(II)/Ni(III) redox couple of [CpNiBr(NHC)] (**1**-**9**), how it relates to the observed catalytic activity, and the determination of the locus of the observed redox processes by means of density functional theory (DFT) calculations. This study also correlates DFT calculated electronic energies from which linear relationships with the experimental electronic redox potentials are obtained.

2. Experimental

2.1 General

All experiments were carried out under an argon atmosphere using standard Schlenk techniques. All solvents used were dried prior to use using standard techniques.[32,33] Column

[32] R. J. Errington, *Advanced Practical Inorganic and Metalorganic Chemistry*, Blackie Academic & Professional, London, 1997.

chromatography was carried out under inert argon atmospheres using silica gel (particle size 0.063-0.200 mm) as the stationary phase. The synthesis, purification, and characterisation of complexes [CpNiBr(NHC)] (**1**-**9**) (Figure 1) were performed as previously reported by our group.[30] All other chemicals were purchased from Sigma-Aldrich and used without further purification.

2.2 Cyclic voltammetry

Cyclic voltammetry measurements were performed using 0.002 or saturated mol.dm^{-3} solutions of the complexes in dry acetonitrile (Aldrich, Biotech grade, 99.93% purity, anhydrous, kept under argon) containing 0.1 mol.dm^{-3} tetra-*N*-butylammonium hexafluorophosphate [NBu_4][PF_6] (Fluka, electrochemical grade) as supporting electrolyte under a purified argon atmosphere at 25 ºC. A three electrode cell, with a glassy carbon (surface area = 7.07 × 10^{-6} m^2) working electrode, a Pt auxiliary electrode, and a Ag/Ag$^+$ (0.010 mol.dm^{-3} $AgNO_3$ in CH_3CN) reference electrode mounted on a Luggin capillary, was used. Successive experiments under identical experimental conditions revealed all redox potentials were reproducible within 5 mV. All reported potentials were referenced against the IUPAC suggested FcH/FcH$^+$ couple. Ferrocene exhibited a formal reduction potential of $E^{0\prime}$ = 0.084 V *vs.* Ag/Ag$^+$, a peak separation of $\Delta E_p = E_{pa} - E_{pc}$ = 0.066 V, and i_{pa}/i_{pc} = 1.00, under our experimental conditions. E_{pa} (E_{pc}) = anodic (cathodic) peak potential and i_{pa} (i_{pc}) = anodic (cathodic) peak current. $E^{0\prime}$ (Fc/Fc$^+$) = 0.400 V *vs.* NHE. Decamethyl ferrocene (Fc*, -0.508 V *vs.* FcH/FcH$^+$) was used as internal standard.

2.3 Computational methods

All calculations were carried out using DFT with the B3LYP hybrid functional,[34,35] and were implemented in the gas phase using the Gaussian 09 program.[36] The triple-ζ basis set 6-311G

[33] D.F. Shriver, M.A. Drezdzon, *The Manipulation of Air-Sensitive Compounds*, 2nd ed., Wiley, New York, 1986.
[34] A. D. Becke, *J. Chem. Phys.*, 1993, **98**, 5648-5652.
[35] C. Lee, W. Yang, R. G. Parr, *Phys. Rev. B.*, 1988, **37**, 785-789.
[36] M. J. Frisch, G. W. Trucks, H. B. Schlegel, G. E. Scuseria, M. A. Robb, J. R. Cheeseman, G. Scalmani, V. Barone, B. Mennucci, G. A. Petersson, H. Nakatsuji, M. Caricato, X. Li, H. P. Hratchian, A. F. Izmaylov, J. Bloino, G. Zheng, J. L. Sonnenberg, M. Hada, M. Ehara, K. Toyota, R. Fukuda, J. Hasegawa, M. Ishida, T. Nakajima, Y. Honda, O. Kitao, H. Nakai, T. Vreven, J. A. Montgomery (Jr), J. E. Peralta, F. Ogliaro, M. Bearpark, J. J. Heyd, E. Brothers, K. N. Kudin, V. N. Staroverov, T. Keith, R. Kobayashi, J. Normand, K. Raghavachari, A. Rendell, J. C. Burant, S. S. Iyengar, J. Tomasi, M. Cossi, N. Rega, J. M. Millam, M. Klene, J. E. Knox, J. B. Cross, V. Bakken,

basis set was used for all atoms (C, H, N, Br, O), whereas the Stuttgart/Dresden (SDD) pseudopotential was used to describe the nickel and bromide electronic cores, while the metal valence electrons were described using the def2-TZVPP basis set.[37] All geometries were optimised without any symmetry restrictions, ensuring that the local minima had zero imaginary vibrational frequencies.[38] All of the redox processes involved one-electron transfer processes, and were therefore modelled as calculated electron affinities or ionisation potential, (EA)/(IP), defined as the amount of energy released/absorbed when an electron is added/removed from a neutral molecule. The adiabatic electron affinity (EA) and ionisation potential (IP) were calculated as the difference between the energy of the neutral complex (n electrons), and either the reduced (n + 1 electrons) or oxidised (n – 1 electrons) complexes, all at their respective optimised geometries. The neutral series of [CpNi(II)Br(NHC)] two-legged piano stool complexes were modelled as low spin diamagnetic (singlet multiplicity) d^8 complexes since the singlet calculations resulted in lower energies (0.09-0.12 eV) compared to triplet multiplicity calculations, for all complexes.

3. Results and Discussion

3.1 Synthesis of nickel(II) NHC complexes

The synthesis and full characterisation of the range of investigated [CpNiBr(NHC)] complexes **1-9** containing flexible symmetric and asymmetric NHC ligands, is described in the literature.[30,31] The general synthesis involves the reflux of an anhydrous THF slurry containing imidazolium bromide [HIm]Br and one equivalent of nickelocene ($NiCp_2$) for 3-16 hours (depending on the NHC salt), see Figure 2. The resulting solution is then concentrated *in vacuo*, subjected to column chromatography (DCM/hexane), after which the collected red fraction was concentrated *in vacuo* to obtain red to red-brown powders.[30] Steric and electronic differences within each of these NHC ligands were incorporated by employing *N*-alkyl, -benzyl, and/or -phenethyl moieties, through which the resulting NHCs exhibited a degree of steric bulk and flexibility (Figure 1). The NO_2 group is introduced to reduce the electron donating ability of the NHC ligand and consequently the electron density on the

C. Adamo, J. Jaramillo, R. Gomperts, R. E. Stratmann, O. Yazyev, A. J. Austin, R. Cammi, C. Pomelli, J. W. Ochterski, R. L. Martin, K. Morokuma, V. G. Zakrzewski, G. A. Voth, P. Salvador, J. J. Dannenberg, S. Dapprich, A. D. Daniels, O. Farkas, J. B. Foresman, J. V. Ortiz, J. Cioslowski, D. J. Fox, Gaussian 09, Revision D.01, Gaussian Inc., Wallingford CT, 2010.

[37] F. Weigend, R. Ahlrichs, *Phys. Chem. Chem. Phys.*, 2005, **7**, 3297-3305.

[38] J. W. McIver, A. K. Komornicki, *J. Am. Chem. Soc.*, 1972, **94**, 2625-2633.

coordinated nickel(II) ion for selected complexes; the NO_2 group is strongly electron withdrawing.[39,40]

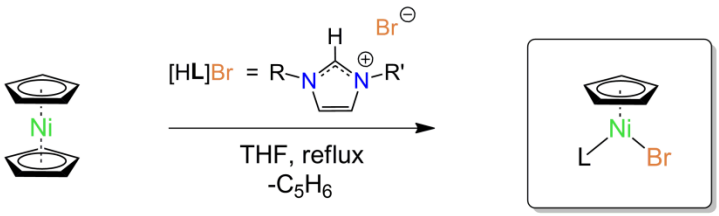


Figure 2: Synthetic route to the complexes [CpNiBr(NHC)] (**1**-**9**). L = NHC ligand with R and R' = Me (methyl), Bn (benzyl), $(CH_2)_2Ph$ (phenethyl) or 4-NO_2-Bn (4-nitrobenzyl), as shown in Figure 1.

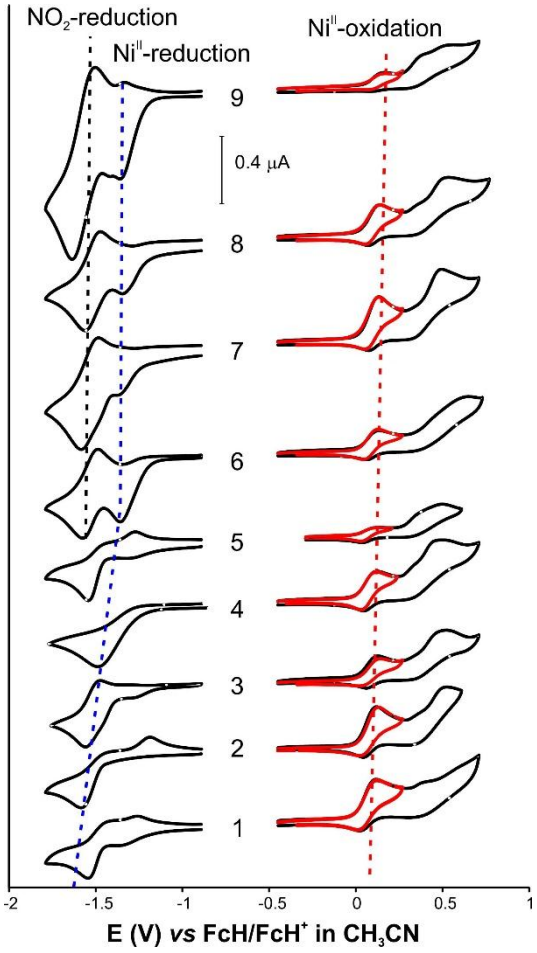


Figure 3: Comparative cyclic voltammograms (*vs.* FcH/FcH^+) at a scan rate of 0.1 $V.s^{-1}$ for complexes [CpNiBr(NHC)] **1**-**9**. Left: The reduction region. Right: The oxidation region. Scans in red indicate the Ni(II)/Ni(III) redox couple. Measured in 0.1 $mol.dm^{-3}$ $[NBu_4][PF_6]/CH_3CN$ on a glassy carbon working electrode at 25 °C. [Ni] = 0.002 $mol.dm^{-3}$ or saturated solution.

[39] J. H. Tocher, D. I. Edwards, *Free Rad. Res. Comms.*, 1987, **4**, 269-276.
[40] A. Kuhn, K. G. von Eschwege, J. Conradie, *J. Phys. Org. Chem.*, 2012, **25**, 58-68.

3.2 Electrochemistry

The cyclic voltammograms at a scan rate of 0.100 V s^{-1} of Ni(II)-NHC complexes **1-9** in the -1.8 V to 0.8 V *vs.* FcH/FcH^+ region are shown in Figure 3, along with a summary of the electrochemical data in Table 1. A graph of scan rates 0.05-5.00 V s^{-1} of the first oxidation peak for **2** is shown in Figure 4 (see Supplementary Information for more results). In the oxidation region, generally three oxidation waves are observed between -0.2 V to 0.8 V for complexes **1-9**, see Figure 4. In the reduction region, depending on the NHC substituents, either one or two reduction processes were observed for complexes **1-9**. The non-NO_2-containing complexes each exhibited one irreversible reduction peak, while the NO_2-containing complexes exhibited one irreversible reduction process, followed by a chemically and electrochemically reversible reduction process.

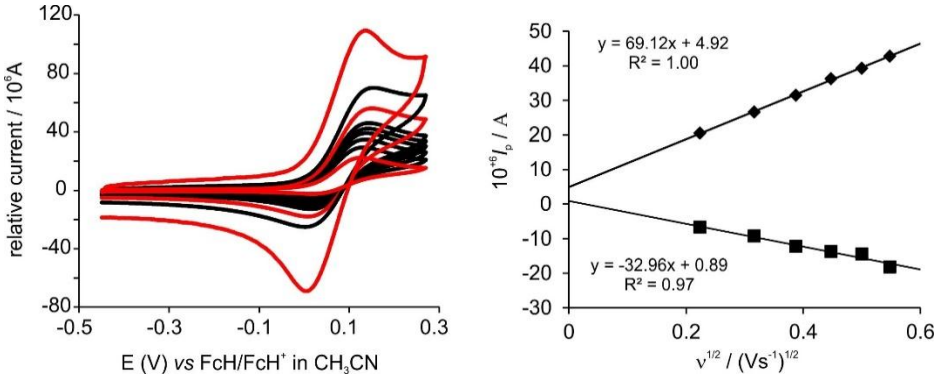


Figure 4: Left: Cyclic voltammograms of complex **2** at scan rates of 0.050 (lowest peak current) - 5.000 (highest peak current) V.s^{-1}. Scans were initiated in the positive direction. The 0.05, 0.5 and 5 V.s^{-1} scans are shown in red. Right: The linear relationship between peak currents (i_p) and (scan rate)^{½} for the oxidation and reduction of complex **2**, is described by the Randles-Sevcik equation.

3.2.1 Oxidation region

The first observed electrochemical process is an electrochemically reversible and chemically quasi-reversible oxidation process, with $0.082 \leq \Delta E_p \leq 0.126$ V, and $0.31 \leq i_{pc}/i_{pa} \leq 0.62$ at a scan rate $\nu = 0.1$ V s^{-1} (Figure 3). The peak separation of the first oxidation process is slightly larger than the Nernstian value of 0.059 V for a one electron process due to uncompensated ohmic drops in the cell.[41] A graph of peak current *vs.* $\nu^{1/2}$ for the first oxidation peak revealed

[41] M. J. Cook, I. Chambrier, G. F. White, E. Fourie, J. C. Swarts, *Dalton Transactions*, 2009, **7**, 1136-1144.

a linear relationship for scan rates in the regions 0.05-0.30 V s^{-1} (Figure 4 for **2**, Supplementary Information for **1** and **3**-**9**), indicating an essentially diffusion-controlled electrochemical process for **1**-**9**. The first oxidation-reduction wave becomes chemically more reversible at increased scan rates (Figure 4 left). The first reversible oxidation peak is associated with the Ni(II)/Ni(III) redox couple. The second and third oxidation peaks are assigned to ligand oxidation (Figure 3). The assignment of the oxidation processes observed are supported by the findings of the DFT study of the frontier orbitals of complexes **1**-**9** presented in section 3.4. The assignment of the Ni(II)/Ni(III) redox couple is also in agreement with published results on related [CpNiX(NHC)] (X = Cl, I) complexes.[25]

From Figure 3 it is clear that the formal reduction potential, $E°'$, of the Ni(II)/Ni(III) redox couple for each of the complexes **1**-**9** is affected by the change of substituents on the coordinated NHC ligand, with $E°'$ varying between 0.068 V and 0.120 V at ν = 0.100 V s^{-1}. Due to the range of *N*-substituents, the overall electron-donating (push) or electron-withdrawing (pull) properties of the NHC ligands differ. These substituents include Me, Bn (benzyl = C_7H_7), phenethyl, $(CH_2)_2Ph$, and 4-NO_2Bn. Of the NHC ligands, the Me substituted derivatives should be the most electron donating,[42,43,44] while the 4-NO_2-Bn substituted ligands will be the most electron withdrawing.[40] Substantial aromatic character exists in the *N*-heterocyclic ring due to the delocalisation of six π-electrons (sextet) within the ring.[45,46,47] Consequently, rapid electronic communication between the two *N*-substituents *via* the *N*-heterocyclic ring to the nickel centre is expected. The electron-donating or electron-withdrawing effect of the two *N*-substituents would thus be summative, resulting in the total electron-donating or electron-withdrawing (push-pull) effect for a specific NHC ligand.

The formal reduction potentials $E°'$ of the Ni(II)/Ni(III) redox couple of complexes **2** and **5** are very similar, indicating that the electron donating properties of Bn and Me are comparable. $E°'$ values of complexes **1** and **3** show that the phenethyl group might be slightly more electron donating than Bn or Me. This notion is confirmed when comparing $E°'$ of

[42] P. R. Wells, *Progress in Physical Organic Chemistry*, John Wiley & Sons Inc., New York, 1968, 6, 111-145.
[43] R. E. Kagarise, *J. Am. Chem. Soc.*, 1955, **47**, 1377–1379.
[44] R. Li, X. Zhang, P. Zhu, D. K. P. Ng, N. Kobayashi, J. Jiang, *Inorg. Chem.*, 2006, **45**, 2327-2334.
[45] C. Heinemann, T. Muller, Y. Apeloig, H. Schwarz, *J. Am. Chem. Soc.*, 1996, **118**, 2023-2038.
[46] C. Boehme, G. Frenking, *J. Am. Chem. Soc.*, 1996, **118**, 2039-2046.
[47] J. F. Lehmann, S. G. Urquhart, L. E. Ennis, A. P. Hitchcock, K. Hatano, S. Gupta, M. K. Denk, *Organometallics*, 1999, **18**, 1862-1872.

complex **2** (0.076 V), containing a Bn substituent, with $E°'$ = 0.068 V for **1**, containing the bis-phenethyl substituent on the NHC ligand. This value for **1** is in fact the lowest for all complexes **1**-**9**. However, the $E°'$ values of the non-NO_2-containing complexes **1**-**5**, all lie in a small range of 0.013 V (0.068-0.081 V), indicative of the similar electron donating properties of Me, Bn and the $(CH_2)_2Ph$ group. The range of four NO_2-containing complexes **6**-**9**, is larger, namely 0.032 V (0.088-0.120 V). Introduction of a NO_2-group as a 4-NO_2Bn substituent on the NHC ligand, leads to an increase (more positive shift) of the formal reduction potential with *ca.* 0.01-0.02 V for the Ni(II)/Ni(III) redox couple (compare **6** with **5**, **7** with **2** or **8** with **4**). The synergy of the two 4-NO_2Bn substituents on the NHC ligand is clearly demonstrated when comparing **9** with **2**, where a 0.03 V increase (more than double the effect of one 4-NO_2Bn substituent alone) is observed. Complex **9**, with two 4-NO_2Bn substituents on the NHC ligand, exhibits the most positive (cathodic) potential (0.120 V) of complexes **1**-**9**.

The $E°'$ values for the Ni(II)/Ni(III) wave obtained for **1**-**9** are in good agreement with those of Crabtree and co-workers.[25] For instance, they found $E_{1/2(ox)}$ = 0.033 V *vs.* FcH/FcH^+ for the complex [CpNiCl(IMes)]. This value, which is less positive compared to the same redox couple for **1**-**9**, is expected when considering the electron donating mesityl substituents on the NHC ligand. Compared to the complex [CpNiCl(IMes)], complexes **1**-**9** all contain less electron-donating NHC ligands. The Ni(II)/Ni(III) redox potential is more negative ($E_{1/2(ox)}$ = -0.130 V) for the complex [CpNiI(IMe)], where the electron-withdrawing chloro ligand was exchanged for the far less electron-withdrawing iodo ligand. Conversely, they found noticeably higher (more positive) $E_{1/2(ox)}$ values when electron-withdrawing functionalities were incorporated on the imidazolyl backbone of the NHC ligand, e.g. $E_{1/2(ox)}$ = 0.073 V (with two Cl-substituents), and $E_{1/2(ox)}$ = 0.124 V (with two CN-substituents). This indicates that substituent variations on the imidazolyl backbone may noticeably affect metal-centred redox processes, apart from the effect of different *N*-alkyl/aryl substituents on NHCs itself.

Table 1: Electrochemical data (*vs.* FcH/FcH^+) for redox processes observed for **1**-**9**.

Complex	R[b]	R'[b]	Ni(II)/Ni(III) (V)				2nd oxidation (V)	3rd oxidation (V)	1st reduction (V)	2nd reduction (V)	Reoxidation[e]
			E_{pa}	E_{pc}	ΔE_p	$E°'$	E_{pa}	E_{pa}	E_{pc}	E_{pc}	E_{pa}
1	$(CH_2)_2Ph$	$(CH_2)_2Ph$	0.124	0.013	0.111	0.068	0.387	0.575	-1.586	-	-
2	Bn	Bn	0.132	0.021	0.111	0.076	0.336	0.538	-1.585	-	-
3	Me	$(CH_2)_2Ph$	0.144	0.018	0.126	0.081	0.34[c]	0.523	-1.579	-	-
4	Bn	$(CH_2)_2Ph$	0.122	0.031	0.091	0.076	0.340	0.501	-1.480	-	-
5	Me	Bn	0.129	0.030	0.099	0.079	0.352	0.498	-1.422	-	-
6	Me	4-NO_2-Bn	0.132	0.045	0.087	0.088	0.49[c]	0.652	-1.396	-1.483	-1.567
7	Bn	4-NO_2-Bn	0.134	0.052	0.082	0.093	0.36[c]	0.495	-1.378	-1.486	-1.584
8	$(CH_2)_2Ph$	4-NO_2-Bn	0.140	0.054	0.086	0.097	0.368	0.534	-1.347	-1.474	-1.562
9	4-NO_2-Bn	4-NO_2-Bn	0.174	0.066	0.108	0.120	0.389	0.552	-1.361	-1.503	-1.636
Nc[a]	-	-	-0.468	-0.356	0.112	-0.412	0.507[d]	-	-2.169	-	-

[a] Nc = nickelocene, $NiCp_2$. [b] Bn = benzyl; $(CH_2)_2Ph$ = phenethyl; NBn = 4-NO_2-benzyl. [c] Cannot determine accurately, 2nd and 3rd oxidation peaks are overlapping. [d] $E°'$ (V). [e] Oxidation of NO_2 group attached to di-anion.

Following the first oxidation process (Ni(II)/Ni(III)), two distinct irreversible oxidation waves are observed for all complexes. The second oxidation process lies at $E_{pa} \approx 0.35$ V (Figure 4) and the third oxidation process at $E_{pa} \approx 0.5$ V. The second oxidation process was assigned as an irreversible halide oxidation by Crabtree[25], where they also observed irreversible oxidation waves between $0.218 \text{ V} \leq E^{\circ\prime} \leq 0.282 \text{ V}$ for their CpNi(NHC) halide complexes, following the Ni(II)/Ni(III) redox couple. After close inspection from DFT studies (see section 3.4) the second and third oxidation processes of complexes **1**-**9** of this study were concluded to be NHC ligand based, and not bromide-based, processes. For the second oxidation process a similar trend as for the Ni(II)/Ni(III) oxidation process is observed, where the electron-donating NHCs exhibit less positive (less cathodic) potentials, compared to the more electron-withdrawing NHCs, which have more cathodic potentials.

3.2.2 Reduction region

Depending on the NHC substituents, either one or two reduction processes were observed for complexes **1**-**9**. The non-NO_2-containing complexes **1**-**5** each exhibited one irreversible reduction peak ($-1.285 \text{ V} \leq E^{\circ\prime} \leq -1.527$ V) assigned to Ni(II)/Ni(I) reduction. This is based on the character of the LUMO of these complexes determined by the DFT study in section 3.4. Crabtree[25] also interpreted a quasi-reversible reduction wave at -1.510 V *vs.* FcH/FcH^+ of the complex [CpNiCl(IMes)] as Ni(II)/Ni(I) reduction.

The four 4-NO_2Bn-containing NHC complexes **6**-**9**, each shows two reduction peaks and one re-oxidation peak. It is expected that Ni(II) in complexes **6**-**9** will be reduced at a higher (less negative potential) than the non-4-NO_2Bn-containing complexes **1**-**5**, due to the electron withdrawing properties of the NO_2 moiety. This explains why the first reduction peak of **9** is much more positive (less negative) than that of **2**, with a similar trend when comparing **7** with **2** and **8** with **1** or **6** with **5**. Reversible NO_2 reduction is expected at *ca.* -1.5 V.[40] This leads to the interpretation that the first reduction peak observed for complexes **6**-**9** is the Ni(II)/Ni(I) reduction, followed by the second reversible couple assigned to NO_2 reduction. For complex **9,** the first reduction peak is followed by a larger second reduction peak, nearly double the peak current of that of the first reduction process. This is consistent with the near simultaneous reduction of the two NO_2 peaks after the initial Ni(II)/Ni(I) reduction.

For further confirmation of the assignment of the observed redox processes for **1**-**9**, the cyclic voltammogram of nickelocene was obtained under the same experimental conditions, with data reported in Table 1. The redox values obtained for nickelocene in this study are in agreement with published data obtained under similar experimental conditions.[48,49] The two oxidation processes are assigned to the reversible Ni(II)/Ni(III) oxidation at -0.468 V, followed by the reversible Ni(III)/Ni(IV) oxidation nearly 1 V higher at 0.507 V. One irreversible reduction process (Ni(II)/Ni(I)) is observed at -2.169 V, *ca.* 1.7 V more negative than the Ni(II)/Ni(III) oxidation. The difference between the Ni(II)/Ni(III) oxidation and the Ni(II)/Ni(I) reduction for the non-NO_2-containing complexes **1**-**5** is 1.6-1.7 V, similar to the difference obtained for nickelocene. However, the difference between the Ni(II)/Ni(III) oxidation and the second and the third oxidation processes for **1**-**9** is *ca.* 0.2 V and 0.4 V, respectively. Analogous to nickelocene, the second and third oxidation processes for **1**-**9** are therefore far too low to be metal-based, and thus in agreement with the NHC ligand based assignment for the second and third oxidation processes.

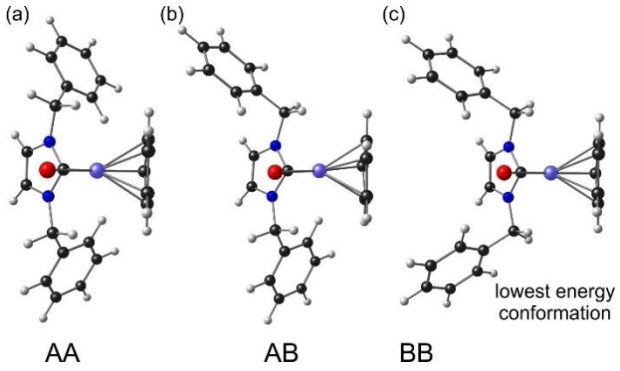


Figure 5: The three different *N*-substituent orientations possible for **5**. Colour code used for atoms: Ni (violet), N (dark blue), Br (red), C (grey), and H (white).

3.3 DFT studies

In order to better understand the oxidation and reduction processes observed, a density functional theory (DFT) study of complexes **1**-**9** is presented. Different orientations for the benzyl, phenethyl, and 4-nitrobenzyl *N*-substituents for each of the complexes **1**-**9** were evaluated, in order to find the conformation of global minimum energy. It is possible for the phenyl ring of the benzyl, phenethyl, or 4-nitrobenzyl *N*-substituents to be orientated 'above'

[48] J. D. L. Holloway, W. E. Geiger, Jr., *J. Am. Chem. Soc.*, 1979, **101**, 2038-2044.
[49] S. P. Gubin, S. A. Smirnova, L. I. Denisovich, *J. Organomet. Chem.*, 1971, **30**, 257-265.

(A) or 'below' (B) the imidazolylidene ligand plane, see Figure 5 for complex **5** as an example. For all complexes **1**-**9**, conformation BB with both *N*-substituents situated below the plane of the imidazolylidene ligand was the lowest in energy.

Table 2: Relative energies (eV) of the optimised isomers of complexes **1**-**9**.

Complex	*E* (eV)	Isomer[a]	X-ray structure reference
1	0.00	BB	[31]
	0.07	AB	
	0.15	AA	
2	0.00	BB	[30]
	0.04	AB	
	0.10	AA	
3	0.00	B	[30]
	0.07	A	
4	0.00	BB	
	0.05	BA	
	0.07	AB	
	0.13	AA	
5	0.00	B	[30]
	0.05	A	
6	0.00	B	[30]
	0.08	A	
7	0.00	BB	[31]
	0.06	BA	
	0.04	AB	
	0.12	AA	
8	0.00	BB	[31]
	0.07	BA	
	0.07	AB	
	0.14	AA	
9	0.00	BB	
	0.05	AB	
	0.14	AA	

[a] The terms above (A) and below (B) refer to the relative conformation of the relevant *N*-substituent with respect to the imidazolylidene ring.

This implies the conformer with the phenyl ring(s) of either the benzyl, phenethyl, or 4-nitrobenzyl *N*-substituents directed away from the Cp ring (Figure 5(c)), minimised the energy of the resultant complex, while conformation AA was found to have the highest energy (Table 2). The conformations of the lowest energy gas phase calculated isomers did

not always correspond to solid state X-ray structures, where intrinsic forces such as π-π stacking between phenyl rings and other stabilisation interactions may lead to a lower energy isomer as the one calculated.

3.3.1 Non-NO_2-containing Ni(II)-NHCs

To understand the electrochemical origin of the first oxidation and first reduction processes observed for the non-NO_2-containing complexes **1**-**5**, selected frontier molecular orbitals (MOs) of complex **2** are shown in Figure 6 as a representative example. Since oxidation involves removal of an electron from the HOMO of the neutral complex, the HOMO of the neutral complex or the LUMO of the oxidised species (MO where the electron was removed), suggests the origin of the first oxidation process. The Mulliken spin density plot of the oxidised complex indicates the locus of the remaining unpaired electron of the cation. The HOMO of neutral **2** has 32% Ni d_π, 17% Br and 34% Cp character, the LUMO of oxidised **2** has 55% Ni d_π, 11% Br and 22% Cp character, while the spin density plot of oxidised **2** has 72% Ni d_π, 8% Br and *ca.* 25% Cp character (Table 3). The first oxidation process of complexes **1**-**5** is thus mainly Ni-metal based, involving the Ni(II)/Ni(III) redox couple with a minor amount of radical character on the Cp ring.[50] The oxidation processes following the Ni(II)/Ni(III) redox couple are proposed to be centred on the phenyl substituent of the NHC ligand. This conclusion was drawn based on the character of the near degenerate HOMO (α-HOMO) and HOMO-1 (β-HOMO) of oxidised **2**, *i.e.* $[\mathbf{2}]^+$ (**2**-$1e^-$), both of similar NHC ligand character (Figure 6(c)).

Similarly, the LUMO of the neutral species (Figure 6a), 45% Ni-$d_{x^2-y^2}$) suggests metal-centred reduction (Ni(II)/Ni(I)), for **2**. Since molecular orbitals often re-arrange after reduction,[51] the inspection of the characters of the HOMOs and spin density profile of the reduced compound becomes important. The spin density of the reduced compound shows the distribution of the added unpaired electron. For the reduced species of **2**, the HOMO (β-HOMO of d_π + Cp character) is *ca.* 0.25 eV higher than the HOMO-1 (α-HOMO of $d_{x^2-y^2}$ + Cp character), with both exhibiting Ni-d character. The spin density profile of 86% Ni and 5% Br character indicates that the nature of the electron added upon reduction is mainly Ni-d-

[50] S. K. Ritter, *Chemical & Engineering News*, 2016, **94**, 6-6.
[51] J. Ferrando-Soria, O. Fabelo, M. Castellano, J. Cano, S. Fordham, H-C. Zhou, *Chem. Commun.*, 2015, **51**, 13381-13384.

based, thereby confirming the first observed reduction process for **2** to be Ni(II)/Ni(I) reduction. Similarly, the anions of **1**-**5** all have 86-90% Mulliken spin density of Ni-d character, whereas the cations of **1**-**5** all have *ca.* 72% Mulliken spin density of Ni-d_π character (Table 3). The DFT results thus clearly indicate that the first oxidation and the first reduction processes observed for the Ni(II)-NHC complexes **1**-**5**, involve Ni(II)/Ni(III) oxidation and Ni(II)/Ni(I) reduction respectively.

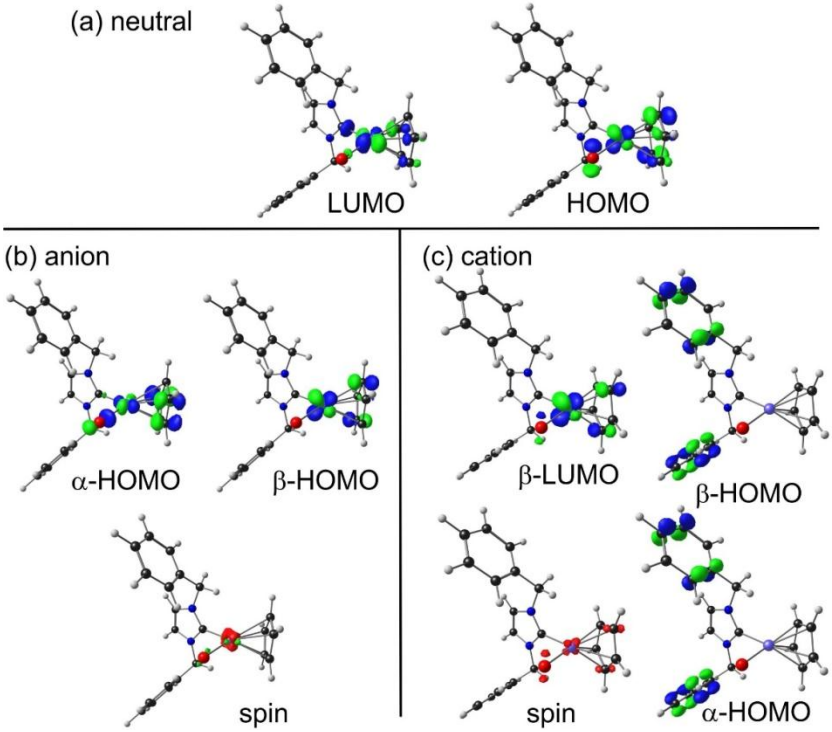


Figure 6: Selected molecular orbitals (green and blue) and Mulliken spin plots (red) of **2**: (a) neutral, (b) reduced ($1e^-$ addition) and (c) oxidised ($1e^-$ removal). Colour code used for atoms: Ni (violet), N (dark blue), Br (red), C (grey) and H (white).

3.3.2 NO_2-containing Ni(II)-NHCs

The HOMO of the neutral complex, the LUMO of oxidised species (removed electron) as well as the Mulliken spin density plot of the oxidised complex of the NO_2-containing Ni(II)-NHC complexes **6**-**9** provide insight in the origin of the first oxidation process of complexes **6**-**9** (complex **6** as representative example, Figure 7). A comparison of Figure 6(a, c) with Figure 7(a, c), as well as the data in Table 3 reveals a similar character of the HOMO of **6**-**9** to that of the non-NO_2-containing Ni(II)-NHC complexes **1**-**5**. The first oxidation process of complexes **6**-**9** is mainly Ni-metal based, involving the Ni(II)/Ni(III) redox couple. However, the oxidations following the Ni(II)/Ni(III) redox couple of **6**-**9**, are proposed to be centred on the NO_2-group of the NHC ligand. This proposal is based on the character of the near

degenerate HOMO (α-HOMO) and HOMO-1 (β-HOMO) of oxidised **6**, *i.e.* $[\mathbf{6}]^{+}$ (**6**-$1e^{-}$), with both of mainly NO_2 character (Figure 7(c)).

The LUMO and LUMO+1 of **6** are NO_2 and Ni-based respectively, suggesting the first reduction of **6** is NO_2-based. However, the HOMO (β-spin) of reduced **6** has 49% Ni character with some NO_2 contribution, suggesting that the electron removed upon reduction involved Ni(II)/Ni(I) reduction of a complex containing a non-innocent NO_2-moiety. The spin density of reduced **6** is 96% Ni-localised, with a spin density profile similar to that of the non-NO_2-containing Ni(II)-NHC complexes **1**-**5**; compare Figure 6(b) with Figure 7(b), as well as the data in Table 3. The LUMO (β-spin) of reduced **6** has 51% NO_2 character with only 13% Ni character, strongly suggesting that the second reversible reduction observed involves NO_2 (Figure 7). This interpretation also applies to the reduction of complexes **7** and **8**, (Table 3), and is in agreement with the experimental observation that the first reduction for complexes **6**-**8** involves the Ni(II)/Ni(I) couple, followed by the second reversible couple assigned to NO_2 reduction. With virtually no spin density on Ni for the anion of complex **9**, the interpretation follows that charge transfer took place after Ni reduction of **9** to the two electron withdrawing NO_2 groups, before reduction of the two NO_2 groups occurs.

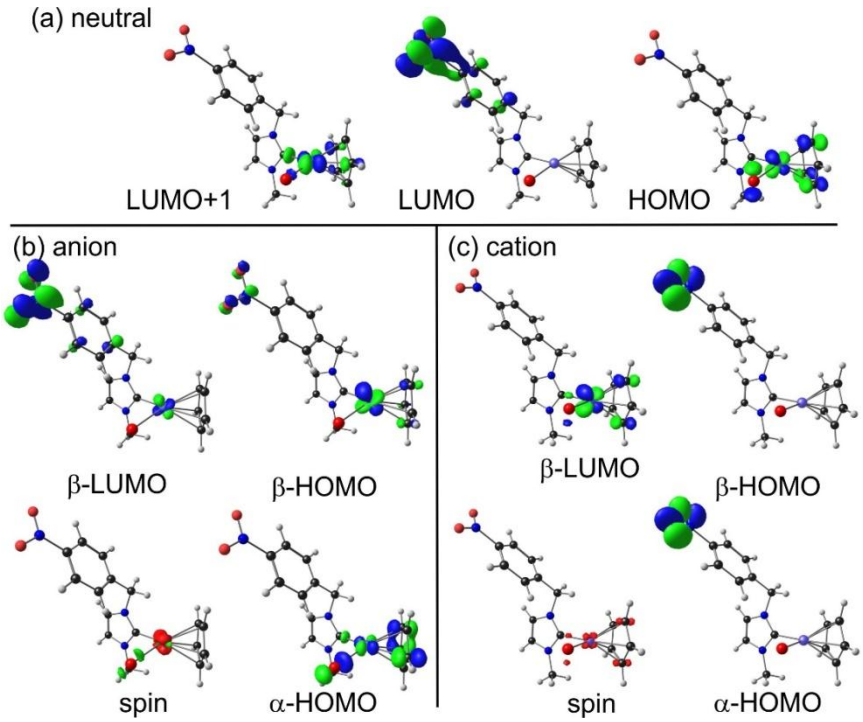


Figure 7: Selected molecular orbitals (green and blue) and Mulliken spin plots (red) of **6**: (a) neutral, (b) reduced ($1e^{-}$ addition) and (c) oxidised ($1e^{-}$ removal). Colour code used for atoms: Ni (violet), N (dark blue), O (red), Br (red), C (grey) and H (white).

Table 3: DFT calculated energies (eV) of the neutral and atomic Mulliken spin density of reduced (anion) and oxidised (cation) of **1**-**9**.

	Neutral			Cation				Anion						
	E_{HOMO}	E_{LUMO}	IP	Ni	Br	C_{NHC}	Cp ring total	Ni	Br	N	O	O	C_{NHC}	Cp ring total
1	-5.114	-1.761	6.281	0.721	0.076	-0.030	-0.092	0.860	0.045	-	-	-	0.030	0.042
2	-5.107	-1.742	6.273	0.724	0.075	-0.032	-0.002	0.863	0.047	-	-	-	0.030	0.076
3	-5.065	-1.713	6.300	0.719	0.079	-0.030	-0.091	0.901	0.045	-	-	-	0.020	0.011
4	-5.126	-1.768	6.284	0.723	0.076	-0.031	-0.091	0.875	0.046	-	-	-	0.025	0.012
5	-5.071	-1.707	6.304	0.719	0.079	-0.031	0.013	0.884	0.047	-	-	-	0.025	0.053
6	-5.305	-2.657	6.536	0.719	0.078	-0.029	-0.005	0.956	0.061	-0.050	-0.041	-0.037	0.040	0.041
7	-5.336	-2.650	6.496	0.722	0.076	-0.030	-0.002	0.934	0.057	-0.037	-0.031	-0.033	0.037	0.058
8	-5.347	-2.673	6.502	0.721	0.076	-0.029	-0.093	0.920	0.055	-0.030	-0.029	-0.026	0.035	0.006
9	-5.556	-2.794	6.703	0.720	0.076	-0.029	-0.093	0.000	0.000	0.096	0.089	0.094	0.002	0.000

3.3.3 Catalytic activities, redox potentials and DFT energies

A simple plot of molecular orbital energies of complexes **1**-**9** clearly illustrated the effect of the electron-withdrawing 4-NO_2-benzyl substituent (Figure 8): A slight lowering of HOMO energies, combined with noticeable lowering of LUMO energies resulted in smaller HOMO-LUMO energy gaps, which necessarily indicate less stable and more reactive species for **6**-**9**.[52] This was also confirmed in catalytic studies involving complexes **1**-**9**, where the 4-NO_2Bn-containing Ni-NHC complexes exhibited the lowest substrate conversions along with the lowest TOFs in the Suzuki-Miyaura coupling of 4-chlorophenyl carboxaldehyde with phenylboronic acid,[30] as well as in the anaerobic oxidation of secondary alcohols.[31] In these catalytic studies, the more electron-donating Ni-NHC complexes were the most efficient, because they were the least susceptible to catalyst deactivation/decomposition throughout the course of the reactions.[31]

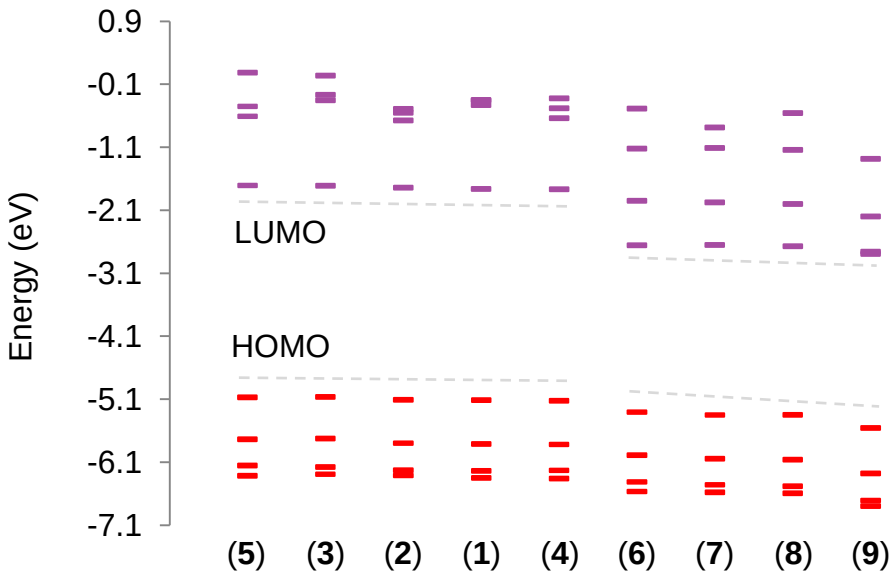


Figure 8: Molecular orbital energy levels (eV) of **1**-**9**. (1 eV = 96.485 kJ.mol^{-1})

The graph of the formal reduction potential, $E^{0'}$ (V), of the Ni(II)/Ni(III) couple, as a function of the C-C coupling product yield (%) from the Suzuki-Miyaura reaction,[30] is shown in Figure 9(a). A direct relationship between these two parameters is observed, as might be expected: The Suzuki-Miyaura mechanism relies on the capability of the Ni(II) catalyst to be constantly oxidised and reduced in solution, the ease of which could be probed using cyclic

[52] S. Thangavel, S. Boopathi, N. Mahadevaiah, P. Kolandaivel, P. B. Pansuriya, H. B. Friedrich, *J. Mol. Catal. A.*, 2016, **423**, 160-171.

voltammetry. The more donating the bound NHC ligand, the higher electron density resides on the metal. Therefore, oxidation should occur faster and be more facile than those bearing electron-withdrawing NHC ligands. Electron-donating NHCs render the Ni(II)/Ni(III) redox couple more cathodic (easier to oxidise at a lower potential), and hence lead to more efficient catalysts. The graph of the formal reduction potential, $E^{o'}$ (V), of the Ni(II)/Ni(III) couple, as a function of the % conversion when used as pre-catalysts in the chemoselective anaerobic oxidation of secondary aryl alcohols, shows a similar trend, Figure 9(b).

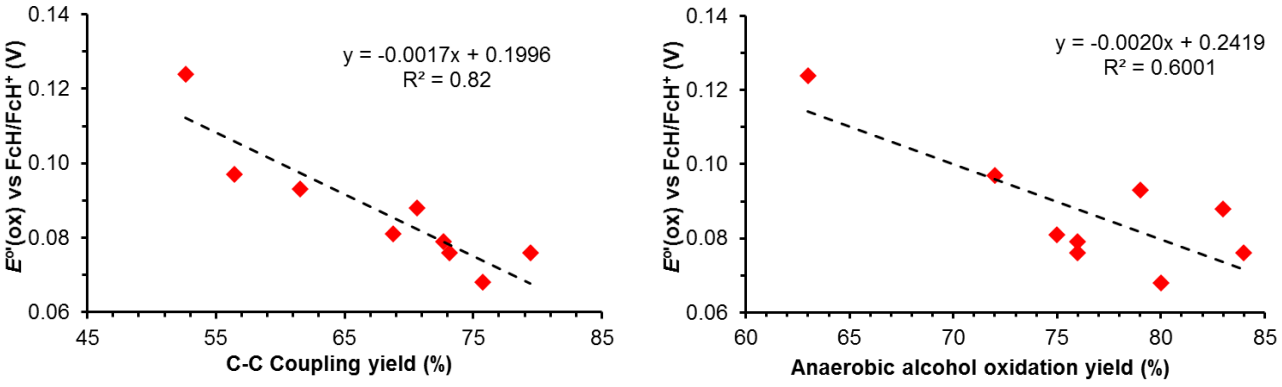
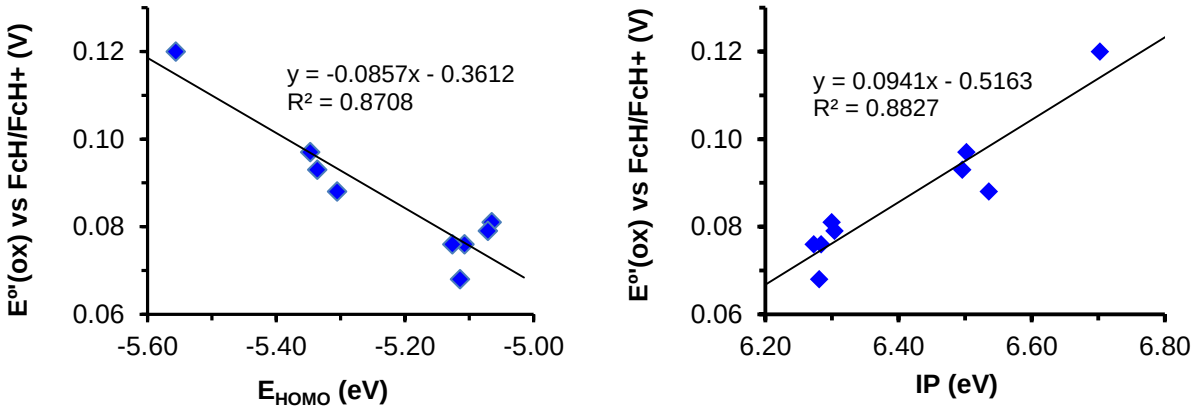


Figure 9: Relationship between the formal reduction potential, $E^{0'}$ (V), of the Ni(II)/Ni(III) couple, as a function of (a) the C-C coupling product yield (%) from the Suzuki-Miyaura reaction and (b) % conversion when used as pre-catalysts in the chemoselective anaerobic oxidation of secondary aryl alcohols. Dotted lines indicate trend lines with the given formulae and correlation coefficients.

Electro-oxidation of a metal complex involves removal of electron(s) from the HOMO of the neutral complex, whereas electro-reduction involves the addition of electron(s) to the LUMO of the neutral complex. Therefore a relationship between the energy of the HOMO (E_{HOMO}), and $E^{o'}$ (Ni(II)/Ni(III)) exists. From Figure 10 these linear relationships are evident with relatively good correlation coefficients, and are in good agreement with the DFT-Koopmans' theorem that states that the first (vertical) ionisation energy of a system is related to the negative of the corresponding E_{HOMO}.[53,54] The DFT calculated energy needed to remove one electron from the HOMO of the neutral complex ($IP_{1\acute{e}}$), *i.e.* the one-electron adiabatic ionisation potential, is also linearly related to $E^{o'}$ of the 1-electron redox couple

[53] J. P. Perdew, M. Levy, *Physical Review B.*, 1997, **56**, 16021-16028.
[54] U. Salzner, R. Baer, *J. Chem. Phys.*, 2009, **131**, 231101.

(Ni(II)/Ni(III)). Hence, it is clear that the electron-withdrawing 4-NO_2Bn-containing NHC complexes require more energy for oxidation (more positive E_{pa} for Ni(II)/Ni(III), more negative ionisation potential), as compared to the non-4-NO_2Bn-containing NHC complexes. This shows once more how electron-donating *N*-substituents on NHC ligands evidently better stabilise the metal species, which may allow for the observation of higher oxidation state metal species.[55]



(a) (b)

Figure 10: Graphs of electrochemical formal reduction potential, *E*°', of the Ni(II)/Ni(III) couple, and the DFT calculated (a) E_{HOMO} and (b) $IP_{1é}$, energies of **1**-**9**. Dotted lines indicate trend lines with the given formulae and correlation coefficients.

To test the applicability of the relationship $E^{o'}$ (Ni(II)/Ni(III)) = -0.09 E_{HOMO} – 0.27 (Figure 10 left), we optimised [CpNiCl(IMes)] that was reported to have a reversible $E^{o'}$ (Ni(II)/Ni(III)) at 0.723 V *vs* NHE = 0.033 V vs FcH/FcH^+.[25] The calculated E_{HOMO} of the DFT optimised [CpNiCl(IMes)] is -4.727 eV, giving a $E^{o'}$ (Ni(II)/Ni(III)) value of 0.055 V that is within 0.022 V of the experimental value considering a range of *ca.* 2.5 V studied.

4. Conclusion

The range of flexible, electron-withdrawing and -donating NHC-containing [CpNiBr(NHC)] complexes were synthesised, and their electrochemical properties investigated by means of cyclic voltammetry and DFT methods. From the CVs several redox active oxidation waves and couples were observed and systematically concluded to be the quasi-reversible

[55] M. M. Rogers, S. S. Stahl, *Topics in Organometallic Chemistry*, Springer, 2006, **21**, 21-46.

Ni(II)/Ni(III) redox couple followed by irreversible ligand-centred oxidations. During reduction the irreversible Ni(II)/Ni(I) reduction wave was observed (first for complexes **1**-**9**). The second reduction process of the NO_2-containing complexes **6**-**9** involves NO_2-reduction. DFT studies supported these findings by providing further insight into the electrochemical nature of the specific electrochemical processes observed for each of the complexes **1**-**9**. Electrochemically and computationally, the push-pull effect of the electron-donating *vs.* electron-withdrawing NHC ligands was evident and largely determines the ease of oxidation of Ni(II) and related electrochemical events observed for complexes **1**-**9**.

Acknowledgements

This work has received support from the South African National Research Foundation (JC Grant nr. 96111, ML Grant nr. 95764, FPM Grant nr. 88594) and the Central Research Fund of the University of the Free State, Bloemfontein (JC) and the University of Pretoria (ML). The High Performance Computing facility of the UFS and the Norwegian Supercomputing Program (NOTUR Grant nr. NN4654K) (JC) are acknowledged for computer time.

CHAPTER 6

Base-free glucose dehydration catalysed by NHC-stabilised heterohalo cyclopentadienyl Cr(III) complexes

Chapter 6 contains work that has been prepared for publication in Dalton Trans.:

Authors: Frederick P. Malan, Eric Singleton, Petrus H. van Rooyen, Jeanet Conradie, Marilé Landman

Status: To be submitted

Contributions:

Frederick P. Malan: Author, synthesis, characterisation, crystallography, electrochemistry (experiment and analysis), DFT study (full optimisation, calculation of HOMOs/LUMOs, energy calculations), catalytic study

Eric Singleton: Co-author, co-supervisor

Petrus H. van Rooyen: co-author, crystallography

Jeanet Conradie: Corresponding author, electrochemistry (supervision of results), DFT study (supervision of calculations, provision of DFT facilities and execution of input files created by FP Malan)

Marilé Landman: Corresponding author, supervisor

6

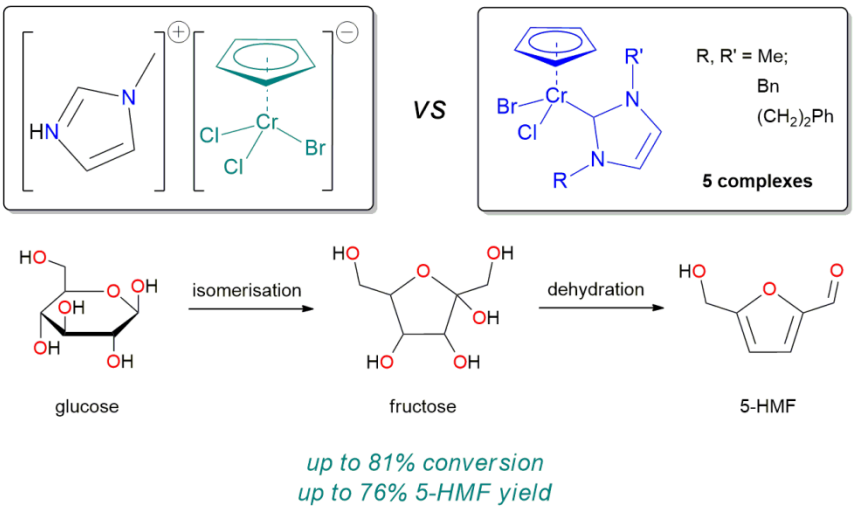
Base-free glucose dehydration catalysed by NHC-stabilised heterohalo cyclopentadienyl Cr(III) complexes

Frederick P. Malan,[a] Eric Singleton,[a] Petrus H. van Rooyen,[a] Jeanet Conradie[b,*] and Marilé Landman[a,*]

[a] *Department of Chemistry, University of Pretoria, 02 Lynnwood Road, Hatfield, Pretoria, 0002, South Africa.*

[b] *Department of Chemistry, University of the Free State, Bloemfontein 9300, South Africa.*

Graphical abstract



Abstract

A range of five air-stable heterohalo Cr(III)-NHC complexes (**1**-**5**) have been synthesised from chromocene and the corresponding imidazolium salts. Employment of an *N*-4-NO_2-benzyl imidazolium salt led to a side reaction where C-N bond cleavage occurred to form an imidazolium Cr(III) complex salt (**6**). The electrochemical processes of all six complexes were studied by means of cyclic voltammetry and a detailed conformational DFT analysis, which showed metal-centred redox behaviour. Furthermore, the Cr(III) complex salt (**6**) was electrochemically oxidised to Cr(IV) and electrochemically reduced to Cr(II) more readily than the related Cr(III)-NHC complexes (**1**-**5**). All complexes (**1**-**6**) were active (up to 81%

conversion) as catalysts in the dehydration of glucose to form 5-hydroxymethylfurfural in moderate yields (up to 76%). This homogeneous system does not require oxidants or stoichiometric amounts of strong bases such as KO^{t}Bu, often required in related catalytic systems, which is important for the development of greener catalytic processes employing naturally abundant precursors.

Keywords: chromium(III); cyclopentadienyl; *N*-heterocyclic carbene; glucose dehydration.

1. Introduction

Biomass has been considered a promising and essential renewable feedstock for chemicals and fuels, especially in the light of a looming energy crisis and global warming.[1-5] The utilisation, activation, and derivatisation of the main constituents of biomass, carbohydrates, is therefore of interest.[2,4,6] Although fructose can be transformed into 5-hydroxymethylfurfural (5-HMF) with relative ease, the more difficult conversion of its abundant precursor, glucose, continues to attract interest (Figure 1).[2,5] Being listed as one of the top ten value-added bio-based chemicals,[3,6] the use of 5-HMF and its 2,5-disubstituted analogues may act as versatile synthons for a variety of sought after chemicals and fuels.[7] The conversion of glucose into 5-HMF is a sensitive reaction that has a strong dependence on solvent, catalyst and temperature variables.[5,8] The formed 5-HMF is susceptible to further reaction/degradation, which includes isomerisation, rehydration,

[1] E. A. Pidko, V. Degirmenci, R. A. van Santen, E. J. M. Hensen, *Angew. Chem. Int. Ed.*, 2010, **49**, 2530-2534.
[2] (a) J. Li, Y. Ma, L. Wang, Z. Song, H. Li, T. Wang, H. Li, W. Eli, *Catalysts*, 2016, **6**, 1-12. (b) L. Hu, Y. Sun, L. Lin, *Ind. Eng. Chem. Res.*, 2012, **51**, 1099-1104.
[3] (a) H. Wang, S. Liu, Y. Zhao, H. Zhang, J. Wang, *ACS Sustainable Chem. Eng.*, 2016, **4**, 6712-6721. (b) M. E. Zakrzewska, E. Bogel-Łukasik, R. Bogel-Łukasik, *Chem. Rev.*, 2011, **111**, 397-417. (c) Z. Xue, M-G. Ma, Z. Li, T. Mu, *RSC Adv.*, 2016, **6**, 98874-98892.
[4] (a) F. D'Anna, S. Marullo, P. Vitale, C. Rizzo, P. L. Meo, R. Noto, *Appl. Catal. A: General*, 2014, **482**, 287-293. (b) Y. Qu, L. Li, Q. Wei, C. Huang, P. Oleskowicz-Popiel, J. Xu, *Scientific Reports*, 2016, **6**, Article number: 26067, doi:10.1038/srep26067.
[5] (a) X. Yi, I. Delidovich, Z. Sun, S. Wang, X. Wang, R. Palkovits, *Catal. Sci. Technol.*, 2015, **5**, 2496-2502. (b) Y. Wang, Z. Gu, W. Liu, Y. Yao, H. Wang, X-F. Xia, W. Li, *RSC Adv.*, 2015, **5**, 60736-60744. (c) S. Xu, X. Yan, Q. Bu, H. Xia, *RSC Adv.*, 2016, **6**, 8048-8052.
[6] P. Zhou, Z. Zhang, *Catal. Sci. Technol.*, 2016, **6**, 3694-3712.
[7] G. Yong, Y. Zhang, J. Y. Ying, *Angew. Chem. Int. Ed.*, 2008, **47**, 9345-9348.
[8] J. Zhang, Y. Cao, H. Li, X. Ma, *Chem. Eng. J.*, 2014, **237**, 55-61.

reversion, fragmentation, and additional dehydration reactions.[11] Various experimental and theoretical studies involving the activation of cellulosic biomass including glucose have been conducted whereby the majority made explicit use of Cr(II) and Cr(III) species in combination with ionic liquids.[1,8,9]

Zhao *et al.*[10] has to date been one of the few groups that could efficiently and selectively convert glucose into 5-HMF without a base in high yield (68-70%) using $CrCl_2$ (10 mol%) in the ionic liquid 1-ethyl-3-methylimidazolium chloride (EMIMCl). Generally, it is proposed that the ionic liquid media provide a non-coordinating polar environment that helps stabilise coordinatively unsaturated metal species.[1,13] However, we suspect that the highly viscous nature of the ionic liquids used may lead to a negative diffusion effect. This results in lower catalyst efficiency, where possible metal coordination of the ionic liquid precursors might compete with substrates due to their unique and tuneable stereo-electronic properties.[3,7] Furthermore, the separation of the formed 5-HMF from ionic liquids remains a technical and economical difficulty that limits the scalability and application in the preparation of 5-HMF.[3,6]

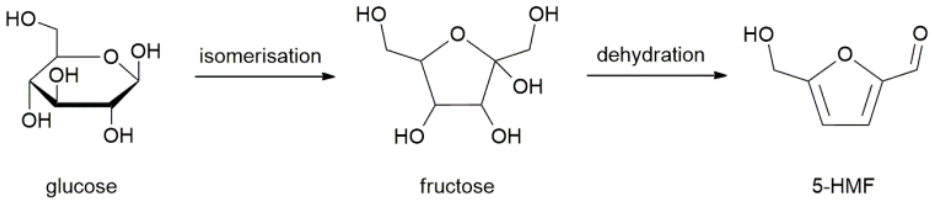


Figure 1: Conversion of glucose into 5-hydroxymethylfurfural (5-HMF) *via* fructose.

Lewis acid catalysed glucose transformations in ionic liquid media have been proposed to involve mononuclear chromium species, of which the $CrCl_3^-$ anion[1] (for Cr(II) species) and $CrCl_4^-$ anion[11] (for Cr(III) species), each coordinated to an enediolate species, was proposed to be an important intermediate. A number of DFT-supported mechanistic studies further support transient Cr(II)- or Cr(III)-alkoxy species to be important catalytically active species.[1,11]

[9] B. Kim, J. Jeong, D. Lee, S. Kim, H-J. Yoon, Y-S. Lee, J. K. Cho, *Green Chem.*, 2011, **13**, 1503-1506.
[10] H. Zhao, J. E. Holladay, H. Brown, Z. C. Zhang, *Science*, 2007, **316**, 1597-1600.
[11] Y. Zhang, E. A. Pidko, E. J. M. Hensen, *Chem. Eur. J.*, 2011, **17**, 5281-5288.

In addition to numerous accounts indicating a higher activity of Cr(III) over Cr(II) species,[11] it has also been shown that $CrCl_3$-catalysed systems exhibited the highest catalytic activity in the transformation of cellulose into 5-HMF.[6] In contrast, Yong *et al.*[12] found that the *in situ* formed *N*-heterocyclic carbene (NHC) NHC-$CrCl_x$ complex (NHC = 1-butyl-3-methylimidazolyl, BMIM; x = 2, 3) was the active catalyst responsible for the transformation of glucose into 5-HMF. Chen and co-workers[13] found, however, a rate- and efficiency-impeding effect that bulky coordinated NHC ligands had on chromium species in the 5-HMF formation process. They found through quantitative NHC titration experiments of $CrCl_x$ (x = 2, 3) with IMes and IPr, that stoichiometric amounts of 2.3 (IMes, Cr(II)), 3.2 (IMes, Cr(III)), and 3.1 (IPr, Cr(II)) were required to completely quench the catalytic reaction. This might be surprising since coordination of highly donating NHCs is expected to stabilise the sensitive catalytic intermediates, and facilitate rapid catalysis.[14] However, since NHCs form some of the strongest M-C bonds,[15] coordination of more than two equivalents of bulky NHCs might significantly contribute to a sterically crowded chromium species, which encumbers substrate coordination and subsequent conversion.

Few studies report on the catalytic use of pre-isolated Cr-NHC complexes in 5-HMF formation, and none without the use of ionic liquids. Generally, most 'one-pot synthesis' studies on the transformation of glucose into 5-HMF necessitates the use of a tandem catalytic system whereby the isomerisation of glucose into fructose (using chromium salts, a Lewis acid) is followed by dehydration (using ionic liquids, a Brønsted acid).[6] We were therefore interested in conducting a study whereby pre-isolated half-sandwich Cr(III)-NHC complexes were employed as catalysts in the conversion of glucose into 5-HMF, without the use of ionic liquids. Herein we report the synthesis, characterisation, electrochemistry, DFT studies, and the results of the catalytic glucose dehydration studies.

[12] G. Yong, Y. Zhang, J. Y. Ying, *Angew. Chem.*, 2008, **120**, 9485-9488.
[13] E. F. Dunn, D. J. Liu, E. Y.-X. Chen, *Appl. Catal. A: General*, 2013, **460-461**, 1-7.
[14] K. A. Kreisel, G. P. A. Yap, K. H. Theopold, *Organometallics*, 2006, **25**, 4670-4679.
[15] (a) P. Daw, R. Petakamsetty, A. Sarbajna, S. Laha, R. Ramapanicker, *J. Am. Chem. Soc.*, 2014, **136**, 13987-13990. (b) J. Witt, A. Pöthig, F. E. Kühn, W. Baratta, *Organometallics*, 2013, **32**, 4042-4045.

2. Results and discussion

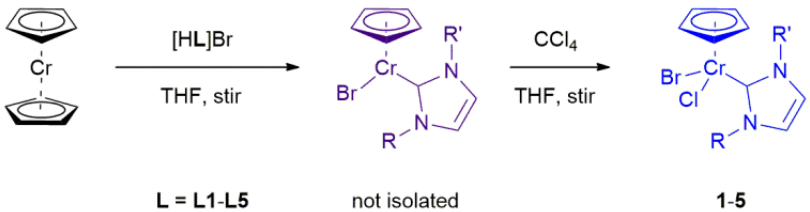
2.1 Synthesis of Cr(III)-NHC complexes

In light of the reported findings of Chen and co-workers,[13] whereby a catalysis-inhibiting effect was observed when bulky Cr-NHC complexes were employed, NHC ligands containing flexible *N*-substituents were used for this study (Figure 2). These imidazolium bromide ligands were synthesised as reported previously.[28] The imidazolium ring and *N*-phenyl substituents of each of the ligand precursor of **L1**-**L6** are connected by either methylene or ethylene linker moieties to facilitate flexibility of the *N*-substituents in order to alleviate the steric bulk associated with each of these ligands. Ligands **L1**-**L5** all contain combinations of the electron donating groups of Me, Bn (benzyl), and C_2H_4Ph, whereas an electron-withdrawing 4-NO_2Bn substituent has been incorporated into ligand **L6** to probe a possible electrochemical effect post coordination.

Dark red THF solutions of freshly synthesised chromocene ($CrCp_2$) were found to react with the imidazolium bromide ligands [H**L1**]Br-[H**L5**]Br in a protonolysis reaction whereby a molecule of cyclopentadiene is formed along with Cr(II) complexes of the type [CpCrBr(NHC)] (NHC = **L1**-**L5**). The purple solutions containing the latter Cr(II)-NHC complexes are highly air-sensitive and darken upon exposure to air.[16] Addition of 0.5 mL of CCl_4 to the purple solutions leads to an immediate oxidation of Cr(II) to Cr(III) metal species, as signified by the colour change from purple to royal blue.[14,17,18] The formed Cr(III)-NHC complexes of the type [CpCrBrCl(NHC)] (**1**-**5**) are moderately air stable in the solid state, and less so in solution. Sensitivity of carbene reactivity to substituent changes[19] is demonstrated by the different outcome when the set of reactions described above is repeated with ligand **L6**: A red THF solution of chromocene reacts with ligand **L6** to slowly yield a blue-green mixture, which upon addition of 0.5 mL CCl_4

[16] (a) M. H. Voges, C. Rømming, M. Tilset, *Organometallics*, 1999, **18**, 529-533. (b) C. Jones, D. P. Mills, R. P. Rose, A. Stasch, W. D. Woodul, *J. Organomet. Chem.*, 2010, **695**, 2410-2417.
[17] (a) W. Zhou, J. A. Therrien, D. L. K. Wence, E. N. Yallits, J. L. Conway, B. O. Patrick, K. M. Smith, *Dalton Trans.*, 2011, **40**, 337-339. (b) A. Döhring, J. Göhre, P. W. Jolly, B. Kryger, J. Rust, G. P. J. Verhovnik, *Organometallics*, 2000, **19**, 388-402.
[18] (a) S. Bellemin-Laponnaz, S. Dagorne, *Chem. Rev.*, 2014, **114**, 8747-8774. (b) Z. Wang, L. Jiang, D. K. B. Mohamed, J. Zhao, T. S. A. Hor, *Coord. Chem. Rev.*, 2015, **293**-**294**, 292-326.
[19] C. D. Abernethy, J. A. C. Clyburne, A. H. Cowley, R. A. Jones, *J. Am. Chem. Soc.*, 1999, **121**, 2329-2330.

immediately turns turquoise. Upon inspection of the single crystal molecular structure (*vide infra*) it was realised that N-C bond cleavage of the NHC ligand occurred, after which a protonation reaction formed a Cr(III) NHC complex salt (Figure 3). Complex **6** is one of the few half-sandwich Cr(III) complex salts isolated, and is only the second to be structurally characterised by SCXRD.



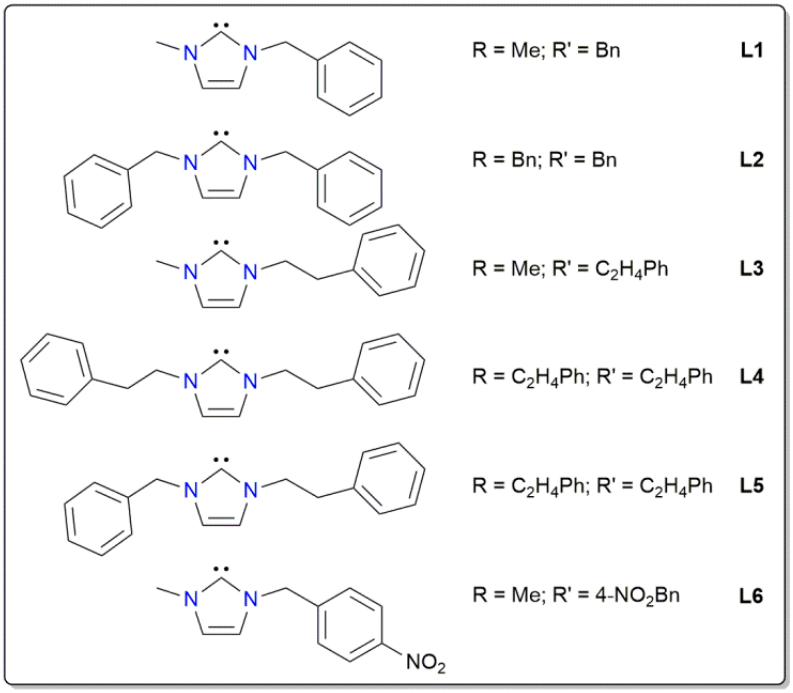
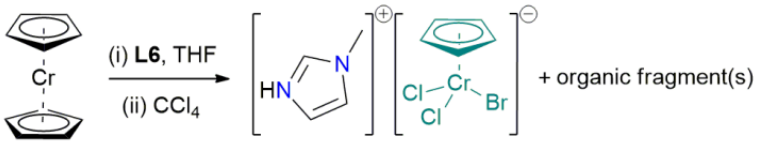


Figure 2: Synthesis of complexes **1**-**5** from chromocene and ligand salts [H(**L1**-**L5**)]Br.

Degradation of **L6** occurred *via* C-N bond cleavage to form the protonated *N*-methyl imidazolium cation as one of the organic by-products. The activation of the C-N bond has been

reported[20] and reviewed[21] in literature, and predominately yields heteroatom-inserted or ring-expanded heterocycles. In general, nucleophilic attack of a halide anion from an imidazolium halide salt occurs in a reverse Menschutkin-type reaction to form the neutral *N*-methylimidazole along with the 4-nitrobenzyl bromide.[22] However, because of the lack of bromido reactivity in a reverse Menschutkin-type reaction using ligands **L1**-**L5**, another similar side reaction involving a Lewis basic cyclopentadienyl ring and electron-poor *N*-4-nitrobenzyl substituent is proposed. Similarly, the neutral *N*-methylimidazole and substituted cyclopentadiene may be formed as transient species, which after protonation forms the *N*-methylimidazolium cation. The imidazolium cation serves to balance the charge on the Cr(III) anion. Tilset and co-workers[16] encountered a similar phenomenon: the sluggish reaction of the bulky $CrCp^*_2$ with [HIMes]Cl led to the formation of [$HIMes^+$][$Cp^*CrCl_3^-$]. The authors suggested sterically demanding substituents on both the cyclopentadienyl and NHC ligands to inhibit carbene coordination. The bulky nature of the *N*-aryl groups might have precluded a similar reverse Menschutkin reaction, and hence prevented *N*-dealkylation.



6

Figure 3: Formation of complex **6**.

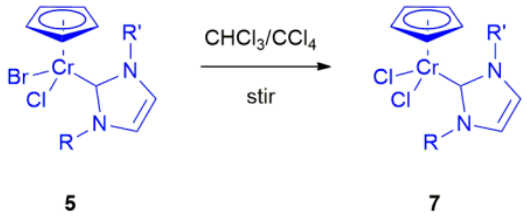
Because of the paramagnetic nature of **1**-**6**, characterisation was performed by means of FT-IR spectroscopy, UV-Vis spectroscopy, MS (EI), microanalysis, and single crystal diffractometry. The IR spectra of **1**-**6** revealed several bending and stretching frequencies expected for saturated and unsaturated hydrocarbon ligands: 3221-3053 cm^{-1} (ν{=CH}, w), 3025-2919 cm^{-1} (ν(-CH),

[20] (a) A. W. Waltman, T. Ritter, R. H. Grubbs, *Organometallics*, 2006, **25**, 4238-4239. (b) S. Haslinger, A. Pöthig, M. Cokoja, F. E. Kühn, *Acta Cryst.*, 2015, **C71**, 1096-1099. (c) P. Hemberger, A. Bodi, J. H. J. Berthel, U. Radius, *Chem. Eur. J.*, 2015, **21**, 1434-1438. (d) F. Hering, U. Radius, *Organometallics*, 2015, **34**, 3236-3245. (e) D. Schmidt, J. H. J. Berthel, S. Pietsch, U. Radius, *Angew. Chem. Int. Ed.*, 2012, **51**, 8881-8885.

[21] (a) K. J. Iversen, D. J. D. Wilson, J. L. Dutton, *Dalton Trans.*, 2014, **43**, 12820-12823. (b) S. Würtemberger-Pietsch, U. Radius, T. B. Marder, *Dalton Trans.*, 2016, **45**, 5880-5895.

[22] S. Sowmiah, V. Srinivasadesikan, M-C. Tseng, Y-H. Chu, *Molecules*, 2009, **14**, 3780-3813.

w), 1521-1493 cm^{-1} (δ(-CH), sym, m), and 1453-1410 cm^{-1} (δ(-CH), asym, m). In addition, strong characteristic C-N stretching frequencies between 1231-1214 cm^{-1} and 1015-1010 cm^{-1} were observed for **1**-**5**, compared to related frequencies of 1262 cm^{-1} and 1011 cm^{-1} for **6**. During the crystallisation process of **1**-**6**, we noticed that upon using the chlorinated solvents $CHCl_3$ or CCl_4, a slow halide exchange reaction takes place (Figure 4). During this reaction, the bromide anion is exchanged for a chloride anion. The reaction occurs faster in CCl_4 than $CDCl_3$, as well as when chlorinated solvent solutions are heated (> 40 °C). In doing so, the bis-chloro derivative of complex **5**, [$CpCrCl_2$(**L5**)] (**7**), could be isolated.



5 **7**

Figure 4: Synthesis of **7** *via* a halide exchange reaction.

The royal blue complexes **1**-**5** have comparable UV-Vis bands with λ_{max} of 574 nm (**1**), 581 nm (**2**), 577 nm (**3**), 573 nm (**4**), and 577 nm (**5**). All of these peak maxima are consistent with analogous dark blue [$CpCrCl_2$(NHC)] complexes.[16,17] The turquoise coloured complex **6** has a slightly higher energy UV-Vis band with λ_{max} of 648 nm, corresponding to similar Cr(IV) complexes.[23] Deep to bright blue single crystals of all complexes **1**-**6** were obtained from slow evaporation of CH_2Cl_2 solutions. Perspective views of the single crystal X-ray structures are shown in Figure 5. All of the structures **1**-**7** confirm their monometallic, three-legged piano stool structures with the centroid of the cyclopentadienyl ring, the chromium centre, as well as the carbenic carbon atom (**1**-**5**, **7**) all situated in the same plane. The Cr1-Cg (1.886(5)-1.904(5) Å; Cg = cyclopentadienyl centroid), Cr1-C1 (2.102(7)-2.132(2) Å), Cr1-Cl1 (2.321(6)-2.407(2) Å), and Cr1-Br1 (2.324(9)-2.373(2) Å) bond distances all compare well with related chromium

[23] (a) S. Groysman, D. Villagrán, D. G. Nocera, *Inorg. Chem.*, 2010, **49**, 10759-10761. (b) A. R. Barron, J. E. Salt, G. Wilkinson, M. Motevalli, M. B. Hursthouse, *J. Chem. Soc. Dalton Trans.*, 1987, 2947-2954. (c) K. L. Fujdala, T. D. Tilley, *Chem. Mater.*, 2001, **13**, 1817-1827.

complexes.[14,17(a),24] The latter bond distances of **4** and **5** are all noticeably longer than in **1**-**3**, presumably due to increased steric repulsion.

Because of the "closed" NHC conformations that **4** and **5** adopt, an increased amount of steric bulk is present around the chromium centre, leading to a slight elongation of the Cr-ligand bonds. For example: the Cr1-C1 bond lengths of **1**-**3** (2.102(7)-2.108(3) Å), are all slightly shorter than those of **4** and **5** (2.132(2)-2.127(5) Å); the Cr1-Cg bond lengths of **1**-**3** (1.886(5)-1.897(9) Å) are slightly shorter than the corresponding bond lengths of **4** and **5** (1.902(7)-1.904(5) Å). In addition, Danopoulos and co-workers[24(b)] proposed that variation in the predominant σ-contribution (with minimal π-contribution) of the Cr-NHC bonding, as well as the variable interelectronic repulsions involving non-bonding metal and ligand orbitals (see below), also affect the Cr-$C_{carbene}$ bond lengths.

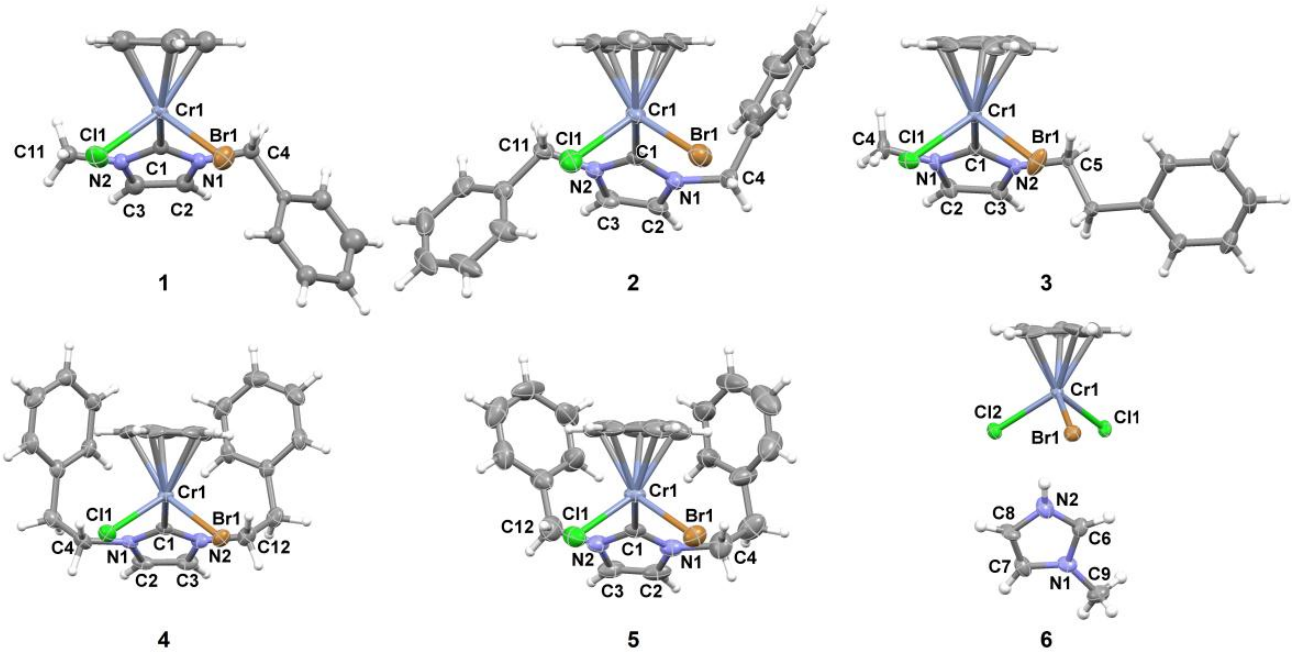


Figure 5: Perspective views of the molecular structures of complexes **1**-**6**. Ellipsoids are drawn at 50% probability level. The representation of complex **1** is obtained from a poor data set, although sufficient for connectivity purposes and completeness.

[24] (a) E. F. van der Eide, M. L. Helm, E. D. Walter, R. M. Bullock, *Inorg. Chem.*, 2013, **52**, 1591-1603. (b) S. Conde-Guadano, A. A. Danopoulos, R. Pattacini, M. Hanton, R. P. Tooze, *Organometallics*, 2012, **31**, 1643-1652.

If the asymmetric nature of the packing of the *N*-substituents of the NHCs in **1**-**5**, and **7** is disregarded, the molecular structures of these complexes exhibit nearly C_s symmetry. This implies the orientation of the NHC ligand is such that the above mentioned mirror plane of Cg-Cr-$C_{carbene}$ bisects the NHC ligand at an angle of θ. The parameter θ, has previously[24(a)] been defined as the absolute value of the absolute value of the dihedral angle between the planes of Cg-Cr-$C_{carbene}$ and Cr-$C_{carbene}$-$(N)_2$. For complexes **1**-**5**, and **7**, θ ranges between 81.1-91.5°. Surprisingly, there appears to be no correlation between θ and the degree of steric repulsion among complexes **1**-**5** and **7**. For complexes **1**, **3**, and **5** the two planes bisect nearly perpendicularly (90.3-91.5°); while for complexes **2**, **4** and **7** the deviation is more prominent which is comparable with the results of Bullock and co-workers[24(a)] (85-88°).

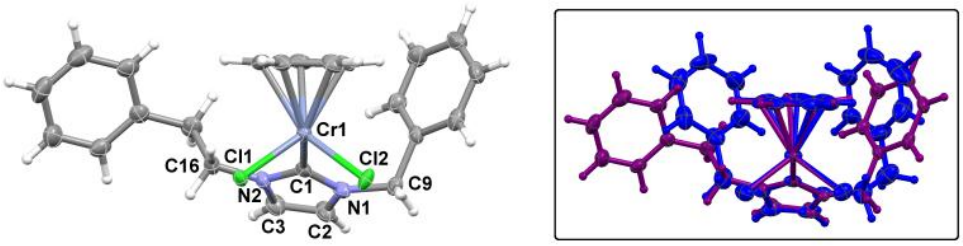


Figure 6: Perspective view of the molecular structure of **7**. Ellipsoids drawn at 50% level. Inset: Overlay of **5** (blue) and **7** (purple) showing their "closed" and "open" configurations, respectively.

The X-ray crystal structure of **7** (Figure 6) exhibits noticeable structural differences compared to **5**: Apart from different unit cells (monoclinic $P2_1/c$ (**7**), orthorhombic $P2_12_12_1$ (**5**)), the *N*-substituents in **7** adopt an "open" configuration whereby one *N*-substituent is situated above the mean imidazolyl plane, and the other one below. The latter is in contrast with the "closed" configuration of **5** whereby both *N*-substituents are situated above the mean imidazolyl plane. All other bond lengths and angles between **5** and **7** are comparable.

2.2 DFT studies

In order to better understand the geometrical and electronic structure of complexes **1**-**5**, a density functional theory (DFT) study of **1**-**5** is presented. Different geometrical isomers are possible for these complexes, depending on the orientation and position of the Cl and Br substituents. For

example, for complex **3**, four geometrical isomers are possible, namely with the phenethyl substituent adjacent to Cl and pointing up (U-Cl), the phenethyl substituent adjacent to Cl and pointing down (D-Cl), the phenethyl substituent on the side of Br and pointing up (U-Br), as well as the phenethyl substituent adjacent to Br and pointing down (D-Br). Figure 7 contains the optimised geometries and relative energies of the four isomers of **3**. The energy of the isomers does not differ significantly, implying all isomers are possible, especially when crystallising in the solid state where packing effects also play a role.

Cr(III) is a d^3 species having either a doublet (q = 0, S = 1/2, spin multiplicity = 2) or a quartet (q = 0, S = 3/2, spin multiplicity = 4) ground state. Energies obtained for the different spin states for one of the lowest energy isomers of neutral **3**, using different functionals and basis sets, are included in Figure 8. The results clearly indicate that the quartet ground state is favoured by more than 1 eV, in agreement with experimental observation for other similar neutral chromium(III) complexes.[25] Table 1 contains the energies obtained for the anion (reduced **3**) and cation (oxidised **3**) using different functionals. The results clearly suggest the d^2 Cr(IV) cation (oxidised) to be a triplet with 2 unpaired electrons (q = +1, S = 1, spin multiplicity = 3) and the d^4 Cr(II) anion to be a pentet with 4 unpaired electrons (q = -1, S = 2, spin multiplicity = 5). The difference between the energy of the neutral complex and either the optimised cation or anion corresponds to the ionisation potential (IP) and electron affinity (EA) of the complex, respectively. Table 2 includes the DFT calculated ionisation potential (IP) and electron affinity (EA)) of the lowest energy isomer of complexes **1**-**5**. The energy level diagram of the frontier molecular orbitals (MOs) of complex **3** is shown in Figure 8. The top three occupied MOs all have some Cr character, while the two alpha (LUMO and LUMO+1) and five of the beta unoccupied MOs (LUMO+2, 3, 4, 6 and 10) have a large % of Cr character.

[25] (a) P. Milko, M. A. Iron, *J. Chem. Theory Comput.*, 2014, **10**, 220-235. (b) M. Wang, J. England, T. Weyhermüller, S-L. Kokatam, C. J. Pollock, S. DeBeer, J. Shen, G. P. A. Yap, K. H. Theopold, K. Wieghardt, *Inorg. Chem.*, 2013, **52**, 4462-4487.

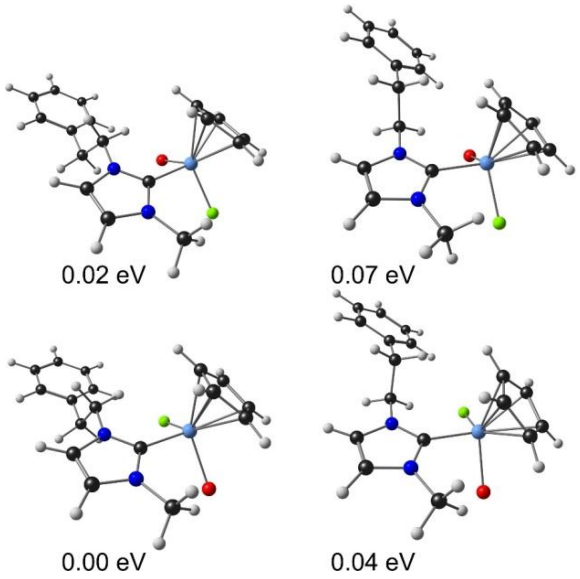


Figure 7: The different isomers possible for Cr(III)-NHC complex [CpCrBrCl(NHC)] (NHC = Im(Me)($(CH_2)_2$Ph), **3**), with the relative energies of the isomers. Colour code used for atoms: Cr (powder blue), N (dark blue), O (red), Br (red), Cl (green), C (grey) and H (white).

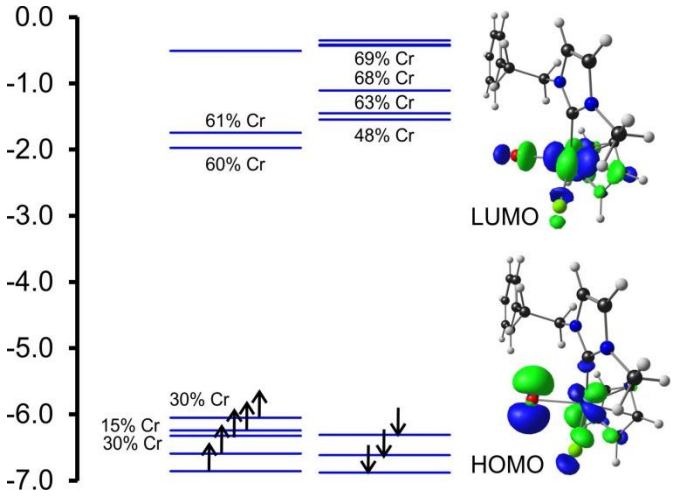


Figure 8: MO energy level diagram of Cr(III)-NHC complex [CpCrBrCl(NHC)] (NHC = Im(Me)($(CH_2)_2$Ph), **3**), with the % Cr character of selected frontier MOs shown. The black arrows represent electrons (up arrow: alpha electron; down arrow: beta electron). The y-axis indicates energy in eV. Right: Visualisation of the LUMO and HOMO. Colour code used for atoms: Cr (powder blue), N (dark blue), O (red), Br (red), Cl (green), C (grey) and H (white).

Table 1: Relative energies (eV) of the optimised neutral complex **3**, cation complex **3** and anion complex **3**, obtained by the indicated basis set and functionals.

	Funct. **Basis set**[a]	**Mult.**	**S**	M06-D3 6-311G(d,p)	LC-BLYP 6-311G(d,p)	CAM-B3LYP 6-311G(d,p)	B3LYP 6-311G(d,p)	B3LYP 6-311G(d,p)/ def2tzvpp/SDD	B3LYP 6-311G(d,p)/ Lanl2dz
Cr(II) d^4	anion	singlet	0	2.19	1.64	1.69	1.59	1.83	1.79
	anion	triplet	1	0.87	[b]	[b]	0.67	[b]	0.85
	anion	pentet	2	**0.00**	**0.00**	**0.00**	**0.00**	**0.00**	**0.00**
Cr(IV) d^2	cation	singlet	0	1.22	0.84	0.87	1.13	1.24	1.20
	cation	triplet	1	**0.00**	**0.00**	**0.00**	**0.00**	**0.00**	**0.00**
Cr(III) d^3	neutral	doublet	1/2	1.67	[b]	[b]	1.31	[b]	[b]
	neutral	quartet	3/2	**0.00**	**0.00**	**0.00**	**0.00**	**0.00**	**0.00**

[a] For more detail on basis sets see Computational details. [b] Geometry did not converge.

Table 2: DFT calculated ionisation potential (IP) and electron affinity (EA) values for **1**-**5**, obtained using B3LYP/6-311G(d,p).

Complex	IP (eV)	EA (eV)
1a	7.23	1.30
1b	7.24	1.26
2	7.21	1.31
3a	7.22	1.24
3b	7.21	1.27
4a	7.18	1.33
4b	7.18	1.52
5	7.16	1.27

2.3 Electrochemistry

Upon oxidation an electron is removed from the HOMO of the neutral quartet complex, resulting in an oxidised triplet cation. Reduction involves the addition of an electron to the LUMO of the neutral complex, leading to the reduced pentet anion. Since both the HOMO and LUMO of the neutral complex has Cr character, the first oxidation and reduction processes observed for complexes **1**-**5** are proposed to be metal-based, *i.e.* Cr(III)/Cr(IV) oxidation and Cr(III)/Cr(II) reduction (Figure 9). Conformation of this assignment is obtained from evaluation of the LUMO of the cation (the MO where the electron was removed upon oxidation) and the HOMO of the anion (the MO where the electron was added upon reduction). The LUMO of the cation has 58% Cr, 11 % Br and *c.a.* 10 % Cl character, confirming Cr(III)/Cr(IV) oxidation for **3**. The HOMO of the anion has 52 % Cr, 16 % Br and *c.a.* 11% Cp character, confirming Cr(III)/Cr(II) reduction for **3**. By analogy, the first oxidation and the first reduction for **1**, **2**, **4**, and **5** will thus involve Cr(III)/Cr(IV) oxidation and Cr(III)/Cr(II) reduction. Figure S1 (Supplementary Information) illustrates the oxidation and reduction processes of the Cr(III) complexes (**1**-**6**) of this study.

The cyclic voltammograms at a scan rate of 0.100 V s^{-1} of the chromium complexes **1**-**6** in the -2.02 V to +1.15 V *vs.* FcH/FcH^+ region are shown in Figure 10, along with a summary of the electrochemical data in Table 3. From Figure 10 two distinct electrochemical processes are observed: (i) In the oxidation (+0.74 V to +0.86 V *vs.* FcH/FcH^+) region, the Cr(III)/Cr(IV) redox couple is observed as either an electrochemically quasi-reversible (**2**, **3**) or electrochemically irreversible (**1**, **4**, **5**, **6**) redox wave; and (ii) in the reduction (-1.25 V to -1.83 V *vs.* FcH/FcH^+) region, a chemically and electrochemically irreversible Cr(III)/Cr(II) reduction peak. The assignment for both the Cr(III)/Cr(IV) and Cr(III)/Cr(II) redox couples are in agreement with published results on related Cr(III) complexes, as well as the DFT-predicted electrochemical events described above (*vide supra*).[26]

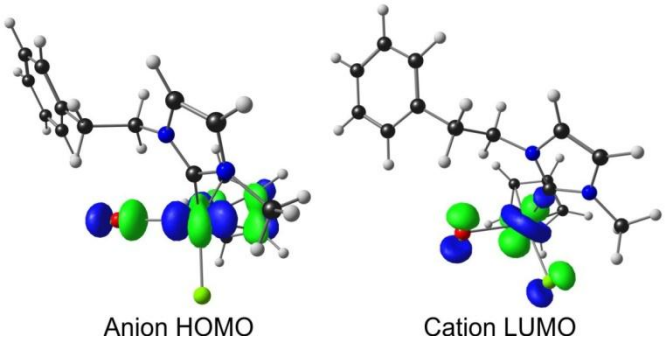


Figure 9: The HOMO of the anion and the LUMO of cation of [CpCrBrCl(NHC)] (NHC = Im(Me)($(CH_2)_2$Ph), **3**). Colour code used for atoms: Cr (powder blue), N (dark blue), O (red), Br (red), Cl (green), C (grey) and H (white).

In general, it is expected that the Cr(III)-NHC complexes featuring more electron-donating *N*-substituents (Me, $(CH_2)_2$Ph) would decrease the Cr(III)/Cr(IV) formal oxidation potential (less positive shift), as compared to a somewhat increased formal oxidation potential (more positively shifted) for the less-donating NHC-bearing Cr(III) complexes. This follows from the expectation that an electron-rich metal centre requires less energy (lower potentials) to be oxidised to a higher oxidation state as compared to relatively electron-poor metal centres. Complexes **1**-**5** all exhibited comparable $E^{\circ\prime}$ (Cr(III)/Cr(IV)) values, which is indicative of the similar electron-

[26] (a) R. F. Higgins, S. M. Fatur, S. G. Shepard, S. M. Stevenson, D. J. Boston, E. M. Ferreira, N. H. Damrauer, A. K. Rappé, M. P. Shores, *J. Am. Chem. Soc.*, 2016, **138**, 5451-5464. (b) R. Liu, J. Conradie, *Electrochim. Acta*, 2015, **185**, 288-296.

donating properties of the three *N*-substituents. Complexes, [CpCrBrCl(**L2**)] (**2**) and [CpCrBrCl(**L5**)] (**5**), containing **L2** = [HIm(Bn)$_2$]Br, and **L5** = [HIm(Bn)(C$_2$H$_4$Ph)]Br, each featuring at least one benzyl substituent, both showed the highest ($E°'$ = 0.86 V) formal oxidation potentials for the Cr(III)/Cr(IV) redox couple. Complexes **1**, **3**, and **4** with Me and C$_2$H$_4$Ph *N*-substituents, exhibited slightly lower $E°'$ (Cr(III)/Cr(IV)) values of 0.84, 0.81, and 0.84 V, respectively. For complex **6**, the Cr(III) centre has a noticeably lower formal oxidation potential for Cr(III)/Cr(IV) oxidation at $E°'$ = 0.74 V.

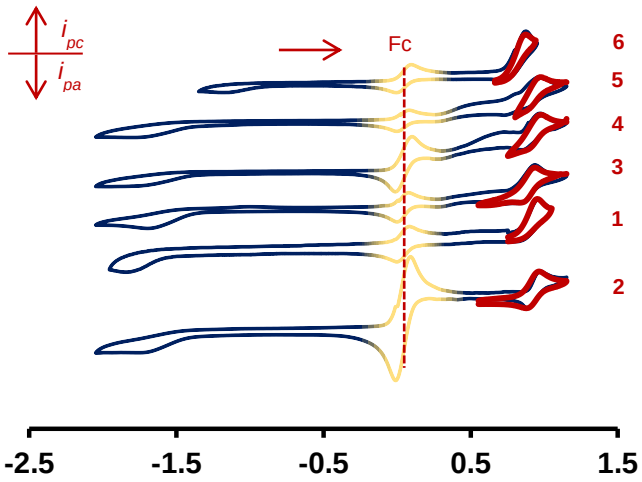


Figure 10: CVs (0.100 V s^{-1}, blue) of complexes **1**-**6** in the -2.02 V to 1.15 V *vs.* FcH/FcH$^+$ region are shown. Ferrocene ($E°'$ (Fc/FcH$^+$) = 0.400 V *vs.* NHE) is used as the internal standard (yellow). Overlay CVs (0.100 V.s^{-1}, red) of complexes **1**-**6** are isolated scans. All scans were initiated in the direction indicated from 0.6-0.8 V depending on the complex.

In the reduction region, complexes **1**-**6** each exhibited a one-electron reduction of Cr(III) to Cr(II). The reduction potentials of complexes **1**-**5** were comparable, with -1.78 V < E_{pc} < -1.83 V. In agreement with the trend observed in the oxidation potentials, complexes **1** and **4** containing the electron-donating **L1** (having a methyl substituent) and **L4** (having two *N*-C$_2$H$_4$Ph substituents) showed the more negative (more anodic shift, E_{pc} = -1.83 V) potentials than **2** and **5**. Furthermore, complex **6** exhibited a significantly less negative E_{pc} of -1.25 V. This shows that less energy is required to reduce the Cr(III) centre to Cr(II). Again, this occurs as a chemically and electrochemically irreversible event, where the electronegative Cr(III) in **6** is able to accept an electron much more readily than complexes **1**-**5**.

Table 3: Electrochemical data (*vs.* FcH/FcH^+) for redox processes observed for **1**-**6**.

Nr	R[a]	R'[a]	Cr(III)/Cr(IV) (V)				Cr(III)/Cr(II) (V)
			E_{pa}	E_{pc}	ΔE_p	$E°'$	E_{pc}
1	Me	Bn	0.89	0.78	0.11	0.84	-1.83
2	Bn	Bn	0.91	0.82	0.08	0.86	-1.81
3	Me	$(CH_2)_2Ph$	0.87	0.75	0.12	0.81	-1.78
4	$(CH_2)_2Ph$	$(CH_2)_2Ph$	0.90	0.78	0.12	0.84	-1.83
5	Bn	$(CH_2)_2Ph$	0.90	0.81	0.09	0.86	-1.81
6	H	Me	0.81	0.68	0.13	0.74	-1.25

[a] Me = methyl, Bn = benzyl, $(CH_2)_2Ph$ = phenethyl.

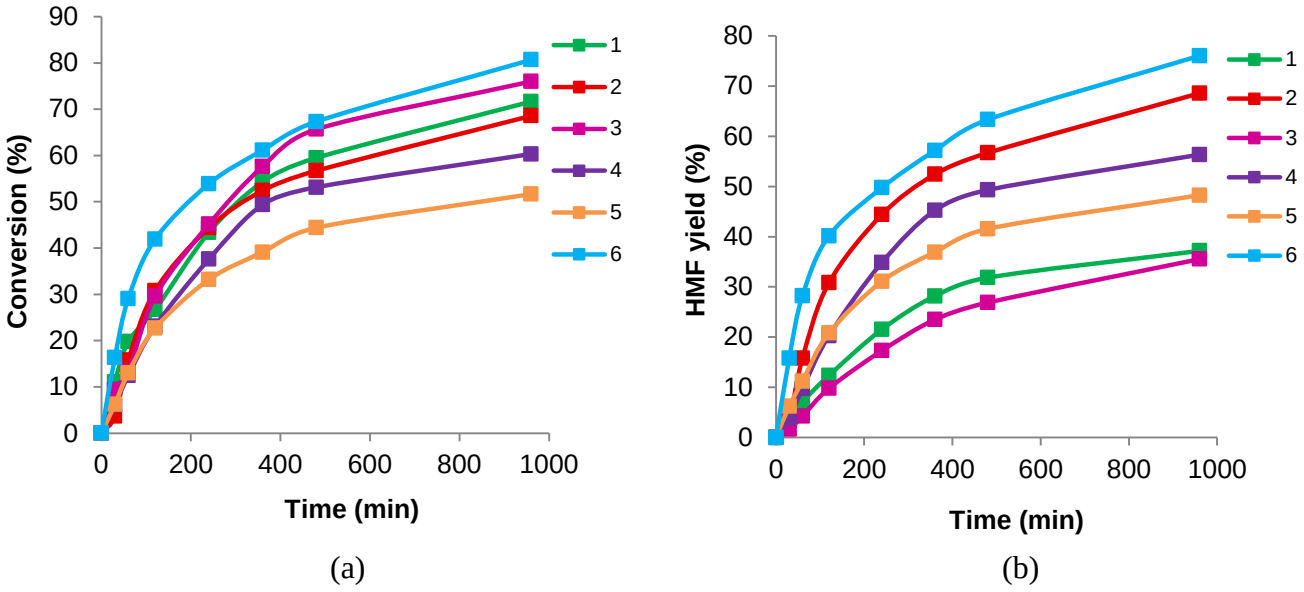
2.4 Glucose dehydration

The catalytic conversion of glucose into 5-HMF using the Cr(III) complexes **1**-**6** as catalysts, were investigated using ^{1}H-NMR spectroscopy. The reaction proceeds through glucose isomerisation, fructose formation, followed by dehydration to yield 5-HMF. We initially investigated the course of the reaction using $CrCl_3(THF)_3$ and **2** (6 mol%) separately as catalysts, with anisole as internal standard in DMSO at 120°C. DMSO conveniently helped provide a polar non-protic medium required for hydrogen transfer and the isomerisation of glucose to fructose to take place. DMSO also protects[3(b),5] the formed 5-HMF from degradation and/or further reaction(s). During the first two hours of the reaction a noticeable colour change from deep blue to light brown was observed in both reactions. A low initial 5-HMF yield of 30.8% was observed after 2 hours, compared to a higher yield of 48.3% for $CrCl_3(THF)_3$. A lowering in 5-HMF formation as the number of coordinated NHC ligands to either Cr(II) or Cr(III) species have previously been reported by Chen and co-workers[13], and is therefore not surprising. However, we reason that the electronic benefits of a coordinated electron-donating NHC ligand, combined with an inherent degree of flexibility of the NHC ligand, might prevail over catalytic inefficiencies due to an associated crowded inner ligand sphere. This reasoning has previously been confirmed by Yong *et al.*,[7] where they found that Cr(II)-NHC and Cr(III)-NHC complexes relied on the use of one equivalent of bulky NHC ligands to protect the chromium centre from reacting with the ionic liquid (imidazolium salt) to form a sterically crowded centre.

During the course of the reaction, a gradual conversion of glucose is observed by the disappearance of signals at δ_H 4.37 (m), 4.46 (d, $^3J_{HH}$ = 4 Hz), 4.64 (d, $^3J_{HH}$ = 4 Hz), 4.77 (d, $^3J_{HH}$ = 4 Hz), 4.87 (m) and 6.20 (d, $^3J_{HH}$ = 4 Hz) ppm, together with the simultaneous appearance of 5-HMF-associated signals at δ_H 6.56 (d, $^3J_{HH}$ = 4 Hz), 7.68 (s), 7.76 (s), and 9.50 (s) ppm. Concomitant formation of fructose was not observed by ^{1}H-NMR spectroscopy, presumably because of rapid fructose dehydration. After 16 hours (*ca.* 1000 min) the glucose is almost completely converted in both reactions, resulting in 5-HMF yields of 68.6% (**2**) and 89.1% ($CrCl_3(THF)_3$). At this stage it is seen that the $CrCl_3(THF)_3$ catalyst is both more active and selective than **2**, and hence provides both higher glucose conversions and higher selectivity towards 5-HMF formation as compared to **2**. During the reaction, the formed excess water in the reaction medium did not seem to notably alter catalyst performance, which is indicative of a level of catalyst robustness towards moisture. This is in contrast to the typically employed catalyst, $CrCl_2$, which spontaneously oxidise in solution having trace amounts of water.[13] Selectivity towards 5-HMF formation is lowered in the dehydration step where condensation reactions of pre-formed fructose intermediates led to the formation of humin-type side products.[8] This was evidenced by the gradual appearance of ^{1}H-NMR signals at δ_H 3.81 (s), 4.46 (s), 7.38 (s), 8.10 (s), and 9.21 (s) ppm. Formation of levulinic and formic acid are excluded due to the absence of characteristic ^{1}H-NMR signals.[3,6] An increase in temperature led to more rapid 5-HMF formation, although signs of 5-HMF degradation appeared for temperatures higher than 120°C. Longer reaction times did not notably increase 5-HMF yields, which is ascribed to eventual catalyst deactivation and include the preferential formation of decomposition products at elevated temperatures for extended periods of time.[5] The decomposition products that formed are most likely humins, as evidenced by the darkening of the reaction mixture.[11]

Following 16 hours reaction time, final conversions of 72% (**1**), 69% (**2**), 76% (**3**), 60% (**4**), 52% (**5**), and 81% (**6**) were achieved. Comparing the activities of the NHC-containing Cr(III) complexes and the Cr(III) complex salt, the latter was more active. Although a decrease in Lewis acidity of the catalyst is expected to decrease the conversion of glucose to 5-HMF,[11] three potential reaction sites within complex **6**, whereas only two exist within complexes **1**-**5**. The additional chloride ions help mediate Lewis-acid-promoted protonation/deprotonation reactions during the isomerisation reactions, as well as help fill the octahedral Cr(III) coordination sphere

and thereby stabilising the catalytically active chromium species. Addition of LiCl as a chloride anion source to a reaction using **2** only slightly improved the 5-HMF yield over a period of 16 hours, although a lowering in 5-HMF yield selectivity is observed. Among the Cr(III)-NHC complexes **1**-**5**, complexes **1** and **3** were the most active by virtue of lower steric bulk of the NHC ligand, which is in favour of the steric requirements for incoming pyranose-like substrates. Increased flexibility of the NHC ligands in **4** and **5** did not seem to compensate for the increased steric bulk of the ligands, and were therefore the least active of the NHC-featured catalysts.



(a) (b)

Figure 11: (a) Time-resolved profile for (+)-D-glucose conversion using complexes **1**-**6** as catalysts. (b) Time-resolved profile for 5-HMF formation using complexes **1**-**6** as catalysts. General conditions: (+)-D-glucose (0.11 mmol), [Cr] (6 mol%), DMSO (4 mL), anisole (0.11 mmol), 120°C.

The final 5-HMF yields for catalysts **1**-**6** are 37% (**1**), 68% (**2**), 36% (**3**), 56% (**4**), 48% (**5**), and 76% (**6**), respectively. Here, too, complex **6** performed the best with the highest 5-HMF selectivity achieved. Interestingly, among the Cr(III)-NHC catalysts, complexes **2** and **4** were the most selective towards 5-HMF formation. It appears as if increased NHC steric bulk assists with the favourable 5-HMF-selectivity of the reaction, albeit a lowering in overall conversion. The high 5-HMF yield obtained using complex **2** could also be ascribed to the higher rate of fructose

dehydration. During the rapid process of fructose dehydration, the relative concentrations of fructose intermediate species remain low, which helps to limit bimolecular condensation reactions from which humins are formed.[6]

3. Experimental

3.1 General considerations

All experiments were carried out under an argon atmosphere using standard Schlenk techniques. Solvents were dried prior to use using standard techniques.[27] Column chromatography was carried out under inert argon atmospheres using silica gel (particle size 0.063-0.200 mm) as the stationary phase. The imidazolium bromide ligands [H(**L1**-**L6**)]Br (**L1** = Im(Me)(Bn), **L2** = $Im(Bn)_2$, **L3** = $Im(Me)(C_2H_4Ph)$, **L4** = $Im(C_2H_4Ph)_2$, **L5** = $Im(Bn)(C_2H_4Ph)$, and **L6** = $Im(Me)(4\text{-}NO_2Bn)$ were synthesised according to literature reports.[28] $CrCp_2$ was synthesised according to the published procedure[29] and used immediately due to its pyrophoric nature. All other chemicals were purchased from Sigma-Aldrich and used without further purification. Infrared (IR) spectra were recorded on a Perkin Elmer Spectrum RXI FT-IR spectrophotometer as potassium bromide pellets. UV-Vis measurements were performed on an Analytic Jena Specord 200 Plus Double Beam UV/Vis spectrophotometer using CH_2Cl_2 solutions. Mass spectra were recorded on a SYNAPT G2 HDMS instrument, using electrospray ionisation as the ion source and a time-of-flight mass analyser. A sampling time of 3 minutes was used, with the direct infusion inlet method.

3.2 General synthesis of [CpCrBrCl(NHC)] complexes

To a THF solution (30 mL) of chromocene (0.5 g, 2.7 mmol), the appropriate imidazolium bromide salt (2.7 mmol, 1 eq., [H(**L1**-**L6**)]Br) was carefully added after which the resulting mixture was stirred for 5 hours. The mixture was filtered under argon, to which CCl_4 (0.5 mL, 5.2 mmol) was added for an immediate colour change from purple to royal blue. The mixture

[27] R. J. Errington, Advanced Practical Inorganic and Metalorganic Chemistry, Blackie Academic & Professional, London, 1997.
[28] F. P. Malan, E. Singleton, P. H. van Rooyen, M. Landman, *J. Organomet. Chem.*, 2016, **813**, 7-14.
[29] R. B. King, Organometallic Syntheses: Vol. 1, Academic Press: New York, NY, 1965; pp 66-67.

was stirred for a further 5 minutes after which it was concentrated in vacuo, and subjected to silica gel column chromatography, using gradient elution with hexane/DCM. Concentration of the collected blue fractions to dryness gave deep blue powders.

*[CpCrBrCl{Im(Me)(Bn)}] (**1**)*

Yield: 72%. FT-IR (cm^{-1}): 3104 (ν(=CH), w), 3053 (ν(=CH), w), 3020 (ν(-CH), w), 2936 (ν(-CH), w), 1639 (ν(=CH), w), 1566 (m), 1493 (δ(-CH), sym, m), 1453 (δ(-CH), sym, s), 1413 (δ(-CH), asym, m), 1359 (δ(-CH), m), 1231 (ν(-CN), m), 1152 (w), 1077 (w), 1029 (w), 1015 (ν(CN), w), 817 (δ(=CH), m), 736 (δ(-CH), s), 702 (s), 562 (w). UV-Vis (DCM; λ_{max}, nm (ε, M^{-1} cm^{-1})): 574 (2133), 468 (565). CHN (%): [$C_{16}H_{17}BrClCrN_2$]: C, 45.92 (45.46), H, 4.22 (4.53), N, 6.32 (6.63). MS (ESI): m/z 367.9970 (**1**$^+$ - Cl), 324.0485 (**1**$^+$ - Br).

*[CpCrBrCl{Im(Bn)$_2$}] (**2**)*

Yield: 76%. FT-IR (cm^{-1}): 3126 (ν(=CH), w), 3087 (ν(=CH), w), 3025 (ν(-CH), w), 2980 (ν(-CH), w), 1603 (ν(=CH), w), 1566 (w), 1496 (δ(-CH), sym, m), 1454 (δ(-CH), sym, s), 1429 (δ(-CH), asym, w), 1413 (δ(-CH), asym, m), 1362 (δ(-CH), m), 1230 (ν(-CN), s), 1169 (w), 1029 (w), 1013 (ν(CN), m), 820 (δ(=CH), s), 731 (δ(-CH), s), 697 (s), 671 (m). UV-Vis (DCM; λ_{max}, nm (ε, M^{-1} cm^{-1})): 581 (1943), 471 (476). CHN (%): [$C_{22}H_{21}BrClCrN_2$]: C, 50.08 (50.19), H, 4.09 (4.17), N, 4.85 (5.15). MS (ESI): m/z 382.0137 (1$^+$ - Cl), 338.0672 (1$^+$ - Br). MS (ESI): m/z 444.0293 (**2**$^+$ - Cl), 400.0170 (**2**$^+$ - Br).

*[CpCrBrCl{Im(Me)(C$_2$H$_4$Ph)}] (**3**)*

Yield: 75%. FT-IR (cm^{-1}): 3221 (ν(=CH), w), 3098 (ν(=CH), w), 2936 (ν(-CH), w), 1631 (ν(=CH), s), 1564 (s), 1494 (δ(-CH), sym, m), 1452 (δ(-CH), sym, s), 1413 (δ(-CH), asym, m), 1357 (δ(-CH), m), 1214 (ν(-CN), s), 1155 (m), 1080 (w), 1032 (m), 1013 (ν(CN), m), 820 (δ(=CH), s), 752 (s), 705 (δ(-CH), s), 562 (s). UV-Vis (DCM; λ_{max}, nm (ε, M^{-1} cm^{-1})): 577 (2159), 473 (660). CHN (%): [$C_{17}H_{19}BrClCrN_2$]: C, 46.25 (46.17), H, 4.17 (4.41), N, 5.91 (6.19). MS (ESI): m/z 382.0137 (**3**$^+$ - Cl), 338.0672 (**3**$^+$ - Br).

*[CpCrBrCl{Im(C$_2$H$_4$Ph)$_2$}] (**4**)*

Yield: 69%. FT-IR (cm^{-1}): 3143 (ν(=CH), w), 3077 (ν(=CH), w), 3019 (ν(-CH), w), 2969 (ν(-CH), w), 2935 (ν(-CH), w), 1572 (w), 1493 (δ(-CH), sym, m), 1453 (δ(-CH), asym, s), 1429 (m), 1401 (w), 1351 (δ(-CH), m), 1225 (ν(-CN), s), 1192 (w), 1077 (w), 1010 (ν(CN), s), 869 (m), 853 (m), 816 (δ(=CH), s), 722 (s), 699 (s), 677 (m). UV-Vis (DCM; λ_{max}, nm (ε, M^{-1} cm^{-1})): 573 (2016), 466 (291). CHN (%): [$C_{24}H_{25}BrClCrN_2$]: C, 53.57 (53.38), H, 4.42 (4.75), N, 5.04 (5.08). MS (ESI): m/z 472.0513 (**4**$^+$ - Cl), 428.1137 (**4**$^+$ - Br).

*[CpCrBrCl{Im(Bn)(C$_2$H$_4$Ph)}] (**5**)*

Yield: 74%. FT-IR (cm^{-1}): 3103 (ν(=CH), m), 3053 (ν(=CH), w), 3025 (ν(-CH), w), 2930 (ν(-CH), w), 1666 (ν(=CH), m), 1600 (m), 1569 (m), 1496 (δ(-CH), sym, m), 1452 (δ(-CH), sym, s), 1410 (δ(-CH), asym, m), 1359 (δ(-CH), m), 1230 (ν(-CN), s), 1183 (w), 1077 (w), 1012 (ν(CN), m), 820 (δ(=CH), s), 737 (δ(-CH), s), 704 (s), 561 (w). UV-Vis (DCM; λ_{max}, nm (ε, M^{-1} cm^{-1})): 577 (2163), 478 (979). CHN (%): [$C_{23}H_{23}BrClCrN_2$]: C, 50.81 (50.80), H, 4.69 (4.41), N, 4.90 (4.98). MS (ESI): m/z 458.0424 (**5**$^+$ - Cl), 414.0928 (**5**$^+$ - Br).

*[C$_4$H$_7$N$_2$][CpCrBrCl$_2$] (**6**)*

In this case the green reaction mixture (after addition of imidazolium salt, [HIm(Me)(4-NO$_2$Bn)]Br, **L6**) turned turquoise upon addition of CCl_4. Yield: 58%. FT-IR (cm^{-1}): 3098 (ν(=CH), m), 3065 (ν(=CH), w), 2964 (ν(-CH), w), 2919 (ν(-CH), w), 2308 (ν(-CH), w), 2284 (ν(-CH), w), 1603 (m), 1521 (δ(-CH), sym, s), 1430 (δ(-CH), asym, s), 1346 (δ(-CH), s), 1262 (ν(-CN), w), 1183 (w), 1152 (w), 1105 (w), 1012 (ν(CN), s), 853 (s), 820 (δ(=CH), s), 716 (m), 610 (m). UV-Vis (DCM; λ_{max}, nm (ε, M^{-1} cm^{-1})): 648 (2871), 477 (898). CHN (%): [$C_9H_{12}BrCl_2CrN_2$]×0.2CH_3CN: C, 31.37 (31.33), H, 3.82 (3.52), N, 8.69 (8.48). MS (ESI): m/z 230.8668 (**6**$^+$ - Cl), 187.1221 (**6**$^+$ - Br).

3.3 General (+)-D-glucose dehydration procedure

To a round-bottom flask containing (+)-D-glucose (20 mg, 0.11 mmol), anisole (12 μL, 0.11 mmol), and chromium complex (10 mol%) was added DMSO (4 mL) and the subsequent reaction mixture was heated under reflux at 120°C for the time indicated. Aliquots (0.05 mL) of the reaction mixture taken at specified times were diluted with d^6-DMSO, and analysed by ^{1}H-

NMR through which conversions were determined relative to anisole as the internal standard. All yields are based on the average of at least two runs.

3.4 Cyclic voltammetry

Cyclic voltammetry measurements were performed using 0.002 or saturated mol.dm^{-3} solutions of the complexes in dry acetonitrile (Aldrich, Biotech grade, 99.93% purity, anhydrous, kept under argon) containing 0.1 mol.dm^{-3} tetra-*N*-butylammonium hexafluorophosphate [NBu_4][PF_6] (Fluka, electrochemical grade) as supporting electrolyte under a purified argon atmosphere at 25 ºC. A three electrode cell, with a glassy carbon (surface area = 7.07 × 10^{-6} m^2) working electrode, a Pt auxiliary electrode, and a Ag/Ag$^+$ (0.010 mol.dm^{-3} $AgNO_3$ in CH_3CN) reference electrode mounted on a Luggin capillary, was used. Successive experiments under identical experimental conditions revealed all redox potentials were reproducible within 10 mV. All reported potentials are referenced against the IUPAC suggested FcH/FcH$^+$ couple. Ferrocene exhibited a formal reduction potential of $E°'$ = 0.084 V vs. Ag/Ag$^+$, a peak separation of ΔEp = $E_{pa} - E_{pc}$ = 0.066 V, and i_{pa}/i_{pc} = 1.00, under our experimental conditions. E_{pa} (E_{pc}) = anodic (cathodic) peak potential and i_{pa} (i_{pc}) = anodic (cathodic) peak current. $E°'$ (Fc/FcH$^+$) = 0.400 V *vs.* NHE.

3.5 Computational details

All calculations were carried out using DFT in the gas phase using the Gaussian 09 program.[30] Different basis sets and functionals were used to confirm the spin state of the neutral, anion and cation of the Cr(III)-NHC complexes [CpCrBrCl(NHC)] (**1**–**5**). The functionals used include

[30] M. J. Frisch, G. W. Trucks, H. B. Schlegel, G. E. Scuseria, M. A. Robb, J. R. Cheeseman, G. Scalmani, V. Barone, B. Mennucci, G. A. Petersson, H. Nakatsuji, M. Caricato, X. Li, H. P. Hratchian, A. F. Izmaylov, J. Bloino, G. Zheng, J. L. Sonnenberg, M. Hada, M. Ehara, K. Toyota, R. Fukuda, J. Hasegawa, M. Ishida, T. Nakajima, Y. Honda, O. Kitao, H. Nakai, T. Vreven, J. A. Montgomery (Jr), J. E. Peralta, F. Ogliaro, M. Bearpark, J. J. Heyd, E. Brothers, K. N. Kudin, V. N. Staroverov, T. Keith, R. Kobayashi, J. Normand, K. Raghavachari, A. Rendell, J. C. Burant, S. S. Iyengar, J. Tomasi, M. Cossi, N. Rega, J. M. Millam, M. Klene, J. E. Knox, J. B. Cross, V. Bakken, C. Adamo, J. Jaramillo, R. Gomperts, R. E. Stratmann, O. Yazyev, A. J. Austin, R. Cammi, C. Pomelli, J. W. Ochterski, R. L. Martin, K. Morokuma, V. G. Zakrzewski, G. A. Voth, P. Salvador, J. J. Dannenberg, S. Dapprich, A. D. Daniels, O. Farkas, J. B. Foresman, J. V. Ortiz, J. Cioslowski, D. J. Fox, *Gaussian 09*, Revision D.01, Gaussian Inc., Wallingford CT, 2010.

CAM-B3LYP,[31] LC-BLYP,[32-35] M06-D3[36] (M06 with the D3 correction[37]) and B3LYP (Becke 1993 and Lee-Yang-Parr) hybrid functional[35,38] with the triple-ζ basis set 6-311G(d,p) basis set on all atoms. Additionally the following basis sets were used using the B3LYP functional: (i) triple-ζ basis set 6-311G(d,p) basis set on all atoms; (ii) triple-ζ basis set 6-311G(d,p) basis set was used for the lighter atoms (C, H, N, O, Cl), whereas the LANL2DZ basis set (corresponding to the Los Alamos Effective Core Potential plus DZ) [39] was used for Cr and Br atoms; (iii) triple-ζ basis set 6-311G(d,p) basis set was used for the lighter atoms (C, H, N, O, Cl), whereas the Stuttgart/Dresden (SDD) pseudopotential was used to describe the Cr and Br electronic cores, while the metal valence electrons were described using the def2-TZVPP basis set.[40] Adiabatic electron affinity (EA) and ionisation potential (IP) are calculated as the difference between the energy of the neutral complex (n electrons), and either the reduced (n + 1 electrons) or oxidised (n - 1 electrons) complexes.

*3.6 X-ray crystallography of **1-7***

Single crystal diffraction of compounds 1-7 were performed using Quazar multi-layer optics monochromated Mo Kα radiation (k = 0.71069 Å) on a Bruker D8 Venture kappa geometry diffractometer with duo Iμs sources, a Photon 100 CMOS detector and APEX II control software.[41] All X-ray diffraction measurements were performed at 150(1) K. Data reduction was performed using SAINT+[41] and the intensities were corrected for absorption using SADABS.[42]

[31] T. Yanai, D. Tew, N. Handy, *Chem. Phys. Lett.*, 2004, **393**, 51-57.
[32] B. Miehlich, A. Savin, H. Stoll, H. Preuss, *Chem. Phys. Lett.*, 1989, **157**, 200-206.
[33] H. Iikura, T. Tsuneda, T. Yanai, K. Hirao, *J. Chem. Phys.*, 2001, **115**, 3540-3544.
[34] A. D. Becke, *Phys. Rev. A*, 1988, **38**, 3098-3100.
[35] C. T. Lee, W. T. Yang, R. G. Parr, *Phys. Rev. B*, 1988, **37**, 785-789.
[36] Y. Zhao, D. G. Truhlar, *Theor. Chem. Acc.*, 2008, **120**, 215-241.
[37] S. Grimme, J. Antony, S. Ehrlich, H. Krieg, *J. Chem. Phys*., 2010, 132, 154104-154122.
[38] A. D. Becke, *J. Chem. Phys.*, 1993, **98**, 5648-5652.
[39] (a) T.H. Jr. Dunning, P.J. Hay, in *Modern Theoretical Chemistry*, (Ed. H.F. Schaefer III), Vol. 3, Plenum, New York, 1976. (b) P. J. Hay, W. R. Wadt, *J. Chem. Phys.*, 1985, **82**, 270-283. (c) P. J. Hay, W. R. Wadt, *J. Chem. Phys.*, 1985, **82**, 284-298. (d) P. J. Hay, W. R. Wadt, *J. Chem. Phys.*, 1985, **82**, 299-310.
[40] F. Weigend, R. Ahlrichs, *Phys. Chem. Chem. Phys.*, 2005, **7**, 3297-3305.
[41] APEX2 (including SAINT and SADABS), Bruker AXS Inc., Madison, WI, 2012.
[42] G. M. Sheldrick, SHELXL96, Program for the Refinement of Crystal Structures, University of Göttingen, Germany, 1996.

All structures were solved by direct methods with SHELXS-97[43] using the SHELXL-2014/7[44] interface. All H atoms were placed in geometrically idealised positions and constrained to ride on their parent atoms. For data collection and refinement parameters, see Supplementary Information.

4. Conclusion

A range of five air stable (solid state) heterohalo cyclopentadienyl Cr(III)-NHC complexes (**1**-**5**) have been synthesised and characterised, as well as an imidazolium Cr(III) complex salt by-product (**6**). The complexes **1**-**6** are electrochemically oxidised to Cr(IV) at potentials +0.74-0.86 V, and irreversibly reduced to Cr(II) at potentials of between -1.25 and -1.83 V. All electrochemical events observed correlate to the DFT predicted electrochemical events. One electron oxidation as well as reduction processes were both metal-based. Complexes **1**-**6** act as active glucose dehydration catalysts to form 5-HMF in moderate to good yields. In this respect, they compare well with the first half-sandwich chromium catalysts used in this model catalytic reaction.

Acknowledgements

This work has received support from the Norwegian Supercomputing Program (NOTUR) through a grant of computer time (Grant nr. NN4654K) (JC), the South African National Research Foundation (JC Grant nr. 96111, ML Grant nr. 93638, FPM Grant nr. 88594) and the Central Research Fund of the University of the Free State, Bloemfontein (JC) and the University of Pretoria (ML). The High Performance Computing facility of the UFS is acknowledged for computer time.

[43] G. M. Sheldrick, *Acta Cryst.*, 2008, **A64**, 112.
[44] G. M. Sheldrick, *Acta Cryst.*, 2015, **C71**, 3-8.

CHAPTER 7

Tandem transfer hydrogenation-epoxidation of ketone substrates catalysed by normal alkene-tethered Ru(II)-NHC complexes

Chapter 7 contains work that has been prepared for publication in Eur. J. Inorg. Chem.:

Authors: Frederick P. Malan, Eric Singleton, Petrus H. van Rooyen, Marilé Landman

Status: To be submitted

Contributions:

Frederick P. Malan: Author, synthesis, characterisation, crystallography, DFT study, catalytic study

Eric Singleton: Co-author, co-supervisor

Petrus H. van Rooyen: Co-author, crystallography

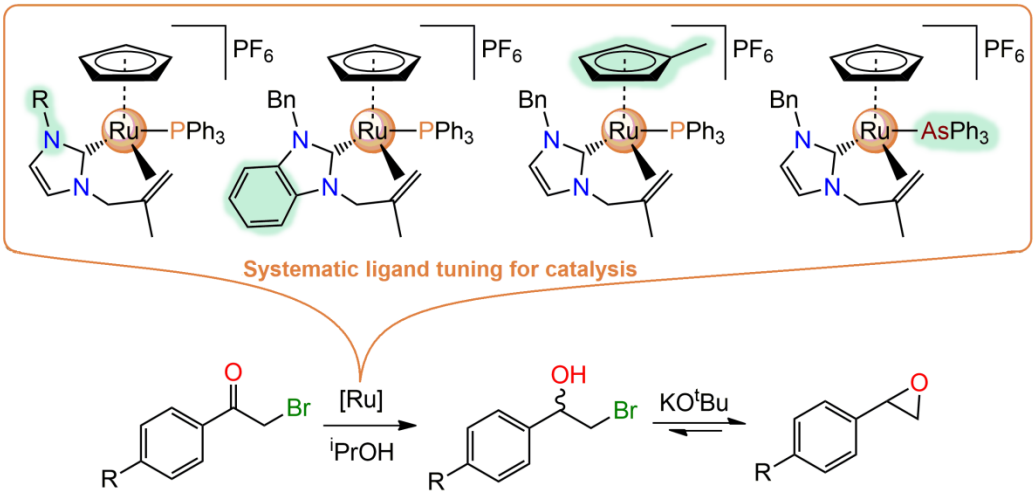
Marilé Landman: Corresponding author, supervisor

7 Tandem transfer hydrogenation-epoxidation of ketone substrates catalysed by normal alkene-tethered Ru(II)-NHC complexes

Frederick P. Malan,[†] Eric Singleton,[†] Petrus H. van Rooyen[†] and Marilé Landman[†*]

[†] Department of Chemistry, University of Pretoria, 02 Lynnwood Road, Hatfield, Pretoria, 0002, South Africa.

Graphical abstract



Abstract

A series of nine cyclopentadienyl Ru(II)-NHC complexes (**1**-**9**) have been synthesised by systematically varying the ligand and ligand substituents: C_5H_4R (R = H, Me), EPh_3 (E = P, As), NHC (Im, BIm), where NHC = Im(R)(R') (R, R' = Me, Bn, 4-NO_2Bn, C_2H_4Ph, C_4H_7). Each of the Ru(II)-NHC complexes features an *N*-alkenyl tether to furnish bidentate NHC ligands. All complexes found application as catalysts in the tandem transfer hydrogenation and epoxidation of carbonyl substrates. The $AsPh_3$-substituted Ru(II)-NHC, [CpRu($AsPh_3$)(**L2**)]PF_6 (**8**), proved most active and efficient (62% conversion, initial TOF = 12 h^{-1}), with the best selectivity (27%(alcohol):73%(epoxide)).

1. Introduction

Alkene epoxidation is recognised as an important reaction in organic synthesis, able to provide enantiopure epoxides, which are important precursors in amongst other, drug synthesis.[1] However, non-atom-economical oxidants such as alkyl hydroperoxides and hypochlorites are often employed in catalytic epoxidation reactions.[13(c)] Much less attention has been devoted to 'greener' oxygen-containing precursors, such as halohydrins. This is mainly because of the undesirable equilibrium that exists between the *vicinal* halohydrin and corresponding epoxide since the expelled mineral acid provides a nucleophilic halide to ring-open the formed epoxide. This problem could, however, be circumvented using acid scavengers or anion exchangers.[1] By making use of the tandem hydrogenation and epoxidation of the more readily available acyl halide precursors, a more efficient catalytic reaction could be devised. This would necessitate the use of highly versatile, transfer-hydrogenation active catalysts capable of withstanding deactivation under oxidative, acidic conditions.[2]

During the last two decades an increasing amount of impetus has been placed on harnessing the synthetic and catalytic advantages that two independent research areas combine: Highly stabilising *N*-heterocyclic carbenes (NHCs), and the hemilability of multi-dentate hybrid ligand systems when coordinated to transition metals.[3] NHCs constitute an ever-expanding ligand class capable of stabilising most transition metals in a range of different oxidation states.[4-6] In

[1] J. H. Schrittwieser, I. Lavandera, B. Seisser, B. Mautner, J. H. Lutje Spelberg, W. Kroutil, *Tetrahedron: Asymmetry*, 2009, **20**, 483-488.
[2] (a) D. Wang, D. Astruc, *Chem. Rev.*, 2015, **115**, 6621-6686. (b) R. H. Crabtree, *Chem. Rev.*, 2015, **115**, 127-150. (c) S. Saha, M. Kaur, K. Singh, J. K. Bera, *J. Organomet. Chem.*, 2016, **812**, 87-94.
[3] (a) F. E. Hahn, A. R. Naziruddin, A. Hepp, T. Pape, *Organometallics*, 2010, **29**, 5283-5288. (b) P. Braunstein, F. Naud, *Angew. Chem. Int. Ed.*, 2001, **40**, 680-699. (c) L. Benhamou, J. Wolf, V. César, A. Labande, R. Poli, N. Lugan, G. Lavigne, *Organometallics*, 2009, **28**, 6981-6993. (d) D. Pugh, A. A. Danopoulos, *Coord. Chem. Rev.*, 2007, **251**, 610-641. (e) F. E. Fernández, M. C. Puerta, P. Valerga, *Inorg. Chem.*, 2013, **52**, 4396-4410.
[4] (a) M. Viciano, M. Feliz, R. Corberán, J. A. Mata, E. Clot, E. Peris, *Organometallics*, 2007, **26**, 5304-5314. (b) S. K. Gupta, J. Choudhury, *Chem. Commun.*, 2016, **52**, 3384-3387. (c) E. Peris, *Chem. Rev.*, 2017, DOI: 10.1021/acs.chemrev.6b00695. (d) V. Leigh, D. J. Carleton, J. Olguin, H. Mueller-Bunz, L. J. Wright, M. Albrecht, *Organometallics*, 2014, **53**, 8054-8060.
[5] (a) M. J. Bitzer, F. E. Kühn, W. Baratta, *J. Catal.*, 2016, **338**, 222-226. (b) F. Hackenberg, H. Müller-Bunz, R. Smith, W. Streciwilk, X. Zhu, M. Tacke, *Organometallics*, 2013, **32**, 5551-5560. (c) A. Kaiho,

addition, NHCs have been shown to act as 'smart' ligands, where their non-innocent, cooperative, switchable, and/or multi-functional properties are exploited in addition to the tailored electronic and steric environments they provide.[4] Bidentate NHCs featuring potentially hemilabile donor groups, capable of reversible dissociation from the metal centre, have stimulated the development thereof to include phosphine,[3(a)] pyrimidine,[7] ether,[8] thioether,[6(c)] carboxylate,[6(c)] indenyl,[9] oxazoline,[10] and pyridine moieties[11]. However, the alkene functional group as secondary donor group received much less attention, despite it featuring in one of the first classical donor NHC complexes synthesised.[3(d),12] To date, only Lavigne,[3(c)] Bera[2(c)] and Albrecht[6(c)] have successfully employed alkene-tethered NHCs in the synthesis of a total of four ruthenium-NHC complexes (Figure 1) for application in catalysis studies.

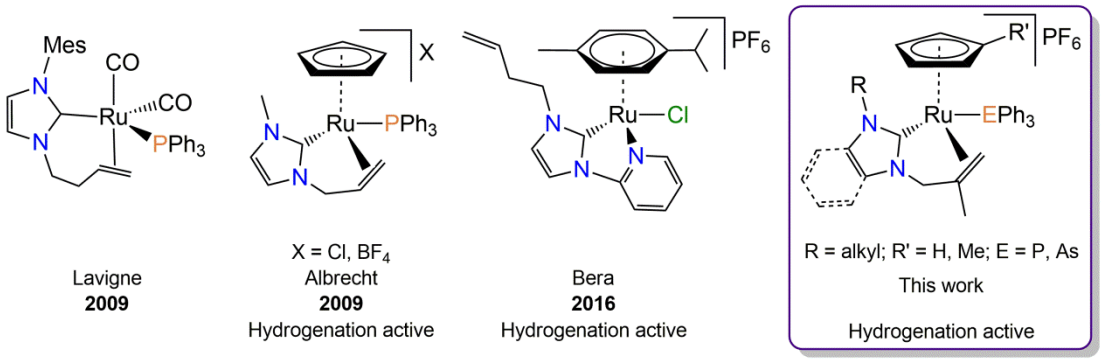


Figure 1: Previously reported alkene-functionalised Ru-NHC complexes, along with the new alkene-tethered Ru-NHC complexes of this study.

H. Suzuki, *Angew. Chem. Int. Ed.*, 2012, **51**, 1408-1411. (d) B. Hildebrandt, C. Ganter, *J. Organomet. Chem.*, 2012, **717**, 83-87.

[6] (a) J. B. Waters, J. M. Goicoechea, *Coord. Chem. Rev.*, 2015, **293-294**, 80-94. (b) T. Steinke, B. K. Shaw, H. Jong, B. O. Patrick, M. D. Fryzuk, J. C. Green, *J. Am. Chem. Soc.*, 2009, **131**, 10461-10466. (c) C. Gandolfi, M. Heckenroth, A. Neels, G. Laurenczy, M. Albrecht, *Organometallics*, 2009, **28**, 5112-5121.

[7] S. Warsink, I. Chang, J. J. Weigend, P. Hauwert, J. Chen, C. J. Elsevier, *Organometallics*, 2010, **29**, 4555-4561.

[8] D. J. Nielsen, K. J. Cavell, B. W. Skelton, A. H. White, *Organometallics*, 2006, **25**, 4850-4856.

[9] D. Takaki, T. Okayama, H. Shuto, S. Matsumoto, Y. Yamaguchi, S. Matsumoto, *Dalton Trans.*, 2011, **40**, 1445-1447.

[10] T. Makino, R. Yamasaki, I. Azumaya, H. Masu, S. Saito, *Organometallics*, 2010, **29**, 6291-6297.

[11] F. E. Fernández, M. C. Puerta, P. Valerga, *Organometallics*, 2012, **31**, 6868-6879.

[12] M. F. Lappert, *J. Organomet. Chem.*, 1988, **258**, 185-214.

The lack of research on potentially hemilabile bidentate NHC ligands as part of half-sandwich ruthenium complexes, prompted us to investigate possible stability and catalytic enhancement effects that these chelating NHC ligands may provide. Half-sandwich ruthenium complexes featuring NHCs are of special interest, given the rich synthetic and catalytic applications that they provide, especially with regards to transfer hydrogenation and epoxidation catalysis.[2(c),3(e),13] Here we report the synthesis of nine new alkene-tethered half-sandwich Ru(II)-NHC complexes, evaluate their application in tandem transfer hydrogenation-epoxidation catalysis, and relate the respective catalytic activities in a DFT study.

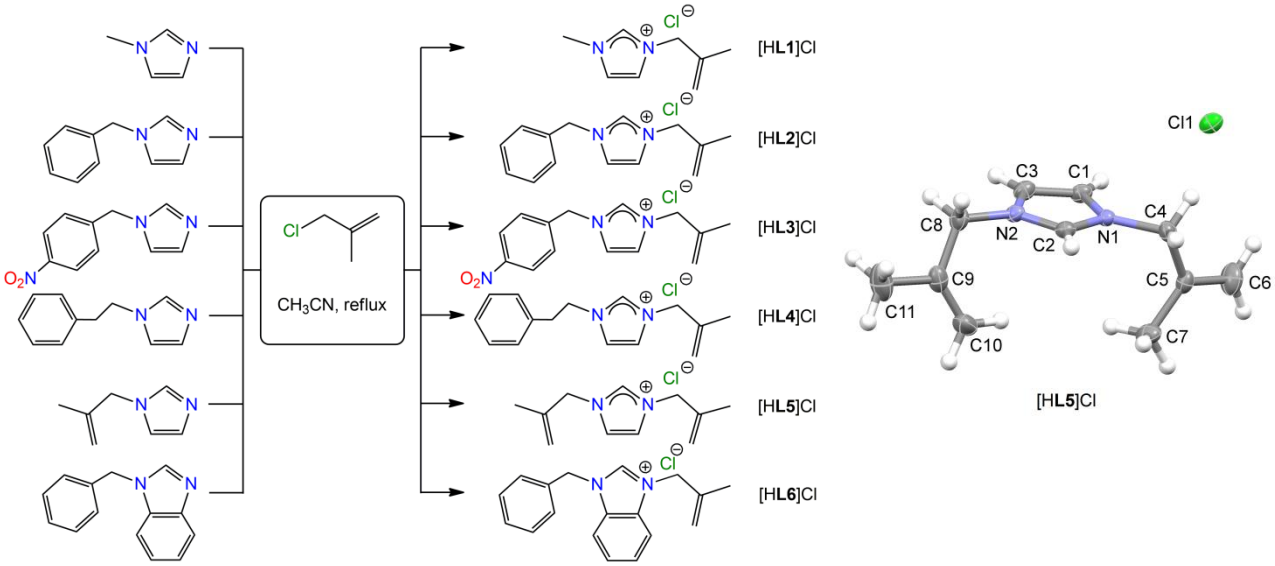
2. Results and Discussion

2.1 Synthesis of the NHC ligands and metal precursors

The NHC ligand precursors of this study were synthesised from *N*-substituted 3-chloro-2-methyl-propene imidazole (Scheme 1). Quarternisation reactions of the functionalised imidazole with the respective alkyl halides produce the corresponding alkene-tethered imidazolium chloride salts in excellent yields (94%, [H**L1**]Cl; 91%, [H**L2**]Cl; 67%, [H**L3**]Cl; 86%, [H**L4**]Cl; 88%, [H**L5**]Cl; 92%, [H**L6**]Cl). The purification of ligand precursors **L1**-**L6** comprised of concentration of the crude reaction mixtures and washing with ethyl acetate to remove unreacted starting material. This was followed by concentration *in vacuo* to give the pure imidazolium salts as white to light yellow crystalline solids or oils. The ^{1}H-NMR spectra of [H(**L1**-**L6**)]Cl all exhibited characteristic signals for the 2-methylpropenyl moiety: δ_H 1.39-1.73 ppm (singlet, methyl), 4.69-5.22 ppm (singlet, methylene protons), and 4.65-5.07 ppm (two singlets, alkene protons). The asymmetrical nature of the imidazolium salts resulted in two singlets for the imidazolium backbone protons ranging between δ_H 6.66-7.81 ppm ([H(**L1**-**L4**)]Cl, [H**L6**]Cl). The only symmetrical ligand precursor, [H**L5**]Cl, exhibited one singlet at δ_H 7.38 ppm (Scheme 1) for these two protons. The acidic C(2)-H proton signals for the salts [H(**L1**-**L6**)]Cl all varied between δ_H 9.40-10.82 ppm. This proton signal may additionally give insight into the respective

[13] (a) V. H. Mai, L. G. Kuzmina, A. V. Churakov, I. Korobkov, J. A. K. Howard, G. I. Nikonov, *Dalton Trans.*, 2016, **45**, 208-215. (b) E. Becker, V. Stingl, G. Dazinger, M. Puchberger, K. Mereiter, K. Kirchner, *J. Am. Chem. Soc.*, 2006, **128**, 6572-6573. (c) Y. Wang, L. Duan, L. Wang, H. Chen, J. Sun, L. Sun, M. S. G. Ahlquist, *ACS Catal.*, 2015, **5**, 3966-3972.

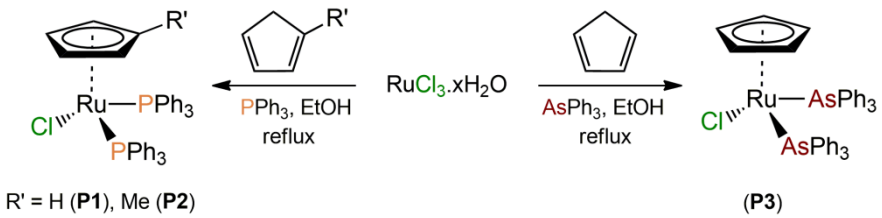
donor capacities of **L1**-**L6** as ligands in terms of proton affinity (PA): **L3** (δ_H 10.82 ppm) < **L5** (δ_H 10.62 ppm) < **L6** (δ_H 10.34 ppm) < **L2** (δ_H 10.14 ppm) ≈ **L4** (δ_H 10.06 ppm) < **L1** (δ_H 9.40 ppm). It is interesting to note that ligand precursors **L1**, **L2**, **L4**, and **L6** have similar donor capacities, while ligand precursors **L3** and **L5** are the least donating. The *N*-methyl imidazolylidene analogue **L1** is the most donating. There is some overlap with this trend when comparing the pseudo-carbenic C(2)-signals in the ^{13}C-NMR spectra: 144.3 ppm (**L6**), 143.4 ppm (**L3**), 139.5 ppm (**L1**), 138.3 ppm (**L5**), 137.4 (**L4**), 136.9 (**L2**).



Scheme 1: Synthesis of ligand precursors [H(**L1**-**L6**)]Cl from the corresponding *N*-functionalised imidazoles. Insert: Perspective view of [H**L5**]Cl. Thermal ellipsoids are drawn at 50% level. The omission of one molecule of H_2O has been done for clarity purposes.

The half-sandwich precursors **P1**-**P3** were synthesised according to a modified version of the literature procedure (Scheme 2). In this modified procedure, an ethanolic solution of $RuCl_3.xH_2O$ is reacted with 2.5 equivalents of the respective pnictogen EPh_3 (E = P, As), and excess (> 2 equivalents) of the respective cyclopentadiene C_5H_4R' (R' = H, Me). Reaction mixtures were allowed to heat under reflux overnight, which upon cooling allowed for the orange $[(C_5H_4R')RuCl(EPh_3)_2]$ (R' = H, Me; E = P, As; **P1**-**P3**) complexes to precipitate. The solid-state molecular structures of **P2** and **P3** are similar in that both assume the classical piano-stool structure with Ru1-Cg = 1.844(3) (**P2**), 1.813(4) (**P3**) (Cg = centroid of Cp ring); as well as Ru1-

E1 = 2.3222(7) (**P2**, E = P), 2.4229(2) (**P3**, E = As). The latter lengths correspond well with related $CpRuCl(PPh_3)_2$ complexes.[14 (b)]



Scheme 2: Synthesis of the ruthenium(II) precursors **P1**-**P3**.

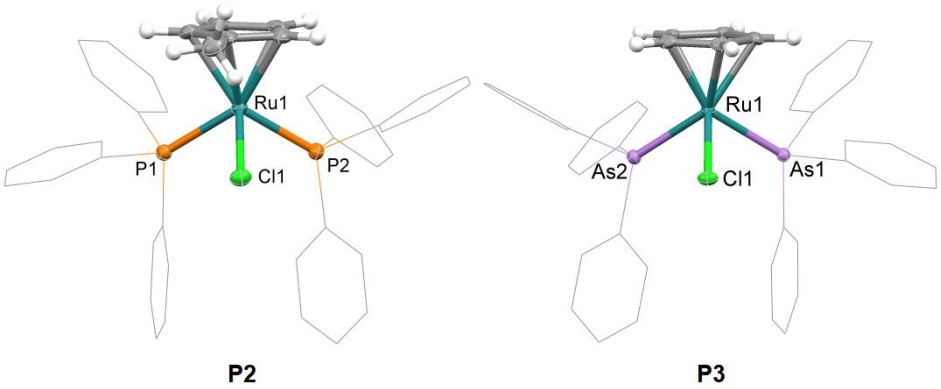
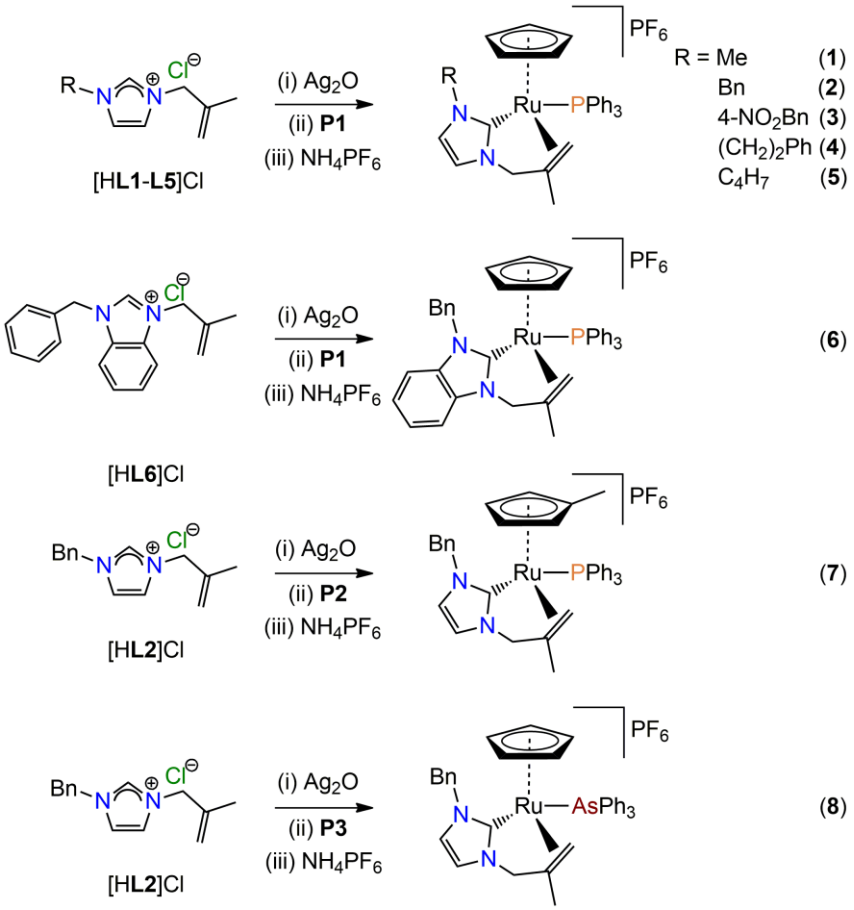


Figure 2: Perspective views of ruthenium precursors **P2** and **P3**. Thermal ellipsoids are drawn at 50% level. The phenyl moieties of the pnictogen moieties have been shown as wireframe presentations, as well as the omission of one molecule of CH_2Cl_2 within each structure have been done for clarity purposes.

2.2 Synthesis of the Ru(II)-NHC complexes

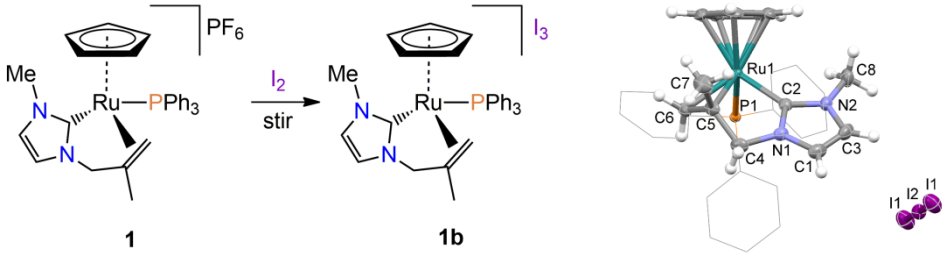
Each of the ligand precursors [H(**L1**-**L6**)]Cl contains an *N*-alkenyl substituent to promote metallation at the normal position of the NHC due to the chelate effect. Ruthenation was carried out using standard literature procedures[2(c),6(c)] which involves reaction of the imidazolium salt with Ag_2O, with the exclusion of light. A biscarbene silver complex is formed, to which the appropriate half-sandwich ruthenium(II) precursor is added *in situ* (Scheme 3). Complexes **1**-**6** resulted from the reaction of ligand precursors [H(**L1**-**L6**)]Cl with $[CpRuCl(PPh_3)_2]$ (**P1**) respectively *via in situ* silver transmetallation, followed by anion exchange with NH_4PF_6 in acetone.



Scheme 3: Syntheses of complexes **1**-**8** from the respective Ru(II) precursors **P1**-**P3**, and ligand precursors [H(**L1**-**L6)]Cl**.

After purification, complexes **1**-**6** were obtained as air and light stable, yellow to dark yellow solids. The yields of complexes **1**-**6** (after purification) were moderate (46-66%), with **3** being the lowest. The decreased reactivity of [H**L3**]Cl is ascribed to the presence of a 4-NO_2Bn moiety on the NHC ligand which renders the ligand less donating than the others. Reactions of [HIm(Bn)(C_4H_7)]Cl (**L2** precursor) with [(C_5H_4R')RuCl(EPh_3)$_2$] (R' = Me, E = P, **P2**; R' = H, E = As, **P3**) in a similar fashion gave solids of **7** (43 %, dark yellow) and **8** (62 %, brown), respectively. Spectroscopic evidence of NHC-coordination for **1**-**8** was obtained from their NMR spectra: Disappearance of the ^{1}H-NMR signal of [H**L1**-**L6**]Cl corresponding to the C(2)-H proton between δ_H 9.40-10.82 ppm, along with the concomitant appearance of the ^{13}C-NMR carbene signal between δ_C 172.9-178.2 ppm were noticed. ^{1}H-NMR signals for the cyclopentadienyl (**1**-**6**, **8**) and methylcyclopentadienyl (**7**) moieties generally appeared in an

equimolar ratio to the respective ligand **L1**-**L6**. Interestingly, other general NMR features include upfield shifts of the *N*-alkyl signals, where for example shifts from δ_H 3.89 ppm (**L1**) to 3.85 ppm (**1**); 4.83 ppm (**L2**) to 4.24 ppm (**2**), and 4.79 ppm (**L3**) to 4.64 ppm (**3**), have been observed. In addition, upfield shifts of the C(4)-H and C(5)-H protons in **L1**-**L5** after complexation have been observed, with the shift of **L1** being the most notable: an upfield shift occurs from δ_H 7.74 and 7.81 ppm (**L1**) to 6.91 and 6.99 ppm (**3**) respectively. This is indicative of a significant degree of electron density perturbation on the C(4) and C(5) carbon atoms after complexation due to higher electron density on the C(2) position. The signal relating to the PPh_3 ligand in the ^{31}P-NMR spectra of complexes **1**-**8** resided in a narrow region between δ_P 6.66-7.81 ppm. ^{1}H-NMR signals for the alkenyl moiety were in general similar for complexes **1**-**8**: the methyl protons resonated between δ_H 1.46-1.91 ppm, the unsymmetrical alkene protons between δ_H 3.68-4.50 and 4.14-4.97 ppm, and the methylene protons between δ_H 4.24-5.61 ppm. In complex **5** containing both free and bound *N*-alkenyl moieties, signals pertaining to the bound tether were observed to resonate more downfield as compared to the free tether which has little to no interaction with the metal centre. Negligent shifts of these signals were observed when recorded at variable temperatures (-5 to +30°C), suggesting a low degree of fluxionality of the tether in solution.



Scheme 4: Reaction of **1** with I_2 to form **1b**. Inset: Perspective view of **1b**. Thermal ellipsoids are drawn at 50% level. The phenyl moieties of PPh_3 have been shown as wireframe presentations for clarity purposes.

In an attempt to further probe the hemilability and subsequent reactivity of the *N*-alkenyl moiety, C=C bond cleavage *via* halogenation were attempted. Reaction of a DCM solution of **1** with slight excess of I_2 resulted in an anion exchange with PF_6^- to form the complex

[CpRu(PPh$_3$){Im(Me)(C$_4$H$_7$)}]I$_3$ (**1b**, Scheme 4). Furthermore, no reaction was observed after heating the sample for several hours. This indicates a level of robustness in the Ru-alkene bond, and hence a lower degree of hemilability that exists in solution than originally anticipated.

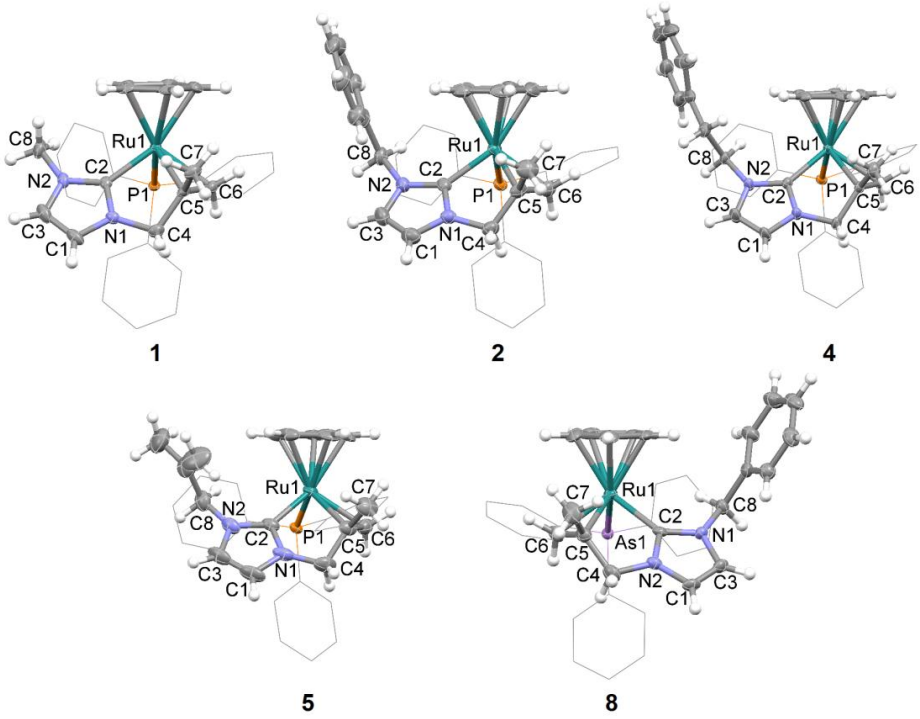


Figure 3: Perspective views of Ru(II)-NHC complexes **1**, **2**, **4**, **5**, and **8**. Thermal ellipsoids are drawn at 50% level. For clarity purposes, the phenyl moieties of the pnictogen moieties have been shown as wireframe presentations, as well as the omission of one molecule of PF_6 within each structure, including the omission of one molecule of CH_2Cl_2 (**2** and **8**).

The proposed molecular structures of the Ru-NHC complexes were supported by SCXRD studies from which C(2)-carbene coordination for complexes **1**, **2**, **4**, **5**, **8** and **1b** were confirmed (Figure 3, Scheme 4). All of the half-sandwich Ru(II) complexes assumed pseudo three-legged piano stool structures, where the η^2-alkene moiety is considered as one leg.[2(c),6(c)] Selected bond lengths and angles are summarised in Table S4 in the Supplementary Information. If chelation of the alkene-tether in complexes **1**-**4** is considered to form pseudo-five membered ruthenacyles, the resulting acute bite angles are almost identical for all complexes, and varies between 89.38(1)° (**8**) and 89.71(1)° (**4**). While the tether and imidazolium planes are essentially co-planar in related five-membered metallacycles,[6(c)] the alkene-containing complexes exhibit

anticlinal torsion angles of either between 24.7(3)° and 28.3(3)° (**1**, **2**, **4**, **5**), or -22.6(7) (**8**) and -26.8(3) (**1b**). It is also interesting to note that the Ru-C(2) bond distances of the complexes have a narrow distribution which fall between 2.033(2) Å (**1**) and 2.042(2) Å (**2**), which is indicative of the slight electronic effect the different NHC ligands have on the Ru-NHC bond. However, the Ru-C bond distances are in good agreement with similar Ru-C bond distances of related normally bound Ru(II)-NHC complexes.[6(c),13(a),14]

2.3 Catalysis studies

The ability of catalysts to mediate tandem reactions are highly attractive since multistep transformations allow for the minimisation of follow-up batch reactions, employment of less catalyst(s), and a rapid increase in molecular complexity from readily available starting material.[15] Transfer hydrogenation in particular has been widely studied by numerous groups over the years, although the added benefits of employing metal-NHC complexes as catalysts were only realised in the last two decades.[2(a)] Very few studies have been concerned with the functionalisation of post-hydrogenation products. We were therefore interested in the base-mediated epoxidation of the formed halohydrins as a secondary reaction. Complexes **1**-**8** were all transfer hydrogenation active, as have been found with numerous other reported half-sandwich Ru(II) complexes.[11,16] Standard conditions were employed, *i.e.* excess isopropanol as a hydrogen donor, base (KOH/KO^{t}Bu) as activator, and 4'-bromophenacylbromide (BPAB) as substrate. ^{1}H-NMR analyses on reaction mixtures in the presence of anisole (internal standard) taken over a period of 18 hours suggested a tandem reaction, whereby after 18 hours a mixture of secondary alcohol (halohydrin) and the ring-closed epoxide products were observed. No induction time was observed for all reactions. All complexes except **3** showed similar activity, with initial TOFs of 8-12 h^{-1} (total conversion) were observed (determined after the first 15 minutes reaction time),

[14] (a) E. Becker, V. Stingl, G. Dazinger, K. Mereiter, K. Kirchner, *Organometallics*, 2007, **26**, 1531-1535. (b) V. Miranda-Soto, D. B. Grotjahn, A. L. Cooksy, J. A. Golen, C. E. Moore, A. L. Rheingold, *Angew. Chem. Int. Ed.*, 2011, **50**, 631-635.
[15] T. Suzuki, *Chem. Rev.*, 2011, **111**, 1825-1845.
[16] (a) J. DePasquale, M. Kumar, M. Zeller, E. T. Papish, *Organometallics*, 2013, **32**, 966-979. (b) F. E. Fernández, M. C. Puerta, P. Valerga, *Organometallics*, 2011, **30**, 5793-5802. (c) G. I. Nikonov, *Organometallics* **2016**, *35*, 943-949. (d) K. Y. Wan, M. M. H. Syng, A. L. Lough, R. H. Morris, *ACS Catal.*, 2017, **7**, 6827-6842. (e) A. G. Nair, R. T. McBurney, D. B. Walker, M. J. Page, M. R. D. Gatus, M. Bhadbhade, B. A. Messerle, *Dalton Trans.*, 2016, **45**, 14335-14342.

under typical conditions (Table 1). The latter TOFs compare poorly with some of the best-performing half-sandwich ruthenium-based catalysts,[16(a),17] where TOFs of up to 3003 h^{-1} have been reported. However, the TOFs of **1**-**8** fall within the lower range of related half-sandwich bidentate NHC-Ru(II) analogues.[11,16]

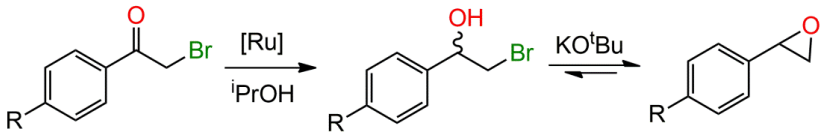
Chelation generally stabilises catalysts to render them more robust and therefore less prone to catalyst deactivation by means of catalyst poisons. However, chelation may also inhibit fast substrate conversion through the occupation of required vacant sites, and hence could reduce the overall yield.[18] This effect might be prevalent in the catalytic activities of **1**-**8**, where a slow transfer hydrogenation reaction of BPAB occurs during the initial few hours of reaction, followed by the concomitant epoxidation reaction of the alcohol substrate. After reaction optimisation (see Table S5 in the Supplementary Information), complexes **1**-**8** were screened for their catalytic activity. After two hours reaction time, complexes **1**, **2**, **4**, **5**, and **7** all exhibited comparable activity, having converted between 27% (**5**) and 34% (**1**) of substrate. Initial TOFs of the latter reactions vary between 8 and 12 h^{-1} (calculated after the first 15 minutes reaction time). Complex **3**, bearing the *N*-4-NO_2-benzyl NHC ligand, fared the worst, with a conversion of 23% (initial TOF = 4 h^{-1}). In contrast, the triphenylarsine functionalised complex **8** was the most active after two hours (37 % conversion, initial TOF = 12 h^{-1}). It is reasoned that generation of vacant coordination site(s) through reversible $AsPh_3$ and alkene dissociation is largely responsible for the slightly better performance. The efficiency of the transfer hydrogenation-epoxidation reaction was found to be temperature and base-dependent. At room temperature, the reaction proceeds sluggishly (9% conversion after 18 hours). Without addition of a base, low (< 31 %) conversions were obtained. Furthermore, the low conversions obtained when using KOH as base necessitated the use of the stronger KO^tBu base, for which better conversions were obtained.

In general it is seen that the similar *N*-alkyl groups (methyl, benzyl, phenethyl) on the NHC ligand have little effect on the catalytic activity (entries 1, 2 and 4). The lower conversion of complex **5** is attributed to the secondary *N*-alkenyl group on the NHC ligand: the presence of a

[17] P. Kumar, R. K. Gupta, D. S. Pandey, *Chem. Soc. Rev.*, 2014, **43**, 707-733.
[18] M. Hollering, M. Albrecht, F. E. Kühn, *Organometallics*, 2016, **35**, 2980-2986.

potentially chelating group competes with substrate coordination once an available site on the ruthenium centre is generated. Furthermore, a slight steric effect may play a role, especially if an inner sphere mechanism is considered. Both *N*-alkyl and the backbone moiety of the NHC ligand may contribute to the overall steric bulk of the resulting Ru-NHC complex, for which complex **1** (*N*-Me) is sterically less demanding than **4** (*N*-$(CH_2)_2$Ph) or **6** (benzimidazole *vs.* imidazole). The resulting effect is seen in the final substrate conversions observed (60% (**1**) *versus* 55% (**4**) and 51% (**6**)). Electronic properties of the substrate marginally affected the conversions, *i.e.* more electron-donating substituents (H *versus* Br) resulted in slightly lower conversions (56%, entry 9). The presence of the electron-withdrawing *para*-bromide moiety (entries 1-8) appears to activate the carbonyl moiety due to resonance effects.

Table 1: Tandem transfer hydrogenation-epoxidation of BPAB using **1**-**8** as catalyst.



Entry	Complex	R	Conversion[a] (%)			Selectivity[b] (%, alc:epox)	TOF_{15}[c] (h^{-1})
			2h	6h	18h		
1	**1**	Br	34	52	60	35:65	12
2	**2**	Br	32	48	58	43:57	10
3	**3**	Br	23	36	39	62:38	4
4	**4**	Br	33	49	55	40:60	10
5	**5**	Br	27	43	45	38:62	8
6	**6**	Br	26	46	51	29:71	8
7	**7**	Br	29	48	52	38:62	10
8	**8**	Br	37	56	62	27:73	12
9[d]	**1**	H	29	49	56	41:59	10

General conditions: 4'-bromophenacylbromide (BPAB, 0.6 mmol), iPrOH (4 mL), base (1.2 eq.), anisole as internal standard (65 µL, 0.6 mmol), [Ru] (2 mol%), 110 °C. [a] Determined by ^{1}H-NMR, based on the average of at least two runs. [b] Selectivity (%): alc:epox = alcohol:epoxide. [c] Determined after the first 15 minutes reaction time, based total conversion. [d] Phenacylbromide (PAB, 0.6 mmol) is used as substrate.

A lack of selectivity is observed in the catalytic conversions using complexes **1**-**8**. It appears that the equilibrium between the halohydrin and corresponding epoxide lies towards the halohydrin during the initial two hours reaction time (69-84%(alcohol):17-31%(epoxide)). After about six hours reaction time, near equimolar amounts of the halohydrin and corresponding epoxide are observed (48-61%(alcohol):39-52%(epoxide)). A shift towards the formed epoxide is observed after 18 hours reaction time (27-43%(alcohol):57-73%(epoxide)).

2.4 DFT studies

In order to probe the stability, reactivity and subsequent catalytic applicability of complexes **1**-**8**, a DFT study of the frontier orbitals is presented (Figure 4). In Figure 4 the HOMO and LUMO representations, the energies of the HOMO and LUMO, as well as the corresponding energy gap (energy difference between the HOMO and LUMO) of all complexes are presented. In terms of the molecular orbitals, similarities among complexes **1**-**8** could be drawn: Precursor complexes **P1**-**P3** all exhibit a LUMO distributed mainly over the ruthenium centre with a minor contribution from the cyclopentadienyl ligand. The HOMO of **P1**-**P3** is uniquely positioned mainly on the pnictogen moieties.

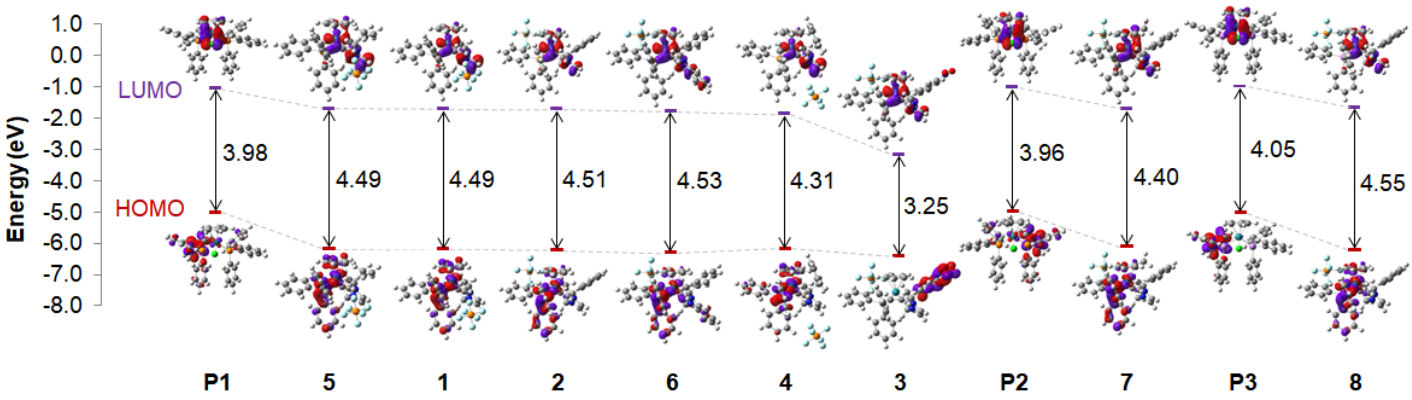


Figure 4: Frontier orbitals of the precursor complexes **P1**-**P3**, and CpRu-NHC complexes **1**-**8**. Representations are ordered according to descending LUMO energy (**1**-**8**) from the respective precursor (**P1**-**P3**).

After NHC-functionalisation, electron density within complexes **1**-**8** is altered such that the LUMO is distributed over the ruthenium and NHC ligand. This might be indicative of the Ru-

NHC bond being prone to reduction, especially in the presence of harsh reducing conditions. In contrast, the HOMO of all the complexes except complex **3** exhibit ruthenium and pnictogen character. The HOMO of complex **3** is exclusively positioned over the 4-NO_2-benzyl moiety of the NHC ligand. This may suggest that a future oxidation process could involve this moiety.

Upon reaction of **P1**, **P2** or **P3** with the respective NHC ligands, the corresponding HOMO and LUMO energies of **1**-**8** are lowered. This is indicative of the stabilisation effect the chelating NHC exerts on the resulting complex. Furthermore, the energy gaps of all complexes except **3** are larger by between 0.34-0.57 eV. The smallest energy gap of 3.25 eV (**3**) corresponds to the least stable (and more reactive) complex of complexes **1**-**8**.[19] This observation corresponds to the experimental catalytic activities of complexes **1**-**8**. Complex **3** being the least active complex, exhibits the smallest energy gap, is the least stable, and is therefore the most susceptible to fast catalyst deactivation. The energy gaps of the remainder of the complexes (4.31-4.55 eV) are comparable, and correspond to similar catalytic activities observed for these complexes. Relating to the Principle of Maximum Hardness (PMH) with respect to molecular orbital (MO) theory, the hardness of a molecule (η) is defined as half the energy gap between the HOMO and the LUMO of that molecule.[19(b)] A chemical system therefore is inclined to maximise the hardness of its respective molecules since a hard molecule tends to have a large(r) energy gap.[19(b)] Comparing the hardness of complexes **1**-**8**, all complexes ($2.16 \leq \eta \leq 2.27$) except complex **3** ($\eta = 1.63$) exhibit relatively hard character, and are therefore more robust against catalyst deactivation than complex **3**.

3. Experimental Section

3.1 General Procedures

All experiments were carried out under an argon atmosphere using standard Schlenk techniques. Solvents were dried and distilled from appropriate drying agents prior to use. The new imidazolium chloride ligands [H(**L1**-**L6**)]Cl, as well as the metal precursors [CpRuCl(PPh_3)$_2$]

[19] (a) S. Thangavel, S. Boopathi, N. Mahadevaiah, P. Kolandaivel, P. B. Pansuriya, H. B. Friedrich, *J. Mol. Catal. A.*, 2016, **423**, 160-171. (b) R. G. Pearson, *Acc. Chem. Res.*, 1993, **26**, 250-255.

(**P1**), [MeCpRuCl(PPh_3)$_2$] (**P2**), and [CpRuCl($AsPh_3$)$_2$] (**P3**) were synthesised and purified according to standard literature procedures.[20] All other chemicals were purchased from commercial suppliers and used without further purification. ^{1}H (300 MHz) and ^{13}C{H} (76 MHz) NMR spectra were recorded on a Bruker Avance-400 spectrometer using $CDCl_3$. All measurements were performed at ambient temperature (~296 K), unless otherwise noted. Chemical shifts were referenced to the internal residual solvent resonances. Microanalytical analyses (%CHNS) were obtained using a Thermo Scientific Flash 2000 elemental analyser fitted with a TCD detector. Electrospray mass spectra (ESI-MS) were recorded on a MicromassQuatro LC instrument.

*3.2 General synthesis of half-sandwich Ru(II)-NHC complexes (**1**-**8**)*

A suspension of the appropriate imidazolium chloride salt (4 mmol) in CH_2Cl_2 (30 mL) containing Ag_2O (0.93 g, 4 mmol) was stirred at 30°C for 12 hours in the absence of light. The mixture was filtered to which the appropriate half-sandwich Ru(II) precursor ([CpRuCl(PPh_3)$_2$] **P1**, [MeCpRuCl(PPh_3)$_2$] **P2**, or [CpRuCl($AsPh_3$)$_2$] **P3**, 4 mmol) was added and heated under reflux for 36 hours. The crude reaction mixture was filtered, concentrated *in vacuo* (5 mL), to which acetone (15 mL), and NH_4PF_6 (0.65 g, 4 mmol) was added. The reaction mixture was stirred for a further hour after which the mixture was evaporated *in vacuo*, and purified by silica gel column chromatography, using gradient elution with Et_2O/CH_2Cl_2. Yellow to dark-yellow solids were obtained.

[CpRu(PPh_3)(**L1**)]PF_6 (**1**): Yield: 66%. ^{1}H-NMR ($CDCl_3$, δ_H) 1.46 (s, CC*H*$_3$, 3H), 3.58 (s, NC*H*$_3$, 3H), 3.68 (s, =C*H*$_2$, 1H), 4.41 (s, =C*H*$_2$, 1H), 5.10 (s, C$_5$*H*$_5$, 5H), 5.61 (s, C*H*$_2$, 2H), 6.89 (s, NC*H*, 1H), 6.96 (s, NC*H*, 1H), 7.11-7.32 (m, C$_5$*H*$_6$, 15H). ^{13}C{^{1}H}-NMR ($CDCl_3$, δ_C) 19.5 (s, C*C*H$_3$), 34.8 (s, N*C*H$_3$), 53.4 (s, *C*H$_2$), 82.4 (s, *C*$_5$H$_5$), 115.2 (s, =*C*H$_2$), 120.8 (s, N*C*H), 123.7 (s, N*C*H), 127.5 (s, *C*$_6$H$_5$), 128.2 (s, *C*$_6$H$_5$), 128.3 (s, *C*$_6$H$_5$), 128.5 (s, *C*$_6$H$_5$), 129.3 (s, *C*$_6$H$_5$), 133.4 (s, *C*$_6$H$_5$), 135.4 (s, *ipso C*$_6$H$_5$), 137.5 (s, *C*CH$_3$), 177.0 (s, N*C*N). ^{31}P{^{1}H}-NMR ($CDCl_3$, δ_P) -

[20] (a) F. P. Malan, E. Singleton, P. H. van Rooyen, M. Landman, *J. Organomet. Chem.* **2016**, *813*, 7-14. (b) R. Fraser, P. H. van Rooyen, J. de Lange, I. Cukrowski, M. Landman, *J. Organomet. Chem.* **2017**, *840*, 11-22. (c) E. V. Gorbachuk, E. K. Badeeva, R. G. Zinnatullin, P. O. Pavlov, A. B. Dobrynin, A. T. Gubaidullin, M. A. Ziganshin, A. V. Gerasimov, O. G. Sinyashin, D. G. Yakhvarov, *J. Organomet. Chem.* **2016**, *805*, 49-53.

144.1 (sp, $^{1}J_{PF}$ = 713 Hz, *P*F_6), 57.2 (s, *P*Ph_3). CHN (%): [$C_{31}H_{32}F_6N_2P_2Ru$]×0.5C_3H_6O: C, 53.17 (52.85), H, 4.71 (4.78), N, 3.93 (3.79). MS (ESI): m/z 565.1344 (M^+).

[CpRu(PPh_3)(**L2**)]PF_6 (**2**): Yield: 58%. ^{1}H-NMR ($CDCl_3$, δ_H) 1.84 (s, CC*H*$_3$, 3H), 3.83 (s, =C*H*$_2$, 1H), 4.24 (s, C*H*$_2$, 2H), 4.63 (s, =C*H*$_2$, 1H), 4.81 (s, C_5H_5, 5H), 5.21 (s, C*H*$_2$, 2H), 6.83 (s, NC*H*, 1H), 6.91 (s, NC*H*, 1H), 7.04-7.23 (m, C_5H_6, 15H), 7.26-7.39 (m, C_5H_6, 5H). ^{13}C{^{1}H}-NMR ($CDCl_3$, δ_C) 15.2 (s, C*C*H$_3$), 53.4 (s, *C*H$_2$), 57.0 (s, *C*H$_2$), 87.5 (s, *C*$_5$H$_5$), 114.3 (s, =*C*H$_2$), 120.9 (s, N*C*H), 121.1 (s, N*C*H), 126.0 (s, *C*$_6$H$_5$), 127.9 (s, *C*$_6$H$_5$), 128.1 (s, *C*$_6$H$_5$), 128.7 (s, *C*$_6$H$_5$), 128.9 (s, *C*$_6$H$_5$), 129.0 (s, *C*$_6$H$_5$), 129.9 (s, *C*$_6$H$_5$), 133.3 (s, *C*$_6$H$_5$), 133.4 (s, *C*$_6$H$_5$), 133.5 (s, *ipso C*$_6$H$_5$), 133.7 (s, *ipso C*$_6$H$_5$), 142.3 (s, *C*CH$_3$), 176.0 (s, N*C*N). ^{31}P{^{1}H}-NMR ($CDCl_3$, δ_P) -144.1 (sp, $^{1}J_{PF}$ = 713 Hz, *P*F_6), 57.6 (s, *P*Ph_3). CHN (%): [$C_{37}H_{36}F_6N_2P_2Ru$]×0.5CH_2Cl_2: C, 54.54 (54.39), H, 4.42 (4.50), N, 3.17 (3.38). MS (ESI): m/z 641.1656 (M^+).

[CpRu(PPh_3)(**L3**)]PF_6 (**3**): Yield: 46%. ^{1}H-NMR ($CDCl_3$, δ_H) 1.48 (s, CC*H*$_3$, 3H), 4.28 (s, =C*H*$_2$, 1H), 4.64 (s, C*H*$_2$, 2H), 4.85 (s, =C*H*$_2$, 1H), 5.25 (s, C_5H_5, 5H), 5.61 (s, C*H*$_2$, 2H), 6.88 (s, NC*H*, 1H), 6.90 (s, NC*H*, 1H), 6.93-7.32 (m, C_5H_6, 15H), 7.69 (s, C_5H_4, 2H), 8.12 (d, $^{3}J_{HH}$ = 8 Hz, C_5H_4, 3H). ^{13}C{^{1}H}-NMR ($CDCl_3$, δ_C) 18.0 (s, C*C*H$_3$), 57.6 (s, *C*H$_2$), 59.6 (s, *C*H$_2$), 87.5 (s, *C*$_5$H$_5$), 119.7 (s, =*C*H$_2$), 123.9 (s, N*C*H), 124.1 (s, N*C*H), 128.0 (s, *C*$_6$H$_5$), 128.2 (s, *C*$_6$H$_5$), 128.6 (s, *C*$_6$H$_5$), 128.9 (s, *C*$_6$H$_5$), 129.1 (s, *C*$_6$H$_5$), 130.0 (s, *C*$_6$H$_5$), 130.5 (s, *C*$_6$H$_5$), 133.4 (s, *C*$_6$H$_5$), 133.6 (s, *C*$_6$H$_5$), 133.8 (s, *ipso C*$_6$H$_5$), 137.3 (s, *ipso C*$_6$H$_5$), 143.3 (s, *C*CH$_3$), 178.2 (s, N*C*N). ^{31}P{^{1}H}-NMR ($CDCl_3$, δ_P) -144.3 (sp, $^{1}J_{PF}$ = 713 Hz, *P*F_6), 57.1 (s, *P*Ph_3). CHN (%): [$C_{37}H_{35}F_6N_3O_2P_2Ru$]×0.5$H_2O$: C, 52.95 (52.92), H, 4.55 (4.32), N, 5.03 (5.00). MS (ESI): m/z 686.1208 (M^+).

[CpRu(PPh_3)(**L4**)]PF_6 (**4**): Yield: 55%. ^{1}H-NMR ($CDCl_3$, δ_H) 1.82 (s, CC*H*$_3$, 3H), 3.07 (t, $^{3}J_{HH}$ = 8 Hz, C*H*$_2$, 2H), 4.22 (s, =C*H*$_2$, 1H), 4.36 (t, $^{3}J_{HH}$ = 8 Hz, C*H*$_2$, 2H), 4.54 (s, =C*H*$_2$, 1H), 4.87 (s, C_5H_5, 5H), 6.89 (s, NC*H*, 1H), 6.94 (s, NC*H*, 1H), 7.03-7.20 (m, C_6H_5, 15H), 7.46-7.61 (m, C_6H_5, 5H). ^{13}C{^{1}H}-NMR ($CDCl_3$, δ_C) 15.3 (s, C*C*H$_3$), 32.7 (s, *C*H$_2$), 50.9 (s, *C*H$_2$), 56.3 (s, *C*H$_2$), 87.5 (s, *C*$_5$H$_5$), 114.2 (s, =*C*H$_2$), 121.3 (s, N*C*H), 122.9 (s, N*C*H), 127.0 (s, *C*$_6$H$_5$), 128.2 (s, *C*$_6$H$_5$), 128.4 (s, *C*$_6$H$_5$), 128.7 (s, *C*$_6$H$_5$), 129.0 (s, *C*$_6$H$_5$), 129.9 (s, *C*$_6$H$_5$), 130.5 (s, *C*$_6$H$_5$), 131.1 (s, *C*$_6$H$_5$), 133.1 (s, *C*$_6$H$_5$), 133.4 (s, *C*$_6$H$_5$), 133.7 (s, *ipso C*$_6$H$_5$), 133.9 (s, *ipso C*$_6$H$_5$), 137.5 (s,

CCH_3), 174.6 (s, N*C*N). $^{31}P\{^1H\}$-NMR ($CDCl_3$, δ_P) -144.2 (sp, $^1J_{PF}$ = 713 Hz, *P*F_6), 57.4 (s, *P*Ph_3). CHN (%): [$C_{38}H_{38}F_6N_2P_2Ru$]×0.5CH_2Cl_2: C, 54.59 (54.91), H, 4.40 (4.67), N, 3.15 (3.33). MS (ESI): m/z 655.1877 (M^+).

[CpRu(PPh_3)(**L5**)]PF_6 (**5**): Yield: 61%. ^{1}H-NMR ($CDCl_3$, δ_H) 1.54 (s, CC*H*$_3$, 3H), 1.91 (s, CC*H*$_3$, 3H), 3.61-3.71 (m, C*H*$_2$ + =C*H*$_2$, 3H), 3.85 (s, C*H*$_2$, 1H), 4.50 (s, =C*H*$_2$, 1H), 4.97 (s, =C*H*$_2$, 1H), 5.00 (s, C_5H_5, 5H), 5.27 (s, C*H*$_2$, 2H), 7.08 (s, NC*H*, 1H), 7.10 (s, NC*H*, 1H), 7.37-7.47 (m, C_6H_5, 12H), 7.51-7.67 (m, C_6H_5, 3H). $^{13}C\{^1H\}$-NMR ($CDCl_3$, δ_C) 20.1 (s, C*C*H$_3$), 31.0 (s, *C*H$_3$), 32.9 (s, *C*H$_2$), 55.8 (s, *C*H$_2$), 87.7 (s, *C*$_5$H$_5$), 112.1 (s, =*C*H$_2$), 114.3 (s, =*C*H$_2$), 121.1 (s, NC*H*), 124.7 (s, N*C*H), 128.3 (s, *C*$_6$H$_5$), 128.5 (s, *C*$_6$H$_5$), 128.8 (s, *C*$_6$H$_5$), 130.9 (s, *C*$_6$H$_5$), 132.1 (s, *C*$_6$H$_5$), 133.1 (s, *ipso C*$_6$H$_5$), 140.8 (s, *C*CH$_3$), 175.7 (s, N*C*N). $^{31}P\{^1H\}$-NMR ($CDCl_3$, δ_P) -144.2 (sp, $^1J_{PF}$ = 713 Hz, *P*F_6), 57.5 (s, *P*Ph_3). CHN (%): [$C_{34}H_{36}F_6N_2P_2Ru$]×0.25CH_2Cl_2: C, 53.70 (53.36), H, 4.59 (4.77), N, 3.63 (3.66). MS (ESI): m/z 605.1715 (M^+).

[CpRu(PPh_3)(**L6**)]PF_6 (**6**): Yield: 51%. ^{1}H-NMR ($CDCl_3$, δ_H) 1.54 (s, CC*H*$_3$, 3H), 4.32 (s, =C*H*$_2$, 1H), 4.42 (s, C*H*$_2$, 1H), 4.76 (s, =C*H*$_2$, 1H), 5.00 (s, C_5H_5, 5H), 5.27 (s, C*H*$_2$, 2H), 7.07 (s, =C*H*, 1H), 7.19 (s, =C*H*, 1H), 7.23 (s, =C*H*, 1H), 7.25 (s, =C*H*, 1H), 7.27-7.66 (m, C_6H_5, 20H). $^{13}C\{^1H\}$-NMR ($CDCl_3$, δ_C) 15.3 (s, C*C*H$_3$), 49.0 (s, *C*H$_2$), 53.5 (s, *C*H$_2$), 88.2 (s, *C*$_5$H$_5$), 110.6 (s, =*C*H), 110.9 (s, =*C*H), 118.7 (s, =*C*H$_2$), 127.0 (s, *C*$_6$H$_5$), 128.1 (s, *C*$_6$H$_5$), 128.5 (s, *C*$_6$H$_5$), 128.9 (s, *C*$_6$H$_5$), 129.5 (s, *C*$_6$H$_5$), 130.5 (s, *C*$_6$H$_5$), 132.0 (s, *C*$_6$H$_5$), 132.9 (s, *ipso C*$_6$H$_5$), 133.6 (s, *ipso C*$_6$H$_5$), 144.1 (s, *C*CH$_3$), 172.9 (s, N*C*N). $^{31}P\{^1H\}$-NMR ($CDCl_3$, δ_P) -144.2 (sp, $^1J_{PF}$ = 713 Hz, *P*F_6), 56.5 (s, *P*Ph_3). CHN (%): [$C_{41}H_{38}F_6N_2P_2Ru$]×0.9CH_2Cl_2: C, 55.19 (55.26), H, 4.25 (4.40), N, 2.95 (3.08). MS (ESI): m/z 691.1312 (M^+).

[MeCpRu(PPh_3)(**L2**)]PF_6 (**7**): Yield: 43%. ^{1}H-NMR ($CDCl_3$, δ_H) 1.28 (s, C*H*$_3$, 3H), 1.52 (s, CC*H*$_3$, 3H), 3.76 (s, =C*H*$_2$, 1H), 4.14 (s, =C*H*$_2$, 1H), 4.66 (s, C*H*$_2$, 1H), 4.83 (d, $^3J_{HH}$ = 8 Hz, C_5H_4, 2H), 5.03 (d, $^3J_{HH}$ = 8 Hz, C_5H_4, 2H), 5.18 (s, C*H*$_2$, 2H), 6.97 (s, NC*H*, 1H), 7.04 (s, NC*H*, 1H), 7.06-7.39 (m, C_6H_5, 15H), 7.45-7.66 (m, C_6H_5, 5H). $^{13}C\{^1H\}$-NMR ($CDCl_3$, δ_C) 11.2 (s, *C*H$_3$), 17.3 (s, C*C*H$_3$), 47.4 (s, *C*H$_2$), 56.1 (s, *C*H$_2$), 78.8 (s, *C*$_5$H$_4$), 81.7 (s, *C*$_5$H$_4$), 116.1 (s, =*C*H$_2$), 122.1 (s, NC*H*), 123.2 (s, N*C*H), 126.2 (s, *C*$_6$H$_5$), 127.9 (s, *C*$_6$H$_5$), 128.1 (s, *C*$_6$H$_5$), 128.2 (s, *C*$_6$H$_5$), 128.7 (s, *C*$_6$H$_5$), 129.1 (s, *C*$_6$H$_5$), 130.3 (s, *C*$_6$H$_5$), 131.7 (s, *C*$_6$H$_5$), 133.6 (s, *ipso C*$_6$H$_5$),

134.3 (s, *ipso* C_6H_5), 143.4 (s, CCH_3), 174.6 (s, N*C*N). $^{31}P\{^1H\}$-NMR ($CDCl_3$, δ_P) -144.2 (sp, $^1J_{PF}$ = 713 Hz, PF_6), 55.8 (s, PPh_3). CHN (%): $[C_{38}H_{38}F_6N_2P_2Ru]\times0.7CH_2Cl_2$: C, 54.06 (54.23), H, 4.51 (4.63), N, 3.49 (3.27). MS (ESI): m/z 655.1816 (M^+).

[CpRu($AsPh_3$)(**L2**)]PF_6 (**8**): Yield: 62%. ^{1}H-NMR ($CDCl_3$, δ_H) 1.86 (s, CCH_3, 3H), 3.72 (s, =CH_2, 1H), 4.39 (s, =CH_2, 1H), 4.48 (s, CH_2, 2H), 4.81 (s, C_5H_5, 5H), 5.05 (s, CH_2, 2H), 6.70 (s, NC*H*, 1H), 6.85 (s, NC*H*, 1H), 7.04-7.40 (m, C_5H_6, 20H). $^{13}C\{^1H\}$-NMR ($CDCl_3$, δ_C) 17.2 (s, CCH_3), 53.4 (s, CH_2), 61.1 (s, CH_2), 85.0 (s, C_5H_5), 114.2 (s, =CH_2), 122.2 (s, N*C*H), 124.1 (s, N*C*H), 127.4 (s, C_6H_5), 128.5 (s, C_6H_5), 128.6 (s, C_6H_5), 129.0 (s, C_6H_5), 129.2 (s, C_6H_5), 129.6 (s, C_6H_5), 130.8 (s, C_6H_5), 131.3 (s, C_6H_5), 133.6 (s, C_6H_5), 134.8 (s, *ipso* C_6H_5), 135.3 (s, *ipso* C_6H_5), 139.3 (s, CCH_3), 176.2 (s, N*C*N). $^{31}P\{^1H\}$-NMR ($CDCl_3$, δ_P) -144.2 (sp, $^1J_{PF}$ = 713 Hz, PF_6). CHN (%): $[C_{37}H_{36}F_6N_2AsPRu]\times0.5CH_3CN$: C, 53.35 (53.68), H, 4.58 (4.45), N, 4.24 (4.12). MS (ESI): m/z 685.1140 (M^+).

Synthesis of [CpRu(PPh_3)(**L1**)]I_3 (**1b**): To a solution of complex **1** (0.36 g, 0.5 mmol) in CH_2Cl_2 (30 mL) was added I_2 crystals (0.26 g, 1 mmol). The resulting mixture was stirred upon which an immediate darkening of the light yellow solution was observed. After 2 hours reaction time, the mixture was concentrated in vacuo, extracted with hexane (3 × 20 mL). The residue was taken up in CH_2Cl_2, passed through a pad of silica, and cooled. Dark yellow crystals formed overnight. Yield: 77%. ^{1}H-NMR ($CDCl_3$, δ_H) 1.46 (s, CH_3, 3H), 3.38 (s, NCH_3, 3H), 3.69 (d, $^3J_{HH}$ = 12 Hz, =CH_2, 1H), 3.80 (s, =CH_2, 1H), 5.11 (s, C_5H_5, 5H), 5.61 (s, CH_2, 2H), 6.90 (s, NC*H*, 1H), 7.06 (s, NC*H*, 1H), 7.37-7.45 (m, C_6H_5, 15H). $^{13}C\{^1H\}$-NMR ($CDCl_3$, δ_C) 19.4 (s, CCH_3), 34.9 (s, NCH_3), 53.4 (s, CH_2), 82.3 (s, C_5H_5), 115.1 (s, =CH_2), 120.8 (s, N*C*H), 123.3 (s, N*C*H), 127.5 (s, C_6H_5), 128.1 (s, C_6H_5), 128.3 (s, C_6H_5), 128.6 (s, C_6H_5), 129.3 (s, C_6H_5), 133.4 (s, C_6H_5), 134.4 (s, *ipso* C_6H_5), 142.8 (s, CCH_3), 176.9 (s, N*C*N). $^{31}P\{^1H\}$-NMR ($CDCl_3$, δ_P) 57.9 (s, PPh_3). MS (ESI): m/z 565.1344 (M^+).

3.3 Transfer hydrogenation catalysis

To a round-bottom flask containing the carbonyl substrate (0.6 mmol), base (1.2 equivalents), anisole (65 μL, 0.6 mmol), and ruthenium complex (2 mol%, 12 μmol) was added 2-propanol (4 mL) and the subsequent reaction mixture was heated under reflux at 110°C for the time

indicated. Aliquots (0.05 mL) diluted with $CDCl_3$ was analysed with ^{1}H-NMR through which conversions were determined relative to anisole as the internal standard. All yields are based on the average of at least two runs.

*3.4 X-ray crystallography of **L5**, **P2**, **P3**, **1**, **2**, **4**, **5**, **8**, and **1b***

Single crystal diffraction studies of the compounds were done using Quazar multi-layer optics monochromated Mo Kα radiation (k = 0.71073 Å) on a Bruker D8 Venture kappa geometry diffractometer with duo Iμs sources, a Photon 100 CMOS detector and APEX II control software.[21] X-ray diffraction measurements were performed at 150(2) K. Data reduction was performed using SAINT+[21] and the intensities were corrected for absorption using SADABS.[21] The structures were solved by direct methods using *SHELXT*,[22] using the *SHELXL-2014/7*[23] program. The non-hydrogen atoms were refined anisotropically. All H atoms were placed in geometrically idealised positions and constrained to ride on their parent atoms. For a table containing the data collection and refinement parameters, see Tables S1-S4 in the Supplementary Information.

4. Conclusion

Variation of the *N*-alkyl group of the NHC, the ancillary pnictogen ligand, and (substituted) cyclopentadienyl ligand, provided access to eight unique half-sandwich Ru(II)-NHC complexes. The NHC ligands of these complexes were tailored to feature an alkenyl-group to act as a hemi-labile group for catalysis purposes. Preliminary catalytic studies involving the tandem transfer hydrogenation and epoxidation of 4'-bromophenacylbromide suggest a low degree of hemilability provided by the alkenyl-tether. A slight electronic and steric effect of the NHC ligand of the catalysts was observed where the more donating and less sterically demanding NHC ligands proved more efficient. Furthermore, a slight activating effect has been observed for the 4'-Br moiety in the substrate, where lower conversions were recorded for the 4'-H substrate analogue.

[21] APEX2 (including SAINT and SADABS), Bruker AXS Inc., Madison, WI, **2012**.
[22] G. M. Sheldrick, *Acta Crystallogr., Sect. A.: Found. Adv.* **2015**, *A71*, 3-8.
[23] G. M. Sheldrick, *Acta Cryst*. **2015**, *C71*, 3-8.

Acknowledgements

This work has received support from the South African National Research Foundation (ML Grant nr. 93638, FPM Grant nr. 88594) and the Central Research Fund of the University of Pretoria (ML). Selected single crystal X-ray diffraction collections and further assistance by Mr. D. Liles are gratefully acknowledged.

CHAPTER 8

(De)hydrogenation catalysis by normal and abnormal alkene- and picolyl-tethered Ru(II)-NHC complexes

Chapter 8 contains work that has been prepared for publication in Organometallics:

Authors: Frederick P. Malan, Eric Singleton, Petrus H. van Rooyen, Marilé Landman, Martin Albrecht

Status: To be submitted

Contributions:

Frederick P. Malan: Author, synthesis, characterisation, crystallography, ^{1}H-NMR study, catalytic studies

Eric Singleton: Co-author, co-supervisor; Petrus H. van Rooyen: co-author, crystallography

Marilé Landman: Corresponding author, supervisor

Martin Albrecht: Corresponding author, host of research visit

8

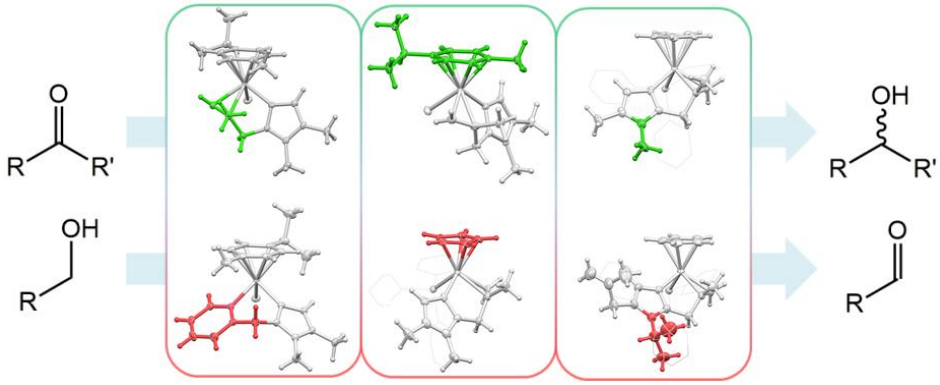
(De)hydrogenation catalysis by normal and abnormal alkene- and picolyl-tethered Ru(II)-NHC complexes

Frederick P. Malan,[†] Eric Singleton,[†] Petrus H. van Rooyen,[†] Marilé Landman[†*] and Martin Albrecht[‡*]

[†] *Department of Chemistry, University of Pretoria, 02 Lynnwood Road, Hatfield, Pretoria, 0002, South Africa.*

[‡] *Department of Chemistry and Biochemistry, Universität Bern, Freiestrasse 3, 3012 Bern, Switzerland.*

Graphical abstract



Abstract

A series of *p*-cymene and cyclopentadienyl Ru(II)-aNHC complexes have been synthesised employing either an *N*-alkene (**1**, **3**) or *N*-picolyl tether (**6**, **7**). The C(5)-Me protected alkene-tethered analogues (**2**, **4**) have also been synthesised. Ag-mediated C(2)-dealkylation was a prominent side reaction that led to the formation of normally bound Ru(II)-NHC complexes, which in selected cases have been isolated as the C(2)-bound Ru(II)-NHCs (**5**, **8**). A C(4)-Ru over C(2)-Ru site selectivity has been established by using a C(2)-iPr protecting group on the imidazolium precursor, for which unique *p*-cymene (**9**) and cyclopentadienyl (**10**) Ru(II)-aNHC derivatives have been synthesised. All complexes found dual application in the transfer hydrogenation of ketones and secondary alcohol oxidation, for which the *p*-cymene over the cyclopentadienyl Ru(II)-aNHC complexes, as well as the alkene- over the picolyl-containing Ru(II)-aNHC complexes, were the most active and efficient.

1. Introduction

N-heterocyclic carbenes (NHCs) remain a favorite choice of stabilising ancillary ligands to a variety of transition metals in a range of different oxidation states, due to their ability to exhibit both innocent and non-innocent behavior in metal-mediated transformation reactions.[1-3] NHCs are known to form some of the strongest M-C bonds,[4,5] and hence attempts have been directed towards the synthesis of highly electron-donating NHCs in order to better stabilise sensitive transition metal species, as well as to access high oxidation state metal species.[6,7] It has also been shown that C(4)/C(5)-bound imidazolylidenes (so-called abnormal NHCs or aNHCs) are significantly stronger donors as opposed to their classical C(2)-bound imidazolylidene counterparts (Figure 1).[1(a),8] The enhanced donor properties imparted by these aNHCs has been

[1] (a) H. Yoo, D. H. Berry, *Inorg. Chem.*, 2014, **53**, 11447-11456. (b) C. Pranckevicius, D. W. Stephan, *Chem. Eur. J.*, 2014, **20**, 6597-6602. (c) M. Viciano, M. Feliz, R. Corberán, J. A. Mata, E. Clot, E. Peris, *Organometallics*, 2007, **26**, 5304-5314. (d) S. K. Gupta, J. Choudhury, *Chem. Commun.*, 2016, **52**, 3384-3387. (e) M. R. Crittall, C. E. Ellul, M. F. Mahon, O. Saker, M. K. Whittlesey, *Dalton Trans.*, 2008, 4209-4211.

[2] (a) M. J. Bitzer, F. E. Kühn, W. Baratta, *J. Catal.*, 2016, **338**, 222-226. (b) F. Hackenberg, H. Müller-Bunz, R. Smith, W. Streciwilk, X. Zhu, M. Tacke, *Organometallics*, 2013, **32**, 5551-5560. (c) A. Kaiho, H. Suzuki, *Angew. Chem. Int. Ed.*, 2012, **51**, 1408-1411. (d) B. Hildebrandt, C. Ganter, *J. Organomet. Chem.*, 2012, **717**, 83-87.

[3] (a) J. B. Waters, J. M. Goicoechea, *Coord. Chem. Rev.*, 2015, **293-294**, 80-94. (b) T. Steinke, B. K. Shaw, H. Jong, B. O. Patrick, M. D. Fryzuk, J. C. Green, *J. Am. Chem. Soc.*, 2009, **131**, 10461-10466.

[4] (a) M. Heckenroth, E. Kluster, A. Neels, M. Albrecht, *Angew. Chem. Int. Ed.*, **2007**, **46**, 6293-6296. (b) A. Krüger, A. Neels, M. Albrecht, *Chem. Commun.*, 2010, **46**, 315-317. (c) P. Daw, R. Petakamsetty, A. Sarbajna, S. Laha, R. Ramapanicker, *J. Am. Chem. Soc.*, 2014, **136**, 13987-13990. (d) J. Witt, A. Pöthig, F. E. Kühn, W. Baratta, *Organometallics*, 2013, **32**, 4042-4045.

[5] (a) V. Leigh, W. Ghattas, R. Lalrempuia, H. Müller-Bunz, M. Albrecht, *Inorg. Chem.*, 2013, **52**, 5395-5402. (b) B. Hildebrandt, W. Frank, C. Ganter, *Organometallics*, 2011, **30**, 3483-3486.

[6] (a) V. Khlebnikov, M. Heckenroth, H. Müller-Bunz, M. Albrecht, *Dalton Trans.*, 2013, **42**, 4197-4207. (b) M. Hollering, M. Albrecht, F. E. Kühn, *Organometallics*, 2016, **35**, 2980-2986. (c) V. Leigh, D. J. Carleton, J. Olguin, H. Mueller-Bunz, L. J. Wright, M. Albrecht, *Inorg. Chem.*, 2014, **53**, 8054-8060. (d) Á. Vivancos, M. Albrecht, *Organometallics*, 2017, **36**, 1580-1590.

[7] (a) B. Hildebrandt, S. Raub, W. Frank, C. Ganter, *Chem. Eur. J.*, 2012, **18**, 6670-6678. (b) J. Ruiz, L. García, C. Mejuto, M. Vivanco, M. R. Díaz, S. García-Granda, *Chem. Commun.*, 2014, **50**, 2129-2132.

[8] (a) A. Prades, M. Viciano, M. Sanaú, E. Peris, *Organometallics*, 2008, **27**, 4254-4259. (b) L. Yang, A. Krüger, A. Neels, M. Albrecht, *Organometallics*, 2008, **27**, 3161-3171. (c) A. Petronilho, H. Mueller-Bunz, M. Albrecht, *J. Organomet. Chem.*, 2015, **775**, 117-123. (d) S. Saha, T. Ghatak, B. Saha, H. Doucet, J. K. Bera, *Organometallics*, 2012, **31**, 5500-5505. (e) S. Gründemann, A. Kovacevic, M. Albrecht, J. W. Faller, R. H. Crabtree, *Chem. Commun.*, 2001, **21**, 2274-2275. (f) A. R. Chianese, B. M. Zeglis, R. H. Crabtree, *Chem. Commun.*, 2004, **19**, 2176-2177.

shown to further enhance the catalytic efficiency of these metal complexes.[1(d),9,10] A range of different backbone- and *N*-functionalised aNHCs have been reported, for which the tunable donor properties have been shown to be significantly influenced by both the number and positions of heteroatoms within the heterocycle (Figure 1), with subsequent catalysis implications.[11,12] For example, the pronounced mesoionic character of the aNHC ligand allows for the usual carbene-type stabilisation when coordinated to low-valent electron-rich metal species, whereas mesoionic character may be dominant in electron-poor, high-oxidation state metal species.[13]

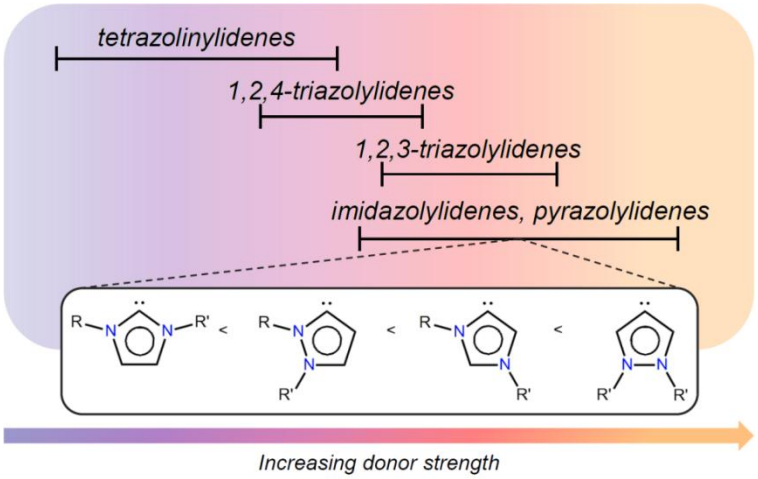


Figure 1: Order of donor strength of imidazolylidene and pyrazolylidene-based NHCs.

[9] (a) M. J. Bitzer, A. Pöthig, C. Jandl, F. E. Kühn, W. Baratta, *Dalton Trans.*, 2015, **44**, 11686-11689. (b) M. Heckenroth, A. Neels, M. G. Garnier, P. Aebi, A. W. Ehlers, M. Albrecht, *Chem. Eur. J.*, 2009, **15**, 9375-9386.

[10] (a) R. Pretorius, M. R. Fructos, H. Müller-Bunz, R. A. Gossage, P. J. Pérez, M. Albrecht, *Dalton Trans.*, 2016, **45**, 14591-14602. (b) M. Albrecht, *Chem. Commun.*, 2008, **31**, 3601-3610. (c) T. K. Sen, S. C. Sau, A. Mukherjee, P. K. Hota, S. K. Mandal, B. Maity, D. Koley, *Dalton Trans.*, 2013, **42**, 14253-14260.

[11] (a) A. Krüger, M. Albrecht, *Aust. J. Chem.*, 2011, **64**, 1113-1117. (b) K. Farrell, P. Melle, R. A. Gossage, H. Müller-Bunz, M. Albrecht, *Dalton Trans.*, 2016, **45**, 4570-4579. (c) C. Segarra, E. Mas-Marzá, J. A. Mata, E. Peris, *Organometallics*, 2012, **31**, 5169-5176. (d) C. L. Deardorff, R. E. Sikma, C. P. Rhodes, T. W. Hudnall, *Chem. Commun.*, 2016, **52**, 9024-9027.

[12] (a) J. C. Bernhammer, G. Frison, H. V. Huynh, *Chem. Eur. J.*, 2013, **19**, 12892-12905. (b) D. Mendoza-Espinosa, G. Ung, B. Donnadieu, G. Bertrand, *Chem. Commun.*, 2011, **47**, 10614-10616. (c) M. Uzelac, A. Hernán-Gómez, D. R. Armstrong, A. R. Kennedy, E. Hevia, *Chem. Sci.*, 2015, **6**, 5719-5728. (d) R. S. Ghadwal, *Dalton Trans.*, 2016, **45**, 16081-16095.

[13] (a) A. Prades, E. Peris, M. Albrecht, *Organometallics*, 2011, **30**, 1162-1167. (b) A. Poulain, D. Canseco-Gonzalez, R. Hynes-Roche, H. Müller-Bunz, O. Schuster, H. Stoeckli-Evans, A. Neels, M. Albrecht, *Organometallics*, 2011, **30**, 1021-1029. (c) L. Y. M. Eymann, R. Scopelliti, F. T. Fadaei, G. Cecot, E. Solari, E.; Severin, K. *Chem. Commun.* **2017**, *53*, 4331-4334. (d) Karthik, V.; Gupta, V.; Anantharaman, G. *Organometallics*, 2014, **33**, 6218-6222.

Despite these attractive advantages of aNHCs, the organometallic chemistry of NHCs remains dominated by far, by normally bound NHCs.[14] A major limitation of aNHC complexes is the synthetic accessibility because of the low acidity of the C(4)/C(5) proton,[15] which requires specific protocols to direct metalation to the imidazolium C(4) position.[16] Even though only a small number of well-defined aNHC complexes of ruthenium have been reported to date, most of these complexes exhibit superior catalytic activities compared to their normally bound analogues.[3(a),17,18]

Protection of the imidazolium C(2) position with alkyl or aryl substituents is probably the most facile and useful route that has been developed for selective metal coordination to the imidazolylidene C(4) atom.[1(d),3(a),19] However, the formation of C(4)-bound aNHCs via transmetallation of the corresponding Ag-aNHCs is generally limited to certain metal precursors because of the sensitive nature of the Ag-aNHC species.[20] The apparent need for more facile routes to access these desirable aNHCs remains relevant, as the preparation of aNHC metal complexes continue to be a challenging synthetic field.[4,21,22] One attractive strategy, particularly

[14] (a) P. L. Arnold, S. Pearson, *Coord. Chem. Rev.*, 2007, **251**, 596-609. (b) R. H. Crabtree, *Coord. Chem. Rev.*, 2013, **257**, 755-766.
[15] (a) S. Saha, P. Daw, J. K. Bera, *Organometallics*, 2015, **34**, 5509-5512. (b) D. Rottschäfer, C. J. Schürmann, J-H. Lamm, A. N. Paesch, B. Neumann, R. S. Ghadwal, *Organometallics*, 2016, **35**, 3421-3429. (c) A. Krüger, G. Michaud, A. Dowling, H. Müller-Bunz, M. Albrecht, *Z. Anorg. Allg. Chem.*, 2015, **641**, 2250-2257. (d) D. Mendoza-Espinosa, B. Donnadieu, G. Bertrand, *J. Am. Chem. Soc.*, 2010, **132**, 7264-7265.
[16] (a) A. Krüger, E. Kluser, H. Müller-Bunz, A. Neels, M. Albrecht, *Eur. J. Inorg. Chem.*, 2012, 1394-1402. (b) O. Schuster, L. Yang, H. G. Raubenheimer, M. Albrecht, *Chem. Rev.*, **2009**, **109**, 3445-3478.
[17] (a) G. A. Filonenko, E. Cosimi, L. Lefort, M. P. Conley, C. Copéret, M. Lutz, E. J. M. Hensen, E. A. Pidko, *ACS Catalysis*, 2014, **4**, 2667-2671. (b) C. E. Ellul, M. F. Mahon, O. Saker, M. K. Whittlesey, *Angew. Chem. Int. Ed.*, 2007, **46**, 6343-6345.
[18] (a) K. Farrel, H. Müller-Bunz, M. Albrecht, *Organometallics*, 2015, **34**, 5723-5733. (b) S. C. Sau, S. Santra, T. K. Sen, S. K. Mandal, D. Koley, *Chem. Commun.*, 2012, **48**, 555-557.
[19] (a) G. Ung, G. Bertrand, *Chem. Eur. J.*, 2011, **17**, 8269-8272. (b) E. Aldeco-Perez, A. J. Rosenthal, B. Donnadieu, P. Parameswaran, G. Frenking, G. Bertrand, *Science*, 2009, **326**, 556-559.
[20] (a) A. S. K. Hashmi, D. Riedel, M. Rudolph, F. Rominger, T. Oeser, *Chem. Eur. J.*, 2012, **18**, 3827-3830. (b) X. Xu, S. H. Kim, X. Zhang, A. K. Das, H. Hirao, S. H. Hong, *Organometallics*, 2013, **32**, 164-171.
[21] (a) L-A. Schaper, K. Öfele, R. Kadyrov, B. Bechlars, M. Drees, M. Cokoja, W. A. Herrmann, F. E. Kühn, *Chem. Commun.*, 2012, **48**, 3857-3859. (b) Y. Kim, E. Lee, *Chem. Commun.*, 2016, **52**, 10922-10925.
[22] (a) G. Song, Y. Zhang, X. Li, *Organometallics*, 2008, **27**, 1936-1943. (b) D. Martin, M. Melaimi, M. Soleilhavoup, G. Bertrand, *Organometallics*, 2011, **30**, 5304-5313.

for aNHCs, is chelate-assisted coordination.[8(d),23,24] Here a variety of main group 4, 5, and 6-based ligands including alkenyl, picolyl, pyridyl, thioether, amine, oxo, and phosphine substituents are grafted onto the C(2)-protected NHC scaffold, usually through *N*-alkylation, essentially forming a bidentate aNHC ligand. Abnormal coordination selectivity has been found to be related to steric control, the tether length, the bite angle, and the nature of the anion of the aNHC precursor.[25] In addition, should these *N*-substituted chelators exhibit hemilability and/or non-innocent behavior in solution, the set of metal-specific catalytic steps within a catalytic cycle is enhanced.[4(d),5(b),26] In light of the latter, the lack of exploitation of potentially hemilabile bidentate NHC ligand systems prompted us to expand upon and evaluate enhancement effects that may be observed when employing these chelating aNHC ligands. Here we report the synthesis of eight new abnormally bound NHC half-sandwich Ru(II) complexes, demonstrate the strong binding of aNHCs through acid stability studies, and evaluate their application in transfer (de)hydrogenation catalysis. Each of these Ru(II) complexes comprises of either an alkene- or picolyl-substituent as one of two possible *N*-functionalised chelating moieties. In addition, selectivity and yield issues typically encountered with Ag_2O-assisted carbene transfer reactions are addressed.

2. Results and Discussion

2.1 Synthesis of the NHC ligands

The aNHC ligand precursors were synthesised from the respective C(2)-protected imidazoles (Scheme 1). For example, 1,2-dimethylimidazole reacts with either 3-chloro-2-methyl-propene

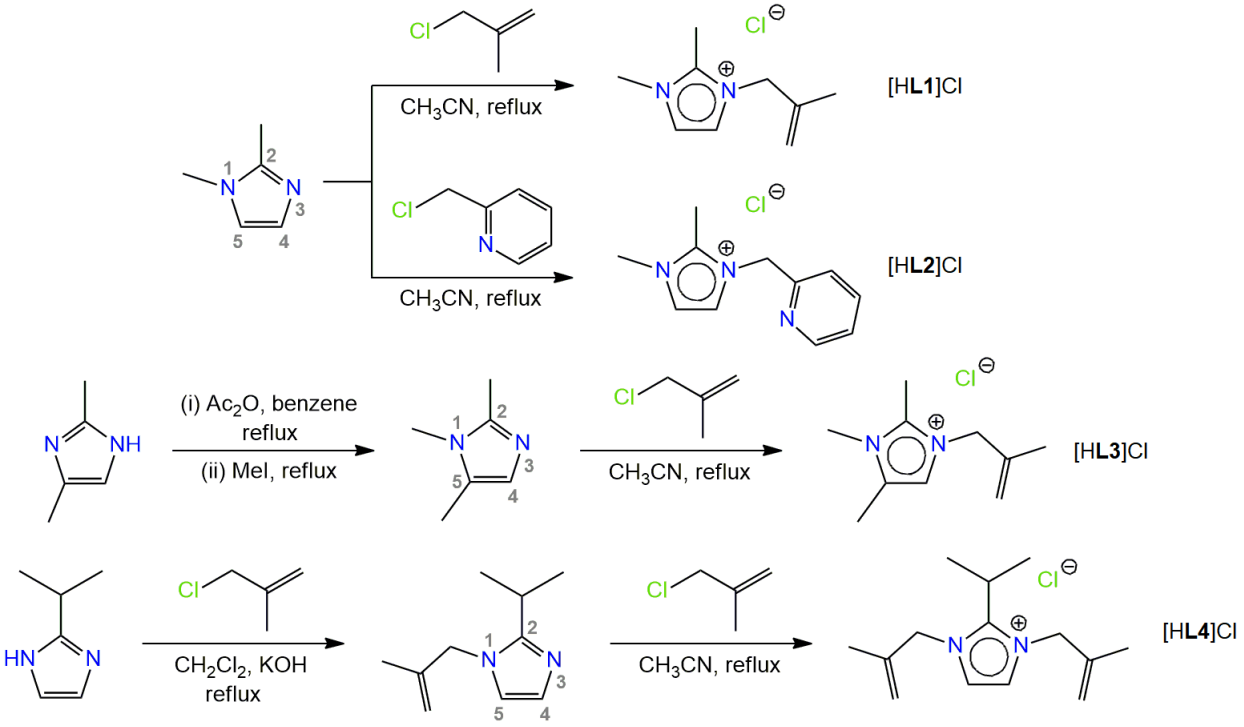
[23] (a) M. Delgado-Rebollo, D. Canseco-Gonzalez, M. Hollering, H. Mueller-Bunz, M. Albrecht, *Dalton Trans.*, 2014, **43**, 4462-4473. (b) M. Hollering, D. T. Weiss, M. J. Bitzer, C. Jandl, F. E. Kühn, *Inorg. Chem.*, 2016, **55**, 6010-6017.

[24] (a) W. Zuo, P. Braunstein, *Dalton Trans.*, 2012, **41**, 636-643. (b) A. R. Chianese, A. Kovacevic, B. M. Zeglis, J. W. Faller, R. H. Crabtree, *Organometallics*, 2004, **23**, 2461-2468.

[25] (a) A. Juzgado, M. M. Lorenzo-García, M. Barrejón, A. M. Rodríguez, J. Rodríguez-López, S. Merino, J. Tejeda, *Chem. Commun.*, 2014, **50**, 15313-15315. (b) V. J. Catalno, M. A. Malwitz, A. O. Etogo, *Inorg. Chem.*, 2004, **43**, 5714-5724. (c) V. Catalano, M. A. Malwitz, *Inorg. Chem.*, 2003, **42**, 5483-5485. (d) F. Cui, P. Yang, X. Huang, X-J. Yang, B. Wu, *Organometallics*, 2012, **31**, 3512-3518. (e) C. Y. Legault, C. Kendall, A. B. Charette, *Chem. Commun.*, 2005, 3826-3828.

[26] (a) S. Sabater, H. Müller-Bunz, M. Albrecht, *Organometallics*, 2016, **35**, 2256-2266. (b) K. F. Donnelly, C. Segarra, L-X. Shao, R. Suen, H. Müller-Bunz, M. Albrecht, *Organometallics*, 2015, **34**, 4076-4084.

or 2-(chloromethyl)pyridine in a quaternisation reaction to produce the C(2)-protected imidazolium chloride salts in good yields (93%, [H**L1**]Cl; 88%, [H**L2**]Cl. The C(2),C(5)-protected imidazolium salt ([H**L3**]Cl) was accessed first by reacting 2,4-dimethylimidazole with acetic anhydride, followed by methyl iodide to selectively yield the 2,3,5-trimethyl imidazole. It was found previously that direct deprotonation and alkylation of 2,4-dimethylimidazole gave mixtures of the 2,3,4-, and 2,3,5-trisubstituted imidazoles.[9(b)] The 2,3,5-trimethylimidazole precursor was further reacted with 3-chloro-2-methyl-propene to obtain [H**L3**]Cl in moderate yield (53%). In an attempt to address selectivity issues (see following section below), the symmetrical aNHC, [H**L4**]Cl, was synthesised in high yield by sequential treatment of 2-isopropylimidazole with KOH and 3-chloro-2-methylpropene, followed by another equivalent of 3-chloro-2-methyl-propene (90%).



Scheme 1: Synthesis of the aNHC ligand precursors.

Purification of ligands [H(**L1**-**L4**)]Cl was facile as the reaction mixture was concentrated *in vacuo*, washed with ethyl acetate to remove any unreacted precursors and concentrated to dryness to afford the pure imidazolium salts. The ^{1}H-NMR spectra of [H**L1**]Cl, [H**L3**]Cl, and [H**L4**]Cl all showed characteristic signals for the 2-methylpropenyl moiety: δ_H 1.53-1.78 ppm

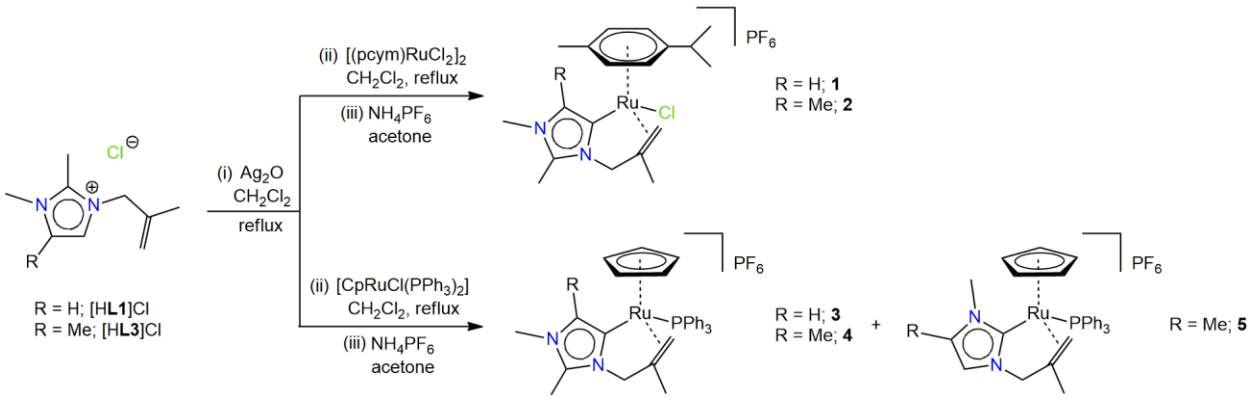
(singlet, C(2)-methyl), 4.60-4.82 ppm (singlet, methylene protons), and 4.51-5.06 ppm (two singlets, alkene protons). Depending on the symmetrical nature of the ligand, the imidazolium backbone protons either appeared as a singlet at δ_H 7.47 ppm ([H**L4**]Cl) and 7.14 ppm ([H**L3**]Cl), or as two singlets ([H(**L1**-**L3**)]Cl) δ_H 7.51 and 7.78 ppm ([H**L1**]Cl), 7.46 and 7.64 ppm ([H**L2**]Cl). The latter series of signals may also serve as a rough indication of proton affinity (PA) and hence donor strength of the ligands **L1**-**L4** relative to one another: **L1** ≈ **L2** < **L4** < **L3**. It is therefore not surprising that **L3** (bearing a C(5)-Me group) is more donating than its C(5)-H counterpart, **L1**. This approximate donor-strength series is supported when comparing the position of the pseudo-carbenic C(4)-signal in the ^{13}C-NMR spectra: 122.9 ppm ([H**L1**]Cl), 122.4 ppm ([H**L2**]Cl), 123.7 ppm ([H**L4**]Cl), 129.7 ppm ([H**L3**]Cl).

2.2 Synthesis of the normal and abnormal NHC Ru(II) complexes

Each of the ligands **L1**-**L4** contains a C(2)-alkyl substituent to inhibit metal coordination at the normal position of the NHC. Metallation was carried out using standard literature procedures[8(f),9,10,20,26(a)] which involves reacting the imidazolium salt with Ag_2O with the exclusion of light to form the biscarbene silver complex, and subsequently treating the *in situ* reaction mixture with the half-sandwich ruthenium(II) precursor (Scheme 2). Complexes **1** and **2** resulted from the reaction of [H**L1**]Cl and [H**L2**]Cl with [(*p*-cymene)$RuCl_2$]$_2$ respectively, whereas treatment of [H**L1**]Cl and [H**L2**]Cl with [CpRuCl(PPh_3)$_2$] gave complexes **3**-**5**. The yields of complexes **1**-**5** were consistently low (19-49%), although **1** and **2** were formed in slightly higher yields (> 38%) owing to the higher reactivity of [(*p*-cymene)$RuCl_2$]$_2$ *vs.* [CpRuCl(PPh_3)$_2$].

In 2004, Crabtree and co-workers[8(f)] described Ag-mediated dealkylation in aNHC systems functionalised with primary alkyl C(2)-protecting groups. Crabtree originally proposed complete C(2)-dealkylation when functionalised with methyl groups, and less so for ethyl and benzyl substituents to give rise to normal C(2)-bound NHC systems after metallation.[8(f),14(b)] It was concluded that when the C(2) moiety is protected by bulky, secondary alkyl/aryl substituents such as *iso*-propyl or phenyl groups, no dealkylation occurs and that the corresponding C(4)/(5)-bound aNHC complexes are obtained.[8(f),16(b)] We were therefore surprised that we were able to observe on ^{1}H-NMR the formation of abnormally bound aNHC-Ru(II) complexes for reactions

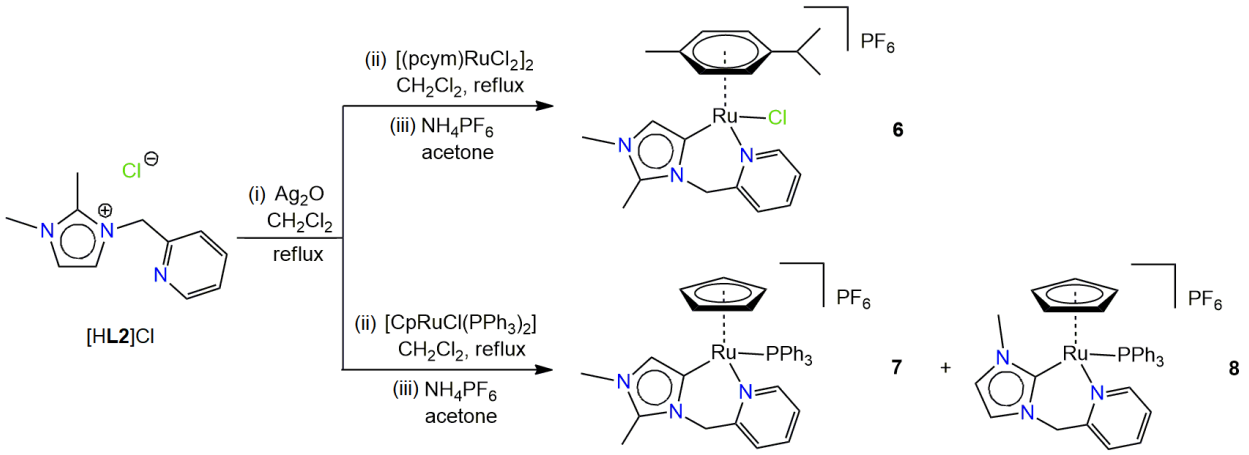
with [H(**L1**-**L3**)]Cl and [CpRuCl(PPh_3)$_2$] using C(2)-methyl substituted aNHC systems, along with the expected C(2)-bound NHC-Ru(II) complexes.



Scheme 2: Synthesis of half-sandwich aNHC-Ru(II) complexes.

Spectroscopic evidence of aNHC-coordination for **1**-**4** was obtained from their NMR spectra: Disappearance of the ^{1}H-NMR signal of [H**L1**]Cl and [H**L3**]Cl corresponding to the C(4)-H proton between δ_H 7.14-7.78 ppm, along with the concomitant appearance of the ^{13}C-NMR carbene signal between δ_C 147.0-174.9 ppm. ^{1}H-NMR signals for either *p*-cymene (**1**, **2**) or cyclopentadienyl (**3**) moieties generally appeared in an equimolar ratio to either **L1** or **L3**. Interestingly, other general NMR features include upfield shifts of the NC*H*$_3$ signals from δ_H 3.91 ppm ([H**L1**]Cl) to 3.85 ppm (**1**) and 3.71 ppm (**3**), respectively. In addition, a slight upfield shift of the C(5)-H proton in [H**L1**]Cl from δ_H 7.51 to 7.41 ppm (**1**) and 7.02 ppm (**3**) respectively. This is indicative of higher electron density on the C(4) position that the C(5)-H proton experiences following coordination. Unfortunately, successive attempts, with column chromatography as well as solvent extraction, at the separation of **4** and **5** failed. The ^{1}H-NMR spectrum of **4**/**5** indicated the presence of both complexes **4** and **5** in a 0.52:0.48 ratio, respectively. Similar to complexes **1**-**3**, signals at δ_H 2.92 (C(2)-CH_3, **4**), 6.74 (C(4)-H, **5**), confirm the normal (**5**) and abnormal (**4**) binding modes of the NHC ligands. The presence of a methyl substituent (C5) leads to substantial increase in the amount of dealkylation to render the normally bound NHC as the major product. This is believed to be due to increased electron density in the imidazolium ring which leads to a decrease in polarisation of the bonds in the ring system and C(2).[12(a)] This results in lower p-character of the imidazolium backbone bonds, and hence activates the C(2)-CH_3 group. During crystallisation in DCM, however, crystals of **5** were

isolated from the crystallisation mixture containing **4** and **5**, upon which its molecular structure was confirmed (see below).



Scheme 3: Synthesis of picolyl-functionalised half-sandwich aNHC-Ru(II) complexes.

Upon changing the mode of chelation, *i.e.* employing an *N*-picolyl substituent, a similar outcome was reached where complexes **6**-**8** were synthesised in 30-46% yields (Scheme 3). The change of chelating *N*-substituent did not appreciably increase the yields of aNHC-Ru(II) complexes, even though picolyl-chelate effects are much more prominent with Ag as opposed to similar alkene-chelate interactions.[25] The ^{1}H-NMR signal of C(4)-H (δ_H 7.64 ppm, [H**L2**]Cl) disappears post-coordination, along with a slight upfield shift of C(5)-H (δ_H 6.58 ppm, **6**; 6.62 ppm, **7**), as well as the appearance of the corresponding ^{13}C-NMR C(4)-Ru carbene signal (δ_C 157.8 ppm, **6**; 159.9 ppm, **7**). Chelation of the picolyl moiety was further confirmed by the characteristic downfield shift of the *ortho* proton of the pyridyl substituent (δ_H 9.35 ppm, **6**; 8.23 ppm, **7**/**8**). Attempts at separation of complexes **7** and **8** failed, even after numerous recrystallisations and application of column chromatography. Distinct NMR signals of C(4)-H/C(5)-H (δ_H 6.32, 6.43 ppm) and C(2)-Ru (δ_C 157.3 ppm) signified the simultaneous presence of the abnormally bound (**7**) and normally bound (**8**) Ru-NHC in the ratio of 0.46(**7**):0.54(**8**).

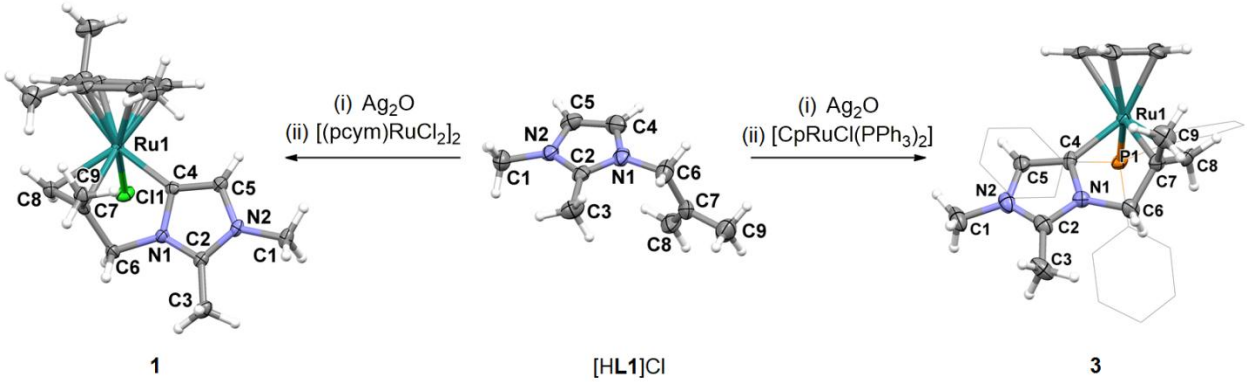


Figure 2: Perspective views of compounds **1**, [H**L1**]Cl, and **3**. Thermal ellipsoids are drawn at 50% level. The phenyl moieties of PPh_3 have been shown as wireframe presentations, as well as the omission of the anions for all compounds have been done for clarity purposes.

The molecular structures deduced from NMR studies were unequivocally supported by X-ray diffraction studies from which the specific mode of carbene coordination for each of the complexes was confirmed (Figure 2-4). All of the half-sandwich Ru(II) complexes assumed the typical three-legged piano stool structures[2(b),5(a),6,8(a),13(a),23(a),26(a)] (complexes **6**-**8**), and pseudo three-legged piano stool structures (**1**, **3**, **5**, **10**). Selected bond lengths and angles are summarised in Table S4 in the Supplementary Information. If chelation of the alkene-tether in complexes **1**-**4** is considered to form pseudo-five membered ruthenacyles, the resulting acute bite angles vary between 89.49(1)° (**1**) and 90.45(2)° (**3**), while the normally bound NHC in **5** resulted in a slightly narrowed bite angle of 89.10(1)°. The picolyl-containing complexes exhibited similar bite angles of 85.7(3)°-86.6(2)° (**6**-**8**). While the tether and imidazolium planes are essentially co-planar in related five-membered metallacycles,[4(c),5(a),9(a),25,26] the picolyl-containing complexes (**6**-**8**) exhibit synclinal torsion angles of between -48.60(3)° and -55.08(6)°, while the alkene-containing complexes (**1**,**3**,**5**) exhibit anticlinal torsion angles of between -108.369(4)° and -122.675(2)°. For the alkene-tethered complexes this inclination renders the two moieties closer towards being parallel to each other with the help of increased flexibility. It is also interesting to note that, in general, the Ru-C(4) bond distances of 2.045(3) Å (**1**), 2.0586(2) Å (**3**), 2.045(2) Å (**6**), and 2.057(6) Å (**7**) are notably shorter than the Ru-C(2) bond distance of 2.099(4) Å (**8**), which might be indicative of a stronger Ru-C(4) bond and hence higher electron density at the ruthenium core. However, both Ru-C bond distances are in good

correlation with the bond distances of other related normal[29(d)] and abnormal[4(d),8(d),14] Ru(II)-NHC complexes. The persistent co-presence of complexes **7** and **8** leads to the co-crystallisation of the two complexes in the x-ray molecular structures in two separate cases: two different unit cells were obtained, each with unique disorders, when either CH_2Cl_2 or $CHCl_3$ was used as crystallisation solvent (see Supplementary Information). Perspective views of the x-ray structures of complexes **6**-**8** are shown in Figure 3.

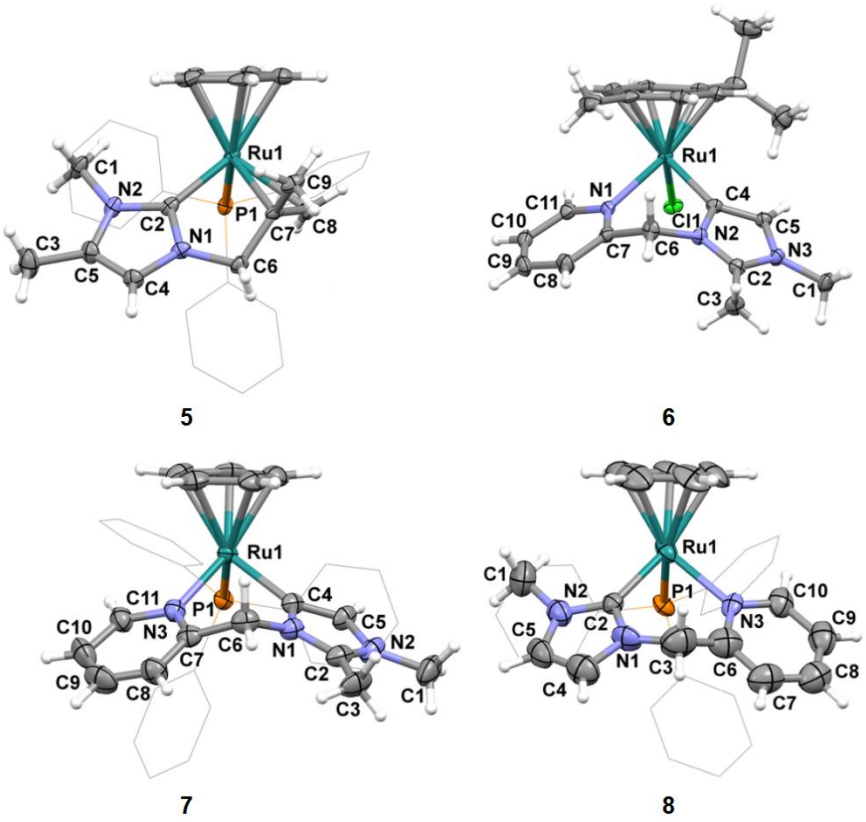
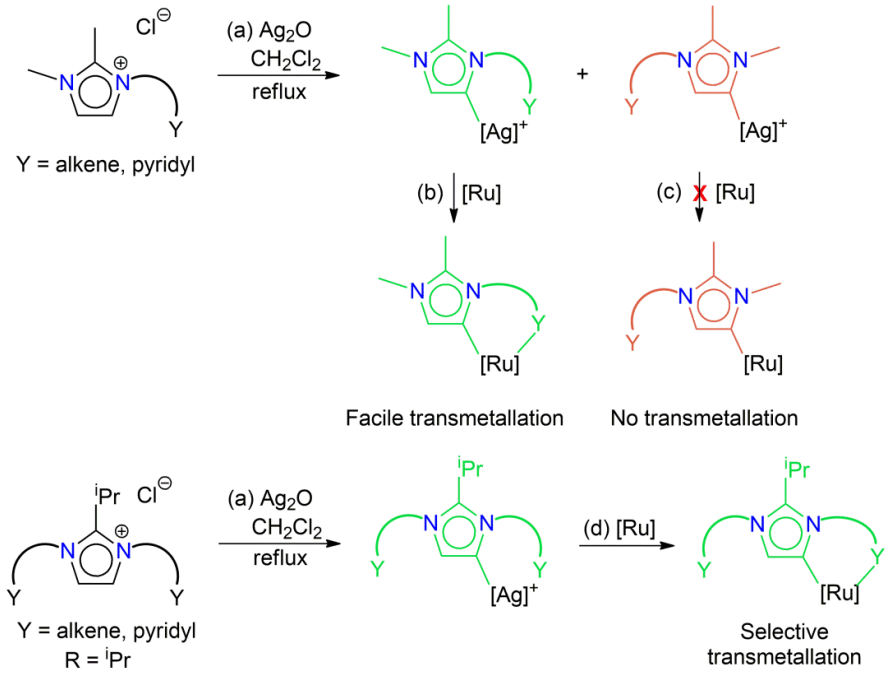


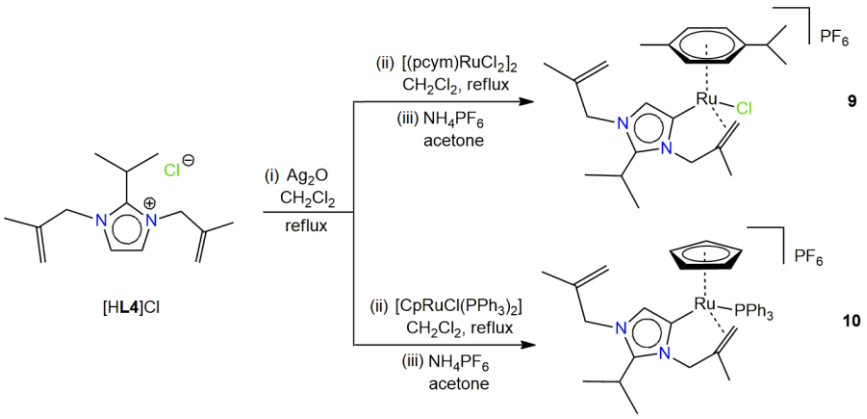
Figure 3: Perspective views of complexes **5**-**8**. Thermal ellipsoids are drawn at 50% level. The phenyl moieties of PPh_3 have been shown as wireframe presentations, as well as the omission of the anions for all compounds have been done for clarity purposes.

The main problem associated with low product formation is proposed to be the lack of selectivity of silver coordination at either the C(4) or C(5) positions (Scheme 4). Metallation of silver at the C(4) position, adjacent to a chelating *N*-substituent (route b), will be the only route that may lead to subsequent ruthenation for the $[CpRuCl(PPh_3)_2]$ precursor. Metallation at the C(5) position (route c) leads to the formation of the carbene with no chelating groups in the near vicinity,

effectively rendering the ligand monodentate and no C(5)-ruthenated product is formed. We reasoned that the symmetric carbene precursor ([H**L4**]Cl), *i.e.* the ligand bearing the *N*,*N*'-2-methyl-propenyl moieties, would resolve this issue. Positions C(4) and C(5) now become equivalent, eliminating losses due to selectivity issues (route d). Furthermore, **L4** features a C(2)-isopropyl substituent which is immune to Ag-mediated dealkylation, which further minimises product formation losses by formation of normal carbene byproducts. Reaction of [H**L4**]Cl with [(*p*-cymene)$RuCl_2]_2$ and [$CpRuCl(PPh_3)_2$] gave complexes **9** and **10**, respectively, all in good yields (62%, **9**; 55%, **10**), with no side-product formation observed (Scheme 5). The better yields for **9** and **10** are ascribed to both the use of the symmetric ligand **L4** as well as the more bulky ^{i}Pr protecting group on C(2).

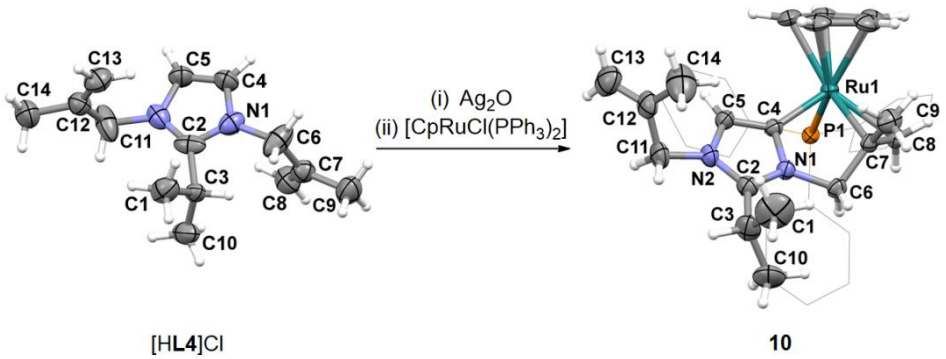


Scheme 4: Site selectivity aNHCs at either the C(4) or C(5) position. [Ru] = [$CpRuCl(PPh_3)_2$].



Scheme 5: Formation of the C(2)-isopropyl functionalised Ru(II)-aNHC complexes **9** and **10**.

Similar to complexes **1** (*p*-cymene) and **3** (cyclopentadienyl), complexes **9** (*p*-cymene) and **10** (cyclopentadienyl) showed distinct signals of bidentate coordination in their respective NMR spectra: Disappearance of the C(4)-H signal at δ_H = 7.47 ppm, an upfield shift of C(5)-H at δ_H = 7.17 ppm (**9**) and 6.75 ppm (**10**), and appearance of the C(4)-Ru signal at δ_C = 152.3 ppm (**9**) and 148.6 ppm (**10**). Due to the coordination of one alkene moiety, desymmetrisation of [H**L4**]Cl leads to a splitting of several alkene-tether signals in the ^{1}H-NMR spectrum of **9** and **10**. Interestingly, notable upfield shifts of the signals relating to the free and coordinating alkene moieties are observed from δ_H = 4.58, 5.06 ppm ([H**L4**]Cl), to 3.99, 4.60 ppm (**9**), as well as δ_H = 1.88, 2.27, 3.84, 4.52 ppm (**10**). The molecular structure of **10** (Figure 4) further confirms the bidentate nature of **L4**, with an average (see above) bite angle of 91.31(8)° and a Ru-C(4) bond distance of 2.046(2) Å, similar to the analogous complexes (**1**, **3**, **6** and **7**) above.



[H**L4**]Cl **10**

Figure 4: Perspective views of compounds [H**L4**]Cl and **10**. Thermal ellipsoids are drawn at 50% level. The phenyl moieties of PPh_3 have been shown as wireframe presentations, as well as the omission of the anions for all compounds have been done for clarity purposes.

2.3 Acid stability studies

In order to probe the robustness of the Ru-C(4) bond in the novel aNHC complexes **1**-**4**, **6**, **7**, **9**, and **10**, the stability of these complexes were evaluated in an acidic environment by ^{1}H-NMR spectroscopy. In addition, the acidic environment provides a means by which possible non-innocent behavior of the aNHC ligand in hydrogen transfer processes could be evaluated. The *p*-cymene complex, [(*p*-cym)RuCl(**L1**)]PF_6 (**1**), served as a representative example which was treated with stoichiometric amounts of DCl (1 M, D_2O solution). Figure 5 shows the ^{1}H-NMR spectra of **1** in $(CD_3)_2CO$ upon addition of various equivalents of the DCl solution. Addition of one equivalent of DCl did not lead to the formation of free aNHC ligand or the corresponding imidazolium salt, even upon heating the solution (40°C) for several hours, which underpins the robustness of the Ru-carbene bond. In addition, no initial alkene fluxionality was observed by inspection of the alkene and methylene linker proton signals.

However, an immediate disappearance of the signal at δ_H 7.41 ppm corresponds to the deuteration of C(5)-H. This phenomenon was observed in similar metal-aNHC complexes, which may be characteristic of non-innocent character of the aNHC ligand.[27] For example, it has been suggested that the strongly mesionic character of the imidazolylidene ligand may facilitate dearomatisation followed by the addition of a proton to a formal metalla-allyl anionic fragment.[27(a)] Addition of more than 1 equivalent of DCl led to a continued gradual disappearance of C(5)-H, along with the appearance of five new signals in the arene region (δ_H 4.7 – 7.3 ppm). The initial partial deuteration of C(5)-H ($\leq$ 4 eq DCl) may also be ascribed due to the moisture present in the solvent (acetone-d_6, DCl in D_2O (35 wt. %)). New signals appearing at δ_H 7.09 ppm (q, $^{3}J_{HH}$ = 6 Hz), 2.84 ppm (m), 2.25 ppm (s), and 1.20 ppm (d, $^{3}J_{HH}$ = 9 Hz), correspond to free *p*-cymene (only aromatic region shown in Figure 5, full spectra in SI). This is coupled to a gradual decrease of the signals corresponding to a coordinated *p*-cymene ligand at δ_H 6.65 ppm (d, $^{3}J_{HH}$ = 6 Hz), 6.50 ppm (d, $^{3}J_{HH}$ = 6 Hz), 5.80 ppm (d, $^{3}J_{HH}$ = 6 Hz), 5.27 (d, $^{3}J_{HH}$ = 6 Hz), and 2.78 (m). The ratio of coordinated versus free *p*-cymene after addition of 1, 4,

[27] (a) A. Petronilho, J. A. Woods, H. Mueller-Bunz, S. Bernhard, M. Albrecht, *Chem. Eur. J.*, 2014, **20**, 15775-15784. (b) K. Hindson, B. de Bruin, *Eur. J. Inorg. Chem.*, 2012, 340−342. (c) E. Peris, *Chem. Rev.*, 2017, DOI: 10.1021/acs.chemrev.6b00695. (d) B. T. Worrel, J. A. Malik, V. V. Fokin, *Science*, 2013, **340**, 457-460.

and 8 equivalents of DCl is 0.83, 0.82, and 0.70 respectively. The signals for the coordinated *p*-cymene ligand never fully disappear, which might be indicative of an equilibrium existing between the non-deutero coordinated and deuterated species. The ratio of deuterio versus protio C(5)-H/D species follows a much more rapid decrease: 0.80 (1 eq), 0.29 (2 eq), 0.13 (4 eq), and 0.01 (8 eq). Therefore, deuteration of the C(5)-H is not expected to affect *p*-cymene dissociation, especially since the signals of coordinated *p*-cymene remain, even after full deuteration of the C(5)-H moiety.

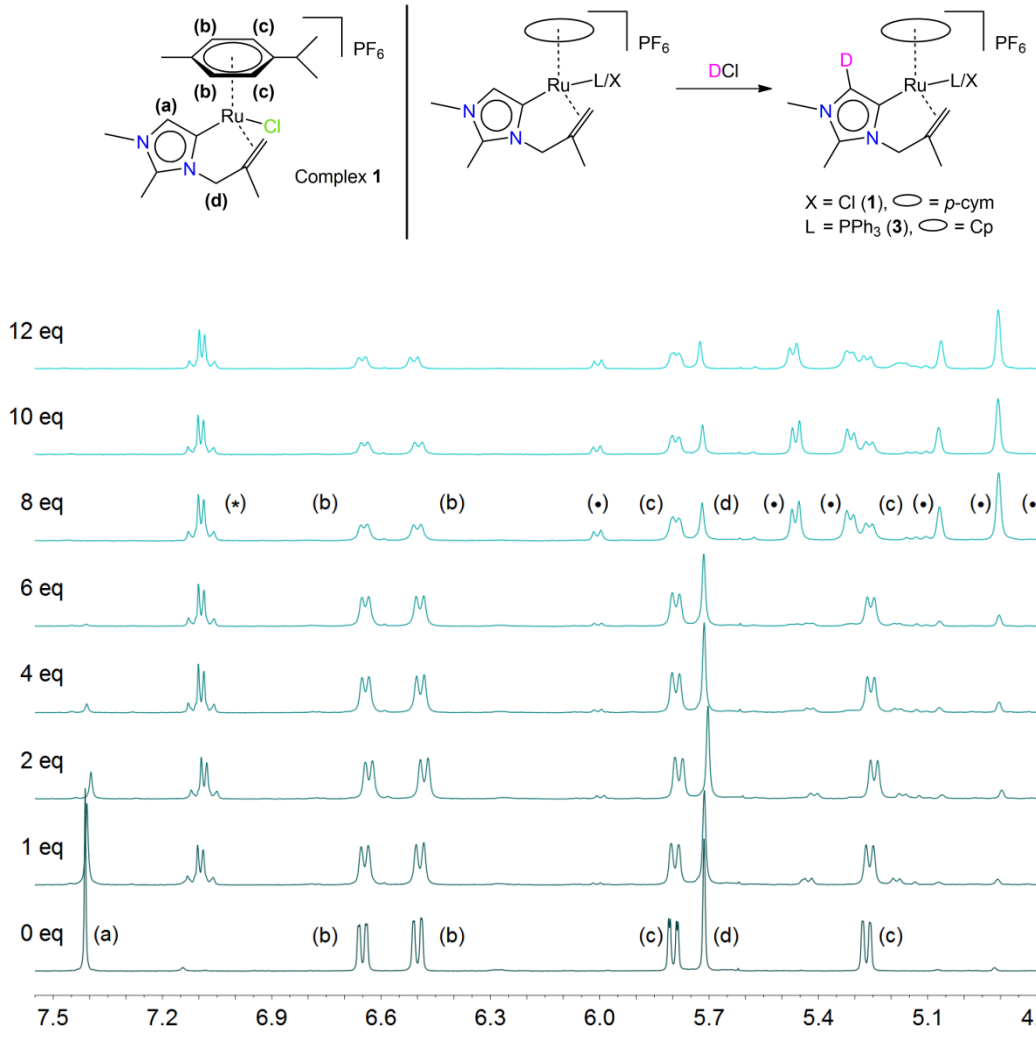


Figure 5: ^{1}H-NMR spectra of complex **1** upon titration with DCl. Signals (a)-(d) correspond to those of complex **1**. The signals (*) and (•) correspond to those of free *p*-cymene and [Ru-aNHC] complex bearing a free *N*-alkenyl substituent, respectively.

The dissociation of the *p*-cymene ligand, along with the aNHC ligand remaining intact suggest three available coordination sites on the ruthenium(II) centre. With increasing amounts of DCl/D_2O the propensity for the formation of (aNHC)Ru-OD_2 and (aNHC)Ru-Cl species increases.[28] After addition of more than 8 equivalents of DCl/D_2O, a series of ten new signals appear: three doublets at δ_H 6.00 ppm ($^3J_{HH}$ = 6 Hz), 5.46 ppm ($^3J_{HH}$ = 6 Hz), and 5.31 ppm ($^3J_{HH}$ = 6 Hz); and seven singlets at δ_H 5.07, 4.91, 4.77, 3.98, 2.75, 2.11, and 1.29 ppm. Of the latter signals, δ_H 3.98, 2.75, 2.11, and 1.29 ppm correspond to the free alkene tether, leaving a monodentate aNHC-Ru(II) complex. Addition of > 12 equivalents of DCl over a period of 10 days leaves complex **1** with several fully and partially deuterated proton signals, along with several unidentified signals related to decomposition products. Remarkably, the signals corresponding to the monodentate abnormally-bound NHC, δ_H 3.98, 2.75, 2.11, and 1.29 ppm remained. In addition, the characteristic signal δ_C 171.1 ppm remain present while no corresponding C(4)-H protons corresponding to free aNHC is observed over the time period of the experiment. A similar trend is seen with the analogous cyclopentadienyl-containing complex **3**, where an immediate deuteration of the C(5)-H proton is observed. No signs of immediate deuteration of the cyclopentadienyl or the alkenyl moieties are observed. However, new signals appearing at δ_H 5.27, 5.35, and 5.62 ppm all suggest reversible alkene coordination. Furthermore no evidence for the subsequent loss of cyclopentadiene could be found, only a gradual deuteration of all signals was observed over a period of two weeks, even upon heating of the sample.

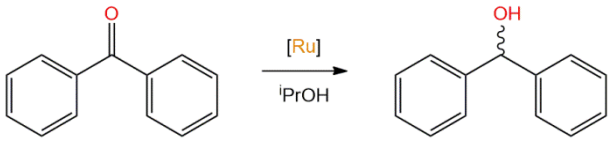
2.4 Transfer hydrogenation

Similar to the series of Ru(II) normal- and abnormal-NHC complexes described in literature,[2,4(d),8(c),6,14(a),23,26] complexes **1**-**10** were active in the (transfer) hydrogenation of selected ketone compounds. Standard conditions were employed, *i.e.* excess isopropanol as a hydrogen donor, base (KOH/KO^tBu) as activator, and benzophenone as substrate. Both ^{1}H-NMR and GC analyses on reaction mixtures in the presence of the suitable internal standards suggested a selective reaction, and hence substrate conversion corresponds to product yields. With complexes **1** (*p*-cymene) and **3** (cyclopentadienyl) as catalysts, initial TOFs of 60 h^{-1} and 26 h^{-1}

[28] (a) L. Bíró, E. Farkas, P. Buglyó, *Dalton Trans.*, 2012, **41**, 285-291. (b) É. A. Enyedy, G. M. Bognár, T. Kiss, M. Hanif, C. G. Hartinger, *J. Organomet. Chem.*, 2013, **734**, 38-44.

were found respectively (determined after the first 15 minutes reaction time), under typical conditions (Table 1, entries 1,3). While these rates are around three orders of magnitude lower than some of the best-performing ruthenium-based catalysts,[23(b)] they are comparable to similar bidentate NHC-Ru(II) analogues.[23(a),26(a)] Evaluation of the enantioselectivity of the alcohol product mixtures obtained using ^{1}H-NMR and GC(FID) techniques proved difficult. However, a low enantioselectity is expected due to the use of non-enantiomerically pure chiral-at-metal catalysts.

Table 1: Transfer hydrogenation of benzophenone using **1**-**10**.



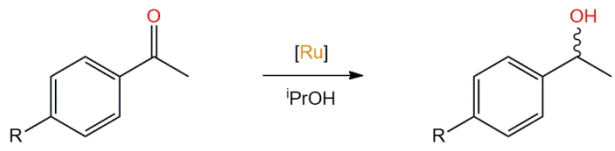
Entry	Complex	Conversion[b] (%)		TOF_{15}[c]
		2h	6h	(h^{-1})
1	**1**	63	93	60
2	**2**	52	76	38
3	**3**	32	69	26
4	**4/5**[a]	37	50	24
5	**6**	52	73	34
6	**7/8**[a]	30	50	22
7	**9**	60	89	58
8	**10**	42	61	46

General conditions: Benzophenone (0.6 mmol), iPrOH (5 mL), base (5 mol%), [Ru] (1 mol%), 110 °C. Base used depending on Ru catalyst: KOH (**1**, **2**, **6**, **9**); KO^{t}Bu (**3**-**5**, **7**, **8**, **10**). [a] Mixture of complexes as isolated after purification. [b] Determined by GC, based on the average of at least two runs. [c] Determined after the first 15 minutes reaction time.

Although chelation generally renders a more robust and longer-lived catalyst, it might inhibit fast substrate conversion and hence could reduce the overall yield.[6(b),26] A low susceptibility to catalyst decomposition is seen by yielding 93% (**1**) and 50% (**3**) conversion after 6 hours (TOF = 15 h^{-1} (**1**), 12 h^{-1} (**3**)), along with activity observed even after 18 hours (total conversion of 81%

using **3**). After reaction optimisation (see Table S5 in the Supplementary Information), complexes **1**-**10** were screened for their catalytic activity. Generally, the *p*-cymene Ru(II) complexes outperformed the cyclopentadienyl Ru(II) complexes (entries 1,2 *vs.* 3,4; 5 *vs.* 6; 7 *vs.* 8) by virtue of the ease of generating vacant coordination site(s) after dehalogenation with KOH. For the cyclopentadienyl Ru(II) complexes to be catalytically active, the most obvious activation pathways would include the somewhat more difficult alkene and/or phosphine dissociation under the catalytic conditions employed. The efficiency of the transfer hydrogenation reaction was found to be temperature and base-dependent. Without addition of a base, low (< 30 %) conversions were obtained. Similarly, very low conversions are obtained (10% after 6 hours) when the reaction is conducted at room temperature.

Table 2: Substrate screening in the transfer hydrogenation reaction



Entry	Substrate	Conversion[a] (%)	
		2h	18h
1	Acetophenone	56	98
2	4'-Chloroacetophenone	34	87
3	4'-Hydroxyacetophenone	24	71
4	4'-Methoxyacetophenone	17	98

General conditions: Ketone (0.6 mmol), ^{i}PrOH (5 mL), KOH (5 mol%), [**1**] (5 mol%), anisole (0.3 mmol), 110 °C. [a] Determined by GC, based on the average of at least two runs.

Furthermore, the low conversions obtained when using KOH as base in the cyclopentadienyl-Ru catalyst reactions, necessitated the use of the stronger base KO^{t}Bu for which better conversions were obtained. It was seen that the C(5)-Me-substituted NHC (**2**) performed somewhat poorer than the C(5)-H NHC complex **1** (entry 2). This is unexpected since **2**, bearing a slightly more donating aNHC, is expected to contribute towards better-stabilised, longer-lived catalytic species. Therefore a slight steric effect in **2** may be dominant, especially if an inner sphere

mechanism is considered. Upon changing the mode of chelation from a potentially hemilabile *N*-alkene tether to an *N*-picolyl substituent (**6**, entry 5), a lowering in catalyst activity is observed, which highlights the importance of the tailoring of the chelating group. The C(2)-^{i}Pr functionalised Ru-NHC **9** containing the *para*-cymene ligand performed better than the cyclopentadienyl analogue **10**, although the catalytic activity of **9** and **10** were comparable to that of **1** and **3**. It does seem as if the C(2)-substituent (Me vs. allyl) on the NHC does not impart on the catalytic activity of the resulting complex. Steric and electrochemical differences in the substrate notably affected the conversions (Table 2), *i.e.* less bulky substrates acetophenone *vs.* benzophenone (entries 1-4) and electron-donating substituents resulted in higher conversions (98%). Conversion of *p*-chloroacetophenone, bearing the electron-withdrawing substituents on the *para*-position, was somewhat lower (entry 2), while a significant retardation in the rate of conversion of these species was observed.

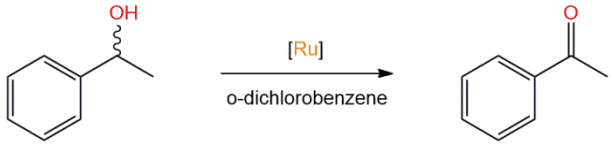
2.5 Alcohol oxidation

The series of complexes **1**-**10** was also tested in the anaerobic secondary alcohol oxidation reaction, where good to excellent activity has been found for related complexes.[26] The catalytic reactions were performed using *ortho*-dichlorobenzene as solvent, hexamethylbenzene (0.1 mmol) as internal standard, at a temperature of 150 °C. Catalyst loadings of less than 5 mol% led to notably low substrate conversions. In general, all complexes catalysed the oxidation whereby good yields of the corresponding ketone compounds were obtained.

Similar trends as with the transfer hydrogenation catalytic reactions were observed: The C(5)-H aNHC complexes **1** and **3** performed somewhat better than their C(5)-Me aNHC counterparts (see Supplementary Info for a time-resolved conversion plot). However, both the *p*-cymene and cyclopentadienyl Ru(II) complexes exhibit higher activity in transfer hydrogenation catalysis as opposed to alcohol oxidation catalysis where, during the oxidation reactions, higher catalyst loadings (5 mol% *vs.* 1 mol%), higher reaction temperatures (150°C *vs.* 110°C), and longer reaction times (4 hours *vs.* 24 hours) are generally required. In the oxidation of ±1-phenylethanol, complex **1** performed best with 77% substrate converted over a period of 24 hours. Similar to the transfer hydrogenation reactions, complexes **1**-**3**, **6**, **9**, and **10** all exhibited similar catalytic activity. The lower performance of complex mixtures **4**/**5** and **7**/**8** may be

attributed the normally-bound NHC content within these mixtures: Using ^{1}H-NMR ratios of **4**(0.52):**5**(0.48) and **7**(0.46):**8**(0.54), the catalytic activities of **4**/**5** and **7**/**8** are roughly lowered by 10% (**4**/**5**) and 17% (**7**/**8**) due to the normally-bound NHC content of **5** and **8**, respectively. Both electrochemical (more electron-rich aNHC) and stereochemical (slightly more bulky aNHC) properties of the complexes employed may play a rate-impeding role on catalysis. However, in light of the above, the normally-bound NHC content in the catalyst mixtures (**4**/**5** and **7**/**8**) has a bigger effect on the overall catalytic efficient. In general, the initial TOFs of all complexes were low (4-11 h^{-1}), with a gradual lowering down to around 1 h^{-1} over the period of 24 h.

Table 3: Oxidation of ±1-phenylethanol using **1**-**10**



Entry	Complex	Conversion[b] (%)		TOF_{10}[c]
		4h	24h	(h^{-1})
1	**1**	63	77	11
2	**2**	60	73	5
3	**3**	58	70	3
4	**4/5**[a]	50	62	2
5	**6**	62	73	6
6	**7/8**[a]	43	56	4
7	**9**	57	74	8
8	**10**	58	68	5

General conditions: ±1-Phenylethanol (1 mmol), *o*-dichlorobenzene (5 mL), KO^{t}Bu (5 mol%), [Ru] (5 mol%), hexamethylbenzene (0.1 mmol), 150 °C. [a] Mixture of complexes as isolated after purification. [b] Determined by GC, based on the average of at least two runs. [c] Determined after the first 10 minutes reaction time.

3. Experimental Section

3.1 General Procedures

All experiments were carried out under an argon atmosphere using standard Schlenk techniques. Solvents were dried and distilled from appropriate drying agents prior to use. The new imidazolium chloride ligands [H(**L1**-**L4**)]Cl were synthesised and purified according to standard literature procedures[29]; see Supplementary Information for characterisation data. The metal precursor [CpRuCl(PPh_3)$_2$] was synthesised according to the reported method.[29(e)] All other chemicals were purchased from commercial suppliers and used without further purification. ^{1}H (300 MHz) and ^{13}C{H} (76 MHz) NMR spectra were recorded on a Bruker ARX-300 spectrometer using $CDCl_3$. All measurements were performed at ambient temperature (~296 K), unless otherwise noted. Chemical shifts were referenced to the internal residual solvent resonances. Solid state FT-IR experiments were carried out on a Perkin Elmer Spectrum RXI FT-IR spectrometer as pressed KBr pellets in air. Microanalytical analyses (%CHNS) were obtained using a Thermo Scientific Flash 2000 elemental analyser fitted with a TCD detector. GC analyses were carried out on a Shimadzu GC-2010 fitted with a flame ionisation detector (FID) using a TRB-780143 capillary column (30 m, 0.25 mm ID, thickness 0.25 µm) and an AOC-20i auto injector. Electrospray mass spectra (ESI-MS) were recorded on a MicromassQuatro LC instrument.

*3.2 General synthesis of half-sandwich Ru(II) complexes (**1**-**10**)*

A suspension of the appropriate imidazolium chloride salt (4 mmol) in CH_2Cl_2 (30 mL) containing Ag_2O (0.93 g, 4 mmol) was stirred at 30°C for 12 hours in the absence of light. The mixture was filtered to which either [(*p*-cym)$RuCl_2$]$_2$ (2 mmol) or [CpRuCl(PPh_3)$_2$] (4 mmol) was added and heated under reflux for either 5 hours ([(*p*-cym)$RuCl_2$]$_2$) or 36 hours ([CpRuCl(PPh_3)$_2$]). The crude reaction mixture was filtered, concentrated *in vacuo* (5 mL), to

[29] (a) F. P. Malan, E. Singleton, P. H. van Rooyen, M. Landman, *J. Organomet. Chem.*, 2016, **813**, 7-14. (b) R. Fraser, P. H. van Rooyen, J. de Lange, I. Cukrowski, M. Landman, *J. Organomet. Chem.*, 2017, **840**, 11-22. (c) R. Fraser, C. G. C. E. van Sittert, P. H. van Rooyen, M. Landman, *J. Organomet. Chem.*, 2017, **835**, 60-69. (d) C. Gandolfi, M. Heckenroth, A. Neels, G. Laurenczy, M. Albrecht, *Organometallics*, 2009, **28**, 5112-5121. (e) E. V. Gorbachuk, E. K. Badeeva, R. G. Zinnatullin, P. O. Pavlov, A. B. Dobrynin, A. T. Gubaidullin, M. A. Ziganshin, A. V. Gerasimov, O. G. Sinyashin, D. G. Yakhvarov, *J. Organomet. Chem.*, 2016, **805**, 49-53.

which acetone (15 mL), and NH_4PF_6 (0.65 g, 4 mmol) was added. The reaction mixture was stirred for a further hour after which the mixture was evaporated *in vacuo*, and purified by silica gel column chromatography, using gradient elution with CH_2Cl_2/acetone. Yellow to dark-yellow solids were obtained.

[(*p*-cym)RuCl(**L1**)]PF_6 (**1**): Yield: 49%. ^{1}H-NMR ($(CD_3)_2CO$, δ_H) 1.33 (t, $^3J_{HH}$ = 6 Hz, *p-cym* (C*H*$_3$)$_2$, 6H), 1.79 (s, CC*H*$_3$, 3H), 1.98 (s, *p-cym* C*H*$_3$, 3H), 2.64 (s, C(2)-C*H*$_3$, 3H), 2.78 (m, C*H*$(CH_3)_2$, 1H), 3.68 (d, $^3J_{HH}$ = 12 Hz, =C*H*$_2$, 1H), 3.85 (s, NC*H*$_3$, 3H), 4.07 (s, C*H*$_2$, 1H), 4.44 (d, $^3J_{HH}$ = 9 Hz, =C*H*$_2$, 1H), 5.27 (d, $^3J_{HH}$ = 6 Hz, *p-cym* C*H*, 1H), 5.71 (s, C*H*$_2$, 1H), 5.80 (d, $^3J_{HH}$ = 6 Hz, *p-cym* C*H*, 1H), 6.50 (d, $^3J_{HH}$ = 6 Hz, *p-cym* C*H*, 1H), 6.65 (d, $^3J_{HH}$ = 6 Hz, *p-cym* C*H*, 1H), 7.41 (s, NC*H*, 2H). ^{13}C{^{1}H}-NMR ($CDCl_3$, δ_C) 14.1 (s, *p*-cym C(*C*H$_3$)$_2$), 19.6 (s, C*C*H$_3$), 21.0 (s, *p-cym C*H$_3$), 22.2 (s, C(2)-*C*H$_3$), 22.6 (s), 29.6 (s, N*C*H$_3$), 31.8 (s, *p-cym C*H), 54.1 (s), 60.3 (s, *C*H$_2$), 80.2 (s, =*C*H), 81.1 (s, =*C*H), 96.6 (s, *p-cym*), 101.7 (s, *p-cym*), 115.2 (s, N*C*H), 121.5 (s, *ipso p-cym*), 122.7 (s, *ipso p-cym*), 137.6 (s, N*C*N), 171.1 (s, N*C*Ru). ^{31}P{^{1}H}-NMR ($CDCl_3$, δ_P) -144.2 (sp, $^1J_{PF}$ = 713 Hz, *P*F_6). CHN (%): [$C_{19}H_{28}ClF_6N_2PRu$]×0.67$CHCl_3$: C, 36.26 (36.59), H, 5.25 (4.48), N, 3.98 (4.34). MS (ESI): m/z 421.096 (M^+) calcd for $C_{19}H_{28}ClN_2Ru$ 421.098.

[(*p*-cym)RuCl(**L2**)]PF_6 (**2**): Yield: 38%. ^{1}H-NMR ($(CD_3)_2CO$, δ_H) 1.21 (dd, $^3J_{HH}$ = 6 and 18 Hz, *p-cym* (C*H*$_3$)$_2$, 6H), 2.18 (s, CC*H*$_3$, 3H), 2.23 (s, *p-cym* C*H*$_3$, 3H), 2.29 (C(5)-C*H*$_3$, 3H), 2.35 (s, C(2)-C*H*$_3$, 3H), 2.79 (m, C*H*$(CH_3)_2$, 1H), 3.31 (s, CH_2, 1H), 3.87 (s, NC*H*$_3$, 3H), 4.31 (q, $^3J_{HH}$ = 6 Hz, =C*H*$_2$, 2H), 4.75 (s, C*H*$_2$, 1H), 5.64 (d, $^3J_{HH}$ = 6 Hz, *p-cym* C*H*, 1H), 5.82 (d, $^3J_{HH}$ = 9 Hz, *p-cym* C*H*, 1H), 6.55 (d, $^3J_{HH}$ = 6 Hz, *p-cym* C*H*, 1H), 6.64 (d, $^3J_{HH}$ = 6 Hz, *p-cym* C*H*, 1H). ^{13}C{^{1}H}-NMR ($CDCl_3$, δ_C) 10.1 (s, *p-cym* C(*C*H$_3$)$_2$), 18.4 (s), 18.9 (s), 19.7 (s, C*C*H$_3$), 20.6 (s, *p-cym C*H$_3$), 22.0 (s, C(2)-*C*H$_3$), 23.9 (s), 27.8 (s, N*C*H$_3$), 31.1 (s, C(5)-*C*H$_3$), 31.4 (s, *p-cym C*H), 34.9 (s), 54.5 (s, *C*H$_2$), 70.2 (s, *p-cym*), 78.1 (s, =*C*H), 78.9 (s, =*C*H), 95.0 (s, *p-cym*), 97.1 (s, *p-cym*), 101.7 (s, *p-cym*), 108.9 (s, N*C*CH$_3$), 117.2 (s, *ipso p-cym*), 133.4 (s, N*C*N), 168.8 (s, N*C*Ru). ^{31}P{^{1}H}-NMR ($CDCl_3$, δ_P) -144.3 (sp, $^1J_{PF}$ = 713 Hz, *P*F_6). CHN (%): [$C_{20}H_{30}ClF_6N_2PRu$]×CH_2Cl_2: C, 38.24 (37.94), H, 4.30 (4.85), N, 4.31 (4.21). MS (ESI): m/z 435.1152 (M^+) calcd for $C_{20}H_{30}ClN_2Ru$ 435.114.

[CpRu(PPh_3)(**L1**)]PF_6 (**3**): Yield: 23%. ^{1}H-NMR ($(CD_3)_2CO$, δ_H) 1.80 (s, CC*H*$_3$, 3H), 2.34 (s, C(2)-C*H*$_3$, 3H), 3.23 (s, =C*H*$_2$, 1H), 3.71 (s, NC*H*$_3$, 3H), 3.80 (s, =C*H*$_2$, 1H), 3.88 (d, $^3J_{HH}$ = 12 Hz, C*H*$_2$, 1H), 5.34 (s, C*H*$_2$, 1H), 4.97 (s, C_5H_5, 5H), 7.02 (s, NC*H*, 1H), 7.38-7.49 (m, $P(C_6H_5)_3$, 15H). $^{13}C\{^1H\}$-NMR ($CDCl_3$, δ_C) 10.2 (s, C*C*H$_3$), 14.0 (s), 31.2 (s, C(2)-*C*H$_3$), 33.9 (s, N*C*H$_3$), 45.7 (s), 56.8 (s, *C*H$_2$), 76.3 (s, =*C*H$_2$), 76.6 (s, =*C*H$_2$), 87.8 (s, *C*$_5$H$_5$), 128.0 (s, N*C*CH$_3$), 128.1 (s, *C*$_6$H$_5$), 128.2 (s, *C*$_6$H$_5$), 128.3 (s, *C*$_6$H$_5$), 128.6 (s, *C*$_6$H$_5$), 128.7 (s, *C*$_6$H$_5$), 130.3 (s), 133.4 (s, N*C*N), 133.5 (s, *C*$_6$H$_5$), 134.6 (s, *C*$_6$H$_5$), 135.1 (s, *ipso*-*C*$_6$H$_5$), 135.2 (s, *ipso*-*C*$_6$H$_5$), 139.2 (s, N*C*N), 147.0 (s, N*C*Ru). $^{31}P\{^1H\}$-NMR ($CDCl_3$, δ_P) -144.2 (sp, $^1J_{PF}$ = 708 Hz, *P*F$_6$), 56.8 (s, *P*Ph$_3$). CHN (%): $[C_{32}H_{34}F_6N_2P_2Ru]\times(CH_3)_2CO$: C, 54.06 (53.78), H, 5.98 (5.16), N, 3.23 (3.58). MS (ESI): m/z 579.1514 (M^+) calcd for $C_{32}H_{34}N_2PRu$ 579.150.

[CpRu(PPh_3)(**L2**)]PF_6 (**4**): Complex **5**, [CpRu(PPh_3)(**L2***)]PF_6, coordinated as a C(2)-NHC of **L2** less one methyl group, is obtained as a by-product that co-elutes with **4**. Combined yield: 38%. **4**/**5**: ^{1}H-NMR ($CDCl_3$, δ_H) 1.85 (s, CC*H*$_3$, 3H), 2.19 (s, C(5)-C*H*$_3$, 1.7H), 2.25 (s, C(5)-C*H*$_3$, 1.8H), 2.47 (s, NC*H*$_3$, 1.5H), 2.51 (s, NC*H*$_3$, 1.5H), 2.92 (s, C(2)-C*H*$_3$, 2H), 3.53 (d, $^3J_{HH}$ = 12 Hz, =C*H*$_2$, 1H), 3.78 (s, C*H*$_2$, 1H), 4.36 (s, =C*H*$_2$, 0.5H), 4.49 (s, C*H*$_2$, 1H), 4.64 (s, =C*H*$_2$, 0.5H), 5.02 (s, C_5H_5, 5H), 6.74 (s, C(5)-*H*, 0.8H), 7.33-7.49 (m, C_6H_5, 15H). $^{13}C\{^1H\}$-NMR ($(CD_3)_2CO$, δ_C) 10.3 (C*C*H$_3$), 32.6 (C(2)-*C*H$_3$), 34.7 (N*C*H$_3$), 57.4 (s, *C*H$_2$), 76.6 (s, =*C*H$_2$), 79.2 (s, =*C*H$_2$), 80.6 (s, =*C*H$_2$), 82.2 (s, =*C*H$_2$), 89.0 (s, *C*$_5$H$_5$), 118.6 (s, N*C*H), 129.3 (s, *C*$_6$H$_5$), 129.4 (s, *C*$_6$H$_5$), 129.5 (s, *C*$_6$H$_5$), 131.3 (s, *C*$_6$H$_5$), 132.6 (s, *C*$_6$H$_5$) 132.7 (s, *C*$_6$H$_5$), 133.8 (s, *ipso*-*C*$_6$H$_5$), 134.3 (s, *ipso*-*C*$_6$H$_5$), 134.4 (s, N*C*(Ru)N), 174.9 (s, N*C*Ru). $^{31}P\{^1H\}$-NMR ($CDCl_3$, δ_P) -144.2 (sp, $^1J_{PF}$ = 708 Hz, *P*F$_6$), 24.9 (s, *P*Ph$_3$ of **5**), 58.3 (s, *P*Ph$_3$ of **4**). CHN (%): $[C_{33}H_{36}F_6N_2P_2Ru]\times4[C_{32}H_{34}F_6N_2P_2Ru]\times0.1H_2O$: C, 53.22 (53.11), H, 4.26 (4.79), N, 4.01 (3.85). MS (ESI): m/z 593.1619 ([**4**]$^+$), 579.1501 ([**5**]$^+$) calcd for $C_{33}H_{36}N_2PRu$ (**4**) 593.166, $C_{32}H_{34}N_2PRu$ (**5**) 579.150.

[(*p*-cym)RuCl(**L3**)]PF_6 (**6**): Yield: 37%. ^{1}H-NMR ($CDCl_3$, δ_H) 1.21 (t, $^3J_{HH}$ = 6 Hz, *p-cym* (C*H*$_3$)$_2$, 6H), 1.85 (s, C(2)-C*H*$_3$, 3H), 2.62 (s, *p-cym* C*H*$_3$, 3H), 2.75 (pent, $^3J_{HH}$ = 9 Hz, *p-cym* C*H*(CH$_3$)$_2$, 1H), 3.62 (s, NC*H*$_3$, 3H), 4.88 (d, $^3J_{HH}$ = 15 Hz, *p-cym* C*H*, 1H), 5.17 (d, $^3J_{HH}$ = 6 Hz, *p-cym* C*H*, 1H), 5.35 (d, $^3J_{HH}$ = 15 Hz, *p-cym* C*H*, 1H), 5.52 (s, C*H*$_2$, 2H), 5.57 (d, $^3J_{HH}$ = 6 Hz, *p-cym* C*H*, 1H), 6.58 (s, NC*H*, 1H), 7.32 (t, $^3J_{HH}$ = 6 Hz, C_5H_4N, 1H), 7.61 (d, $^3J_{HH}$ = 9 Hz,

C_5H_4N, 1H), 7.77 (t, $^3J_{HH}$ = 6 Hz, C_5H_4N, 1H), 9.36 (d, $^3J_{HH}$ = 9 Hz, C_5H_4N, 1H). $^{13}C\{^1H\}$-NMR ($CDCl_3$, δ_C) 9.52 (s, *p-cym* (CH_3)$_2$), 18.1 (s, CCH_3), 22.4 (s, *p-cym* CH_3), 30.6 (s, NCH_3), 34.4 (s, $CH(CH_3)_2$), 53.0 (s, CH_2), 82.0 (s, *p-cym*), 86.0 (s, *p-cym*), 88.8 (s, *p-cym*), 99.5 (s, *p-cym*), 107.1 (s, C_5H_4N), 124.6 (s, NCH), 125.1 (s, *ipso p-cym*), 125.5 (s, C_5H_4N), 139.1 (s, NCN), 141.9 (s, C_5H_4N), 150.0 (s, C_5H_4N), 156.0 (s, C_5H_4N), 157.8 (s, NCRu). $^{31}P\{^1H\}$-NMR ($CDCl_3$, δ_P) -144.3 (sp, $^1J_{PF}$ = 709 Hz, PF_6). CHN (%): $[C_{21}H_{27}ClF_6N_3PRu]\times 0.4CH_2Cl_2$: C, 40.52 (40.36), H, 4.52 (4.40), N, 6.17 (6.60). MS (ESI): m/z 458.0948 (**6**$^+$) calcd for $C_{21}H_{27}ClN_3Ru$ 458.094.

[CpRu(PPh_3)(**L3**)]PF_6 (**7**): Complex **8**, [CpRu(PPh_3)(**L3***)]PF_6, coordinated as a C(2)-NHC of **L3** less one methyl group, is obtained as a by-product that co-elutes with **7**. Yield: 26% (**4**, by NMR); 25% (**5**, by NMR). **7**/**8**: ^1H-NMR ($CDCl_3$, δ_H) 2.15 (s, C(2)-CH_3, 1.5H), 2.99 (s, NCH_3, 2H), 3.33 (s, NCH_3, 1H), 4.73 (s, C_5H_5, 5H), 4.78 (d, $^2J_{HH}$ = 15Hz, CH_2, 1H), 5.36 (d, $^2J_{HH}$ = 18 Hz, CH_2, 1H), 6.32 (s, NCH, 0.5H), 6.43 (s, NCH, 0.5H), 6.62 (s, NCH, 0.6H), 6.87 (m, C_5H_4N and C_6H_5, 7H), 7.21-7.34 (m, C_6H_5, 8H), 7.42-7.48 (m, C_6H_5, 4H), 8.23 (d, $^3J_{HH}$ = 6 Hz, C_5H_4N, 1H). $^{13}C\{^1H\}$-NMR ($CDCl_3$, δ_C) 9.6 (s, CCH_3), 33.9 (s, NCH_3), 37.3 (s, NCH_3), 53.9 (s, CH_2), 55.1 (s, CH_2), 77.6 (s, C_5H_5), 122.5 (s, NCH), 123.3 (s, NCH), 125.3 (s, NCH), 125.4 (s, C_6H_5), 128.1 (s, C_6H_5), 128.4 (s, C_6H_5), 128.5 (C_6H_5), 129.4 (C_5H_4N), 129.8 (C_5H_4N), 133.0 (C_5H_4N), 133.1 (s, C_5H_4N), 133.5 (s, C_5H_4N), 135.3 (s, C_5H_4N), 135.9 (s, NCN), 137.0 (s, C_5H_4N), 137.6 (s, *ipso*-C_6H_5), 157.3 (s, NC(Ru)N), 159.9 (s, NCN), 184.4(s, NCRu). $^{31}P\{^1H\}$-NMR ($CDCl_3$, δ_P) -144.2 (sp, $^1J_{PF}$ = 708 Hz, PF_6), 55.96 (s, PPh$_3$ of **8**), 56.8 (s, PPh$_3$ of **7**). CHN (%): $[C_{34}H_{33}F_6N_3P_2Ru]\times$ $[C_{33}H_{31}F_6N_3P_2Ru]\times 1.33CHCl_3$: C, 49.03 (49.25), H, 4.47 (3.95), N, 5.23 (5.04). MS (ESI): m/z 616.1520 (**7**$^+$), 602.1279 (**8**$^+$) calcd for $C_{34}H_{33}N_3PRu$ (**7**) 616.146, $C_{33}H_{31}N_3PRu$ (**8**) 602.130.

[(*p*-cym)RuCl(**L4**)]PF_6 (**9**): Yield: 62%. ^1H-NMR ($CDCl_3$, δ_H) 1.22-1.35 (m, CH(CH_3)$_2$, 12H), 1.66 (s, CCH_3, 3H), 1.74 (s, CCH_3, 3H), 1.88 (s, *p-cym* CH_3, 3H), 2.69 (pent, $^3J_{HH}$ = 6 Hz, *p-cym* CH(CH$_3$)$_2$, 1H), 3.23 (pent, $^3J_{HH}$ = 6 Hz, CH(CH$_3$)$_2$, 1H), 3.73 (d, $^2J_{HH}$ = 15 Hz, =CH_2, 1H), 4.03 (s, CH_2, 1H), 4.26 (d, $^2J_{HH}$ = 15 Hz, =CH_2, 1H), 4.57 (s, CH_2, 1H), 4.60 (d, $^3J_{HH}$ = 6 Hz, =CH_2, 2H), 4.96 (s, CH_2, 1H), 5.02 (d, $^3J_{HH}$ = 6 Hz, *p-cym*, 1H), 5.51 (s, CH_2, 1H), 5.63 (d, $^3J_{HH}$ = 6 Hz, *p-cym*, 1H), 6.28 (d, $^3J_{HH}$ = 6 Hz, *p-cym*, 1H), 6.42 (d, $^3J_{HH}$ = 6 Hz, *p-cym*, 1H), 7.17 (s, NCH, 1H). $^{13}C\{^1H\}$-NMR ($CDCl_3$, δ_C) 15.2 (s, *p-cym* (CH_3)$_2$), 18.8 (s, *p-cym* (CH_3)$_2$), 19.4 (s, CCH_3),

19.6 (s, C*C*H$_3$), 24.2 (s, *p-cym C*H$_3$), 24.9 (s), 26.6 (s, *C*H(CH$_3$)$_2$), 30.7 (s, *C*H(CH$_3$)$_2$), 53.2 (s, *C*H$_2$), 56.1 (s, *C*H$_2$), 90.5 (s, =*C*H), 93.4 (s, =*C*H), 95.6 (s, =*C*H), 98.2 (s, =*C*H), 99.4 (s, *p-cym*), 103.5 (s, *p-cym*), 113.4 (s, *p-cym*), 118.7 (s, *p-cym*), 125.7 (s, N*C*H), 139.5 (s, N*C*N), 146.8 (s, *ipso p-cym*), 148.0 (s, *ipso p-cym*), 152.3 (s, N*C*Ru). ^{31}P{^{1}H}-NMR (CDCl$_3$, δ_P) -144.2 (sp, $^{1}J_{PF}$ = 710 Hz, *P*F$_6$). CHN (%): [C$_{24}$H$_{36}$ClF$_6$N$_2$PRu]: C, 42.15 (42.43), H, 3.95 (5.40), N, 3.70 (3.99). MS (ESI): m/z 489.1451 (**9**$^+$) calcd for C$_{24}$H$_{36}$ClN$_2$Ru 489.161.

[CpRu(PPh$_3$)(**L4**)]PF$_6$ (**10**): Yield: 55%. ^{1}H-NMR (CDCl$_3$, δ_H) 1.01 (d, $^{3}J_{HH}$ = 9 Hz, CH(C*H*$_3$)$_2$, 3H), 1.24 (d, $^{3}J_{HH}$ = 9 Hz, CH(C*H*$_3$)$_2$, 3H), 1.55 (s, CC*H*$_3$, 3H), 1.74 (s, CC*H*$_3$, 3H), 1.88 (d, $^{3}J_{HH}$ = 12 Hz, =C*H*$_2$, 1H), 2.27 (d, $^{3}J_{HH}$ = 15 Hz, =C*H*$_2$, 1H), 3.11 (pent, $^{3}J_{HH}$ = 9 Hz, C*H*(CH$_3$)$_2$, 1H), 3.65 (s, C*H*$_2$, 1H), 3.84 (d, $^{3}J_{HH}$ = 12 Hz, =C*H*, 1H), 4.48 (s, C*H*$_2$, 2H), 4.52 (d, $^{3}J_{HH}$ = 18 Hz, =C*H*, 1H), 4.79 (s, C$_5$*H*$_5$, 5H), 5.28 (s, C*H*$_2$, 1H), 6.75 (s, NC*H*, 1H), 7.19-7.36 (m, C$_6$*H*$_5$, 15H). ^{13}C{^{1}H}-NMR (CDCl$_3$, δ_C) 19.4 (s, C*C*H$_3$), 24.6 (s, C*C*H$_3$), 25.6 (s, *C*H(CH$_3$)$_2$), 30.7 (s, =C*H*), 45.1 (s, =C*H*), 53.0 (s, *C*H$_2$), 53.4 (s, *C*H$_2$), 58.2 (s, =C*H*), 68.0 (s, =C*H*), 88.3 (s, *C*$_5$H$_5$), 112.7 (s, N*C*H), 128.1 (s, *C*$_6$H$_5$), 128.2 (s, *C*$_6$H$_5$), 130.3 (s, *C*$_6$H$_5$), 133.3 (s, *C*$_6$H$_5$), 134.9 (s, *C*$_6$H$_5$), 135.5 (s, *C*$_6$H$_5$), 140.1 (s, *ipso*-*C*$_6$H$_5$), 146.3 (s, N*C*N), 148.6 (s, N*C*Ru). CHN (%): [C$_{37}$H$_{42}$F$_6$N$_2$P$_2$Ru]: C, 55.35 (55.03), H, 5.62 (5.27), N, 3.13 (3.45). MS (ESI): m/z 647.2039 (**10**$^+$) calcd for C$_{37}$H$_{42}$N$_2$PRu 647.213.

3.3 Transfer hydrogenation catalysis

To a round-bottom flask containing the carbonyl substrate (0.6 mmol), base (5 mol%, 0.03 mmol), anisole (22 μL, 0.2 mmol), and ruthenium complex (1 mol%, 6 μmol) was added 2-propanol (4 mL) and the subsequent reaction mixture was heated under reflux at 110°C for the time indicated. Aliquots (0.05 mL) of the reaction mixture taken at specified times were diluted with 2-propanol, and analysed by GC through which conversions were determined relative to anisole as the internal standard. Aliquots (0.05 mL) diluted with CDCl$_3$ was analysed with ^{1}H-NMR for selected catalytic experiments through which conversions were determined relative to anisole as the internal standard. All yields are based on the average of at least two runs.

3.4 Secondary alcohol oxidation catalysis

To a round-bottom flask containing ±1-phenylethanol (1 mmol), KO^{t}Bu (5 mol%, 0.05 mmol), hexamethylbenzene (18 mg, 0.1 mmol), and the ruthenium complex (5 mol%, 0.05 mmol) and *ortho*-dichlorobenzene (4 mL) and the subsequent reaction mixture was stirred at 150°C for the time indicated. Aliquots (0.05 mL) of the reaction mixture were diluted with 2-propanol, and analysed by GC through which conversions were determined relative to anisole as the internal standard. All yields are based on the average of at least two runs.

*3.5 X-ray crystallography of [H**L1**]Cl, [H**L4**]Cl, **1**, **3**, **4**, **5**, **6**, **7/8a**, **7/8b** and **10***

Single crystal diffraction studies of the compounds were done using either Quazar multi-layer optics monochromated Mo Kα radiation (k = 0.71073 Å) on a Bruker D8 Venture kappa geometry diffractometer with duo Iμs sources, a Photon 100 CMOS detector and APEX II control software[30] ([H**L1**]Cl, [H**L4**]Cl, **3**, **6**, **7/8a**, **7/8b**, and **10**), or an Oxford Diffraction SuperNova area-detector diffractometer[31] using mirror optics monochromated Mo Kα radiation (λ = 0.71073 Å) and Al filtered[32] (**1**, **5**). X-ray diffraction measurements were performed at either 123(2) K (**1**, **5**), 150(2) K ([H**L1**]Cl, **3**, **6**, **7/8a**, **7/8b**), or 298(2) K ([H**L4**]Cl, **10**). Data reduction was performed using the *CrysAlisPro*[31] program. The intensities were corrected for Lorentz and polarisation effects, and an absorption correction based on the multi-scan method using SCALE3 ABSPACK in *CrysAlisPro*[31] was applied (**1**, **5**). For the remaining compounds: Data reduction was performed using SAINT+[30] and the intensities were corrected for absorption using SADABS.[30] The structures were solved by direct methods using *SHELXT*[33] using the *SHELXL-2014/7*[34] program. The non-hydrogen atoms were refined anisotropically. All H atoms were placed in geometrically idealised positions and constrained to ride on their parent atoms. For a table containing the data collection and refinement parameters, see Tables S1-S3 in the Supplementary Information.

[30] APEX2 (including SAINT and SADABS), Bruker AXS Inc., Madison, WI, 2012.
[31] Oxford Diffraction (2010). CrysAlisPro (Version 1.171.34.44). Oxford Diffraction Ltd., Yarnton, Oxfordshire, UK.
[32] P. Macchi, H. B. Bürgi, A. S. Chimpri, J. Hauser, J.; Z. Gal, *J. Appl. Cryst.*, 2011, **44**, 763-771.
[33] G. M. Sheldrick, *Acta Cryst.*, 2015, **A71**, 3-8.
[34] G. M. Sheldrick, *Acta Cryst*. 2015, **C71**, 3-8.

4. Conclusion

Variation of the half-sandwich (*p*-cymene, cyclopentadienyl) and chelating tether of the aNHCs employed, provided access to six unique half-sandwich Ru(II)-aNHC complexes. In addition, Ag-mediated C(2)-demethylation resulted in the isolation of two normally-bound Ru(II)-NHC side-products. Symmetrisation of the *N*-alkene substituents of the aNHC ligand, as well as employing an ^{i}Pr-group on the C(2)-position of the imidazolium precursor, prevented C(2)-dealkylation and allowed for the selective C(4)-ruthenation for both the *p*-cymene and cyclopentadienyl Ru(II) precursors. Preliminary catalytic studies involving transfer hydrogenation suggest a greater dependence on the presence of a vacant coordination site *via* dehalogenation (*p*-cymene Ru(II) complexes) as opposed to relying on reversible alkene and/or phosphine dissociation (cyclopentadienyl Ru(II) complexes). Furthermore, a slight deactivating effect has been observed for both *p*-cymene and cyclopentadienyl Ru(II)-aNHC complexes employing the less labile *N*-picolyl tether and the presence of a methyl group on the aNHC ligand C(5) position. These potentially hemi-labile aNHC ligand systems provide a dynamic platform for the optimisation of highly active, selective, and long-lived catalysts. Further research studies on the ability of the tethers in **1**-**10**, and other similar ligand systems, to synergistically help with metal stabilisation as well as assist with reversible coordination, remain of interest.

Acknowledgements

This work has received support from the South African National Research Foundation (ML Grant nr. 93638, FPM Grant nr. 88594) and the Central Research Fund of the University of Pretoria (ML). Single crystal X-ray diffraction collections and further assistance by Mr. D. Liles (University of Pretoria), Dr. Jürg Hauser and Dr. Piero Macchi (Universität Bern) are gratefully acknowledged.

9 Conclusion

The aim of the research outlined in this thesis focusses on the development of robust, yet highly active catalysts for different metal-specific catalytic transformations. Moreover, consideration was given to employ and develop the earth-abundant, economical analogues of PGM metals, as well as finding suitable model catalysts to evaluate the effect of normal *versus* abnormal binding of the NHC ligands. To this end, the study investigated the use of cyclopentadienyl and imidazolylidene (NHC) ligands on complexes of nickel(II), chromium(III), and ruthenium(II) to stabilise the resultant complexes, as well as their corresponding sensitive catalytic intermediates.

A range of nine (three symmetric, six asymmetric) novel imidazolium bromide salts were synthesised and characterized as ligand precursors to metal-NHC complexes. Consideration was taken to include a range of electron-donating and electron-withdrawing *N*-substituents to probe the electrochemical effect the *N*-substituents have on the overall donating capacity that the NHC ligand exhibits. Complexation of these ligands to nickel(II) allowed for the isolation and characterization of nine [CpNiBr(NHC)] complexes. These complexes found successful application as catalysts in two separate catalytic reactions: (a) firstly the Suzuki-Miyaura cross-coupling reaction for which moderate to good activity (53-79% conversion, maximum TOF = 320 h^{-1}) was observed, (b) secondly the anaerobic oxidation of secondary alcohols where moderate activity (52-84% conversion, TOF = 14-86 h^{-1}) was observed using conventional heating, and excellent activity (90-98% conversion) using microwave heating. A combination of electrochemical and DFT studies provided insight for the better catalytic performance of the complexes featuring electron-donating NHCs as opposed to those with electron-withdrawing NHC ligands. In general, complexes with electron-withdrawing *N*-substituent NHCs exhibited smaller HOMO/LUMO energy gaps, were more reactive, less stable, more prone to catalyst deactivation, and as a result yielded less efficient catalysts.

The formation of bis-carbene Ni(II) complexes as by-products during synthesis of the above mentioned nickel complexes prompted further investigation. From these studies mono- and bis-carbene complexes of [CpNi(SPh)(NHC)], [$Ni(SPh)_2(NHC)_2$], and [$NiBr_2(NHC)_2$] were isolated

and characterised. A detailed DFT-supported structural and conformational analysis, as well as an electronic structure study indicated the preference of the *N*-substituents to assume a "downwards" configuration, *i.e.* with the *N*-substituents facing away from the cyclopentadienyl ring, below the imidazolylidene ring plane. The electronic differences among the [CpNiBr(NHC)] were further highlighted in a DFT-supported electrochemistry study, which showed electrochemical differences in the nickel complexes due to the diverse *N*-alkyl substituents present. From these studies, various electrochemical processes were identified: a quasi-reversible Ni(II)/Ni(III) couple ($0.068\ V \leq E^{\circ\prime} \leq 0.120\ V$) is followed by electrochemically and chemically irreversible ligand based oxidation peaks (E_{pa} ~ 0.35 V and ~0.405 V). Depending on the *N*-substituents, either one (non-NO_2-containing NHCs) or two (NO_2-containing NHCs) reduction processes were observed below -1.3 V. The non-NO_2-containing NHCs exhibited a Ni(II)/Ni(I) reduction peak, whereas the NO_2-containing NHC complexes exhibited a NO_2 reduction peak first, followed by a Ni(II)/Ni(I) reduction peak. Furthermore, these results indicated electron-donating NHC complexes of nickel required less energy for oxidation, and were therefore more applicable to analogous palladium catalysed reactions relying on facile metal-based oxidation/reduction processes.

In order to evaluate the stabilising effect of the above mentioned imidazolium bromide ligands, the series of metal-NHC complexes were extended to include chromium(III) complexes. It was found that the NHC salts with non-NO_2-containing *N*-substituents (five ligands) could be complexes to chromium(II), which, after chromium oxidation, formed five complexes of the type [CpCrBrCl(NHC)]. Exposure of these heterohalo complexes to an excess of $CHCl_3$ or CCl_4 leads to the formation of complexes [$CpCrCl_2$(NHC)]. Complexation of NO_2-containing NHC salts were unsuccessful, since ligand decomposition resulted in the formation of an ionic complex [$C_4H_7N_2$][$CpCrBrCl_2$]. All six Cr(III) complexes were found to be catalytically active in the base-free glucose dehydration reaction. Moderate activity (52-81% conversion) was observed. Findings from the supplementary DFT and electrochemical studies corresponded to the observation that the Cr-NHC complexes featuring electron-donating *N*-substituents were slightly more active and longer-lived catalysts than those with electron-withdrawing *N*-substituents. The complex salt, [$C_4H_7N_2$][$CpCrBrCl_2$], was found to exhibit the highest catalytic activity among

six Cr(III) complexes, by virtue of its increased Lewis acidity, and increased number of potential reaction sites.

As part of developing NHCs that strongly bind to a metal without sacrifice of vacant sites required for catalysis, potentially hemilabile NHC ligand systems were investigated. A range of six new bidentate (benz)imidazolium chloride salts (one symmetric, five asymmetric), each bearing a *N*-2-methylallyl substituent were synthesised and complexed to ruthenium(II) (three different Ru(II) precursors) *via* silver transmetallation. In order to further evaluate additional stereoelectronic effects that ancillary ligands might have on the overall stability and reactivity of the ruthenium complexes, variations to the inner coordination sphere of the resulting Ru-NHC complexes were made. These included different cyclopentadienyl, pnictogen, and NHC ligands with varied *N*-substituents and imidazolylidene backbone moieties. To this end eight new cationic complexes $[(C_5H_4R)Ru(EPh_3)(NHC)]PF_6$ (R = H, Me; E = P, As; NHC = Im(R')(2-methylallyl), BIm(Bn)(2-methylallyl); R' = alkyl) were isolated, purified and characterised. DFT studies suggested comparable stabilities and reactivities for all complexes except the complex featuring the 4-NO_2Bn containing NHC ligand. This complex exhibited the smallest energy gap, and was predicted to be the least active catalyst. A catalytic study (tandem transfer hydrogenation-epoxidation of ketone substrates) confirmed this prediction where the Ru-NHC complexes were employed as catalysts. While the remainder of Ru-NHC complexes exhibiting moderate activity (45-62% conversion, TOF = 8-12 h^{-1}), the NO_2-featuring Ru-NHC complex was the least active (39% conversion, TOF = 4 h^{-1}).

In an attempt at further stabilising sensitive catalytic intermediates by employing NHC ligands, the mode of coordination of the NHC ligands, as well as the type of chelating functionality were studied. A range of four new C(2)-protected bidentate imidazolium chloride salts (one symmetric, three asymmetric), each bearing either a *N*-2-methylallyl or *N*-picolyl substituent were synthesised and characterised. These ligands were found suitable as ligand precursors to abnormal NHCs, and hence were separately reacted with $[(p\text{-cym})RuCl_2]_2$ and $[CpRuCl(PPh_3)_2]$ to form ten new Ru(II)-NHC complexes (eight Ru-aNHC and two Ru-NHC). The Ru-NHC complexes formed as by-products due to Ag-mediated C(2)-dealkylation were present in selected cases. The added strength of the abnormally bound NHC over the normally bound analogue was

confirmed in a ^{1}H-NMR titration study with DCl, for which the Ru-NHC bond remained intact under corrosive conditions. The catalytic activity of the latter ten complexes was evaluated in both the transfer hydrogenation and alcohol oxidation reactions. The beneficial effect of abnormal *versus* normal mode of coordination was evident in the results where a notable increase in catalytic activity (50-93% conversion, TOF = 22-60 h^{-1}) was observed for transfer hydrogenation, as well as alcohol oxidation (56-77% conversion, TOF = 2-11 h^{-1}).

Overall, the outcomes achieved in this thesis successfully addressed the aim and objectives set in the study. Several relatively stable Cr(III), Ru(II) and Ni(II) complexes that were all moderately to highly active in six different organic transformation reactions were developed, as set out in the original aim of this project. Further objectives outlined for this project were systematically achieved through (i) the synthesis of three different ranges of symmetric (R = R') and asymmetric (R ≠ R') imidazolium halide salts featuring both monodentate and bi-dentate *N*-substituents; (ii) the synthesis, purification, and full characterisation of three different ranges of Cr(III)-NHC, Ru(II)-NHC, and Ni(II)-NHC complexes; (iii) the evaluation of the catalytic activity of each of the different complexes in metal-specific transformation reactions, and how the NHC ligands influence the overall selectivity and efficiency of the employed catalysts; (iv) the evaluation of the catalytic effect of introducing hemilability by *N*-chelating NHC ligands, and by changing the mode of NHC coordination (normal *vs.* abnormal); (v) the identification of structure-activity relationships (if any) for each set of complexes and their associated catalytic activity by employment of DFT en electrochemical methods.

Future research following from the work in this study will focus on:

- Incorporation of more electron donating ligands in the Ni(II) environment such as substituting Cp for Cp* and *p*-cymene. The complexes containing electron-donating NHC ligands were shown to exhibit the best catalytic activity.
- Expanding the Cr(III) project to include more complex salts with variation in both the cationic part (different *N*-substituents on the imidazolium moiety, addition of backbone substituents) as well as the anionic part (different halide and pseudo-halide ligands as well as modification of the π-bonded ligand).

- Substitution of the PPh_3 moieties on the normal Ru(II) complexes for $AsPPh_3$ or $SbPPh_3$ ligands, which should have higher propensity for reversible dissociation.
- Employment of electrochemistry in the evaluation of the electronic effect of different NHC ligands of Ru(II) complexes.
- Employment of more electron-donating NHC ligands such as pyrazolylidene ligands for the abnormal Ru(II) complexes.

Supplementary Information

Chapter 2
Facile Suzuki-Miyaura coupling of activated aryl halides using new CpNiBr(NHC) complexes

Frederick P. Malan, Eric Singleton, Petrus. H. van Rooyen, Marilé Landman*

Department of Chemistry, University of Pretoria, 02 Lynnwood Road, Hatfield, Pretoria, 0002, South Africa.

Supplementary Information

1. General synthesis for imidazolium bromide salts ([H**L1**]Br, [H**L2**]Br):
2. **Table 1**: Crystal data and experimental parameters for compounds [H**L1**]Br, [H**L2**]Br, **1**, **2**, **3**, **4**.

1. General synthesis for imidazolium bromide salts ([H**L1**]Br, [H**L2**]Br):

To a slurry of imidazole (2.05 g, 30 mmol), KOH (3.38 g, 60 mmol), and K_2CO_3 (4.16 g, 30 mmol), in CH_3CN (20 mL) was added the aryl halide (RX, 30 mmol) and the resulting mixture was heated under reflux for 3 hours. The mixture was concentrated to dryness, extracted with DCM (20 mL), which was washed with H_2O (3 x 8 mL). The combined organic extracts was concentrated *in vacuo* to which the second aryl halide (R'X, 30 mmol) was added in CH_3CN (20 mL) and heated under reflux overnight. The resulting mixture was concentrated to dryness and washed several times with hexane (3 x 10 mL), Et_2O (3 x 10 mL), and EtOAc (3 x 10 mL) to give the precursor imidazolium salts in high yield (> 85%).

[*Im(Me)(EtPh)]Br ([H**L1**]Br)*: Yield: 87%. ^{1}H-NMR ($(CD_3)_2CO$, δ_H) 3.32 (t, $^3J_{HH}$ = 8 Hz, NC*H*$_2$CH$_2$, 2H), 4.04 (s, C*H*$_3$, 3H), 4.72 (t, $^3J_{HH}$ = 8 Hz, NCH$_2$C*H*$_2$, 2H), 7.18 – 7.30 (m, C$_6$*H*$_5$, 3H), 7.39 – 7.75 (m, C$_6$*H*$_5$, 2H), 7.76 (s, NC*H*, 1H), 7.92 (s, NC*H*, 1H), 10.16 (s, NC*H*N, 1H). ^{13}C{^{1}H}-NMR ($(CD_3)_2CO$, δ_C) 36.5 (s, *C*H$_2$), 37.0 (s, *C*H$_3$), 51.2 (s, *C*H$_2$), 123.4 (s, N*C*H), 124.1 (s, s, N*C*H), 127.6 (s, *C*$_6$H$_5$), 129.4 (s, *C*$_6$H$_5$), 129.9 (s, *C*$_6$H$_5$), 137.9 (s, *ipso*-*C*$_6$H$_5$), 138.4 (s, N*C*N).

[*Im(Me)(4-NO_2Bn)]Br ([H**L1**]Br)*: Yield: 86%. ^{1}H-NMR ($(CD_3)_2CO$, δ_H) 3.75 (s, C*H*$_3$, 3H), 6.00 (s, C*H*$_2$, 2H), 6.96 (s, NC*H*, 1H), 7.09 (s, NC*H*, 1H), 7.99 (m, C_6H_5, 2H), 8.24 (m, C_6H_5, 2H), 10.34 (s, NC*H*N, 1H). ^{13}C{^{1}H}-NMR ($(CD_3)_2CO$, δ_C) 36.7 (s, *C*H$_3$), 51.9 (s, *C*H$_2$), 124.7 (s, N*C*H), 124.8 (s, s, N*C*H), 128.5 (s, *C*$_6$H$_4$), 131.5 (s, *C*$_6$H$_4$), 136.5 (s, *ipso*-*C*$_6$H$_5$ *trans* to NO_2-group), 138.8 (s, *ipso*-*C*$_6$H$_5$ adjacent to NO_2-group), 143.0 (s, N*C*N).

2. **Table 1**: Crystal data and experimental parameters for compounds [H**L1**]Br, [H**L2**]Br, **1**, **2**, **3**, **4**.

Complex	[H**L1**]Br	**[**H**L2**]Br	**1**	**2**	**3**	**4**
Emp. formula	$C_{12}H_{15}BrN_2$	$C_{11}H_{12}BrN_3O_2$	$C_{22}H_{21}BrN_2Ni$	$C_{16}H_{17}BrN_2Ni$	$C_{20}H_{22}BrN_2Ni$	$C_{16}H_{16}BrN_3NiO_2$
Form. weight (g.mol^{-1})	267.17	298.15	452.03	375.93	429.96	420.94
Crystal system	monoclinic	monoclinic	orthorhombic	triclinic	monoclinic	monoclinic
Space group	*P*2$_1$/*n*	*P*2$_1$/*n*	*Pnma*	*P*-1	*C*2/*c*	*P*2$_1$/*n*
Crystal descr.	colourless block	colourless rod	red fragment	red block	red block	red plate
a (Å)	7.537(2)	5.2343(2)	13.1389(6)	7.3271(5)	13.3223(9)	14.7447(1)
b (Å)	17.252(5)	24.6265(1)	17.3065(8)	9.1441(6)	12.7790(1)	28.446(3)
c (Å)	9.742(3)	19.0455(9)	8.3032(4)	11.4801(7)	22.2205(2)	9.0297(1)
α (°)	90.000	90.000	90.000	87.589(2)	90.000	90.000
β (°)	100.874(9)	94.7320(11)	90.000	82.321(2)	102.963(3)	120.885(2)
γ (°)	90.000	90.000	90.000	85.151(2)	90.000	90.000
Volume (Å^3)	1243.9(6)	2446.64(2)	1888.05(2)	759.17(9)	3686.5(5)	3250.3(6)
Z	4	8	4	2	8	8
Abs. coeff. (m.mm^{-1})	3.276	4.553	3.151	3.900	3.223	3.664
F(000)	544.0	1200.0	920.0	380.0	1752.0	1696.0
Independent refl.	4967	4829	4734	12814	4098	7850
Completeness (%)	100	100	99	100	99	100
Data/Restr/Para	4967/0/196	4829/0/309	4734/0/167	12814/0/182	4098/0/218	7850/420/417
Goodness of fit on F^2	1.050	1.116	1.289	1.027	1.046	1.079
Final R$_1$ indices	0.0323	0.0436	0.0573	0.0476	0.0263	0.0622
wR$_2$ indices (all data)	0.0796	0.1099	0.1215	0.1060	0.0592	0.1718
Largest diffr. peak and hole (e.Å^{-3})	1.19/-0.37	1.40/-0.48	1.95/-0.65	1.25/-0.53	0.69/-0.61	1.36/-0.77

Chapter 3

CpNiBr(NHC) complexes as pre-catalysts in the chemoselective anaerobic oxidation of secondary aryl alcohols: Experimental and DFT studies

Frederick P. Malan, Eric Singleton, Bryan Bulling, Ignacy Cukrowski, Petrus H. van Rooyen and Marilé Landman*

Department of Chemistry, University of Pretoria, 02 Lynnwood Road, Hatfield, Pretoria, 0002, South Africa.

Supplementary Information

1. **Table 1:** Crystal data and experimental parameters for compounds **5**, **6**, **8**.
2. **Table 2:** Selected bond distances (Å) and angles (°) for **5**, **6**, and **8**.
3. **Table 3**: TON and TOF for complexes **1-9**.
4. Calculated catalysis intermediates and transition states: Optimized structures and coordinates

1. **Table 1**: Crystal data and experimental parameters for compounds **5**, **6**, **8**.

Complex	**5**	**6**	**8**
Emp. formula	$C_{24}H_{25}N_2BrNi$	$C_{22}H_{20}N_3O_2BrNi$	$C_{24}H_{24}N_3O_2Cl_2BrNi$
Form. weight (g.mol^{-1})	480.08	497.02	595.98
Crystal system	orthorhombic	triclinic	orthorhombic
Space group	*Fdd2*	*P-1*	$P2_12_12_1$
Crystal descr.	red plate	red fragment	red needle
a (Å)	27.8772(2)	7.0558(8)	8.1143(4)
b (Å)	49.387(3)	12.3319(2)	16.4115(8)
c (Å)	6.3979(3)	14.2614(2)	18.7539(1)
α (°)	90	76.889(4)	90
β (°)	90	87.895(4)	90
γ (°)	90	81.707(4)	90
Volume (Å^3)	8808.4(4)	1195.9(3)	2497.4(2)
Z	16	2	4
Abs. coeff. (m.mm^{-1})	2.707	2.501	2.617
F(000)	3936.0	504.3	1208.0
Independent refl.	5529	5471	7680
Completeness (%)	100	95	100

Data/Restr/Para	5529/1/314	5471/0/238	7680/0/370
Goodness of fit on F^2	1.094	0.988	1.049
Final R_1 indexes	0.0360	0.0949	0.0406
wR_2 indices (all data)	0.0709	0.2497	0.0948
Largest diffr. peak and hole ($e.Å^{-3}$)	0.73/-0.35	2.28/-2.46	0.55/-0.48

2. **Table 2**: Selected bond distances (Å) and angles (°) for **5**, **6**, and **8**.

Description	**5**	**6**	**8**
Ni-C6	1.881(4)	2.15(2)	1.881(3)
Ni1-Br1	2.337(1)	2.334(2)	2.3552(5)
Br1-Ni1-C6	94.9(1)	161.0(5)	94.46(8)
N1-C6-Ni1	127.2(3)	129.6(6)	128.8(2)
N2-C6-Ni1	127.8(3)	127.9(6)	127.0(2)
C_α[a]-N1-C6	124.3(3)	123.8(7)	125.2(2)
C_α[a]-N2-C6	124.9(2)	122.3(7)	125.1(2)
C_α[a]-N1-C6-Ni1	-0.7(6)	-13(1)	-0.2(4)
C_α[a]-N2-C6-Ni1	-7.4(6)	10(1)	1.2(4)
C_β[a]-C_α[a]-N1-C6	-95.9(5)	-95.7(9)	-103.6(3)
C_β[a]-C_α[a]-N2-C6	98.5(4)	-140.3(8)	98.8(3)

[a] α-Carbon atom of the substituent on the adjacent *N*-atom. [b] β-Carbon atom adjacent to the α-carbon on the *N*-substituent. [c] γ-Carbon adjacent to the β-carbon on the *N*-substituent.

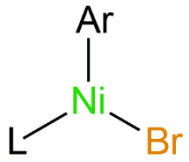
3. **Table 3**: TON and TOF for complexes **1**-**9**.

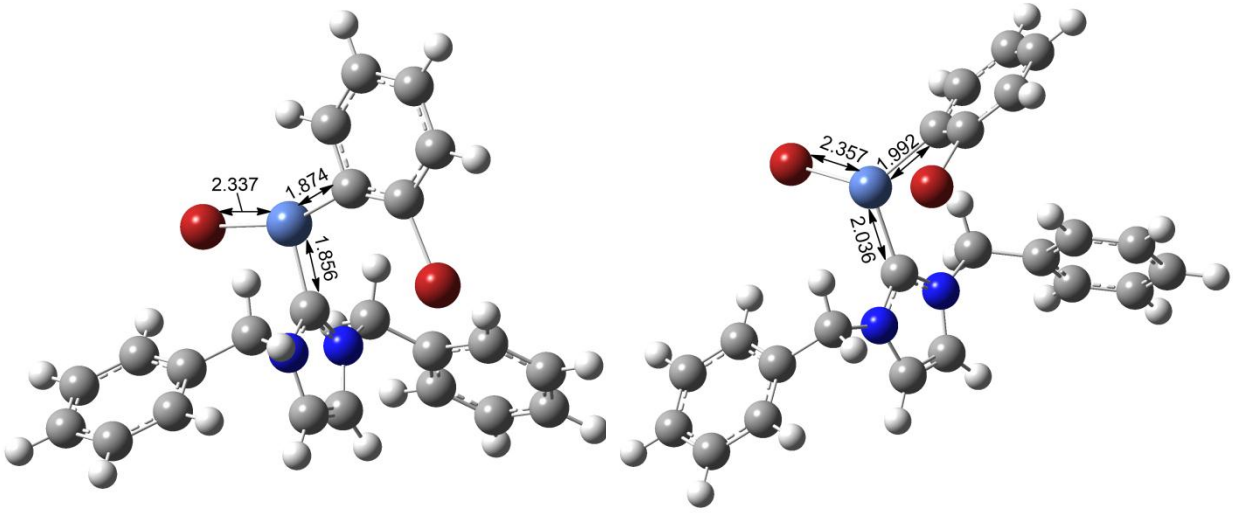
Complex	Initial TON[a]	TON[b]	Initial TOF[c] (h^{-1})
1	5.5	28.2	66.0
2	4.6	26.6	54.9
3	3.8	25.4	45.9
4	2.2	24.7	26.3
5	5.3	26.7	63.8
6	4.5	24.5	54.4
7	5.2	26.5	61.9
8	1.6	23.8	19.6
9	1.2	20.5	14.3

[a] After first 5 min of reaction. Cat conc. = 9 μmol. [b] After 120 min of reaction. Cat conc. = 9 μmol. [c] Based on initial TON within first 5 minutes of reaction.

4. Calculated catalysis intermediates and transition states: Optimized structures and coordinates

Intermediate A:

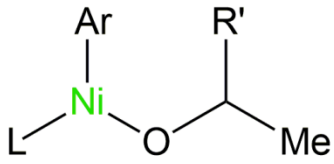


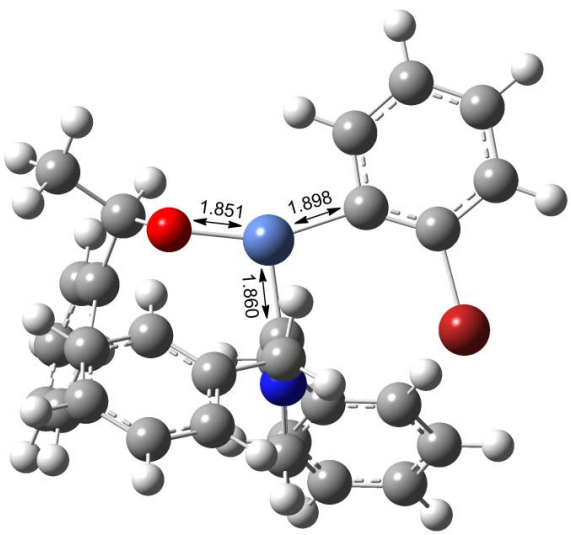


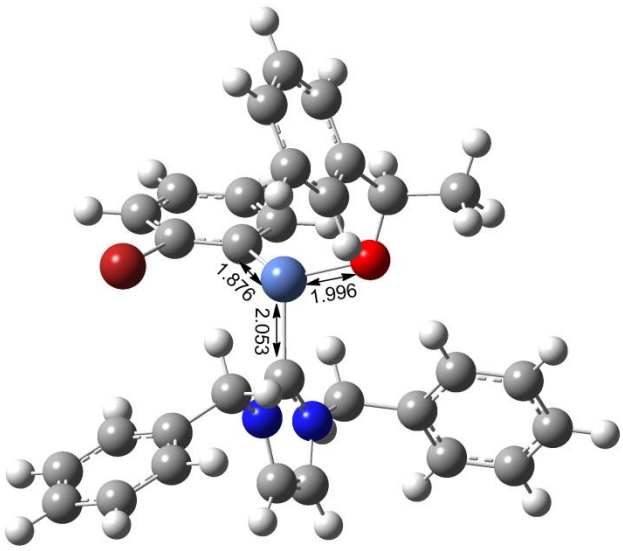
A – Singlet	X	Y	Z	A – Triplet	X	Y	Z
Br	-1.4042	-0.25968	-3.06462	Br	-1.25813	1.552967	-2.65122
Ni	-0.37098	0.895959	-1.31532	Ni	-0.14836	1.204156	-0.60098
N	0.757063	-1.41454	-0.04195	N	0.133505	-1.82731	-0.32576
C	3.106757	-2.08792	-0.52253	C	2.480703	-2.58825	-0.65152
C	3.856867	-1.34997	0.400968	C	3.222455	-1.99109	0.373948
C	1.807027	-1.54411	-1.06783	C	1.285798	-1.87471	-1.24271
C	5.063563	-1.84531	0.884202	C	4.321448	-2.64616	0.919753
C	3.588473	-3.32674	-0.95095	C	2.865079	-3.84521	-1.12355
C	5.538384	-3.08319	0.449339	C	4.695788	-3.90405	0.446213
C	4.799666	-3.82301	-0.46938	C	3.967885	-4.50222	-0.57834
C	-0.18337	-0.44317	-0.0436	C	-0.53235	-0.69782	0.015672
C	0.501364	-2.3282	0.971241	C	-0.45629	-2.94468	0.244795
H	1.424095	-2.17792	-1.87064	H	0.964779	-2.3604	-2.16726
H	3.016917	-3.90551	-1.67085	H	2.305786	-4.31104	-1.93059
H	1.942413	-0.54623	-1.48717	H	1.525666	-0.83984	-1.47965
H	5.164009	-4.78537	-0.81399	H	4.258	-5.47697	-0.95708
H	5.637633	-1.26257	1.597292	H	4.892534	-2.17052	1.710379
H	1.138223	-3.17743	1.148817	H	-0.06432	-3.93778	0.104294
H	3.491205	-0.38649	0.742519	H	2.943814	-1.0061	0.734676
H	6.481847	-3.46657	0.824372	H	5.555885	-4.41157	0.870964
N	-1.02447	-0.74109	0.970652	N	-1.54725	-1.12404	0.808533
C	-3.49089	-0.67882	1.306698	C	-3.96582	-0.55118	0.964176
C	-3.9809	-1.13963	0.078849	C	-4.34132	-0.32428	-0.3652
C	-2.1794	0.072591	1.374949	C	-2.55605	-0.24755	1.422251

C	-5.19594	-1.81458	0.020319	C	-5.6404	-0.59799	-0.78062
C	-4.23685	-0.90243	2.465615	C	-4.90985	-1.04924	1.864309
C	-5.93644	-2.03473	1.182376	C	-6.57822	-1.09793	0.123582
C	-5.45647	-1.57645	2.405707	C	-6.21248	-1.32201	1.447643
C	-0.61379	-1.90271	1.608923	C	-1.51747	-2.50185	0.958896
H	-2.18246	0.937054	0.710439	H	-2.27267	0.773602	1.165017
H	-3.86832	-0.54111	3.422047	H	-4.6306	-1.21787	2.901066
H	-1.99667	0.441175	2.387109	H	-2.47581	-0.33966	2.508136
H	-6.02826	-1.74112	3.313361	H	-6.93795	-1.70613	2.157481
H	-5.5679	-2.16473	-0.93702	H	-5.92293	-0.41368	-1.81186
H	-1.15392	-2.31793	2.442669	H	-2.24965	-3.03476	1.541842
H	-3.41274	-0.96743	-0.83076	H	-3.61948	0.072787	-1.07334
H	-6.88513	-2.55952	1.131938	H	-7.59145	-1.30731	-0.20399
C	0.398684	2.329823	-0.38651	C	1.75597	1.733213	-0.35601
C	0.173798	3.278666	-1.39275	C	2.758191	1.783007	-1.33786
C	1.039147	2.775032	0.759746	C	2.150147	2.110919	0.918003
C	0.56752	4.609618	-1.27062	C	4.063375	2.171923	-1.03401
H	-0.33182	2.96848	-2.31745	H	2.509876	1.526834	-2.36475
C	1.446798	4.0998	0.918282	C	3.433816	2.508497	1.273542
C	1.208114	5.016901	-0.10248	C	4.402487	2.529753	0.270331
H	0.376161	5.315189	-2.07236	H	4.816448	2.20237	-1.81582
H	1.945834	4.411025	1.828533	H	3.674389	2.798692	2.289872
H	1.524827	6.04747	0.019622	H	5.415497	2.836161	0.51137
Br	1.421642	1.576064	2.237081	Br	0.766558	2.114454	2.311719

Intermediate B:



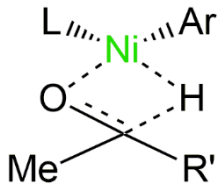


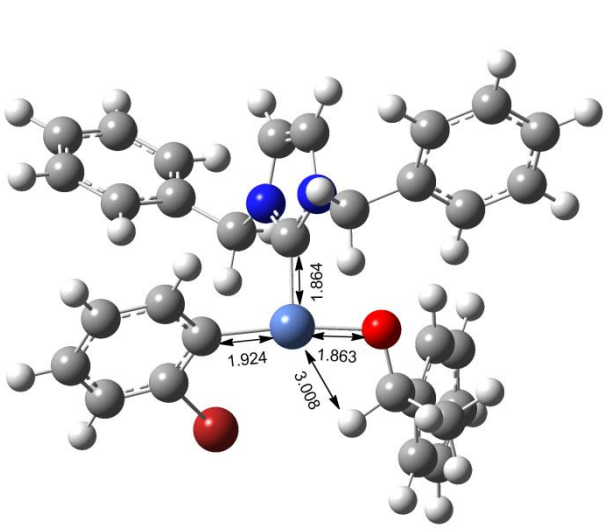


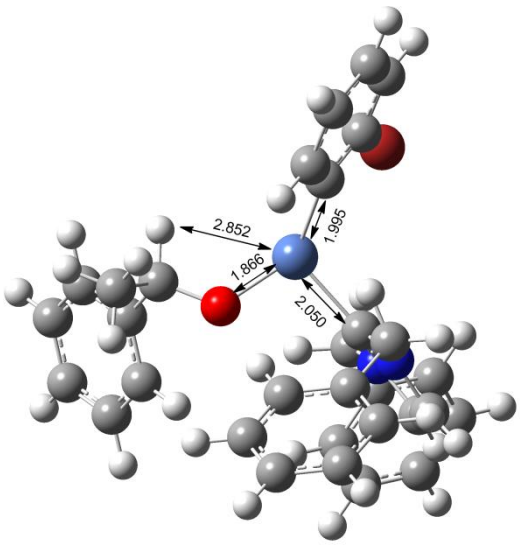
B – Singlet	X	Y	Z	B – Triplet	X	Y	Z
Ni	0.210631	0.869065	1.330184	Ni	0.37595	-0.67488	0.070091
N	-0.54065	-0.88398	-0.85522	N	-0.88518	2.08259	-0.54776
C	-2.40548	-2.52128	-0.63829	C	-3.33698	2.147352	-0.98813
C	-3.52946	-1.7813	-1.0242	C	-3.8678	2.112038	0.30662
C	-1.22613	-1.84719	0.023158	C	-2.00718	1.494277	-1.29385
C	-4.61975	-2.41335	-1.61323	C	-5.10014	2.697295	0.577825
C	-2.39514	-3.9013	-0.85342	C	-4.06246	2.777862	-2.0008
C	-4.6031	-3.79302	-1.82157	C	-5.81959	3.323742	-0.44051
C	-3.48956	-4.53615	-1.44046	C	-5.2997	3.362434	-1.7308
C	0.047936	0.251331	-0.4164	C	0.103453	1.359794	0.039624
C	-0.30062	-1.05925	-2.21063	C	-0.64341	3.444663	-0.43824
H	-0.49552	-2.58695	0.355484	H	-1.78931	1.564378	-2.36286
H	-1.52722	-4.48254	-0.55594	H	-3.66196	2.808471	-3.01034
H	-1.5406	-1.2784	0.900015	H	-2.02565	0.434398	-1.03513
H	-3.46985	-5.60967	-1.59873	H	-5.85378	3.846595	-2.52842
H	-5.4864	-1.82954	-1.90629	H	-5.50356	2.659702	1.58449
H	-0.69207	-1.90039	-2.75596	H	-1.32135	4.184614	-0.82853
H	-3.54492	-0.70729	-0.86687	H	-3.31463	1.620491	1.100701
H	-5.4561	-4.28484	-2.27812	H	-6.78217	3.777091	-0.22714
N	0.652569	0.792142	-1.49827	N	0.958246	2.290257	0.528002
C	2.86755	1.930523	-1.6868	C	3.447015	2.338773	0.456164
C	3.655868	1.390579	-0.66271	C	3.766762	1.626121	-0.70633
C	1.372322	2.073874	-1.50178	C	2.205609	1.984706	1.246822
C	5.032347	1.272587	-0.83486	C	4.909499	1.957931	-1.42873
C	3.477683	2.352828	-2.86962	C	4.286082	3.37085	0.881212
C	5.635964	1.691805	-2.02101	C	5.743611	2.991879	-1.00164
C	4.856912	2.23441	-3.03885	C	5.432286	3.69759	0.156999
C	0.444702	-0.00425	-2.61478	C	0.52076	3.57369	0.24009
H	1.13838	2.551126	-0.54984	H	2.167919	0.921601	1.479048
H	2.874616	2.787095	-3.66291	H	4.05011	3.919551	1.789556
H	0.941544	2.694953	-2.29037	H	2.187468	2.52625	2.195766
H	5.31949	2.569092	-3.96196	H	6.078719	4.499564	0.4993
H	5.637184	0.856492	-0.03543	H	5.153013	1.401335	-2.32837
H	0.842641	0.249826	-3.58267	H	1.071312	4.45087	0.536315
H	3.192523	1.062146	0.265162	H	3.125744	0.81097	-1.03684
H	6.710063	1.600126	-2.14783	H	6.63472	3.242831	-1.56854
C	-1.31914	1.985075	1.456788	C	0.586411	-1.45304	1.896125
C	-1.28187	2.285589	2.831686	C	1.820073	-1.80055	2.476015
C	-2.35802	2.573522	0.746521	C	-0.52451	-1.71815	2.684342
C	-2.21551	3.110236	3.456118	C	1.911839	-2.3607	3.750688
H	-0.48299	1.859496	3.447317	H	2.735879	-1.6363	1.912027
C	-3.3119	3.405497	1.332354	C	-0.49027	-2.27353	3.958422
C	-3.23897	3.67159	2.696981	C	0.756296	-2.59455	4.494095
H	-2.14327	3.312084	4.520286	H	2.883004	-2.61824	4.163625
H	-4.1003	3.842117	0.730479	H	-1.40052	-2.45627	4.517885
H	-3.97888	4.317586	3.158454	H	0.816981	-3.02989	5.48673
Br	-2.56261	2.293104	-1.17046	Br	-2.29205	-1.30282	1.937699

O	1.814648	0.143301	1.900539	O	1.666797	-0.88189	-1.27509
C	1.934754	-1.02437	2.662317	C	1.983984	-2.16939	-1.73874
H	1.074915	-1.14844	3.346697	H	2.438657	-2.76609	-0.92892
C	2.003577	-2.29873	1.819623	C	0.750967	-2.9349	-2.21956
C	2.59368	-2.29653	0.552294	C	-0.2104	-2.29759	-3.01412
C	1.499172	-3.50606	2.314813	C	0.554799	-4.27834	-1.88991
C	2.681049	-3.46868	-0.19658	C	-1.32935	-2.98769	-3.47284
H	2.975958	-1.36436	0.153728	H	-0.0676	-1.25278	-3.27101
C	1.584798	-4.68218	1.570584	C	-0.5661	-4.97276	-2.34401
H	1.030357	-3.5259	3.295834	H	1.283157	-4.78454	-1.26182
C	2.177074	-4.6672	0.308417	C	-1.51183	-4.3296	-3.13839
H	3.144442	-3.44598	-1.17858	H	-2.06205	-2.47971	-4.09344
H	1.187992	-5.60864	1.975389	H	-0.70436	-6.01409	-2.06913
H	2.247545	-5.58055	-0.27438	H	-2.38693	-4.86694	-3.49039
C	3.191814	-0.90378	3.543133	C	3.028391	-2.05293	-2.86043
H	4.079147	-0.8016	2.912535	H	2.629882	-1.45646	-3.68571
H	3.115281	-0.0128	4.171484	H	3.924704	-1.55582	-2.47988
H	3.323529	-1.77918	4.186354	H	3.313068	-3.03501	-3.24989

Transition state 1:





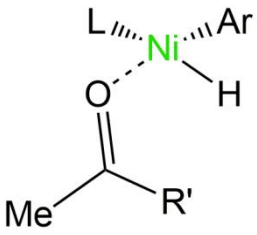


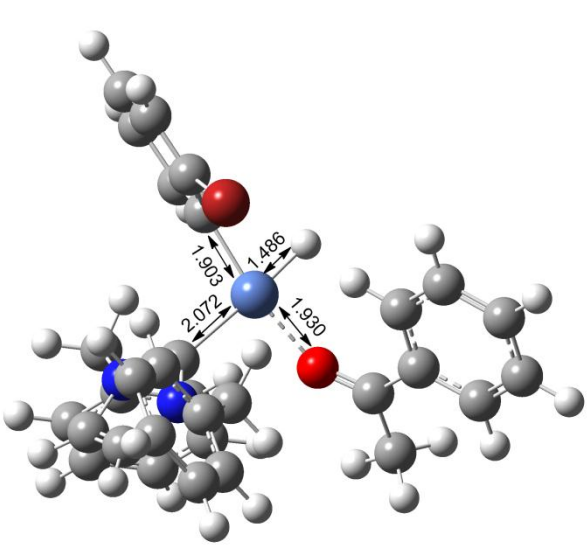
TS1 – Singlet	X	Y	Z	TS1 – Triplet	X	Y	Z
Ni	0.216223	-1.09604	-0.58546	Ni	0.249957	-0.45511	1.007423
N	-0.28998	0.961345	1.34397	N	1.546	1.754586	-0.64886
C	-2.62548	1.83074	1.262362	C	3.636836	2.496531	0.482526
C	-3.12008	0.938607	2.221092	C	4.468109	1.393696	0.255143
C	-1.34302	1.550139	0.509184	C	2.136387	2.32025	0.571588

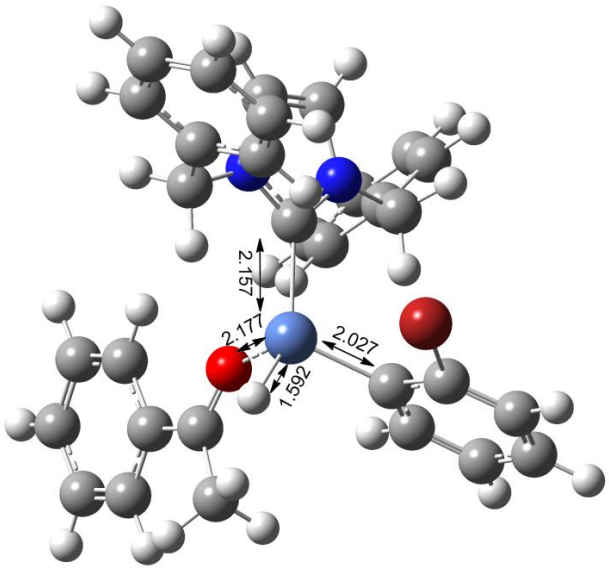
C	-4.33535	1.186875	2.853017	C	5.848087	1.555093	0.193232
C	-3.37494	2.965706	0.944038	C	4.21331	3.7573	0.647567
C	-5.07561	2.324058	2.532179	C	6.41676	2.818359	0.36084
C	-4.59415	3.21122	1.573085	C	5.597393	3.919669	0.589624
C	0.462467	-0.09718	0.969297	C	0.747263	0.648764	-0.67455
C	0.195247	1.504567	2.528418	C	1.714184	2.297206	-1.91407
H	-0.94964	2.460478	0.050681	H	1.656	3.280126	0.781505
H	-3.00176	3.662747	0.199152	H	3.577932	4.620176	0.828696
H	-1.51779	0.841523	-0.30332	H	1.87085	1.638761	1.384096
H	-5.16355	4.098886	1.316707	H	6.031763	4.905446	0.722141
H	-4.70873	0.485797	3.592723	H	6.482569	0.691887	0.020286
H	-0.26358	2.358512	2.996957	H	2.330967	3.161091	-2.09728
H	-2.56517	0.036098	2.458843	H	4.03069	0.408103	0.129189
H	-6.02291	2.515602	3.025846	H	7.494136	2.940857	0.315013
N	1.398347	-0.24282	1.933083	N	0.428043	0.51767	-1.98996
C	3.831279	-0.73189	1.617485	C	-1.74072	-0.05123	-3.07222
C	4.06553	-0.04783	0.418359	C	-2.68181	0.509774	-2.20104
C	2.450918	-1.26848	1.935811	C	-0.41379	-0.55167	-2.54232
C	5.344526	0.420142	0.12949	C	-3.90942	0.954852	-2.68079
C	4.88784	-0.94722	2.504451	C	-2.0566	-0.16054	-4.42758
C	6.396476	0.209467	1.021531	C	-4.21595	0.843176	-4.03763
C	6.167963	-0.47996	2.209007	C	-3.28802	0.282753	-4.91031
C	1.256006	0.750505	2.897016	C	1.004736	1.515954	-2.76067
H	2.146833	-2.01994	1.205444	H	-0.55417	-1.27484	-1.74019
H	4.713435	-1.48466	3.433202	H	-1.33943	-0.60446	-5.11282
H	2.442778	-1.74538	2.919015	H	0.148561	-1.05138	-3.33498
H	6.981553	-0.65355	2.906188	H	-3.51993	0.188159	-5.96644
H	5.523147	0.943903	-0.80439	H	-4.63215	1.382575	-1.99309
H	1.918571	0.826906	3.74276	H	0.858441	1.581074	-3.82614
H	3.256798	0.081518	-0.29891	H	-2.44861	0.589259	-1.14387
H	7.391014	0.576484	0.788092	H	-5.17552	1.187696	-4.40994
C	-1.0331	-2.27046	0.288029	C	0.016557	-2.40234	0.474472
C	-1.33602	-2.59341	1.620808	C	-1.22981	-3.01643	0.246497
C	-1.78943	-2.95035	-0.65479	C	1.105045	-3.25193	0.334444
C	-2.33136	-3.51617	1.948434	C	-1.36041	-4.3684	-0.07636
H	-0.78359	-2.1183	2.428164	H	-2.13738	-2.41747	0.307852
C	-2.79132	-3.87241	-0.39278	C	1.0325	-4.60499	0.01563
C	-3.06459	-4.15062	0.946742	C	-0.22566	-5.16918	-0.18783
H	-2.53578	-3.74377	2.9908	H	-2.34574	-4.7965	-0.24244
H	-3.33934	-4.35591	-1.19347	H	1.93085	-5.20584	-0.07265
H	-3.8433	-4.86292	1.199794	H	-0.311	-6.22305	-0.43457
Br	-1.31542	-2.53199	-2.51075	Br	2.908766	-2.52146	0.591575
O	1.423094	-0.014	-1.50476	O	-1.53778	0.211974	1.297099
C	1.140347	0.725569	-2.65017	C	-2.39665	0.042447	2.178291
C	0.597703	2.118041	-2.30836	H	0.594412	-0.69101	2.554532
C	-0.56119	2.611679	-2.91281	C	-3.54616	0.97972	2.231094
C	1.215747	2.905207	-1.32901	C	-3.47989	2.182624	1.507767
C	-1.0883	3.85526	-2.56092	C	-4.70677	0.695659	2.966541

H	-1.06157	2.013754	-3.67021	C	-4.53982	3.07851	1.529336
C	0.69627	4.146713	-0.97259	H	-2.58158	2.401695	0.943656
H	2.114997	2.538107	-0.84585	C	-5.77437	1.587827	2.973327
C	-0.46168	4.628097	-1.58682	H	-4.79015	-0.23233	3.51942
H	-1.98707	4.219277	-3.05013	C	-5.69192	2.782061	2.260481
H	1.198526	4.745735	-0.21809	H	-4.47125	4.010426	0.977756
H	-0.86394	5.599013	-1.31402	H	-6.67027	1.351646	3.537764
C	2.4152	0.815943	-3.51576	H	-6.52186	3.481117	2.274212
H	3.101831	1.581859	-3.14379	C	-2.23724	-1.06217	3.175433
H	2.928865	-0.14749	-3.48909	H	-2.45674	-2.02673	2.707565
H	2.178353	1.05546	-4.55717	H	-1.17222	-1.1003	3.437496
H	0.36581	0.246051	-3.27316	H	-2.85389	-0.94389	4.064403

Intermediate Ca:





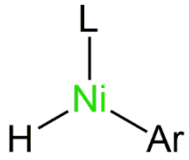


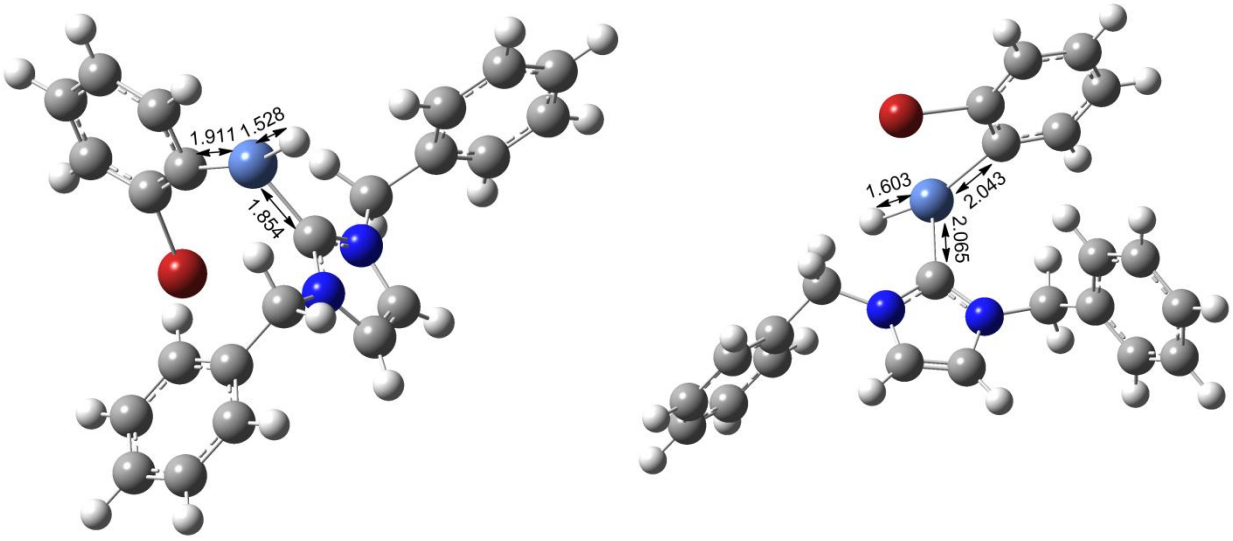
Ca – Singlet	X	Y	Z	Ca – Triplet	X	Y	Z
Ni	-0.61633	0.192529	1.10754	Ni	-0.33569	-0.48125	-1.06532
N	0.15821	-0.25483	-1.86305	N	-1.61248	1.821245	0.6433
C	2.561963	-0.44702	-2.48972	C	-3.68397	2.537717	-0.54009
C	2.808734	-1.81671	-2.33665	C	-4.48899	1.402008	-0.39529
C	1.520124	0.248627	-1.64128	C	-2.17628	2.408024	-0.57884
C	3.778362	-2.44884	-3.1082	C	-5.87461	1.519963	-0.37988
C	3.306067	0.271461	-3.42808	C	-4.29233	3.78748	-0.67005
C	4.517499	-1.72244	-4.04249	C	-6.47507	2.772708	-0.5116

C	4.281029	-0.36006	-4.20017	C	-5.68194	3.906752	-0.65808
C	-0.77587	-0.38176	-0.8773	C	-0.84485	0.69626	0.668491
C	-0.36096	-0.57582	-3.11077	C	-1.78757	2.351046	1.913539
H	1.536134	1.323564	-1.84319	H	-1.71677	3.386934	-0.74189
H	3.125919	1.335513	-3.55511	H	-3.67755	4.675836	-0.78804
H	1.724554	0.107949	-0.58028	H	-1.86194	1.759833	-1.40061
H	4.852533	0.212975	-4.92343	H	-6.1413	4.884518	-0.76283
H	3.96263	-3.51015	-2.97579	H	-6.4882	0.631548	-0.27132
H	0.234774	-0.55803	-4.00745	H	-2.38354	3.229009	2.099202
H	2.24353	-2.38283	-1.60406	H	-4.0271	0.424413	-0.29719
H	5.275004	-2.21724	-4.64193	H	-7.55667	2.86162	-0.50224
N	-1.88402	-0.80595	-1.54514	N	-0.54817	0.538117	1.984755
C	-4.17968	0.05282	-1.06637	C	1.571366	-0.10561	3.120361
C	-3.95776	1.278885	-0.42821	C	2.569731	0.420977	2.292474
C	-3.18214	-1.07849	-0.92003	C	0.255507	-0.56493	2.529597
C	-4.88702	2.308352	-0.54066	C	3.785039	0.833612	2.829396
C	-5.34653	-0.11762	-1.81372	C	1.817684	-0.215	4.490126
C	-6.04966	2.13007	-1.29132	C	4.021366	0.723648	4.20032
C	-6.27841	0.913931	-1.92798	C	3.036334	0.196391	5.030065
C	-1.6514	-0.92357	-2.9084	C	-1.11154	1.540748	2.760588
H	-2.98145	-1.29318	0.127462	H	0.412419	-1.2625	1.707589
H	-5.53608	-1.06822	-2.30534	H	1.055582	-0.63426	5.14159
H	-3.58074	-1.99316	-1.3654	H	-0.34236	-1.08032	3.285346
H	-7.18146	0.764307	-2.51132	H	3.214195	0.1021	6.096643
H	-4.70933	3.250972	-0.03209	H	4.553512	1.233752	2.175476
H	-2.41193	-1.24816	-3.5992	H	-0.97917	1.589496	3.828734
H	-3.05566	1.42205	0.158496	H	2.391072	0.498583	1.224527
H	-6.7741	2.934083	-1.3743	H	4.971435	1.04271	4.617076
C	-0.9135	-1.48971	1.946398	C	0.016224	-2.41326	-0.56253
C	-2.17613	-1.84363	2.471202	C	1.288008	-2.99314	-0.3953
C	0.053813	-2.48296	2.085429	C	-1.04048	-3.29419	-0.38201
C	-2.44327	-3.08971	3.034194	C	1.468019	-4.34232	-0.08606
H	-2.97202	-1.10302	2.46108	H	2.174454	-2.3699	-0.50023
C	-0.16534	-3.7397	2.645108	C	-0.92023	-4.64617	-0.07533
C	-1.43693	-4.05021	3.117999	C	0.361339	-5.17468	0.07075
H	-3.43555	-3.30538	3.421306	H	2.470571	-4.74519	0.033694
H	0.641573	-4.46045	2.71365	H	-1.797	-5.27245	0.04662
H	-1.62859	-5.02368	3.558417	H	0.486968	-6.22689	0.30727
Br	1.887086	-2.13107	1.499397	Br	-2.87082	-2.60073	-0.5607
O	-0.46677	2.056507	0.629923	O	1.668921	0.336796	-1.29053
C	0.163141	3.112293	0.69808	C	2.512578	0.206483	-2.17993
H	-0.53804	0.530459	2.552209	H	-0.6309	-0.64647	-2.62065
C	1.532038	3.192169	1.261951	C	3.719031	1.081727	-2.15958
C	2.124838	2.052784	1.830727	C	3.73804	2.196486	-1.30695
C	2.254963	4.398242	1.250906	C	4.842902	0.81435	-2.95363
C	3.403172	2.120503	2.371466	C	4.850177	3.026218	-1.25666
H	1.566707	1.124046	1.868993	H	2.865661	2.401004	-0.69815
C	3.535813	4.459526	1.785931	C	5.962738	1.638151	-2.89063

H	1.821287	5.295455	0.825151	H	4.854568	-0.04684	-3.61137
C	4.112818	3.320144	2.347037	C	5.966864	2.74655	-2.04655
H	3.842532	1.232592	2.813055	H	4.850001	3.892429	-0.60315
H	4.083993	5.395696	1.768434	H	6.830869	1.416545	-3.50234
H	5.112797	3.369476	2.766096	H	6.837456	3.393135	-2.00448
C	-0.50911	4.370299	0.18978	C	2.334187	-0.81928	-3.26432
H	0.0623	4.828685	-0.62245	H	2.835572	-1.7494	-2.97509
H	-1.50166	4.117592	-0.17828	H	1.268363	-1.03636	-3.35651
H	-0.59977	5.116806	0.984064	H	2.745353	-0.49446	-4.22087

Intermediate C:

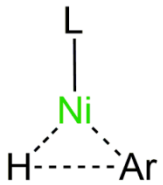


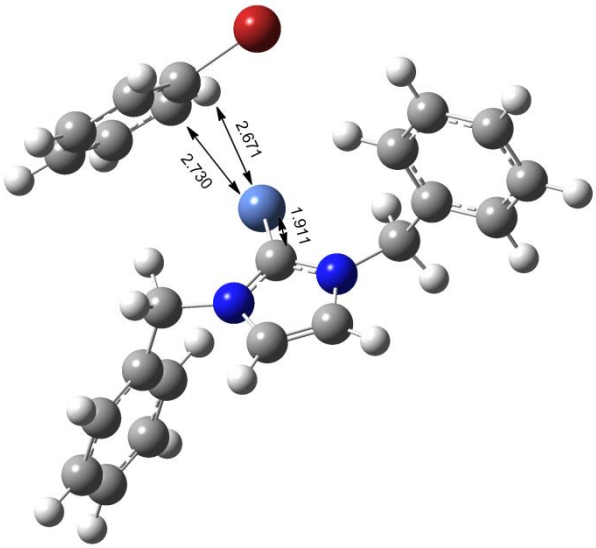


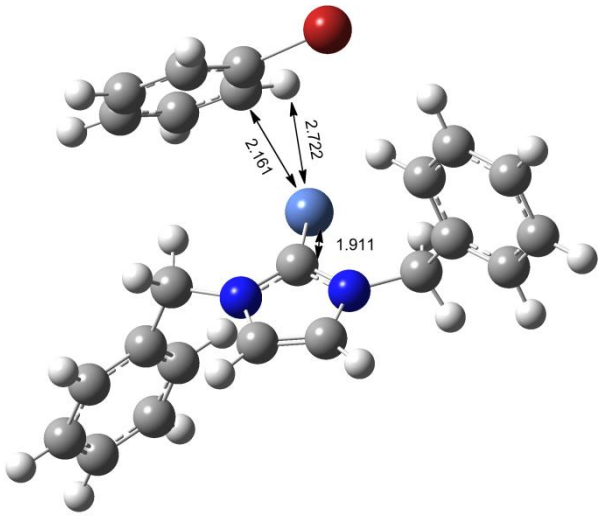
C – Singlet	X	Y	Z	C – Triplet	X	Y	Z
Ni	-0.21996	0.347215	-1.64607	Ni	-0.09718	1.316923	-1.41206
N	0.424115	-2.13406	-0.31184	N	-0.05379	-1.66001	-0.50889
C	2.89708	-2.30936	-0.58181	C	2.228622	-2.63614	-0.33557
C	3.300113	-1.08718	-0.03183	C	2.892292	-1.91194	0.66145
C	1.530184	-2.45472	-1.21805	C	1.202934	-1.95594	-1.2144
C	4.564442	-0.95401	0.532588	C	3.835656	-2.53523	1.471792
C	3.782661	-3.38838	-0.55839	C	2.532657	-3.98818	-0.50889
C	5.445039	-2.03615	0.549405	C	4.129458	-3.88782	1.296085
C	5.052765	-3.25398	0.001774	C	3.478331	-4.61388	0.302826
C	-0.34669	-1.02072	-0.40097	C	-0.67092	-0.44969	-0.50868
C	0.024893	-2.92267	0.759807	C	-0.7907	-2.60023	0.19754
H	1.385884	-3.47563	-1.58076	H	0.97412	-2.57763	-2.08454
H	3.481822	-4.34163	-0.98503	H	2.033905	-4.55645	-1.28972
H	1.412505	-1.78779	-2.07376	H	1.579868	-0.99848	-1.57108

H	5.731254	-4.10112	0.011529	H	3.707109	-5.66453	0.155681
H	4.863024	-0.00147	0.957846	H	4.349026	-1.96201	2.23687
H	0.527933	-3.84019	1.014975	H	-0.46191	-3.61831	0.319815
H	2.621122	-0.24049	-0.04087	H	2.675793	-0.85637	0.791491
H	6.431903	-1.92855	0.988106	H	4.868016	-4.37083	1.92781
N	-1.2329	-1.12242	0.62125	N	-1.80465	-0.65057	0.211577
C	-3.66412	-0.59442	0.509985	C	-4.208	-0.01731	0.293753
C	-3.95304	-0.85521	-0.83464	C	-4.67108	-0.18709	-1.01641
C	-2.27928	-0.13943	0.921074	C	-2.77801	0.403859	0.542523
C	-5.2285	-1.2612	-1.21291	C	-5.98908	-0.56311	-1.25364
C	-4.67497	-0.74092	1.461436	C	-5.08987	-0.22539	1.356221
C	-6.23355	-1.40586	-0.25577	C	-6.86273	-0.77252	-0.18582
C	-5.95556	-1.14316	1.082287	C	-6.41213	-0.60129	1.119884
C	-1.02115	-2.29245	1.339117	C	-1.89159	-1.96138	0.655789
H	-1.98856	0.774745	0.402425	H	-2.51345	1.256687	-0.083
H	-4.46429	-0.53373	2.507258	H	-4.74455	-0.08406	2.376898
H	-2.24367	0.073039	1.991549	H	-2.63576	0.690082	1.587678
H	-6.7323	-1.25111	1.832676	H	-7.08762	-0.75636	1.955106
H	-5.44091	-1.4603	-2.25845	H	-6.3393	-0.68557	-2.27356
H	-1.63215	-2.56526	2.183005	H	-2.72295	-2.31768	1.240189
H	-3.17393	-0.74154	-1.58257	H	-3.99411	-0.01095	-1.84662
H	-7.22871	-1.71993	-0.5541	H	-7.89161	-1.06266	-0.37318
C	0.352524	1.924954	-0.7314	C	1.876793	1.63837	-0.99544
C	0.267916	2.481883	-2.00432	C	3.048249	1.376542	-1.73388
C	0.763402	2.765645	0.281589	C	2.107441	2.285732	0.210231
C	0.573069	3.810308	-2.29022	C	4.319683	1.729621	-1.27918
H	-0.06362	1.83366	-2.86044	H	2.970684	0.885532	-2.70321
C	1.081852	4.105789	0.060047	C	3.343387	2.664212	0.719214
C	0.984387	4.622864	-1.23296	C	4.469486	2.370761	-0.05025
H	0.495415	4.205971	-3.29784	H	5.195319	1.509359	-1.88336
H	1.401661	4.739672	0.879425	H	3.43431	3.173531	1.671885
H	1.231837	5.66451	-1.41033	H	5.45437	2.65062	0.310622
Br	0.922658	2.094379	2.104131	Br	0.508769	2.732716	1.277966
H	-0.66961	-0.64266	-2.7202	H	-1.53334	1.639372	-2.04653

Transition state 3:



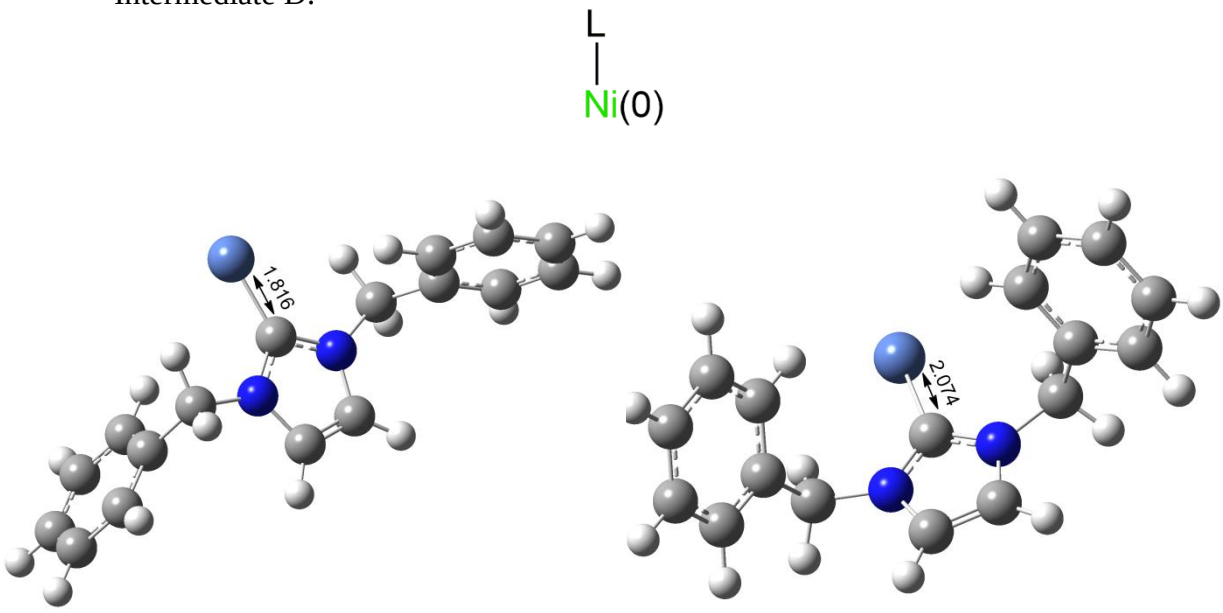




TS3 – Singlet	X	Y	Z	TS3 – Triplet	X	Y	Z
Ni	0.276155	0.613902	-1.73693	Ni	0.309449	1.271433	-0.8897
N	-0.17312	-2.11371	-0.75821	N	0.019274	-1.66399	-1.06773
C	2.289552	-2.74117	-0.15904	C	2.344932	-2.42136	-0.36312
C	2.120241	-2.61595	1.220134	C	1.906178	-2.78382	0.90984
C	1.159694	-2.55544	-1.15626	C	1.412865	-1.88131	-1.43163
C	3.196784	-2.80935	2.086704	C	2.80536	-3.2833	1.852582
C	3.558272	-3.06147	-0.6553	C	3.700683	-2.56673	-0.67679
C	4.454681	-3.12942	1.585281	C	4.151651	-3.42673	1.533017
C	4.632321	-3.25446	0.207546	C	4.59779	-3.06499	0.261812
C	-0.64974	-0.85364	-0.93548	C	-0.53225	-0.44275	-0.80972
C	-1.14553	-2.93889	-0.2069	C	-0.93409	-2.67122	-0.9928
H	1.007211	-3.50568	-1.67722	H	1.412573	-2.56429	-2.28751
H	3.707257	-3.15446	-1.72746	H	4.058241	-2.28086	-1.66241
H	1.470921	-1.83422	-1.91273	H	1.784225	-0.92198	-1.79777
H	5.609297	-3.49869	-0.19599	H	5.646684	-3.1671	0.003
H	3.048046	-2.70719	3.156719	H	2.448728	-3.55746	2.8403
H	-0.96509	-3.98003	0.000584	H	-0.69374	-3.70659	-1.16758
H	1.148704	-2.35924	1.626681	H	0.862092	-2.66646	1.177237
H	5.290944	-3.27822	2.259838	H	4.850261	-3.81348	2.267537
N	-1.92846	-0.90387	-0.48701	N	-1.84468	-0.71768	-0.56427
C	-4.22765	-0.11647	0.061426	C	-4.20804	-0.178	0.079367
C	-4.97737	-1.16415	-0.48589	C	-4.95561	-0.92369	-0.84091
C	-2.86426	0.22657	-0.5018	C	-2.8323	0.338569	-0.27284
C	-6.23349	-1.46734	0.030979	C	-6.23025	-1.37627	-0.51292
C	-4.7563	0.618115	1.125071	C	-4.76742	0.109686	1.326482
C	-6.75748	-0.72819	1.09168	C	-6.77928	-1.08471	0.735635
C	-6.01694	0.316035	1.639064	C	-6.04588	-0.33912	1.654576
C	-2.25012	-2.17854	-0.03577	C	-2.10728	-2.0756	-0.67763
H	-2.93895	0.538	-1.54451	H	-2.8758	0.984914	-1.1537
H	-4.18069	1.432234	1.556826	H	-4.19934	0.689834	2.047775
H	-2.41929	1.051926	0.061174	H	-2.43435	0.933516	0.549501
H	-6.41836	0.896605	2.46307	H	-6.46723	-0.10394	2.626425
H	-6.80717	-2.27952	-0.40277	H	-6.79955	-1.94954	-1.23733

H	-3.23226	-2.42769	0.327566	H	-3.09156	-2.4885	-0.54475
H	-4.57715	-1.74433	-1.31206	H	-4.54143	-1.14503	-1.82013
H	-7.74026	-0.96355	1.486419	H	-7.77579	-1.43257	0.987144
C	1.143529	3.068885	-0.91623	C	1.245109	3.211941	-0.72134
C	1.702059	2.705711	0.30958	C	1.634894	2.335335	0.314002
C	-0.11149	3.676097	-0.95822	C	0.081241	4.026584	-0.51791
C	1.005358	2.949118	1.493042	C	0.815265	2.097437	1.40418
C	-0.80811	3.920544	0.22558	C	-0.71785	3.81974	0.592881
H	-0.55177	3.962562	-1.92426	H	-0.18575	4.776996	-1.26128
C	-0.24998	3.557054	1.451103	C	-0.40229	2.840423	1.53708
H	1.445258	2.662318	2.459236	H	1.116983	1.390233	2.173669
H	-1.79744	4.399693	0.192196	H	-1.61756	4.423774	0.727597
H	-0.79909	3.748925	2.384356	H	-1.04095	2.675645	2.404026
Br	3.420063	1.873044	0.366394	Br	3.333284	1.430196	0.192568
H	1.692183	2.875894	-1.84872	H	1.890962	3.376764	-1.57901

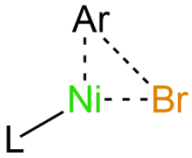
Intermediate D:

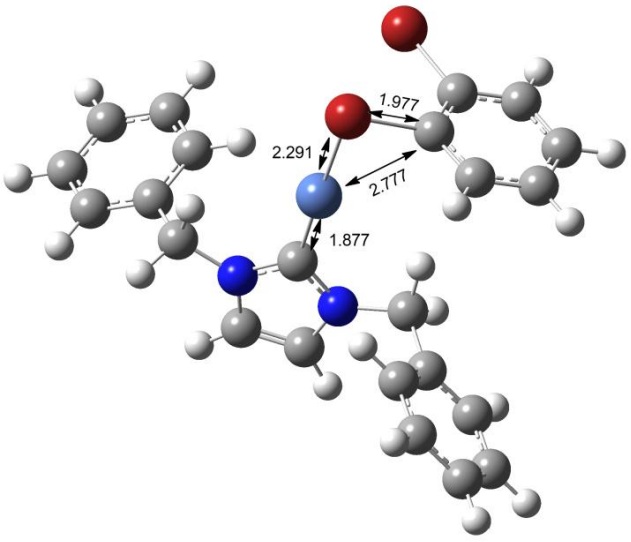


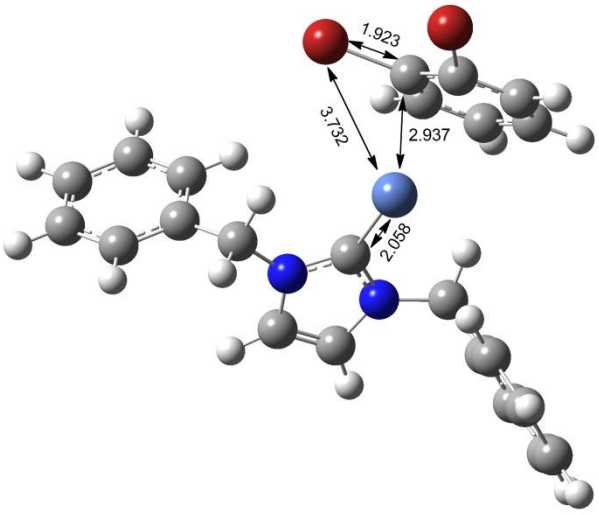
D – Singlet	X	Y	Z	D – Triplet	X	Y	Z
Ni	-0.00017	2.290691	0.000117	Ni	0.000558	2.274144	1.520765
N	-0.91563	-0.37595	0.567835	N	1.069816	0.997548	-1.09841
C	-3.40254	-0.22015	0.56678	C	3.114221	-0.12168	-0.21586
C	-3.61974	0.284839	-0.72062	C	2.672265	-0.75987	0.948498
C	-2.10461	0.06911	1.291885	C	2.462856	1.167731	-0.66783
C	-4.82193	0.044922	-1.37756	C	3.268212	-1.94266	1.372893
C	-4.41194	-0.96481	1.179389	C	4.164732	-0.68682	-0.94099
C	-5.82576	-0.70073	-0.75793	C	4.314859	-2.5033	0.640039
C	-5.61923	-1.20437	0.522877	C	4.763861	-1.87263	-0.5168
C	-0.00006	0.475016	0.000119	C	0.000212	1.354039	-0.33816
C	-0.57635	-1.70444	0.35327	C	0.676838	0.419583	-2.29717
H	-2.10963	-0.39911	2.2805	H	3.02492	1.612953	-1.49232

H	-4.25711	-1.35869	2.180534	H	4.524047	-0.19496	-1.84117
H	-1.96771	1.144601	1.433583	H	2.437099	1.896988	0.145264
H	-6.39442	-1.78551	1.012396	H	5.580793	-2.30023	-1.08929
H	-4.97922	0.443549	-2.37491	H	2.919918	-2.4255	2.280259
H	-1.1844	-2.5201	0.70816	H	1.381796	0.064832	-3.03105
H	-2.83983	0.868817	-1.19995	H	1.861352	-0.32058	1.522872
H	-6.76312	-0.88675	-1.27256	H	4.779824	-3.42567	0.973023
N	0.91567	-0.37576	-0.56766	N	-1.06976	0.997564	-1.0979
C	3.402563	-0.21991	-0.5668	C	-3.1143	-0.12138	-0.21535
C	3.619933	0.284838	0.720669	C	-4.16518	-0.68579	-0.9405
C	2.104569	0.069564	-1.29169	C	-2.46261	1.16804	-0.66678
C	4.822171	0.044734	1.377448	C	-4.7646	-1.87163	-0.51678
C	4.41185	-0.96454	-1.17964	C	-2.67227	-0.76032	0.948576
C	5.825889	-0.70088	0.757577	C	-4.31552	-2.50305	0.639616
C	5.619189	-1.20429	-0.52329	C	-3.2685	-1.94314	1.372504
C	0.576624	-1.70432	-0.35317	C	-0.67737	0.419614	-2.29685
H	1.96761	1.145102	-1.43299	H	-3.02476	1.613969	-1.49083
H	4.256888	-1.35822	-2.18084	H	-1.86107	-0.3216	1.522963
H	2.1095	-0.39831	-2.28047	H	-2.43629	1.89681	0.146733
H	6.394285	-1.78539	-1.01299	H	-2.92014	-2.42657	2.279528
H	4.979595	0.443182	2.374843	H	-5.58182	-2.29865	-1.08929
H	1.184819	-2.51985	-0.7081	H	-1.38269	0.064739	-3.03032
H	2.840103	0.868779	1.200183	H	-4.52456	-0.19335	-1.84033
H	6.763287	-0.88705	1.272079	H	-4.7807	-3.42543	0.97224

Transition state 4:



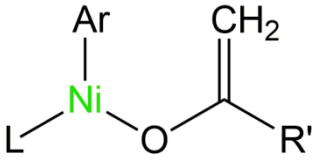


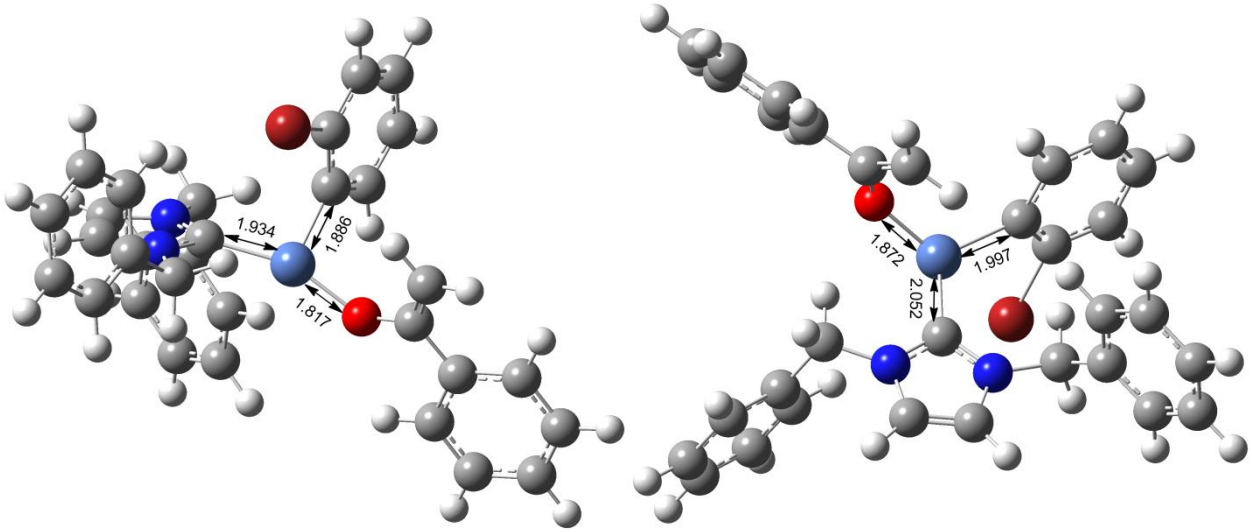


TS4 – Singlet	X	Y	Z	TS4 – Triplet	X	Y	Z
Ni	-0.21063	-0.1716	-0.938	Ni	0.033056	4.398163	1.36197
N	-2.00761	2.04186	-0.24437	N	-2.52062	4.073651	-0.30923
C	-4.26453	0.988584	-0.32337	C	-2.03015	1.695689	-1.26955
C	-4.08911	-0.12738	0.503354	C	-2.94242	1.035717	-0.44573
C	-3.09153	1.554744	-1.09677	C	-1.84273	3.202465	-1.26394
C	-5.16677	-0.6631	1.200473	C	-3.07588	-0.35207	-0.50521
C	-5.53667	1.551613	-0.43817	C	-1.25145	0.93973	-2.1531
C	-6.4352	-0.09327	1.081131	C	-2.29913	-1.09623	-1.38785
C	-6.61898	1.01451	0.259083	C	-1.38351	-0.44384	-2.2133
C	-0.80008	1.407392	-0.11166	C	-1.92831	4.625947	0.781864
C	-2.08123	3.180503	0.545847	C	-3.83749	4.500472	-0.42818
H	-3.42149	2.372987	-1.74334	H	-2.12021	3.582651	-2.25189
H	-5.68702	2.414407	-1.08191	H	-0.53106	1.438913	-2.79514
H	-2.63778	0.78974	-1.73153	H	-0.78357	3.426412	-1.13241
H	-7.60256	1.462795	0.159145	H	-0.76857	-1.01339	-2.90209
H	-5.01866	-1.53082	1.83555	H	-3.78955	-0.84975	0.14324
H	-2.962	3.799813	0.589363	H	-4.47386	4.181679	-1.23625
H	-3.10251	-0.57254	0.591424	H	-3.5495	1.599713	0.253142
H	-7.27496	-0.51349	1.625549	H	-2.40291	-2.17501	-1.43219
N	-0.12969	2.198662	0.785774	N	-2.89154	5.399531	1.340902
C	2.257873	2.902798	0.660452	C	-3.95649	6.984174	2.941484
C	2.359413	3.086297	-0.72365	C	-4.57231	7.859398	2.039252
C	1.23597	1.940929	1.233324	C	-2.7095	6.223257	2.541806
C	3.320171	3.94227	-1.25248	C	-5.71255	8.562275	2.417047
C	3.135837	3.592192	1.498625	C	-4.49737	6.829703	4.219764
C	4.19566	4.62558	-0.40736	C	-6.24658	8.405963	3.696253
C	4.102293	4.448021	0.969892	C	-5.63738	7.537979	4.598428
C	-0.89589	3.283905	1.188663	C	-4.07175	5.334493	0.609646
H	1.457528	0.915895	0.927078	H	-1.89076	6.906759	2.313059
H	3.067784	3.458429	2.575082	H	-4.02655	6.151488	4.92608
H	1.259384	1.970838	2.326341	H	-2.3834	5.575135	3.360187
H	4.776736	4.977926	1.635236	H	-6.04579	7.412282	5.595717
H	3.388013	4.076408	-2.3276	H	-6.18	9.240176	1.710774
H	-0.53102	4.026976	1.87864	H	-4.94359	5.90723	0.875283
H	1.679672	2.551802	-1.38047	H	-4.16287	7.987345	1.041583
H	4.943737	5.293843	-0.82197	H	-7.13135	8.961608	3.988673
C	2.998059	-1.14545	-0.75441	C	2.500153	4.082389	2.207002
C	1.882142	-1.94167	-0.48875	C	2.272261	2.706135	2.228487
C	4.035181	-1.07256	0.167902	C	2.353995	4.831777	3.374308
C	1.819009	-2.68675	0.688888	C	1.897642	2.0796	3.416904
C	3.967871	-1.80421	1.353636	C	1.980226	4.205047	4.563391
H	4.890979	-0.43962	-0.04039	H	2.533743	5.916461	3.357593
C	2.864299	-2.61059	1.610941	C	1.75191	2.829202	4.58484
H	4.774488	-1.75472	2.077059	H	1.717387	0.994925	3.433776
H	2.806128	-3.18721	2.526444	H	1.865463	4.796097	5.483697
Br	0.52465	-2.10881	-1.91585	H	1.456585	2.334973	5.521759
Br	0.327447	-3.80572	1.113076	Br	2.472615	1.673633	0.618483

H	3.041795	-0.58193	-1.6777	Br	3.01114	4.940337	0.578837

Intermediate E:

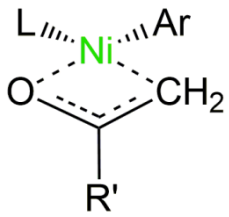


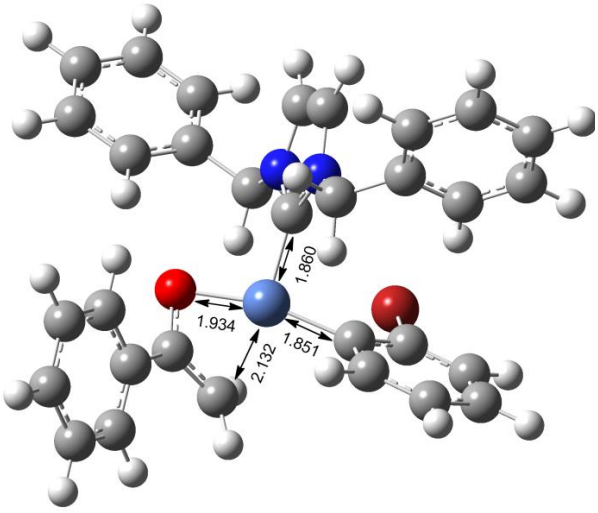


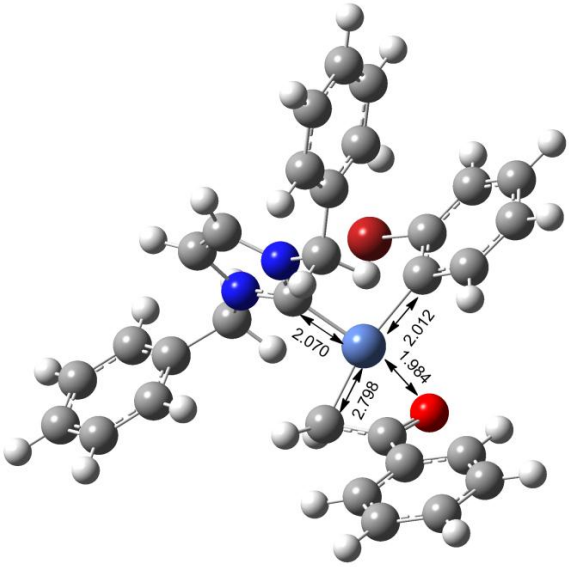
E – Singlet	X	Y	Z	E – Triplet	X	Y	Z
Ni	-0.48887	-0.12004	0.081151	Ni	0.145814	-0.61835	-0.64264
N	2.227238	0.592287	0.905183	N	0.568189	1.97671	0.906666
C	3.797664	-1.16285	1.736327	C	2.643584	2.964593	-0.04727
C	4.562934	-1.42506	0.593547	C	3.553249	3.866743	0.507445
C	2.366245	-0.68993	1.6207	C	2.032936	1.867275	0.798425
C	5.869961	-1.8863	0.711197	C	4.132608	4.865765	-0.2746
C	4.368431	-1.37074	2.993817	C	2.322092	3.078644	-1.40445
C	6.430283	-2.09555	1.971649	C	3.802919	4.973309	-1.62223
C	5.676971	-1.83806	3.113124	C	2.895361	4.07594	-2.18593
C	1.129983	0.933838	0.172089	C	-0.32424	1.084092	0.402034
C	3.13456	1.637158	0.965946	C	-0.07743	3.015822	1.554975
H	1.928571	-0.5813	2.616392	H	2.446558	1.887878	1.808925
H	3.785044	-1.17251	3.88848	H	1.619041	2.382198	-1.85188
H	1.759428	-1.412	1.071108	H	2.24155	0.877949	0.389825
H	6.104603	-1.99891	4.097358	H	2.639209	4.15019	-3.23785
H	6.450999	-2.08955	-0.18251	H	4.840992	5.556952	0.170624
H	4.072735	1.556729	1.487136	H	0.45856	3.829132	2.014854
H	4.131069	-1.26552	-0.38884	H	3.820237	3.783555	1.557404
H	7.448727	-2.45927	2.061116	H	4.252265	5.749227	-2.23347
N	1.382187	2.205208	-0.23606	N	-1.53724	1.582993	0.754871
C	-0.32684	4.019899	-0.17936	C	-3.77219	0.858387	1.574266
C	-1.35176	3.564197	0.657581	C	-3.47327	-0.0056	2.634106

C	0.463957	3.04223	-1.02371	C	-2.8331	0.980725	0.395301
C	-2.08402	4.460855	1.429123	C	-4.3433	-0.12811	3.712162
C	-0.05564	5.388607	-0.2313	C	-4.96001	1.591137	1.615325
C	-1.80309	5.826097	1.373534	C	-5.52746	0.609138	3.7448
C	-0.78869	6.289277	0.540497	C	-5.83585	1.467577	2.693818
C	2.601877	2.651608	0.245197	C	-1.40485	2.767623	1.460929
H	-0.19284	2.363151	-1.56242	H	-2.60746	0.004274	-0.03024
H	0.727959	5.758566	-0.88717	H	-5.20836	2.257828	0.794136
H	1.062385	3.575202	-1.7656	H	-3.28582	1.585555	-0.39383
H	-0.56834	7.350601	0.487275	H	-6.75734	2.040562	2.709716
H	-2.87989	4.094064	2.068961	H	-4.10168	-0.80474	4.525421
H	2.978939	3.637682	0.031494	H	-2.25447	3.306087	1.845235
H	-1.58212	2.503286	0.700098	H	-2.55733	-0.58801	2.610221
H	-2.37708	6.524761	1.973539	H	-6.20712	0.509863	4.584935
C	-0.68707	-0.18283	-1.79322	C	-1.32337	-1.87641	-1.14029
C	-1.80365	0.47376	-2.33577	C	-1.64426	-3.0528	-0.44119
C	0.136943	-0.85129	-2.69208	C	-2.07343	-1.64389	-2.28476
C	-2.05745	0.476588	-3.70657	C	-2.65265	-3.91418	-0.87361
H	-2.50411	0.968438	-1.67076	H	-1.08221	-3.30724	0.454239
C	-0.09497	-0.86822	-4.0672	C	-3.0868	-2.4696	-2.75903
C	-1.19736	-0.18922	-4.57647	C	-3.37543	-3.6222	-2.02972
H	-2.93451	0.989254	-4.08968	H	-2.87297	-4.81748	-0.31218
H	0.572966	-1.4109	-4.72593	H	-3.63155	-2.23113	-3.6653
H	-1.38676	-0.19675	-5.64497	H	-4.1603	-4.28939	-2.37217
Br	1.65724	-1.87973	-2.0668	Br	-1.66288	-0.02473	-3.31884
O	-2.04148	-0.88249	0.636002	O	1.746544	-1.32445	0.024468
C	-2.02907	-3.16365	-0.01387	C	1.223805	-2.01747	2.225348
C	-2.6158	-2.08508	0.54508	C	2.077676	-1.88886	1.184008
H	-2.51552	-4.12863	-0.05004	H	1.499784	-2.52895	3.137221
H	-1.04394	-3.08863	-0.45825	H	0.209904	-1.64085	2.151998
C	-3.98195	-2.14011	1.1548	C	3.485448	-2.3921	1.234263
C	-4.8934	-3.17092	0.879027	C	4.161109	-2.61934	2.442246
C	-4.38681	-1.12505	2.032657	C	4.170185	-2.63903	0.036709
C	-6.15062	-3.1948	1.47294	C	5.466411	-3.09958	2.451769
H	-4.62806	-3.95101	0.174609	H	3.669894	-2.39866	3.383579
C	-5.6443	-1.14942	2.630556	C	5.475712	-3.12258	0.045744
H	-3.69645	-0.31684	2.238523	H	3.659347	-2.45045	-0.89919
C	-6.53336	-2.18541	2.356263	C	6.130141	-3.35774	1.252642
H	-6.83955	-4.00068	1.237438	H	5.971208	-3.26493	3.398957
H	-5.93116	-0.35388	3.312445	H	5.983749	-3.3154	-0.89447
H	-7.51605	-2.20406	2.817601	H	7.149613	-3.73089	1.26074

Transition state 2:





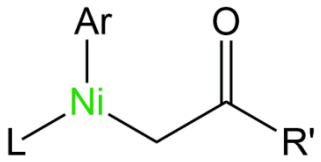


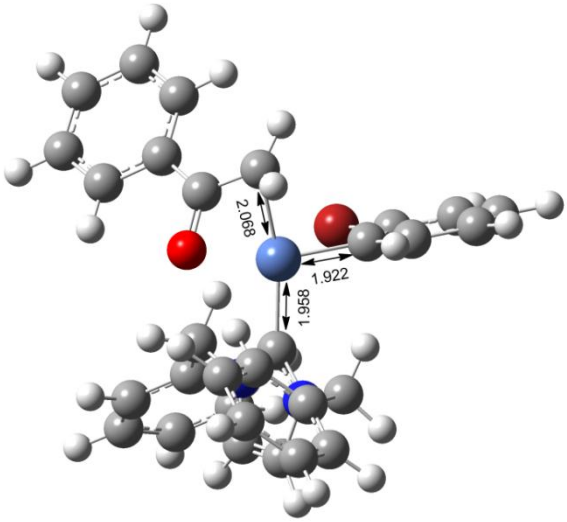
TS2 – Singlet	X	Y	Z
Ni	-0.38865	0.718619	0.654018
N	0.772548	-0.90647	-1.50337
C	3.044993	-0.33432	-2.34302
C	3.896858	-0.68964	-1.2905
C	1.63746	0.142631	-2.06099
C	5.194421	-1.11755	-1.5513
C	3.519229	-0.4117	-3.65429
C	5.659869	-1.19393	-2.8645
C	4.820936	-0.83841	-3.91656
C	-0.07086	-0.74654	-0.44641
C	0.625355	-2.16199	-2.07685
H	1.175658	0.519558	-2.9781
H	2.86927	-0.13041	-4.47863
H	1.640789	0.951284	-1.33385
H	5.176563	-0.89144	-4.94064
H	5.846772	-1.38502	-0.72638
H	1.215988	-2.48061	-2.91876
H	3.543687	-0.62119	-0.26695
H	6.673693	-1.5258	-3.06457
N	-0.74759	-1.92625	-0.37747
C	-3.07122	-2.71949	0.026726
C	-3.92844	-1.78968	-0.57412
C	-1.76154	-2.26661	0.634433
C	-5.13431	-2.20676	-1.12956
C	-3.44781	-4.06398	0.067065
C	-5.50055	-3.55266	-1.09157
C	-4.6564	-4.48153	-0.48982
C	-0.32738	-2.80339	-1.36545
H	-1.9026	-1.37217	1.236119
H	-2.79728	-4.79105	0.546275
H	-1.34707	-3.04215	1.282825
H	-4.93786	-5.52903	-0.44855
H	-5.79557	-1.47775	-1.58743
H	-0.74705	-3.78897	-1.47466

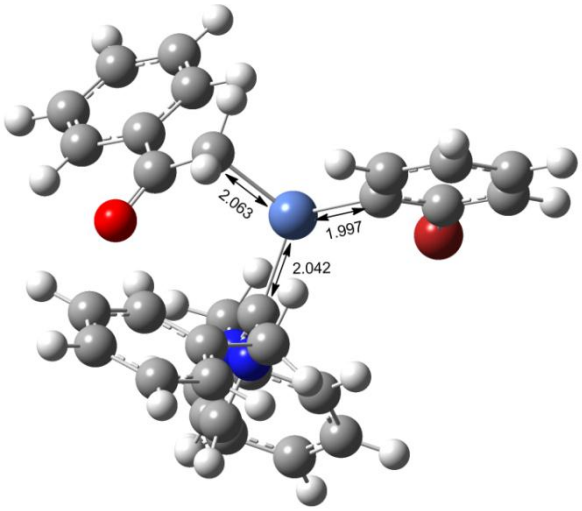
TS2 – Triplet	X	Y	Z
Ni	-0.30769	0.571054	0.500958
N	0.888794	-1.21973	-1.78115
C	3.161185	-0.64787	-2.62114
C	4.013172	-1.00338	-1.56878
C	1.75377	-0.17073	-2.33885
C	5.310628	-1.43147	-1.82983
C	3.635191	-0.72524	-3.93249
C	5.775846	-1.50784	-3.14311
C	4.936791	-1.15213	-4.19501
C	0.045585	-1.05974	-0.72403
C	0.741319	-2.4752	-2.35467
H	1.291871	0.206321	-3.25586
H	2.985137	-0.44381	-4.75671
H	1.75734	0.637883	-1.61166
H	5.29224	-1.20516	-5.21915
H	5.963076	-1.69908	-1.00503
H	1.331765	-2.79386	-3.1967
H	3.660181	-0.93494	-0.54517
H	6.789587	-1.83985	-3.34337
N	-0.63131	-2.23935	-0.65505
C	-2.95499	-3.03227	-0.25052
C	-3.81217	-2.1023	-0.85117
C	-1.64514	-2.57962	0.356999
C	-5.0182	-2.51916	-1.40643
C	-3.33177	-4.3767	-0.21019
C	-5.38463	-3.86501	-1.36846
C	-4.54052	-4.79404	-0.7669
C	-0.2114	-3.11649	-1.64315
H	-1.78597	-1.68519	0.958761
H	-2.68127	-5.1039	0.268868
H	-1.23068	-3.35526	1.005278
H	-4.82213	-5.84151	-0.72564
H	-5.67942	-1.79003	-1.86415
H	-0.63123	-4.10201	-1.75235

H	-3.64713	-0.74158	-0.58691	H	-3.53071	-1.05424	-0.86394
H	-6.44331	-3.87339	-1.52348	H	-6.32751	-4.18557	-1.80023
C	1.401855	0.895056	1.364803	C	1.554706	0.75424	1.239922
C	2.198643	1.993839	0.979878	C	2.351593	1.852927	0.854928
C	1.998624	0.051583	2.299722	C	2.151505	-0.08938	2.174693
C	3.484758	2.208814	1.472487	C	3.637822	2.067682	1.347336
H	1.793508	2.718991	0.277055	H	1.94645	2.57818	0.152214
C	3.281254	0.227636	2.818026	C	3.434247	0.086456	2.692794
C	4.034483	1.318138	2.392046	C	4.187568	1.176871	2.266752
H	4.054786	3.072021	1.141039	H	4.207924	2.930823	1.015843
H	3.680756	-0.4693	3.54584	H	3.833766	-0.61059	3.420501
H	5.034609	1.470715	2.785301	H	5.187782	1.329276	2.659849
Br	1.008164	-1.47537	3.004546	Br	1.160935	-1.61622	2.879594
O	-2.17289	0.952104	0.221687	O	-2.22384	1.030705	0.270002
C	-2.20296	3.333867	-0.13565	C	-2.25391	3.412468	-0.08733
C	-2.47168	3.159218	-1.4991	C	-2.52263	3.237819	-1.45078
C	-2.22682	4.628443	0.398074	C	-2.27778	4.707044	0.446389
C	-2.73703	4.255123	-2.31319	C	-2.78799	4.333724	-2.26488
H	-2.4697	2.153561	-1.90221	H	-2.52066	2.232162	-1.8539
C	-2.48817	5.725192	-0.41748	C	-2.53913	5.803793	-0.36916
H	-2.05862	4.778247	1.458818	H	-2.10957	4.856848	1.507133
C	-2.74157	5.541939	-1.77591	C	-2.79253	5.62054	-1.72759
H	-2.94182	4.106922	-3.36889	H	-2.99278	4.185523	-3.32057
H	-2.50407	6.722998	0.009185	H	-2.55502	6.801599	0.0575
H	-2.94993	6.397262	-2.41089	H	-3.00089	6.475863	-2.36258
C	-1.94526	2.1387	0.717958	C	-1.99621	2.217301	0.766273
C	-1.27108	2.17485	1.937794	C	-1.46027	2.480923	2.186488
H	-0.81844	3.080397	2.319426	H	-1.00783	3.386559	2.568142
H	-1.43473	1.375651	2.653246	H	-1.62393	1.681741	2.901959

Intermediate F:



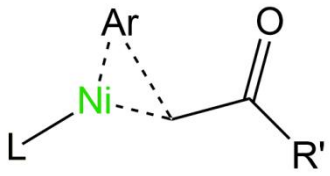


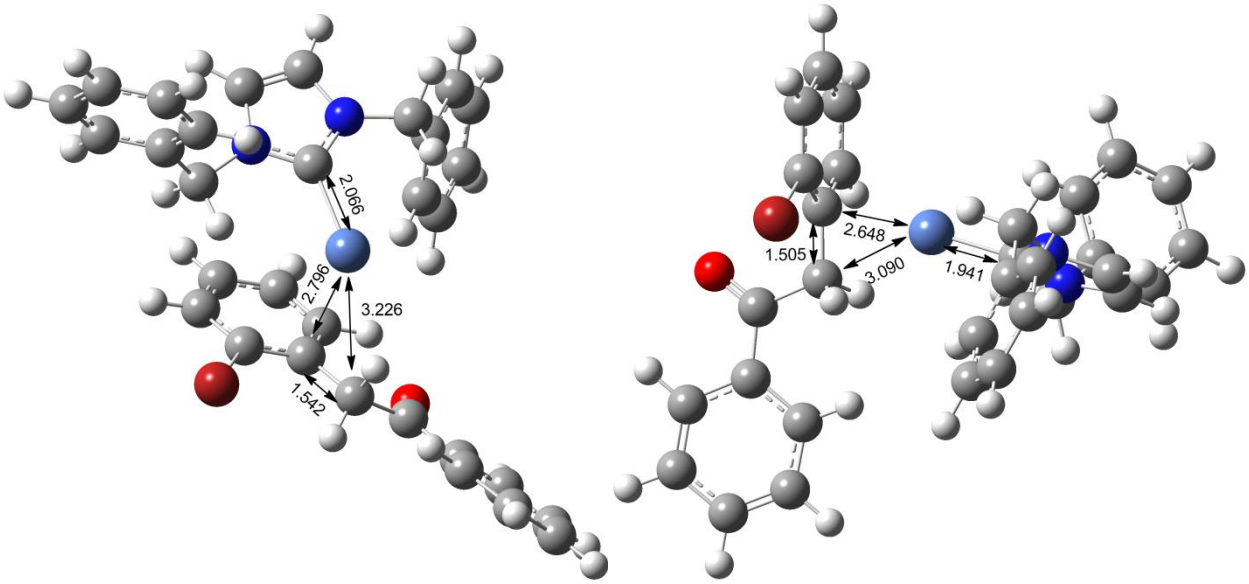


F – Singlet	X	Y	Z	F – Triplet	X	Y	Z
Ni	0.599296	-0.93735	-0.2364	Ni	-0.3526	-0.69434	0.827778
N	-0.01462	1.951511	0.063331	N	0.700219	0.993405	-1.49822
C	-2.36805	2.76372	0.060927	C	3.153271	0.870947	-1.90584
C	-2.73493	2.739928	1.412009	C	3.25566	-0.32708	-2.62263
C	-1.37025	1.768247	-0.48518	C	2.041117	1.072791	-0.9014
C	-3.66123	3.651967	1.907629	C	4.289877	-0.51727	-3.53284
C	-2.94922	3.716122	-0.77917	C	4.105062	1.870202	-2.11668
C	-4.23669	4.599424	1.060395	C	5.237908	0.486177	-3.73667
C	-3.88054	4.629142	-0.28477	C	5.144804	1.679467	-3.02661
C	0.877525	0.940857	0.243486	C	-0.34926	0.351068	-0.92621
C	0.565348	3.186053	0.317926	C	0.306796	1.680198	-2.63674
H	-1.30973	1.842015	-1.57286	H	2.138724	2.038641	-0.40086
H	-2.67519	3.742333	-1.83013	H	4.037343	2.801903	-1.56236
H	-1.66339	0.747273	-0.24474	H	2.079734	0.304499	-0.12666
H	-4.32574	5.361124	-0.95105	H	5.879082	2.463832	-3.17914
H	-3.94027	3.619509	2.955948	H	4.360557	-1.45143	-4.08053
H	0.012047	4.106642	0.248415	H	0.998063	2.248174	-3.23574
H	-2.29609	1.998542	2.071845	H	2.522219	-1.11197	-2.46412
H	-4.96146	5.308117	1.448186	H	6.045982	0.335542	-4.44518
N	2.01958	1.568967	0.628214	N	-1.40127	0.635709	-1.73106
C	4.258147	0.98838	-0.30429	C	-3.76611	1.290763	-1.29804
C	3.874161	0.540227	-1.5739	C	-3.4847	2.34745	-0.42329
C	3.30193	0.904502	0.870146	C	-2.77279	0.165809	-1.51014
C	4.770573	0.594547	-2.63692	C	-4.43163	3.347035	-0.21466
C	5.550001	1.486185	-0.12352	C	-4.99877	1.257022	-1.95441
C	6.060684	1.09023	-2.44759	C	-5.66345	3.30459	-0.86721
C	6.449924	1.535335	-1.18766	C	-5.94655	2.256145	-1.73841
C	1.847266	2.944719	0.673289	C	-1.01902	1.452099	-2.78419
H	3.0717	-0.12859	1.122099	H	-2.72979	-0.49877	-0.64696
H	5.860184	1.835646	0.857768	H	-5.22405	0.44255	-2.6379
H	3.752294	1.355101	1.757653	H	-3.07097	-0.44644	-2.36552
H	7.450944	1.924573	-1.03093	H	-6.90047	2.216606	-2.25478
H	4.459758	0.245351	-3.61633	H	-4.20245	4.161177	0.465322
H	2.641816	3.615692	0.954124	H	-1.71823	1.799809	-3.52593
H	2.87194	0.155759	-1.73729	H	-2.53024	2.401961	0.093915
H	6.75718	1.129683	-3.27905	H	-6.39735	4.086428	-0.69883
C	0.796003	-1.73396	1.50126	C	-1.26788	-2.46906	0.840434
C	2.015545	-2.331	1.879816	C	-2.58603	-2.73493	1.247706
C	-0.21195	-1.82115	2.458286	C	-0.54419	-3.57819	0.427335
C	2.210064	-2.93242	3.122404	C	-3.12346	-4.02224	1.221008
H	2.841133	-2.34832	1.171538	H	-3.20893	-1.91737	1.604167
C	-0.05989	-2.41136	3.711688	C	-1.02864	-4.88055	0.383156
C	1.170721	-2.96717	4.048828	C	-2.34612	-5.09482	0.786214
H	3.17058	-3.37954	3.362577	H	-4.14678	-4.19165	1.543487
H	-0.88923	-2.44208	4.409032	H	-0.40602	-5.70317	0.050627
H	1.306463	-3.43054	5.020909	H	-2.75605	-6.09972	0.764417
Br	-1.98864	-1.12547	2.059043	Br	1.323208	-3.29013	-0.11427

O	0.340373	-0.67024	-2.20271	O	-0.58151	2.677276	1.419525
C	-1.63214	-2.00459	-2.47875	C	1.028687	1.87639	2.95477
C	-2.20018	-1.02018	-3.29779	C	1.660488	3.126357	2.979354
C	-2.39032	-3.14045	-2.16693	C	1.633791	0.807286	3.628695
C	-3.49386	-1.16324	-3.78822	C	2.85719	3.307357	3.66415
H	-1.60315	-0.15161	-3.54829	H	1.184874	3.945118	2.452026
C	-3.68956	-3.2764	-2.64484	C	2.83885	0.983673	4.305272
H	-1.97396	-3.92003	-1.54008	H	1.171235	-0.17329	3.626091
C	-4.24495	-2.29014	-3.45881	C	3.452511	2.234378	4.327868
H	-3.91745	-0.39512	-4.42769	H	3.327668	4.28574	3.682523
H	-4.26913	-4.15612	-2.38404	H	3.297401	0.143163	4.816795
H	-5.25671	-2.40148	-3.83579	H	4.387967	2.372479	4.861084
C	0.488439	-2.74576	-1.23292	C	-1.06338	0.542968	2.318126
H	0.0441	-3.66374	-0.8737	H	-0.96544	-0.01086	3.250599
H	1.569769	-2.75507	-1.33769	H	-2.10515	0.694173	2.039286
C	-0.22327	-1.81833	-2.01636	C	-0.2722	1.753482	2.185955

Transition state 5:





TS5 – Singlet	X	Y	Z	TS5 – Triplet	X	Y	Z
Ni	-1.4062	1.101592	0.044193	Ni	-1.74503	0.990298	0.394697
N	-2.70648	3.466141	-1.41704	N	-3.0291	3.238152	-1.02477
C	-5.123	3.39311	-2.01156	C	-5.44561	3.165121	-1.6193
C	-5.75998	3.973829	-0.90812	C	-6.0826	3.74584	-0.51585
C	-3.83596	2.619162	-1.84024	C	-4.15858	2.391173	-1.44798
C	-6.94966	4.676731	-1.06964	C	-7.27227	4.448743	-0.67737

C	-5.70335	3.52992	-3.27452	C	-6.02597	3.301931	-2.88225
C	-7.52195	4.807591	-2.33534	C	-7.84456	4.579602	-1.94307
C	-6.89775	4.231428	-3.43788	C	-7.22037	4.00344	-3.04562
C	-1.67427	3.030332	-0.64606	C	-1.99689	2.802344	-0.25379
C	-2.48273	4.756746	-1.8748	C	-2.80534	4.528757	-1.48253
H	-3.55851	2.123518	-2.77271	H	-3.88112	1.89553	-2.38044
H	-5.22035	3.080856	-4.13786	H	-5.54297	2.852867	-3.74559
H	-3.94161	1.846037	-1.08047	H	-4.26422	1.618048	-0.68821
H	-7.33793	4.326166	-4.42541	H	-7.66054	4.098177	-4.03314
H	-7.43547	5.117916	-0.20521	H	-7.75809	4.889927	0.187052
H	-3.1969	5.282473	-2.48474	H	-3.51951	5.054484	-2.09248
H	-5.32239	3.866294	0.079082	H	-5.645	3.638305	0.471349
H	-8.45171	5.353662	-2.45894	H	-8.77432	5.125674	-2.06667
N	-0.81048	4.079183	-0.62159	N	-1.13309	3.851195	-0.22933
C	1.648716	3.808912	-0.93327	C	1.326102	3.580924	-0.541
C	1.658186	2.667847	-1.74449	C	1.335571	2.439858	-1.35222
C	0.502963	4.069507	0.025903	C	0.180348	3.841518	0.41817
C	2.729403	2.424236	-2.59869	C	2.406788	2.196247	-2.20643
C	2.727995	4.69255	-0.9942	C	2.405381	4.464561	-0.60193
C	3.805632	3.310169	-2.65147	C	3.483018	3.082181	-2.25921
C	3.803935	4.445314	-1.84619	C	3.48132	4.217325	-1.45393
C	-1.2877	5.142543	-1.37388	C	-1.61032	4.914554	-0.98162
H	0.457306	3.31198	0.805533	H	0.134691	3.083991	1.1978
H	2.732736	5.581012	-0.36819	H	2.410121	5.353023	0.024075
H	0.639044	5.031557	0.52538	H	0.316429	4.803568	0.917646
H	4.635844	5.141576	-1.88169	H	4.313229	4.913588	-1.48942
H	2.723595	1.536782	-3.22334	H	2.40098	1.308793	-2.83107
H	-0.74124	6.064924	-1.47863	H	-1.06385	5.836935	-1.08637
H	0.825527	1.971502	-1.71724	H	0.502913	1.743514	-1.32497
H	4.639754	3.115798	-3.31815	H	4.317139	2.88781	-2.92588
C	-2.21473	-1.25367	-1.22639	C	-1.34178	-1.60392	0.740741
C	-1.7763	-0.41292	-2.26945	C	-0.04021	-1.65307	0.201714
C	-3.59838	-1.32892	-1.08737	C	-2.36083	-1.60037	-0.20846
C	-2.65375	0.264357	-3.115	C	0.209376	-1.72457	-1.16802
H	-0.70913	-0.26133	-2.41684	H	0.814871	-1.61223	0.873075
C	-4.51024	-0.67058	-1.91052	C	-2.15593	-1.67205	-1.58518
C	-4.02919	0.130311	-2.9421	C	-0.85276	-1.7425	-2.06871
H	-2.26215	0.901569	-3.90291	H	1.232975	-1.75871	-1.53033
H	-5.57627	-0.77629	-1.74481	H	-2.99837	-1.66634	-2.26731
H	-4.72548	0.649918	-3.59268	H	-0.67527	-1.79913	-3.13799
Br	-4.36985	-2.37711	0.363864	Br	-4.21738	-1.44456	0.36507
O	0.30767	-1.36812	-1.4421	O	-1.33705	-3.77888	2.008108
C	0.954361	-2.69709	0.445527	C	-2.66734	-3.22505	3.924121
C	2.306198	-2.44782	0.175371	C	-2.56443	-4.54109	4.393202
C	0.626376	-3.55214	1.505513	C	-3.45256	-2.31403	4.64226
C	3.30501	-3.04136	0.940005	C	-3.23279	-4.93895	5.546277
H	2.553151	-1.77329	-0.63556	H	-1.94303	-5.23676	3.842296
C	1.625434	-4.15774	2.260524	C	-4.13322	-2.71581	5.786889

H	-0.41116	-3.75826	1.740173	H	-3.54544	-1.28843	4.305277
C	2.967583	-3.90282	1.982398	C	-4.02395	-4.02826	6.244309
H	4.347904	-2.83258	0.722878	H	-3.13727	-5.96038	5.901118
H	1.355762	-4.82795	3.070415	H	-4.74806	-2.00175	6.32535
H	3.745313	-4.37154	2.577047	H	-4.55092	-4.33777	7.141351
C	-1.46553	-2.11535	-0.19006	C	-1.86298	-1.54886	2.151644
H	-2.07338	-2.87522	-0.66152	H	-2.69586	-1.10205	1.626448
H	-1.95696	-1.53137	0.583119	H	-1.03786	-0.88063	2.381865
C	-0.07618	-1.99819	-0.38088	C	-1.89285	-2.84263	2.70455

Chapter 4
Synthesis, structure and DFT conformation analysis of CpNiX(NHC) and $NiX_2(NHC)_2$ (X = SPh or Br) complexes

Frederick P. Malan,[a] Eric Singleton,[a] Petrus H. van Rooyen,[a] Jeanet Conradie[b,*] and Marilé Landman[a,*]

[a] *Department of Chemistry, University of Pretoria, 02 Lynnwood Road, Hatfield, Pretoria, 0002, South Africa.* [b] *Department of Chemistry, University of the Free State, Bloemfontein 9300, South Africa.*

Supplementary Information

1. **Table S1:** Crystal data and experimental parameters for compounds **1**, **3**, **4**, and **5**.
2. **Table S2:** Optimised coordinates of complexes **A**-**D**, **1**-**5**.
3. **Table S3:** Experimental and Calculated IR data.
4. **Table S4:** Experimental and Calculated ^{1}H-NMR data.

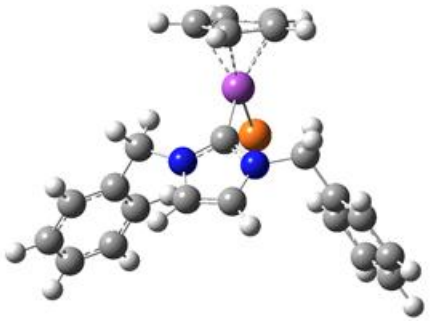
1. **Table S1**: Crystal data and experimental parameters for compounds **1**, **3**, **4**, and **5**.

Complex	**1**	**3**	**4**	**5**
Emp. formula	$C_{28}H_{26}N_2SNi$	$C_{34}H_{30}N_6O_4Br_2Ni$	$C_{36}H_{36}N_4Br_2Ni$	$C_{34}H_{32}N_6O_4S_2Ni$
Form. weight (g.mol^{-1})	481.28	805.17	743.18	711.47
Crystal system	triclinic	monoclinic	monoclinic	monoclinic
Space group	*P-1*	*$P2_1/c$*	*$P2_1$*	*C2/c*
Crystal descr.	bronze needle	orange block	orange fragment	bronze block
a (Å)	12.6753(6)	8.6414(1)	7.7172(5)	24.7600(4)
b (Å)	13.8158(7)	12.1962(2)	15.1745(9)	8.3110(1)
c (Å)	15.1434(8)	15.5053(2)	14.1412(8)	17.6200(3)
α (°)	92.956(3)	90	90	90
β (°)	110.431(2)	99.176(4)	92.557(2)	99.510(4)

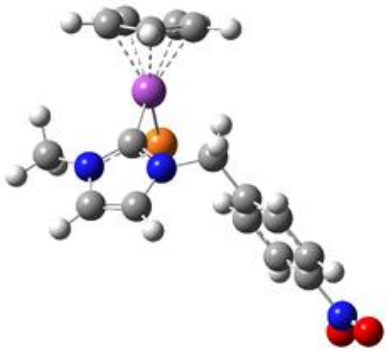
γ (°)	106.967(2)	90	90	90
Volume (Å^3)	2341.8(2)	1613.2(4)	1654.4(2)	3576.0(1)
Z	4	2	2	4
Abs. coeff. (m.mm^{-1})	0.936	3.128	3.033	0.704
F(000)	1008.0	812.0	756.0	1480.0
Independent refl.	10477	3328	10133	4607
Completeness (%)	99.6	99.9	100	99.7
Data/Restr/Para	10477/0/577	3328/0/214	10133/1/388	4607/0/214
Goodness of fit on F^2	1.024	1.072	1.105	1.099
Final R$_1$ indexes	0.0420	0.0213	0.0436	0.0361
wR$_2$ indices (all data)	0.0857	0.0496	0.0854	0.0972
Largest diffr. peak and hole (e.Å^{-3})	0.34/-0.36	0.36/-0.26	1.24/-0.80	0.42/-0.39

2. **Table S2:** Optimised coordinates of complexes **A**-**D**, **1**-**5**. All of the below conformations have been calculated with a singlet multiplicity.

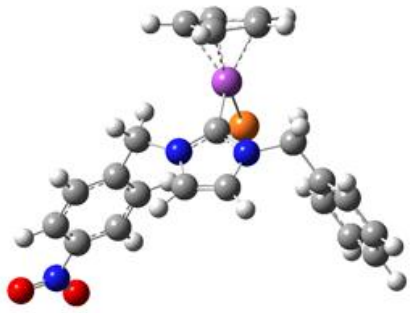
Complex	Element	Coordinates		
		x	y	z
A	Br	-0.00012	0.877169	-2.06301
	Ni	-0.00009	1.910546	0.050772
	N	1.074889	-0.47817	1.3361
	C	3.283106	-1.18296	0.431443
	C	3.002207	-1.5615	-0.88689
	C	2.47438	-0.09263	1.098911
	C	3.752377	-2.55854	-1.50157
	C	4.324907	-1.81315	1.115117
	C	4.79065	-3.18615	-0.8121
	C	5.078018	-2.81108	0.496899
	C	0.000009	0.259496	0.95364
	C	0.676185	-1.65723	1.950251
	C	-0.00012	3.240127	1.64458
	C	1.168349	3.574322	0.877828
	C	0.722976	3.914491	-0.40244
	H	-9.3E-05	2.926377	2.67849
	H	2.429011	0.798169	0.472126
	H	4.554851	-1.51874	2.134712



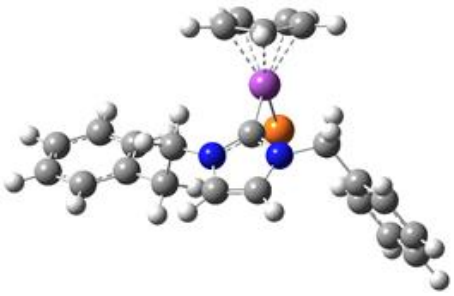
	H	2.928768	0.186518	2.053618
	H	5.886284	-3.29104	1.03722
	H	3.530118	-2.84245	-2.524
	H	2.19225	3.496028	1.209101
	H	1.38166	-2.39071	2.298862
	H	2.199282	-1.06822	-1.42595
	H	1.339889	4.132134	-1.26078
	H	5.374522	-3.96109	-1.29602
	N	-1.07479	-0.47825	1.336159
	C	-3.28297	-1.18318	0.43153
	C	-3.00206	-1.56162	-0.88683
	C	-2.47432	-0.09282	1.099043
	C	-3.75216	-2.55869	-1.50155
	C	-4.3247	-1.8135	1.115188
	C	-4.79036	-3.18643	-0.8121
	C	-5.07774	-2.81146	0.496926
	C	-0.67596	-1.65732	1.950232
	H	-2.42904	0.798014	0.472302
	H	-4.55465	-1.51917	2.134805
	H	-2.92871	0.186239	2.053776
	H	-5.88595	-3.29152	1.037234
	H	-3.5299	-2.84251	-2.52401
	H	-1.38135	-2.39088	2.298836
	H	-2.19919	-1.06824	-1.42588
	H	-5.37418	-3.96139	-1.29605
	C	-1.16862	3.574245	0.877856
	C	-0.72329	3.914437	-0.40242
	H	-2.19251	3.495882	1.209149
	H	-1.34024	4.132035	-1.26075
B	Br	1.34601	-1.6417	-1.3534
	N	0.11511	1.69845	0.18541
	C	-2.0184	0.65418	0.91156
	C	-2.1665	-0.3266	-0.0783
	C	-0.6385	1.13636	1.30848
	C	-3.4307	-0.781	-0.4297
	C	-3.1521	1.16843	1.54632
	C	-4.5415	-0.2481	0.21753
	C	-4.4243	0.72059	1.2053
	C	1.29874	1.20569	-0.2688
	C	-0.3093	2.77088	-0.5881
	C	3.16033	0.41226	2.08189
	C	2.6321	-0.8668	2.41155
	C	3.22913	-1.7823	1.52305
	H	2.90085	1.34701	2.55752
	H	-0.0362	0.30749	1.684
	H	-3.0442	1.92465	2.31653



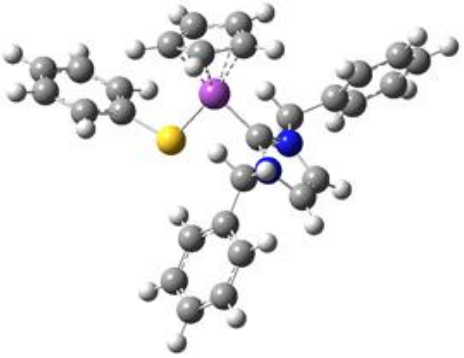
	H	-0.7119	1.88702	2.09961
	H	-5.3139	1.10628	1.68273
	H	-3.5679	-1.5392	-1.188
	H	1.85793	-1.0792	3.13264
	H	-1.2316	3.29181	-0.3997
	H	-1.2914	-0.7387	-0.5718
	H	2.98908	-2.8306	1.43356
	N	1.61051	1.99304	-1.329
	C	0.632	2.95179	-1.5426
	H	0.69093	3.66768	-2.3439
	C	4.23922	0.23823	1.13014
	C	4.26407	-1.1071	0.77543
	H	4.86978	1.0254	0.74538
	H	4.8944	-1.569	0.0314
	C	2.74932	1.75087	-2.2112
	H	2.84421	2.58866	-2.9012
	H	3.66022	1.66166	-1.6217
	H	2.59216	0.82375	-2.7639
	N	-5.8921	-0.7261	-0.1567
	O	-5.9688	-1.5813	-1.027
	O	-6.8484	-0.234	0.42785
	Ni	2.2624	-0.287	0.33633
C	Br	-0.7369	-0.7402	-2.0575
	Ni	-1.4128	-1.8505	-0.0962
	N	-1.5789	0.68022	1.3447
	C	-3.1522	2.32956	0.34656
	C	-2.5695	2.67298	-0.8791
	C	-2.9634	0.94139	0.91551
	C	-2.7454	3.94984	-1.4021
	C	-3.9153	3.2787	1.02987
	C	-3.5059	4.89497	-0.7127
	C	-4.0934	4.55772	0.50313
	C	-0.8662	-0.4223	0.99917
	C	-0.8262	1.53273	2.13998
	C	-2.0869	-3.2135	1.3155
	C	-3.2312	-2.9292	0.48795
	C	-2.8871	-3.2941	-0.8142
	H	-2.0317	-3.0433	2.38104
	H	-3.1847	0.17797	0.16974
	H	-4.3796	3.01604	1.97565
	H	-3.6285	0.78572	1.76924
	H	-4.6907	5.28538	1.04095
	H	-2.2935	4.20629	-2.3536
	H	-4.146	-2.4557	0.80934
	H	-1.2078	2.47352	2.49572
	H	-1.9853	1.93391	-1.4182



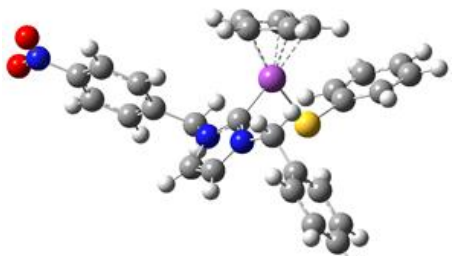
	H	-3.4769	-3.1377	-1.7043
	N	0.34602	-0.2436	1.59029
	C	2.72707	-0.5368	0.93487
	C	2.73925	0.01732	-0.352
	C	1.46794	-1.1797	1.47676
	C	3.89922	0.58901	-0.8576
	C	3.8929	-0.5135	1.70511
	C	5.04405	0.59989	-0.066
	C	5.06266	0.05414	1.21045
	C	0.38494	0.95275	2.29535
	H	1.12484	-1.9722	0.8101
	H	3.89196	-0.946	2.69994
	H	1.66098	-1.6229	2.4573
	H	5.97484	0.08239	1.78953
	H	3.93256	1.01756	-1.8494
	H	1.26449	1.288	2.81657
	H	1.84048	-0.0097	-0.9602
	C	-1.1194	-3.9293	0.53642
	C	-1.5733	-3.8986	-0.7875
	H	-0.1866	-4.3384	0.89247
	H	-1.0452	-4.2634	-1.6551
	N	6.28327	1.21016	-0.5994
	O	7.27281	1.20336	0.12094
	O	6.24125	1.68436	-1.7256
	H	-3.6429	5.88818	-1.1252
D	Ni	0.14702	1.62371	0.16104
	Br	-0.0816	0.5554	-1.9223
	C	0.53496	0.01454	1.0555
	C	1.62637	-1.7207	2.0168
	C	0.30078	-1.9717	2.11246
	H	2.47905	-2.2966	2.33112
	H	-0.2262	-2.8065	2.54089
	C	0.11215	3.67484	-0.4762
	C	-1.1807	3.39303	0.10197
	C	1.09726	3.56239	0.52363
	H	0.27904	3.96099	-1.5033
	C	-0.9833	3.01283	1.42626
	H	-2.1187	3.41606	-0.4309
	C	0.44502	3.02797	1.66946
	H	2.15381	3.75057	0.41176
	H	-1.7385	2.70945	2.13535
	H	0.91425	2.79544	2.61445
	N	-0.3548	-0.9004	1.52213
	N	1.7531	-0.5007	1.36808
	C	-1.8029	-0.8259	1.31125
	H	-2.3066	-0.9607	2.27255



	H	-2.0098	0.1824	0.9568
	C	-2.2996	-1.8556	0.28037
	H	-1.7121	-1.7263	-0.6315
	H	-2.1178	-2.8683	0.65371
	C	-3.7711	-1.6696	-0.0148
	C	-4.7482	-2.3787	0.6905
	C	-4.1808	-0.7503	-0.9879
	C	-6.1028	-2.1769	0.43335
	H	-4.4471	-3.1037	1.4411
	C	-5.534	-0.5474	-1.2469
	H	-3.4302	-0.202	-1.5485
	C	-6.4993	-1.259	-0.5364
	H	-6.847	-2.7401	0.98582
	H	-5.8344	0.1626	-2.0095
	H	-7.5526	-1.1035	-0.7413
	C	3.03764	0.12844	1.0322
	H	2.78545	1.04572	0.49916
	H	3.54554	0.40568	1.95996
	C	3.92963	-0.7595	0.19135
	C	5.16831	-1.181	0.67833
	C	3.52957	-1.1514	-1.092
	C	6.00163	-1.9835	-0.1007
	H	5.48848	-0.8761	1.67009
	C	4.36022	-1.9547	-1.8664
	H	2.57073	-0.8241	-1.4828
	C	5.5971	-2.3727	-1.374
	H	6.96248	-2.3018	0.28798
	H	4.04317	-2.2502	-2.8601
	H	6.24227	-2.9964	-1.9826
1	Ni	-0.1591	0.72493	0.93413
	S	-1.3449	0.91786	-0.944
	N	0.10292	-2.133	0.3523
	N	1.66152	-0.9841	-0.5804
	C	0.57126	-0.8628	0.22432
	C	0.88678	-3.0293	-0.3608
	H	0.66769	-4.082	-0.3981
	C	1.86627	-2.3062	-0.9491
	H	2.68323	-2.6071	-1.5813
	C	-1.0835	-2.5094	1.13527
	H	-1.5027	-1.5712	1.49969
	H	-0.7589	-3.0948	2.00003
	C	-2.1041	-3.2846	0.33033
	C	-2.7968	-2.6645	-0.717
	H	-2.596	-1.6234	-0.9534
	C	-3.7432	-3.3783	-1.4452
	H	-4.2768	-2.8889	-2.2522

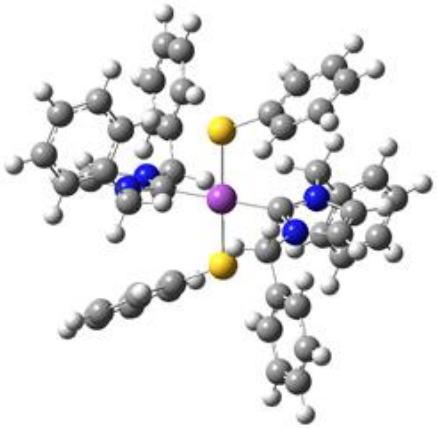


	C	-4.0119	-4.7125	-1.1377
	H	-4.7522	-5.2635	-1.707
	C	-3.3296	-5.333	-0.0955
	H	-3.5356	-6.3683	0.15211
	C	-2.3787	-4.6196	0.63401
	H	-1.852	-5.1044	1.45056
	C	2.43642	0.14914	-1.0945
	H	2.0316	1.03015	-0.5936
	H	2.22469	0.26084	-2.1606
	C	3.92561	0.01599	-0.8603
	C	4.8219	0.21895	-1.9115
	H	4.44173	0.44082	-2.9036
	C	6.19777	0.1429	-1.6985
	H	6.88072	0.30377	-2.525
	C	6.69141	-0.1443	-0.4294
	H	7.76058	-0.2067	-0.2616
	C	5.80356	-0.3535	0.626
	H	6.18208	-0.577	1.61713
	C	4.43133	-0.2726	0.41234
	H	3.74443	-0.4379	1.23511
	C	-2.1182	2.53242	-0.9696
	C	-1.4781	3.61814	-1.583
	H	-0.4868	3.47572	-1.9971
	C	-2.1047	4.85921	-1.6689
	H	-1.5922	5.68697	-2.1481
	C	-3.3862	5.03834	-1.1507
	H	-3.8747	6.00387	-1.2198
	C	-4.0365	3.96265	-0.5482
	H	-5.0378	4.0879	-0.1493
	C	-3.4106	2.7211	-0.4603
	H	-3.9206	1.88283	0.00017
	C	0.16505	2.6956	1.80817
	H	0.23678	3.59607	1.21776
	C	-1.0679	2.11239	2.28437
	H	-2.0497	2.52653	2.11429
	C	-0.7643	0.96559	3.04152
	H	-1.4665	0.32522	3.55264
	C	0.63501	0.74725	2.90215
	H	1.18928	-0.0732	3.33499
	C	1.2176	1.87362	2.21622
	H	2.26859	2.01765	2.01618
[CpNi(SPh){Im(Bn)(4-NO_2Bn)}]	Ni	0.72258	0.70184	0.87444
	S	1.97036	1.00674	-0.9486
	N	-0.8937	-1.087	-0.7703
	N	0.65799	-2.1609	0.25696
	C	0.13392	-0.9161	0.10786



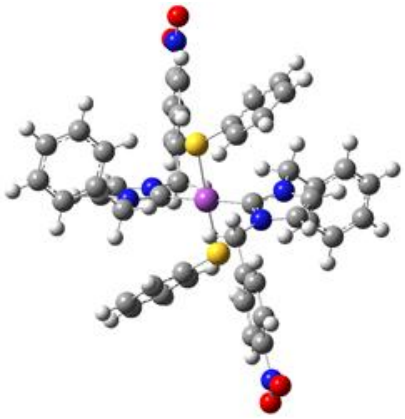
C	-1.0042	-2.4155	-1.1601
H	-1.7554	-2.754	-1.8524
C	-0.0282	-3.0903	-0.5123
H	0.25199	-4.1286	-0.5458
C	-1.6985	0.00449	-1.3103
H	-1.5628	0.04001	-2.3938
H	-1.2637	0.92082	-0.9036
C	-3.1696	-0.0885	-0.965
C	-3.5948	-0.5404	0.28962
H	-2.8632	-0.8706	1.01671
C	-4.9452	-0.5744	0.61196
H	-5.2922	-0.9204	1.57554
C	-5.8706	-0.1489	-0.3348
C	-5.4809	0.30602	-1.5884
H	-6.2327	0.62362	-2.2973
C	-4.1258	0.32947	-1.8964
H	-3.8094	0.67673	-2.8739
C	1.82249	-2.4788	1.09889
H	1.48557	-3.0822	1.94614
H	2.17455	-1.521	1.48318
C	2.91779	-3.1981	0.34238
C	3.2529	-4.5148	0.66449
H	2.72089	-5.0255	1.46148
C	4.2707	-5.1764	-0.0221
H	4.52349	-6.1978	0.23904
C	4.95906	-4.5223	-1.0395
H	5.75108	-5.0331	-1.5755
C	4.63009	-3.2058	-1.3649
H	5.16837	-2.6905	-2.1524
C	3.61727	-2.5433	-0.679
H	3.36924	-1.5156	-0.9286
C	2.68972	2.64533	-0.8834
C	3.9501	2.85558	-0.307
H	4.4657	2.018	0.14836
C	4.53839	4.11827	-0.3232
H	5.51537	4.26041	0.12677
C	3.882	5.19357	-0.9197
H	4.34138	6.17554	-0.9332
C	2.63245	4.99325	-1.5039
H	2.11625	5.82099	-1.9789
C	2.04331	3.73111	-1.4894
H	1.07756	3.57296	-1.955
C	1.50592	2.08254	2.31029
H	2.48421	2.52733	2.2143
C	0.29047	2.63944	1.76039
H	0.23293	3.55003	1.18416

	C	-0.7657	1.78578	2.08774
	H	-1.8057	1.91047	1.82719
	C	-0.1976	0.66034	2.78368
	H	-0.7551	-0.1821	3.1676
	C	1.18569	0.91195	3.01896
	H	1.86894	0.27935	3.56428
	O	-8.1007	0.19444	-0.8525
	N	-7.311	-0.1871	0.00043
	O	-7.6225	-0.5982	1.10977
2	Ni	5E-06	-0.1108	-3E-06
	S	-0.7953	-0.0379	2.09483
	N	-2.6105	0.93144	-0.919
	N	-2.6973	-1.1824	-0.5578
	C	-1.8462	-0.1222	-0.5309
	C	-3.9106	0.53393	-1.194
	H	-4.6706	1.22939	-1.5039
	C	-3.9655	-0.7971	-0.9691
	H	-4.7821	-1.493	-1.0445
	C	-2.3143	-2.5702	-0.2637
	H	-1.3151	-2.5174	0.16738
	H	-2.2494	-3.1189	-1.2073
	C	-3.2677	-3.2697	0.68045
	C	-3.3226	-2.899	2.02926
	H	-2.6715	-2.1069	2.38612
	C	-4.1939	-3.5492	2.89715
	H	-4.2275	-3.2568	3.94072
	C	-5.0166	-4.576	2.43251
	H	-5.6933	-5.0812	3.11272
	C	-4.9627	-4.9533	1.09378
	H	-5.5954	-5.7536	0.72643
	C	-2.136	2.312	-1.0639
	H	-2.2306	2.59441	-2.1146
	H	-1.0712	2.29112	-0.8312
	C	-2.8765	3.29782	-0.184
	C	-3.5567	4.37492	-0.7559
	H	-3.5624	4.49365	-1.8351
	C	-4.2239	5.30134	0.04518
	H	-4.747	6.13356	-0.4127
	C	-4.2195	5.15297	1.42882
	H	-4.7397	5.86949	2.05471
	C	-3.5426	4.07852	2.00705
	H	-3.5345	3.95886	3.08478
	C	-2.873	3.15621	1.2091
	H	-2.3428	2.32508	1.66481
	C	0.45641	-0.074	3.37277
	C	0.6903	1.06915	4.15111



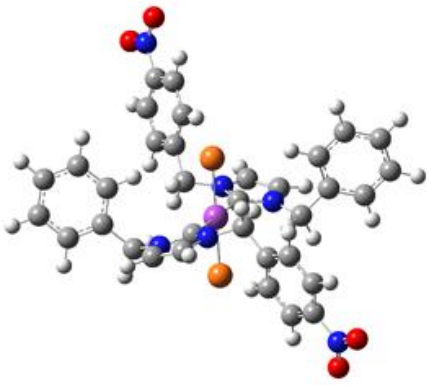
H	0.14285	1.97701	3.92483
C	1.59738	1.04196	5.20861
H	1.75684	1.93712	5.80106
C	2.29302	-0.1272	5.51079
H	2.99765	-0.149	6.33448
C	2.06114	-1.2729	4.751
H	2.58336	-2.1945	4.98689
C	1.14976	-1.2485	3.69848
H	0.95024	-2.1497	3.1306
S	0.79525	-0.0376	-2.0948
N	2.69838	-1.1799	0.55763
N	2.60949	0.93387	0.91897
C	1.84618	-0.1205	0.53091
C	3.96625	-0.7933	0.96887
H	4.78353	-1.4884	1.04415
C	3.91002	0.53765	1.1939
H	4.66938	1.23386	1.50372
C	2.31674	-2.5681	0.26352
H	1.3176	-2.5161	-0.1679
H	2.25198	-3.1167	1.20721
C	3.27102	-3.2667	-0.6803
C	4.0955	-4.2966	-0.2218
H	4.0519	-4.5962	0.82105
C	4.96842	-4.9482	-1.0928
H	5.60221	-5.7474	-0.725
C	5.02173	-4.5715	-2.4317
H	5.69908	-5.0761	-3.1117
C	4.19756	-3.546	-2.8968
H	4.23065	-3.2541	-3.9406
C	3.32535	-2.8966	-2.0292
H	2.67317	-2.1056	-2.3865
C	2.13369	2.314	1.06389
H	1.06886	2.29211	0.83136
H	2.22825	2.59653	2.11459
C	2.87317	3.30046	0.18381
C	3.55211	4.37845	0.75558
H	3.55758	4.4974	1.83472
C	4.2183	5.30547	-0.0457
H	4.74041	6.13836	0.41204
C	4.21409	5.15682	-1.4293
H	4.73354	5.87382	-2.0553
C	3.5385	4.08149	-2.0073
H	3.53057	3.96161	-3.0851
C	2.86987	3.15857	-1.2093
H	2.34063	2.32675	-1.6648
C	-0.4564	-0.0749	-3.3728

	C	-1.1485	-1.2501	-3.6986
	H	-0.948	-2.1511	-3.1307
	C	-2.0598	-1.2755	-4.7511
	H	-2.581	-2.1976	-4.987
	C	-2.2929	-0.13	-5.5109
	H	-2.9975	-0.1525	-6.3346
	C	-1.5985	1.03993	-5.2086
	H	-1.7589	1.93493	-5.8011
	C	-0.6915	1.06808	-4.1511
	H	-0.145	1.97652	-3.9248
	C	-4.0907	-4.3009	0.22248
	H	-4.0467	-4.601	-0.8202
$[Ni(SPh)_2\{Im(Bn)(4\text{-}NO_2Bn)\}_2]$	Ni	0.05024	-0.1652	0.07261
	S	-1.1365	-0.6144	1.91872
	N	-2.1475	-1.309	-1.538
	N	-0.9251	-2.8528	-0.6855
	C	-1.0452	-1.5013	-0.7654
	C	-2.6943	-2.5186	-1.9436
	H	-3.5755	-2.576	-2.5583
	C	-1.9237	-3.4902	-1.4084
	H	-2.0021	-4.5616	-1.4603
	C	0.16283	-3.5581	0.01049
	H	0.66623	-2.8045	0.61484
	H	0.86964	-3.9259	-0.7383
	C	-0.3214	-4.6985	0.87822
	C	-1.0106	-4.4338	2.06761
	H	-1.1882	-3.4027	2.35749
	C	-1.4487	-5.4834	2.86879
	H	-1.9797	-5.2693	3.78952
	C	-1.2022	-6.8051	2.49574
	H	-1.5441	-7.6202	3.12373
	C	-0.5116	-7.0748	1.31764
	H	-0.3117	-8.0994	1.02476
	C	-2.6873	-0.0053	-1.9231
	H	-2.6769	0.06294	-3.0127
	H	-1.984	0.74024	-1.549
	C	-4.0832	0.25306	-1.3919
	C	-5.1006	0.63952	-2.2692
	H	-4.8925	0.72854	-3.33
	C	-6.381	0.91534	-1.801
	H	-7.1803	1.21523	-2.464
	C	-6.6289	0.79271	-0.4402
	C	-5.6372	0.40844	0.45746
	H	-5.873	0.32876	1.50949
	C	-4.3623	0.13993	-0.0234
	H	-3.5769	-0.1467	0.66939



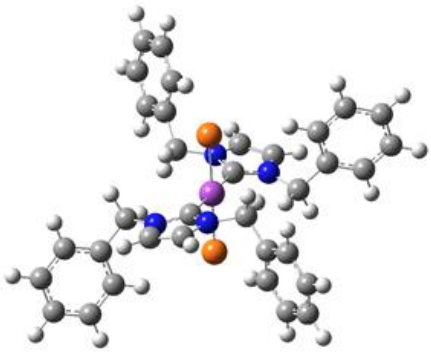
C	-0.6658	0.33455	3.3622
C	-1.4892	1.37473	3.81568
H	-2.3775	1.62537	3.24754
C	-1.1873	2.06708	4.98669
H	-1.8433	2.8633	5.32294
C	-0.0562	1.7348	5.72983
H	0.17684	2.27102	6.64272
C	0.76339	0.69424	5.29536
H	1.63595	0.41325	5.87604
C	0.45937	-0.0018	4.12801
H	1.08043	-0.8319	3.8121
S	1.14259	0.39696	-1.7984
N	2.42358	0.99616	1.39495
N	0.87162	2.45833	1.15891
C	1.15718	1.15293	0.92253
C	2.90897	2.18128	1.93267
H	3.8953	2.26396	2.35384
C	1.93166	3.10109	1.7811
H	1.89824	4.14437	2.04118
C	3.16174	-0.2698	1.39872
H	2.54794	-0.9779	0.84219
H	3.2401	-0.6263	2.42907
C	4.53902	-0.1626	0.77759
C	5.68257	-0.3107	1.56761
H	5.58339	-0.4996	2.63119
C	6.95274	-0.2247	1.00641
H	7.84942	-0.3354	1.59964
C	7.05812	0.0111	-0.358
C	5.93793	0.15657	-1.1711
H	6.06709	0.33044	-2.2302
C	4.67645	0.06824	-0.5975
H	3.78688	0.16714	-1.2126
C	-0.4016	3.11461	0.83565
H	-1.0214	2.3502	0.36689
H	-0.886	3.39585	1.77304
C	-0.2425	4.32425	-0.0612
C	-0.6668	5.58079	0.37574
H	-1.0992	5.68726	1.36586
C	-0.5454	6.69869	-0.4492
H	-0.8805	7.66806	-0.0978
C	0.00843	6.56705	-1.7191
H	0.10728	7.43435	-2.3622
C	0.43547	5.31455	-2.1617
H	0.86554	5.20676	-3.1513
C	0.31028	4.19769	-1.3415
H	0.63546	3.2229	-1.6927

	C	0.69493	-0.5507	-3.2493
	C	1.0913	-1.8847	-3.4179
	H	1.65125	-2.3703	-2.6274
	C	0.79932	-2.5735	-4.5925
	H	1.11969	-3.6042	-4.7036
	C	0.11508	-1.9416	-5.6299
	H	-0.1041	-2.4762	-6.5471
	C	-0.2709	-0.611	-5.4803
	H	-0.7904	-0.1025	-6.286
	C	0.01382	0.07701	-4.3023
	H	-0.2768	1.11571	-4.1934
	C	-0.0736	-6.0235	0.5127
	H	0.47038	-6.2364	-0.4026
	N	8.40563	0.10474	-0.9645
	O	9.37058	-0.0233	-0.2225
	O	8.47178	0.30451	-2.1692
	N	-7.9882	1.08124	0.06819
	O	-8.8393	1.41387	-0.7462
	O	-8.1786	0.97064	1.27154
3	Br	-0.7887	0.04361	1.73784
	Ni	0.18844	-0.332	-0.3831
	O	8.27214	0.0641	-1.5928
	N	2.12692	-2.0045	1.10761
	N	0.72915	-3.2132	0.01803
	O	9.00057	0.35729	0.42915
	C	1.05294	-1.9224	0.27933
	C	2.46792	-3.3286	1.35646
	H	3.29879	-3.6019	1.98338
	C	1.58489	-4.0885	0.67277
	H	1.47802	-5.1569	0.60255
	N	8.11657	0.10998	-0.3805
	C	2.82465	-0.8618	1.69268
	H	2.86824	-1.0016	2.77508
	H	2.19325	0.01024	1.51778
	C	4.2177	-0.6445	1.13514
	C	4.45812	-0.6886	-0.2439
	H	3.64969	-0.9083	-0.9328
	C	5.73073	-0.4427	-0.7438
	H	5.93531	-0.469	-1.8049
	C	6.75913	-0.1523	0.14681
	C	6.55038	-0.1018	1.51911
	H	7.37787	0.12418	2.17675
	C	5.27241	-0.3528	2.00545
	H	5.09545	-0.3195	3.07506
	C	-0.3663	-3.6457	-0.8554
	H	0.05263	-4.2768	-1.6425

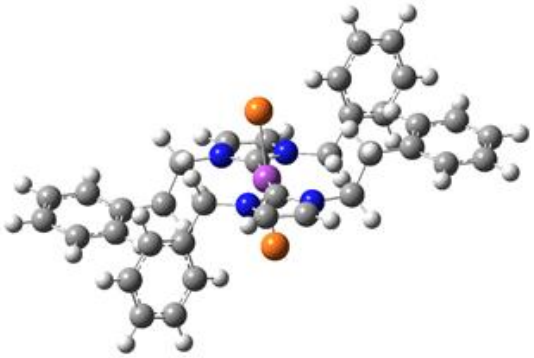


H	-0.737	-2.7445	-1.3435
C	-1.4715	-4.3786	-0.1227
C	-1.9241	-5.6116	-0.597
H	-1.4588	-6.0535	-1.4727
C	-2.9701	-6.2779	0.04035
H	-3.311	-7.2345	-0.3393
C	-3.5692	-5.7166	1.16421
H	-4.3809	-6.2331	1.66388
C	-3.1193	-4.4873	1.64624
H	-3.5825	-4.0445	2.52079
C	-2.0782	-3.8198	1.00831
H	-1.7368	-2.8635	1.39148
Br	1.15457	-0.6789	-2.5043
O	-8.0735	2.05889	1.87587
N	-1.954	1.36864	-1.4948
N	-0.1246	2.46843	-1.2786
O	-9.0143	1.6837	-0.0424
C	-0.67	1.24563	-1.0706
C	-2.2007	2.64916	-1.9772
H	-3.1627	2.94949	-2.3535
C	-1.0495	3.34152	-1.8355
H	-0.8103	4.3666	-2.0586
N	-8.0415	1.72841	0.69873
C	-2.9268	0.27252	-1.5207
H	-3.039	-0.0785	-2.5496
H	-2.4914	-0.538	-0.9353
C	-4.2694	0.66482	-0.9426
C	-4.3691	1.05354	0.39971
H	-3.4775	1.06981	1.01719
C	-5.5988	1.40153	0.94117
H	-5.6999	1.70062	1.975
C	-6.7274	1.35572	0.12748
C	-6.6604	0.96946	-1.2043
H	-7.5626	0.94642	-1.799
C	-5.4204	0.6246	-1.7335
H	-5.3512	0.31913	-2.7719
C	1.27047	2.82556	-0.9999
H	1.75704	1.90941	-0.6658
H	1.74659	3.10909	-1.9414
C	1.4146	3.93328	0.02277
C	0.82461	3.82022	1.28726
H	0.23849	2.94035	1.53274
C	0.98816	4.83135	2.22886
H	0.52715	4.73384	3.20533
C	1.74384	5.96351	1.92292
H	1.86966	6.7491	2.65941

	C	2.33507	6.08086	0.66853
	H	2.92321	6.95777	0.42252
	C	2.16765	5.0699	-0.2773
	H	2.63024	5.16514	-1.2547
$[NiBr_2\{Im(Bn)_2\}_2]$	Br	1.05625	0.12026	2.1121
	Ni	9.3E-05	0.11743	-8E-05
	N	-2.3605	-0.9294	1.44198
	N	-2.5324	1.17975	1.08703
	C	-1.7137	0.11916	0.8752
	C	-3.5638	-0.5281	2.00721
	H	-4.2324	-1.2208	2.4877
	C	-3.6706	0.80111	1.78728
	H	-4.4492	1.49877	2.04045
	C	-1.8448	-2.2999	1.49824
	H	-1.7196	-2.5779	2.54745
	H	-0.8464	-2.2646	1.06245
	C	-2.7251	-3.3055	0.7854
	C	-3.0747	-3.1246	-0.5581
	H	-2.7315	-2.244	-1.0916
	C	-3.859	-4.0706	-1.2105
	H	-4.1225	-3.921	-2.2516
	C	-4.3015	-5.2078	-0.5342
	C	-3.9569	-5.3942	0.80115
	H	-4.2977	-6.2743	1.33498
	C	-3.1739	-4.4445	1.45668
	H	-2.9063	-4.5934	2.49823
	C	-2.2121	2.56079	0.69933
	H	-1.3874	2.48751	-0.0098
	H	-1.8536	3.097	1.58202
	C	-3.3816	3.28839	0.07454
	C	-3.8717	2.88991	-1.1747
	H	-3.4036	2.05547	-1.6864
	C	-4.9408	3.56448	-1.7547
	H	-5.311	3.25108	-2.7244
	C	-5.5314	4.64463	-1.0975
	H	-6.3635	5.16969	-1.5532
	C	-5.0464	5.04901	0.14279
	H	-5.4979	5.88997	0.65716
	C	-3.9756	4.37143	0.72561
	H	-3.596	4.69074	1.69137
	Br	-1.0561	0.12098	-2.1122
	N	2.53361	1.17763	-1.0871
	N	2.35977	-0.9313	-1.4423
	C	1.7139	0.11776	-0.8754
	C	3.67146	0.79806	-1.7874
	H	4.45063	1.49504	-2.0404

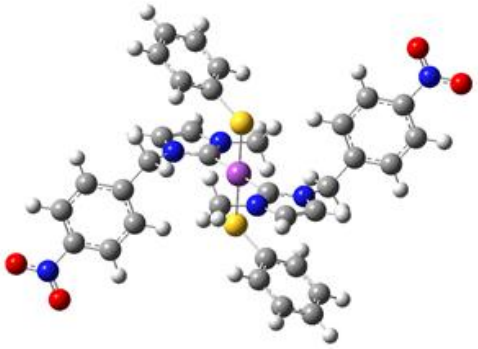


	C	3.5634	-0.531	-2.0075
	H	4.23135	-1.2243	-2.4881
	C	2.21452	2.5589	-0.6991
	H	1.85646	3.09557	-1.5817
	H	1.38991	2.48628	0.01006
	C	3.38482	3.28531	-0.0743
	C	3.87481	2.88599	1.17471
	H	3.40611	2.0518	1.68623
	C	4.94465	3.55943	1.75465
	H	5.31469	3.24539	2.72421
	C	5.53603	4.63928	1.09772
	C	5.05112	5.04449	-0.1423
	H	5.50325	5.88523	-0.6565
	C	3.97957	4.36805	-0.7252
	H	3.60014	4.688	-1.6907
	C	1.84288	-2.3013	-1.4988
	H	0.8443	-2.2652	-1.0633
	H	1.7178	-2.5793	-2.548
	C	2.72197	-3.3078	-0.7856
	C	3.07103	-3.1272	0.55812
	H	2.72833	-2.2463	1.09148
	C	3.8541	-4.074	1.21088
	H	4.11724	-3.9246	2.25208
	C	4.29598	-5.2115	0.53476
	H	4.90532	-5.9473	1.04758
	C	3.95182	-5.3975	-0.8008
	H	4.29206	-6.278	-1.3345
	C	3.17002	-4.4471	-1.4567
	H	2.90284	-4.5958	-2.4984
	H	6.36864	5.16346	1.55346
	H	-4.9118	-5.943	-1.0468
4	Br	0.52981	0.32381	2.27379
	Ni	3.7E-05	5.4E-05	-0.0002
	N	0.70022	-2.8778	0.12581
	N	-1.3081	-2.5264	0.79145
	C	-0.2074	-1.8884	0.31862
	C	0.17589	-4.1133	0.48294
	H	0.73991	-5.0259	0.39659
	C	-1.0902	-3.8931	0.9004
	H	-1.8532	-4.5731	1.2362
	C	2.07062	-2.6822	-0.3456
	H	2.29863	-3.4752	-1.0621
	C	-2.559	-1.8648	1.16794
	H	-2.4156	-0.8063	0.95084
	H	-2.6934	-1.9549	2.24867
	C	-3.7627	-2.4148	0.43198



C	-3.7808	-2.4585	-0.9677
H	-2.9186	-2.1089	-1.5273
C	-4.9003	-2.9413	-1.6384
H	-4.9047	-2.9684	-2.7222
C	-6.0135	-3.3852	-0.9233
H	-6.8833	-3.7623	-1.4495
C	-6.0018	-3.3437	0.46801
H	-6.8613	-3.6897	1.03132
C	-4.879	-2.8617	1.14107
H	-4.8731	-2.8304	2.22609
Br	-0.5297	-0.3238	-2.2741
N	-0.7002	2.8779	-0.126
N	1.30787	2.52657	-0.7922
C	0.20739	1.88848	-0.319
C	-0.1761	4.11337	-0.4834
H	-0.7402	5.02591	-0.397
C	1.08981	3.89322	-0.9013
H	1.8527	4.57323	-1.2374
C	-2.0705	2.68221	0.34599
H	-2.092	1.74043	0.89255
H	-2.2981	3.47503	1.06288
C	2.55871	1.8651	-1.169
H	2.41542	0.80652	-0.9522
H	2.69307	1.95545	-2.2498
C	3.76257	2.41482	-0.4331
C	3.78065	2.45855	0.96663
H	2.91838	2.10913	1.5262
C	4.90022	2.94123	1.63727
H	4.9047	2.96831	2.72111
C	6.01351	3.38492	0.92222
H	6.88339	3.76182	1.44836
C	6.00185	3.34341	-0.4691
H	6.86139	3.68927	-1.0324
C	4.87894	2.86155	-1.1422
H	4.87298	2.83022	-2.2272
C	3.09253	-2.6826	0.8068
H	2.84435	-1.869	1.49274
H	2.98976	-3.6172	1.36794
C	4.51076	-2.5431	0.30007
C	5.21449	-3.6563	-0.1744
C	5.14111	-1.2952	0.26889
C	6.50959	-3.5272	-0.6694
H	4.74775	-4.6366	-0.1466
C	6.43723	-1.1615	-0.2256
H	4.62018	-0.4214	0.64517
C	7.1248	-2.2769	-0.6978

	H	7.04026	-4.4027	-1.0271
	H	6.90725	-0.1847	-0.2355
	H	8.13443	-2.175	-1.0797
	C	-3.0929	2.68312	-0.806
	H	-2.845	1.86978	-1.4924
	H	-2.9904	3.61794	-1.3668
	C	-4.5109	2.54324	-0.2987
	C	-5.2143	3.65611	0.17693
	C	-5.1412	1.2954	-0.2681
	C	-6.5092	3.52668	0.67247
	H	-4.7476	4.63646	0.1496
	C	-6.4371	1.16134	0.22696
	H	-4.6205	0.42183	-0.6453
	C	-7.1244	2.27642	0.70029
	H	-7.0397	4.40196	1.03111
	H	-6.9071	0.18447	0.23643
	H	-8.1338	2.17421	1.08267
	H	2.09233	-1.7406	-0.8925
5	Ni	0.00011	6.7E-05	-0.0002
	S	-0.9588	-1.7222	1.05965
	N	-0.836	1.45666	2.4054
	N	-2.3183	1.6254	0.86517
	C	-1.0972	1.08924	1.12607
	C	-1.8728	2.21171	2.93256
	H	-1.8509	2.60075	3.93556
	C	-2.8069	2.32194	1.96158
	H	-3.7595	2.8214	1.9521
	C	-3.0179	1.51456	-0.4152
	H	-2.3429	0.97204	-1.0785
	H	-3.1457	2.51683	-0.8289
	C	-4.3546	0.80775	-0.3103
	C	-4.4377	-0.4964	0.19672
	H	-3.5405	-1.011	0.52875
	C	-5.664	-1.1443	0.26721
	H	-5.7493	-2.1508	0.6525
	C	-6.8041	-0.4793	-0.1742
	C	-6.7519	0.8114	-0.6837
	H	-7.6618	1.29164	-1.0148
	C	0.3559	1.05012	3.1413
	H	0.34815	-0.0316	3.28087
	H	0.35925	1.54955	4.10965
	C	-0.1892	-3.3066	0.73581
	C	0.60244	-3.9024	1.72823
	H	0.76548	-3.367	2.65652
	C	1.15542	-5.1674	1.53934
	H	1.75671	-5.6132	2.32504



C	0.92922	-5.8639	0.35336
H	1.35535	-6.85	0.20661
C	0.13348	-5.2867	-0.6351
H	-0.0648	-5.8268	-1.555
C	-0.4245	-4.025	-0.4445
H	-1.0649	-3.595	-1.2052
S	0.95918	1.72245	-1.0597
N	0.83651	-1.4563	-2.4058
N	2.31842	-1.6255	-0.8653
C	1.09752	-1.0891	-1.1264
C	1.87323	-2.2115	-2.9328
H	1.85153	-2.6003	-3.9359
C	2.80712	-2.322	-1.9617
H	3.75968	-2.8216	-1.9521
C	3.01791	-1.5149	0.41513
H	2.34272	-0.9726	1.07852
H	3.14565	-2.5172	0.82864
C	4.35456	-0.808	0.3106
C	5.51732	-1.4497	0.74694
H	5.46035	-2.4587	1.14104
C	6.75173	-0.8115	0.68462
H	7.66161	-1.2917	1.016
C	6.80407	0.47915	0.17511
C	5.66409	1.1441	-0.2667
H	5.74939	2.15049	-0.6521
C	4.43774	0.49616	-0.1965
H	3.54066	1.01075	-0.5289
C	0.18905	3.30661	-0.7363
C	-0.6029	3.90193	-1.7288
H	-0.7659	3.36627	-2.6569
C	-1.1563	5.16682	-1.5402
H	-1.7578	5.6122	-2.3259
C	-0.9302	5.86369	-0.3544
H	-1.3567	6.84962	-0.2078
C	-0.1342	5.28695	0.63418
H	0.06405	5.82741	1.55387
C	0.42429	4.02543	0.44374
H	1.06492	3.59584	1.20447
C	-5.5175	1.44958	-0.7463
H	-5.4605	2.45856	-1.1403
N	-8.1133	-1.1659	-0.1001
O	-9.0976	-0.5525	-0.4916
O	-8.1315	-2.3041	0.34725
N	8.1132	1.16582	0.10131
O	9.09747	0.55256	0.4932
O	8.13157	2.30388	-0.3463

H	1.24852	1.33881	2.58562
C	-0.3552	-1.0495	-3.1419
H	-1.248	-1.3385	-2.5868
H	-0.3474	0.03232	-3.2809
H	-0.3581	-1.5483	-4.1106

3. **Table S3**: Experimental and Calculated IR data.

Complex	Frequency (cm^{-1})[a]								
	ν(=CH), w	ν(-CH), w	δ(-CH), m	δ(-CH), w	δ(-CH), w	δ(-CH), m	ν(-CN), m	δ(=CH), m	δ(-CH), m
1	3094 (3171)	3058 (3047)	1495 (1500)	1455 (1451)	1407 (1390)	1359 (1374)	1238 (1242)	783 (765)	728 (726)
2	3097 (3154)	3059 (3048)	1519 (1531)	1455 (1430)	1408 (1391)	1342 (-)	1233 (1246)	784 (745)	727 (710)
3	3098 (3171)	3058 (3063)	1519 (1530)	1449 (1433)	1401 (-)	1339 (1378)	1233 (1253)	786 (818)	726 (727)
4	3104 (3179)	2930 (3063)	1519 (1529)	- (1437)	1410 (1387)	1346 (1376)	1259 (1236)	803 (750)	- (704)
5	3087 (3150)	2925 (3052)	1572 (1579)	1455 (1439)	1409 (-)	- (1379)	1261 (1252)	806 (820)	749 (701)

[a] Experimental frequencies, values in parentheses indicate calculated frequencies.

4. **Table S4**: Experimental and Calculated ^{1}H-NMR data.

Complex	Signal (ppm)[a]				
	C_5H_5	CH_2	NC*H*	SC_6H_5	C_6H_5
1	5.07 (3.60)	5.48 (5.09) 6.28 (5.46)	6.66 (5.94)	6.91 (5.99) 7.15 (6.25)	7.17 (5.99), 7.33 (6.33), 7.36 (6.56),7.43 (6.59)

[a] Experimental resonances, referenced to the internal deuterated solvent signal ($CDCl_3$: δ_H 7.24 ppm). Values in parentheses indicate calculated resonances, referenced to TMS (δ_H 0.00 ppm); using SCRF (solvent = chloroform).

Chapter 5

Electrochemistry of a series of symmetric and asymmetric CpNiBr(NHC) complexes: Probing the electrochemical environment due to push-pull effects

Frederick P. Malan,[a] Eric Singleton,[a] Jeanet Conradie[b,*] and Marilé Landman[a,*]

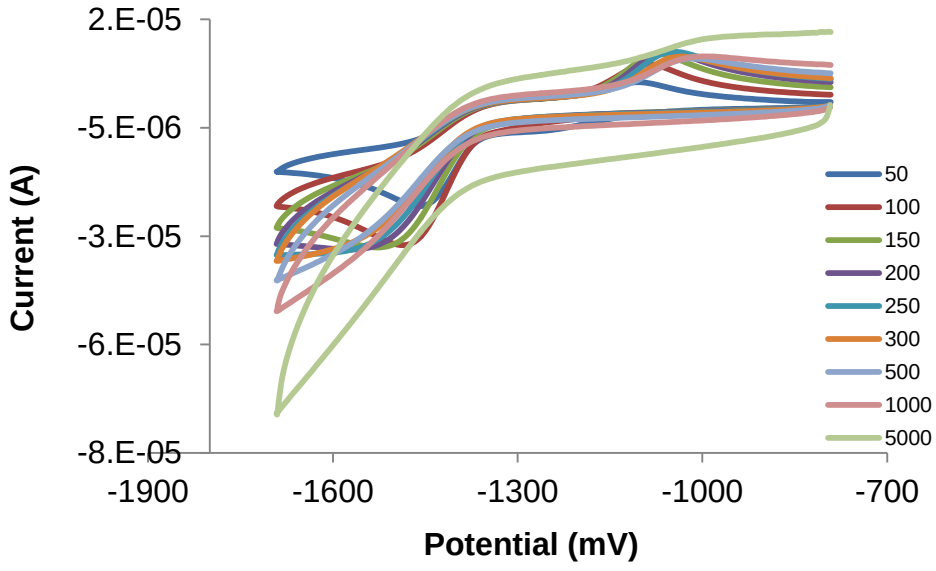
[a] *Department of Chemistry, University of Pretoria, 02 Lynnwood Road, Hatfield, Pretoria, 0002, South Africa.* [b] *Department of Chemistry, University of the Free State, Bloemfontein 9300, South Africa.*

Supplementary Information

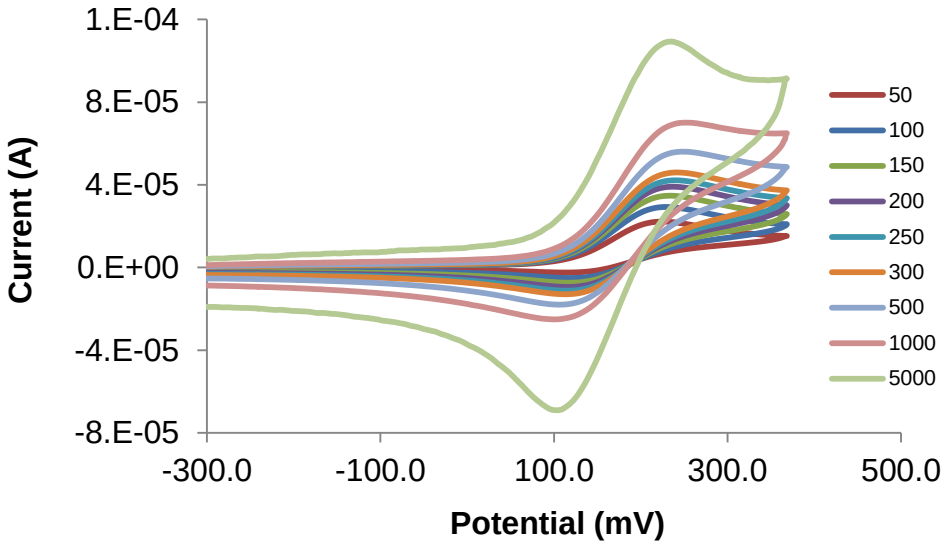
1. CVs of **2** as a function of scan speed (regions I, II, and III).
2. Graphs of **1**-**9** (region II): $v^{½}$ vs. I_{pa} (blue) and I_{pc} (red).
3. Tables of **1**-**9** (region II) with electrochemical data.
4. Optimized coordinates (DFT calculations) of **1**-**9.**

1. CVs of **2** as a function of scan speed (regions I, II, and III).

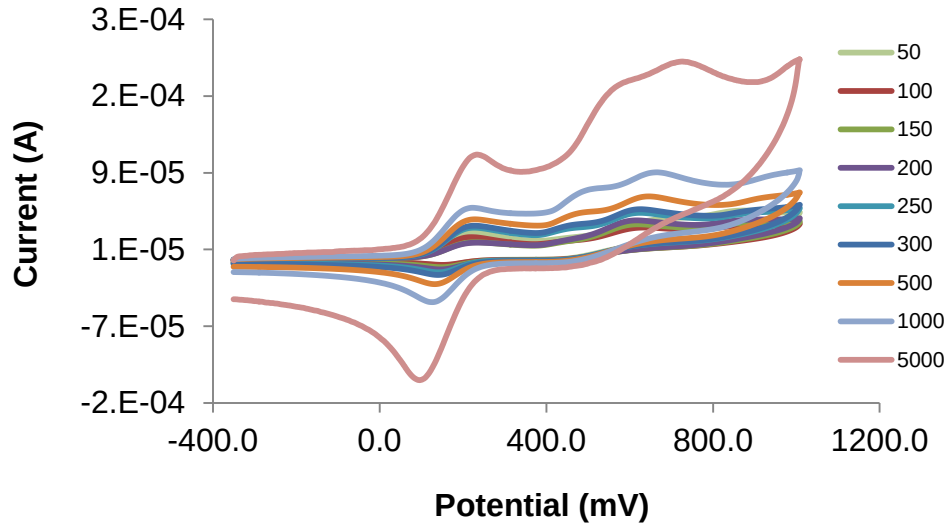
Region I:



Region II:

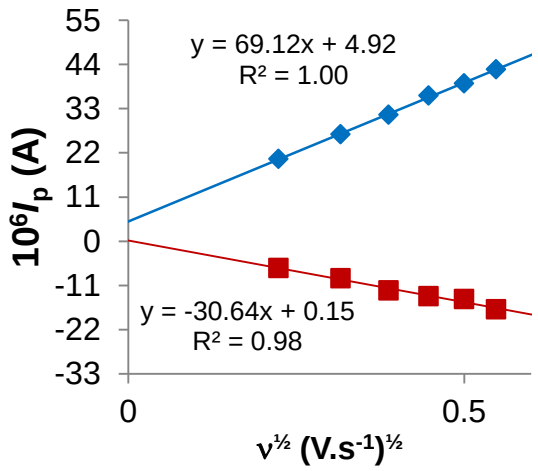


Region III:

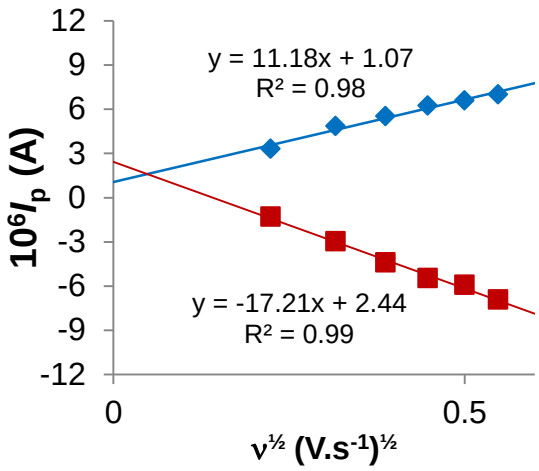


2. Graphs of **1**-**9** (region II): $\nu^{1/2}$ *vs.* I_{pa} (blue) and I_{pc} (red).

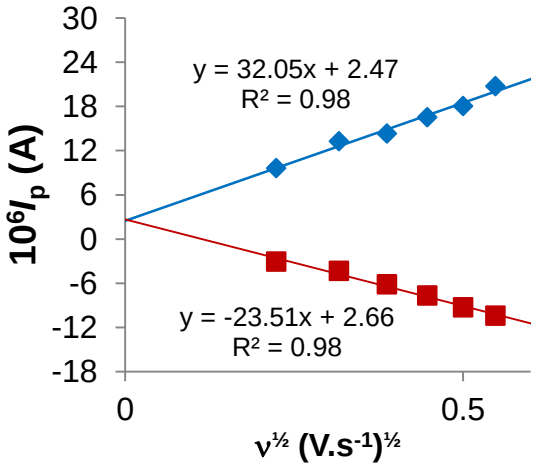
Complex **2**



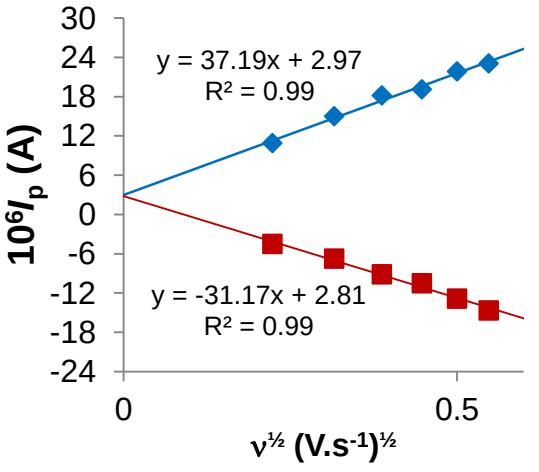
Complex **5**



Complex **3**

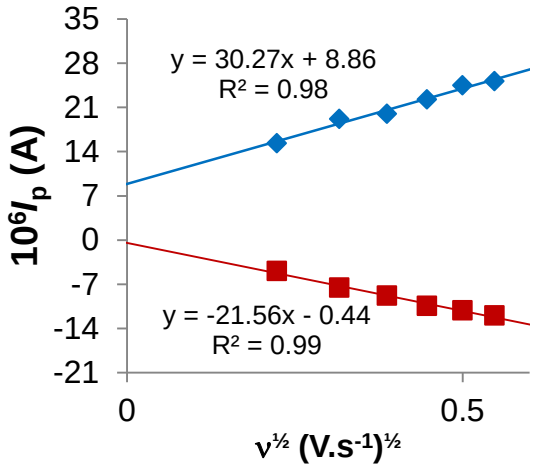


Complex **6**

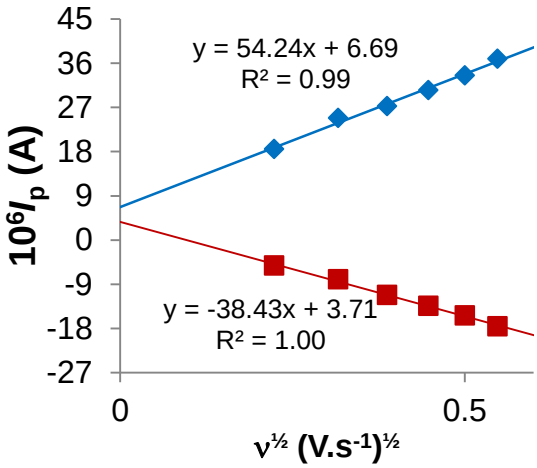


Complex **1**

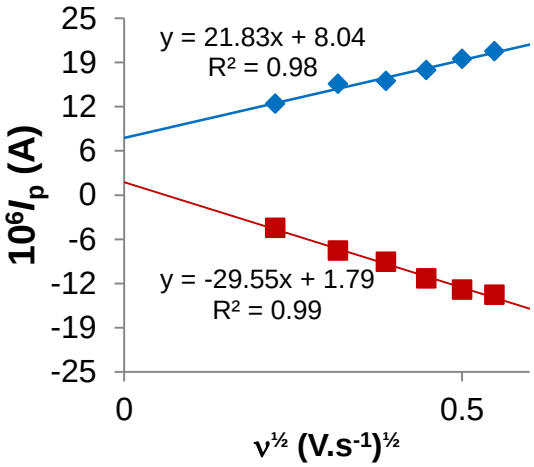
Complex **7**



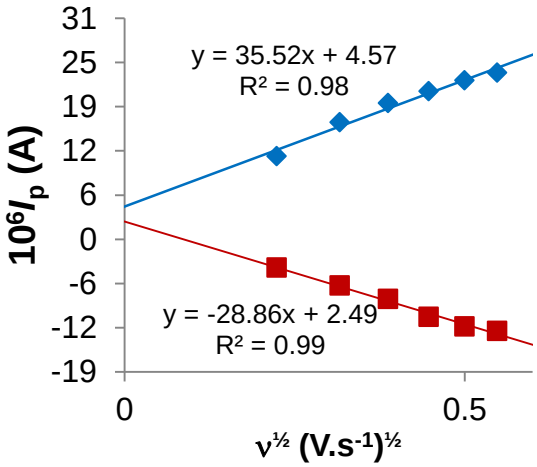
Complex **4**

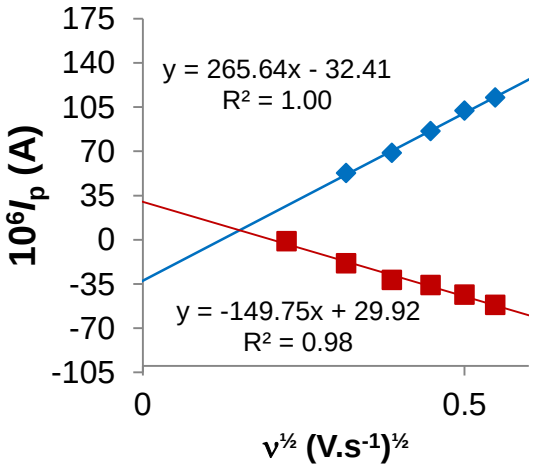


Complex **8**



Complex **9**





3. Tables of **1**-**9** (region II) with electrochemical data.

Complex **2**:

Scan rate; υ ($V.s^{-1}$)	I_{pa} (A)	I_{pc} (A)	I_{pc}/I_{pa}	E_{pc} (V)	E_{pa} (V)	ΔE (V)	E°' (V)
0.05	2.050E-05	6.700E-06	0.33	0.0145	0.1265	0.112	0.071
0.10	2.662E-05	9.265E-06	0.35	0.0205	0.1315	0.111	0.076
0.15	3.145E-05	1.226E-05	0.39	0.0195	0.1365	0.117	0.078
0.20	3.628E-05	1.372E-05	0.38	0.0175	0.1385	0.121	0.078
0.25	3.930E-05	1.442E-05	0.37	0.0165	0.1425	0.126	0.080
0.30	4.279E-05	1.698E-05	0.40	0.0145	0.1445	0.130	0.080
0.50	5.118E-05	2.353E-05	0.46	0.0085	0.1495	0.141	0.079
1.00	6.400E-05	2.920E-05	0.46	0.0025	0.1545	0.152	0.079
5.00	8.968E-05	5.806E-05	0.65	0.0055	0.1375	0.132	0.072

Complex **5**:

Scan rate; υ ($V.s^{-1}$)	I_{pa} (A)	I_{pc} (A)	I_{pc}/I_{pa}	E_{pc} (V)	E_{pa} (V)	ΔE (V)	E°' (V)
0.05	3.294E-06	1.294E-06	0.39	0.0205	0.1245	0.104	0.073
0.10	4.837E-06	2.977E-06	0.62	0.0295	0.1285	0.099	0.079
0.15	5.529E-06	4.412E-06	0.80	0.0245	0.1315	0.107	0.078
0.20	6.235E-06	5.471E-06	0.88	0.0225	0.1315	0.109	0.077
0.25	6.588E-06	5.941E-06	0.90	0.0225	0.1315	0.109	0.077
0.30	7.000E-06	6.933E-06	0.99	0.0195	0.1335	0.114	0.077
0.50	8.083E-06	7.583E-06	0.94	0.0125	0.1355	0.123	0.074
1.00	1.200E-06	1.145E-06	0.95	0.0135	0.1175	0.104	0.066
5.00	1.883E-06	1.093E-06	0.58	0.0075	0.1125	0.105	0.060

Complex **3**:

Scan rate; υ ($V.s^{-1}$)	I_{pa} (A)	I_{pc} (A)	I_{pc}/I_{pa}	E_{pc} (V)	E_{pa} (V)	ΔE (V)	E°' (V)
0.05	9.622E-06	3.081E-06	0.32	0.0335	0.1355	0.102	0.085
0.10	1.325E-05	4.333E-06	0.33	0.0175	0.1435	0.126	0.081
0.15	1.431E-05	6.176E-06	0.43	0.0335	0.1415	0.108	0.088
0.20	1.651E-05	7.674E-06	0.46	0.0305	0.1405	0.110	0.086
0.25	1.802E-05	9.302E-06	0.52	0.0285	0.1425	0.114	0.086
0.30	2.074E-05	1.044E-05	0.50	0.0305	0.1445	0.114	0.088
0.50	2.683E-05	1.533E-05	0.57	0.0215	0.1465	0.125	0.084
1.00	3.279E-05	1.837E-05	0.56	0.0145	0.1435	0.129	0.079
5.00	5.360E-05	2.280E-05	0.43	-0.0075	0.1615	0.169	0.077

Complex **6**:

Scan rate; υ ($V.s^{-1}$)	I_{pa} (A)	I_{pc} (A)	I_{pc}/I_{pa}	E_{pc} (V)	E_{pa} (V)	ΔE (V)	E°' (V)
0.05	1.085E-05	4.545E-06	0.42	0.0425	0.1305	0.088	0.087
0.10	1.500E-05	6.800E-06	0.45	0.0445	0.1315	0.087	0.088
0.15	1.814E-05	9.186E-06	0.51	0.0405	0.1325	0.092	0.087
0.20	1.908E-05	1.053E-05	0.55	0.0395	0.1355	0.096	0.088
0.25	2.182E-05	1.288E-05	0.59	0.0385	0.1365	0.098	0.088
0.30	2.303E-05	1.470E-05	0.64	0.0375	0.1375	0.100	0.088
0.50	2.780E-05	1.900E-05	0.68	0.0305	0.1385	0.108	0.085
1.00	3.474E-05	2.842E-05	0.82	0.0285	0.1365	0.108	0.083
5.00	5.842E-05	4.000E-05	0.68	0.0085	0.1465	0.138	0.078

Complex **1**:

Scan rate; υ ($V.s^{-1}$)	I_{pa} (A)	I_{pc} (A)	I_{pc}/I_{pa}	E_{pc} (V)	E_{pa} (V)	ΔE (V)	E°' (V)
0.05	1.533E-05	4.917E-06	0.32	0.0125	0.1165	0.104	0.065
0.10	1.919E-05	7.568E-06	0.39	0.0125	0.1235	0.111	0.068
0.15	2.000E-05	8.837E-06	0.44	0.0125	0.1305	0.118	0.072
0.20	2.227E-05	1.045E-05	0.47	0.0115	0.1335	0.122	0.073
0.25	2.450E-05	1.117E-05	0.46	0.0085	0.1345	0.126	0.072
0.30	2.516E-05	1.194E-05	0.47	0.0075	0.1365	0.129	0.072
0.50	4.088E-05	1.618E-05	0.40	-0.0005	0.1425	0.143	0.071
1.00	4.667E-05	2.067E-05	0.44	-0.0055	0.1365	0.142	0.066
5.00	8.061E-05	2.727E-05	0.34	-0.0255	0.1435	0.169	0.059

Complex **7**:

Scan rate; υ ($V.s^{-1}$)	I_{pa} (A)	I_{pc} (A)	I_{pc}/I_{pa}	E_{pc} (V)	E_{pa} (V)	ΔE (V)	E°' (V)
0.05	1.850E-05	5.200E-06	0.28	0.0455	0.1315	0.086	0.089
0.10	2.485E-05	8.030E-06	0.32	0.0515	0.1335	0.082	0.093
0.15	2.727E-05	1.121E-05	0.41	0.0525	0.1375	0.085	0.095
0.20	3.054E-05	1.339E-05	0.44	0.0515	0.1405	0.089	0.096
0.25	3.349E-05	1.535E-05	0.46	0.0505	0.1445	0.094	0.098
0.30	3.690E-05	1.762E-05	0.48	0.0495	0.1455	0.096	0.098
0.50	4.333E-05	2.182E-05	0.50	0.0455	0.1515	0.106	0.099
1.00	5.680E-05	3.400E-05	0.60	0.0405	0.1525	0.112	0.097
5.00	9.754E-05	5.328E-05	0.55	0.0235	0.1595	0.136	0.092

Complex **4**:

Scan rate; υ ($V.s^{-1}$)	I_{pa} (A)	I_{pc} (A)	I_{pc}/I_{pa}	E_{pc} (V)	E_{pa} (V)	ΔE (V)	E°' (V)
0.05	1.279E-05	4.643E-06	0.36	0.0295	0.1205	0.091	0.075
0.10	1.558E-05	7.791E-06	0.50	0.0305	0.1215	0.091	0.076
0.15	1.600E-05	9.400E-06	0.59	0.0295	0.1285	0.099	0.079
0.20	1.750E-05	1.171E-05	0.67	0.0275	0.1285	0.101	0.078
0.25	1.908E-05	1.329E-05	0.70	0.0265	0.1305	0.104	0.079
0.30	2.017E-05	1.400E-05	0.69	0.0245	0.1315	0.107	0.078
0.50	2.380E-05	1.860E-05	0.78	0.0195	0.1295	0.110	0.075
1.00	2.897E-05	2.538E-05	0.88	0.0175	0.1175	0.100	0.068
5.00	5.070E-05	3.256E-05	0.64	0.0055	0.1165	0.111	0.061

Complex **8**:

Scan rate; υ ($V.s^{-1}$)	I_{pa} (A)	I_{pc} (A)	I_{pc}/I_{pa}	E_{pc} (V)	E_{pa} (V)	ΔE (V)	E°' (V)
0.05	1.165E-05	4.000E-06	0.34	0.0535	0.1405	0.087	0.097
0.10	1.640E-05	6.512E-06	0.40	0.0535	0.1395	0.086	0.097
0.15	1.907E-05	8.372E-06	0.44	0.0535	0.1435	0.090	0.099
0.20	2.076E-05	1.091E-05	0.53	0.0525	0.1475	0.095	0.100
0.25	2.227E-05	1.227E-05	0.55	0.0525	0.1495	0.097	0.101
0.30	2.333E-05	1.288E-05	0.55	0.0495	0.1505	0.101	0.100
0.50	2.640E-05	1.720E-05	0.65	0.0455	0.1535	0.108	0.100
1.00	3.316E-05	2.368E-05	0.71	0.0425	0.1485	0.106	0.100
5.00	6.158E-05	3.895E-05	0.63	0.0315	0.1505	0.119	0.091

Complex **9**:

Scan rate; υ ($V.s^{-1}$)	I_{pa} (A)	I_{pc} (A)	I_{pc}/I_{pa}	E_{pc} (V)	E_{pa} (V)	ΔE (V)	E°' (V)
0.05	6.200E-06	1.267E-06	0.20	0.0615	0.1665	0.105	0.114
0.10	5.267E-05	1.867E-05	0.35	0.0655	0.1735	0.108	0.120
0.15	6.867E-05	3.200E-05	0.47	0.0735	0.1695	0.096	0.122
0.20	8.600E-05	3.600E-05	0.42	0.0755	0.1715	0.096	0.124
0.25	1.021E-05	4.357E-05	0.43	0.0725	0.1715	0.099	0.122
0.30	1.125E-05	5.167E-05	0.46	0.0735	0.1715	0.098	0.123
0.50	1.221E-05	6.047E-06	0.50	0.0735	0.1745	0.101	0.124
1.00	1.697E-05	1.197E-05	0.71	0.0695	0.1815	0.112	0.126
5.00	2.618E-05	1.618E-05	0.62	0.0655	0.1875	0.122	0.127

4. Optimized coordinates (DFT calculations) of **1**-**9**.

All of the following optimized coordinates are based on calculations of nickel in the singlet multiplicity (lowest energy) and lowest energy conformers (see manuscript for details).

Complex 1 (neutral):

Ni	0.04435400	1.07738900	0.60798000
Br	-0.15176000	0.73800400	-1.71691800
C	0.03181400	-0.79230300	1.00763500
C	0.69320400	-2.91506200	1.41050100
C	-0.66068500	-2.90377600	1.41505800
H	1.39070100	-3.71930200	1.56944200
H	-1.36929600	-3.69688200	1.58005900
C	0.31594900	3.25218100	0.70510600
C	-1.00634000	3.01746100	1.23187300
C	1.26618800	2.66229300	1.56666800
H	0.53700000	3.83755700	-0.17496100
C	-0.87826500	2.18718900	2.33774700
H	-1.92642800	3.37626300	0.79589000
C	0.53586200	1.90399100	2.51357400
H	2.33963000	2.70233700	1.46250800
H	-1.67562500	1.79673500	2.95283500
H	0.95393700	1.31224800	3.31546100
N	-1.04988800	-1.59437000	1.17011900
N	1.10147700	-1.61155800	1.16482100
C	-2.43434300	-1.15026900	0.98638100
H	-3.03222100	-1.50676500	1.82971000
H	-2.41285000	-0.06189600	1.01929900
C	-3.02845500	-1.62695400	-0.35158000
H	-2.34015500	-1.32919900	-1.14586700
H	-3.09241300	-2.71983300	-0.35633500
C	-4.39438600	-1.02460500	-0.59280500
C	-5.55906900	-1.67124700	-0.16778200
C	-4.50977100	0.21864300	-1.22605600
C	-6.81079600	-1.09211900	-0.36720200
H	-5.48736100	-2.64176500	0.31449400
C	-5.75973700	0.79892600	-1.42669700
H	-3.61206000	0.72324200	-1.56941400
C	-6.91387400	0.14613800	-0.99686500
H	-7.70439000	-1.61016300	-0.03662700
H	-5.83262200	1.75900600	-1.92560000
H	-7.88706500	0.59661000	-1.15686500
C	2.49007800	-1.18922300	0.96899800
H	2.51255400	-0.11202200	1.12979400
H	3.10832900	-1.66224200	1.73636600
C	3.01002700	-1.52264000	-0.44178900
H	3.00867700	-2.60830700	-0.58216300
H	2.31292400	-1.09533400	-1.16694100
C	4.40031200	-0.96920400	-0.65802900
C	5.53653700	-1.71692900	-0.33257500
C	4.57244200	0.32619800	-1.15948500

C	6.81364500	-1.18540600	-0.49874800
H	5.42162100	-2.72862500	0.04529600
C	5.84794200	0.86017200	-1.32644400
H	3.69875100	0.91053000	-1.43006300
C	6.97243500	0.10659500	-0.99493700
H	7.68365100	-1.78173900	-0.24653000
H	5.96351200	1.86295900	-1.72258900
H	7.96547800	0.52076900	-1.12839500

Complex 1 (cation, oxidized):

Ni	0.00002100	1.15972600	0.53976700
Br	0.00002100	0.89533100	-1.73062600
C	-0.00000500	-0.75634500	0.87130900
C	0.67717900	-2.86336300	1.20604100
C	-0.67724200	-2.86334000	1.20607900
H	1.37965000	-3.66700700	1.34410700
H	-1.37973300	-3.66696100	1.34417600
C	0.00008800	3.32269900	0.74435800
C	-1.15824400	2.81753400	1.40636600
C	1.15836500	2.81745700	1.40640000
H	0.00012100	3.99188900	-0.10285400
C	-0.72380500	1.92511700	2.40578600
H	-2.18260100	3.02721200	1.13653500
C	0.72383600	1.92506800	2.40580700
H	2.18274400	3.02706700	1.13659900
H	-1.34961600	1.35989000	3.07992500
H	1.34959000	1.35979700	3.07996200
N	-1.08128500	-1.55281000	0.99765000
N	1.08125500	-1.55283500	0.99767100
C	-2.48397900	-1.12512700	0.85734900
H	-3.04041900	-1.49863300	1.71967600
H	-2.49030700	-0.03670800	0.90459400
C	-3.12976800	-1.59799700	-0.45642700
H	-2.51371700	-1.25732100	-1.29212600
H	-3.14062200	-2.69153200	-0.48458700
C	-4.53750300	-1.05639600	-0.58386600
C	-5.61907800	-1.72757000	-0.00453600
C	-4.77446300	0.14539300	-1.25936400
C	-6.90817700	-1.20804900	-0.09431300
H	-5.45779700	-2.67176000	0.50699800
C	-6.06322900	0.66615400	-1.35168300
H	-3.94820700	0.66598800	-1.73409100
C	-7.13258000	-0.00859100	-0.76679000
H	-7.73785500	-1.74430700	0.35144000
H	-6.23415400	1.59109800	-1.89041800
H	-8.13649800	0.39192900	-0.84375700
C	2.48396000	-1.12518500	0.85738100
H	2.49031900	-0.03676900	0.90468000
H	3.04040000	-1.49875000	1.71968200

C	3.12971800	-1.59800500	-0.45642800
H	3.14055900	-2.69153800	-0.48463600
H	2.51365500	-1.25728400	-1.29210000
C	4.53745600	-1.05641200	-0.58387100
C	5.61903600	-1.72762400	-0.00459500
C	4.77441500	0.14540600	-1.25931700
C	6.90813900	-1.20811200	-0.09437400
H	5.45775600	-2.67183700	0.50689800
C	6.06318300	0.66615900	-1.35163800
H	3.94815400	0.66603200	-1.73400200
C	7.13254000	-0.00862400	-0.76679900
H	7.73782100	-1.74440000	0.35133600
H	6.23410700	1.59112700	-1.89033200
H	8.13646100	0.39188900	-0.84376700

Complex 1 (anion, reduced):

Ni	0.06804500	1.03414200	0.57615600
Br	-0.50109000	0.62408700	-1.91765700
C	-0.05587200	-0.85504900	1.16655400
C	0.50283000	-3.00912700	1.67031600
C	-0.84996500	-2.92982700	1.68713500
H	1.16089600	-3.84000800	1.86307600
H	-1.59421100	-3.67879900	1.90013800
C	1.83771500	3.00772400	0.78976300
C	0.45261300	3.28999900	0.66325500
C	2.05778900	2.42738300	2.05770900
H	2.59157600	3.21385700	0.04018600
C	-0.18695900	2.87952200	1.86973000
H	-0.02340500	3.78003300	-0.17428100
C	0.81118800	2.33312500	2.72006300
H	3.01186300	2.09231500	2.44773000
H	-1.22593700	3.04127900	2.12655800
H	0.64414800	1.92601400	3.70981900
N	-1.17100500	-1.61260600	1.38544500
N	0.96756000	-1.73805200	1.36190500
C	-2.52040000	-1.09514300	1.18294400
H	-3.15334500	-1.39911700	2.02382400
H	-2.42446400	-0.00842200	1.19354600
C	-3.12353100	-1.55506800	-0.15870000
H	-2.40092100	-1.30198100	-0.94033400
H	-3.25561600	-2.64312300	-0.14759000
C	-4.44209200	-0.87380500	-0.44120000
C	-5.65975300	-1.43698100	-0.04472600
C	-4.45702300	0.36817400	-1.09050900
C	-6.86627100	-0.78084200	-0.28458900
H	-5.66321200	-2.40401900	0.45107600
C	-5.66186900	1.02425400	-1.33010400
H	-3.51356100	0.80154600	-1.41216900
C	-6.86993200	0.45491500	-0.92784500
H	-7.80119600	-1.23565500	0.02755600
H	-5.65564100	1.98333300	-1.83732700
H	-7.80683200	0.96856800	-1.11778000
C	2.35741800	-1.38291300	1.08918400

H	2.47543000	-0.33580200	1.37150000
H	3.00681500	-1.99053700	1.72711500
C	2.70962700	-1.57326300	-0.39968500
H	2.61107100	-2.63189000	-0.66310500
H	1.97047200	-1.01815700	-0.98659300
C	4.10426900	-1.08795500	-0.71619900
C	5.17544800	-1.97628600	-0.85569400
C	4.35317300	0.28402000	-0.85626300
C	6.46244000	-1.51426400	-1.12904500
H	4.99674000	-3.04344800	-0.75806600
C	5.63728200	0.74782800	-1.12763700
H	3.53017200	0.98349700	-0.74912700
C	6.69723800	-0.14838800	-1.26559500
H	7.27871700	-2.22127600	-1.23913000
H	5.80864200	1.81358400	-1.23513100
H	7.69661600	0.21561300	-1.48047800

Complex 2 (neutral):

Br	0.00028700	0.83455400	2.09159700
Ni	0.00022000	1.88736400	-0.01590900
N	-1.07482000	-0.49568600	-1.36286000
C	-3.28649600	-1.17723100	-0.44627100
C	-2.99066800	-1.55557500	0.86883100
C	-2.47282500	-0.10171900	-1.13198300
C	-3.74755000	-2.53803400	1.49880600
C	-4.34856100	-1.79322000	-1.11144700
C	-4.80662700	-3.15108300	0.82819800
C	-5.10809300	-2.77643200	-0.47774300
C	-0.00002200	0.23177200	-0.96913500
C	-0.67653200	-1.66668700	-1.99388600
C	0.00025800	3.23864800	-1.64429500
C	-1.16675500	3.59129500	-0.88381200
C	-0.72302100	3.97668100	0.38166900
H	0.00017300	2.90551400	-2.67259300
H	-2.42467900	0.80334700	-0.52560800
H	-4.58913700	-1.49949300	-2.12880200
H	-2.92567800	0.15740400	-2.09321300
H	-5.93201100	-3.24561500	-1.00371600
H	-3.51384400	-2.82193400	2.51871900
H	-2.19111800	3.50363900	-1.21238200
H	-1.38254200	-2.39383200	-2.35475400
H	-2.17097500	-1.07404300	1.39357400
H	-1.34182300	4.23267300	1.22874300
H	-5.39533800	-3.91468300	1.32417500
N	1.07458200	-0.49588900	-1.36300300
C	3.28615300	-1.17777300	-0.44646300
C	2.99028400	-1.55589600	0.86869400
C	2.47268100	-0.10218000	-1.13227400
C	3.74698100	-2.53843400	1.49876700
C	4.34807200	-1.79406000	-1.11159500
C	4.80591400	-3.15178000	0.82820300
C	5.10742100	-2.77734900	-0.47779300
C	0.67599600	-1.66683900	-1.99393100
H	2.42474200	0.80295700	-0.52598700
H	4.58867900	-1.50050600	-2.12899300

H	2.92553800	0.15675800	-2.09355400
H	5.93122800	-3.24676500	-1.00373200
H	3.51324300	-2.82216700	2.51872000
H	1.38182000	-2.39413800	-2.35485600
H	2.17069800	-1.07413900	1.39339900
H	5.39448000	-3.91544200	1.32425500
C	1.16741500	3.59107200	-0.88393300
C	0.72388300	3.97654000	0.38159600
H	2.19172900	3.50322100	-1.21260700
H	1.34282100	4.23241100	1.22860600

Complex 2 (cation, oxidized):

Br	0.01685500	1.10708400	2.10307800
Ni	0.01536600	1.95515400	-0.01934500
N	-1.08743800	-0.54112800	-1.14771100
C	-3.36298400	-1.21395900	-0.37373700
C	-3.17864600	-1.65232400	0.94268000
C	-2.49322400	-0.11934200	-0.94405300
C	-3.99100100	-2.65188500	1.46666200
C	-4.37131300	-1.78639300	-1.15232600
C	-4.99615000	-3.22049200	0.68357900
C	-5.18691200	-2.78666100	-0.62508700
C	0.00023300	0.19182400	-0.83532600
C	-0.69629900	-1.75757800	-1.68789800
C	0.74867000	3.17808000	-1.62056400
C	-0.69859500	3.18229200	-1.62502100
C	-1.13498500	3.78662800	-0.42977200
H	1.37601500	2.80618900	-2.41648300
H	-2.45447700	0.73814500	-0.27089500
H	-4.52898700	-1.44587300	-2.17089100
H	-2.88988100	0.21735200	-1.90490600
H	-5.96981900	-3.22165700	-1.23483500
H	-3.84606800	-2.98373100	2.48797000
H	-1.32301500	2.81397700	-2.42489000
H	-1.41035200	-2.50461600	-1.98703500
H	-2.40225200	-1.20849300	1.55709500
H	-2.15960000	3.92421900	-0.11812800
H	-5.63044300	-3.99627800	1.09582000
N	1.07323500	-0.55522600	-1.16438000
C	3.34219200	-1.25217400	-0.39266000
C	3.15376600	-1.66460900	0.93154300
C	2.48771000	-0.15480800	-0.98095000
C	3.95268800	-2.66626400	1.47181900
C	4.34074300	-1.85278300	-1.16255500
C	4.94829300	-3.26299100	0.69747300
C	5.14286900	-2.85519900	-0.61894900
C	0.65783300	-1.76649600	-1.69810800
H	2.47013400	0.71848400	-0.32759600
H	4.50143200	-1.53270300	-2.18727100

H	2.88259300	0.15284300	-1.95219800
H	5.91826300	-3.31215300	-1.22220300
H	3.80470100	-2.97803700	2.49900400
H	1.35738700	-2.52305700	-2.00746100
H	2.38455800	-1.19941200	1.53920100
H	5.57213300	-4.04038200	1.12243600
C	1.18090100	3.77903800	-0.42244300
C	0.02137500	4.09940900	0.34410000
H	2.20426300	3.90987900	-0.10381600
H	0.01968000	4.52762700	1.33519000

Complex 2 (anion, reduced):

Br	-0.00087500	0.46621600	2.33381400
Ni	0.00549000	1.79620500	0.07233000
N	-1.07187400	-0.48436000	-1.59727600
C	-3.24375600	-1.12774500	-0.56860700
C	-2.87210700	-1.46924600	0.73853100
C	-2.45537200	-0.08763200	-1.33623500
C	-3.60789600	-2.41721900	1.44318100
C	-4.35651900	-1.74556000	-1.14435600
C	-4.71740300	-3.03342600	0.86188600
C	-5.09326700	-2.69462400	-0.43498600
C	0.00044200	0.21866700	-1.12616300
C	-0.68219900	-1.59840400	-2.32946100
C	0.02511700	3.89397300	-1.59610200
C	-1.13075100	3.90435000	-0.77937000
C	-0.70735300	3.90555900	0.57656000
H	0.03537000	3.85956800	-2.67917000
H	-2.37661500	0.84659700	-0.77327200
H	-4.65256500	-1.47896100	-2.15526100
H	-2.94965300	0.12948600	-2.28902900
H	-5.95594700	-3.16569500	-0.89530200
H	-3.31275800	-2.66806400	2.45643700
H	-2.15717600	3.91995600	-1.12445800
H	-1.38802200	-2.28974700	-2.75759100
H	-2.01418700	-0.98552500	1.20498600
H	-1.34700800	3.94181400	1.44756600
H	-5.28678300	-3.77072000	1.41886700
N	1.06825500	-0.48979800	-1.59938800
C	3.23702500	-1.14282300	-0.57010800
C	2.86347700	-1.47865100	0.73795400
C	2.45427100	-0.10053600	-1.34059200
C	3.59422100	-2.42847200	1.44536000
C	4.34653200	-1.76811700	-1.14403600
C	4.70052200	-3.05212500	0.86590900
C	5.07823400	-2.71901200	-0.43190400
C	0.67147400	-1.60187900	-2.33074400
H	2.38158900	0.83592400	-0.78049200
H	4.64406100	-1.50594200	-2.15566300
H	2.94909300	0.11059500	-2.29444100
H	5.93843800	-3.19595400	-0.89080600
H	3.29762100	-2.67487200	2.45927700
H	1.37290700	-2.29683100	-2.76025700

H	2.00799100	-0.98930500	1.20301600
H	5.26599100	-3.79080800	1.42503200
C	1.16514100	3.89751900	-0.75737300
C	0.71568000	3.90124100	0.59027000
H	2.19811000	3.90773600	-1.08254700
H	1.33870900	3.93352600	1.47335400

Complex 3 (neutral):

Ni	1.55512800	-0.62977000	-0.20158300
Br	0.80493900	-0.76267100	2.02462800
C	1.26535400	1.25569200	-0.28818500
C	1.56606500	3.49030000	-0.13120000
C	0.27771500	3.27782800	-0.48814200
H	2.10730300	4.40412300	0.04365900
H	-0.51984500	3.97276100	-0.68656500
C	2.26306700	-2.67627000	-0.55357800
C	1.06477600	-2.55257900	-1.34630400
C	3.24160600	-1.79238300	-1.05833300
H	2.40093300	-3.37633700	0.25684100
C	1.26211000	-1.51638000	-2.25051000
H	0.16054700	-3.12548800	-1.20681700
C	2.59757000	-0.98996200	-2.03125200
H	4.25526200	-1.68725000	-0.70291000
H	0.55453700	-1.14486400	-2.97702800
H	3.05379500	-0.19921100	-2.60975400
N	0.11117900	1.90385000	-0.58590100
N	2.15759900	2.24030700	-0.01806900
C	-1.16620400	1.23162600	-0.83972900
H	-1.62550900	1.67620300	-1.72696100
H	-0.92790400	0.19271900	-1.06346400
C	-2.11479700	1.30805600	0.37017300
H	-1.57415600	0.92876400	1.24053700
H	-2.37427400	2.35342200	0.56645000
C	-3.36898900	0.49616600	0.13706700
C	-4.50616200	1.06774500	-0.44238800
C	-3.39886300	-0.86212300	0.47438500
C	-5.64656900	0.30390800	-0.68238900
H	-4.50363500	2.12311900	-0.69903100
C	-4.53769500	-1.62746700	0.23565600
H	-2.52545100	-1.31226900	0.93569900
C	-5.66449000	-1.04735800	-0.34452200
H	-6.52165500	0.76501300	-1.12716500
H	-4.54717000	-2.67666300	0.50965300
H	-6.55221300	-1.64271900	-0.52641800
C	3.52460400	2.00779900	0.43153600
H	3.61558600	2.23394300	1.49559800
H	3.75406400	0.95644900	0.27369200
H	4.21730600	2.62862400	-0.13959800

Complex 3 (cation, oxidized):

Ni	1.55587100	-0.63897700	-0.24370800
Br	1.17169700	-0.81415700	2.00008600
C	1.17611500	1.26678400	-0.25813400

C	1.39714900	3.48955400	-0.08380600
C	0.10597700	3.22886800	-0.39795300
H	1.90770700	4.42231000	0.08356400
H	-0.72660300	3.89289800	-0.55333100
C	2.04961500	-2.68259000	-0.78349000
C	0.97384200	-2.25881600	-1.61636000
C	3.18775300	-1.86501900	-1.05984400
H	2.01793800	-3.49917000	-0.07804500
C	1.40712600	-1.12131000	-2.32704000
H	-0.01611700	-2.68950000	-1.63946400
C	2.79194300	-0.87880100	-1.98218500
H	4.15475000	-1.95015100	-0.58701300
H	0.82864700	-0.54741500	-3.03539400
H	3.41031900	-0.09437100	-2.39167700
N	-0.01437400	1.85090800	-0.50282400
N	2.04407300	2.26601000	0.00447800
C	-1.28750200	1.14334500	-0.72769600
H	-1.75940700	1.56824400	-1.61607700
H	-1.04056100	0.10490100	-0.94610600
C	-2.23246800	1.21669700	0.48391400
H	-1.70828400	0.82894500	1.36091900
H	-2.47954500	2.26240600	0.68939900
C	-3.49530800	0.42214700	0.22812700
C	-4.57992900	0.99885500	-0.44049500
C	-3.58633200	-0.91357700	0.63304600
C	-5.72907000	0.25688400	-0.70214300
H	-4.53497800	2.04020600	-0.74509100
C	-4.73535300	-1.65732100	0.37349700
H	-2.76197800	-1.36796000	1.17431200
C	-5.80817500	-1.07383100	-0.29686500
H	-6.56548900	0.71993600	-1.21260100
H	-4.79800000	-2.68732500	0.70528400
H	-6.70514800	-1.64932000	-0.49292100
C	3.45917200	2.09984300	0.33944600
H	3.75353400	2.88590900	1.03305900
H	3.59754600	1.13691800	0.82657400
H	4.07668000	2.16072300	-0.55826700

Complex 3 (anion, reduced):

Ni	-1.61316000	-0.49673300	0.12035300
Br	0.07178200	-1.65421600	-1.45085300
C	-1.08789700	1.41233300	-0.04259900
C	-1.16084000	3.65736000	-0.45069900
C	0.10025700	3.36124200	-0.05529500
H	-1.60712600	4.59649100	-0.73244700
H	0.96127600	3.99500500	0.07586400
C	-3.38477800	-2.09499000	0.28747000
C	-2.62302500	-1.89803500	1.47651700
C	-4.44802700	-1.15956400	0.29143900

H	-3.20946700	-2.86507100	-0.45104900
C	-3.21357500	-0.81550800	2.18992900
H	-1.81572100	-2.52952200	1.82463200
C	-4.34041800	-0.37562600	1.46075000
H	-5.20399200	-1.05849500	-0.47897300
H	-2.87814500	-0.42864400	3.14442500
H	-4.99511900	0.44265600	1.74096500
N	0.12723000	1.99631800	0.19131700
N	-1.86833000	2.46426600	-0.43629700
C	1.30985900	1.25483700	0.62299900
H	1.72793100	1.74276400	1.51047600
H	0.95848300	0.26078000	0.89865500
C	2.37167800	1.13986900	-0.48582600
H	1.90635500	0.60447300	-1.31821500
H	2.65807700	2.14082100	-0.82808600
C	3.59678100	0.39353900	-0.00847800
C	4.73960400	1.07287800	0.42697600
C	3.59419100	-1.00778800	0.02998100
C	5.85666200	0.37842400	0.88975100
H	4.75698400	2.15905000	0.39676400
C	4.70964300	-1.70150000	0.49275500
H	2.70922100	-1.53798500	-0.31443500
C	5.84396400	-1.01394400	0.92465700
H	6.73514400	0.92436700	1.21948800
H	4.69212000	-2.78628800	0.51256800
H	6.71133600	-1.55905200	1.28302300
C	-3.26567200	2.33145700	-0.82059000
H	-3.39666100	2.59460800	-1.87460700
H	-3.56449200	1.29563000	-0.65932900
H	-3.89282800	2.98049000	-0.20331000

Complex 4 (neutral):

Ni	-0.13182400	1.59185200	-0.13411100
Br	0.04772900	0.51697700	1.95626600
C	-0.53253300	-0.02111300	-1.08043900
C	-1.64451500	-1.73259600	-2.05451100
C	-0.32129900	-1.99680200	-2.15571100
H	-2.50413300	-2.29502400	-2.37449800
H	0.19660300	-2.83227700	-2.59412800
C	0.03996700	3.70047600	0.45184400
C	1.29249900	3.38687000	-0.19396300
C	-1.00151200	3.59913500	-0.49331900
H	-0.06558700	4.01575400	1.47916400
C	1.01074100	2.98468600	-1.49262100
H	2.26174700	3.40580200	0.28105900
C	-0.42977000	3.04282200	-1.66554300
H	-2.04557400	3.81350400	-0.32405200
H	1.71862100	2.65808100	-2.24000500
H	-0.95237500	2.82116500	-2.58524200
N	0.34695000	-0.93662400	-1.55814200
N	-1.75575300	-0.51662200	-1.39477000
C	1.79648400	-0.87273300	-1.35138700
H	2.29363700	-1.08877400	-2.30107200
H	2.02444200	0.15571800	-1.07476400

C	2.27276100	-1.83617900	-0.24905400
H	1.68477400	-1.63084600	0.64859500
H	2.07062300	-2.86826500	-0.55332100
C	3.74652700	-1.65737900	0.03797700
C	4.71508900	-2.38764600	-0.65802900
C	4.16793500	-0.72548000	0.99377500
C	6.07228100	-2.19286800	-0.40979000
H	4.40490100	-3.12382300	-1.39395400
C	5.52397300	-0.52958500	1.24395500
H	3.42369900	-0.16203400	1.54779800
C	6.48036900	-1.26132600	0.54217700
H	6.80949200	-2.77224900	-0.95481400
H	5.83344200	0.19093300	1.99299700
H	7.53577700	-1.11108800	0.74002200
C	-3.02737600	0.13911700	-1.05938400
H	-2.75273400	1.05935000	-0.54181000
H	-3.53510700	0.41183800	-1.98870100
C	-3.93270700	-0.72089400	-0.20393600
C	-5.18191500	-1.12238300	-0.68108400
C	-3.53448700	-1.10696400	1.08164900
C	-6.02781300	-1.89909100	0.11033800
H	-5.50062700	-0.82168400	-1.67464500
C	-4.37801700	-1.88454500	1.86843700
H	-2.56721900	-0.79447200	1.46416500
C	-5.62543500	-2.28242800	1.38619800
H	-6.99673800	-2.20198600	-0.27051300
H	-4.06244500	-2.17559300	2.86397400
H	-6.28050700	-2.88594200	2.00447700

Complex 4 (cation, oxidized):

Ni	-0.02899400	1.64556700	-0.15739900
Br	-0.10203200	0.89822000	2.00095200
C	-0.48286500	-0.09487900	-0.89379100
C	-1.63736300	-1.86855700	-1.62610500
C	-0.31994700	-2.16405700	-1.73041000
H	-2.51348300	-2.44868400	-1.85710000
H	0.17476700	-3.05237200	-2.08339900
C	0.52640000	3.73199500	0.09913800
C	1.47781000	3.12752700	-0.77231800
C	-0.75586200	3.68959100	-0.52789700
H	0.74148500	4.16809500	1.06300900
C	0.77562000	2.61999300	-1.88448100
H	2.53375000	3.01514900	-0.57641200
C	-0.61939800	2.97587000	-1.73300500
H	-1.67448400	4.07561600	-0.11183400
H	1.19853200	2.09080000	-2.72507500
H	-1.40315000	2.75163600	-2.44056000
N	0.38217800	-1.05729900	-1.27423700
N	-1.72068500	-0.58681300	-1.10357700
C	1.84709500	-1.00240900	-1.13272700
H	2.29053100	-1.30876900	-2.08256600
H	2.11281500	0.04085600	-0.96464200

C	2.37324900	-1.87361400	0.02107400
H	1.87169500	-1.57315200	0.94449200
H	2.11215300	-2.91942300	-0.16496000
C	3.87316800	-1.72613100	0.16079900
C	4.74427000	-2.53555100	-0.57519300
C	4.41265700	-0.75284600	1.00852300
C	6.12370300	-2.37443500	-0.46959300
H	4.34400100	-3.30886700	-1.22396800
C	5.79190200	-0.59002300	1.11600200
H	3.74930000	-0.13384800	1.60517200
C	6.65025200	-1.39942800	0.37491400
H	6.78667500	-3.01566000	-1.03874500
H	6.19660200	0.15886400	1.78709000
H	7.72349600	-1.27853200	0.46291600
C	-2.98852200	0.13365200	-0.83687100
H	-2.72586700	0.97920800	-0.20001700
H	-3.36283000	0.52363200	-1.78646600
C	-4.03334800	-0.73527700	-0.17880600
C	-5.18250000	-1.10476100	-0.88140400
C	-3.86769500	-1.16515000	1.14290800
C	-6.15561300	-1.89710100	-0.27404200
H	-5.32551700	-0.76646800	-1.90287500
C	-4.83772200	-1.95768800	1.74674200
H	-2.98194000	-0.87637100	1.69911000
C	-5.98274300	-2.32495400	1.03905300
H	-7.04633300	-2.17483300	-0.82490400
H	-4.70572700	-2.28359500	2.77169600
H	-6.73926300	-2.93866500	1.51354400

Complex 4 (anion, reduced):

Ni	-0.41059400	1.47795700	-0.18418700
Br	0.51495000	0.43459300	2.02995500
C	-0.49483600	-0.18248000	-1.26577800
C	-1.29641200	-2.04256100	-2.32065600
C	0.05557000	-2.11175600	-2.35232900
H	-2.04526700	-2.71931500	-2.69607000
H	0.70961500	-2.85513300	-2.77625200
C	-1.20978800	3.50897200	0.58904000
C	-0.16766000	3.68249000	-0.36726300
C	-2.42004300	3.29012700	-0.11791500
H	-1.10047500	3.58177800	1.66181900
C	-0.74216400	3.54020600	-1.66055300
H	0.85732100	3.95117100	-0.14804200
C	-2.12964400	3.30954700	-1.49978200
H	-3.39263100	3.12683200	0.32996200
H	-0.21416600	3.62620400	-2.60202800
H	-2.84098400	3.15057600	-2.30249400
N	0.52590000	-0.97349300	-1.71108600
N	-1.61331500	-0.86145800	-1.66409600
C	1.93200400	-0.67207900	-1.45823700
H	2.48561300	-0.72591900	-2.40221500

H	1.95289900	0.35718800	-1.09892700
C	2.55226900	-1.60754900	-0.40392800
H	1.93745100	-1.52660600	0.49712700
H	2.51466700	-2.64285200	-0.76147400
C	3.97940300	-1.22257700	-0.08944900
C	5.06083700	-1.82934400	-0.73689200
C	4.23916000	-0.21716700	0.85204500
C	6.37215800	-1.44727300	-0.45675300
H	4.87330000	-2.61560400	-1.46317300
C	5.54877200	0.16511900	1.13183800
H	3.40051800	0.24781700	1.36434600
C	6.61965800	-0.44603100	0.47955400
H	7.19824500	-1.93307700	-0.96663800
H	5.73250600	0.94230400	1.86636500
H	7.63876900	-0.14625300	0.70165100
C	-2.97066500	-0.42544800	-1.33588600
H	-2.88913200	0.63481900	-1.08123400
H	-3.59230100	-0.51432300	-2.23193800
C	-3.58616800	-1.20602500	-0.19103900
C	-4.76991800	-1.92481400	-0.36996300
C	-2.98045700	-1.19124900	1.07211500
C	-5.34800700	-2.62330000	0.69055700
H	-5.24774000	-1.93491700	-1.34582900
C	-3.55596700	-1.89179700	2.12750500
H	-2.06059400	-0.63378300	1.23199900
C	-4.73915800	-2.60868600	1.94249100
H	-6.26876500	-3.17699800	0.53661800
H	-3.07356500	-1.86939700	3.09850400
H	-5.18364400	-3.15134100	2.77067300

Complex 5 (neutral):

Br	0.96148000	-1.17166200	-1.79984400
N	-0.87983800	1.37812100	0.52134200
C	-2.84902600	-0.12294600	0.78051000
C	-2.82041400	-0.83538700	-0.42444800
C	-1.56689400	0.40837800	1.38477300
C	-3.99952700	-1.33890600	-0.96413700
C	-4.06933900	0.07171300	1.43020600
C	-5.21618500	-1.14195000	-0.30985100
C	-5.25006000	-0.43690800	0.88950400
C	0.38280400	1.22327300	0.04959600
C	-1.44540200	2.55418000	0.04880400
C	2.23416300	0.02557800	2.28813900
C	1.98977300	-1.36543400	2.15927900
C	2.83931000	-1.82957700	1.13425500
H	1.74378300	0.69639300	2.97927800
H	-0.84784200	-0.39539800	1.54876000
H	-4.09895900	0.61830400	2.36801800
H	-1.77211800	0.88166200	2.34902700
H	-6.19126100	-0.28129800	1.40481900
H	-3.96700600	-1.89219100	-1.89591500
H	1.23534000	-1.93809400	2.67666300
H	-2.44975200	2.85056300	0.29575100
H	-1.87513200	-0.99568800	-0.93472400
H	2.85609700	-2.83050400	0.72958100

H	-6.13206100	-1.53873600	-0.73338000
N	0.60698900	2.32355700	-0.70911900
C	-0.50945800	3.14702500	-0.72833100
H	-0.53785800	4.06749400	-1.28554300
C	3.37798600	0.37042200	1.46445600
C	3.74229800	-0.76860000	0.75744800
H	3.83514500	1.34716100	1.40554800
H	4.51903100	-0.84649300	0.01165400
C	1.80052900	2.52071000	-1.52476600
H	2.00628500	3.58799400	-1.61430400
H	2.63711200	2.02243800	-1.04027500
Ni	1.56418400	-0.25802300	0.28367800
H	1.65681600	2.07803900	-2.51161100

Complex 5 (cation, oxidized):

Br	1.13351200	-1.41543900	-1.61121300
N	-0.91487700	1.17845100	0.30997800
C	-2.94972700	-0.20839300	0.70538500
C	-3.13099100	-0.93069300	-0.47981100
C	-1.56157900	0.15888000	1.17124600
C	-4.41170700	-1.27130100	-0.90109100
C	-4.06423500	0.16132500	1.46165100
C	-5.52141500	-0.89753300	-0.14221500
C	-5.34750800	-0.18308300	1.03951000
C	0.36380600	1.14501300	-0.11456300
C	-1.54986000	2.30745200	-0.18499800
C	2.02682000	-0.03327700	2.36729400
C	2.29689900	-1.37309500	2.03297900
C	3.34589900	-1.37652900	1.06403500
H	1.28049000	0.31835100	3.06340200
H	-0.90122900	-0.70894800	1.15751300
H	-3.93247100	0.71149000	2.38807600
H	-1.59391400	0.54875000	2.19138200
H	-6.20638800	0.10342000	1.63462100
H	-4.54584900	-1.83397500	-1.81733700
H	1.76280000	-2.24238600	2.38669800
H	-2.58585100	2.51479300	0.01751200
H	-2.27016700	-1.22798700	-1.07003100
H	3.74792600	-2.25104200	0.57489700
H	-6.51795500	-1.16785500	-0.47073300
N	0.53863700	2.24060700	-0.88252400
C	-0.63779900	2.97430600	-0.93137600
H	-0.72114500	3.88726700	-1.49536700
C	2.95663000	0.80329200	1.63921700
C	3.79135300	-0.03657900	0.87354900
H	3.01657600	1.87887200	1.70955900
H	4.57915300	0.27894100	0.20607400
C	1.77238600	2.59839700	-1.58427900
H	1.52081200	3.20875800	-2.44982200
H	2.43876600	3.16282700	-0.92977500

Ni	1.69110500	-0.22479800	0.25479000
H	2.26442300	1.69093000	-1.92973500

Complex 5 (anion, reduced):

Br	-1.41813500	0.80423400	2.22391900
N	0.91229000	0.89092300	-1.57627700
C	2.63964900	-0.48945800	-0.44248000
C	2.22410000	-0.38586100	0.89149500
C	1.62232300	-0.38789600	-1.56277400
C	3.15446300	-0.49336100	1.92026800
C	3.99093300	-0.70663500	-0.71908100
C	4.50384900	-0.71108800	1.63740000
C	4.92214500	-0.81955600	0.31394800
C	-0.33588100	1.05613000	-1.04031100
C	1.45761400	2.09473100	-2.00051900
C	-1.36172800	-2.70386200	-1.83442800
C	-1.00043700	-3.06308800	-0.51783200
C	-1.97927300	-2.54414500	0.36541100
H	-0.80291800	-2.93695700	-2.73430400
H	0.85479800	-1.15952900	-1.45547900
H	4.31855800	-0.79287200	-1.75159500
H	2.11198000	-0.52486400	-2.53173300
H	5.96911800	-0.98942700	0.08323400
H	2.81531100	-0.40853700	2.94684500
H	-0.11895500	-3.62143200	-0.22614800
H	2.44583500	2.17099700	-2.42125700
H	1.17571100	-0.21836300	1.12535600
H	-2.00813100	-2.67472200	1.43816100
H	5.22391300	-0.79639900	2.44503700
N	-0.55285000	2.39737000	-1.16366700
C	0.52618800	3.04481100	-1.74607200
H	0.53937000	4.10713700	-1.92388600
C	-2.56494900	-1.96199100	-1.77983100
C	-2.96592900	-1.87501800	-0.41673000
H	-3.11010300	-1.56440300	-2.62697800
H	-3.89721100	-1.46459400	-0.04838500
C	-1.77434400	3.04522100	-0.70211000
H	-1.57235000	4.10461300	-0.53050800
H	-2.57047800	2.94154600	-1.44451100
Ni	-1.44765900	-0.30373600	-0.12269600
H	-2.07369200	2.57254900	0.23597400

Complex 6 (neutral):

Br	1.28734900	-1.65207400	-1.37786800
N	0.11552400	1.71673900	0.18340600
C	-2.00997200	0.65965700	0.91854600
C	-2.15735900	-0.33562300	-0.05661400
C	-0.62996600	1.14659100	1.30865800
C	-3.42209500	-0.79161300	-0.40454400
C	-3.14369400	1.18638300	1.54314400
C	-4.53313400	-0.24603000	0.23180300
C	-4.41611900	0.73682000	1.20553800
C	1.29363800	1.22350500	-0.27819400
C	-0.29852000	2.80556300	-0.57316600

C	3.12478800	0.35171600	2.13876600
C	2.68953600	-0.97228900	2.38779600
C	3.37153200	-1.79986600	1.46879300
H	2.79591300	1.24003600	2.65922100
H	-0.01887800	0.32112200	1.67779900
H	-3.03575200	1.95336900	2.30269900
H	-0.70408800	1.89568600	2.10136400
H	-5.30605900	1.13140800	1.67511500
H	-3.55943100	-1.56059200	-1.15182000
H	1.92119000	-1.27997800	3.08048000
H	-1.21510600	3.33331600	-0.37543300
H	-1.28068200	-0.75662700	-0.54089900
H	3.22012400	-2.86112600	1.33955400
N	1.61765400	2.02443100	-1.32129900
C	0.64705800	2.99539700	-1.52202900
H	0.71501400	3.72516300	-2.31031000
C	4.21854800	0.30485900	1.18402400
C	4.36903700	-1.01632300	0.78194600
H	4.79010500	1.15705400	0.84680900
H	5.05788300	-1.39347300	0.04122200
C	2.75306200	1.78867000	-2.20768600
H	3.14122900	2.74373600	-2.56341600
H	3.52242200	1.26157200	-1.64833500
H	2.44682500	1.16707300	-3.05041300
N	-5.88419500	-0.72570700	-0.13872200
O	-5.96134400	-1.59311400	-0.99695900
O	-6.84056500	-0.22276000	0.43636300
Ni	2.24237200	-0.32360400	0.31436200

Complex 6 (cation, oxidized):

Br	1.50441300	-1.70970000	-1.29895100
N	0.03460200	1.50738800	0.16351300
C	-2.10482600	0.44790100	0.87808000
C	-2.34587900	-0.47765600	-0.14471300
C	-0.68711300	0.81899900	1.25361300
C	-3.64634700	-0.82957000	-0.48047200
C	-3.18056400	1.01455800	1.56599500
C	-4.69698700	-0.24668500	0.21949600
C	-4.48936400	0.66888200	1.24043900
C	1.25764200	1.17626800	-0.30075700
C	-0.46364100	2.59488000	-0.53963900
C	2.97178700	0.29491600	2.24761600
C	2.91592300	-1.11219000	2.24971400
C	3.82991900	-1.58272800	1.26046000
H	2.39696700	0.96282900	2.87135900
H	-0.10476800	-0.07197400	1.49114600
H	-3.00312100	1.72568600	2.36546200
H	-0.68507300	1.46966600	2.13083300
H	-5.33852400	1.09265500	1.75834500
H	-3.86108000	-1.54368400	-1.26327700
H	2.25357400	-1.72747400	2.84031700
H	-1.43284200	3.01530400	-0.33603900

H	-1.51609400	-0.92676900	-0.67917900
H	3.98522000	-2.61536400	0.98613900
N	1.53087400	2.04501000	-1.29646600
C	0.47492900	2.93032400	-1.45552900
H	0.48505300	3.70710600	-2.20052200
C	3.98035300	0.70076900	1.29117800
C	4.52870100	-0.46261100	0.71844300
H	4.27678900	1.71946500	1.09105200
H	5.28975600	-0.50395900	-0.04640600
C	2.72231200	2.00844400	-2.14861900
H	2.64430900	2.80139400	-2.88919700
H	3.62077500	2.17108400	-1.55378300
H	2.78245900	1.04724200	-2.65844800
N	-6.09197600	-0.61937000	-0.13836100
O	-6.23712500	-1.43409000	-1.03540600
O	-6.99014600	-0.08249600	0.48936700
Ni	2.38052700	-0.30532900	0.27468500

Complex 6 (anion, reduced):

Br	1.13790000	-1.85882700	-1.41556300
N	0.08793100	1.83167000	0.00292100
C	-2.00263700	0.80854600	0.86895800
C	-2.15069100	-0.27145700	-0.01799900
C	-0.63189000	1.35545400	1.18242900
C	-3.41012100	-0.78570400	-0.28795000
C	-3.13995700	1.35072900	1.48021600
C	-4.53146900	-0.22239100	0.32933100
C	-4.40622400	0.84482800	1.21943900
C	1.28094100	1.29824700	-0.38780400
C	-0.34581300	2.82263500	-0.86852000
C	3.29028100	0.28829300	2.49150800
C	2.90349500	-1.07756900	2.39027200
C	3.69452000	-1.67851700	1.37443200
H	2.87467200	1.01638700	3.17626000
H	0.01715100	0.57580000	1.60160700
H	-3.03155900	2.18165800	2.17070900
H	-0.70780600	2.16661900	1.91367400
H	-5.29420400	1.25415200	1.67975200
H	-3.54107200	-1.61861500	-0.96439600
H	2.17107500	-1.58178500	3.00606700
H	-1.27508300	3.35026500	-0.73846700
H	-1.27459600	-0.71255900	-0.49109000
H	3.64427600	-2.70996800	1.05814100
N	1.58728600	1.99610300	-1.51464300
C	0.60242800	2.92114900	-1.83099400
H	0.65763500	3.55712900	-2.69851600
C	4.32131400	0.52297900	1.55239400
C	4.56909600	-0.68614300	0.85683900
H	4.81173700	1.47150800	1.37332100
H	5.30362200	-0.83633100	0.07678800
C	2.72593300	1.65760500	-2.35655600
H	3.13236100	2.56306900	-2.81371100

H	3.47713400	1.18554400	-1.72565800
H	2.42566100	0.94316900	-3.12591700
N	-5.85737800	-0.75258800	0.04202400
O	-5.95113400	-1.69418500	-0.75211400
O	-6.82817000	-0.23140400	0.60762400
Ni	2.20274300	-0.31288500	0.33978500

Complex 7 (neutral):

Br	0.68272200	-0.68965000	2.08144100
Ni	1.35277700	-1.84697800	0.14039700
N	1.58452000	0.66978600	-1.36646700
C	3.16043200	2.30242800	-0.34401600
C	2.53161800	2.67208000	0.85083500
C	2.96354700	0.91432400	-0.91097100
C	2.71957600	3.94794500	1.37227500
C	3.97934100	3.22472100	-0.99881900
C	3.53730200	4.86585300	0.71205800
C	4.16937200	4.50257300	-0.47344800
C	0.84908300	-0.41502200	-1.02184700
C	0.86357900	1.51603900	-2.19817400
C	1.86012000	-3.35830400	-1.26830200
C	3.13153900	-2.94241500	-0.70558400
C	3.09984600	-3.22835600	0.65266600
H	1.59610000	-3.29568600	-2.31450600
H	3.16423700	0.14810400	-0.16178700
H	4.47749400	2.94208500	-1.92133900
H	3.64105300	0.75136800	-1.75371000
H	4.81004200	5.20914400	-0.98894000
H	2.23208600	4.22482700	2.30017200
H	3.93419200	-2.46945400	-1.25153600
H	1.26642800	2.44484000	-2.56209100
H	1.90299700	1.95371000	1.36787000
H	3.86171600	-2.99504900	1.38112600
N	-0.34192200	-0.23870200	-1.64989500
C	-2.72147900	-0.52676200	-0.98430700
C	-2.70874000	0.02960800	0.30145400
C	-1.47151100	-1.16691100	-1.55129900
C	-3.86016800	0.59926800	0.82862200
C	-3.90226700	-0.50833400	-1.73154100
C	-5.02074700	0.60515000	0.06040200
C	-5.06348900	0.05685100	-1.21452100
C	-0.34951300	0.94580800	-2.37678300
H	-1.12961200	-1.98139000	-0.91015400
H	-3.91996200	-0.94177100	-2.72582000
H	-1.67695100	-1.57962200	-2.54261500
H	-5.98704800	0.08182600	-1.77540700
H	-3.87449600	1.03005400	1.81998900
H	-1.21042800	1.27961800	-2.92932700
H	-1.79760900	0.00674500	0.89216300
C	1.11167000	-4.01356700	-0.25599800
C	1.82126900	-3.83217600	0.94778400
H	0.14511600	-4.48032300	-0.36851600
H	1.49466800	-4.14140900	1.92942400
N	-6.25050000	1.21370500	0.61698200
O	-7.25478100	1.20159600	-0.08267600

O	-6.18688400	1.69202600	1.74049300
H	3.68331900	5.85820300	1.12365100

Complex 7 (cation, oxidized):

Br	0.81200300	-0.98624200	2.10790100
Ni	1.48713200	-1.87599600	0.11365100
N	1.53029800	0.76458300	-1.21052000
C	3.14287300	2.44002600	-0.30659400
C	2.59070000	2.83051300	0.91892400
C	2.93631300	1.03743900	-0.82585900
C	2.79171100	4.12093500	1.39634000
C	3.90077500	3.35491600	-1.04090600
C	3.54862500	5.03103000	0.65752600
C	4.10433100	4.64738100	-0.55948800
C	0.83942800	-0.35309800	-0.91047100
C	0.73049700	1.63590000	-1.93563900
C	1.60862100	-3.40550300	-1.38445600
C	2.89224700	-2.74991500	-1.24825200
C	3.37457800	-3.00443700	0.05030900
H	1.00474600	-3.41845100	-2.27926200
H	3.18938800	0.29744100	-0.06555100
H	4.34231100	3.05786000	-1.98700300
H	3.56700200	0.85960600	-1.70008000
H	4.69768600	5.34947000	-1.13298400
H	2.36513300	4.41635400	2.34757100
H	3.39686100	-2.19533700	-2.02487800
H	1.08420400	2.59887500	-2.26003000
H	2.00664700	2.12367300	1.49930900
H	4.29797200	-2.63905400	0.47435800
N	-0.39486700	-0.18901800	-1.43263900
C	-2.79426800	-0.53037000	-0.84583900
C	-2.86874400	0.03089900	0.43480100
C	-1.50575400	-1.15602500	-1.33331100
C	-4.05694100	0.58663300	0.88977800
C	-3.92484100	-0.53213700	-1.66629300
C	-5.16529700	0.57163300	0.05016100
C	-5.12318200	0.01947000	-1.22149100
C	-0.47604500	1.03876000	-2.07579200
H	-1.17262400	-1.93463200	-0.64593000
H	-3.87865300	-0.97031400	-2.65734300
H	-1.65492000	-1.61158000	-2.31489300
H	-6.01193400	0.02890500	-1.83699400
H	-4.14275300	1.02274500	1.87532400
H	-1.38025000	1.37891200	-2.54961700
H	-1.99729100	0.03018000	1.07989900
C	1.31998500	-4.05197500	-0.16726800
C	2.37811100	-3.75440500	0.74263500
H	0.42784200	-4.61444200	0.06466000
H	2.42713700	-4.06551800	1.77534900
N	-6.43982000	1.16705200	0.53243600
O	-7.39140300	1.14021500	-0.23118500
O	-6.44203800	1.64137100	1.65715800
H	3.70761400	6.03463800	1.03374600

Complex 7 (anion, reduced):

Br	0.52127400	-0.48856100	2.24504400
Ni	1.45982800	-1.71570200	0.17563000
N	1.51292800	0.74025000	-1.62937400
C	3.05568500	2.34934900	-0.52195200
C	2.45948100	2.50168300	0.73664100
C	2.90122400	1.05036600	-1.28549100
C	2.61807000	3.69201100	1.43971900
C	3.80670800	3.40039100	-1.05273100
C	3.36949500	4.73925900	0.90421500
C	3.96632800	4.59177700	-0.34471100
C	0.85573000	-0.35063100	-1.14432000
C	0.69828300	1.51362000	-2.44733800
C	3.31760000	-3.03872100	-1.00211600
C	3.63185700	-2.82618400	0.36345200
C	2.60804800	-3.42320400	1.14644900
H	3.89452100	-2.68889500	-1.84900700
H	3.24304700	0.19977500	-0.69088200
H	4.27545400	3.28559100	-2.02610200
H	3.49520600	1.08204400	-2.20451100
H	4.55353100	5.39959700	-0.76919200
H	2.15424700	3.79583500	2.41458900
H	4.50515000	-2.31557900	0.74707200
H	1.03189300	2.43193100	-2.89969500
H	1.87733200	1.68835100	1.16692600
H	2.56044000	-3.44028300	2.22532500
N	-0.38851000	-0.23872700	-1.69183500
C	-2.72133000	-0.64630200	-0.93831300
C	-2.75248700	-0.00116400	0.30895400
C	-1.43470900	-1.23452800	-1.46148200
C	-3.94016100	0.52652700	0.79365800
C	-3.90487900	-0.75818000	-1.67885900
C	-5.10589700	0.40926400	0.03121600
C	-5.10078400	-0.23557400	-1.20495100
C	-0.50415400	0.89314600	-2.48940900
H	-0.99318300	-1.93420200	-0.74083100
H	-3.88910100	-1.26284800	-2.63992700
H	-1.62257800	-1.77916600	-2.39255600
H	-6.02196700	-0.31065600	-1.76510800
H	-3.98341700	1.02063300	1.75413200
H	-1.41863500	1.16480900	-2.98827000
H	-1.84261400	0.06536900	0.90333000
C	2.10171200	-3.75896000	-1.06903500
C	1.66146500	-4.00499300	0.26097800
H	1.59713600	-4.07373400	-1.97338800
H	0.78587700	-4.57008500	0.55044900
N	-6.35712100	0.96928100	0.53235000
O	-7.37013800	0.84558300	-0.16569000
O	-6.34315100	1.54035300	1.62553600
H	3.48942000	5.66394900	1.45926500

Complex 8 (neutral):

Ni	-0.80074100	1.75483700	-0.14361200
Br	-0.47723200	0.21551600	-1.89953900

C	-0.24996200	0.51457500	1.20559800
C	1.01117400	-0.66678500	2.66865200
C	-0.24359500	-1.17068200	2.71099800
H	1.90381700	-0.95015900	3.19855200
H	-0.65717900	-1.97505200	3.29444000
C	-1.30717100	3.56664800	-1.26010900
C	-2.53632700	3.16308300	-0.62178700
C	-0.36931600	3.92704900	-0.26730900
H	-1.15699400	3.63743800	-2.32705800
C	-2.31578700	3.15470300	0.74931900
H	-3.43770900	2.86189800	-1.13364600
C	-0.94102700	3.56721700	0.97637500
H	0.62404600	4.31454000	-0.43390400
H	-3.02030800	2.87693900	1.51927800
H	-0.48681400	3.69531100	1.94867100
N	-1.00409900	-0.43365000	1.81342900
N	0.98974400	0.36664400	1.74074000
C	-2.40345400	-0.71447100	1.47532000
H	-2.97374000	-0.80384200	2.40391600
H	-2.76924700	0.15705800	0.93438100
C	-2.55598400	-1.97906400	0.61100600
H	-1.89925300	-1.87171700	-0.25544300
H	-2.22158000	-2.85346600	1.17835200
C	-3.98772000	-2.16698100	0.16142500
C	-4.88995100	-2.92904800	0.91009900
C	-4.44144200	-1.54952100	-1.01012400
C	-6.21499700	-3.07086100	0.50260000
H	-4.55076500	-3.42559900	1.81450400
C	-5.76524200	-1.68963900	-1.41908700
H	-3.74506400	-0.96802500	-1.60600100
C	-6.65648400	-2.44940600	-0.66320500
H	-6.89970500	-3.67110000	1.09162100
H	-6.09887000	-1.21136800	-2.33333700
H	-7.68592200	-2.56189500	-0.98427200
C	2.14945800	1.18352900	1.37311300
H	1.78008800	1.91171400	0.64888800
H	2.49195800	1.72820900	2.25687100
C	3.28741900	0.37368800	0.78690400
C	4.54264100	0.38048900	1.40132100
C	3.09697900	-0.36713600	-0.38689200
C	5.60349500	-0.34006600	0.86238200
H	4.69812600	0.95660200	2.30725900
C	4.14674100	-1.09327800	-0.93393500
H	2.12795000	-0.36824100	-0.87719900
C	5.38495400	-1.06901500	-0.29890000
H	6.58199900	-0.34797800	1.32138900
H	4.02362500	-1.66891200	-1.84061400
N	6.50711400	-1.84289800	-0.87746900
O	6.28951300	-2.47724200	-1.89979800
O	7.58294800	-1.80046900	-0.29534300

Complex 8 (cation, oxidized):

Ni	0.92803600	1.81232300	0.05667400
Br	0.49769100	0.70139900	2.00700400
C	0.25969600	0.35638300	-1.04818400

C	-1.09098000	-0.99610700	-2.22025000
C	0.15745400	-1.51716500	-2.26992300
H	-2.01808400	-1.34272100	-2.64227700
H	0.52841900	-2.40439400	-2.75329500
C	1.74274800	3.69004000	0.78103900
C	2.72603800	3.07703500	-0.05151700
C	0.59495100	3.98500100	-0.01345900
H	1.85697300	3.91499400	1.83079600
C	2.15563400	2.89903400	-1.32652800
H	3.70335600	2.74425500	0.26496900
C	0.82367300	3.46584500	-1.30259600
H	-0.31005800	4.45884600	0.33636900
H	2.62965000	2.45057600	-2.18659800
H	0.14785500	3.50944900	-2.14332700
N	0.98067800	-0.67056600	-1.54073600
N	-1.01212000	0.16041500	-1.45711700
C	2.40585300	-0.92843000	-1.26638800
H	2.91233200	-1.08526400	-2.22116600
H	2.81174900	-0.02187400	-0.81888100
C	2.62948500	-2.12473500	-0.32536400
H	2.06038500	-1.96031600	0.59298500
H	2.23850900	-3.03375500	-0.79191100
C	4.10129700	-2.28978000	-0.01217900
C	4.93952600	-3.00656900	-0.87219400
C	4.65298800	-1.70078400	1.13033300
C	6.29976400	-3.12900000	-0.59941000
H	4.52571500	-3.48794000	-1.75327500
C	6.01310400	-1.82333800	1.40588800
H	4.01092900	-1.16125500	1.82000000
C	6.83971300	-2.53552500	0.53973300
H	6.93524500	-3.69584700	-1.26978400
H	6.42463400	-1.37400100	2.30236200
H	7.89644800	-2.63729500	0.75677200
C	-2.15669900	1.04348600	-1.15512500
H	-1.80927500	1.74629500	-0.39674400
H	-2.40308300	1.60989300	-2.05614900
C	-3.37138900	0.28791000	-0.66322700
C	-4.56203500	0.32916800	-1.39262800
C	-3.31785600	-0.43437000	0.53522800
C	-5.69397100	-0.34211200	-0.93832600
H	-4.61515100	0.89169600	-2.31840800
C	-4.43825000	-1.11162800	0.99752500
H	-2.39956100	-0.46466200	1.11093600
C	-5.60900500	-1.05323500	0.24941600
H	-6.62740600	-0.32343400	-1.48345500
H	-4.42474400	-1.67438700	1.92057300
N	-6.81185200	-1.77737400	0.74022100
O	-6.70117600	-2.39363600	1.78792700
O	-7.82212600	-1.70473000	0.05954200

Complex 8 (anion, reduced):

Ni	0.72876700	1.70982600	0.23933100
Br	0.56336200	-0.21563700	1.97174200
C	0.24451200	0.59604000	-1.33925900
C	-0.98931600	-0.47409000	-2.93352200

C	0.26943800	-0.97091600	-2.99219600
H	-1.86988600	-0.71758700	-3.50313300
H	0.69534700	-1.72502800	-3.63247700
C	1.47495900	3.40311000	1.54441900
C	2.48948400	3.32931400	0.55152500
C	0.29233000	3.89167500	0.92723400
H	1.58540000	3.14408100	2.58713500
C	1.93342600	3.77054500	-0.67486800
H	3.51060200	3.01042100	0.71192800
C	0.57965700	4.11384600	-0.44772400
H	-0.64528800	4.09684400	1.42605700
H	2.44749300	3.81214100	-1.62665200
H	-0.11452700	4.48935200	-1.18895100
N	1.00597100	-0.30433100	-2.02188600
N	-0.98337900	0.48038800	-1.92422900
C	2.38975900	-0.59803400	-1.65569800
H	3.00084300	-0.63164400	-2.56381000
H	2.72028200	0.24469300	-1.04768400
C	2.51314200	-1.90849700	-0.85523800
H	1.80698600	-1.84639000	-0.02178400
H	2.22559100	-2.75465400	-1.48939500
C	3.91425500	-2.10729200	-0.32559800
C	4.87667200	-2.82311600	-1.04532600
C	4.27843400	-1.54315100	0.90432200
C	6.17352500	-2.97316800	-0.55609000
H	4.60498900	-3.27477400	-1.99552200
C	5.57372400	-1.69216700	1.39359600
H	3.52926800	-0.99976900	1.47340100
C	6.52615700	-2.40548900	0.66616200
H	6.90540400	-3.53595000	-1.12682900
H	5.83743600	-1.25293000	2.34986200
H	7.53392800	-2.52181700	1.05126200
C	-2.13736600	1.25864900	-1.48079800
H	-1.72911900	1.96673700	-0.74888400
H	-2.53399900	1.82920900	-2.32617900
C	-3.22885400	0.41734000	-0.86277800
C	-4.52198600	0.42867800	-1.39880800
C	-2.96533100	-0.36036500	0.27674100
C	-5.54250900	-0.32045700	-0.82805300
H	-4.73308600	1.03394400	-2.27502100
C	-3.97583900	-1.11384100	0.85674500
H	-1.96933300	-0.37001200	0.71608300
C	-5.25577300	-1.09095900	0.29759300
H	-6.54523800	-0.32572200	-1.23109700
H	-3.79041500	-1.71393400	1.73653800
N	-6.32271600	-1.88806600	0.90015900
O	-6.05234400	-2.56781600	1.89155800
O	-7.44390100	-1.84055100	0.38348300

Complex 9 (neutral):

Br	-0.00016900	1.02978400	-2.05546600
Ni	-0.00012900	2.56572200	-0.26784800
N	1.07404300	0.57232700	1.61070200
C	3.27708900	-0.27953600	0.82693300

C	2.94354100	-0.92930600	-0.36870100
C	2.46859600	0.90932100	1.30067700
C	3.69691900	-2.00788900	-0.81319100
C	4.37659000	-0.72178200	1.56756900
C	4.78466300	-2.42715000	-0.05316200
C	5.14118900	-1.79967600	1.13280700
C	-0.00001700	1.18766600	1.05503800
C	0.67605200	-0.41696700	2.50165300
C	-0.00015200	4.27319800	0.97857900
C	1.16737100	4.42564300	0.15456800
C	0.72362700	4.48416800	-1.16695400
H	-0.00012400	4.20796900	2.05753300
H	2.42135200	1.67876700	0.52871200
H	4.64521100	-0.21874200	2.49033500
H	2.92947500	1.34845000	2.18951200
H	5.99596900	-2.15741300	1.68924300
H	3.46091700	-2.52106300	-1.73492800
H	2.19166300	4.42721300	0.49517100
H	1.37975000	-1.03452200	3.03197700
H	2.09793800	-0.58113700	-0.95425300
H	1.34201200	4.52361100	-2.05119700
N	-1.07399100	0.57226400	1.61079300
C	-3.27699600	-0.27972200	0.82707300
C	-2.94343300	-0.92938700	-0.36861300
C	-2.46858200	0.90917000	1.30085700
C	-3.69673700	-2.00800200	-0.81315100
C	-4.37643700	-0.72210500	1.56771600
C	-4.78442400	-2.42740400	-0.05311600
C	-5.14096000	-1.80003300	1.13290600
C	-0.67587100	-0.41697800	2.50174300
H	-2.42142300	1.67865100	0.52891900
H	-4.64506900	-0.21914600	2.49052200
H	-2.92945700	1.34823100	2.18972800
H	-5.99569100	-2.15787700	1.68934700
H	-3.46072300	-2.52109400	-1.73493100
H	-1.37949000	-1.03455100	3.03215200
H	-2.09787600	-0.58111000	-0.95416800
C	-1.16771800	4.42556700	0.15462200
C	-0.72403500	4.48411400	-1.16692100
H	-2.19199700	4.42707000	0.49526900
H	-1.34246300	4.52351400	-2.05113600
N	5.59144900	-3.57760500	-0.52243000
N	-5.59113200	-3.57789400	-0.52243500
O	-6.54256400	-3.91954400	0.16713000
O	-5.25543100	-4.11453500	-1.56821600
O	5.25573200	-4.11436000	-1.56815000
O	6.54292600	-3.91913300	0.16713700

Complex 9 (cation, oxidized):

Br	-0.00073000	1.45104500	2.13210900
Ni	0.00016400	2.69159200	0.21259800
N	-1.07955200	0.45185300	-1.39446300
C	-3.32940800	-0.37687000	-0.71156300
C	-3.08317300	-1.02819500	0.50342400
C	-2.48866500	0.81003200	-1.12531800

C	-3.86334400	-2.10920000	0.89148100
C	-4.37088900	-0.81596600	-1.53256100
C	-4.89047300	-2.52569700	0.05184500
C	-5.16232200	-1.89709600	-1.15421400
C	0.00007000	1.11566000	-0.93105100
C	-0.67648900	-0.63083400	-2.16441200
C	0.00125100	4.71754500	0.99142700
C	1.15900900	4.56079900	0.17226800
C	0.72347600	4.20822200	-1.11955100
H	0.00205400	4.94194900	2.04751800
H	-2.46834900	1.56010500	-0.33393000
H	-4.57574500	-0.31164900	-2.47064900
H	-2.90281400	1.27279200	-2.02394200
H	-5.97519700	-2.25475700	-1.77083500
H	-3.69744900	-2.62769300	1.82559300
H	2.18321100	4.63395700	0.50651400
H	-1.38078900	-1.30574200	-2.61861600
H	-2.28242400	-0.68784400	1.15062000
H	1.34798300	4.00684400	-1.97680000
N	1.07968600	0.45181500	-1.39442900
C	3.32952300	-0.37691800	-0.71145200
C	3.08327100	-1.02821100	0.50355000
C	2.48879200	0.80997600	-1.12525100
C	3.86343500	-2.10920700	0.89164400
C	4.37100900	-0.81603900	-1.53242900
C	4.89056900	-2.52572600	0.05202600
C	5.16243500	-1.89716100	-1.15404700
C	0.67661600	-0.63080400	-2.16447000
H	2.46846000	1.56006900	-0.33387900
H	4.57587700	-0.31174700	-2.47052700
H	2.90296900	1.27272400	-2.02386800
H	5.97531600	-2.25484300	-1.77064900
H	3.69752900	-2.62767800	1.82576700
H	1.38090800	-1.30569300	-2.61871500
H	2.28251400	-0.68784900	1.15073300
C	-1.15780900	4.56141300	0.17390900
C	-0.72437000	4.20868700	-1.11852900
H	-2.18147900	4.63509200	0.50967200
H	-1.35022700	4.00765600	-1.97487400
N	-5.72887600	-3.68407300	0.46269600
N	5.72896400	-3.68409000	0.46291300
O	6.62194000	-4.02181500	-0.29690600
O	5.46124100	-4.21325900	1.52947600
O	-5.46112500	-4.21332800	1.52920800
O	-6.62180900	-4.02182800	-0.29715900

Complex 9 (anion, reduced):

Br	0.25026000	1.85824100	2.23801700
Ni	0.21991700	2.67571800	0.03558000
N	-1.11456900	0.22582400	-0.86265700
C	-3.47929100	-0.33680100	-0.27510600
C	-3.51632500	-1.11314800	0.89768400
C	-2.44748500	0.74028800	-0.45134000
C	-4.46198300	-2.10958600	1.06611300
C	-4.42987800	-0.59415800	-1.27659600

C	-5.40312700	-2.35086400	0.05032400
C	-5.38572500	-1.58590100	-1.12664900
C	0.03056700	0.93026600	-0.70445000
C	-0.85420700	-1.01473200	-1.42567600
C	0.46932100	3.83277500	-1.74058500
C	-0.84920100	4.18964100	-1.25823800
C	-0.69047200	4.78663900	-0.01274200
H	0.67754100	3.37652800	-2.69798500
H	-2.27542600	1.28432600	0.47847300
H	-4.41970900	0.00008900	-2.18576200
H	-2.77327600	1.45820700	-1.20820700
H	-6.12651900	-1.79033600	-1.88639200
H	-4.50577500	-2.71062100	1.96318700
H	-1.78038800	3.98397500	-1.76518500
H	-1.63198600	-1.73544200	-1.60393400
H	-2.79160800	-0.92303300	1.68287900
H	-1.47723500	5.10833800	0.65317600
N	1.01163600	0.12194800	-1.17159600
C	3.35813300	-0.62595800	-0.77166700
C	3.39838200	-1.04889600	0.56943900
C	2.44302800	0.49019400	-1.19713600
C	4.24634100	-2.06790900	0.96697400
C	4.19605800	-1.25844500	-1.70187600
C	5.07856200	-2.68701600	0.01964100
C	5.05349300	-2.27967800	-1.32152000
C	0.48492000	-1.08090800	-1.61969400
H	2.52623800	1.35262700	-0.53400300
H	4.17942800	-0.93831900	-2.73980000
H	2.69549700	0.81772800	-2.21017800
H	5.70833300	-2.77313700	-2.02535100
H	4.29327900	-2.40277400	1.99342300
H	1.10718100	-1.87489100	-1.99317400
H	2.75514800	-0.56726100	1.29924400
C	1.43400000	4.33407300	-0.82693700
C	0.72002800	4.82185000	0.28491500
H	2.50672400	4.25992900	-0.91994300
H	1.15180100	5.20156100	1.19906400
N	-6.38892300	-3.37575400	0.21734300
N	5.96656900	-3.73949700	0.42583700
O	6.69372000	-4.26638100	-0.44404800
O	5.97245600	-4.07783800	1.62788800
O	-6.38323100	-4.03675900	1.27942800
O	-7.21167400	-3.56203000	-0.70803100

Chapter 6
Base-free glucose dehydration catalysed by NHC-stabilised heterohalo cyclopentadienyl Cr(III) complexes

F. P. Malan,[a] E. Singleton,[a] P. H. van Rooyen,[a] J. Conradie,[b] and M. Landman[a]

[a] *Department of Chemistry, University of Pretoria, 02 Lynnwood Road, Hatfield, Pretoria, 0002, South Africa.* [b] *Department of Chemistry, University of the Free State, Bloemfontein 9300, South Africa.*

Supporting Information

1. Crystal data and structure refinement for **1-7** (**Tables S1**,**S2**)
2. Selected bond lengths and angles for **1-7** (**Table S3**)
3. Schematic representation of the oxidation and reduction processes (**Figure S1**)
4. Glucose dehydration using **1-6** (**Table S4**)
5. ^{1}H-NMR spectrum of glucose dehydration reaction mixture

1. Crystal data and structure refinement for **1-7** (**Tables S1**,**S2**)

Table S1

Complex	**1**	**2**	**3**	**4**
Emp. formula	$C_{16}H_{17}N_2Cl_{1.82}Br_{0.18}Cr$	$C_{22}H_{21}N_2Cl_{1.36}Br_{0.64}Cr$	$C_{16}H_{17}N_2ClBrCr$	$C_{24}H_{25}N_2Cl_{1.35}Br_{0.65}Cr$
Form. weight (g.mol^{-1})	368.11	464.71	404.67	493.15
Crystal system	monoclinic	monoclinic	orthorhombic	orthorhombic
Space group	*P2$_1$/c*	*P2$_1$/c*	*Pbca*	*P2$_1$2$_1$2$_1$*
Crystal descr.	blue blade	blue blade	blue needle	blue block
a (Å)	22.494(6)	11.578(3)	7.8759(5)	9.9270(1)
b (Å)	6.2985(2)	20.917(5)	16.9413(11)	14.6703(1)
c (Å)	22.856(6)	16.763(4)	25.1308(16)	15.1733(2)
α (°)	90	90	90	90
β (°)	95.878(6)	91.965(5)	90	90
γ (°)	90	90	90	90
Volume (Å^3)	3221.1(2)	4057.2(2)	3353.2(4)	2209.7(4)

Z	8	8	8	4
Abs. coeff. ($m.mm^{-1}$)	1.447	2.010	3.219	1.865
F(000)	1506.0	1892.0	1624.0	1011.0
Independent refl.	4518	7419	5221	4546
Completeness (%)	98.4	100.0	99.4	100.0
Data/Restr/Para	4518/0/205	7419/0/491	5221/0/200	4546/0/264
Goodness of fit on F^2	1.121	0.990	0.982	1.055
Final R_1 indexes	0.1568	0.0722	0.0695	0.0211
wR_2 indices (all data)	0.3369	0.1436	0.1954	0.0481
Largest diffr. peak and hole ($e.Å^{-3}$)	1.07/-0.90	0.57/-0.42	1.41/-1.23	0.25/-0.28

Table S2

Complex	**5**	**6**	**7**
Emp. formula	$C_{23}H_{23}N_2Cl_{1.24}Br_{0.76}Cr$	$C_{18}H_{22}N_4Cl_{5.0}Br_{0.8}Cr_2$	$C_{23}H_{23}N_2Cl_2Cr$
Form. weight ($g.mol^{-1}$)	484.23	493.15	450.33
Crystal system	orthorhombic	monoclinic	monoclinic
Space group	$P2_12_12_1$	$P2_1$	$P2_1/c$
Crystal descr.	blue block	blue block	blue block
a (Å)	9.920(4)	7.7436(1)	9.3840(6)
b (Å)	14.406(6)	7.0456(9)	14.9768(1)
c (Å)	14.898(6)	11.7412(2)	14.9659(1)
α (°)	90	90	90
β (°)	90	92.740(4)	92.549(2)
γ (°)	90	90	90
Volume ($Å^3$)	2129.0(2)	639.85(2)	2101.3(2)
Z	4	1	4
Abs. coeff. ($m.mm^{-1}$)	2.135	2.596	0.810
F(000)	987.0	322.0	932.0
Independent refl.	4388	2831	4752
Completeness (%)	99.8	99.9	99.6
Data/Restr/Para	4388/0/255	2831/1/141	4752/0/253
Goodness of fit on F^2	1.066	1.097	0.904
Final R_1 indexes	0.0439	0.0738	0.0446
wR_2 indices (all data)	0.1035	0.2152	0.1419
Largest diffr. peak and hole ($e.Å^{-3}$)	0.82/-0.40	1.29/-1.08	0.66/-0.68

2. Selected bond lengths and angles for **1-7** (**Table S3**)

Description	1	2	3	4	5	6	7
Cr1-C1	2.107(2)	2.102(7)	2.108(3)	2.132(2)	2.127(5)	-	2.117(3)
Cr1-Cg[a]	1.886(5)	1.897(9)	1.891(9)	1.904(5)	1.902(7)	1.895(6)	1.888(9)
Cr1-Cl1	2.321(6)	2.3988(2)	2.3471(9)	2.3933(6)	2.4066(2)	2.324(4)	2.3225(9)
Cr1-Br1	2.328(5)	2.3548(2)	2.3254(9)	2.3584(7)	2.3730(2)	2.360(3)	2.3242(9)[c]
Cr1-C1-Cl1	97.239(2)	96.450(2)	97.804(3)	100.486(2)	82.817(3)	-	97.478(3)
Cr1-C1-Br1	100.114(2)	99.832(2)	97.724(3)	98.161(2)	99.652(3)	-	98.551(3)[d]
C_β-C_α-N1-C1[b]	127.841(2)	-77.168(5)	-	128.727(2)	-127.029(6)	-	-72.823(4)
C_β-C_α-N2-C1[b]	-	-132.343(5)	112.056(5)	-134.143(2)	81.480(6)	-	112.804(3)
C_γ-C_β-C_α-N1[b]	119.699(2)	-54.622(6)	-	-74.162(2)	71.272(5)	-	152.008(3)
C_γ-C_β-C_α-N2[b]	-	-124.305(6)	175.804(5)	71.238(2)	-163.136(5)	-	-179.548(3)

[a] Cg = centroid of cyclopentadienyl moiety. [b] C_α, C_β, and C_γ denotes the primary, secondary, and tertiary carbon atoms attached to the NX (X = 1, 2) atom, in the former respective order. [c] The Cr1-Cl2 bond distance refers. [d] The Cr1-C1-Cl2 bond angle refers.

3. Schematic representation of the oxidation and reduction processes (**Figure S1**)

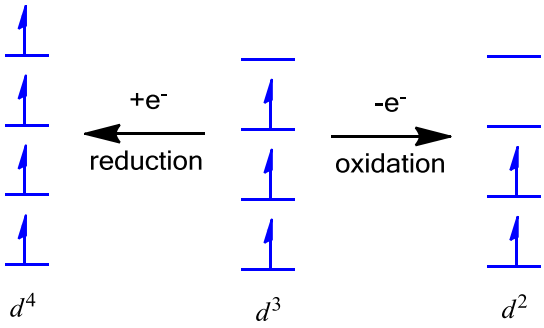


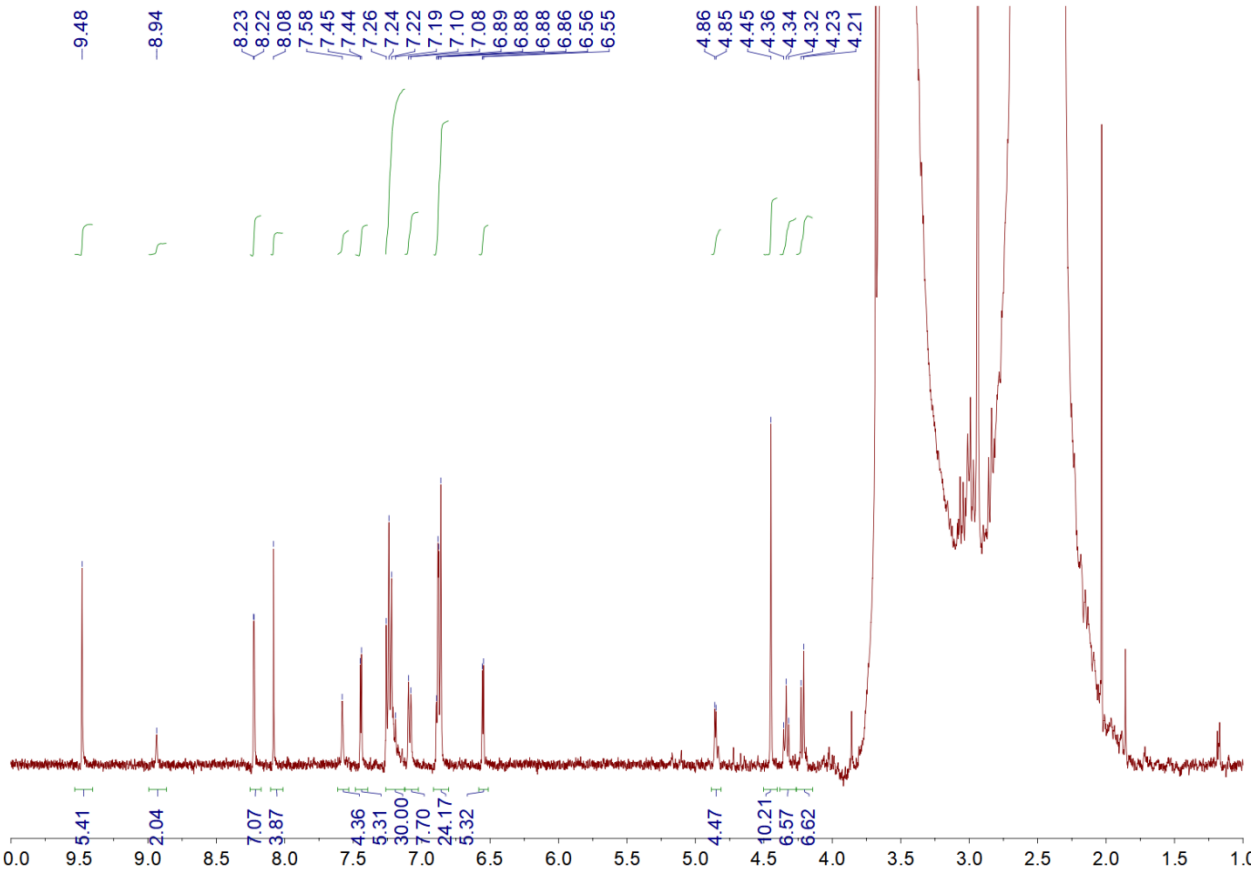
Figure S1: Schematic representation of the oxidation and reduction process of the Cr(III)-NHC complexes [CpCrBrCl(NHC)] (**1**–**5**). The blue arrows represent electrons (up arrow is an alpha up-spin electron).

4. Glucose dehydration using **1-6** (**Table S4**)

Entry	Catalyst (5 mol%)	Conversion (%)	HMF Yield (%)	Other (%)	TOF (h^{-1})
1	-	14.9	3.8	11.1	0.0
2	$CrCl_3(THF)_3$	89.8	89.8	0.0	9.9
3	**2** (room temperature)	34.0	34.0	0.0	0.2
4	**2** (3 mol%)	48.1	34.8	13.3	1.22
5	**2** (10 mol%)	92.3	73.1	19.2	3.00
6	**2**	68.6	68.6	0.00	2.62
7	**2** (THF)	64.7	51.3	13.4	3.82
8	**1**	71.7	37.2	34.5	3.69
9	**3**	76.0	35.5	40.5	3.13
10	**4**	60.3	56.3	4.0	2.02
11	**5**	51.7	48.3	3.4	2.08
12	**6**	80.6	76.0	4.6	5.44

General conditions: (+)-D-glucose (0.11 mmol), [Cr] (6 mol%), DMSO (4 mL), anisole (0.11 mmol), 120 °C.

5. ^{1}H-NMR spectrum of glucose dehydration reaction mixture



General conditions: (+)-D-glucose (0.11 mmol), [**1**] (6 mol%), anisole (0.11 mmol), 120 °C. Aliquot taken after 1 hour reaction time, analysed using d_6-DMSO.

Chapter 7
Tandem transfer hydrogenation-epoxidation of ketone substrates catalysed by alkene-tethered Ru(II)-NHC complexes

Frederick P. Malan,[†] Eric Singleton,[†] Petrus H. van Rooyen[†] and Marilé Landman[†*]

[†] *Department of Chemistry, University of Pretoria, 02 Lynnwood Road, Hatfield, Pretoria, 0002, South Africa.*

Supporting Information

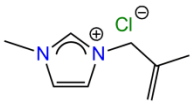
1. Synthesis, characterization, and NMR spectra of [H(**L1**-**L6**)]Cl
2. ^{1}H-, ^{13}C-, ^{31}P-NMR spectra of **1**-**8**
3. Crystal data and structure refinement for [H**L5**]Cl, **P2**, **P3**, **1**,**2**,**4**,**5**,**8** (**Tables S1**,**S2**,**S3**)
4. Selected bond lengths and angles for [H**L5**]Cl, **P2**, **P3**, **1**,**2**,**4**,**5**,**8** (**Table S4**)
5. Time-resolved conversion profiles in the transfer hydrogenation-epoxidation catalysis
6. Optimization of transfer hydrogenation-epoxidation conditions (**Table S5**)
7. ^{1}H-NMR spectrum of catalysis reaction mixture

1. Synthesis, characterization, and NMR spectra of [H(**L1**-**L6**)]Cl

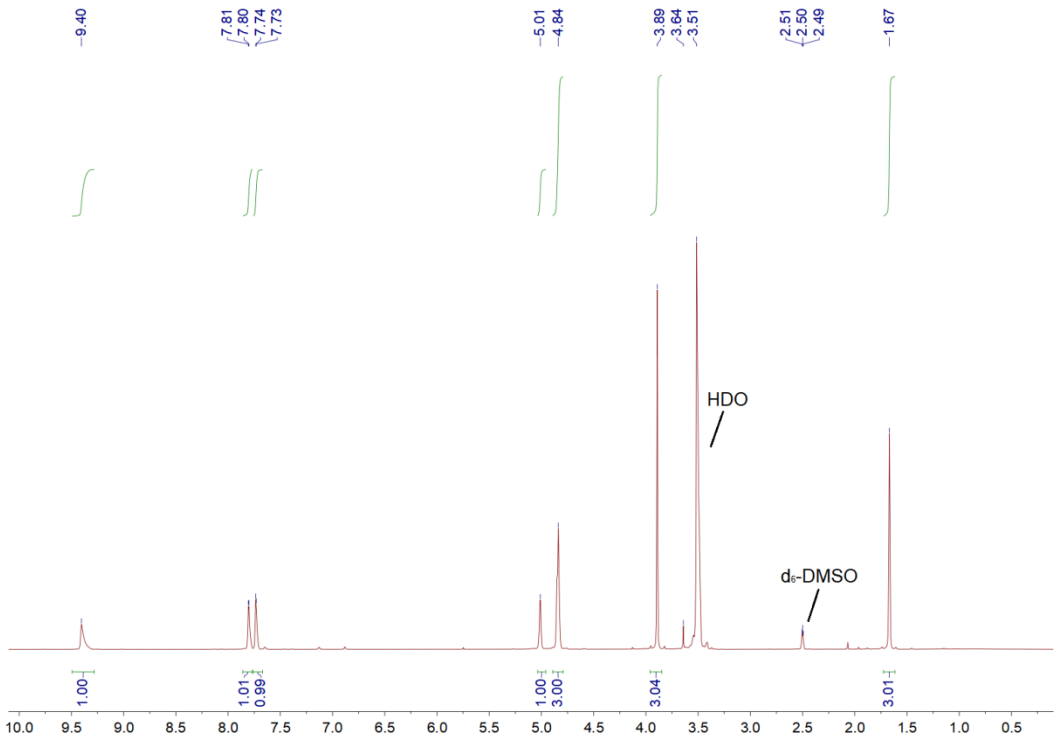
General synthesis of imidazolium salts: To an acetonitrile (20 mL) solution of the respective *N*-alkyl imidazole (42 mmol, [H**L1**]Cl, [H**L2**]Cl) was added 1-chloro-2-methylpropene (1 equivalent), and the resulting mixture heated under reflux overnight. After cooling, the reaction mixture was concentrated *in vacuo*, and washed with a 1:1 v/v Et_2O/Et_2OAc mixture (3 × 15 mL). The resulting oil/solid was concentrated in vacuo to give the respective ligands [H(**L1**-**L6**)]Cl.

Ligand [H**L1**]Cl: Yield: 94%. ^{1}H-NMR ($(CD_3)_2SO$, δ_H) 1.67 (s, CH_3, 3H), 3.89 (s, NCH_3, 3H), 4.84 (s, =C*H* + CH_2, 3H), 5.01 (s, =C*H*, 1H), 7.74 (d, $^{3}J_{HH}$ = 2 Hz, NC*H*, 1H), 7.81 (d, $^{3}J_{HH}$ = 2 Hz, NC*H*, 1H), 9.40 (s, NC*H*N, 1H). ^{13}C{^{1}H}-NMR ($(CD_3)_2SO$, δ_C) 19.5 (s, *C*H_3), 35.9 (s, N*C*H_3), 54.0 (s, *C*H_2), 114.9 (s, =*C*H_2), 122.6 (s, N*C*H), 123.9 (s, N*C*H), 137.0 (s, *C*CH_2), 139.5 (s, N*C*N).

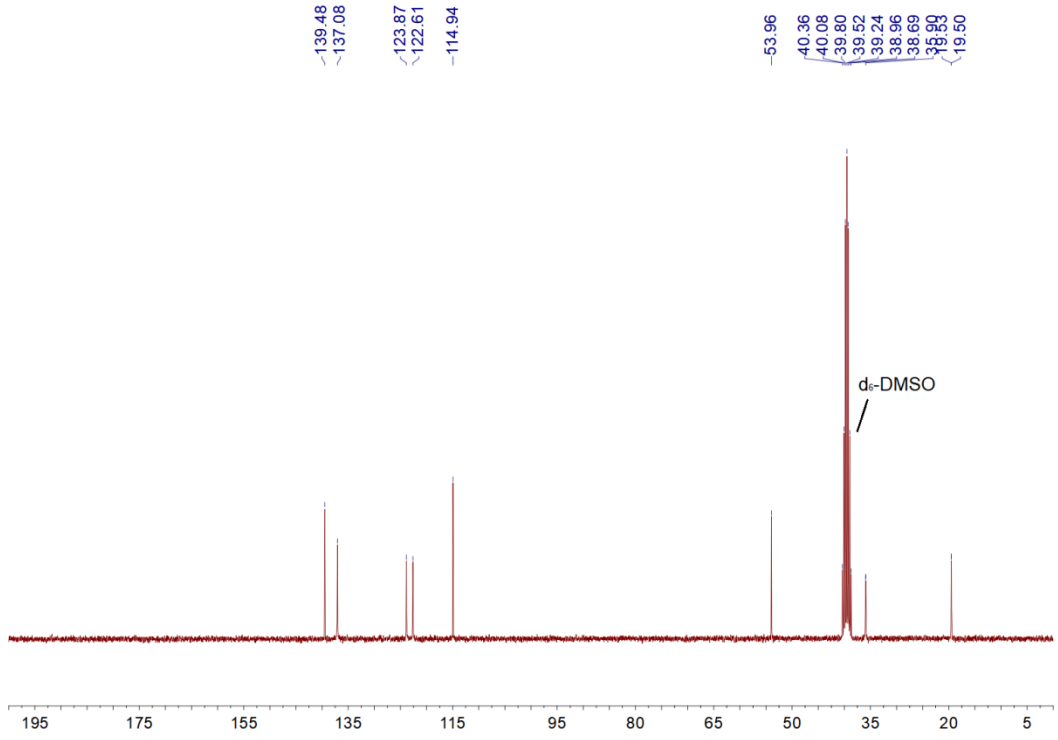
^{1}H-NMR



[HL1]Cl

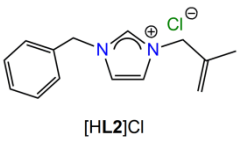


^{13}C-NMR

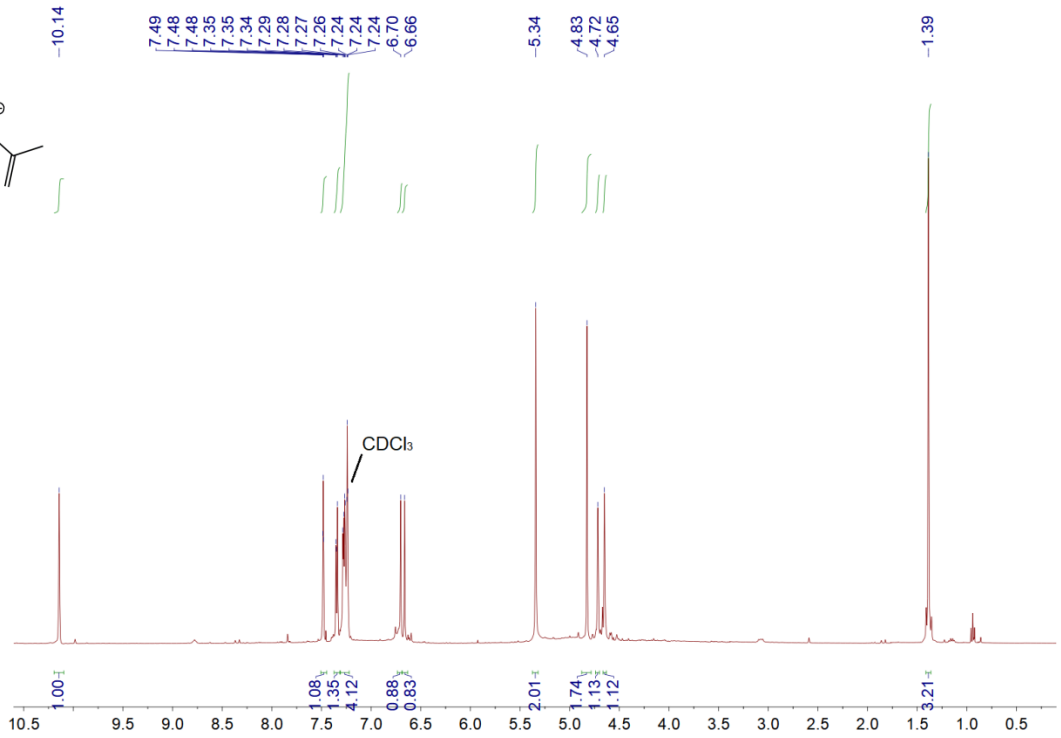


Ligand **L2**: Yield: 91%. ^{1}H-NMR ($CDCl_3$, δ_H) 1.39 (s, CH_3, 3H), 4.65 (s, =CH_2, 1H), 4.72 (s, =CH_2, 1H), 4.83 (s, CH_2, 2H), 5.34 (s, CH_2, 2H), 6.66 (s, NCH, 1H), 6.70 (s, NCH, 1H), 7.26 (m, C_6H_5, 4H), 7.49 (m, C_6H_5, 1H), 10.14 (s, NCHN, 1H). ^{13}C{^{1}H}-NMR ($CDCl_3$, δ_C) 18.5 (s, CH_3), 51.6 (s, CH_2), 53.9 (s, CH_2), 115.5 (s, =CH_2), 121.4 (s, NCH), 121.4 (s, NCH), 132.6 (s, C_6H_5), 135.1 (s, C_6H_5), 135.7 (s, *ipso* C_6H_5), 136.0 (s, CCH$_2$), 136.9 (s, NCN).

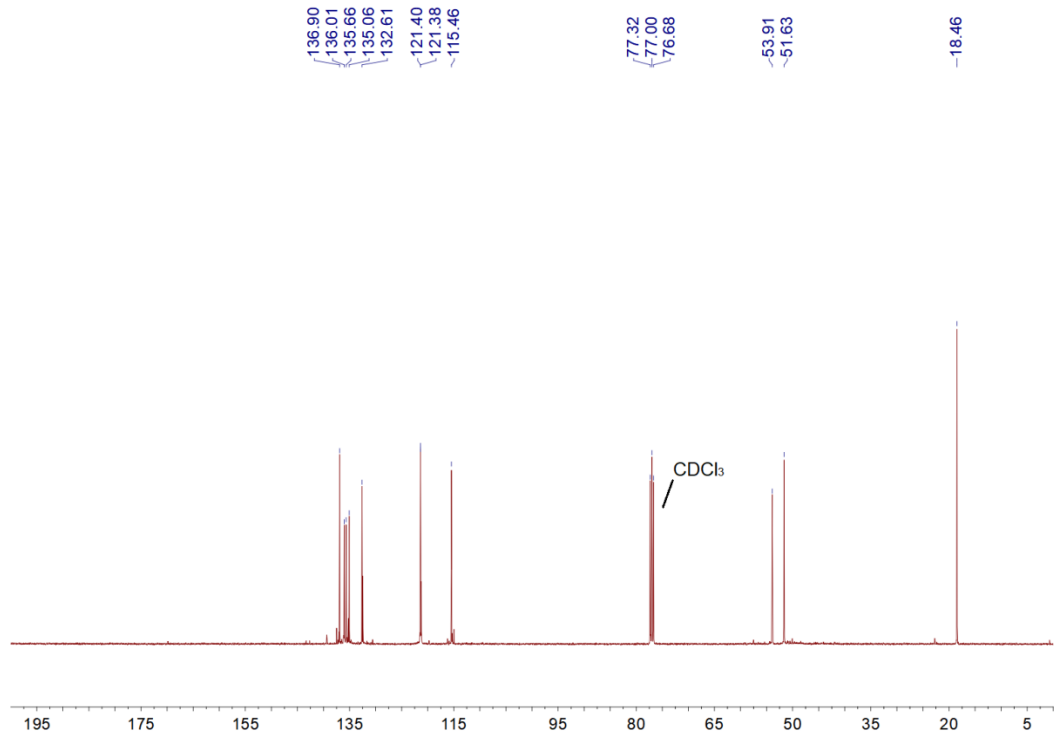
^{1}H-NMR



[H**L2**]Cl

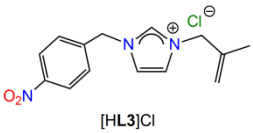


^{13}C-NMR

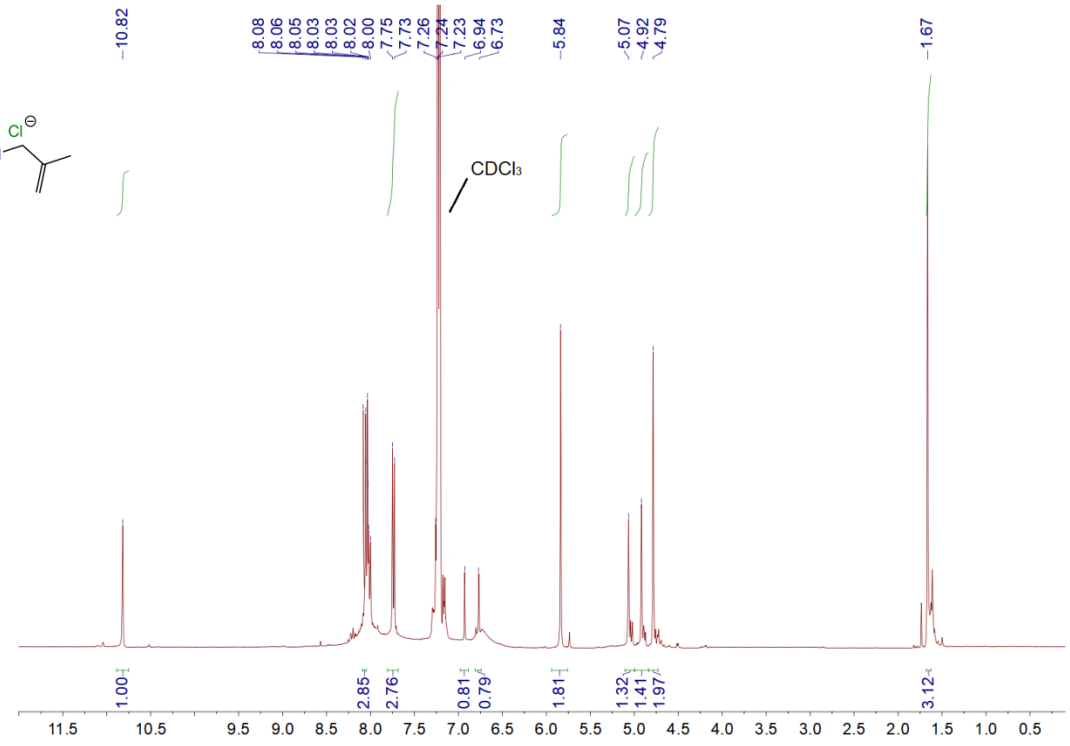


Ligand **L3**: Yield: 67%. ^{1}H-NMR ($CDCl_3$, δ_H) 1.67 (s, CH_3, 3H), 4.79 (s, CH_2, 2H), 4.92 (s, =C*H*, 1H), 5.07 (s, =C*H*, 1H), 5.84 (s, CH_2, 2H), 6.74 (s, NC*H*, 1H), 6.94 (s, NC*H*, 1H), 7.74 (d, $^{3}J_{HH}$ = 6 Hz, C_6H_4, 2H), 8.05 (m, C_6H_4, 2H), 10.82 (s, NC*H*N, 1H). ^{13}C{^{1}H}-NMR ($CDCl_3$, δ_C) 19.5 (s, *C*H_3), 51.9 (s, *C*H_2), 53.6 (s, *C*H_2), 117.4 (s, =*C*H_2), 122.0 (s, N*C*H), 122.3 (s, N*C*H), 129.1 (s, *C*$_6$H$_4$), 129.5 (s, *C*$_6$H$_4$), 129.9 (s, *ipso C*$_6$H$_4$), 137.4 (s, *C*CH_2), 143.4 (s, N*C*N).

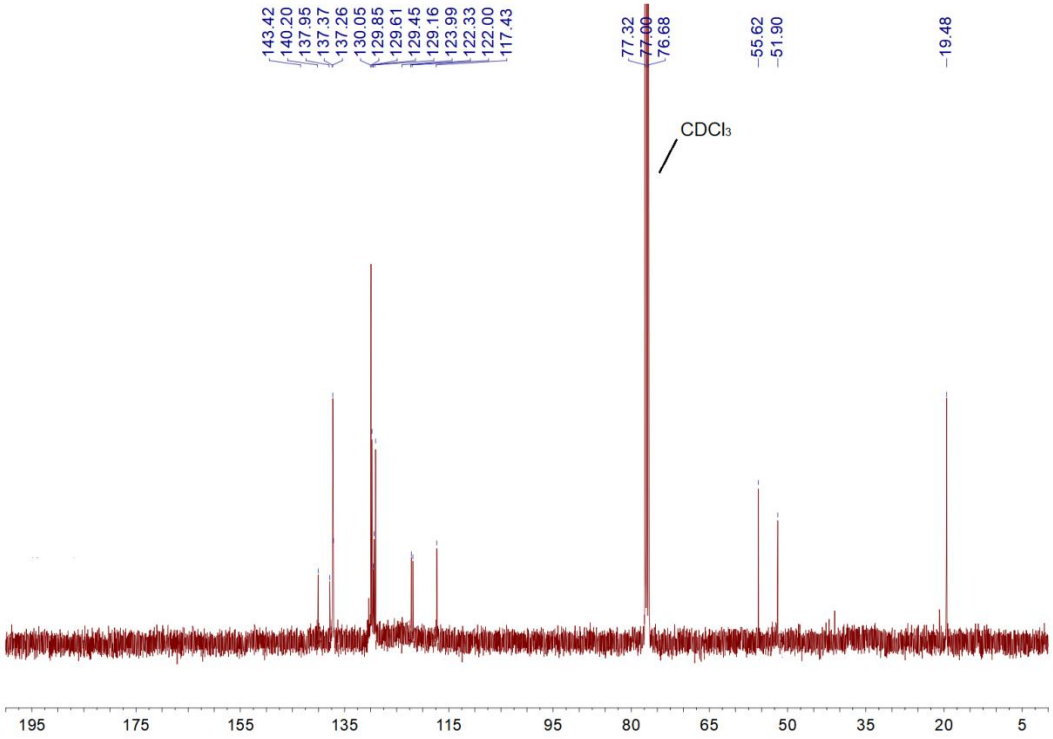
^{1}H-NMR



[HL3]Cl

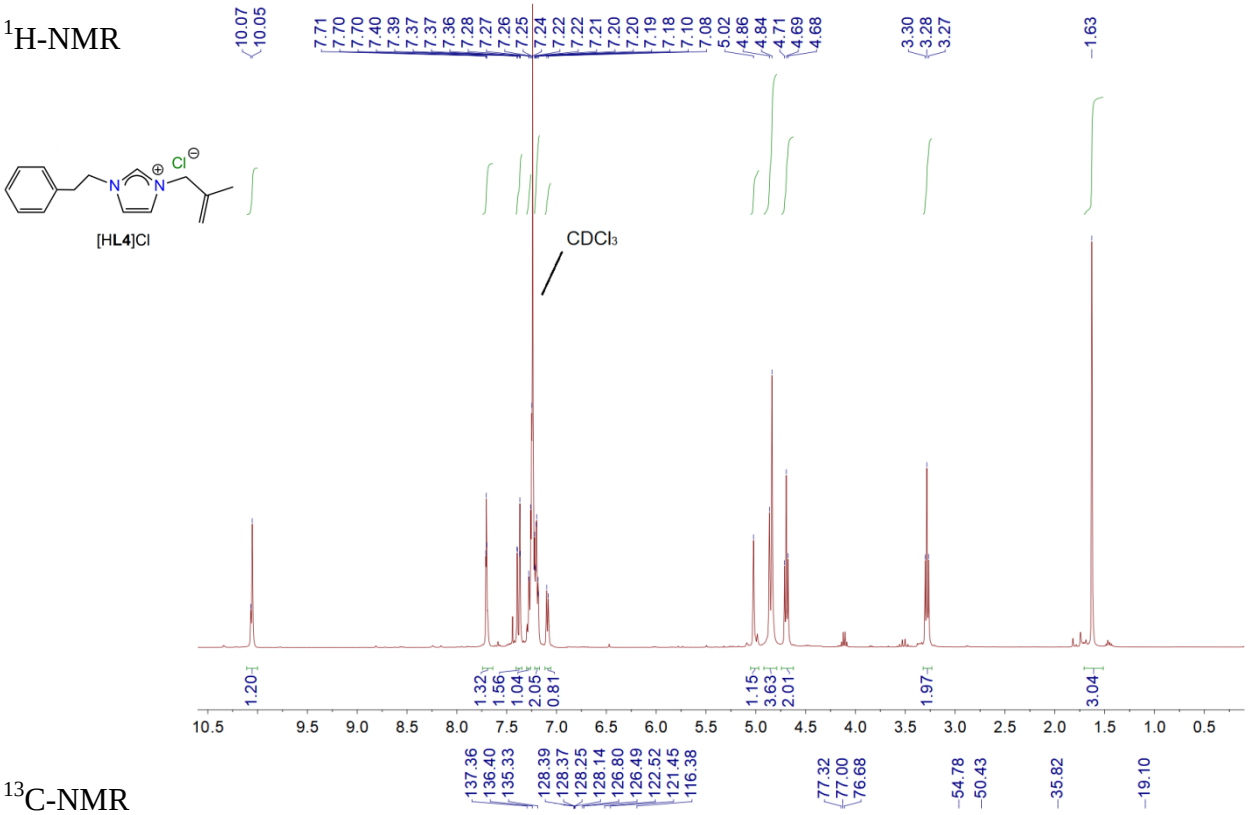


^{13}C-NMR

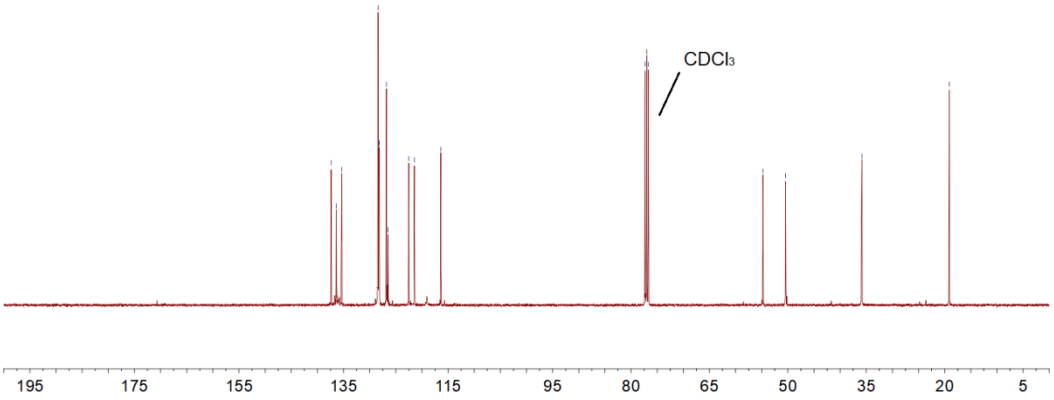


Ligand **L4**: Yield: 86%. ^{1}H-NMR ($CDCl_3$, δ_H) 1.63 (s, CH_3, 3H), 1.97 (t, $^{3}J_{HH}$ = 8 Hz, CH_2, 2H), 4.69 (t, $^{3}J_{HH}$ = 8 Hz, CH_2, 2H), 4.84 (m, =CH_2 + CH_2, 4H), 5.02 (s, =CH_2, 1H), 7.09 (d, $^{3}J_{HH}$ = 8 Hz, NCH, 1H), 7.18-7.28 (m, NCH + C_6H_5, 3H), 7.37 (m, C_6H_5, 1H), 7.40 (m, C_6H_5, 1H), 7.70 (m, C_6H_5, 1H), 10.06 (s, NCHN, 1H). ^{13}C{^{1}H}-NMR ($CDCl_3$, δ_C) 19.1 (s, CH$_3$), 35.8 (s, CH$_2$), 50.4 (s, CH$_2$), 54.8 (s, CH$_2$), 116.4 (s, =CH$_2$), 121.5 (s, NCH), 122.5 (s, NCH), 126.5 (s, C_6H$_5$), 126.8 (s), 128.1 (s), 128.3 (s, C_6H$_5$), 128.4 (s, C_6H$_5$), 135.3 (s, *ipso* C_6H$_5$), 136.4 (s, CCH$_2$), 137.4 (s, NCN).

^{1}H-NMR

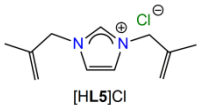


^{13}C-NMR

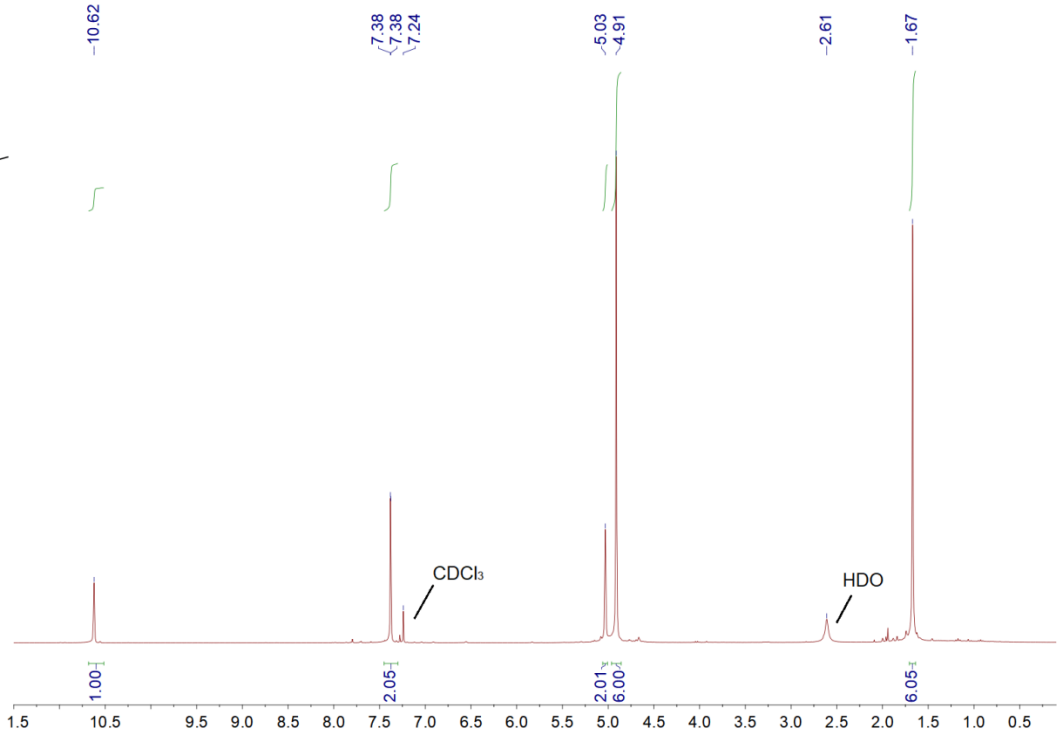


Ligand **L5**: Yield: 88%. ^{1}H-NMR ($CDCl_3$, δ_H) 1.67 (s, CH_3, 6H), 4.91 (s, CH_2 + =CH_2, 6H), 5.03 (s, =CH_2, 2H), 7.38 (s, NC*H*, 2H), 10.62 (s, NC*H*, 1H). ^{13}C{^{1}H}-NMR ($CDCl_3$, δ_C) 19.5 (s, *C*H_3), 19.6 (s, *C*H_3), 55.4 (s, *C*H_2), 116.9 (s, =*C*H_2), 122.0 (s, N*C*H), 137.9 (s, *C*$(CH_3)_2$), 138.3 (s, N*C*N).

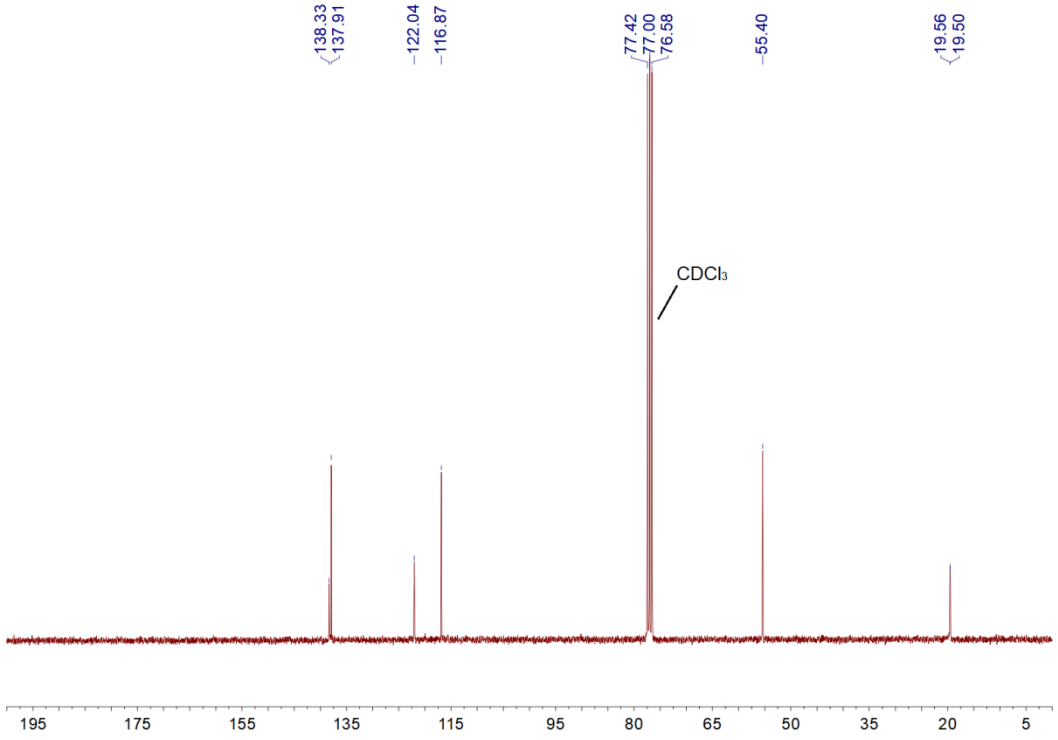
^{1}H-NMR



[HL**5**]Cl

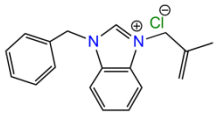


^{13}C-NMR

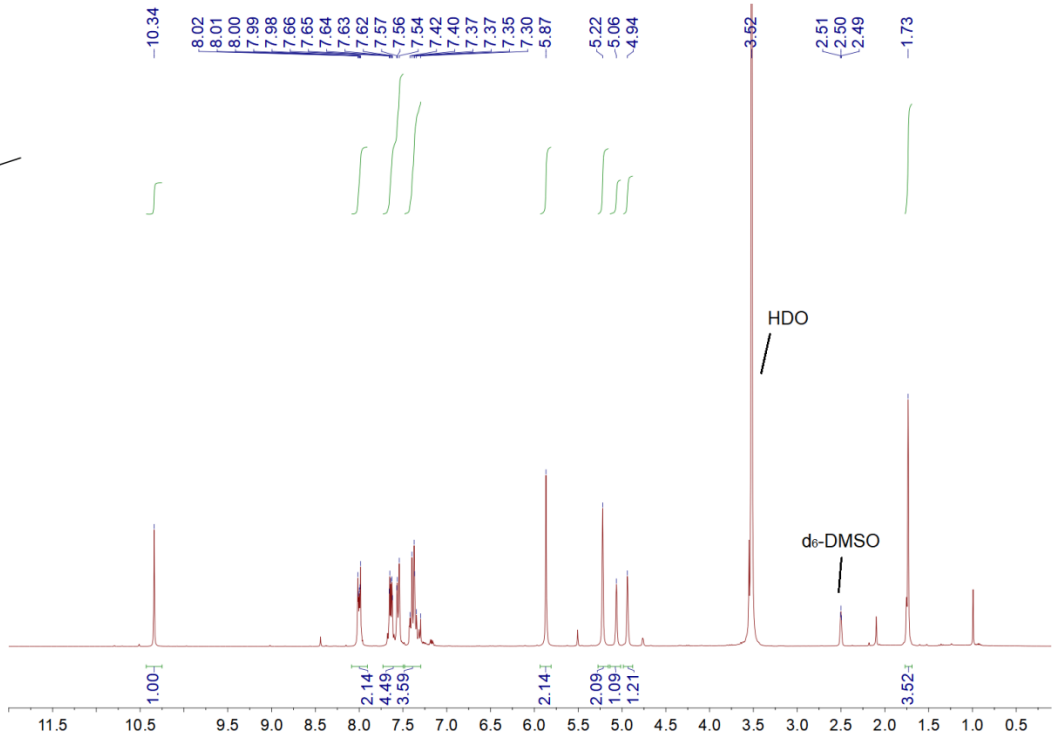


Ligand **L6**: Yield: 92%. ^{1}H-NMR ($(CD_3)_2SO$, δ_H) 1.73 (s, C*H*$_3$, 3H), 4.94 (s, =C*H*$_2$, 1H), 5.06 (s, =C*H*$_2$, 1H), 5.22 (s, C*H*$_2$, 2H), 5.87 (s, C*H*$_2$, 2H), 7.30-7.42 (m, C_6H_4, 3H), 7.54-7.66 (m, C_6H_4 + C_6H_5, 4H), 8.00 (m, C_6H_5, 2H), 10.34 (s, NC*H*N, 1H). ^{13}C{^{1}H}-NMR ($(CD_3)_2SO$, δ_C) 19.8 (s, *C*H$_3$), 47.8 (s, *C*H$_2$), 51.5 (s, *C*H$_2$), 110.8 (s, *C*$_6$H$_4$), 119.6 (s, =*C*H$_2$), 121.8 (s, N*C*H), 122.6 (s, N*C*H), 127.5 (s, *C*$_6$H$_5$), 127.8 (s, *C*$_6$H$_5$), 128.8 (s, *C*$_6$H$_5$), 133.7 (s, *C*$_6$H$_4$), 137.0 (s, *ipso* *C*$_6$H$_5$), 143.6 (s, *C*CH$_2$), 144.3 (s, NC*N*).

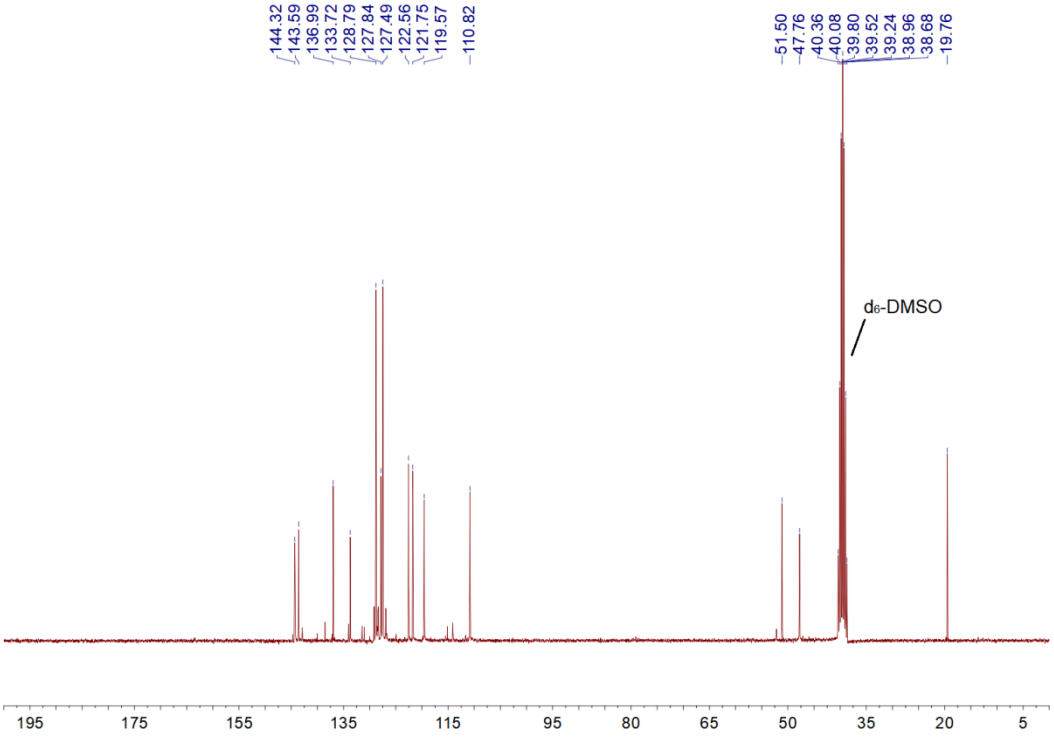
^{1}H-NMR



[H**L6**]Cl



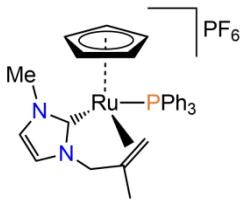
^{13}C-NMR

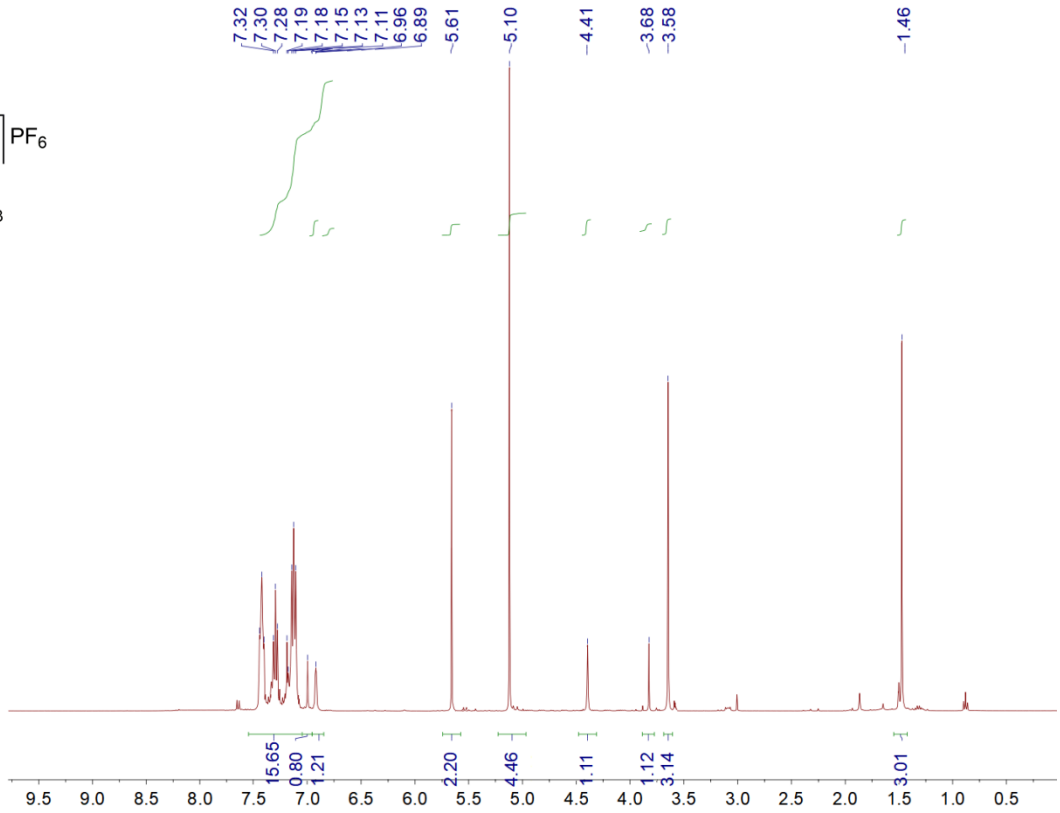


2. ^{1}H-, ^{13}C-, ^{31}P-NMR spectra of **1-9**

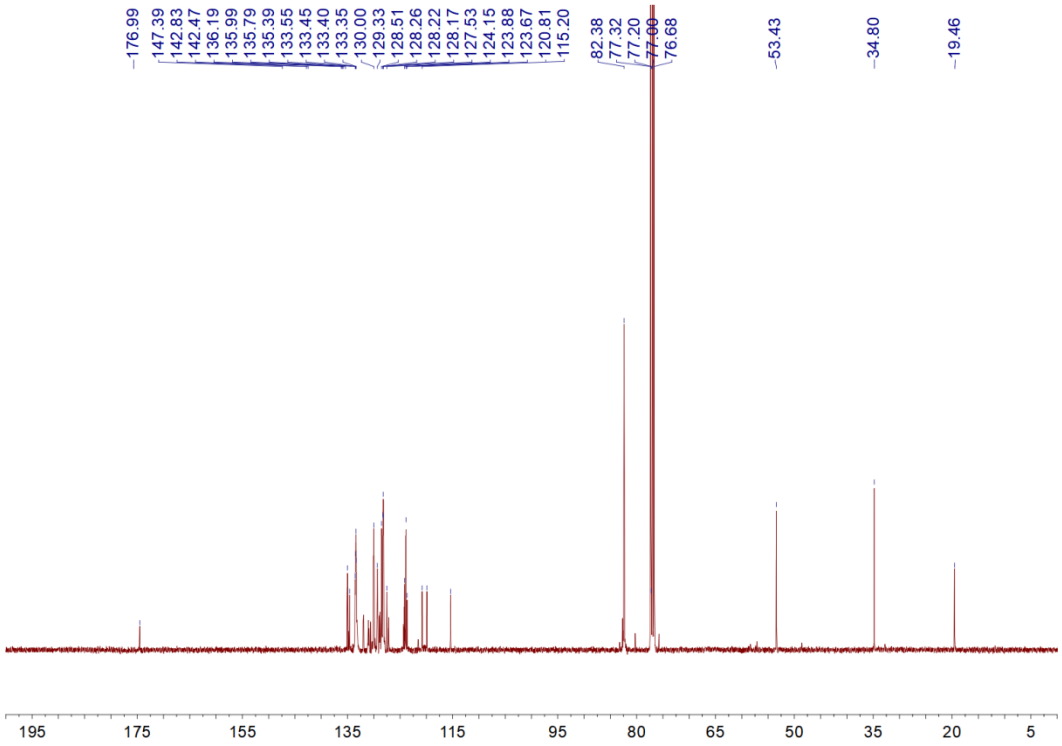
Complex **1**

^{1}H-NMR

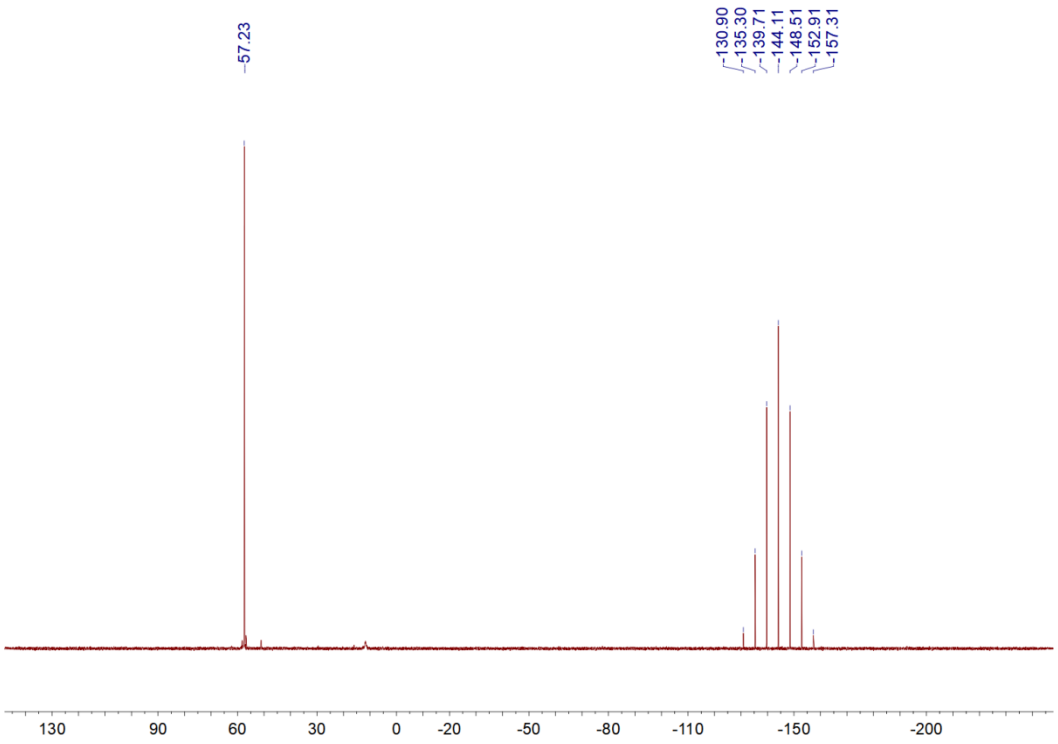




^{13}C-NMR

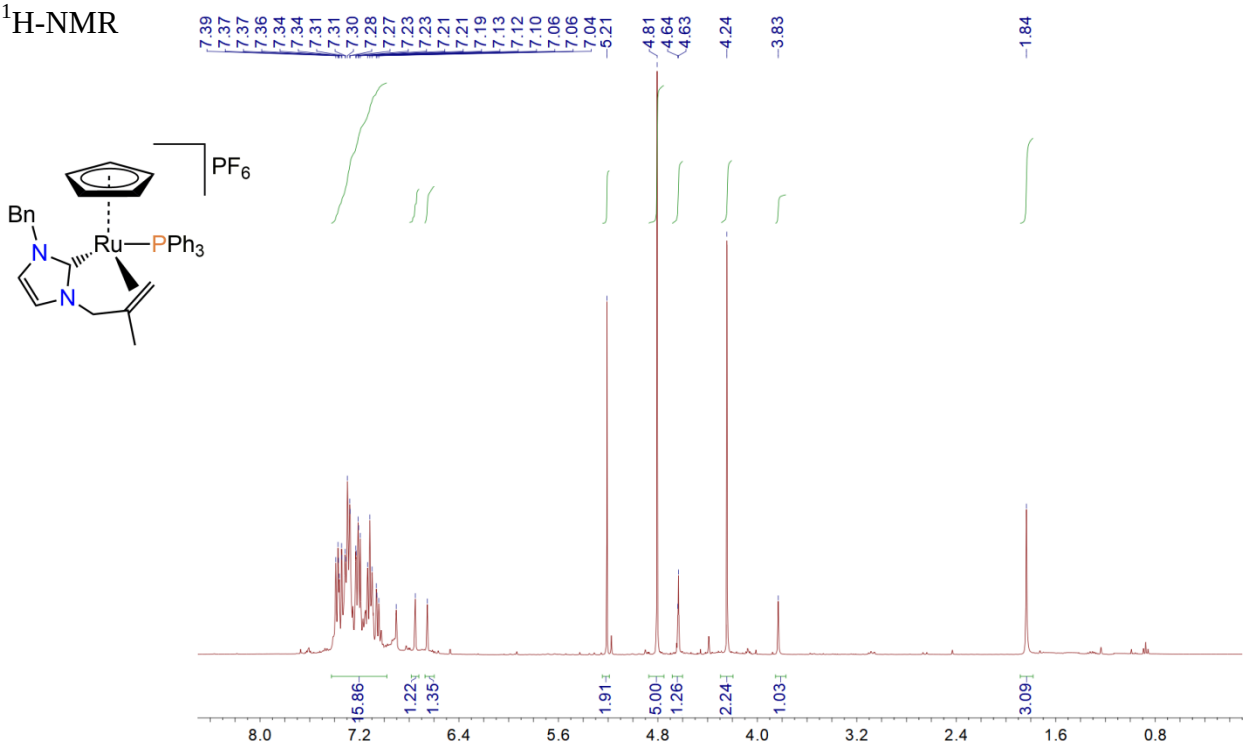


^{31}P-NMR

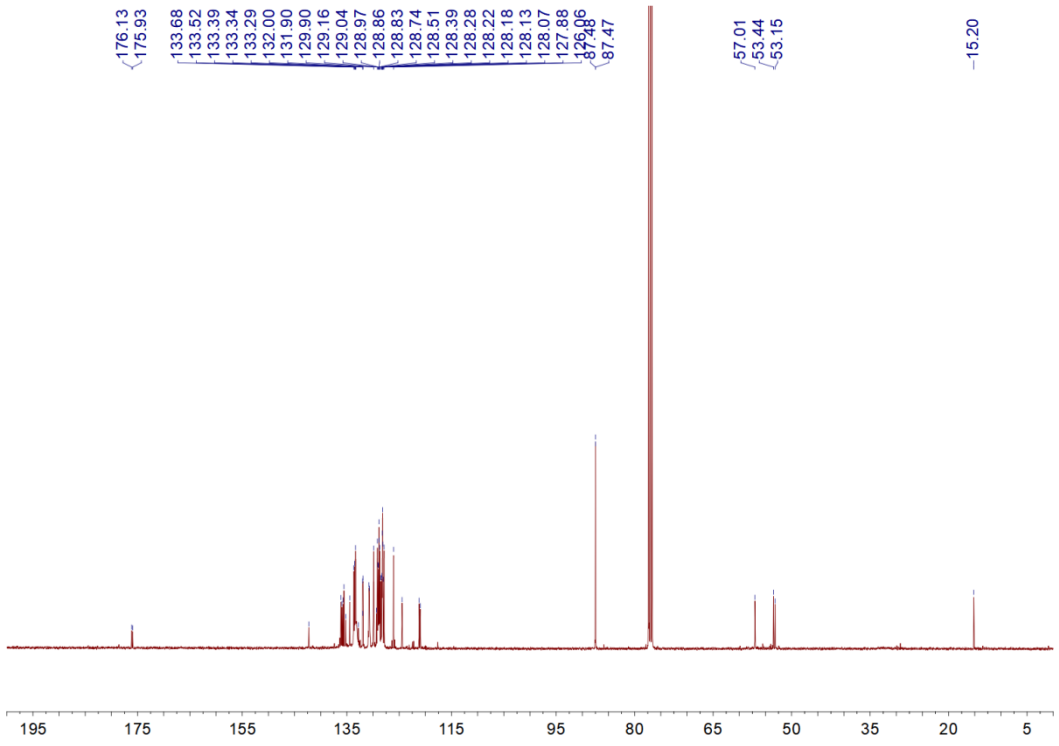


Complex **2**

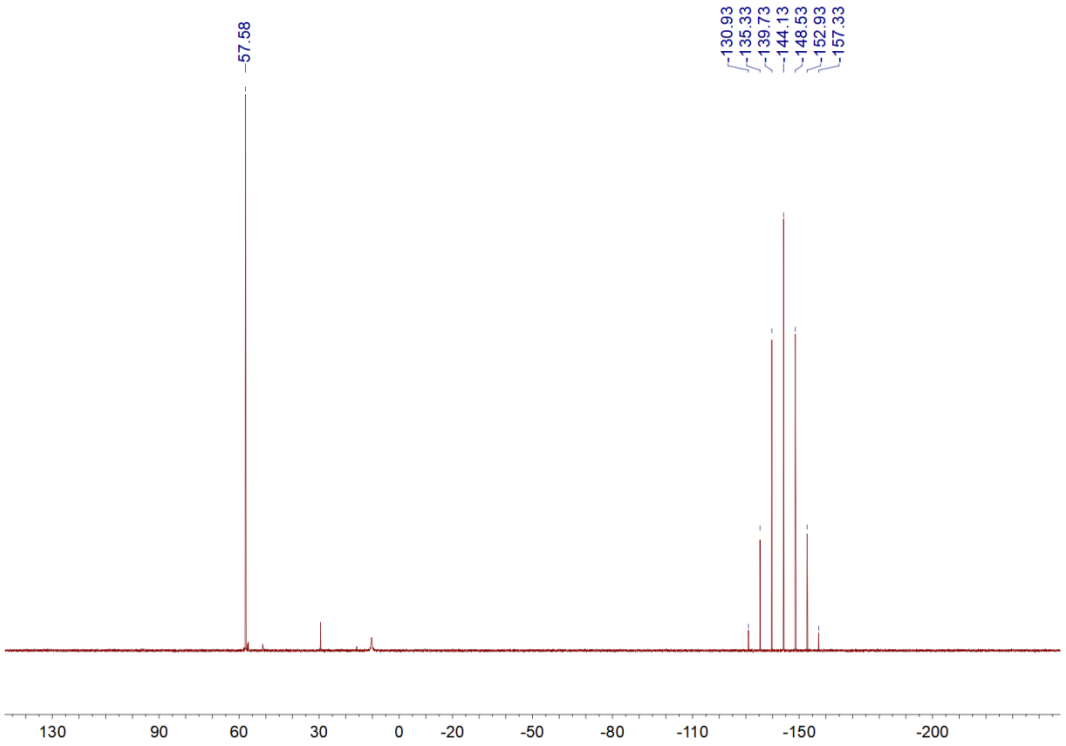
^{1}H-NMR



^{13}C-NMR

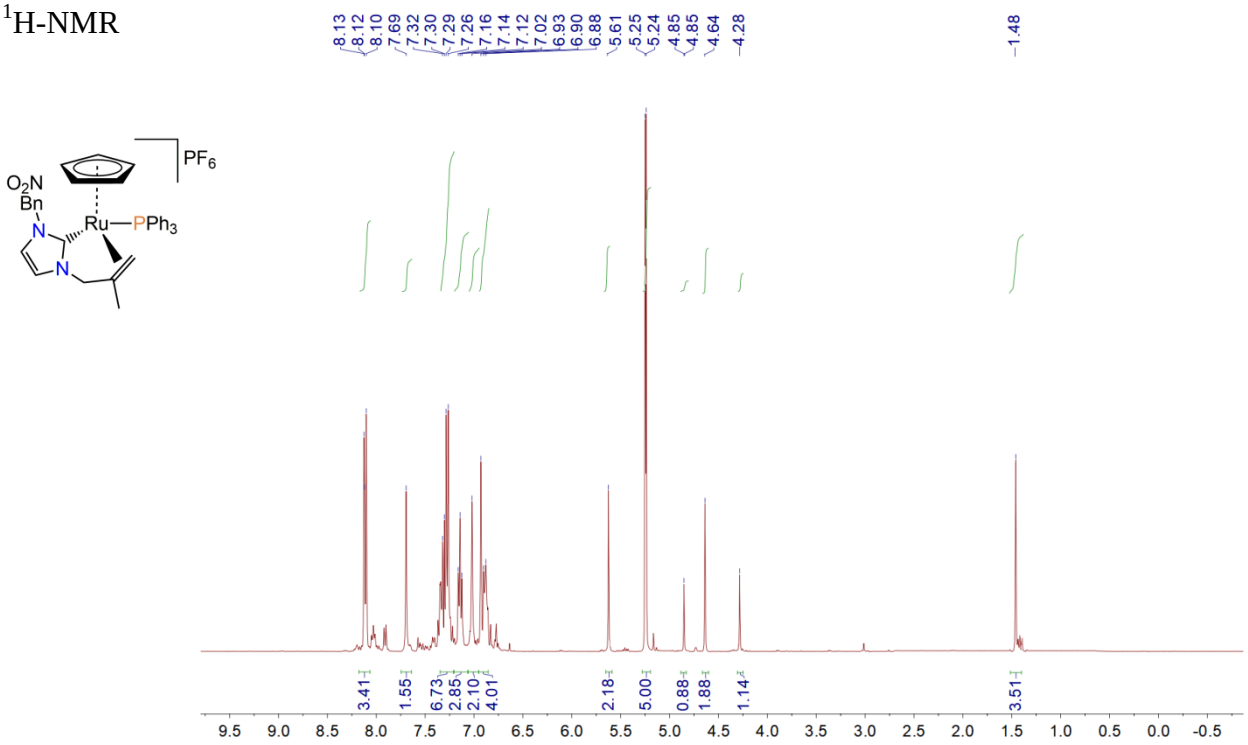


^{31}P-NMR

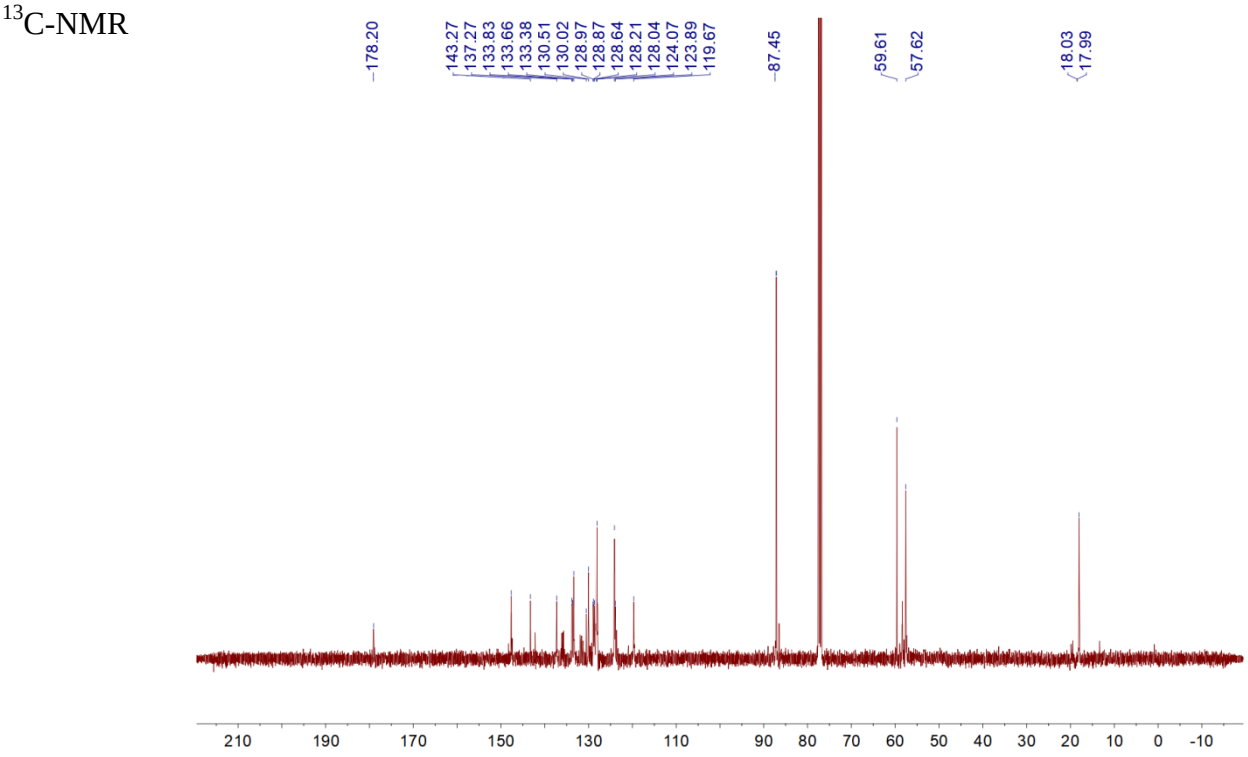


Complex **3**

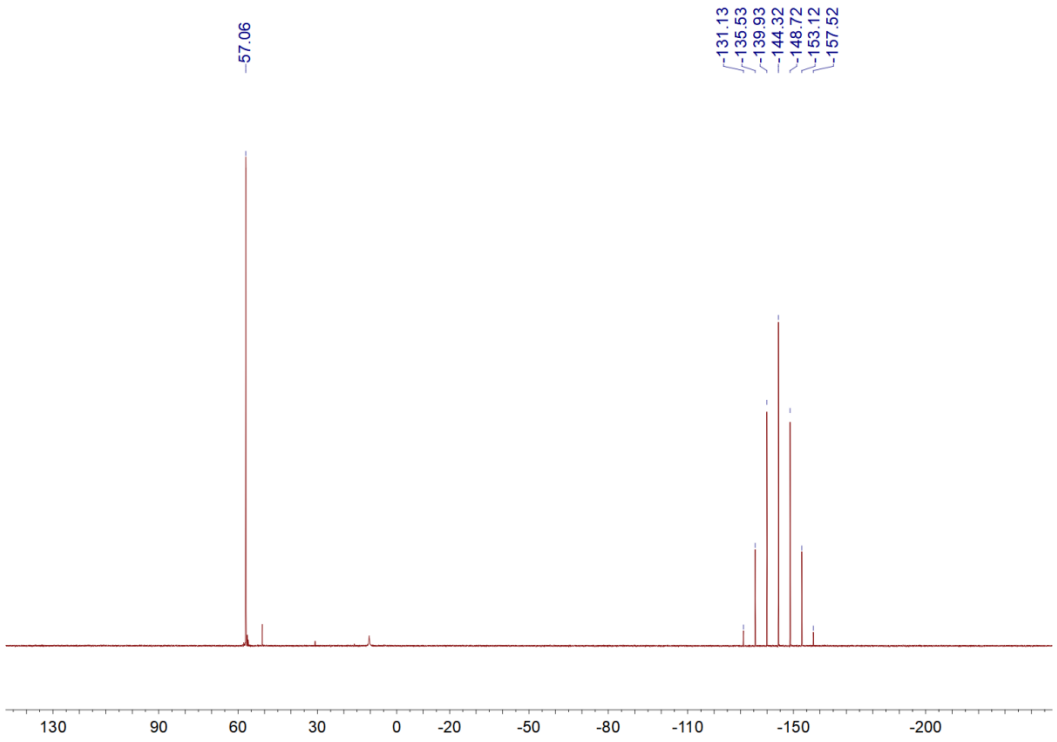
^{1}H-NMR



^{13}C-NMR

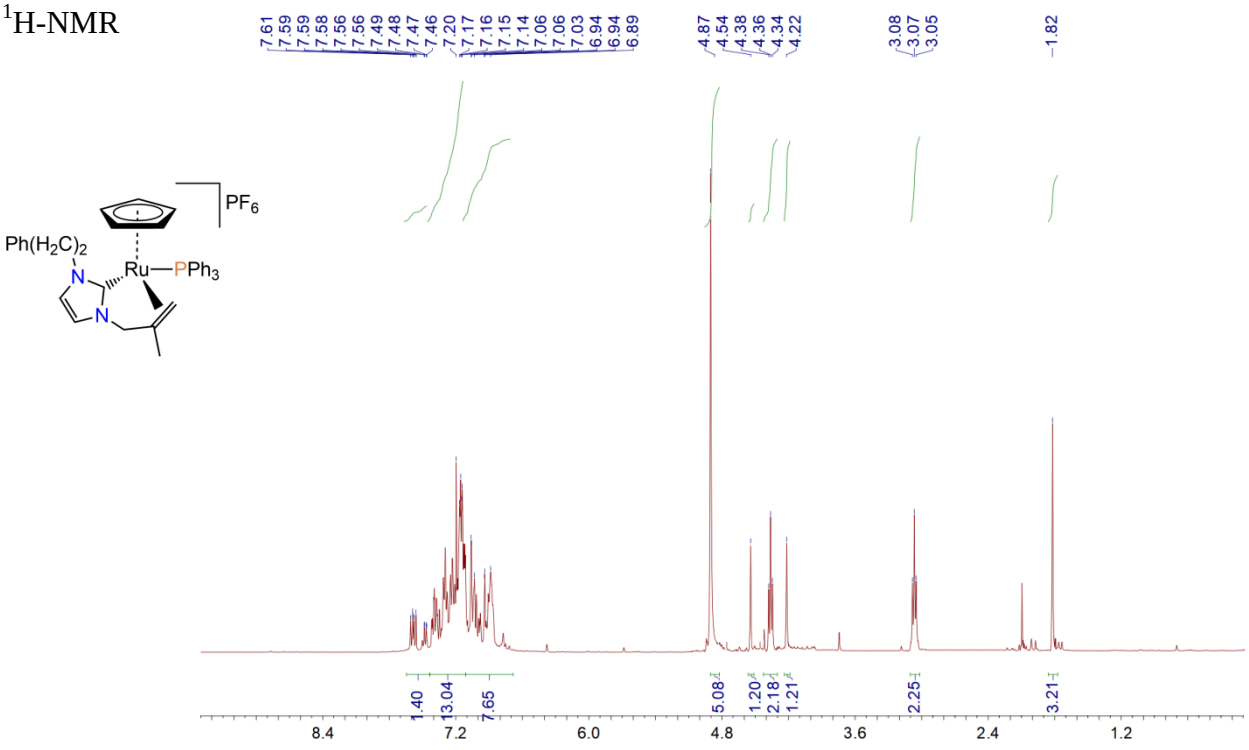


^{31}P-NMR

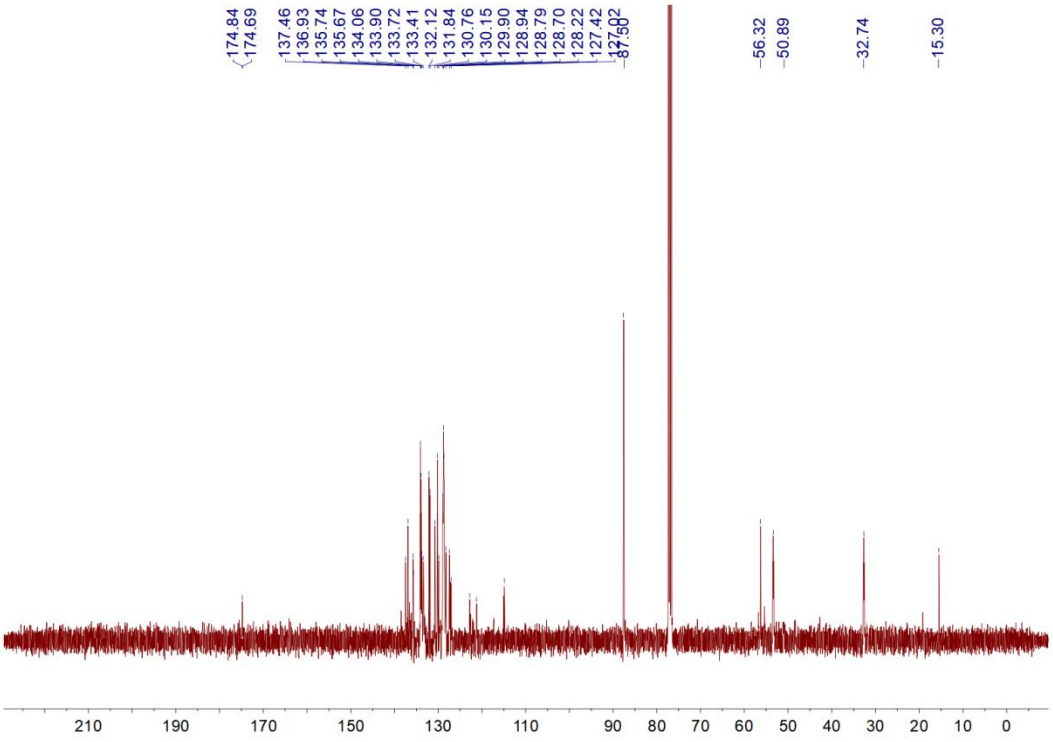


Complex **4**

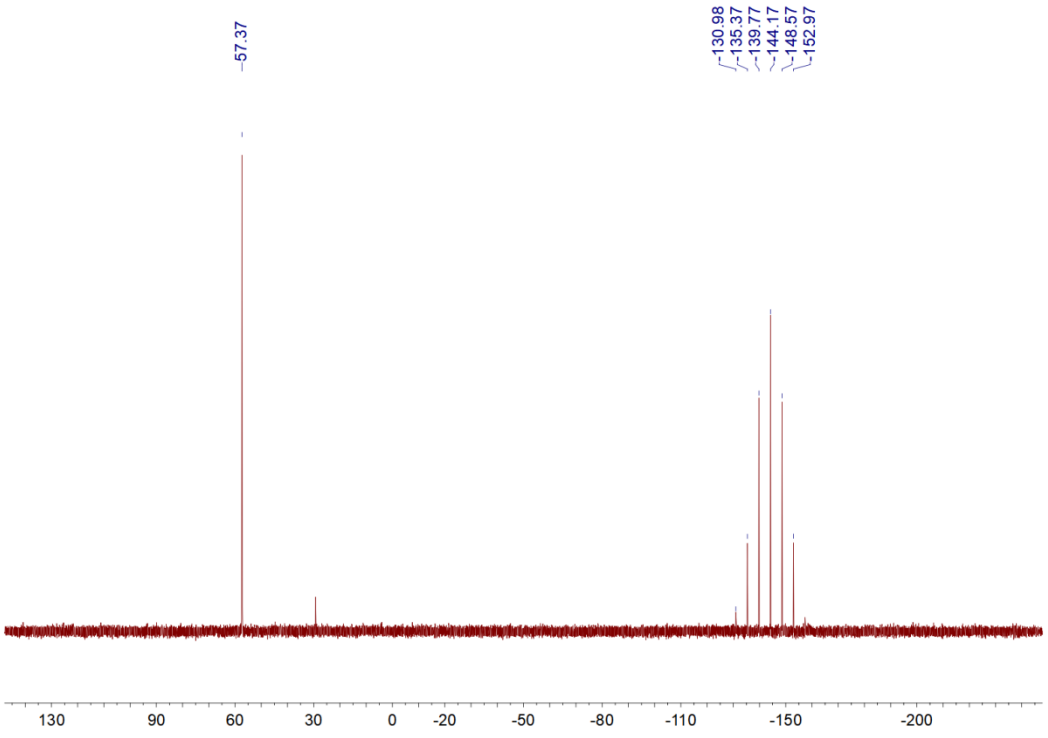
^{1}H-NMR



^{13}C-NMR

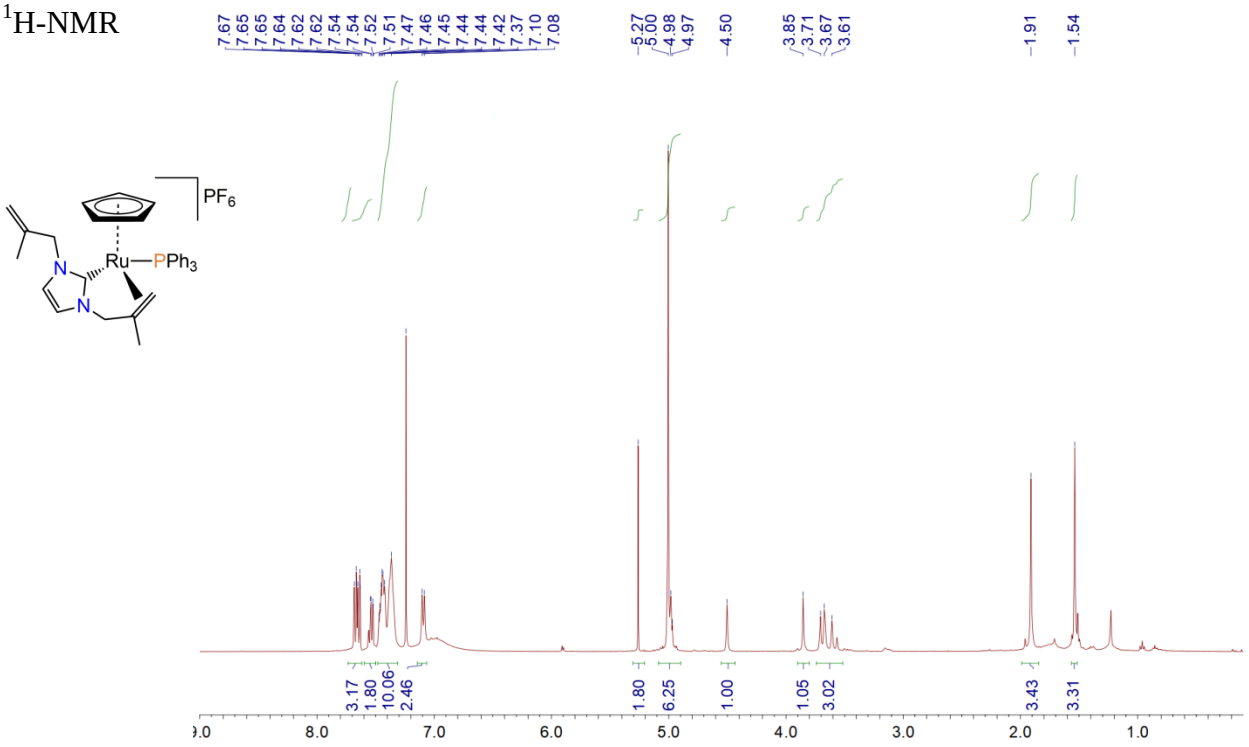


^{31}P-NMR

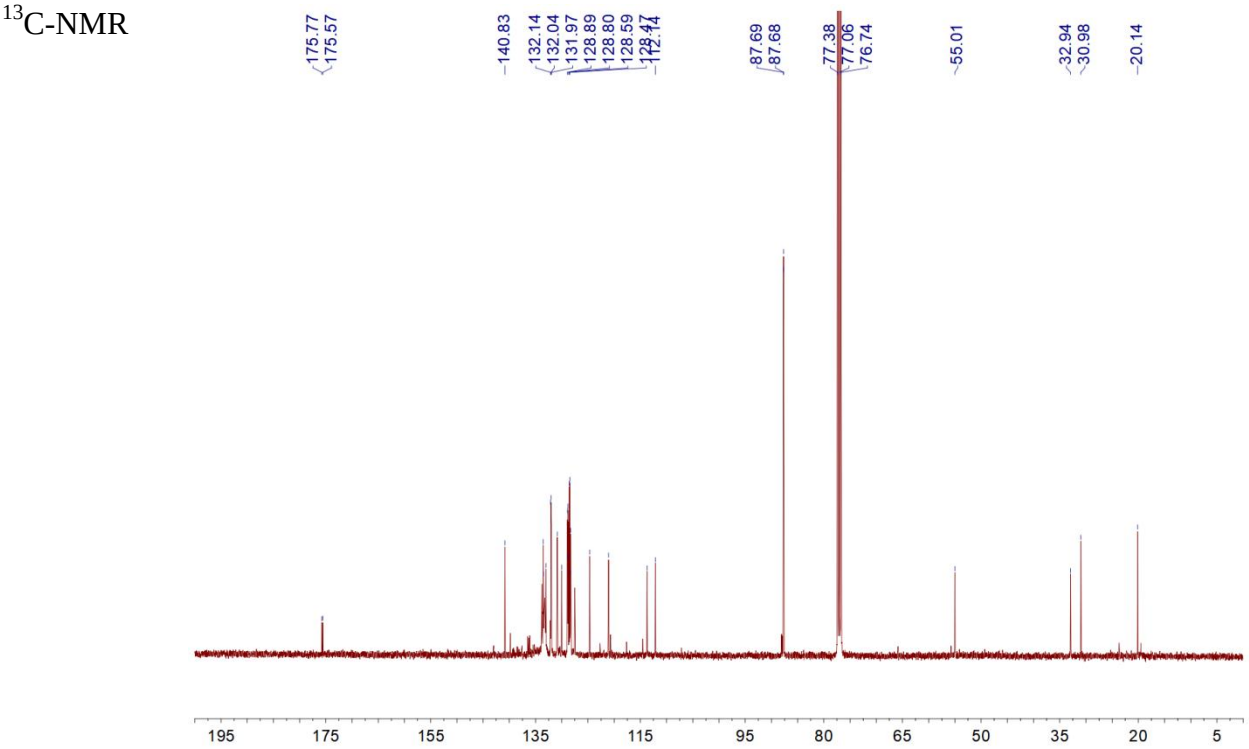


Complex **5**

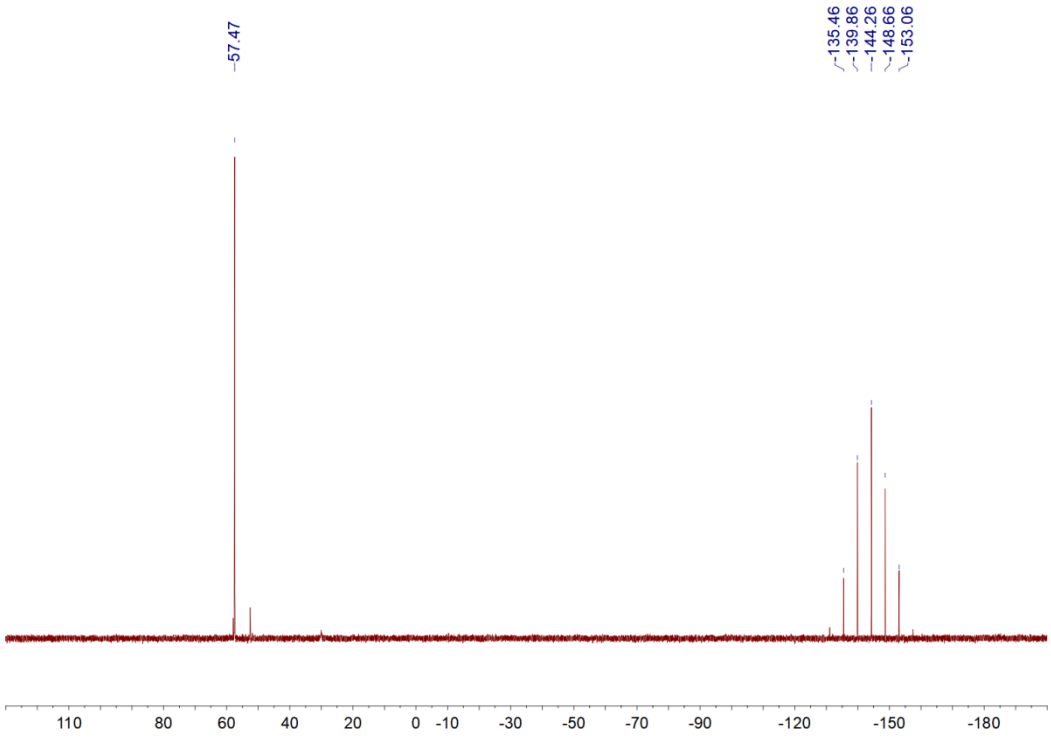
^{1}H-NMR



^{13}C-NMR

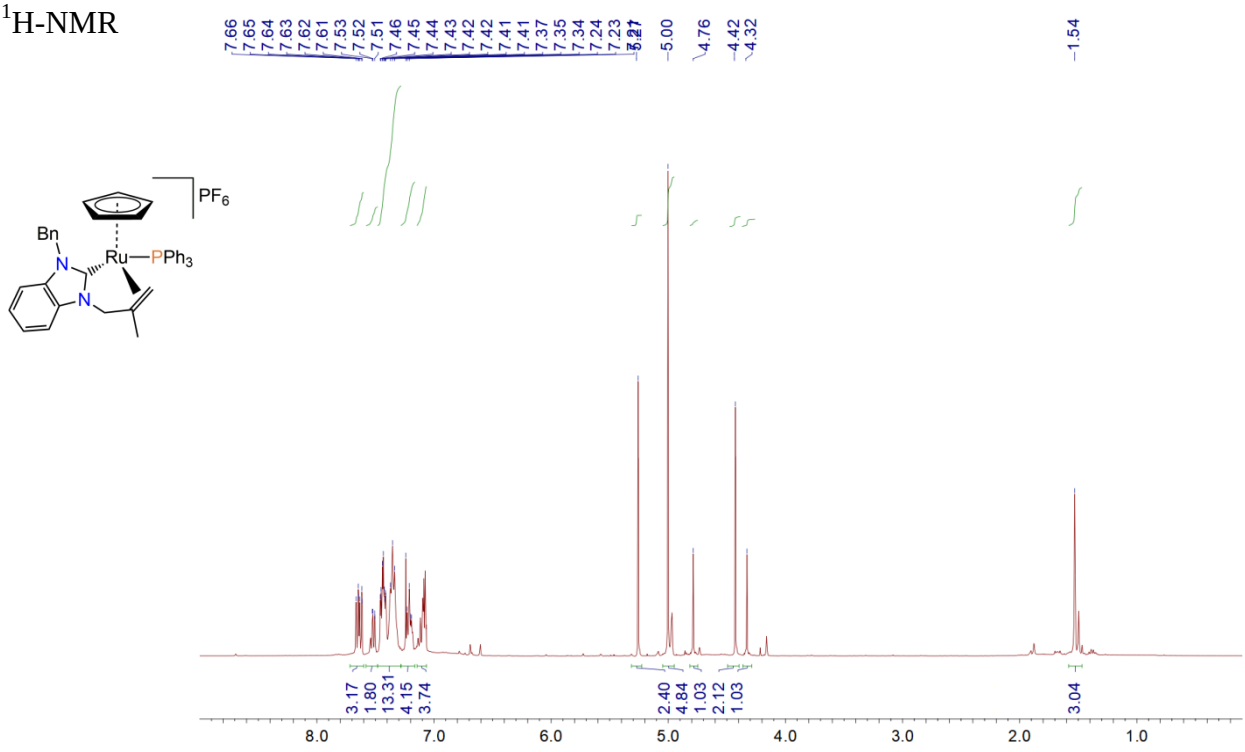


^{31}P-NMR

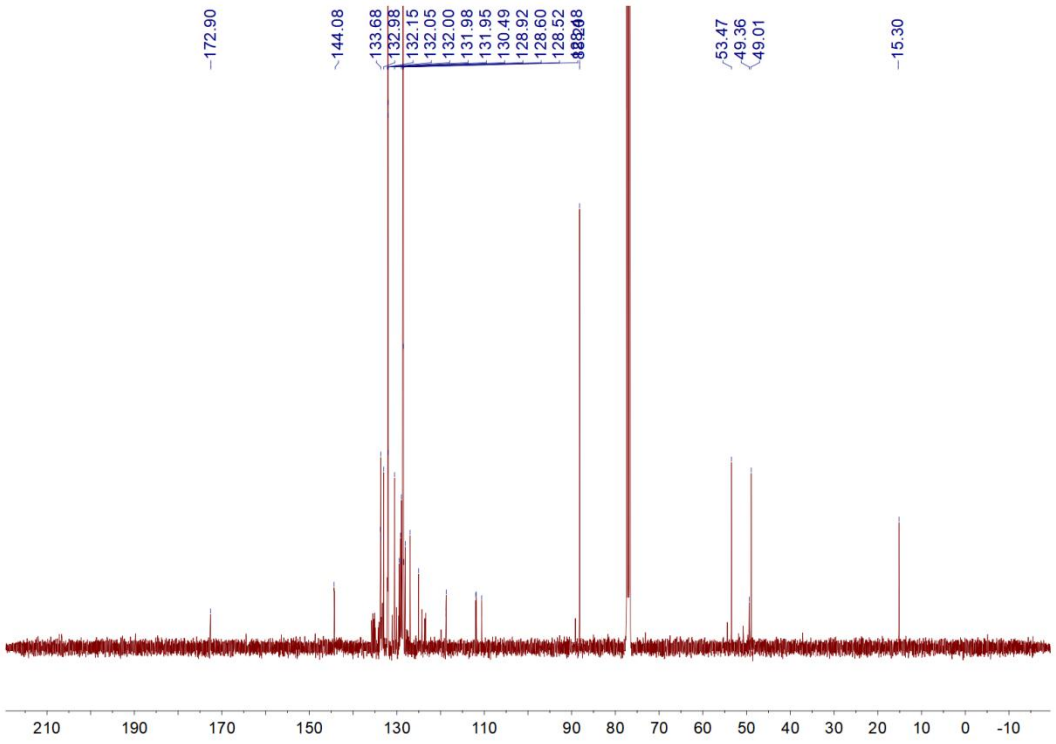


Complex **6**

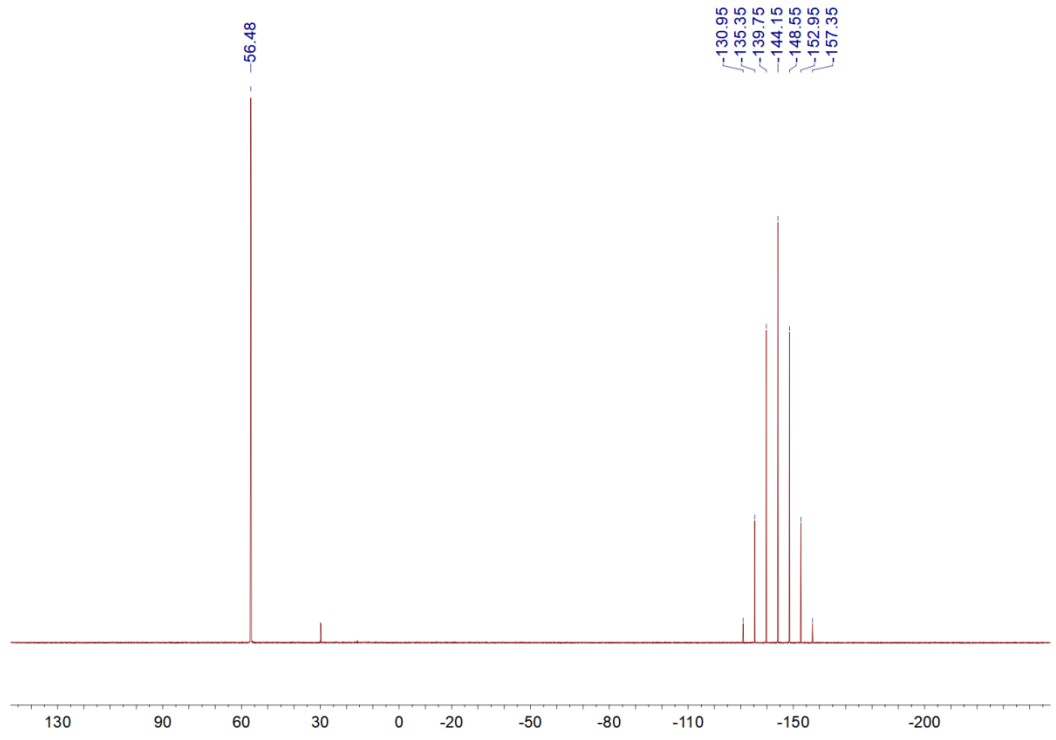
^{1}H-NMR



^{13}C-NMR

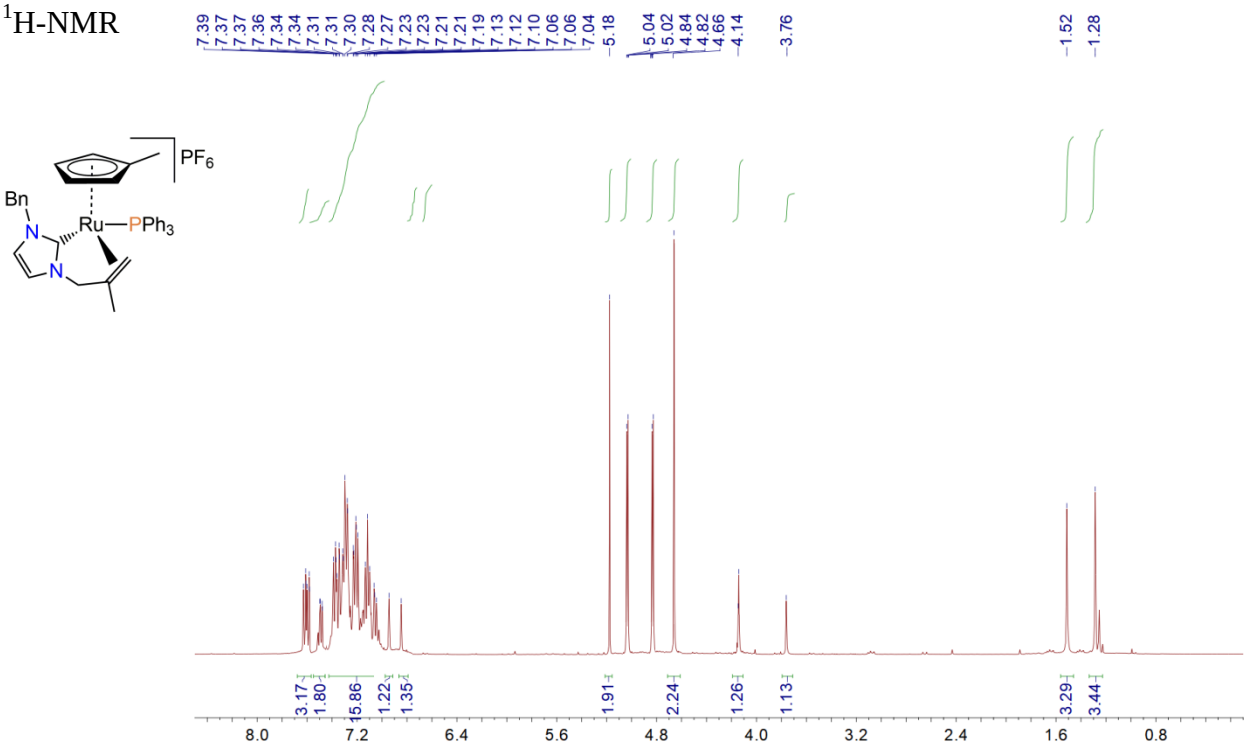


^{31}P-NMR

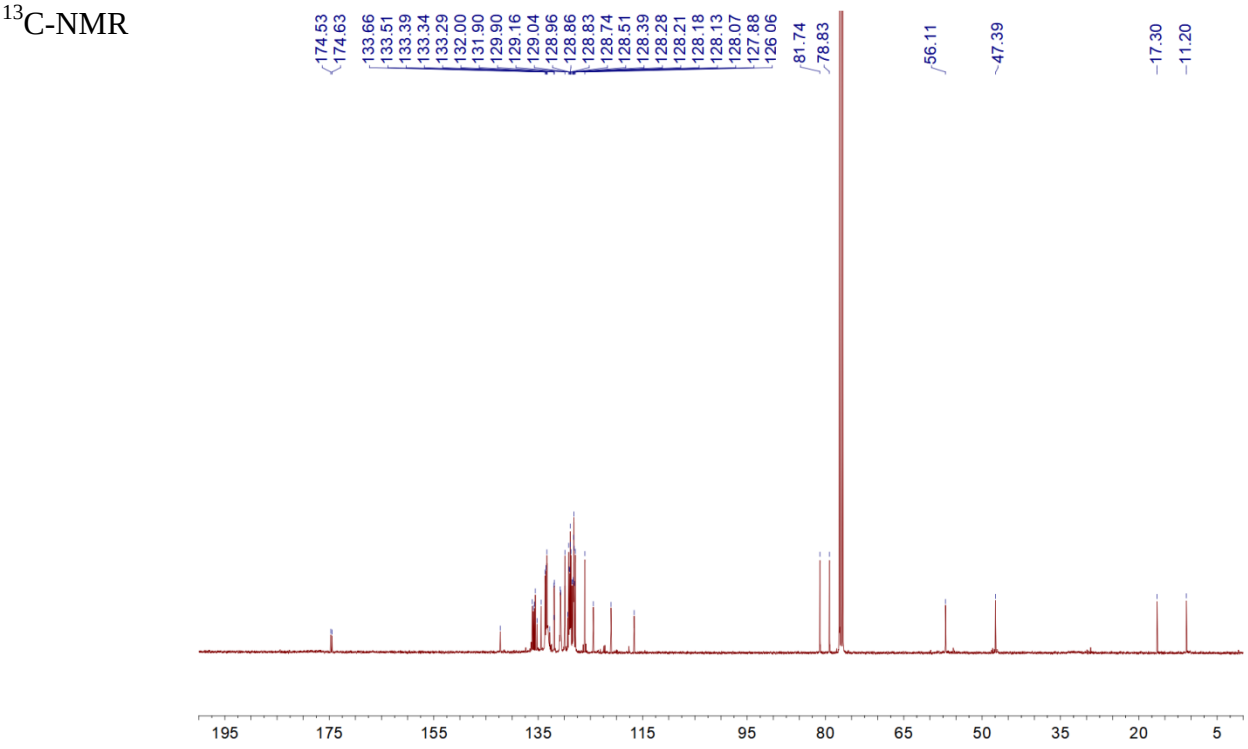


Complex **7**

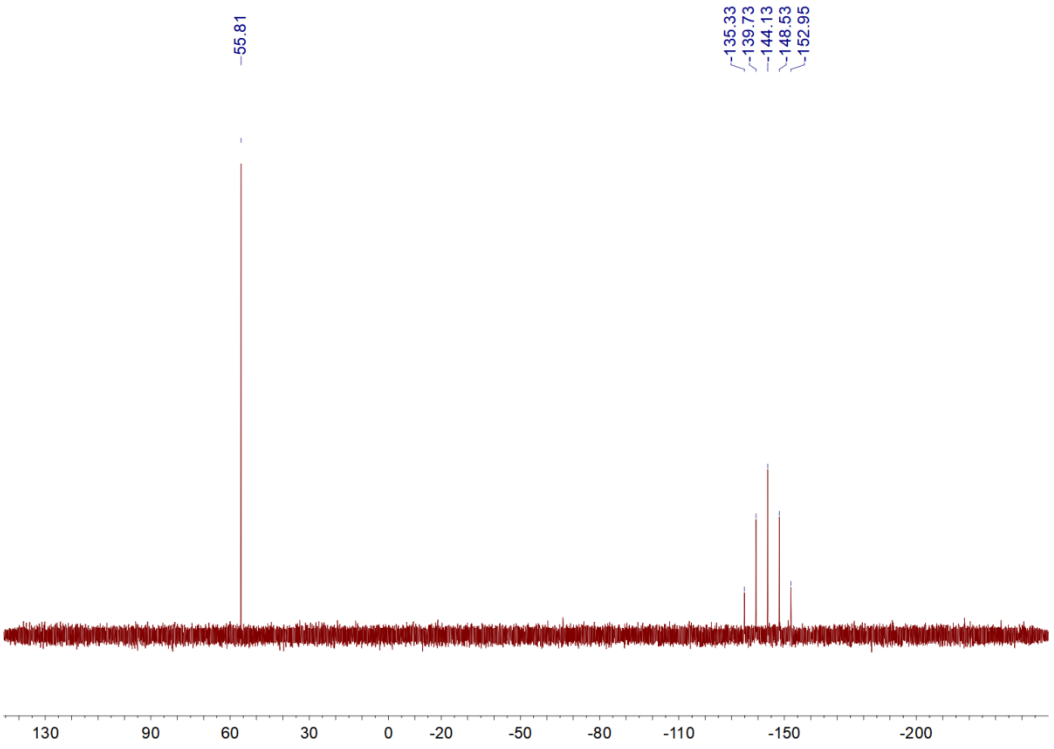
^{1}H-NMR



^{13}C-NMR

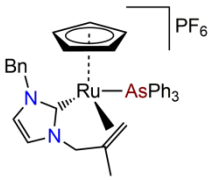


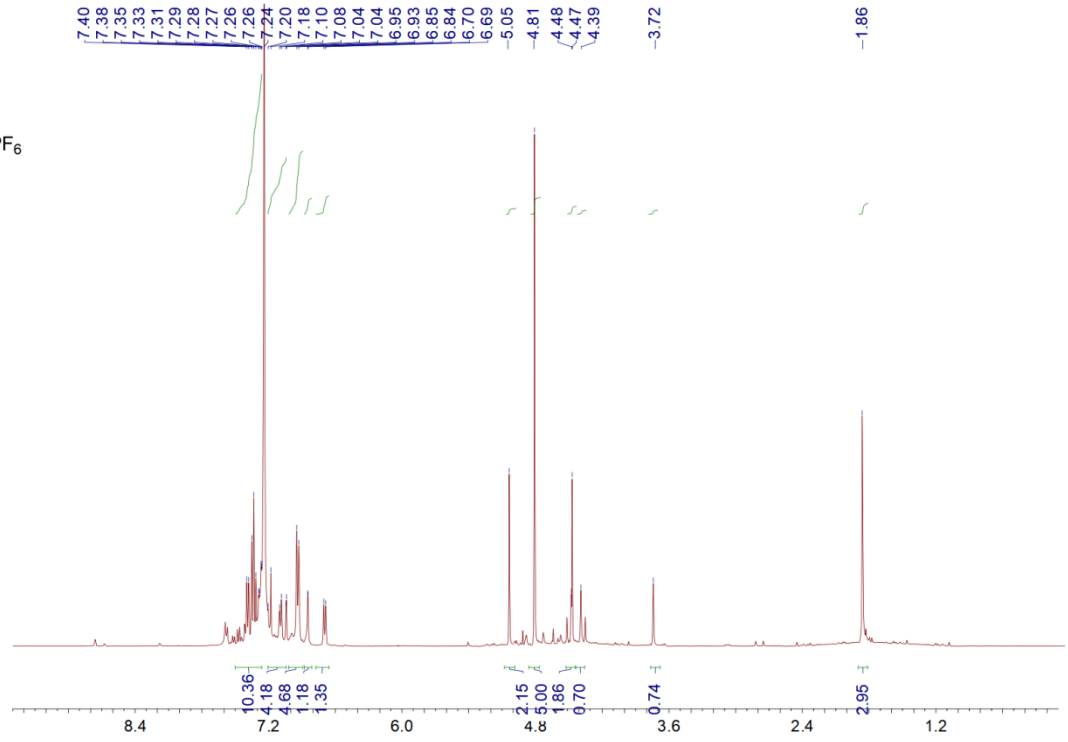
^{31}P-NMR



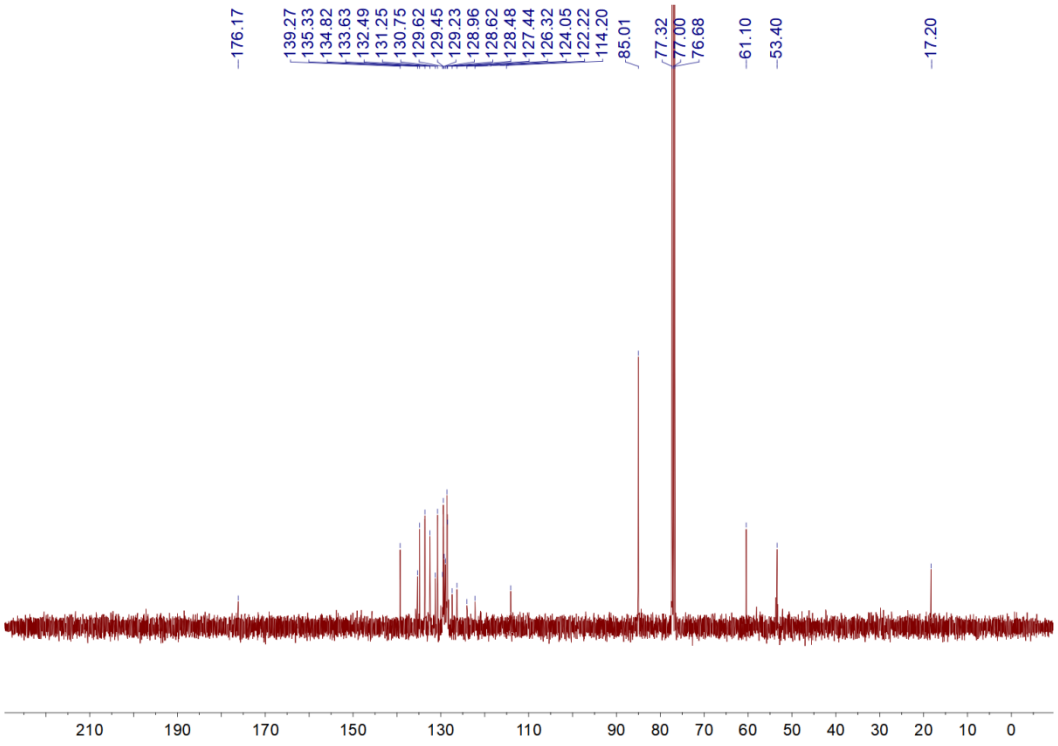
Complex **8**

^{1}H-NMR

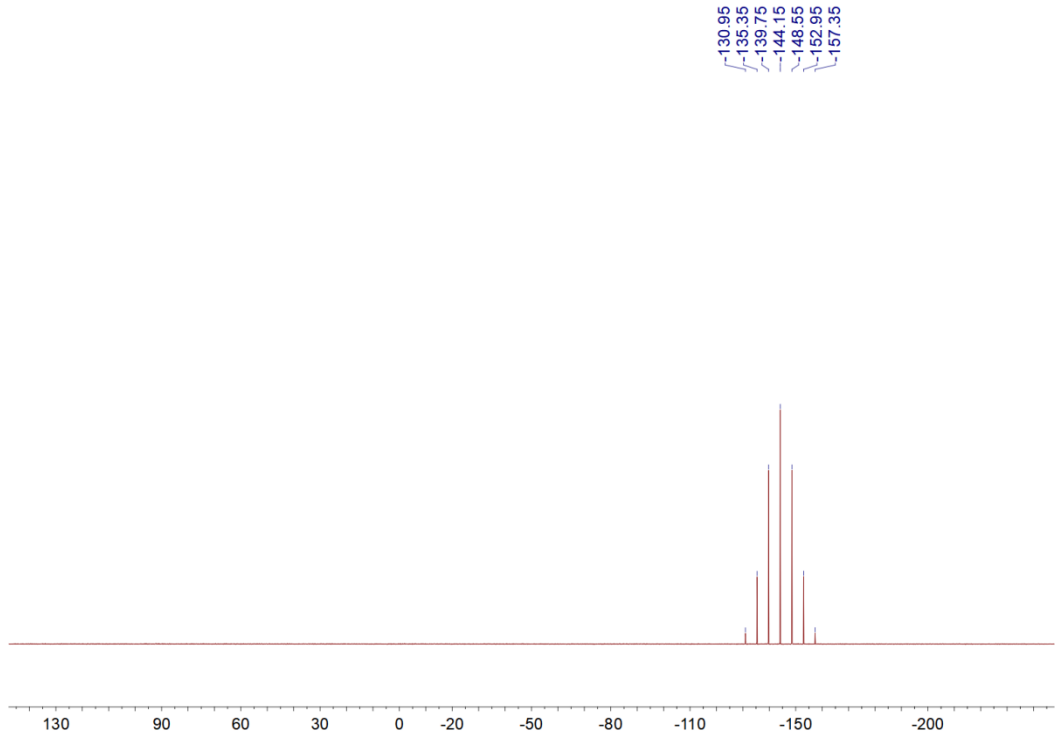




^{13}C-NMR

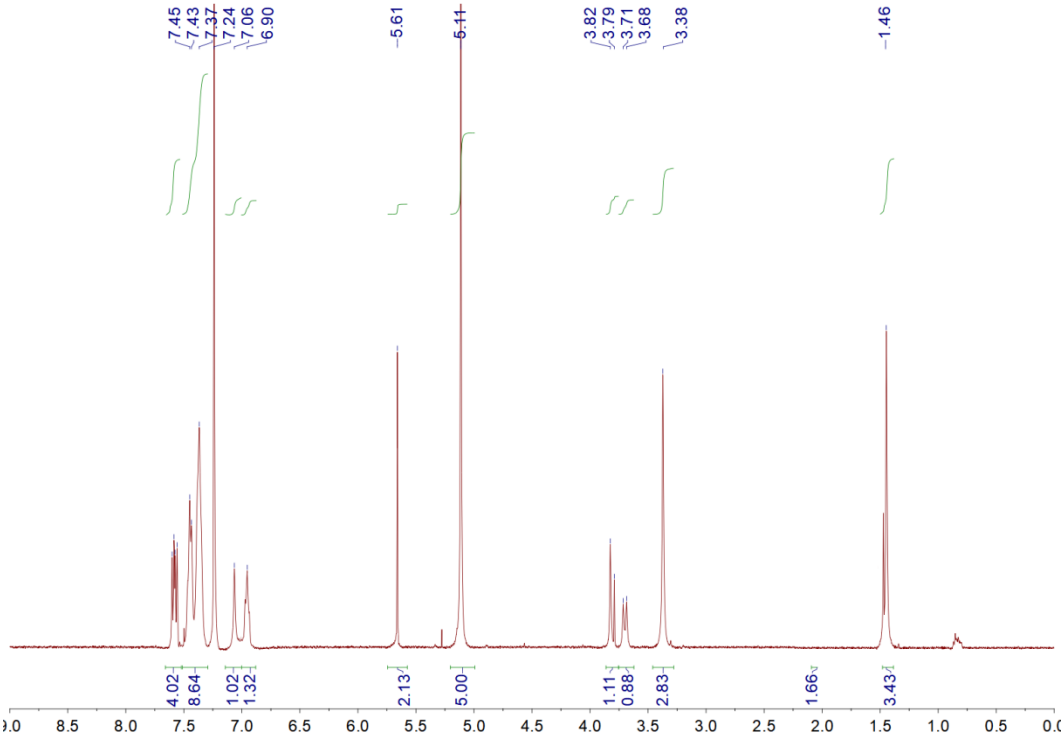


^{31}P-NMR

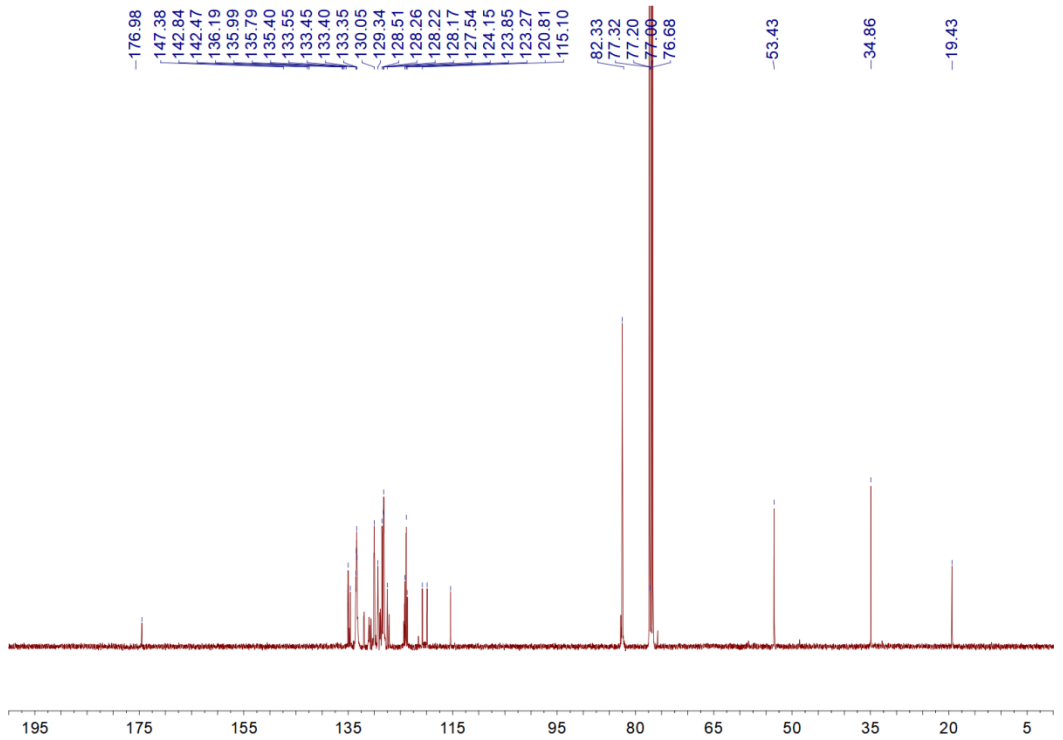


Complex **1b**

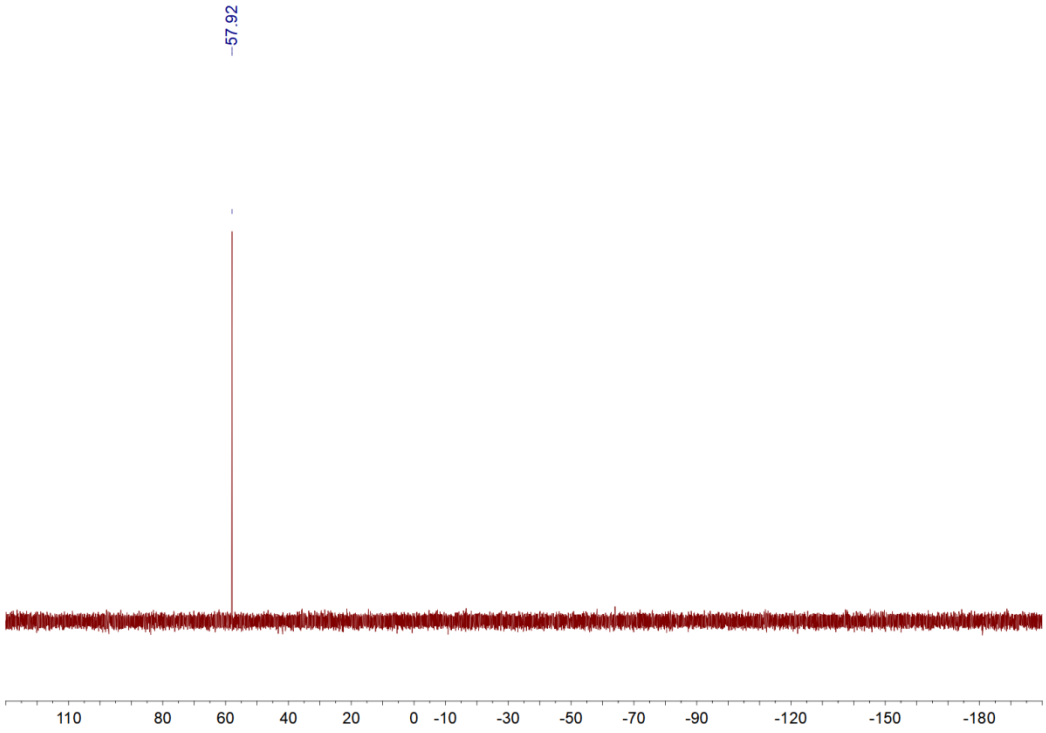
^{1}H-NMR



^{13}C-NMR



^{31}P-NMR



3. Crystal data and structure refinement for **L5**, **P2**,**P3**,**1**,**2**,**4**,**5**,**8** (**Tables S1**,**S2**, **S3**)

Table S1

Complex	**L5**	**P2**	**P3**	**1**
Emp. formula	$C_{14.7}H_{24}N_{2.7}O_{0.7}Cl_{1.3}$	$C_{43}H_{39}Cl_3P_2Ru$	$C_{42}H_{37}Cl_3As_2Ru$	$C_{31}H_{32}N_2F_6P_2Ru$
Form. weight (g.mol^{-1})	295.64	740.17	898.97	709.59
Crystal system	orthorhombic	triclinic	triclinic	monoclinic
Space group	*Pbcn*	*P-1*	*P-1*	*P2$_1$/c*
Crystal descr.	colourless blade	yellow block	orange block	yellow plate
a (Å)	16.1278(8)	9.8196(2)	9.931(7)	16.2788(2)
b (Å)	12.2682(5)	14.155(3)	14.018(1)	9.1026(9)
c (Å)	12.5817(6)	14.978(3)	14.536(1)	19.875(2)
α (°)	90	73.264(8)	102.99(2)	90
β (°)	90	71.924(7)	104.958(2)	96.086(3)
γ (°)	90	78.353(7)	98.90(2)	90
Volume (Å^3)	2489.4(2)	1880.8(6)	1856.0(2)	2928.5(5)
Z	6	2	2	4
Abs. coeff. (m.mm^{-1})	0.280	0.600	2.438	0.708
F(000)	953.5	760.0	900.0	1440.0
Independent refl.	2565	7775	9240	6046
Completeness (%)	99.9	99.2	99.6	99.6
Data/Restr/Para	2565/0/138	7775/0/443	9240/0/433	6046/0/381
Goodness of fit on F^2	1.034	0.963	1.037	1.045

Final R_1 indexes	0.0376	0.0318	0.0264	0.0307
wR_2 indices (all data)	0.1331	0.1153	0.0524	0.0666
Largest diffr. peak and hole (e.Å^{-3})	0.31/-0.32	1.25/-0.97	0.47/-0.63	1.83/-1.02

Table S2

Complex	**2**	**4**	**5**	**8**
Emp. formula	$C_{38}H_{38}N_2F_6P_2Cl_2Ru$	$C_{38}H_{38}N_2F_6P_2Ru$	$C_{34}H_{36}N_2F_6P_2Ru$	$C_{150}H_{148}N_8F_{24}P_4As_4Cl_4Ru$
Form. weight (g.mol^{-1})	870.61	799.71	749.66	3488.51
Crystal system	monoclinic	triclinic	monoclinic	monoclinic
Space group	*$P2_1/n$*	*P-1*	*C2/c*	*$P2_1$*
Crystal descr.	yellow block	yellow needle	yellow block	yellow block
a (Å)	13.8600(6)	11.0881(7)	18.0319(9)	9.910(2)
b (Å)	13.9831(7)	13.1574(8)	13.2824(6)	24.910(5)
c (Å)	18.9389(9)	14.6115(8)	29.0663(1)	15.236(3)
α (°)	90	113.867(2)	90	90
β (°)	93.545(2)	95.538(2)	99.842(2)	108.51(3)
γ (°)	90	111.568(2)	90	90
Volume (Å^3)	3663.4(3)	1735.89(2)	6859.1(6)	3566.6(1)
Z	4	2	8	1
Abs. coeff. (m.mm^{-1})	0.723	0.607	0.609	1.542
F(000)	1768.0	816.0	3056.0	1753.0
Independent refl.	7590	7167	7046	14652
Completeness (%)	99.7	99.9	99.8	99.7
Data/Restr/Para	7590/0/461	7167/0/443	7046/0/408	14652/1/905
Goodness of fit on F^2	1.535	1.096	1.132	0.843
Final R_1 indexes	0.0532	0.0367	0.0351	0.0289
wR_2 indices (all data)	0.1895	0.1288	0.0842	0.0637
Largest diffr. peak and hole (e.Å^{-3})	1.98/-1.82	1.08/-0.87	0.73/-0.80	0.63/-0.54

Table S3

Complex	**1b**
Emp. formula	$C_{15.5}H_{16}NP_{0.5}I_{1.5}Ru_{0.5}$
Form. weight (g.mol^{-1})	472.66
Crystal system	triclinic
Space group	*P-1*
Crystal descr.	yellow block
a (Å)	9.4358(2)
b (Å)	9.7889(2)
c (Å)	18.948(4)

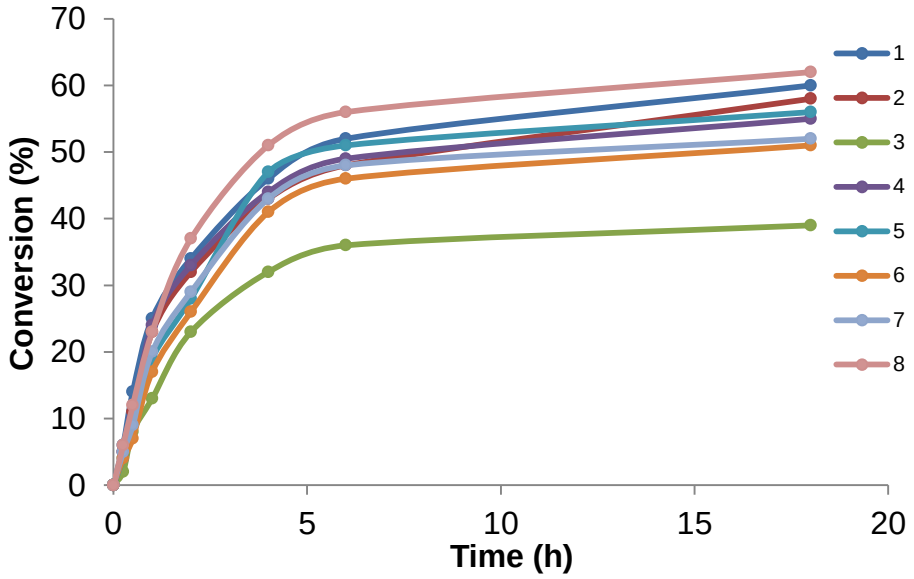
α (°)	91.365(6)
β (°)	94.352(6)
γ (°)	114.451(5)
Volume ($Å^3$)	1585.6(5)
Z	4
Abs. coeff. ($m.mm^{-1}$)	3.488
F(000)	900.0
Independent refl.	6706
Completeness (%)	98.4
Data/Restr/Para	6706/0/348
Goodness of fit on F^2	1.047
Final R_1 indexes	0.0218
wR_2 indices (all data)	0.0467
Largest diffr. peak and hole ($e.Å^{-3}$)	1.31/-1.27

4. Selected bond lengths and angles for **L5**, **P2**,**P3**,**1**,**2**,**4**,**5**,**8**,**1b** (**Table S4**)

Description	**L5**	**P2**	**P3**	**1**	**2**	**4**	**5**	**8**	**1b**
Ru1-C2	-	-	-	2.033(2)	2.042(4)	2.040(3)	2.038(3)	2.035(4)	2.033(3)
Ru1-Cg[a]	-	1.844(3)	1.813(4)	1.899(3)	1.894(3)	1.892(4)	1.889(6)	1.874(6)	1.907(7)
Ru-E1[b]	-	2.3222(7)	2.4229(2)	2.3262(6)	2.2993(1)	2.3135(7)	2.3168(6)	2.4190(7)	2.3155(8)
Ru1-C2-N1	-	-	-	120.23(2)	119.90(3)	119.95(2)	119.60(2)	119.7(3)	120.81(2)
C2-Ru1-E1[b]	-	-	-	87.32(7)	88.98(1)	86.84(7)	87.19(7)	85.92(1)	87.51(7)
E1-Ru1-Ca[b,c]	-	-	-	93.99(7)	95.33(1)	95.34(7)	96.08(8)	94.50(9)	93.14(7)
C2-Ru1-Ca[c]	-	-	-	89.65(1)	89.58(1)	89.71(1)	89.66(1)	89.38(2)	89.38(1)
C2-N1-C4	125.22(1)			130.7(2)	118.0(3)	129.6(2)	118.4(2)	118.8(3)	117.6(2)
C2-N2-C8	126.14(2)	-	-	126.30(2)	127.00(3)	125.8(2)	126.4(2)	125.5(3)	126.1(2)
C2-N1-C4-C5	104.65(2)	-	-	28.3(3)	26.6(5)	24.7(3)	27.5(3)	-22.6(7)	-26.8(3)
C2-N2-C8-C9	-68.92(2)	-	-	-	-91.4(5)	-104.4(3)	-99.9(3)	100.9(7)	-

[a] Cg = centroid of arene/cyclopentadienyl moiety. [b] E = P (1-7), As (8). [c] Average position between two carbon atoms belonging to the alkene moiety.

5. Time-resolved conversion profiles in the transfer hydrogenation-epoxidation catalysis



General conditions: 4'-bromophenylphenacylbromide (BPAB, 0.6 mmol), iPrOH (4 mL), base (1.2 eq), [Ru] (2 mol%), 110 °C. Determined by ^{1}H-NMR, based on the average of at least two runs.

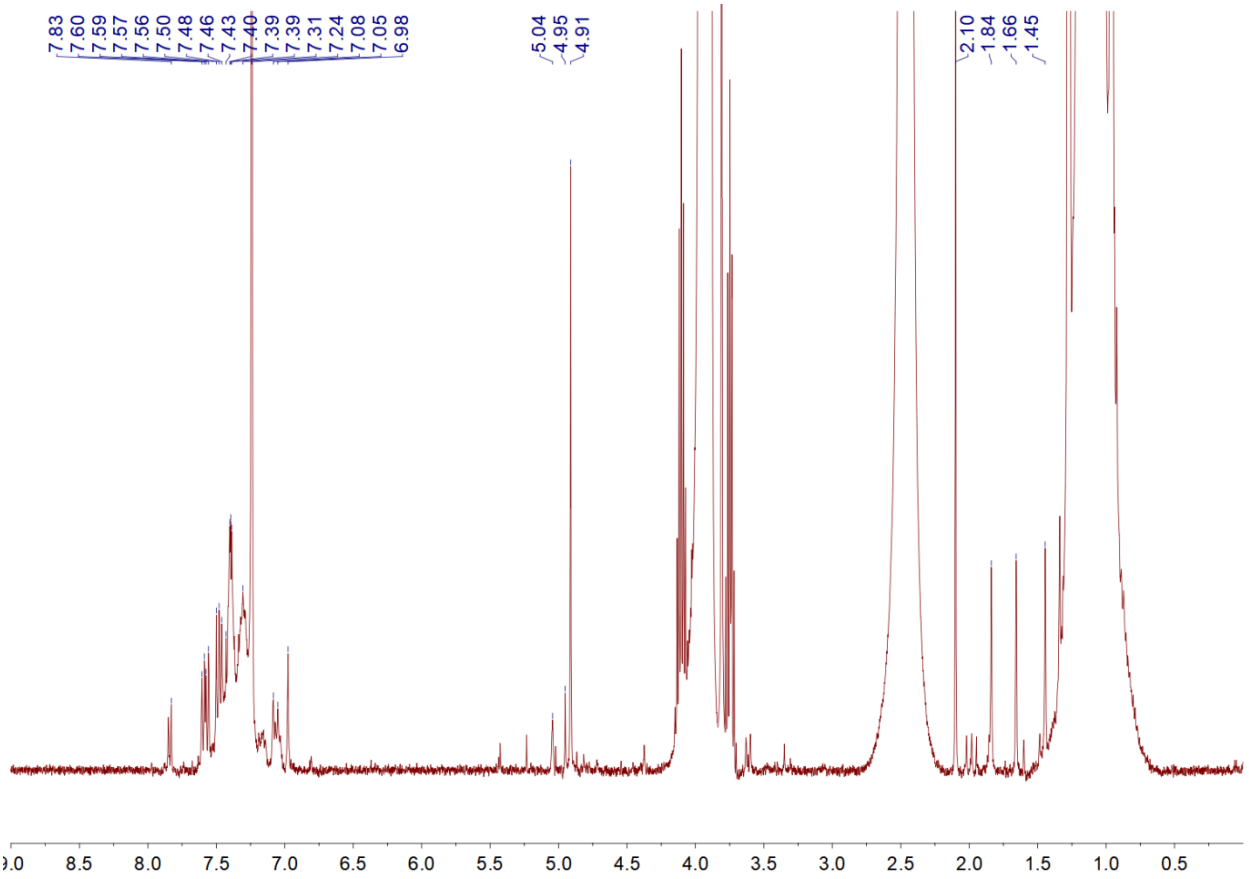
6. Optimization of transfer hydrogenation-epoxidation conditions (**Table S5**)

Table S5: Optimization of transfer hydrogenation-epoxidation conditions.

Entry	Complex	Temp (°C)	Base	Conversion[a] (%)			Selectivity[b] (%)
				2h	6h	18h	
1	-	110	-	0	1	2	0:0:100
2	-	110	KO^{t}Bu	0	2	3	0:0:100
3	**1**	110	-	20	36	41	90:3:7
4	**1**[c]	110	KOH	19	31	38	49:51:0
5	**1** (3 mol%)	110	KO^{t}Bu	37	55	63	29:71:0
6	**1** (1 mol%)	110	KO^{t}Bu	21	37	43	47:53:0
7	**1**	110	KOH	26	44	49	43:57:0
8	**1**	25	KOH	7	8	9	89:11:0

General conditions: 4'-bromophenylphenacylbromide (BPAB, 0.6 mmol), iPrOH (4 mL), base (1.2 eq), [Ru] (2 mol%), 110 °C. [a] Determined by ^{1}H-NMR, based on the average of at least two runs. [b] Selectivity (A:E:O) = alcohol:epoxide:other, after 18 hours.

7. ^{1}H-NMR spectrum of catalysis reaction mixture



General conditions: 4'-bromophenylphenacylbromide (BPAB, 0.6 mmol), iPrOH (4 mL), base (1.2 eq), [**1**] (2 mol%), anisole (0.6 mmol), 110 °C. Aliquot taken after 6 hours reaction time, analysed using $CDCl_3$.

Chapter 8
(De)hydrogenation catalysis by normal and abnormal alkene- and picolyl-tethered Ru(II)-NHC complexes

Frederick P. Malan,[†] Eric Singleton,[†] Petrus H. van Rooyen,[†] Marilé Landman[†*] and Martin Albrecht[‡*]

[†] *Department of Chemistry, University of Pretoria, 02 Lynnwood Road, Hatfield, Pretoria, 0002, South Africa.* [‡] *Department of Chemistry and Biochemistry, Universität Bern, Freiestrasse 3, 3012 Bern, Switzerland.*

Supporting Information

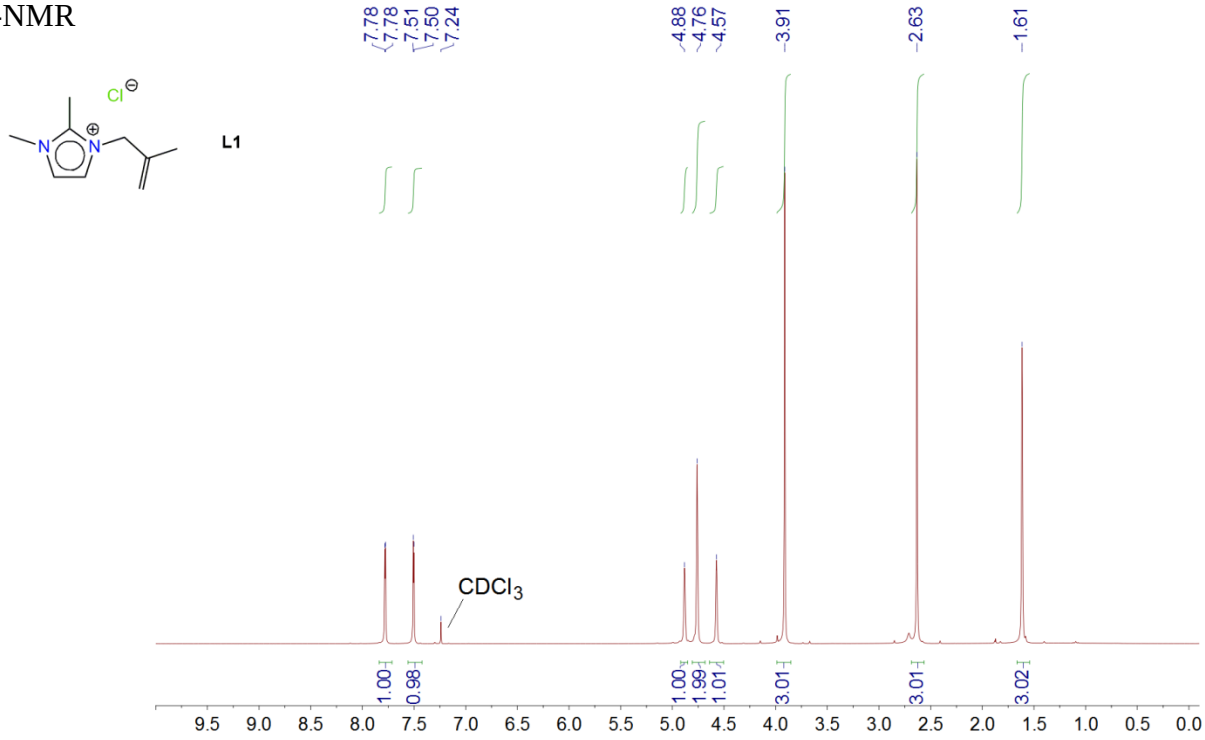
1. Synthesis, characterization, and NMR spectra of [H(**L1**-**L4**)]Cl
2. ^{1}H-, ^{13}C-, ^{31}P-NMR spectra of **1**-**10**
3. Crystal data and structure refinement for [H**L1**]Cl, [H**L4**]Cl, **1**,**3**,**5**,**6**,**7**,**8**,**10** (**Tables S1**,**S2**,**S3**)
4. Selected bond lengths and angles for [H**L1**]Cl, [H**L4**]Cl, **1**,**3**,**5**,**6**,**7**,**8**,**10** (**Table S4**)
5. **Figure S1**, **S2**: Perspective views of the crystal structures of **7** and **8**
6. Stacked ^{1}H-NMR of the stoichiometric addition of DCl to **1** (**Figure S3**)
7. Stacked ^{1}H-NMR of the stoichiometric addition of DCl to **3** (**Figure S4**)
8. Time-resolved conversion profiles in the transfer hydrogenation reactions
9. Time-resolved conversion profiles in the alcohol oxidation reactions
10. Optimization of transfer hydrogenation conditions (**Table S5**)
11. ^{1}H-NMR spectrum of transfer hydrogenation reaction mixture
12. ^{1}H-NMR spectrum of alcohol oxidation reaction mixture

1. Synthesis, characterization, and NMR spectra of [H(**L1**-**L4**)]Cl

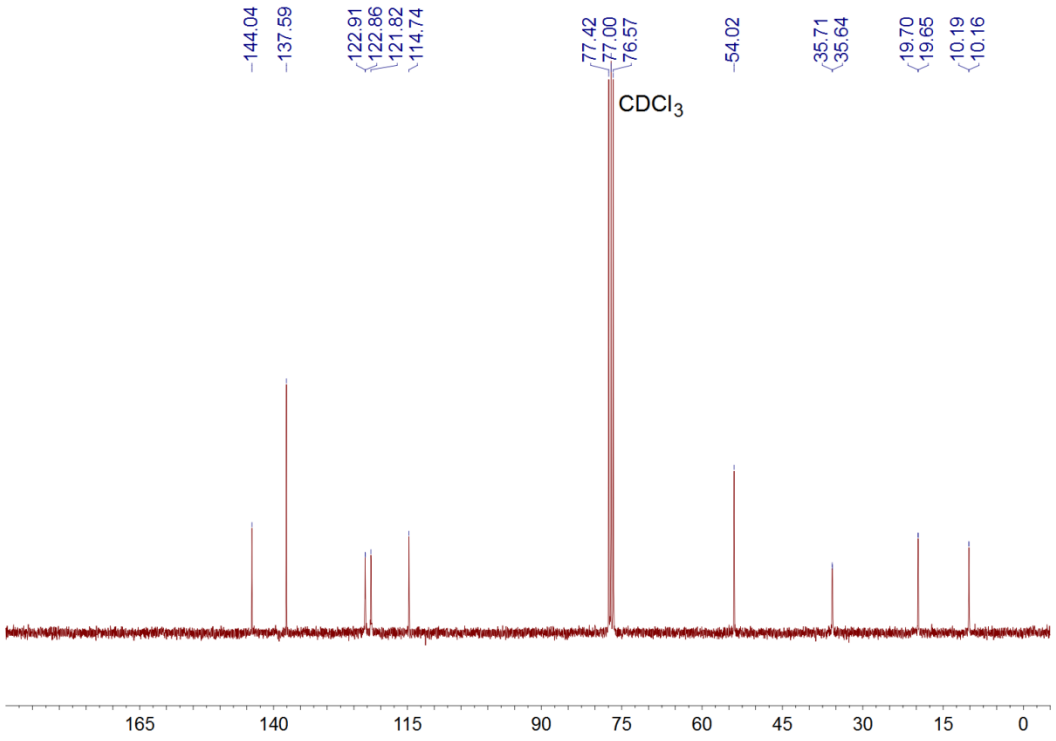
General synthesis of imidazolium salts: To an acetonitrile (20 mL) solution of 1,2-dimethylimidazole (42 mmol, **L1**, **L2**)/2,3,5-trimethylimidazole (42 mmol, **L3**)/1-(2-methylpropenyl)-2-isopropylimidazole (50 mmol, **L4**) was added the respective alkyl halide (1-chloro-2-methylpropene (**L1**, **L3**, **L4**) or picolyl chloride (**L2**)) (1 equivalent), and the resulting mixture heated under reflux overnight. After cooling, the reaction mixture was concentrated *in vacuo*, and washed with a 1:1 v/v Et_2O/Et_2OAc mixture (3 × 15 mL). The resulting oil/solid was concentrated in vacuo to give the respective ligand precursors [H(**L1**-**L4**)]Cl.

Ligand [H**L1**]Cl: Yield: 93%. ^{1}H-NMR ($CDCl_3$, δ_H) 1.61 (s, CH_3, 3H), 2.63 (s, CH_3, 3H), 3.91 (s, NCH_3, 3H), 4.57 (s, =CH, 1H), 4.76 (s, CH_2, 2H), 4.88 (s, =CH, 1H), 7.51 (d, $^{3}J_{HH}$ = 2 Hz, NCH, 1H), 7.78 (d, $^{3}J_{HH}$ = 2 Hz, NCH, 1H). ^{13}C{^{1}H}-NMR ($CDCl_3$, δ_C) 10.2 (s, CH$_3$), 19.7 (s, CH$_3$), 35.7 (s, =CH), 54.0 (s, CH$_2$), 114.7 (s, =CH), 121.8 (s, NCH), 122.9 (s, NCH), 137.6 (s, NCH$_3$), 144.0 (s, NCN).

^{1}H-NMR

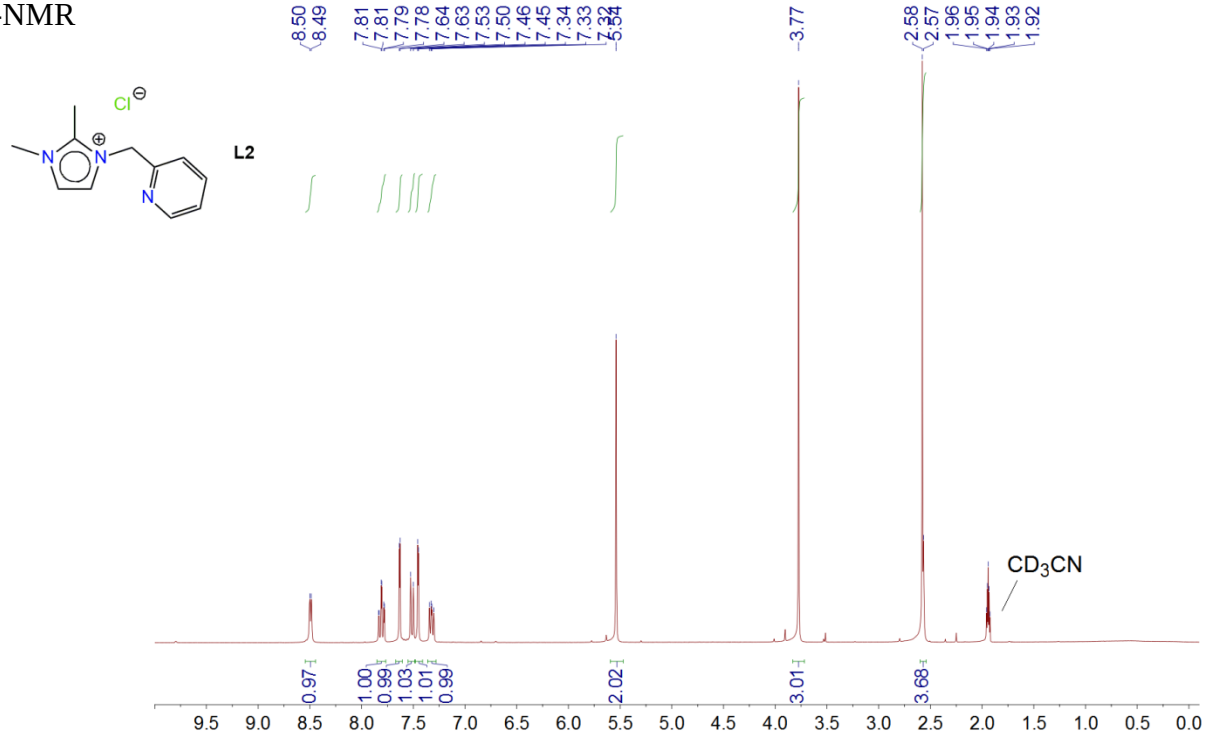


^{13}C-NMR

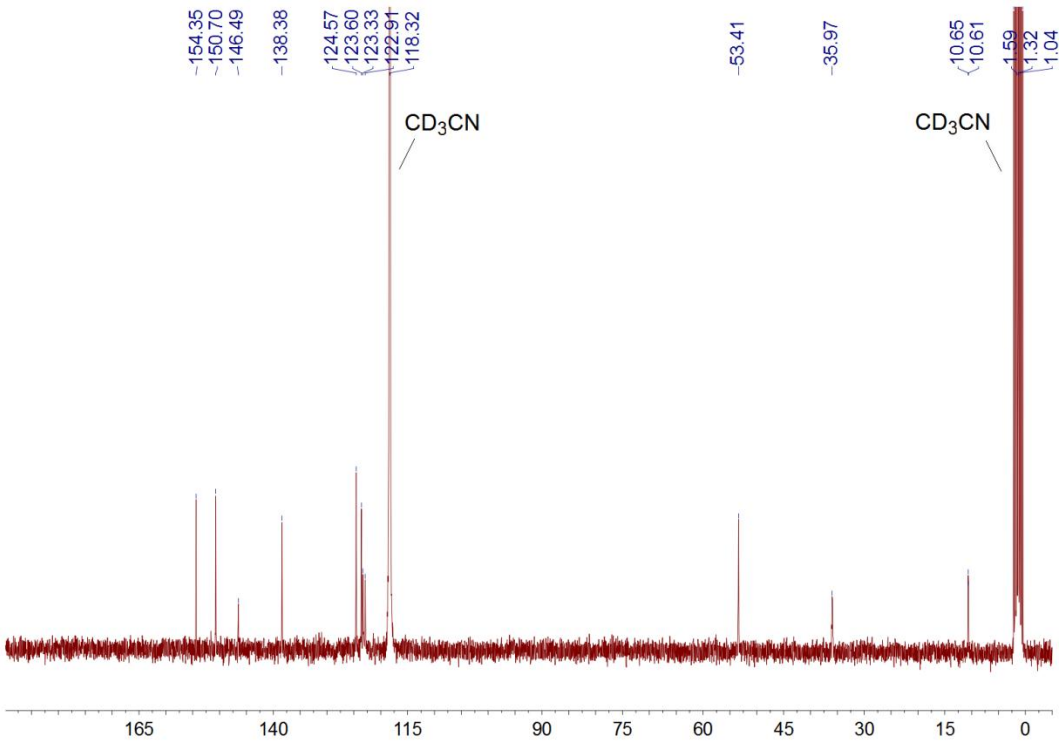


Ligand [H**L2**]Cl: Yield: 88%. ^{1}H-NMR (CD_3CN, δ_H) 2.60 (s, CH_3, 3H), 3.80 (s, NCH_3, 3H), 5.57 (s, CH_2, 2H), 7.33 (dd, $^{3}J_{HH}$ = 3 and 6 Hz, C_5H_4N, 1H), 7.46 (d, $^{3}J_{HH}$ = 2 Hz, NCH, 1H), 7.52 (d, $^{3}J_{HH}$ = 8 Hz, C_5H_4N, 1H), 7.64 (d, $^{3}J_{HH}$ = 2 Hz, NCH, 1H), 7.84 (ddd, $^{3}J_{HH}$ = 2 and 8 Hz, C_5H_4N, 1H), 8.52 (d, $^{3}J_{HH}$ = 4 Hz, NCH, 1H). ^{13}C{^{1}H}-NMR (CD_3CN, δ_C) 9.7 (s, CH_3), 35.0 (s, CH_3), 52.0 (s, CH_2), 121.9 (s, NCH), 122.4 (s, NCH), 122.6 (s, py), 123.6 (s, py), 137.4 (s, NCH_3), 145.5 (s, py), 149.7 (s, py), 153.4 (s, NCN).

^{1}H-NMR

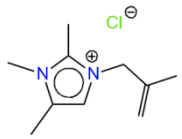


^{13}C-NMR

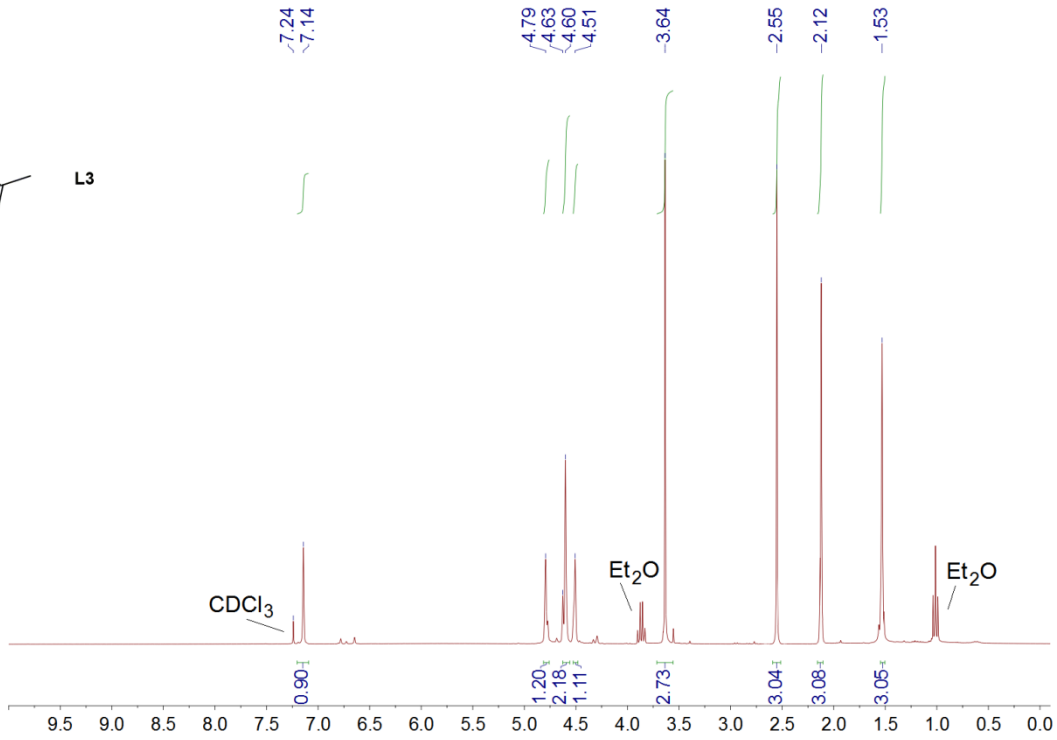


Ligand [H**L3**]Cl: Yield: 53%. ^{1}H-NMR ($CDCl_3$, δ_H) 1.53 (s, C*H*$_3$, 3H), 2.12 (s, C*H*$_3$, 3H), 2.55 (s, C*H*$_3$, 3H), 3.64 (s, NC*H*$_3$, 3H), 4.51 (s, =C*H*, 1H), 4.60 (s, C*H*$_2$, 2H), 4.79 (s, =C*H*, 1H), 7.14 (s, NC*H*, 1H). ^{13}C{^{1}H}-NMR ($CDCl_3$, δ_C) 10.4 (s, *C*H$_3$), 13.7 (s, *C*H$_3$), 19.5 (s, *C*H$_3$), 32.3 (s, =*C*H), 53.6 (s, *C*H$_2$), 114.5 (s, =*C*H), 118.7 (s, N*C*H), 129.7 (s, N*C*H), 137.4 (s, N*C*H$_3$), 143.6 (s, N*C*N).

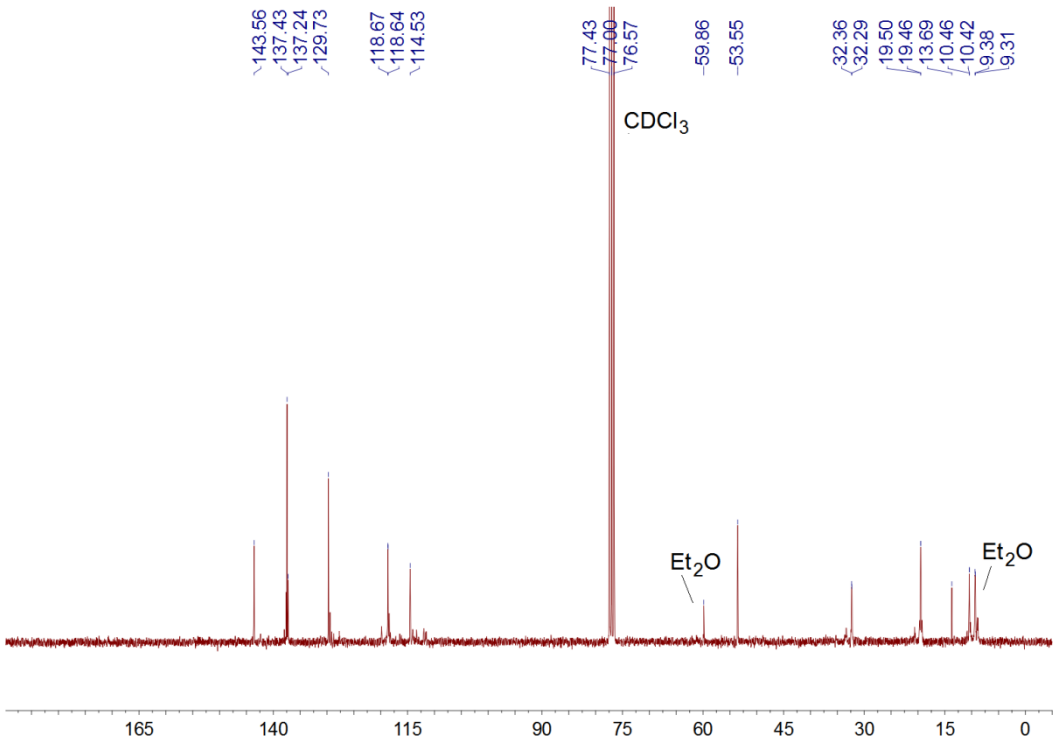
^{1}H-NMR



L3

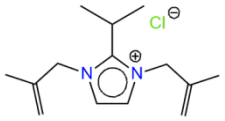


^{13}C-NMR

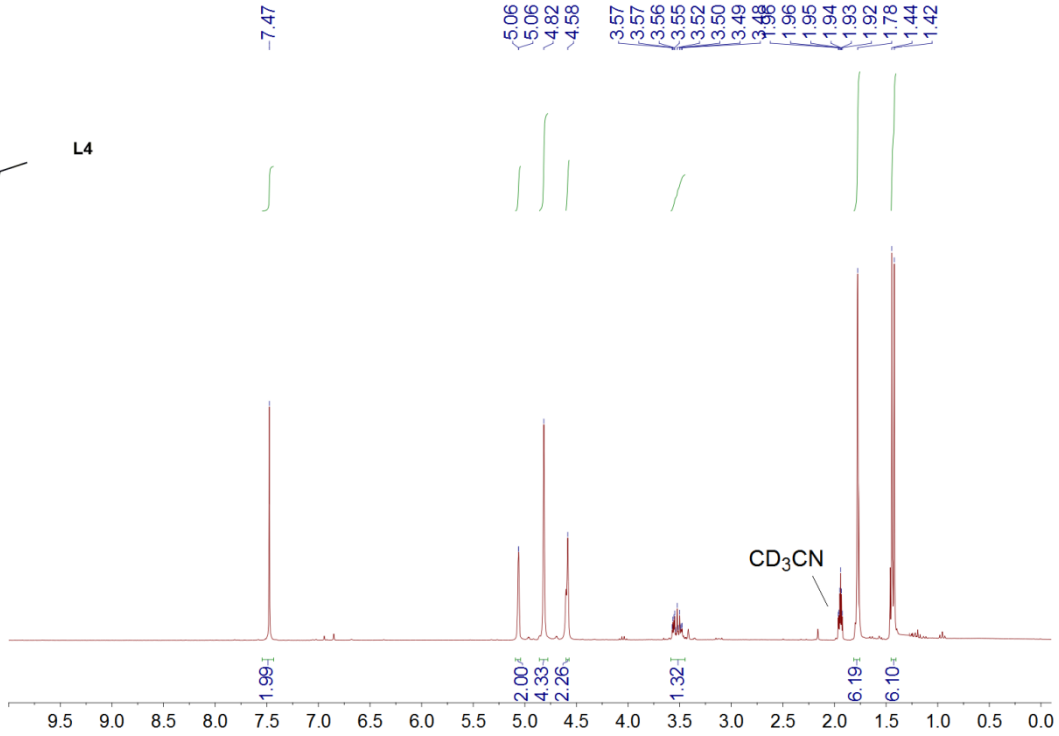


Ligand [H**L4**]Cl: Yield: 90%. ^{1}H-NMR (CD_3CN, δ_H) 1.43 (d, $^{3}J_{HH}$ = 7 Hz, CH_3, 6H), 1.78 (s, CH_3, 6H), 3.52 (m, CH, 1H), 4.58 (s, =CH, 2H), 4.82 (s, CH_2, 4H), 5.06 (s, =CH, 2H), 7.47 (s, NCH, 2H). ^{13}C{^{1}H}-NMR (CD_3CN, δ_C) 19.2 (s, CH$_3$), 20.0 (s, CH$_3$), 26.2 (s, =CH), 54.6 (s, CH$_2$), 114.0 (s, =CH), 123.7 (s, NCH), 140.8 (s, C(CH$_3$)$_2$), 151.4 (s, NCN).

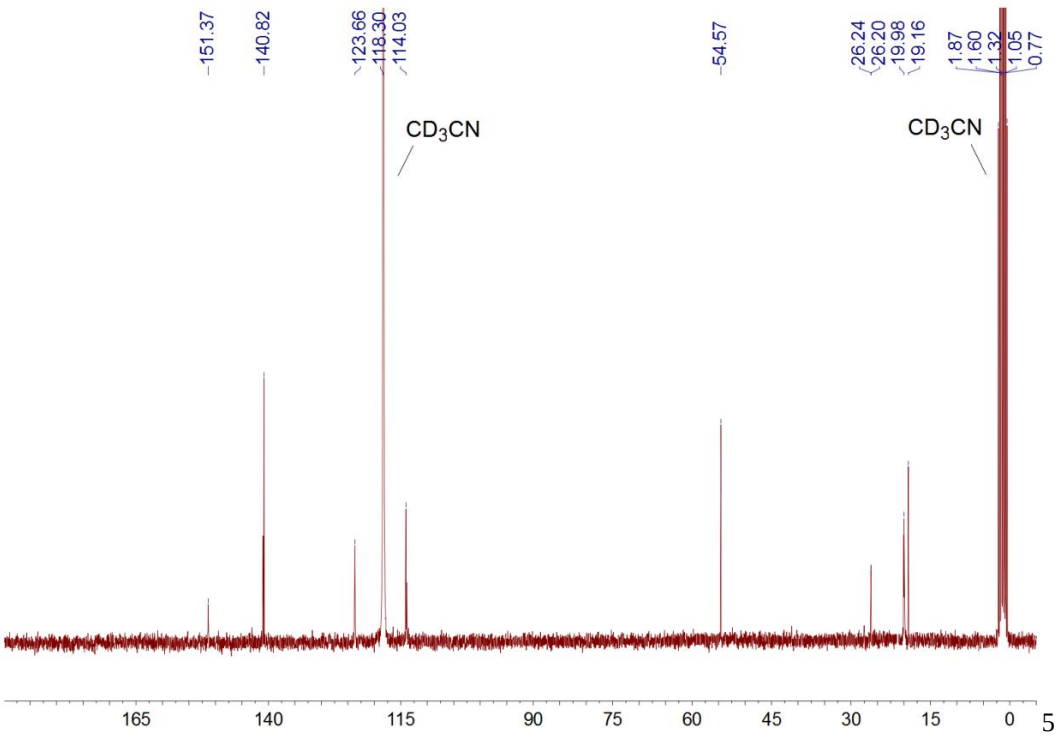
^{1}H-NMR



L4



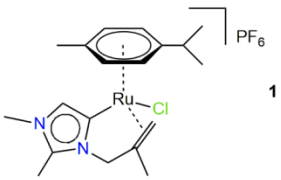
^{13}C-NMR



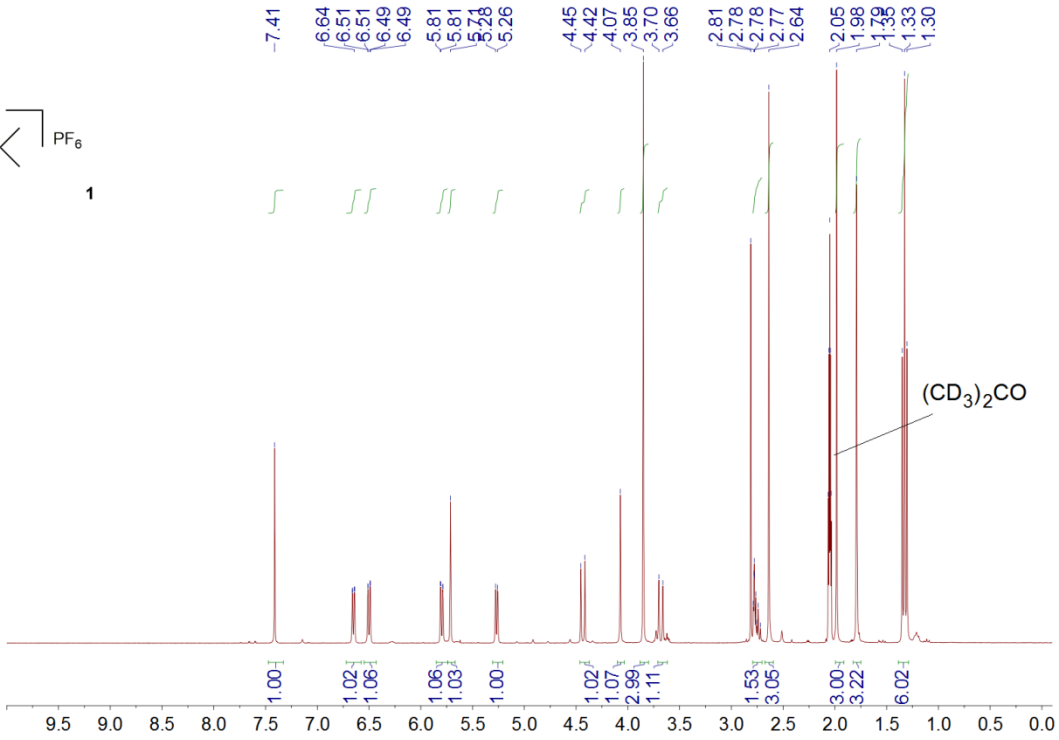
2. ^{1}H-, ^{13}C-, ^{31}P-NMR spectra of **1-10**

Complex **1**

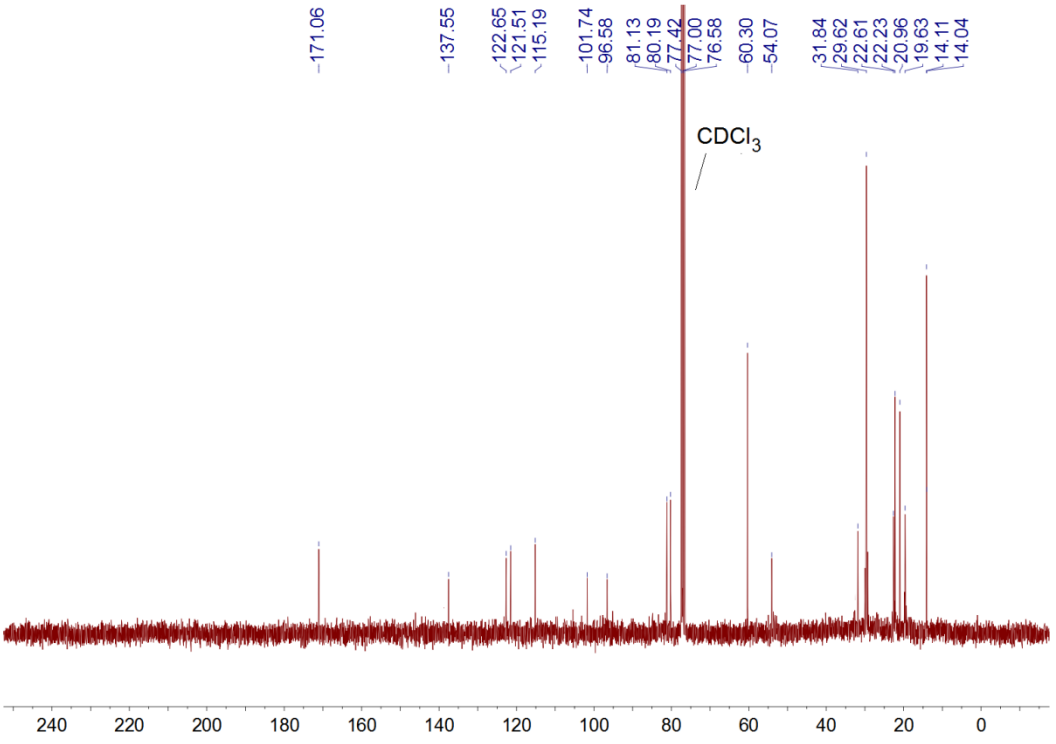
^{1}H-NMR



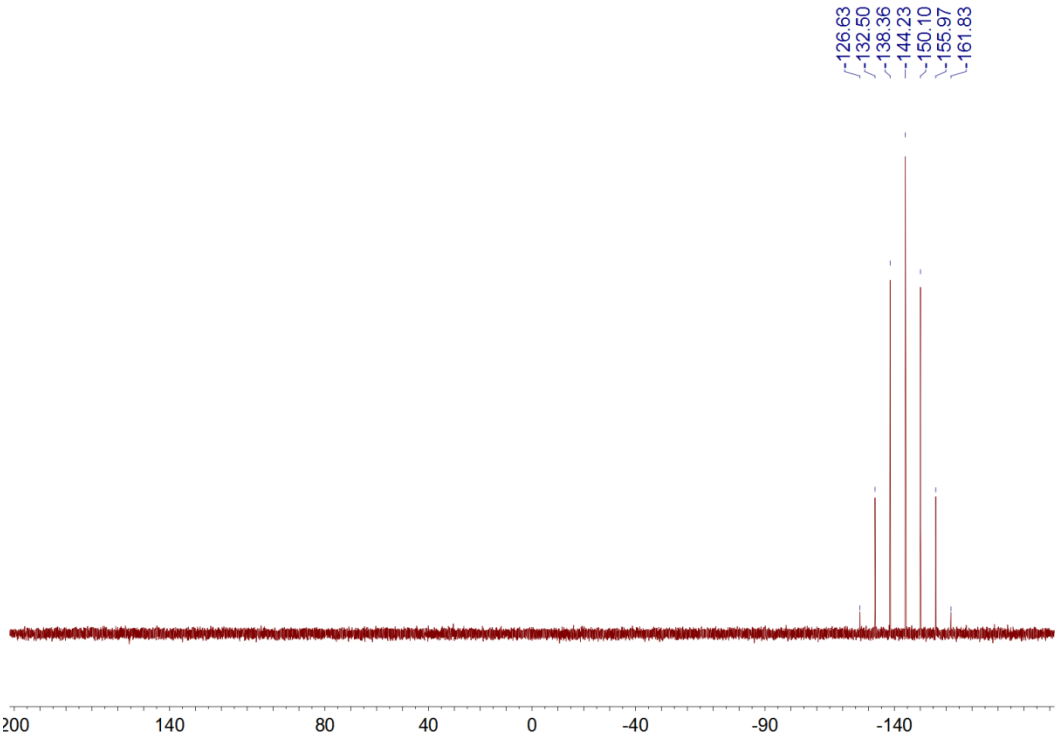
1



^{13}C-NMR

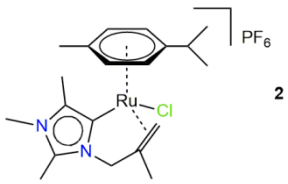


^{31}P-NMR

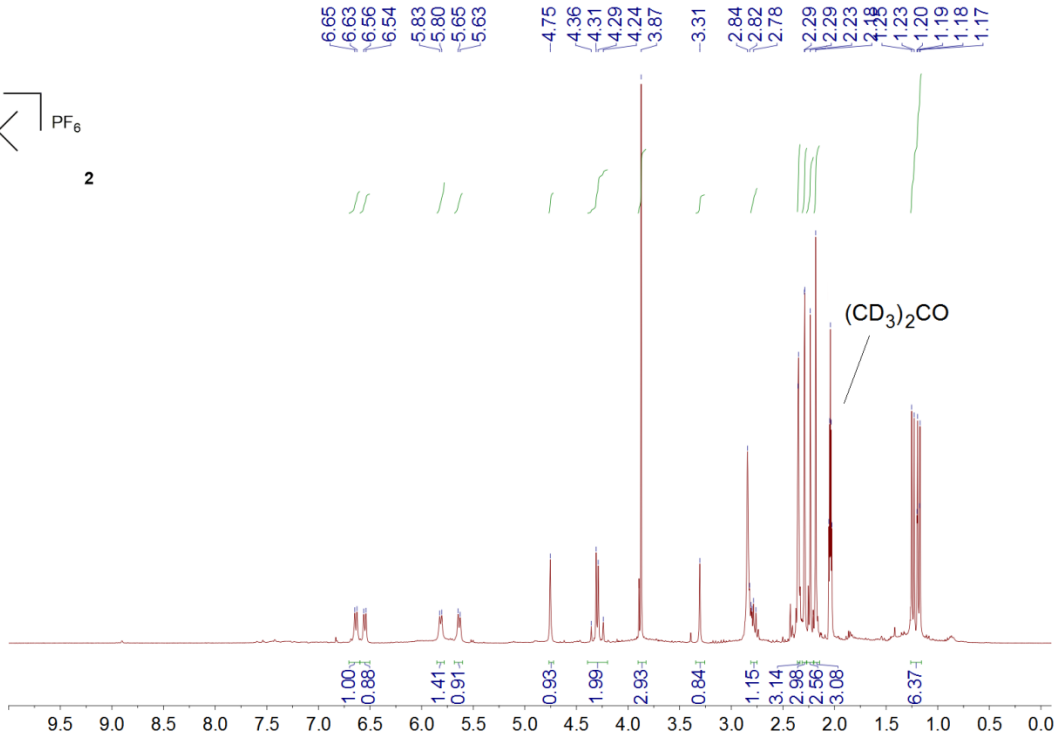


Complex **2**

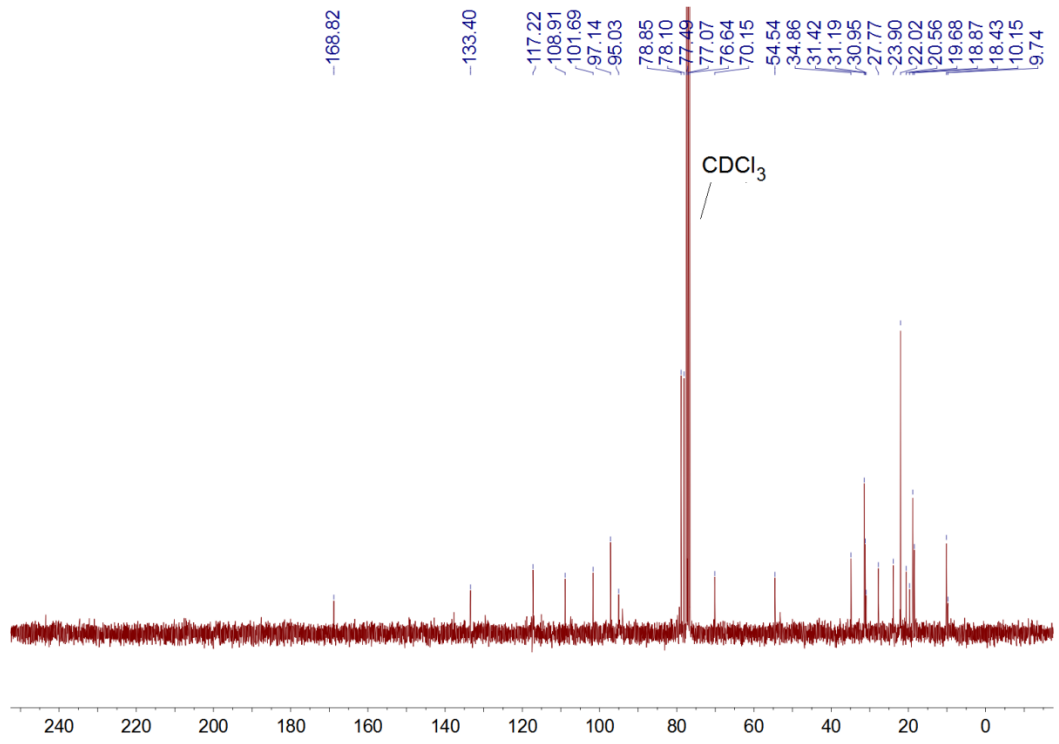
^{1}H-NMR



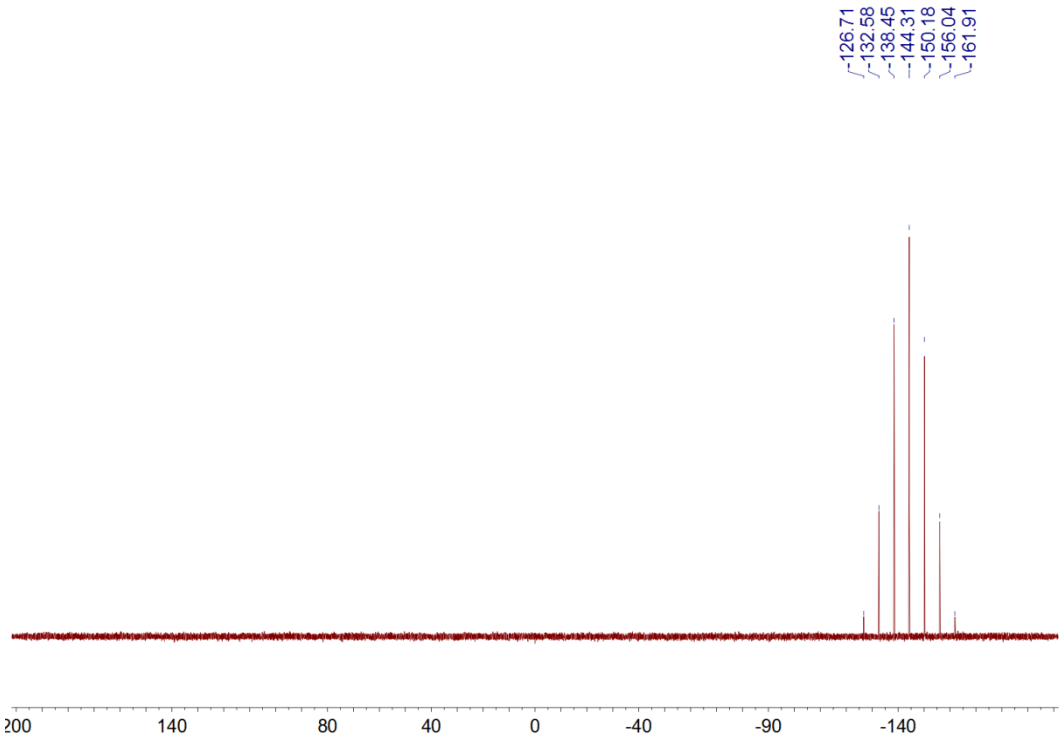
2



^{13}C-NMR

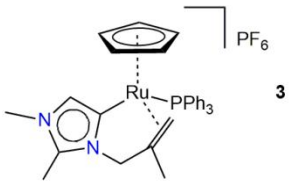


^{31}P-NMR

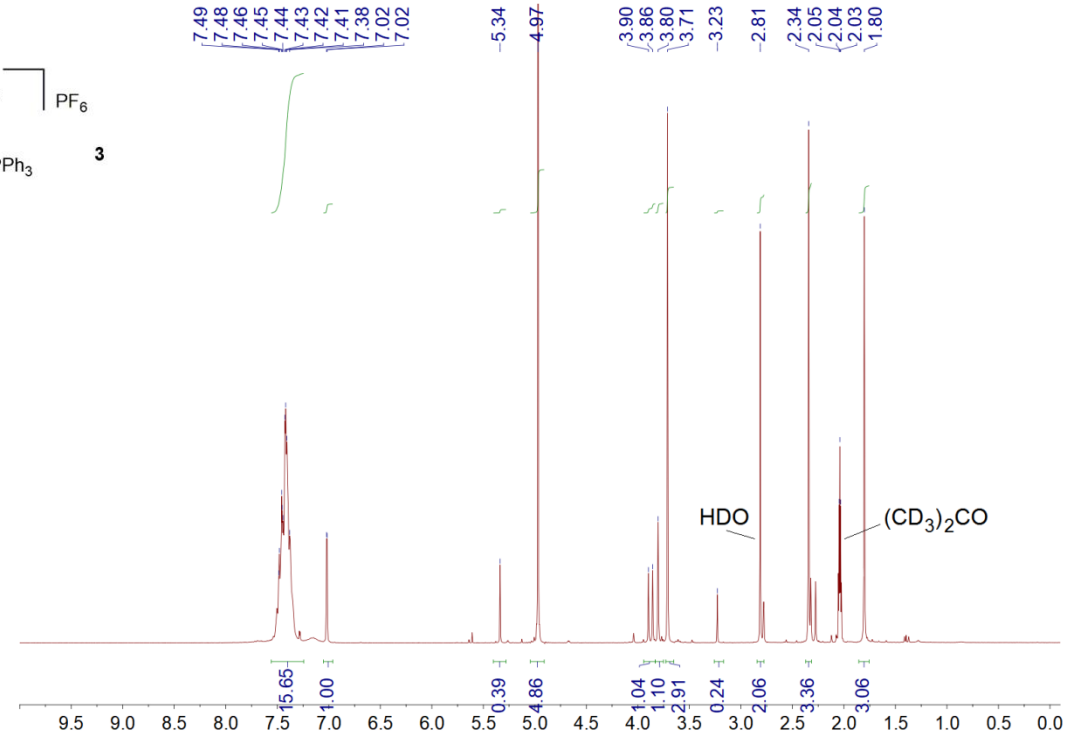


Complex **3**

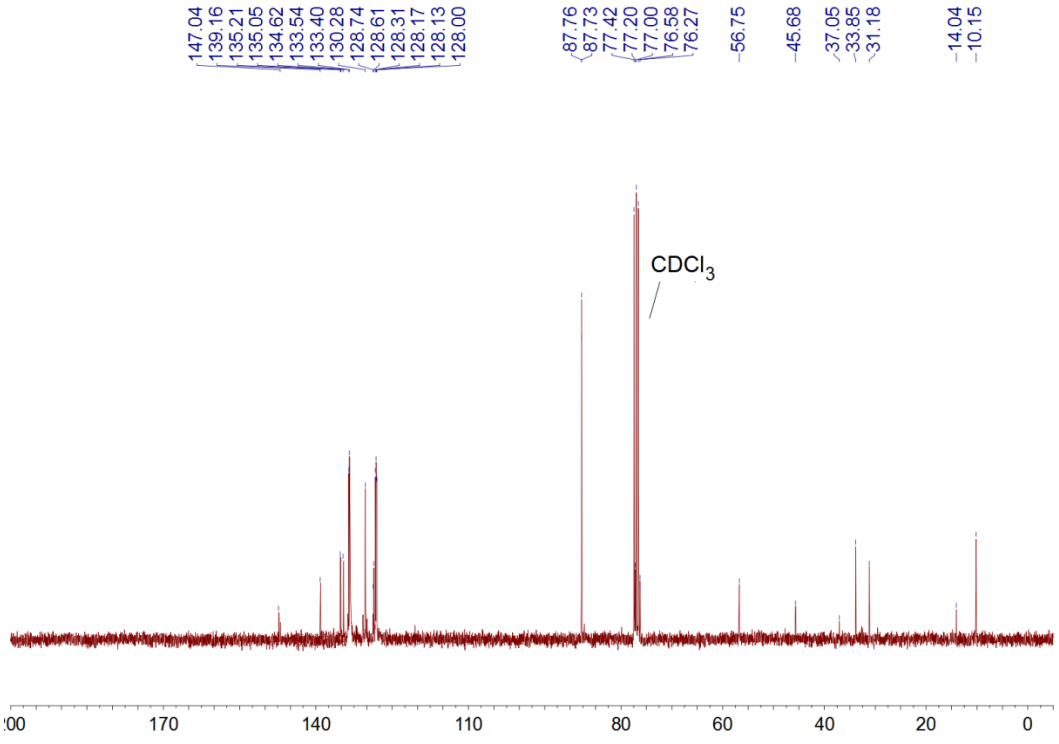
^{1}H-NMR



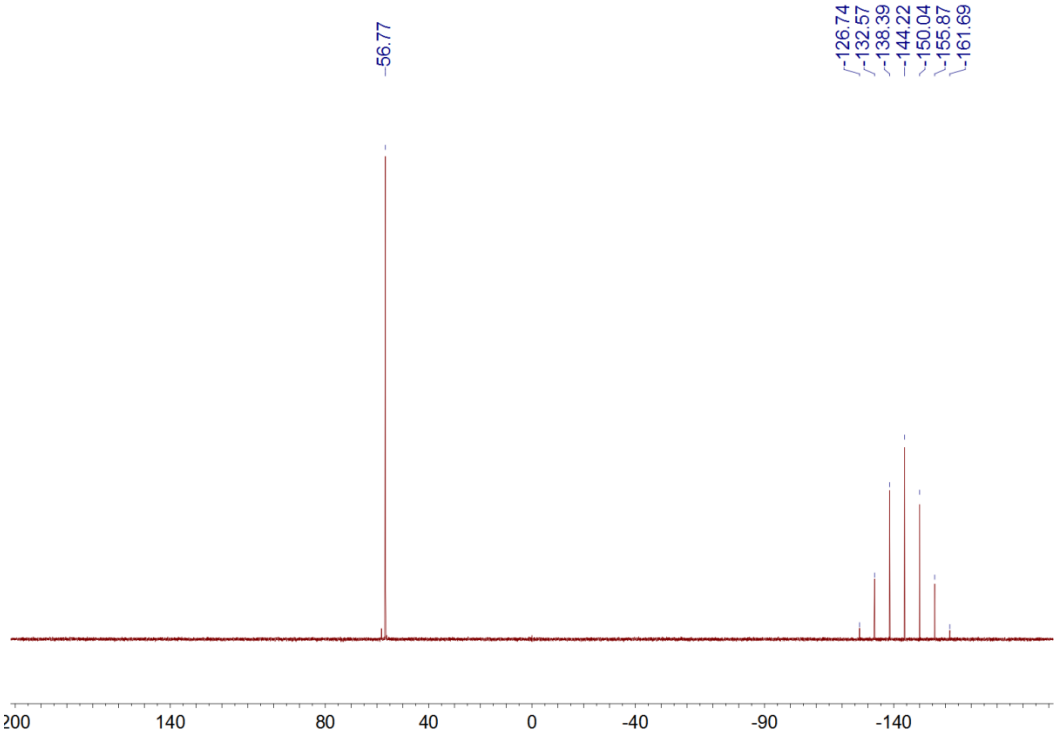
3



^{13}C-NMR

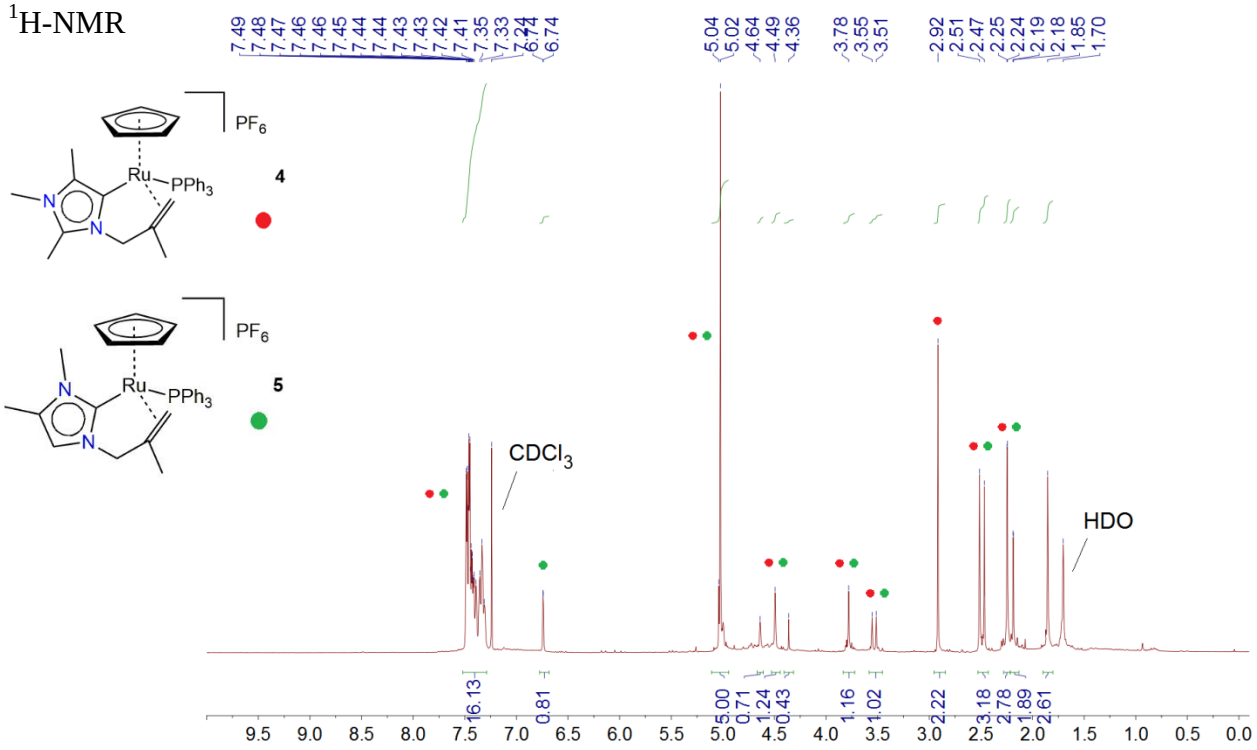


^{31}P-NMR

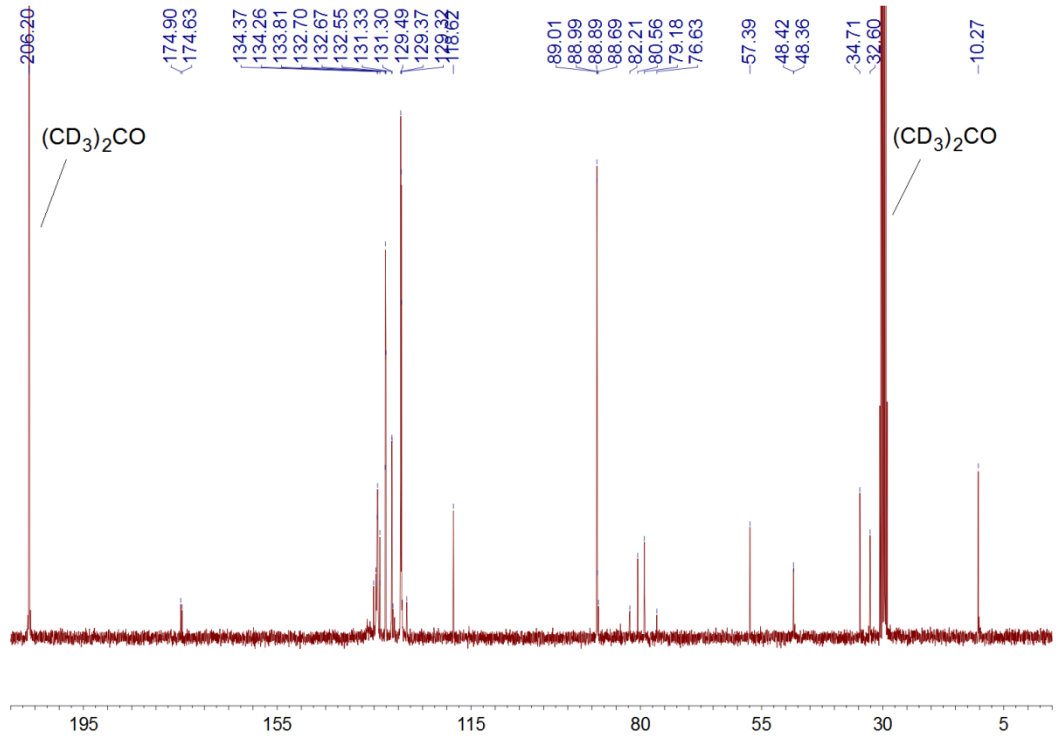


Complex **4,5**

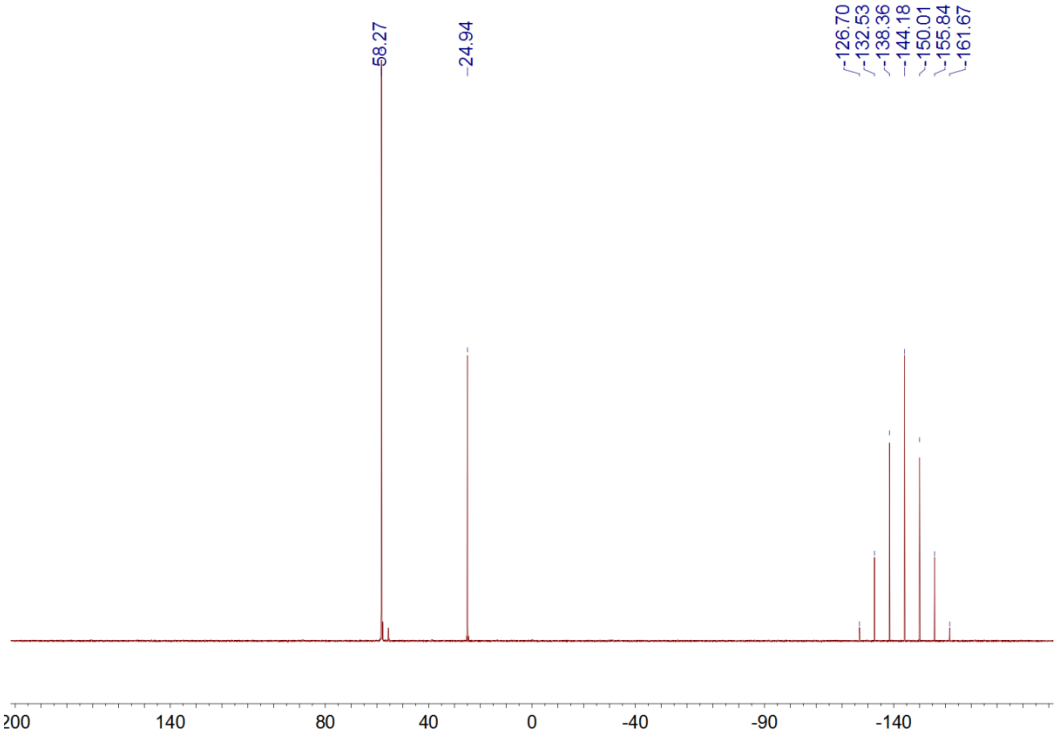
^{1}H-NMR



^{13}C-NMR

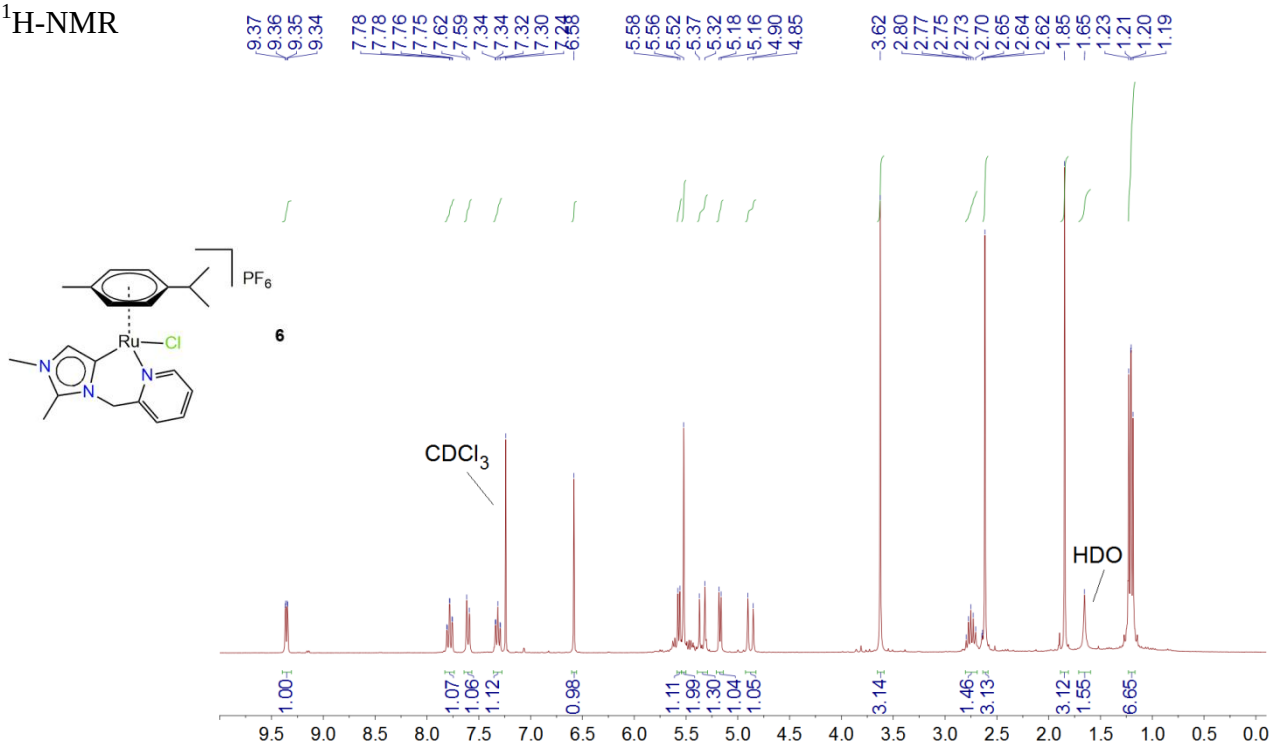


^{31}P-NMR

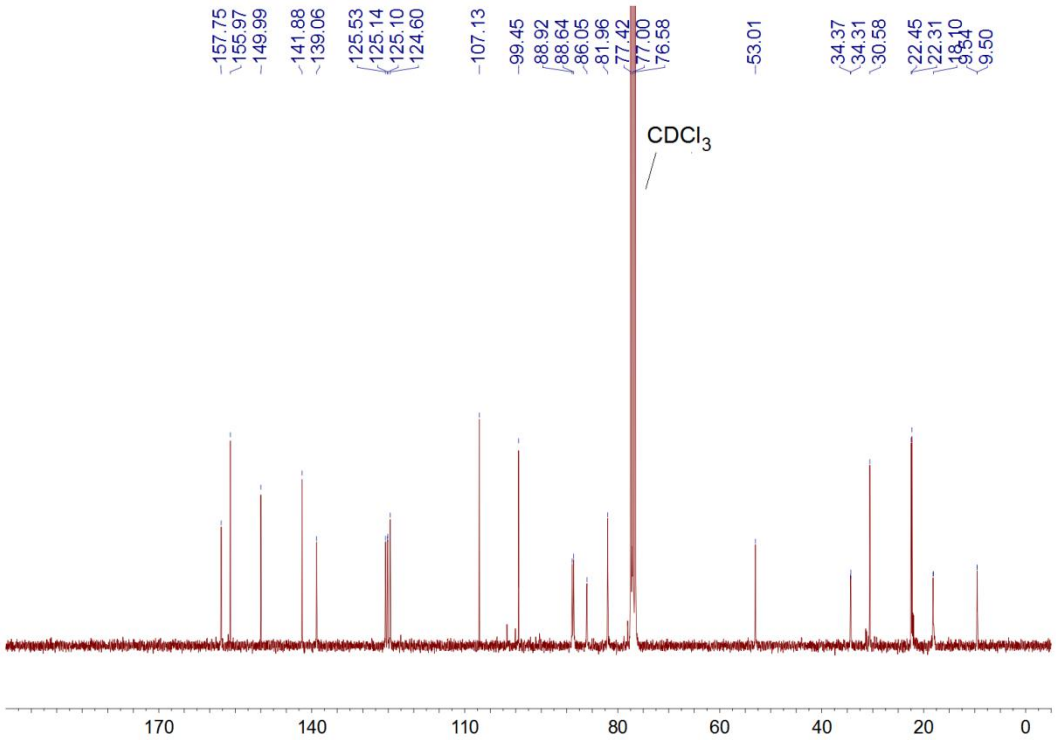


Complex **6**

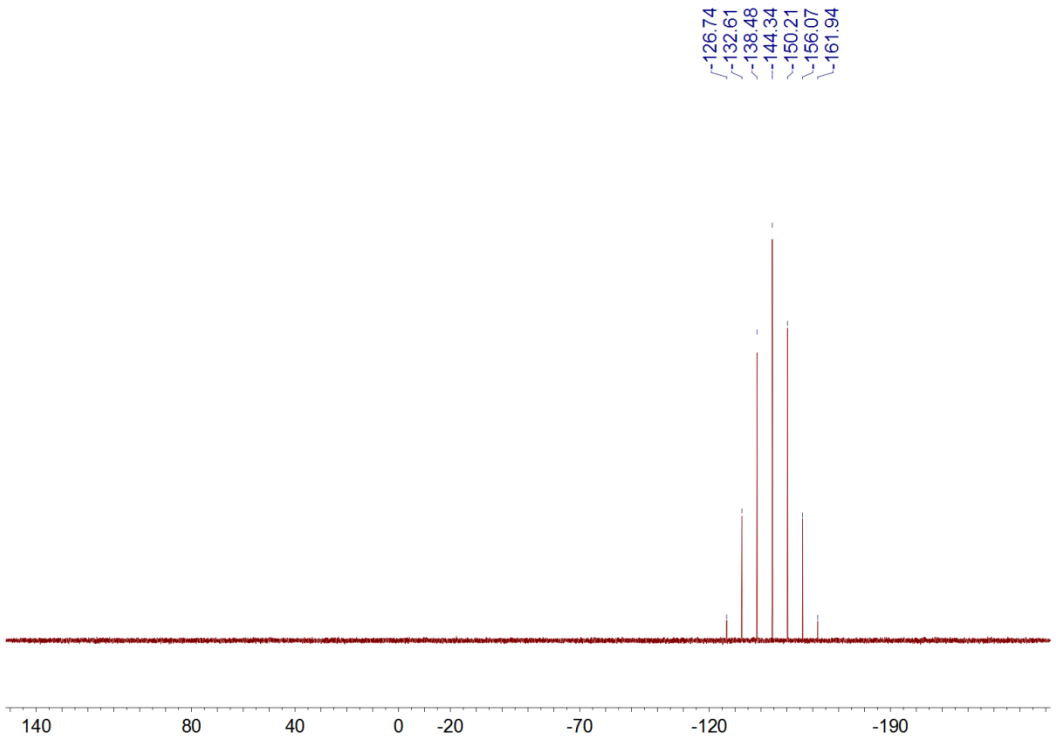
^{1}H-NMR



^{13}C-NMR

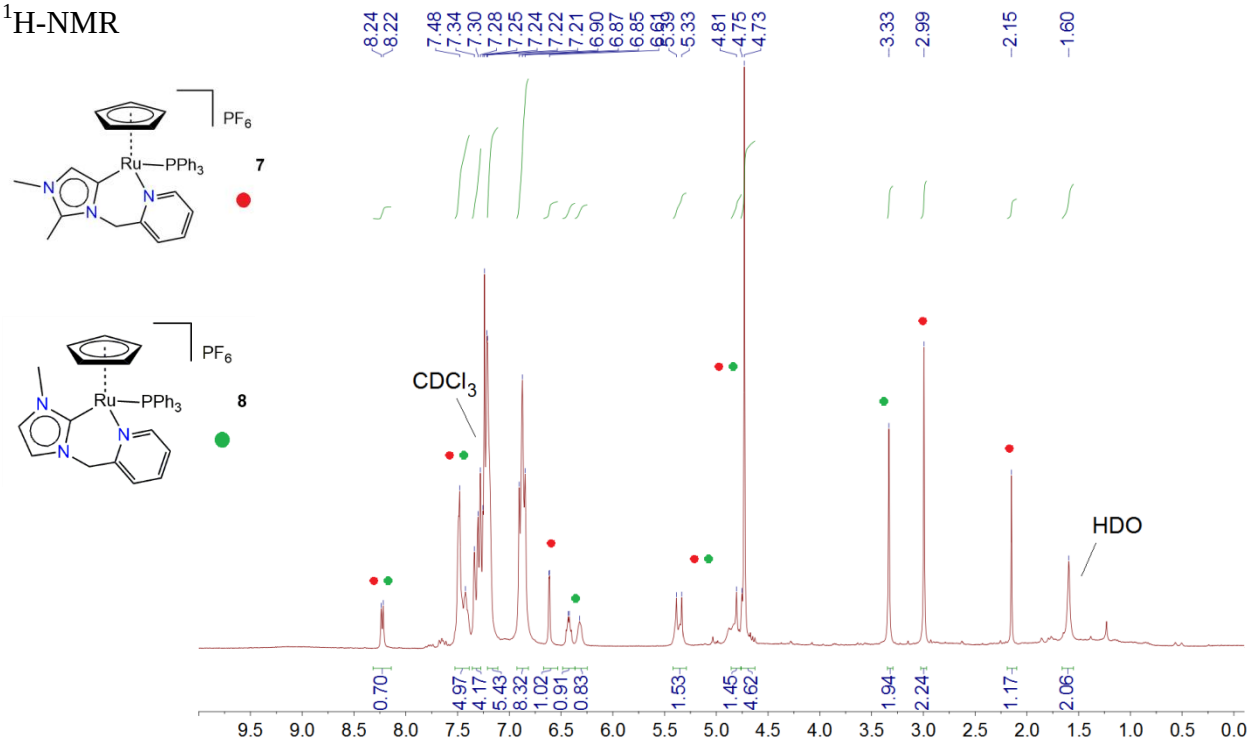


^{31}P-NMR

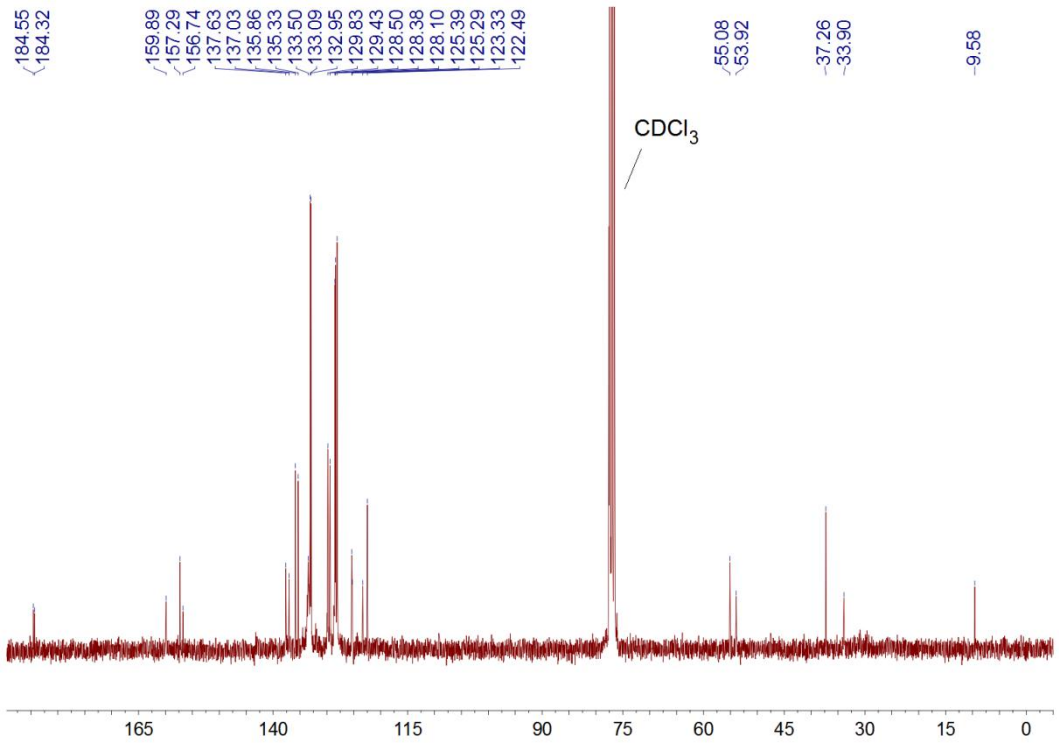


Complex **7,8**

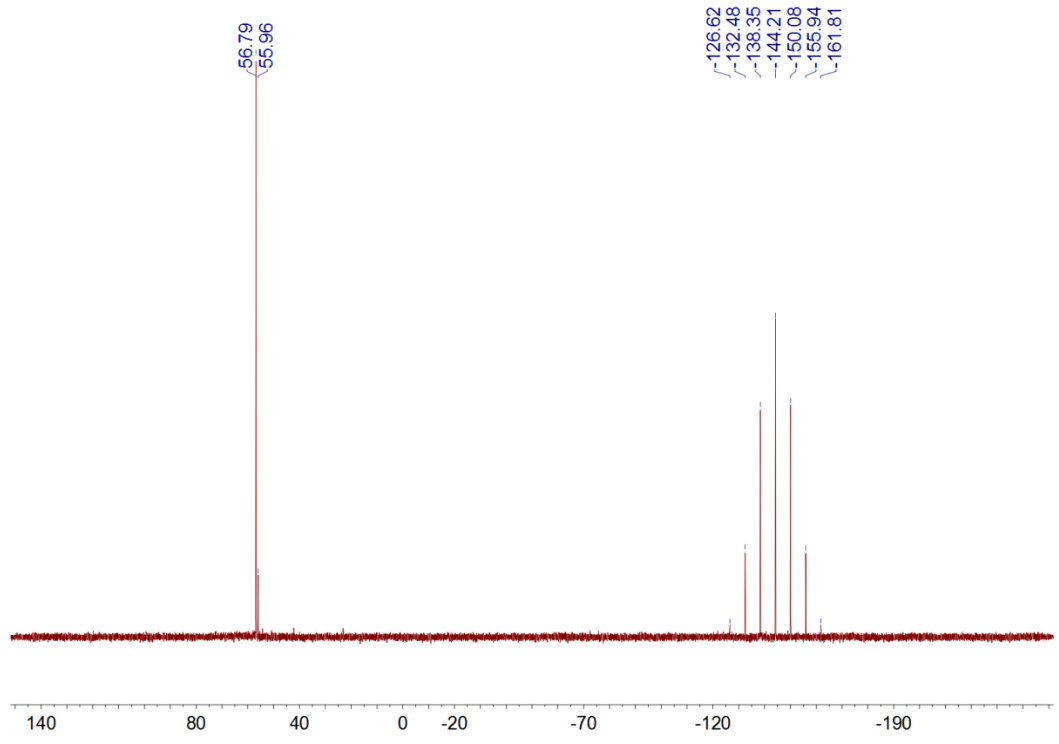
^{1}H-NMR



^{13}C-NMR

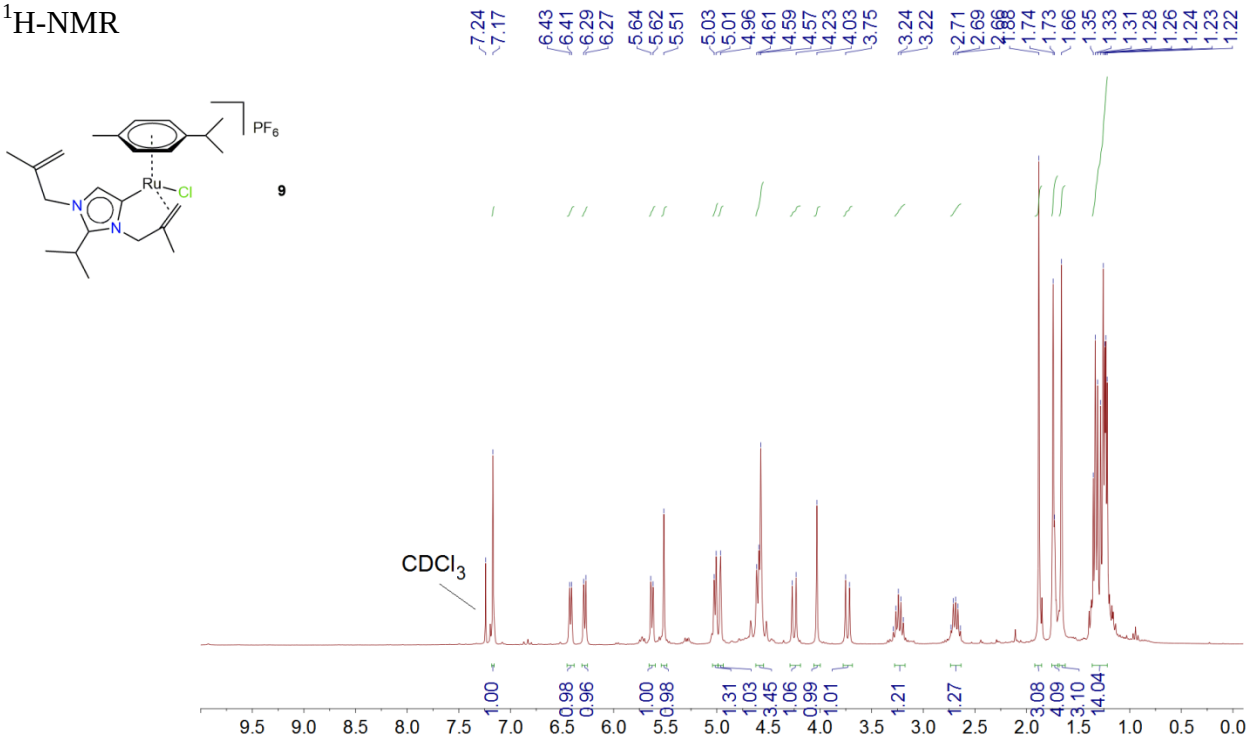


^{31}P-NMR

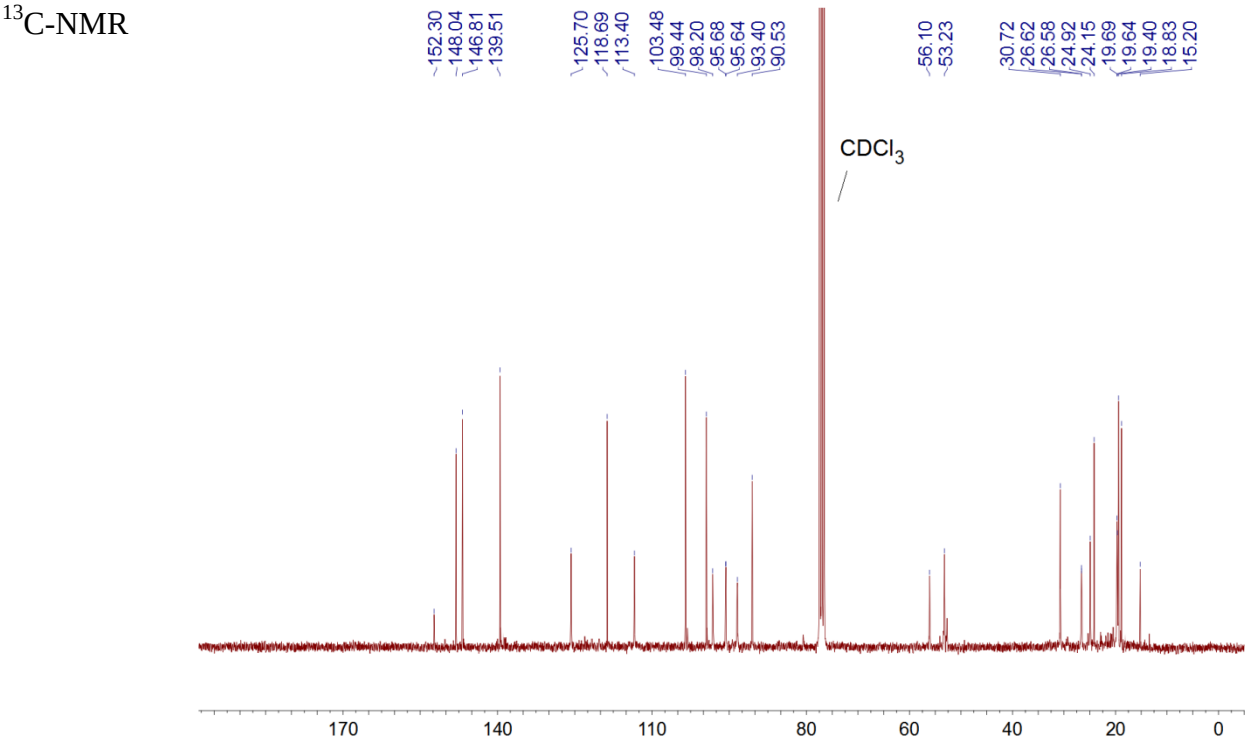


Complex **9**

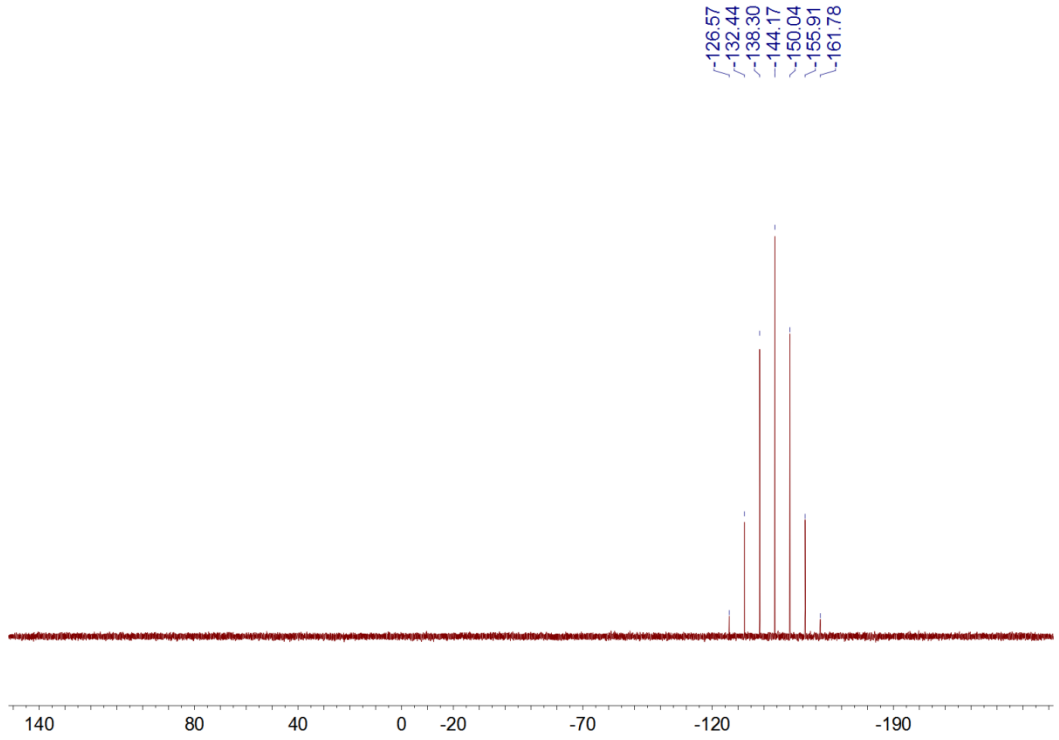
^{1}H-NMR



^{13}C-NMR

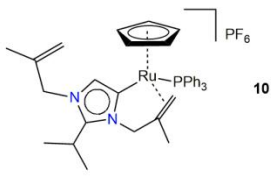


^{31}P-NMR

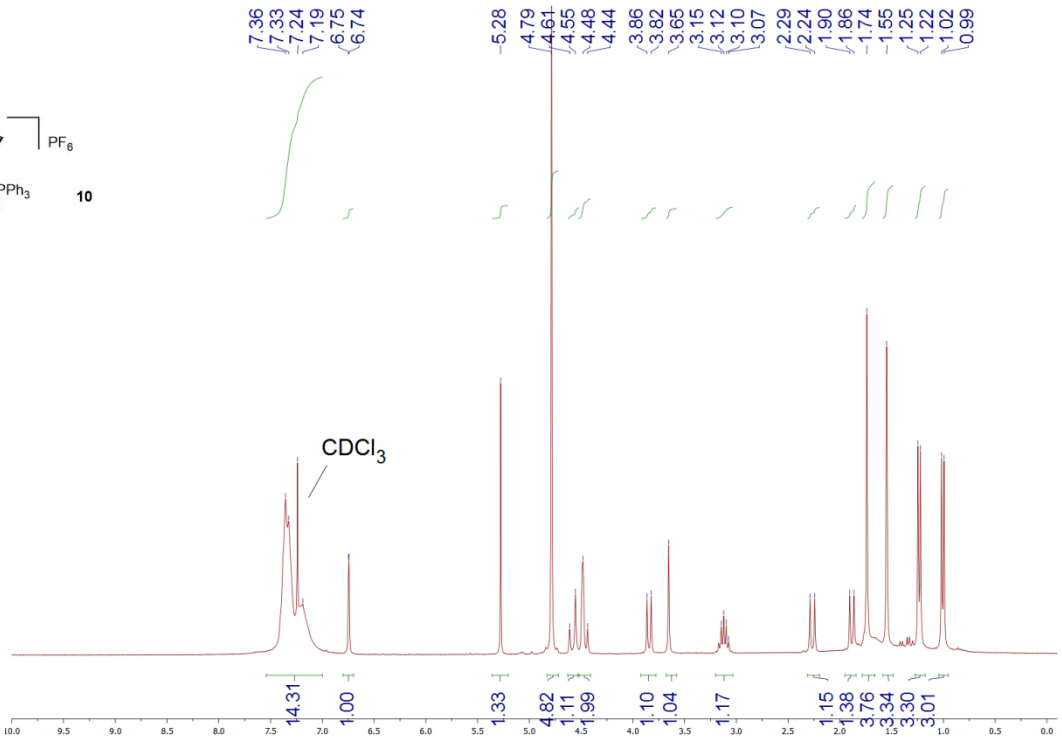


Complex **10**

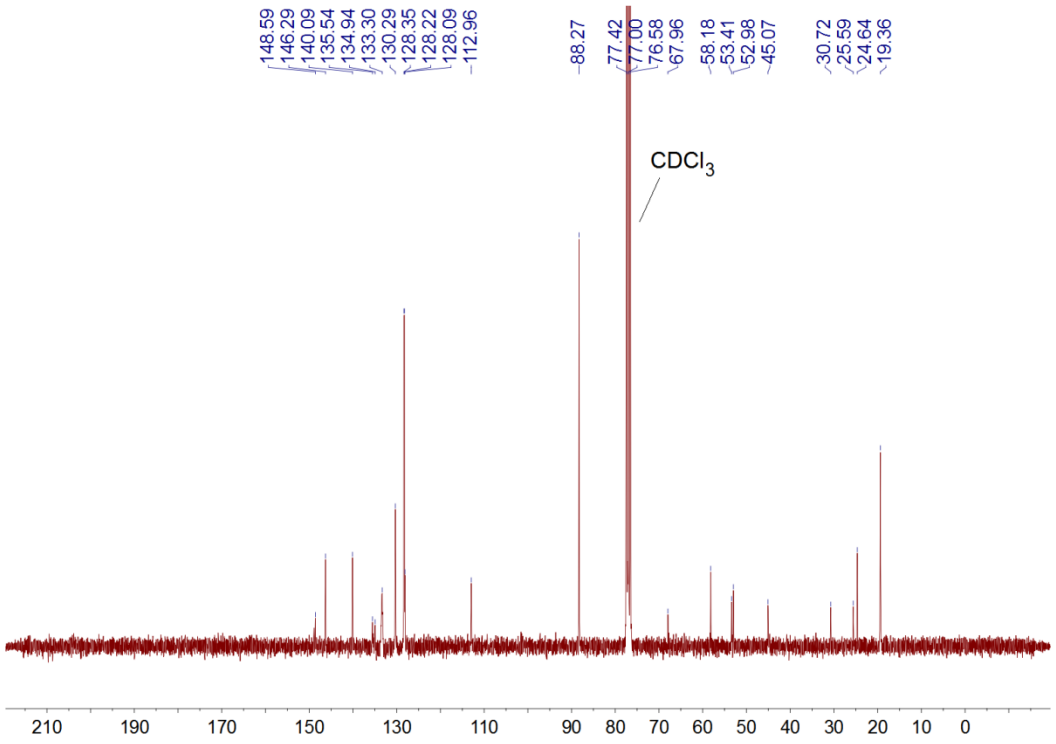
^{1}H-NMR



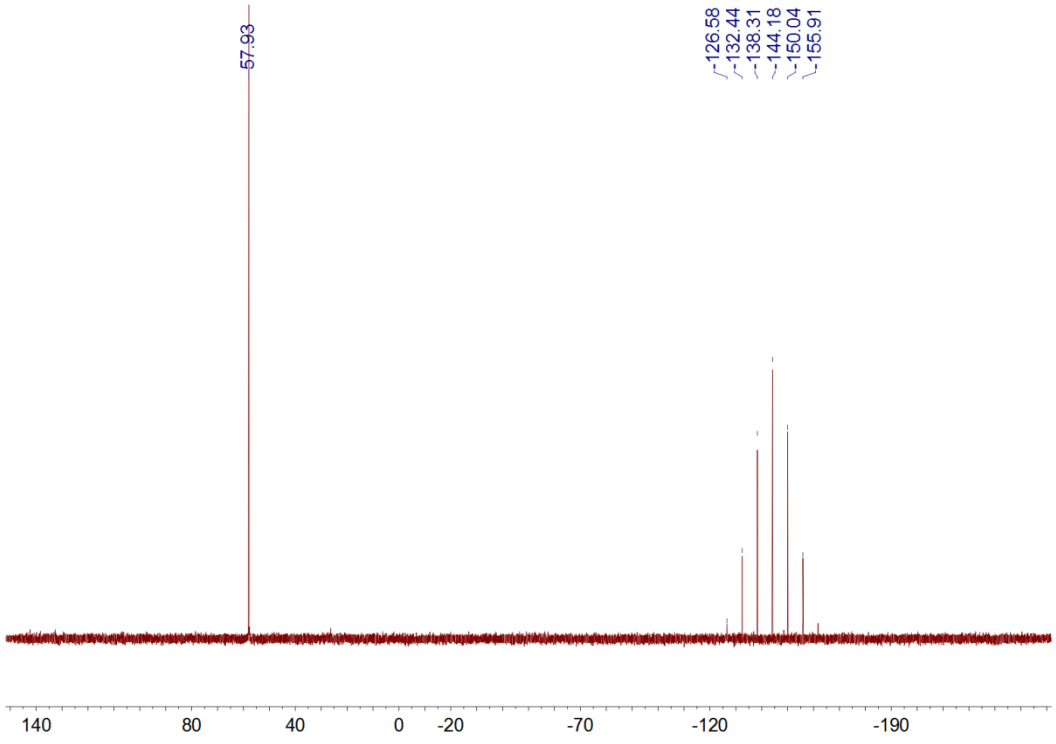
10



^{13}C-NMR



^{31}P-NMR



3. Crystal data and structure refinement for [H**L1**]Cl, [H**L4**]Cl, **1**,**3**,**5**,**6**,**7**,**8**,**10** (**Tables S1**,**S2**,**S3**)

Table S1

Complex	[H**L1**]Cl	[H**L4**]Cl	**1**	**3**
Emp. formula	$C_9H_{15}N_2F_6P$	$C_{14}H_{23}ClN_2$	$C_{19}H_{28}ClF_6N_2PRu$	$C_{128}H_{136}F_{24}N_8P_8Ru_4$
Form. weight (g.mol^{-1})	296.20	254.79	565.92	2894.48
Crystal system	monoclinic	trigonal	monoclinic	monoclinic
Space group	*$P2_1/c$*	*$P3_221$*	*$P2_1/c$*	*Cc*
Crystal descr.	yellow block	colourless block	yellow prism	gold block
a (Å)	6.5921(4)	7.8674(1)	13.4504(2)	20.1114(1)
b (Å)	13.8855(7)	7.8674(2)	13.8832(3)	19.4730(1)
c (Å)	14.0294(8)	21.086(2)	11.9684(3)	31.887(2)
α (°)	90	90	90	90
β (°)	92.682(3)	90	100.215(2)	100.516(2)
γ (°)	90	120	90	90
Volume (Å^3)	1282.77(1)	1130.3(4)	2199.49(8)	12278.2(2)
Z	4	3	4	4
Abs. coeff. (m.mm^{-1})	0.272	0.237	0.966	0.677
F(000)	608.0	414.0	1144.0	5888.0
Independent refl.	2625	1592	4527	25310
Completeness (%)	99.8	99.6	91.9	99.8
Data/Restr/Para	2625/0/166	1592/0/122	4527/0/277	25310/2/1562
Goodness of fit on F^2	1.064	1.043	1.031	1.049
Final R_1 indexes	0.0418	0.0418	0.0325	0.0333
wR_2 indices (all data)	0.1065	0.1054	0.0744	0.0730
Largest diffr. peak and hole (e.Å^{-3})	0.33/-0.28	0.20/-0.20	1.11/-0.63	0.59/-0.42

Table S2

Complex	**5**	**6**	**7/8a**	**7/8b**
Emp. formula	$C_{32}H_{34}F_6N_2P_2Ru$	$C_{24}H_{30}N_3F_6PClRu$	$C_{33.5}H_{20}F_6N_3P_2Ru$	$C_{68}H_{65}Cl_3F_{12}N_6P_4Ru_2$
Form. weight (g.mol^{-1})	723.62	642.00	741.44	1626.63
Crystal system	monoclinic	monoclinic	monoclinic	triclinic
Space group	*$P2_1/n$*	*$P2_1/c$*	*$P2_1/n$*	*P-1*
Crystal descr.	yellow prism	yellow blade	yellow fragment	yellow block
a (Å)	17.8511(6)	8.2722(1)	13.6883(9)	14.8003(7)
b (Å)	9.6153(2)	11.3526(1)	14.8014(9)	15.2415(1)
c (Å)	18.9847(6)	27.375(4)	15.5452(1)	16.7390(1)
α (°)	90	90	90	85.024(2)
β (°)	111.505(4)	91.752(4)	96.467(2)	80.728(2)
γ (°)	90	90	90	77.631(2)
Volume (Å^3)	3031.76(2)	2569.6(6)	3129.5(3)	3634.8(4)

Z	4	4	4	2
Abs. coeff. ($m.mm^{-1}$)	0.686	0.839	0.668	0.688
F(000)	1472.0	1300.0	1480.0	1644.0
Independent refl.	6195	4699	6443	13308
Completeness (%)	90.4	99.7	99.5	99.7
Data/Restr/Para	6195/60/428	4699/3/347	6443/156/479	13308/71/841
Goodness of fit on F^2	1.023	1.049	1.032	1.058
Final R_1 indexes	0.0460	0.0245	0.0495	0.0866
wR_2 indices (all data)	0.0995	0.0615	0.1153	0.1975
Largest diffr. peak and hole ($e.Å^{-3}$)	0.63/-0.63	0.57/-0.55	1.07/-1.81	4.62/-4.10

Table S3

Complex	**10**
Emp. formula	$C_{37}H_{42}F_6N_2P_2Ru$
Form. weight ($g.mol^{-1}$)	791.73
Crystal system	orthorhombic
Space group	*Pbca*
Crystal descr.	yellow prism
a (Å)	14.8783(9)
b (Å)	18.7535(2)
c (Å)	25.0075(2)
α (°)	90
β (°)	90
γ (°)	90
Volume ($Å^3$)	6977.6(7)
Z	8
Abs. coeff. ($m.mm^{-1}$)	0.603
F(000)	3248.0
Independent refl.	7200
Completeness (%)	99.9
Data/Restr/Para	7200/0/474
Goodness of fit on F^2	1.043
Final R_1 indexes	0.0311
wR_2 indices (all data)	0.0661
Largest diffr. peak and hole ($e.Å^{-3}$)	0.35/-0.40

4. Selected bond lengths and angles for [H**L1**]Cl, [H**L4**]Cl, **1**,**3**,**5**,**6**,**7**,**8**,**10** (**Table S4**)

Table S4

Description	[H**L1**]Cl	[H**L4**]Cl	**1**	**3**	**5**	**6**	**7**	**8**	**10**
Ru1-C4	-	-	2.045(3)	2.0586(2)	2.032(4)[c]	2.045(2)	2.057(6)	2.099(4)[c]	2.046(2)
Ru1-Cg[a]	-	-	1.728(3)	1.866(3)	1.905(3)	1.691(2)	1.853(6)	1.856(6)	1.899(4)
Ru-Cl1	-	-	2.4114(7)	-	-	2.4075(6)	-	-	-
Ru-P1	-	-	-	2.2948(2)	2.307(1)	-	2.2863(2)	2.3102(1)	2.3175(6)
Ru1-C4-C5	-	-	138.5(2)	139.1(5)	135.2(3)[c]	135.04(2)	137.3(5)	130.5(4)[c]	109.31(1)
N1-C3-C2	113.6(2)	114.4(3)	105.4(2)	107.6(5)	108.2(3)	-	-	-	106.95(2)
N3-C6-C7	-	-	-	-	-	112.97(2)	128.4(7)	121.3(7)	-
C4-Ru1-Ca[b]	-	-	89.49(1)	90.45(2)	89.10(1)[c]	-	-	-	91.31(8)
C4-Ru1-N3	-	-	-	-	-	85.94(8)	86.6(2)	85.7(3)[c]	-
Cl1-Ru1-C4	-	-	83.69(8)	-	-	87.17(6)	-	-	-
P1-Ru1-C4	-	-	-	85.01(2)	86.71(1)[c]	-	89.72(2)	89.1(2)[c]	87.62(6)
C1-C2-C3-N1	10.2(3)	4.3(5)	-122.675(2)	-112.194(4)	-108.369(4)	-	-	-	-116.977(2)
N3-C7-C6-N1	-	-	-	-	-	-48.60(3)	-55.077(6)	-51.739(4)	-

[a] Cg = centroid of arene/cyclopentadienyl moiety. [b] Ca = Average position between two carbon atoms belonging to the alkene moiety. [c] C2 replaces C4 for C(2)-bound (normal) NHC.

5. **Figure S1**, **S2**: Perspective views of the crystal structures of **7** and **8**

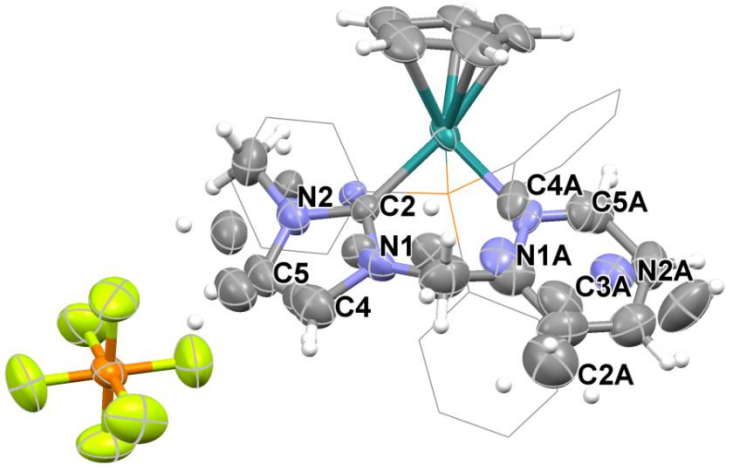


Figure S1: Perspective view of **7** and **8** when CH_2Cl_2 is used as crystallising solvent.

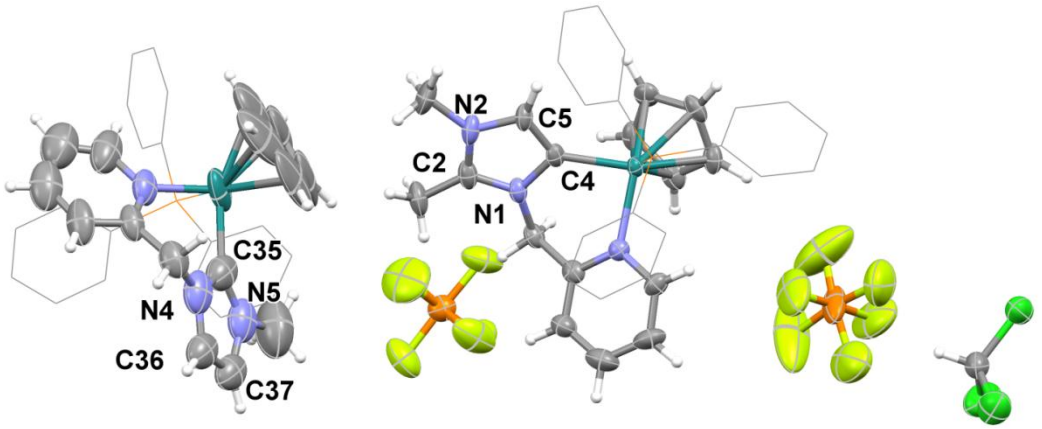


Figure S2: Perspective view of **7** and **8** when $CHCl_3$ is used as crystallising solvent.

6. Stacked ^{1}H-NMR of the stoichiometric addition of DCl to **1** (**Figure S3**)

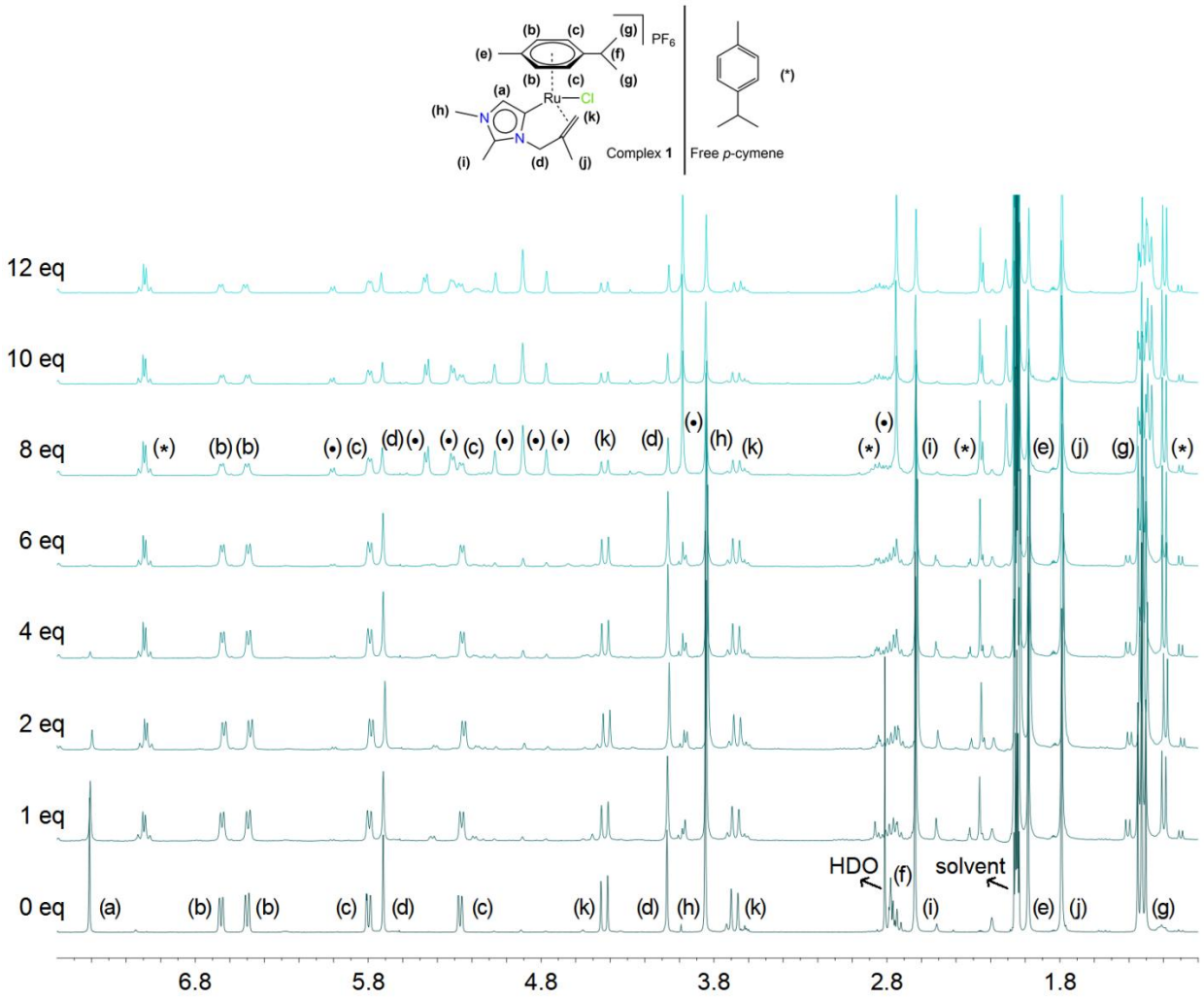


Figure S3: ^{1}H-NMR spectra (δ_H 1.0 – 7.6 ppm) of complex **1** with stoichiometric addition of DCl. Signals (a)-(j) correspond to those of complex **1**. The signals (*) and (•) correspond to those of free p-cymene and [Ru-aNHC] complex bearing a free *N*-alkenyl substituent, respectively.

7. Stacked ^{1}H-NMR of the stoichiometric addition of DCl to **3** (**Figure S4**)

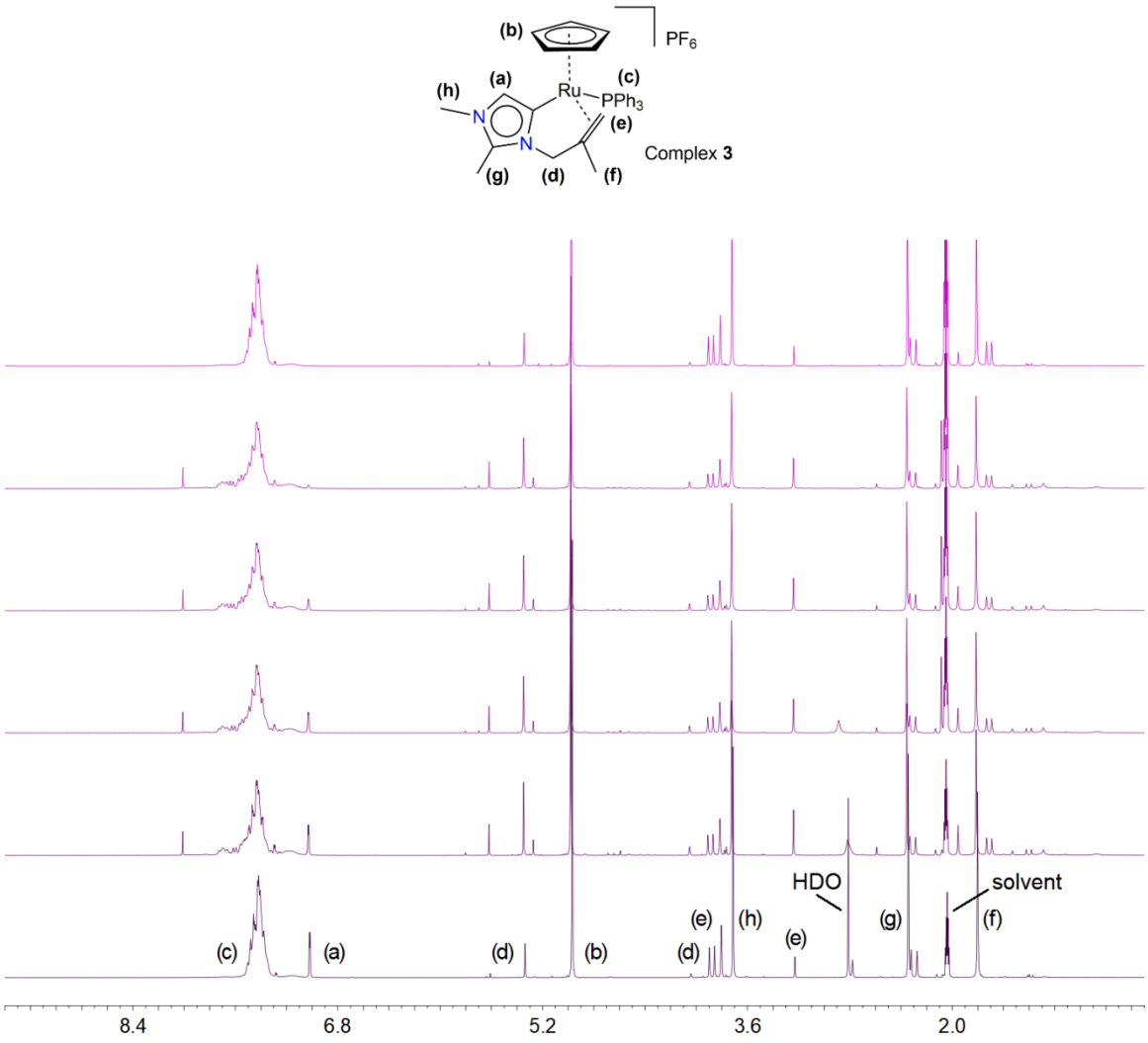
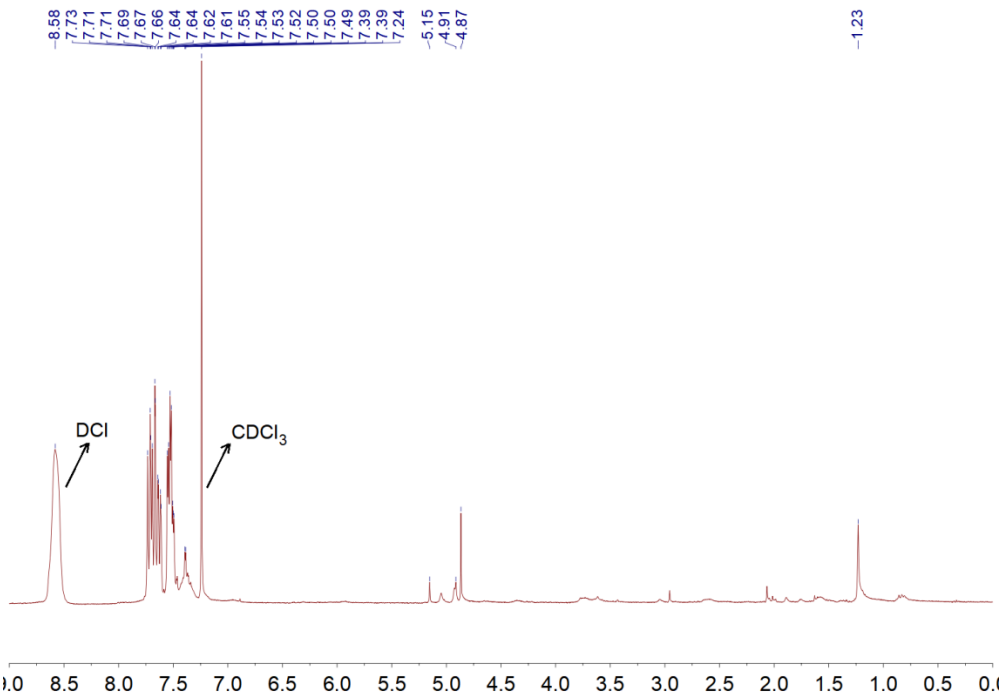
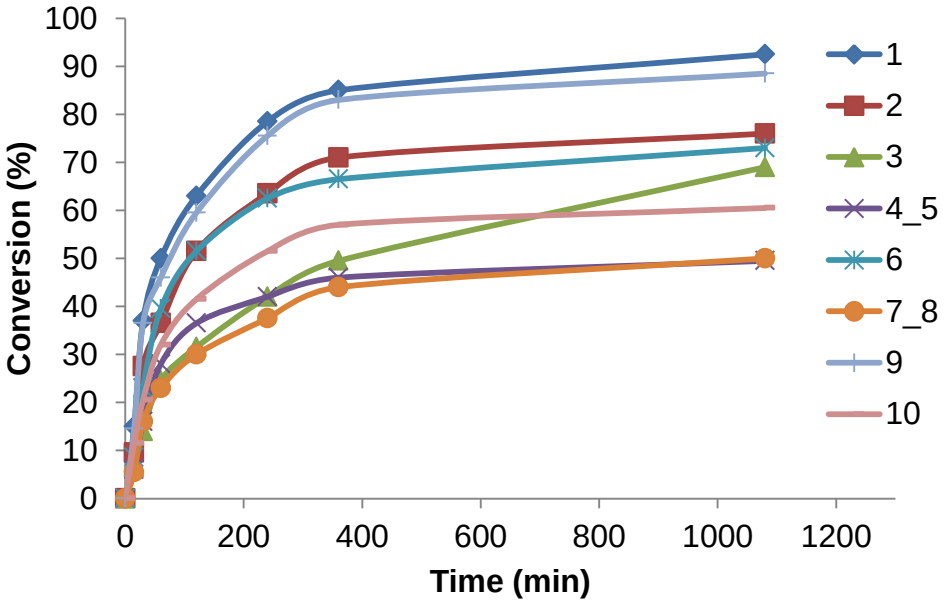


Figure S4: ^{1}H-NMR spectra (δ_H 0.5 – 9.4 ppm) of complex **3** with stoichiometric addition of DCl. Signals (a)-(g) correspond to the different moieties indicated of complex **3**. Solvent = acetone-d_6.



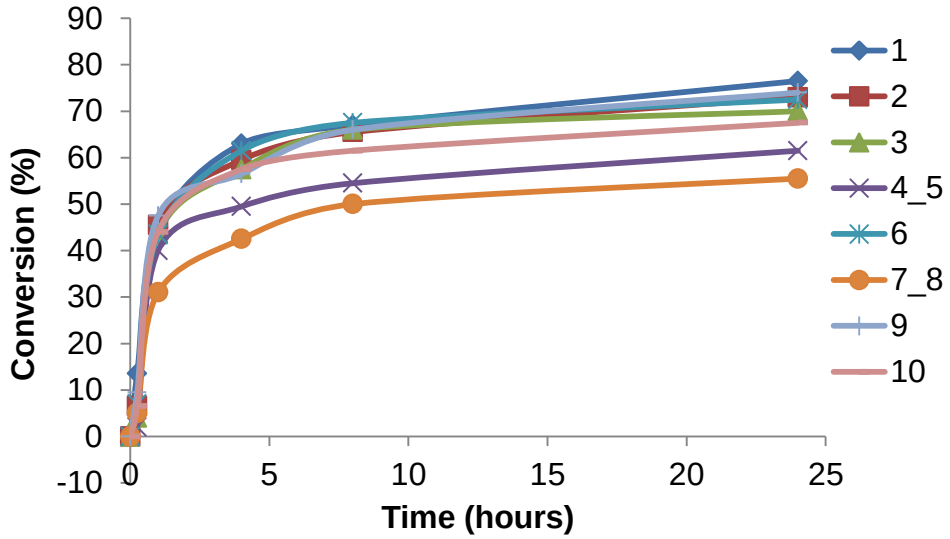
Inset: ^{1}H-NMR of **3** after addition of 12 eq. DCl over a period of two weeks. Solvent: $CDCl_3$.

8. Time-resolved conversion profiles in the transfer hydrogenation reactions



General conditions: benzophenone (0.6 mmol), iPrOH (5 mL), base (5 mol%), [Ru] (1 mol%), 110 °C. Base used depending on Ru catalyst: KOH (**1**, **2**, **6**, **9**); KO^{t}Bu (**3**-**5**, **7**, **8**, **10**). Complexes 4_5 and 7_8 were used as a ~50/50 mixture of complexes as isolated after purification. Conversions determined by GC, based on the average of at least two runs.

9. Time-resolved conversion profiles in the alcohol oxidation reactions



General conditions: ±1-phenylethanol (1 mmol), o-dichlorobenzene (5 mL), KOtBu (5 mol%), [Ru] (5 mol%), hexamethylbenzene (0.1 mmol), 150 °C. Complexes 4_5 and 7_8 were used as a ~50/50 mixture of complexes as isolated after purification. Conversions determined by GC, based on the average of at least two runs.

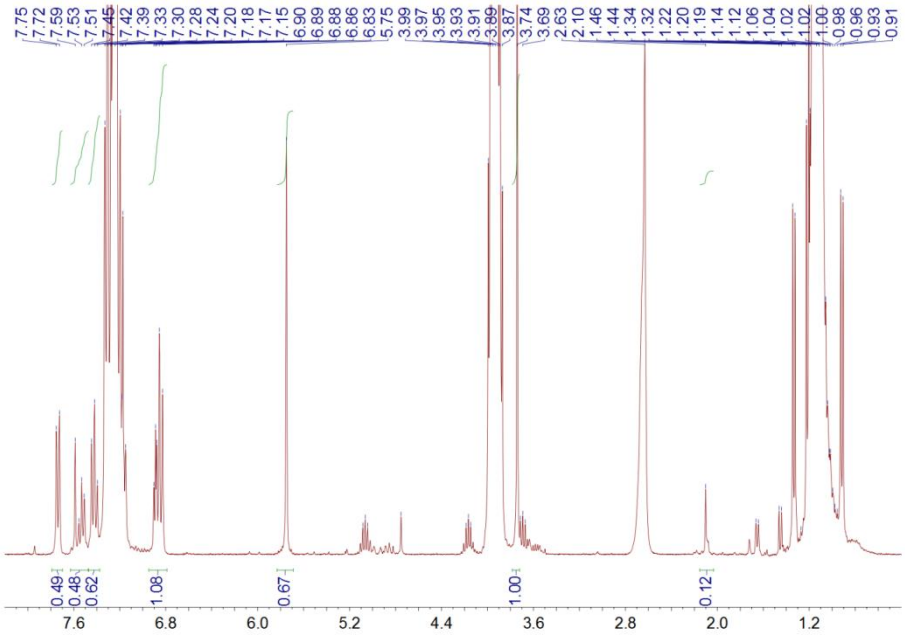
10. Optimization of transfer hydrogenation conditions (**Table S5**)

Table S5: Transfer hydrogenation of benzophenone using **1**,**3**.

Entry	Complex	Temp (ºC)	Base	Conversion[b] (%)	
				2h	6h
1	-	110	KOH	1	2
2	-	110	KO^{t}Bu	3	6
3	**1**	110	-	5	28
4	**3**	110	-	2	5
5	**1** (3 mol%)	110	KOH	72	95
6	**1** (0.5 mol%)	110	KOH	9	37
7	**1**	110	KOH (10 mol%)	64	92
8	**1**	25	KOH	4	10

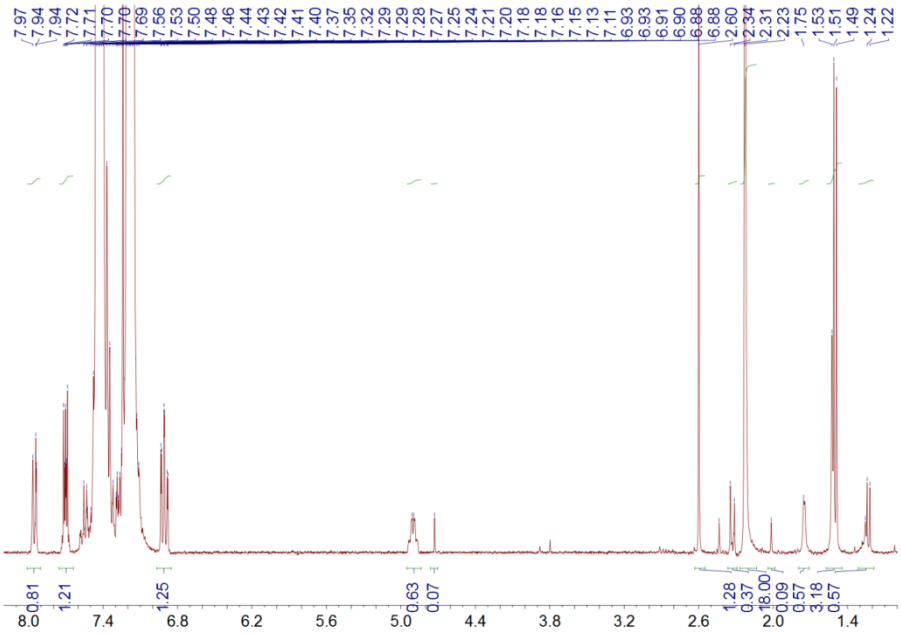
General conditions: benzophenone (0.6 mmol), iPrOH (5 mL), base (5 mol%), [Ru] (1 mol%), 110 °C. Base used depending on Ru catalyst: KOH (**1**); KO^{t}Bu (**3**). [a] Mixture of complexes as isolated after purification. [b] Determined by GC, based on the average of at least two runs. Yields in parentheses are based on ^{1}H-NMR.

11. ^{1}H-NMR spectrum of transfer hydrogenation reaction mixture



General conditions: Benzophenone (0.6 mmol), iPrOH (5 mL), KOH (5 mol%), [**1**] (1 mol%), 110 °C. Aliquot taken after 2 hours reaction time, analysed using $CDCl_3$.

12. ^{1}H-NMR spectrum of alcohol oxidation reaction mixture



General conditions: ±1-Phenylethanol (1 mmol), *o*-dichlorobenzene (5 mL), KO^{t}Bu (5 mol%), [**1**] (5 mol%), hexamethylbenzene (1 mmol), 150 °C. Aliquot taken after 4 hours reaction time, analysed using $CDCl_3$.